



## CONTENTS

	<b>Page No.</b>
<b>FOREWORD</b>	0.7
<b>EXECUTIVE SUMMARY</b>	0.9
<b>1. INTRODUCTION</b>	1.1
1.1 BACKGROUND	1.1
1.2 LOADCASE 1 OBJECTIVES	1.2
1.3 REPORT LAYOUT	1.5
<b>2. LOADCASE 1 TEST</b>	2.1
2.1 CONFIGURATION	2.1
2.1.1 Reference Schemes	2.1
2.1.2 Component Properties	2.2
2.1.3 Response Data	2.5
2.1.4 Test Procedure	2.6
2.2 RESPONSE	2.7
2.2.1 Preamble	2.7
2.2.2 Global Response	2.9
2.2.3 Detailed Response	2.12
2.2.4 Comparison with Phase II 2D Results	2.18
2.2.5 Local K Joint Responses	2.20
2.3 QUANTIFIED SUMMARY OF RESULTS	2.26
<b>3. COMPONENT TESTING AND ANALYSIS</b>	3.1
3.1 NORSK HYDRO FINITE ELEMENT ANALYSIS	3.1
3.1.1 Background	3.1
3.1.2 Modelling	3.1
3.1.3 Joint Responses	3.2
3.1.4 Joint / Frames Responses	3.2
3.1.5 Comparisons	3.2
3.2 SINTEF ISOLATED STATIC TESTS	3.7
3.2.1 Background	3.7
3.2.2 Test Specimens and Procedures	3.8
3.2.3 Isolated Test Results	3.8
3.2.4 Results Update	3.9
3.3 FRAMES PROJECT PHASE II INFORMATION	3.13



## CONTENTS CONTINUED

	<b>Page No.</b>
3.3.1 Basis of 2D Investigations	3.13
3.3.2 Capacity Results	3.13
3.3.3 Bending Moment Results	3.13
3.4 SAFJAC FRAME RESPONSE PREDICTIONS	3.15
3.4.1 Background	3.15
3.4.2 Comparison between Predicted and Measured Responses	3.15
<b>4. INDUSTRY PRACTICE</b>	<b>4.1</b>
4.1 PREAMBLE	4.1
4.2 PLANAR JOINT CODE CAPACITY FORMULATIONS	4.2
4.3 AS-BUILT JOINT CAPACITY PREDICTIONS	4.2
4.4 MULTIPLANAR JOINT CAPACITY FORMULATIONS	4.4
<b>5. ASSESSMENT OF LOADCASE 1 COMPONENT AND SYSTEM RESPONSES</b>	<b>5.1</b>
5.1 JOINT CAPACITY DATA ASSIMILATION	5.1
5.2 JOINT DEFORMATION COMPARISONS	5.4
5.3 SYSTEM RESPONSE COMPARISONS	5.6
<b>6. CONCLUSIONS</b>	<b>6.1</b>
<b>7. REFERENCES</b>	<b>7.1</b>
<b>APPENDIX A AS-BUILT DRAWINGS RELEVANT TO LOADCASE 1 TEST</b>	
<b>APPENDIX B INSTRUMENTATION LAYOUT DRAWINGS</b>	
<b>APPENDIX C FRAME RESPONSE PLOTS</b>	



## FOREWORD

This report is one of a series describing different aspects of Phase III of the Joint Industry Tubular Frames Project. Each report is self contained providing detailed information in the subject area and summarising relevant data from other documents. The following table lists and briefly describes the focus of each report for cross-referencing purposes.

Report Title	Reference	Circulation
<b>Summary and Conclusions</b> Overview report describing the project and principal findings	C636\04\478R	1
<b>Background, Scope and Development</b> Scene setting report summarising previous work, identified needs and Phase III programme definition and development	C636\04\435R	1
<b>3D Test Set Up</b> Brief description of the 3D test set up and structural configuration	C636\06\313R	1
<b>Material Testing Report</b> Description of material testing procedures, test results and disposition of specific materials within test structure	C636\23\004R	1
<b>Assessment of Locked-In Fabrication Stress</b> Explanation for the build up of locked-in fabrication stresses, description of their measurement and summary of the locked-in force values in key components at the start of each test	C636\21\050R	1
<b>Test Frame Instrumentation</b> Detailed description of all instrumentation systems used in the 3D frame, accuracy, sign conventions etc. Data on CD in final report	C636\25\071R	1
<b>Loadcase 1 Test Report - Multiplanar K Joint Action</b> Detailed description of the Loadcase 1 static test response and interpretation of the results and their significance	C636\37\014R	1
<b>Loadcase 2 Test Report - Interaction Between X-Braced Planes</b> Detailed description of the Loadcase 2 static test response and interpretation of the results and their significance	C636\39\011R	1
<b>Loadcase 3 Test Report - Multiple Member Failures and 3D System Action</b> Detailed description of the Loadcase 3 static test response and interpretation of the results and their significance	C636\40\021R	1



Report Title	Reference	Circulation
<p><b>Philosophy of Cyclic Testing</b> Discussion of the background to cyclic response issues in the context of ultimate system strength and basis for specific loading scenarios</p>	C636\24\021R	1
<p><b>Loadcase 1 Cyclic Test Report</b> Detailed description of the Loadcase 1 cyclic test response and interpretation of the results and their significance. Comparison with LC1 static results</p>	C636\38\010R	1
<p><b>Monotonic and Cyclic testing of Isolated K Joints</b> Description and presentation of results from isolated component tests undertaken by SINTEF in Norway</p>	STF22 F98704 (C636\24)	1/2
<p><b>Loadcases 2 and 3 Cyclic Test Report</b> Detailed description of the Loadcases 2 and 3 cyclic test responses and interpretation of the results and their significance. Comparison with LC2 and LC3 static results</p>	C636\41\011R	2
<p><b>Loadcases 1 and 3 'Alternative' Cyclic Tests</b> Detailed description of the Loadcases 1 and 3 alternative cyclic test responses and interpretation of the results and their significance. Comparison with LC1 and LC3 static and cyclic tests</p>	C636\45\008R	3
<p><b>Multiplanar SCFs</b> Joint BG / BOMEL report describing analytical work and experimental measurements of multiplanar SCFs. Includes comparison with 'standard' empirical approaches</p>	C636\18\018R	1
<p><b>Site Testing Programme results - Report to Benchmark Analysts</b> Comprehensive report describing results for benchmark cases LC1, LC2 and LC3, including all pertinent data and providing response plots 'matching' the contributions from individual analysts</p>	C636\32\066R	4
<p><b>Benchmark Conclusions</b> Report comparing blind and post test analyses with measured responses and assimilating learnings and recommendations for future practice identified by Benchmark Analysts</p>	C636\32\084R	1



Key to circulation.

Circulation	All participants	Participants in 1st extension	Participants contributing finance/analytical results to 2nd extension	Benchmark Analysts
1	✓	-	-	×
2	-	✓	-	×
3	-	-	✓	×
4	✓	-	-	✓



## JOINT INDUSTRY TUBULAR FRAMES PROJECT - PHASE III

### LOADCASE 1 TEST REPORT MULTIPLANAR K JOINT ACTION

#### EXECUTIVE SUMMARY

Phase III of the Joint Industry Tubular Frames Project involves a series of ultimate strength tests of a jacket type structure together with associated analytical and laboratory investigations. This report forms one of a series and addresses the specific results from the first Loadcase 1 ultimate strength test of the frame.

The critical components in the test were a pair of multiplanar K joints. Previous 2D investigations had indicated some 20-40% greater capacity when K joints were loaded within a frame compared with predictions from isolated test databases. The purpose of the investigation was to assess how these factors applied in the more realistic case of multiplanar K joints and to see how the structural system adapts as components fail.

This report provides specific background to the Loadcase 1 test and gives a detailed description of the test. Findings from complementary laboratory tests undertaken by SINTEF, previous Frames Project research, and analyses performed by Norsk Hydro and BOMEL are presented. Current industry practice is assessed in relation to the provisions of recent codes and standards.

It was found that the multiplanar K joints in the frame exhibited strengths as much as twice the level seen in isolated test databases. The potential sources of strength are examined in the context of the supporting tests and it is found that frame constraints dominate over local stiffening or relative force contributions.

Once joint failure occurs forces redistribute through the structure contributing to a global reserve strength ratio of 4.0 with respect to API practice. This is attributable to both the conservatism in joint capacity calculations and system contributions to strength.

The ultimate response was finally determined by buckling of a compression K-brace. The details of the member response are assessed in the Loadcase 3 report alongside other similar component response data.



## 1. INTRODUCTION

### 1.1 BACKGROUND

Phase III of the Joint Industry Tubular Frames Project follows earlier phases of 2D frame tests and analytical investigations. These had indicated that components behave differently within the confines of a frame than in isolated tests on which engineering practice has been based. Furthermore the structural systems exhibit significant reserve of strength beyond design load levels. If these effects could be assured for jacket structures there could be important practical benefits in terms of a reduced need to strengthen existing structures and greater efficiency in future designs.

The purpose of the Frames Project Phase III was therefore to demonstrate the validity of these findings for 3D jacket type structures and in so doing to examine aspects absent from the earlier plane frame tests. The specific objectives were:

- To establish the effects of nonlinear joint/member behaviour on three-dimensional frame behaviour and collapse mechanisms.
- To quantify the reserve and residual strength of three-dimensional frames and to investigate redundancy and load shedding characteristics.
- To investigate the static performance of members and joints within three-dimensional frames and to develop procedures for the exploitation of available component data.
- To carry out comparative isolated joint tests.
- To measure locked-in stresses introduced during construction of three-dimensional frames.
- To calibrate and apply a nonlinear numerical procedure, SAFJAC, to the collapse analysis of the test frame and to provide data for the calibration of other software with similar stated capabilities.
- To benchmark the capabilities of existing 3D nonlinear analysis software.

These objectives have been fulfilled with the conduct of a series of static and cyclic tests of a three dimensional jacket type structure under different loading scenarios denoted Loadcase 1,

Loadcase 2 and Loadcase 3 (LC1, LC2 and LC3). Figure 1.1 shows the test set up and scenarios.

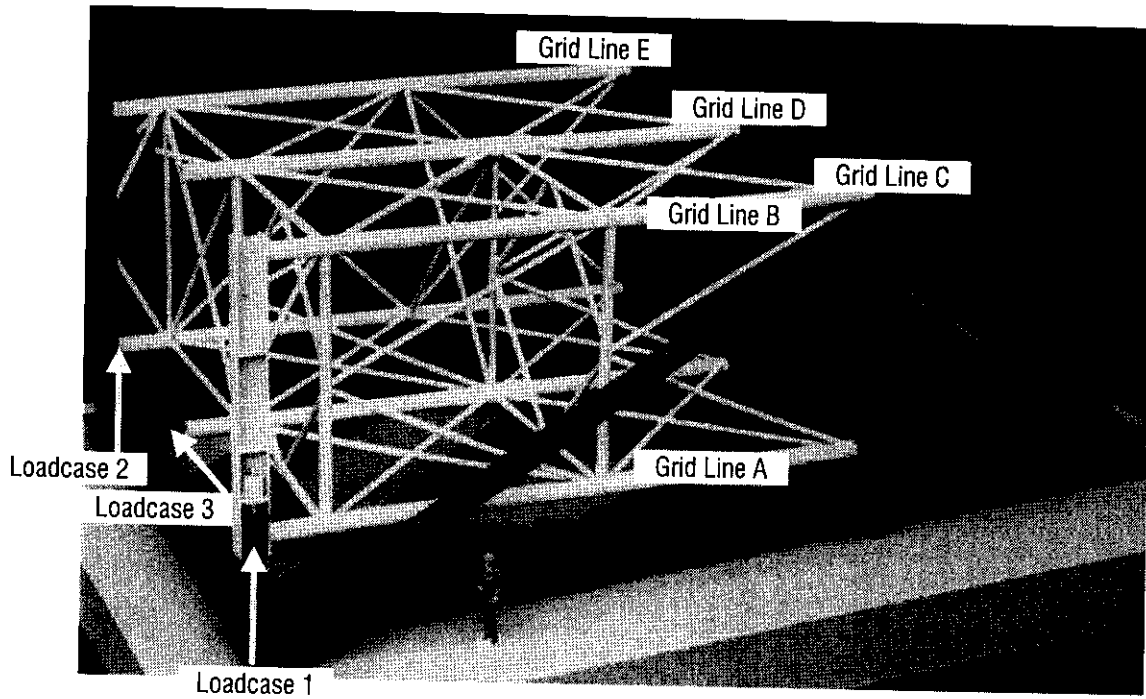


Figure 1.1 3D frame loading configuration

Reference 1 describes in detail how the test structure was designed in the context of the Phase III programme and the range of features embraced. This report focuses on the specific conduct of, and findings from, the Loadcase 1 static test. Appendix A provides structural drawings for the frame pertinent to the LC1 response.

## 1.2 LOADCASE 1 OBJECTIVES

Multiplanar K joint intersections are a common feature of offshore jacket structures. However data on the ultimate strength of multiplanar connections are sparse. Design practice assesses the capacity within individual planes, completely neglecting the benefit or detrimental effects of out-of-plane braces and the loads they transmit.

In Phase II of the Frames Project<sup>(2, 3)</sup> a K-braced plane frame was tested for a number of alternative gap K joint configurations (Figure 1.2). Although isolated tests of K joints generally exhibit a ductile mode of failure with ovalisation of the chord around the compression intersection<sup>(4)</sup>, the peak capacity of the joints in the 2D frame was governed by cracking at the tension brace weld toe in the gap region. Further isolated tests confirmed that this was due to the strong shear across the gap region when both ends of the chord are constrained within the structure (Figure 1.2). In most isolated tests, one end of the chord is often left free.



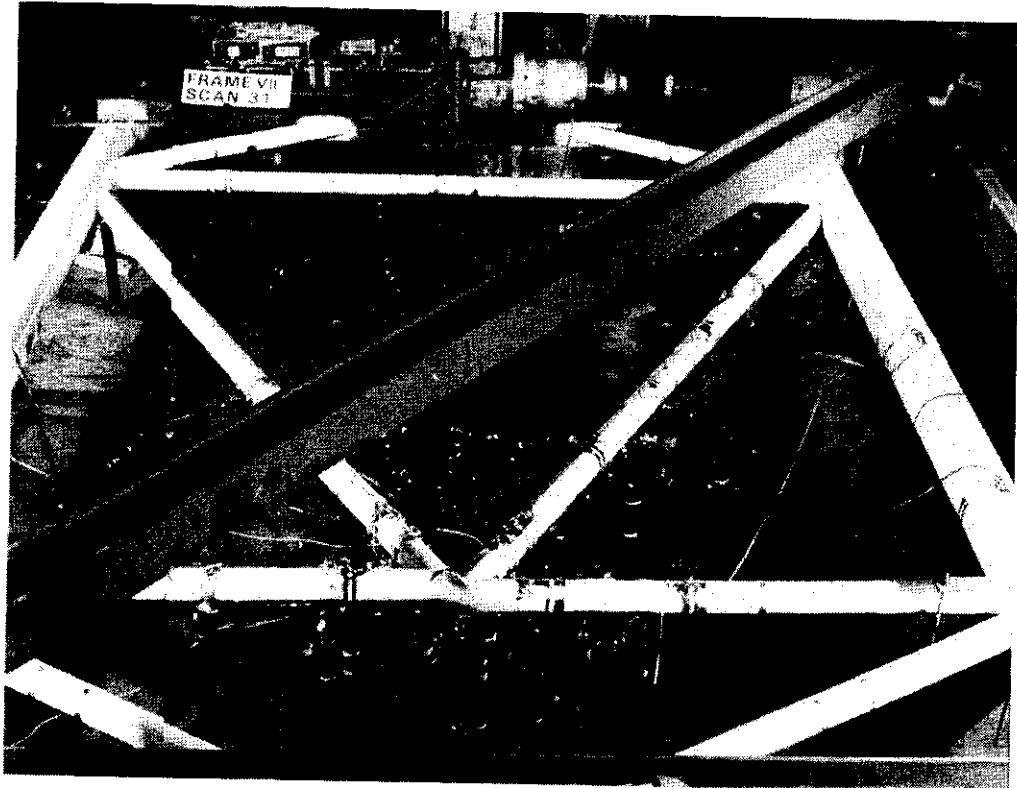


Figure 1.2 Phase II K-braced frame test

The capacity of the K joints in the frame was found to be 17-34% higher than the mean value predicted from the data underlying the then current HSE Guidance<sup>(4)</sup>. However, as described, the mode of failure had a 'brittle' as opposed to 'ductile' characteristic, resulting in rapid load shedding and loss of integrity for the K-braced bay. Figure 1.3 shows the member forces in the primary K braces in the 2D test frame in comparison with the applied load.

One aspect of the Phase III programme was therefore to examine the relevance of these findings for 3D structures and specifically:

- To assess how much out-of-plane bracing modifies the response mode and capacity of K joints within a structure, whether due to local stiffening of the chord wall, the loads in the out-of-plane braces or out-of-plane constraint.
- To assess how applied load transfers via the multiplanar connections to mobilise alternative loadpaths in the 3D structure contributing to the reserve and residual strength of the system

Figure 1.4 shows the Loadcase 1 scenario in which these multiplanar K joint responses were examined (see also Figure 1.1). The actuator is mounted on the K-braced Frame C, pushing the structure upwards. The two K nodes in Frame C both form multiplanar connections at the intersection with the Level 1 and Level 2 diamond bracing. At the Level 1 intersection (closest to the actuator) the out-of-plane diamond braces overlap whereas at Level 2 they do not.

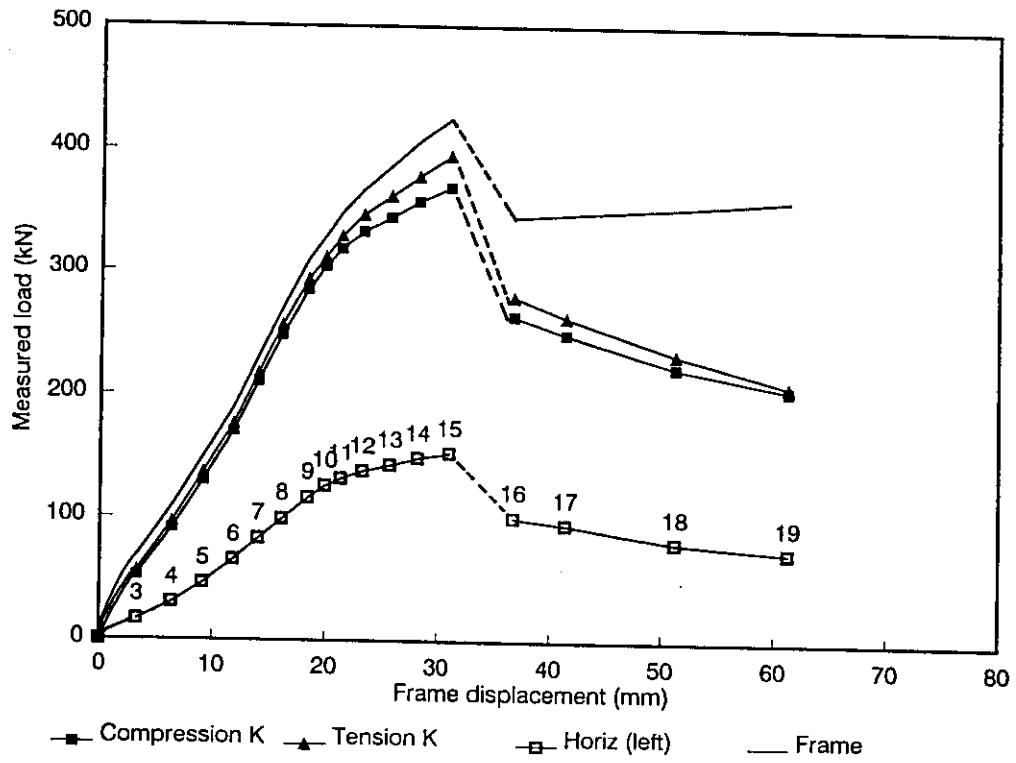


Figure 1.3 Frames Project Phase II - Frame VIII global response in comparison with primary brace loads

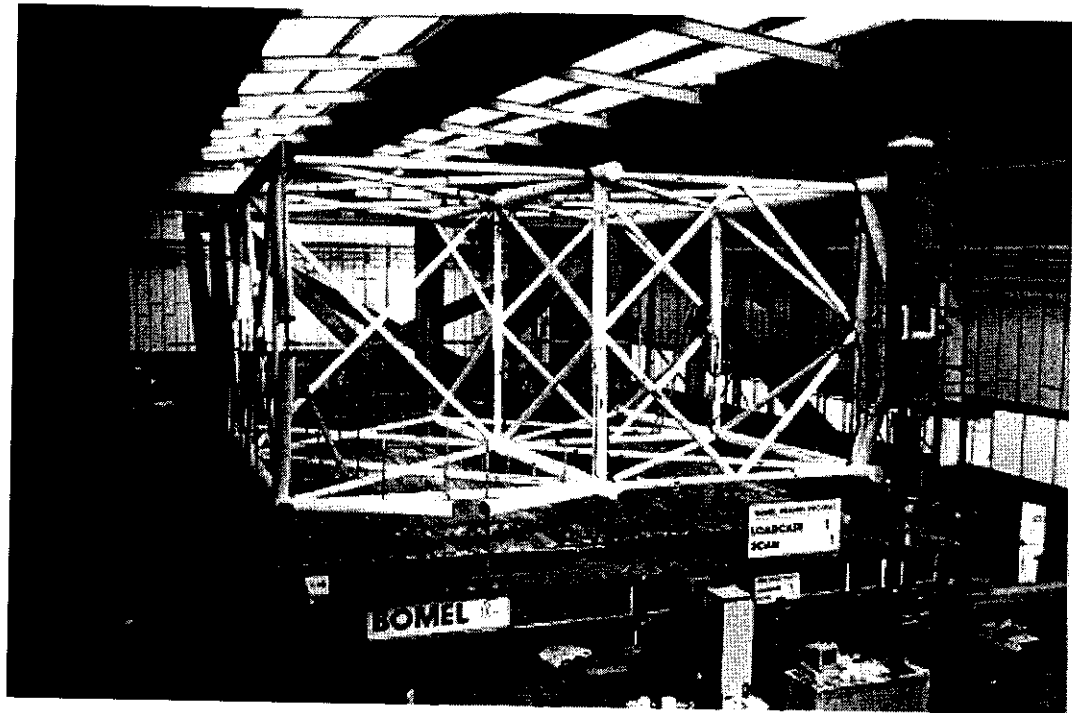


Figure 1.4 Loadcase 1 configuration - start of test



The Loadcase 1 configuration was designed based on an extensive survey of actual jacket configurations from drawings provided by Participants and held by BOMEL in-house. Although space, tubular sizes manufactured and the requirements of other test scenarios imposed some restrictions, the geometry and non-dimensional properties of the K nodes on Line C were chosen to be representative of offshore practice.

A number of other studies within the Phase III programme have provided complementary information, either to aid in the interpretation of the Loadcase 1 test or to help determine the appropriate application of the findings. The studies include:

- Nonlinear shell finite element analysis performed by Norsk Hydro to predict the capacity of the K joints in isolation and analysed within the 3D frame<sup>(5)</sup>.
- Laboratory tests for nominally identical K joints with and without out-of-plane bracing performed by SINTEF<sup>(6)</sup>.
- Component and system response predictions performed by BOMEL using the Frames Project nonlinear software SAFJAC<sup>(7)</sup>.
- Blind predictions using various nonlinear analysis packages contributed by Analysts to the Benchmark<sup>(8)</sup>.

In addition the repeat of the Loadcase 1 static test once the structure was repaired but with cyclic applied loads<sup>(12)</sup>, provides a comparative reference.

It can therefore be seen that the Loadcase 1 test was not only addressing the specific issues surrounding multiplanar K joints but was also contributing to the overall project objectives (see Section 1.1).

### 1.3 REPORT LAYOUT

Having established the purpose of the Loadcase 1 test, Section 2 describes the structural response. Section 3 provides a corresponding factual description of the other analytical and experimental studies contributing to the understanding of the frame behaviour. In Section 4 reference is made to recent codes and standards and, by inference, isolated tubular joint databases. All these aspects are assimilated in Section 5 leading to conclusions in Section 6.

As noted in the Foreword, this report is one of a series describing the Frames Project Phase III results. It assembles data relevant to the interpretation of the Loadcase 1 static test results. More detailed information, for example on the instrumentation or materials, can be found in the companion reports. The draft report is printed in black and white with key plots reproduced in colour in the appendices. Final and electronic issues will be in full colour.



## 2. LOADCASE 1 TEST

### 2.1 CONFIGURATION

#### 2.1.1 Reference Schemes

Figure 1.4 shows the 3D test structure at the start of the Loadcase 1 test. The loading beam and actuator are positioned on Frame C applying positive load upwards in displacement control. The datum position (zero applied load) corresponds to the condition in which the tubular frame cantilevers under its self weight from the reaction rig; the weight of the actuator system is taken directly to ground. A consistent numbering scheme for every member and node within the frame was adopted by all parties and for all aspects of the work. This is shown in Figures 2.1 and 2.2 as it applies for Loadcase 1. The global axis system is also shown.

For internal member axial forces the convention: positive = tension, negative = compression is adopted. A left hand rule defines moment orientations; however, these are also described within the local context.

#### 2.1.2 Component Properties

Appendix A contains as-built structural drawings for the 3D frame. Reference 9 provides information on the disposition of material throughout the structure, together with diameter ( $D$ ) and wall thickness ( $T$ ) measurements from surveys for every member segment within each member and at key nodes. Results are developed from static tensile coupon tests giving yield properties ( $F_y$ ) corresponding to the rate of structural testing. Reference 10 explains the build up of locked-in fabrication forces within the frame. Measured values are presented and combined with calculated member forces due to self weight to give the net force in every component at the start of each test (zero applied load).

For this report, properties for key components in the Loadcase 1 test scenario have been extracted and are presented below. Table 2.1 details the geometric properties and parameters in comparison with nominal and assumed values at the design stage. Table 2.2 shows the contributions to the initial distribution of forces in the structure at the start of the Loadcase 1 test.

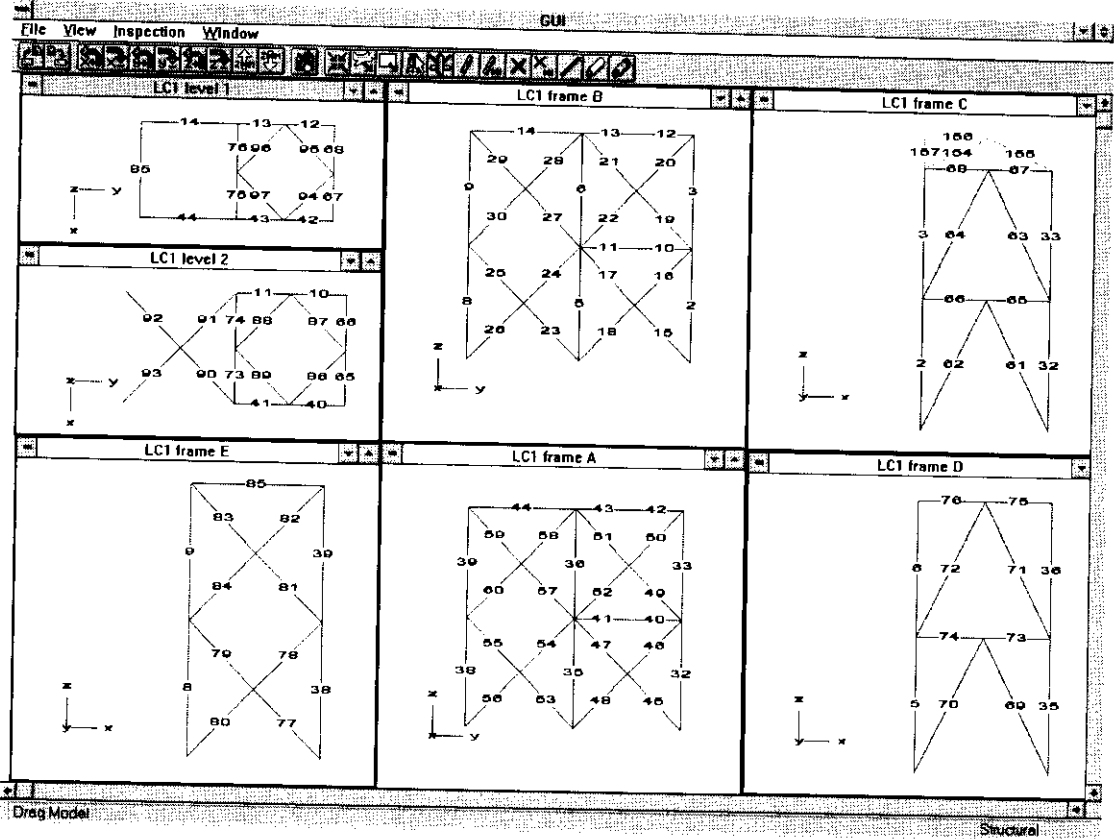


Figure 2.1 Member numbering system Loadcase 1

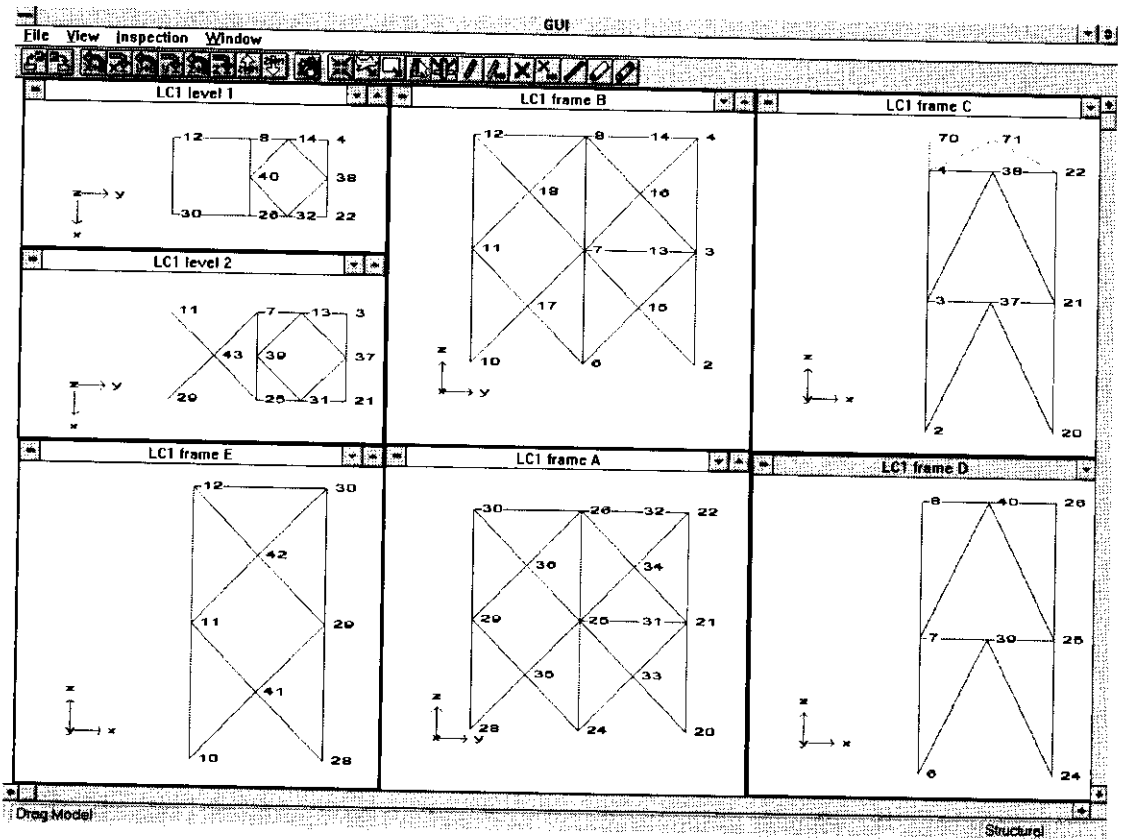


Figure 2.2 Node numbering system Loadcase 1

Table 2.1 Loadcase 1 - Actual compared with nominal component properties

Component	Braces - nominal				Chord - nominal				Chord - actual			
	Member	$\theta$	d (mm)	t (mm)	g (mm)	D (mm)	T (mm)	$F_y$ (N/mm <sup>2</sup> )	g (mm)	D (mm)	T (mm)	$F_y$ (N/mm <sup>2</sup> )
N37 / Frame C	61	64.3°	168.3	5.6	26	273.1	5.6	240	9	273.1	5.61	288.6
	62	64.3°	168.3	5.6								
N37 / Level 2	86	45°	168.3	4.5	-101	273.1	5.6	240	-99	273.1	5.61	288.6
	87	45°	168.3	4.5								
N38 / Frame C	63	64.3°	168.3	5.6	26	273.1	5.6	240	12	273.3	5.61	288.6
	64	64.3°	168.3	5.6								
N38 / Level 1	94	45°	168.3	4.5	35	273.1	5.6	240	28	273.3	5.61	288.6
	95	45°	168.3	4.5								

Component	Brace - nominal				Brace - actual				
	$\theta$	d (mm)	t (mm)	$F_y$ (N/mm <sup>2</sup> )	Imperfection (mm)	d (mm)	t (mm)	$F_y$ (N/mm <sup>2</sup> )	Imperfection (mm)
Member 72	64.3°	168.3	4.5	250	0	168.6	4.58	283.3	In-plane 2mm towards leg Out-of-plane 0mm

Sources:

D, d, T, t and  $F_y$  - C636\06\294w-b.xls

Gap and imperfection data - C636\06\307w.xls



Table 2.2 Loadcase 1 - Initial forces at zero applied load

Member	Forces (kN)				
	Locked in fabrication force - free component to completed, propped structure (DEMEC system)	Forces induced as supports are removed and datum position reached (recorded by instrumentation)	Net force at start of LC1 test	Self weight gravitational component of force (calculated)	Locked-in fabrication component of force
	a	b	a + b	c	a + b - c
61	-9	-72	-81	-76	-5
62	60	70	130	76	54
63	2	-80	-78	-53	-25
64	20	74	94	54	40
65	-	34	-	31	-
66	-31	-36	-67	-32	-35
67	-	106	-	25	-
68	-	-20	-	-24	-
72	-37	32	-5	34	-38
86	18	-3	15	0	14
87	-3	5	2	0	3
94	47	-20	27	-4	31
95	-30	20	-10	4	-14

Source: C636\21\046w.xls

Notes:

- 1 - indicates no value available
- 2 Figures rounded to 0 d.p
- 3 (a) Mechanical DEMEC system accurate to within  $\pm 10$  kN - coarse but suitable for use during fabrication<sup>(10)</sup>. Force values based on nominal properties
- (b) Instrumentation readings use loadcell values where available. Where site installed strain gauges are used, force values based on nominal properties
- (c) Calculated self weight forces taken from BOMEL SAFJAC analysis



### 2.1.3 Response Data

All data for member forces, moments and displacements are taken from the instrumentation installed and monitored on site by AV Technology Limited. Appendix B presents drawings showing the location of instrumentation within the frame. The 880 data channel system includes:

- Integral pre-calibrated loadcells welded into the structure during fabrication. These are exceptionally accurate and are relied upon wherever possible. Four gauges (two opposite pairs) provide redundancy in the axial force calculation.
- Site installed surface mounted linear strain gauges to provide supplementary data on forces and moments (using nominal or local measurements of section properties). Four gauges (two opposite pairs) provide redundancy in the axial force calculation although care is needed in interpreting axial forces when sections distort and hoop strains become significant.
- Displacement transducers record deformations at key nodes and displacements of the frame and reaction rig.

Reference 11 provides a detailed description of the instrumentation techniques and data acquisition and reduction systems. Monitoring of the instrumentation was command activated (ie. not continuous). The raw data were processed online in an Excel spreadsheet programmed by BOMEL and AVT for this purpose. During and after the tests the data were validated and cross-checked wherever possible. Faulty gauges were replaced and/or formulae were altered to eliminate any erroneous values. The need for such corrections was rare and in general the quality and consistency of the data were shown to be excellent.

The final datafile provided by AVT for the Loadcase 1 test was:

LC1a\_test.xls

The updated spreadsheet incorporating BOMEL modifications as detailed on the spreadsheet revision sheet is:

C636\37\011w.xls

Copies of the datafiles are provided with Reference 11. This report presents the load effects determined from the raw data using these spreadsheet systems.





#### 2.1.4 Test Procedure

Prior to the test commencing a number of cycles of load were applied up to 100kN in stages, in order that the functionality of all systems could be checked and the take-up of load in the structure could be compared with predictions. On satisfactory completion of the trial, the actuator ram was withdrawn to leave the structure hanging at the datum position (zero applied load) relative to which all forces and moments were measured.

Throughout the test the following steps and procedures were followed:

- A datum scan of the instrumentation was taken (Scan 1) as the Scan number was displayed on the master board (see Figure 1.4). The scan number associated with each set of measurements uniquely defined the point in the test.
- An increment of load was applied under displacement control at the direction of BOMEL. Once complete, the actuator was locked-off in position. An on-screen trace of actuator load with time was monitored; a flat trace indicated a state of static equilibrium had been achieved. This was almost instantaneous when the structure was elastic but took a couple of minutes to reach once there was extensive plasticity.
- The scan number on the master board was incremented by one.
- The instrumentation system was scanned and backed up. Dial gauges were read manually.
- Throughout, all parties maintained independent logs with respect to Scan number and clock time of key events (eg. physical observations, checks on spurious gauge readings, ramp rate changes, movements in camera position, etc).
- Results within the data acquisition spreadsheet were reviewed by BOMEL. Graphs were generated automatically, plotting incremental measured values against BOMEL predictions. Built-in checks on maximum and minimum strains and functionality were monitored. Based on a review of the data the appropriate value for the next load / displacement increment was determined.

The sequence was repeated until the ultimate capacity of the structure had been attained and the pattern and level of post-peak loading capacity had been determined. The extent of post-peak deformation was limited to ensure extensive plasticity was not generated in distant parts of the structural frame.

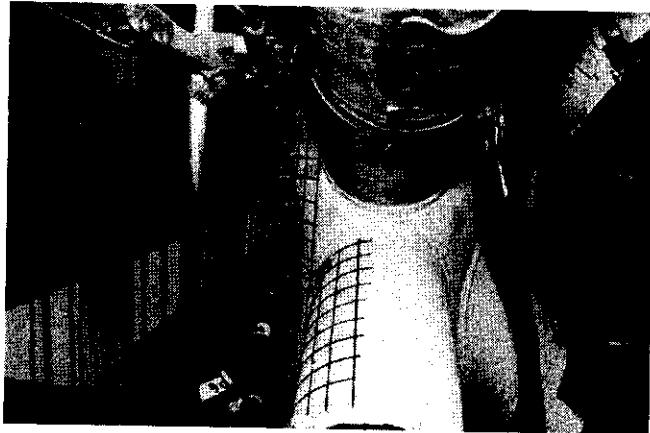
- The applied load was then reduced in three or four decrements with scans of the instrumentation and record keeping at each stage as before.

## 2.2 RESPONSE

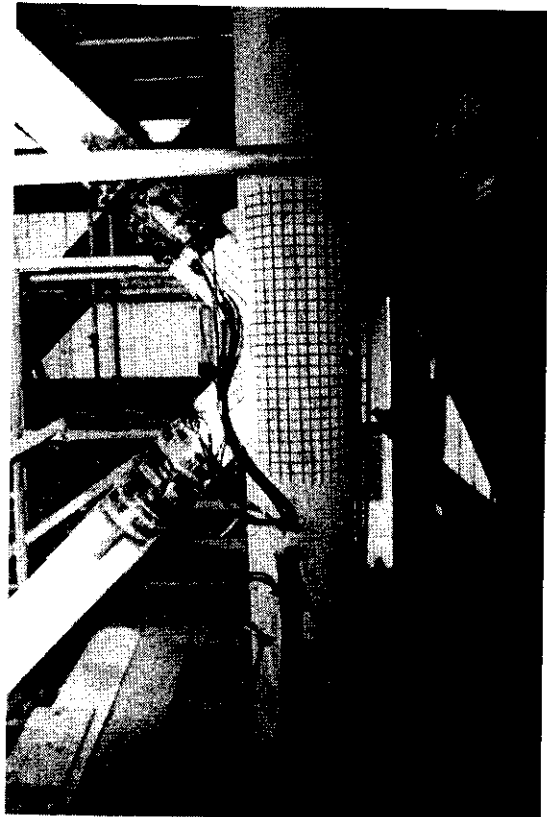
### 2.2.1 Preamble

The test set up for Loadcase 1 is shown in Figure 1.4. The member and node numbering schemes are shown in Figures 2.1 and 2.2. The datum position corresponds to the structure cantilevered from the reaction rig under its self weight with no actuator load.

Load was applied in displacement control on Line C, positive load pushing the frame upwards. Frame C was K-braced. The  $64^\circ \beta=0.6$  K joints at Level 1 (Node 38) and Level 2 (Node 37) have a nominal gap ratio ( $\xi=g/D$ ) of 0.1. Typical of jacket structures, the K nodes form part of a multiplanar connection. In both cases the out-of-plane K joints have  $45^\circ$  brace angles. At Node 37 the configuration is non-overlapping (Figure 2.3) but at Node 38, closest to the loading beam, the brace intersections overlap (Figure 2.4).



(a) Forward view along Line C into gap region



(b) Reverse view along Line C at Level 2 bracing

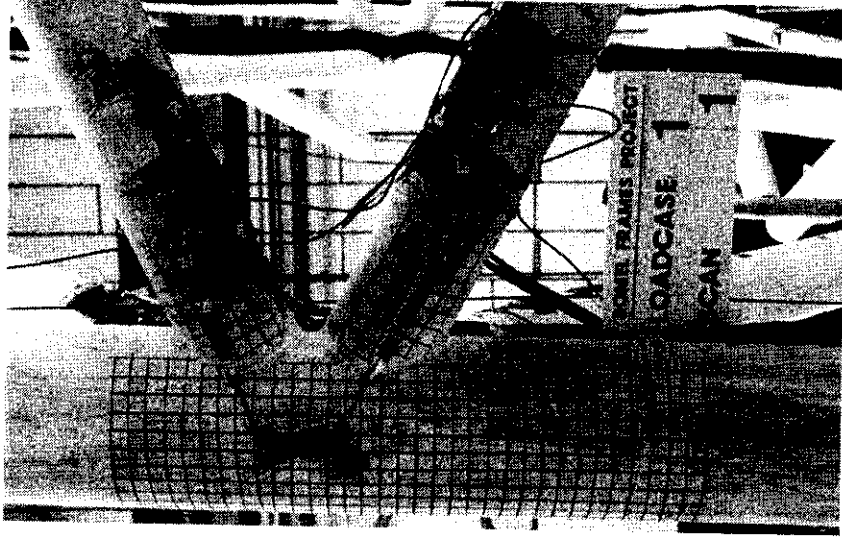
Figure 2.3 Node 37 pre test



(a) Forward view along Line c into gap region



(b) Reverse view along Line C onto Level 1 overlap bracing

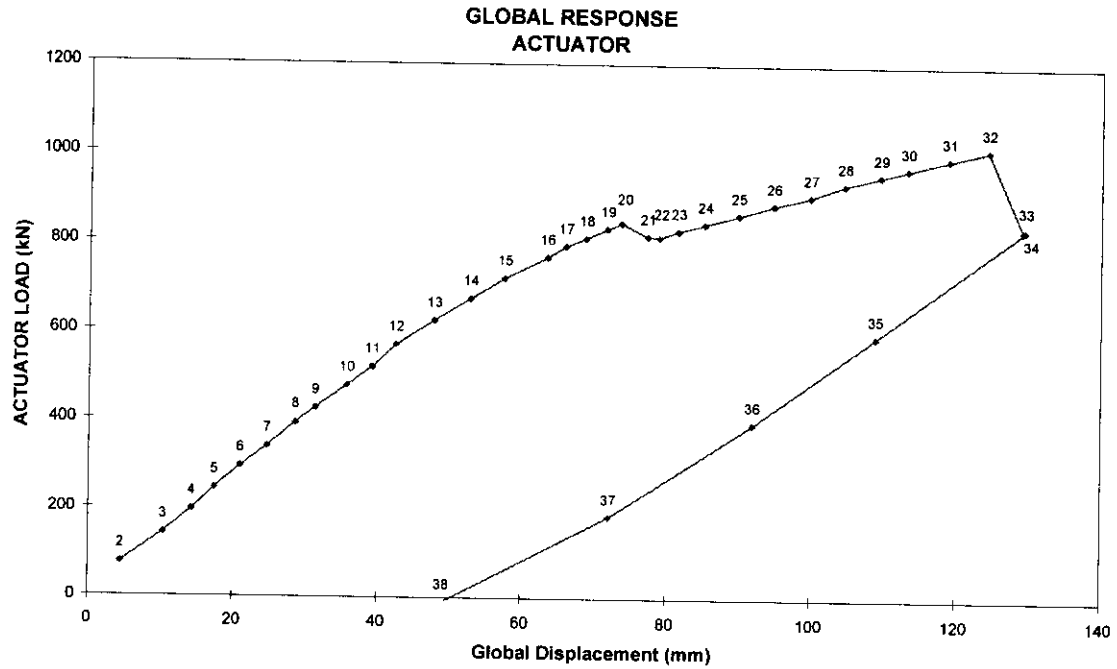


(c) Elevation onto Frame C gap K joints (N37 comparable)

Figure 2.4 Node 38 pre test

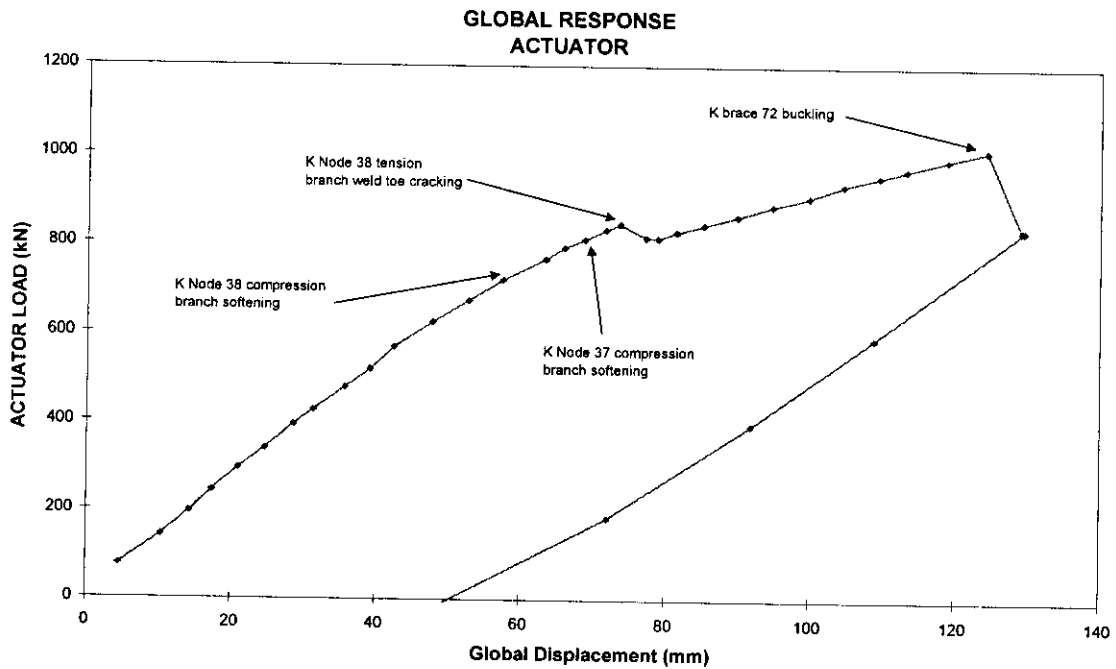
### 2.2.2 Global Response

Figures 2.5 and 2.6 show the loading and unloading trace for the full test. Figure 2.5 is annotated with the scan numbers to which reference will be made. Figure 2.6 highlights key events in the test described in further detail below.



Loadcase 1 - Test

Figure 2.5 Loadcase 1 - Scan numbers through test



Loadcase 1 - Test

Figure 2.6 Loadcase 1 - Key events through test

As described previously these traces correspond to the state of the structure after load has been applied, the actuator has been locked-off and the internal forces have equilibrated. The actuator control system supplied by Bodycote Limited independently recorded the applied load and displacement of the point of load application at one second intervals throughout. Figure 2.7 plots the loads applied by the actuator with those recorded by the logger once the system had equilibrated. The degree of 'relaxation' later in the test as the structure became plastic is evident. Furthermore the actuator system also provides evidence of the peak system capacity in instances where failure occurred as load was being applied between scans.

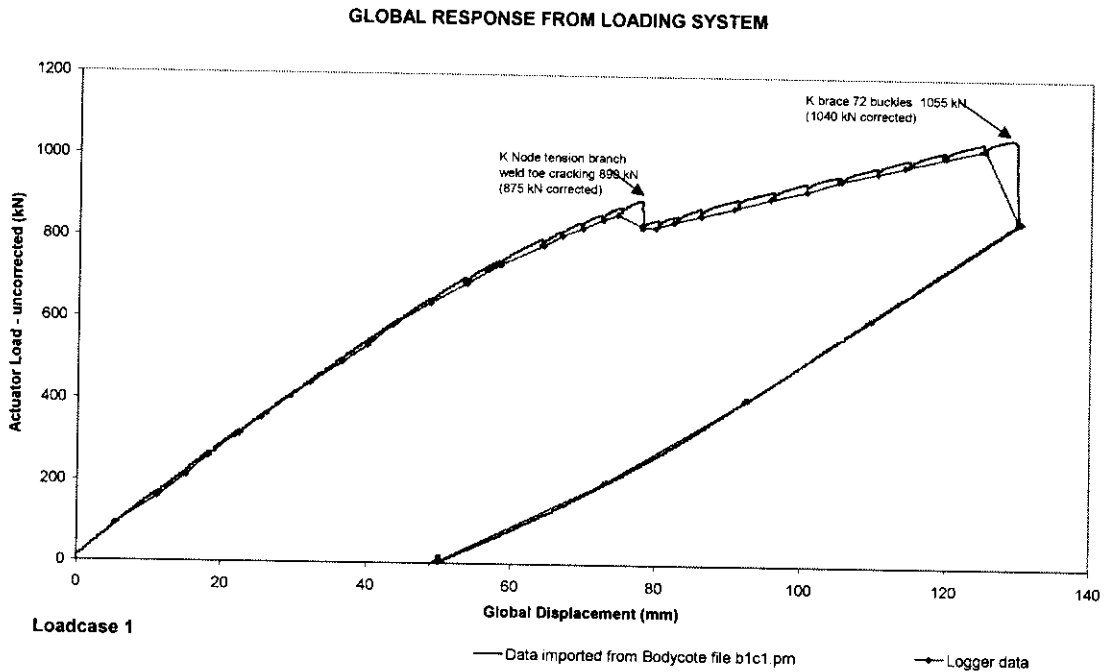


Figure 2.7 Applied actuator loads in comparison with equilibrated forces recorded at each scan

Note: The data in this plot include a 15kN positive load offset due to the self weight of the hinge unit and loadcell. In all other plots and data reported in this document the appropriate correction has been made.

These global response plots are reproduced in colour in Appendix C. Corresponding plots for the member forces in different areas of the structure are also provided and will be referred to in the test descriptions which follow. The main text includes a compilation plot (Figure 2.8) from which the pattern and relative magnitude of forces in primary bracing of interest in the Loadcase 1 test can be seen. Some explanatory notes are presented in the text following the figure.

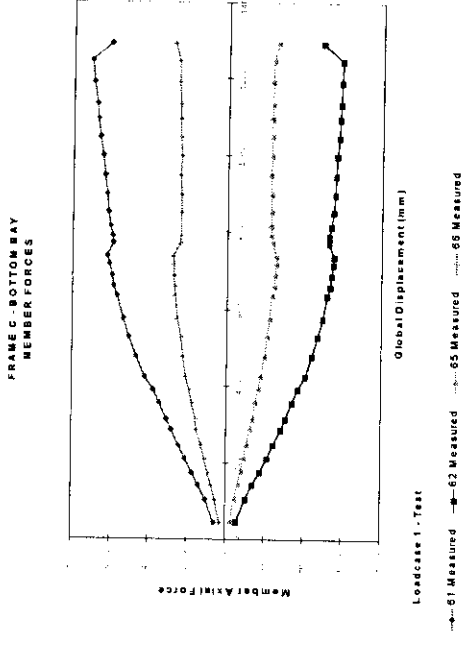
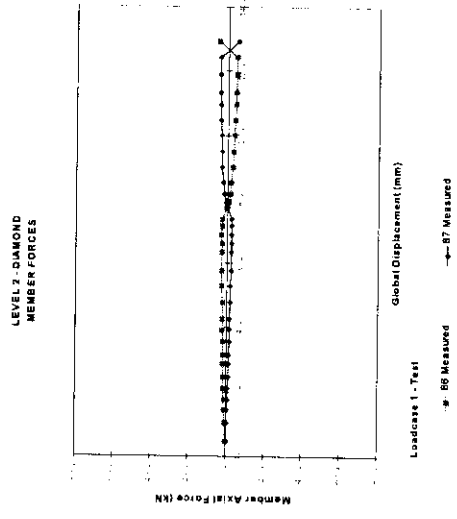
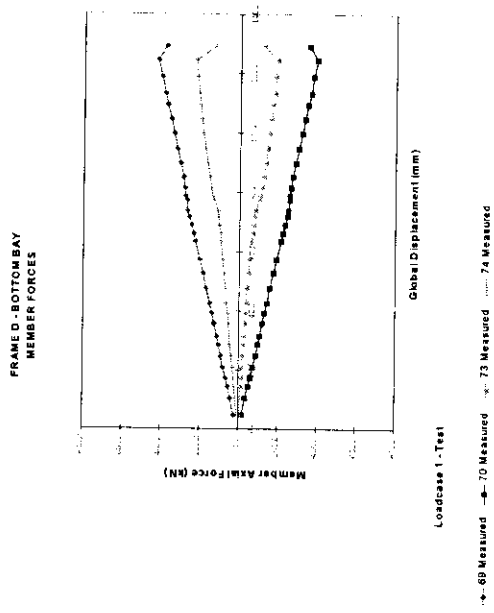
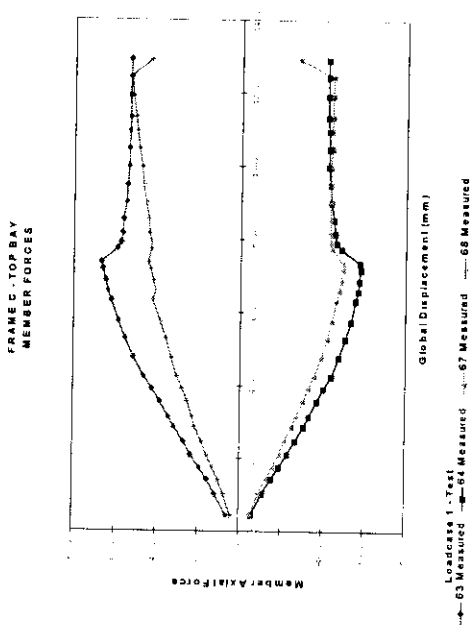
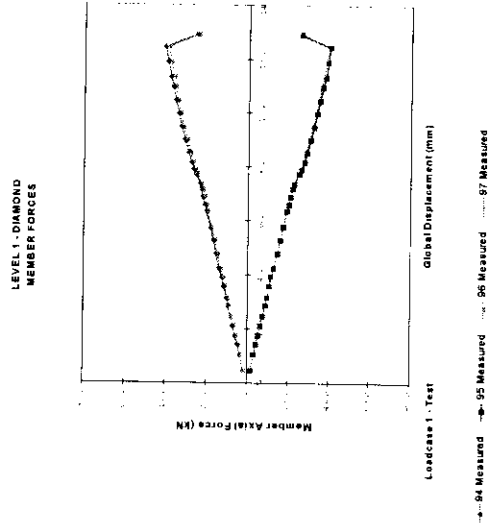
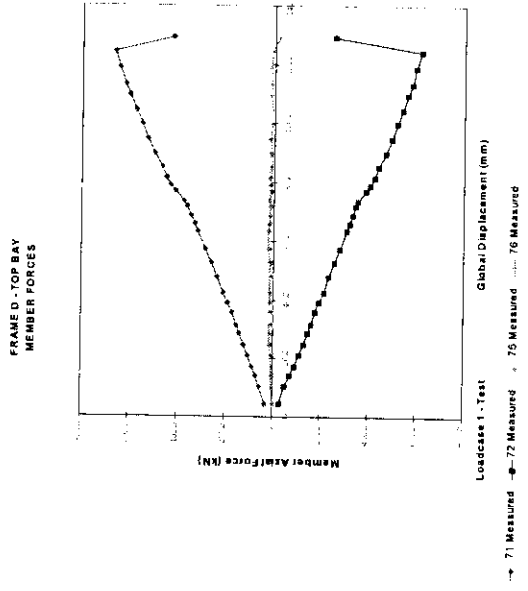


Figure 2.8 Member forces in key braces through the Loadcase 1 test



The plots are arranged as if looking at the structure from the viewpoint in Figure 1.4. The top diagrams relate to the bays closest to the viewer. Those on the right correspond to the loaded Frame C and those to the left give results for Frame D; the intermediate diagrams are for the interconnecting diamond bracing which forms the out-of-plane K bracing at Nodes 37 and 38. All plots are to the same scale to enable direct comparisons to be made. The member forces are plotted with respect to the incremental displacements through the test. Graphs giving a record of the loading in other parts of the structure are included in Appendix C.

### 2.2.3 Detailed Response

During the initial stages of loading the global response was linear and there was negligible relaxation as the actuator displacement (oil volume) was locked-off for each scan. It was not until Scan 16 (see Figure 2.5) that any signs of distress were visible. Initially distortion of the chord around the compression intersections of K Nodes 37 and 38 could be seen as shown in Figure 2.9. Close-up shots of the nodes revealed evidence of surface cracking at the tension weld toe in the gap region (Figure 2.10).

During the early stages of the test, the tension and compression K braces 61/62 and 63/64 in the Frame C plane sustained equal and opposite forces for each increment of applied load (Figure 2.8). However, as the K nodes began to distort the compression loadpaths softened and the relative magnitude of the forces in the tension braces, 61 and 63, increased. A slight softening in the global response was also evident until, as the load was increased beyond Scan 20, the crack at Node 38 went through thickness (Figure 2.11) and the global load fell to the equilibrium position recorded at Scan 21. Logging at one second intervals from the actuator system (as shown in Figure 2.7) indicates a load of 875kN was being applied at the point failure occurred.

Instrumentation output for the equilibrium condition at Scan 20, plotted in Figure 2.8, indicates maximum tension and compression forces in the braces at Node 38 of 670kN (Brace 63) and -578kN (Brace 64). Corresponding values at Node 37, which remained uncracked, were 619kN and -554kN. *When considering the absolute capacities of the components, it is important to remember that the applied load effects are recorded with reference to a zero datum. Self weight effects are additional. For example, self weight forces in Braces 63 and 64 at Node 38 oppose the applied loads and are calculated to be -53 and +54kN. Neglecting locked-in fabrication force effects in the illustration, the net forces acting at Scan 20 just prior to failure are therefore +617kN (670-53) and -524kN (-578+54).*

Once the structure had re-equilibrated at Scan 21 additional actuator loads were sustained by the structure with a greater transfer of applied load through the diamond bracing at Level 1 across into the 3D structure and Frame D. Load transfer through K Node 37 at Level 2 in Frame C also continued. Figure 2.8 shows the pattern of force distribution across the diamond bracing levels to Frame D with increasing displacement of the frame through the test.



Having applied a global load of 1040kN, the actuator system was locked off for Scan 33. However, as the structure equilibrated Brace 72 slowly buckled in-plane and the pressure in the hydraulic system fell to 834kN for the same global displacement (Figure 2.7). The Loadcase 1 test was terminated at this point and the structure was unloaded.

In the original scheme it had only been intended to investigate failures in Frame C and establish the pattern of subsequent load redistribution. In the event the test was continued significantly beyond that point giving information on the subsequent failure modes and specific data on K-braced member buckling which had not been covered in the earlier Frames Project investigations. It was necessary to stop the test at this point to limit the degree of damage and extent (cost) of repairs in view of the subsequent tests to be performed.

Figures 2.12 to 2.16 show the condition of the structure at the end of the test. Figures 2.12 and 2.13 show the condition of Node 38: deformation around the compression intersection, cracking in the gap region and overall deformation of the chord. Despite the damage, the load transferred by the primary K joint had fallen less than 25% below the failure load (see Figure 2.8). At Scan 32 the measured brace forces were still 531 and -418kN. Node 37 (Figure 2.14) remained intact despite surface cracking and chord distortions, sustaining tension/compression brace loads of 706kN / -592kN under the maximum applied actuator load. (630/-516kN when corrected for initial gravitational effects of  $\pm 76$ kN).

Brace 72 can be seen in its buckled state in Figure 2.15. The axial force recorded at Scan 32 prior to the load increment causing failure was -618kN (-584kN corrected for gravity).

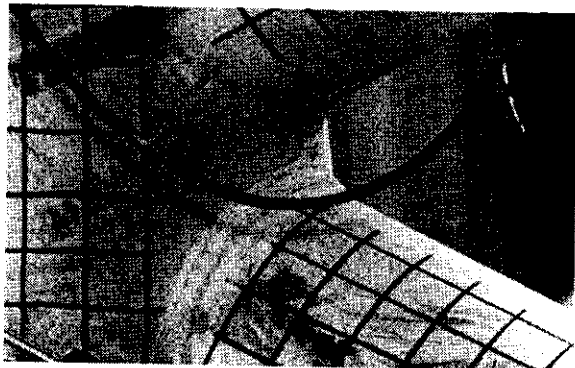
Figure 2.16 shows the structure subsequent to unloading at Scan 38.

Throughout the test uplift of the rig from the support stools was monitored. The reactions were taken out beneath the actuator and at supports to the rear of the rig. However, at the remainder of the supports the rig lifted up by as much as 7mm.

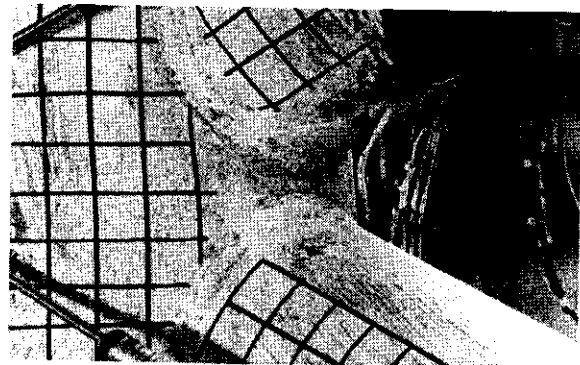




Figure 2.9 Distortion of the Node 38 chord around the compression intersection (upper)



(a) Node 37



(b) Node 38

Figure 2.10 Surface cracking in Frame C K joint gaps at Scan 16



Figure 2.11 Through thickness cracking in gap region of Node 38 at Scan 21

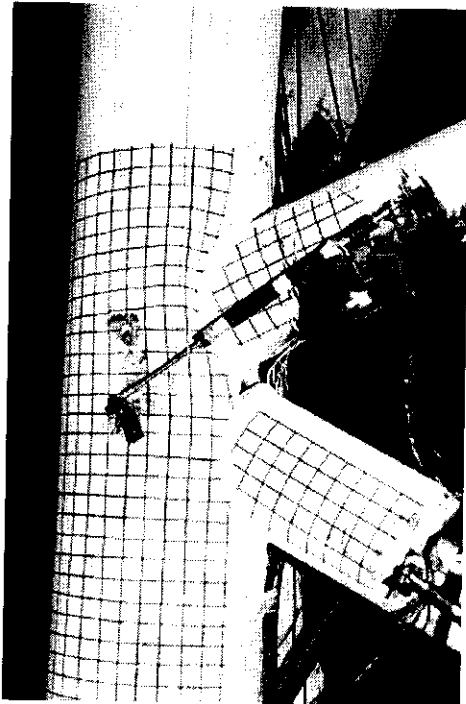


Figure 2.12 Node 38 post failure

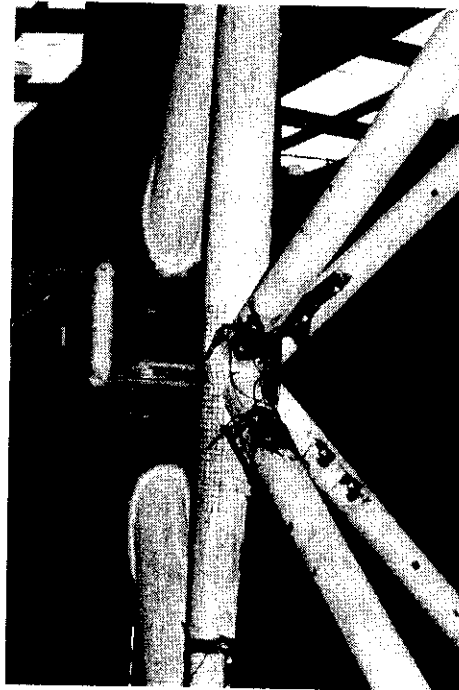


Figure 2.13 Node 38 deformation

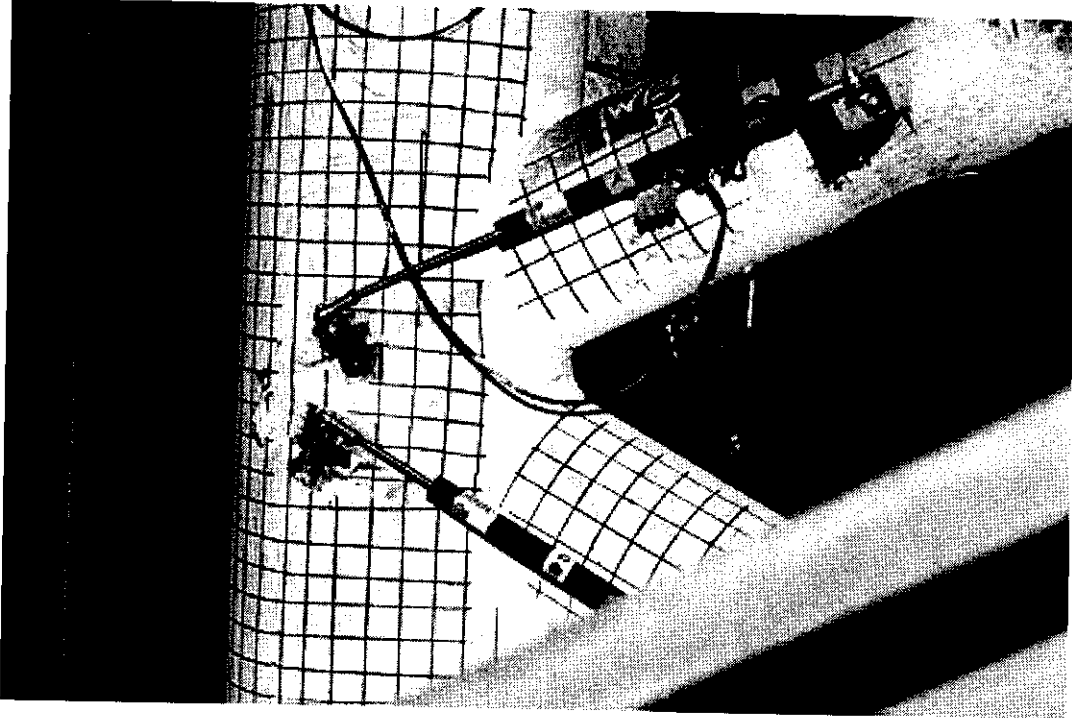


Figure 2.14 Node 37 - Local chord deformation and surface cracking



Figure 2.15 Brace 72 - Buckled

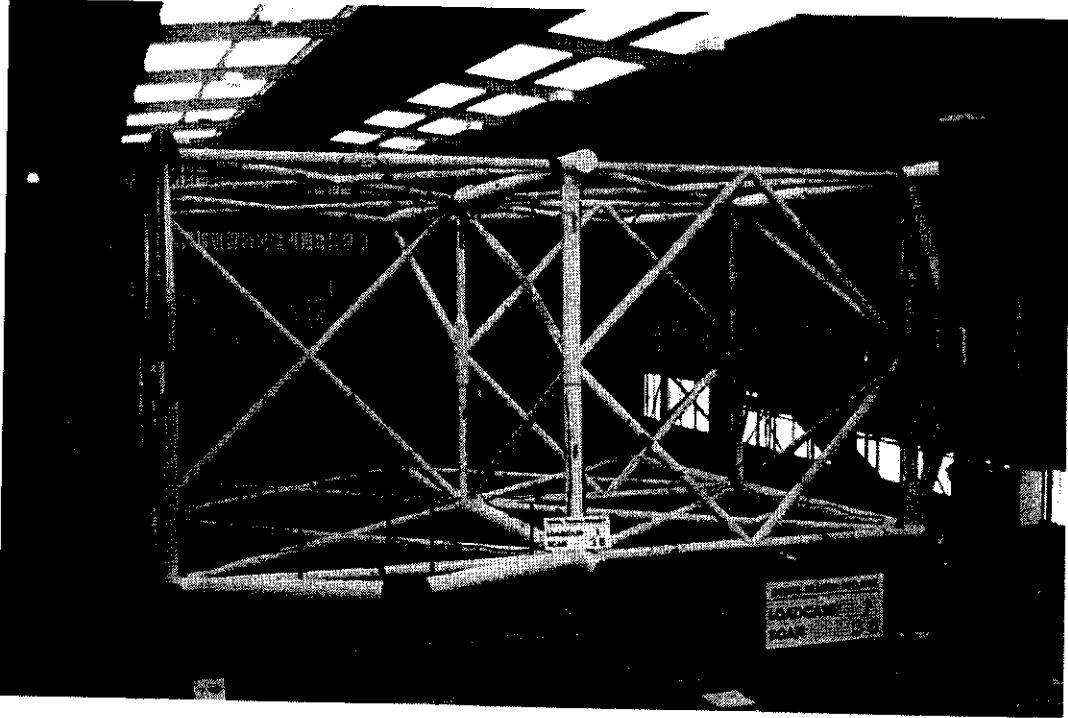


Figure 2.16 3D test frame after Loadcase I test (NB. Brace 72 buckled in Frame D)

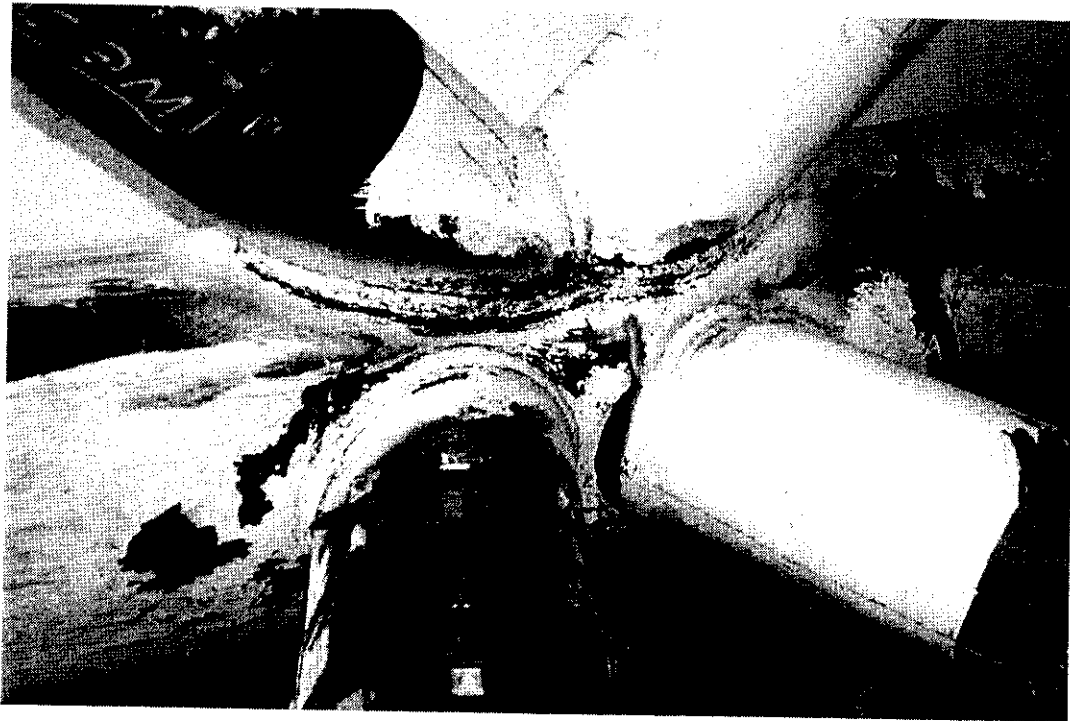


Figure 2.17 View into multiplanar 'gap' region of Node 38 post test



## 2.2.4 Comparison with Phase II 2D Results

From the view onto the structure at the end of the test (Figure 2.16) buckling of brace 72 is evident but distortion of the joints at Nodes 37 and 38 is not discernable. Although the nodes are distant, the deformations are in fact localised to the external face of Frame C away from the diamond bracing.

Indeed, although cracking at the tension weld toe at Node 38 is initiated at the centerline of Frame C, subsequent propagation was predominantly to the outside face of the joint and not into the constrained gap region between the Frame C and Level 1 planes of bracing. Figure 2.17 presents a view into this region once the joint had been removed from the structure. The asymmetry in the damage and constraint afforded by the out-of-plane bracing is evident.

Useful comparison can also be made with symmetric deformations observed in the Frames Project Phase II plane frame tests<sup>(2)</sup>. Figure 2.18 shows a view into the gap region at Scan 19 of the Frame VIII test. The corresponding global and member force plots are shown in Figure 1.3. The brace to chord diameter ratio at the intersection ( $\beta$ ) was 0.77, reasonably comparable with the 0.62  $\beta$  ratio for the K joints of interest in Frame C of the 3D test specimen. The significance of the chord deformations and greater extent of cracking in the 2D test are evident. Figures 2.19 and 2.20 show corresponding views along the chord of the planar joint and in elevation.

Further comparison can be made between the post-peak capacity of the planar and multiplanar joints with reference to Figures 1.3 and 2.8. In the case of the planar joint the relative loss of load carrying capacity is greater. The multiplanar joint in Frame C of the 3D frame continues to sustain some 75% of the peak load (Figure 2.8) whereas in the Phase II test the load had reduced to around 50% of the peak and was continuing to decay at the point the test was terminated (Figure 1.3). Both tests provide evidence that, prior to failure as compression intersection deforms, the tension loadpath transmits higher loads through the joint.

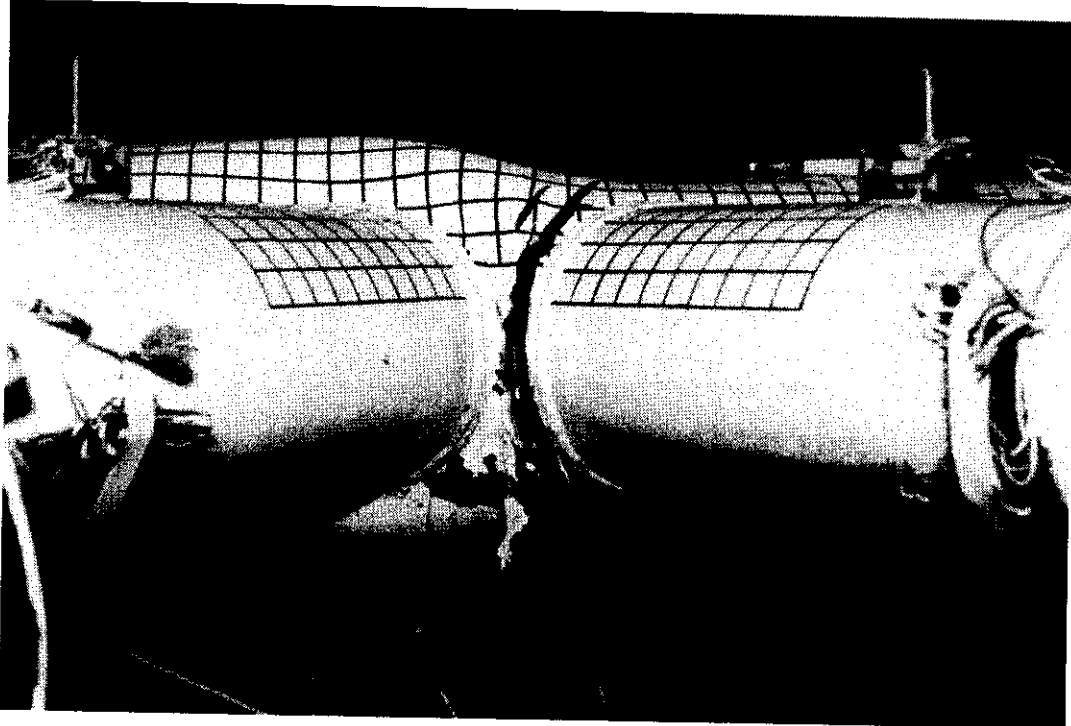


Figure 2.18 Phase II - plane frame test - gap K joint deformation - Frame VIII Scan 19

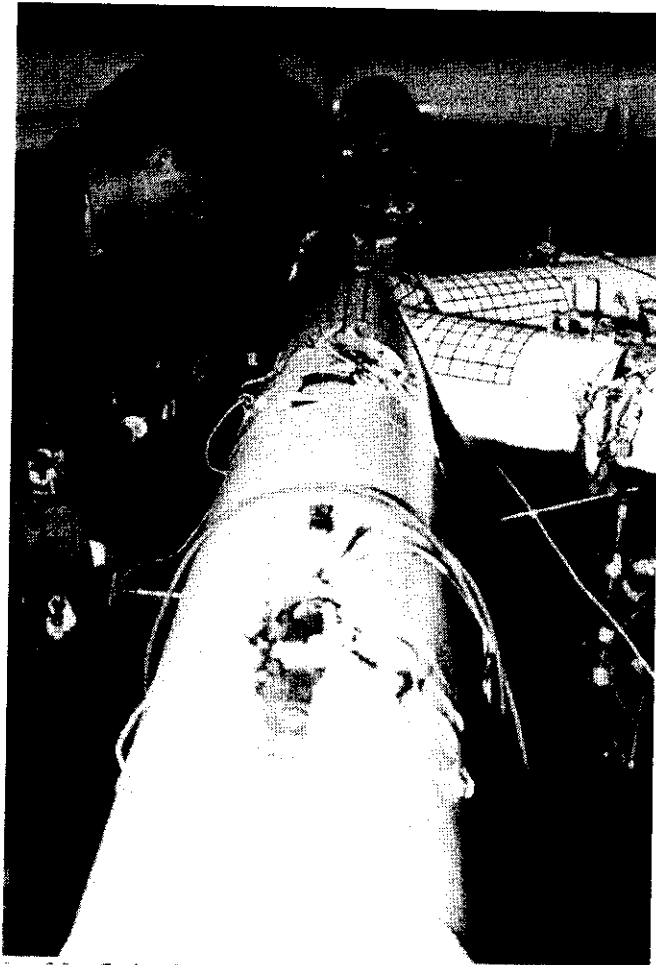


Figure 2.19 Phase II - plane frame test - K joint chord deformation - Frame VIII Scan 19



Figure 2.20 Phase II - plane frame test  $\beta = 0.77$  K joint distortion - Frame VIII Scan 19

### 2.2.5 Local K Joint Responses

The multiplanar K joints on Line C were heavily instrumented for the Loadcase 1 test in order that the mechanisms of load transfer could be examined. Layout drawings on Appendix B show the position of sets of four site-installed strain gauges on the incoming braces in- and out-of-plane. Those closest to the joint are denoted 'Near', the second set 'Far'. In addition displacement transducers straddle the tension and compression intersections along the axis of the braces in Frame C. The instrumentation can be seen clearly in the photographs (Figures 2.3, 2.4 and 2.9 to 2.17). The output provides information on the load deformation response of the joints. This is used for back-analysing the response of the frame and providing recommendations for characterising joint responses in jacket analyses. In addition the strain gauges enable the moments acting at the intersection in addition to axial loads to be quantified up to and beyond the point of failure. They also confirm the pattern of deformations occurring locally and enable the strength manifested by the joints to be determined more completely.

#### 2.2.5.1 Load deformation responses

Figure 2.21 presents the load deformation responses for Nodes 37 (Level 2) and 38 (Level 1) with the tension and compression branch responses separately identified. The scales in all cases are the same to give an immediate comparison of the characteristics. As may be anticipated from the test description and photographic evidence, the tension loadpath is significantly stiffer than compression. Comparing the responses it can be seen that, although generally similar, the degree of deformation at Node 37 is somewhat greater than at Node 38, even though a peak in the Node 37 capacity had not been reached.

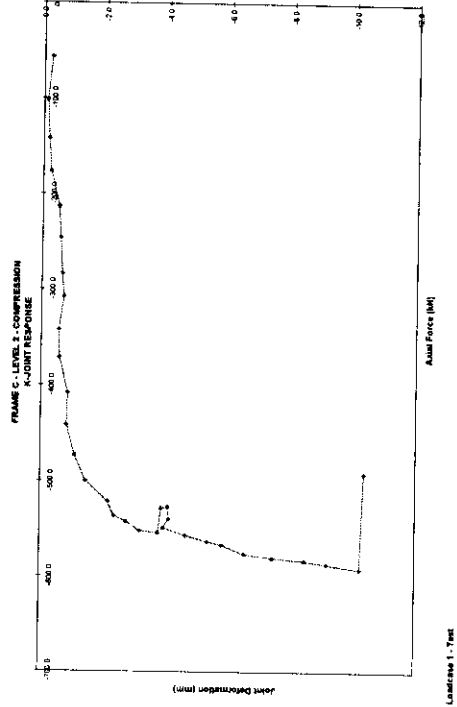
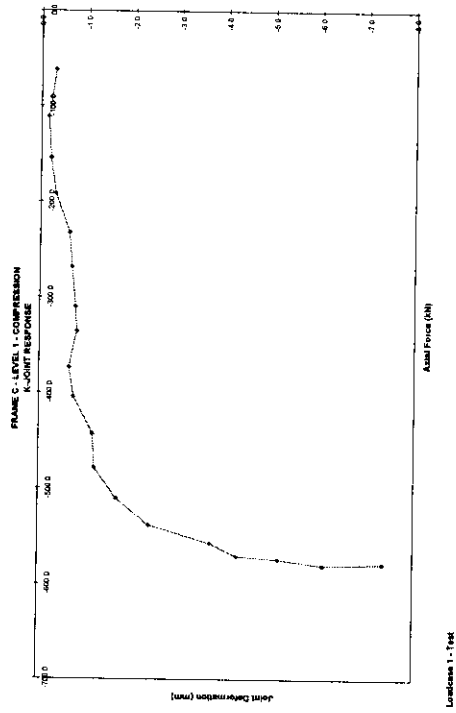
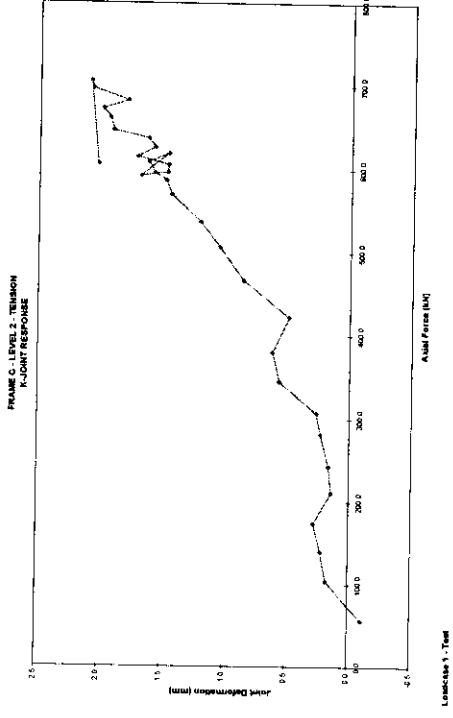
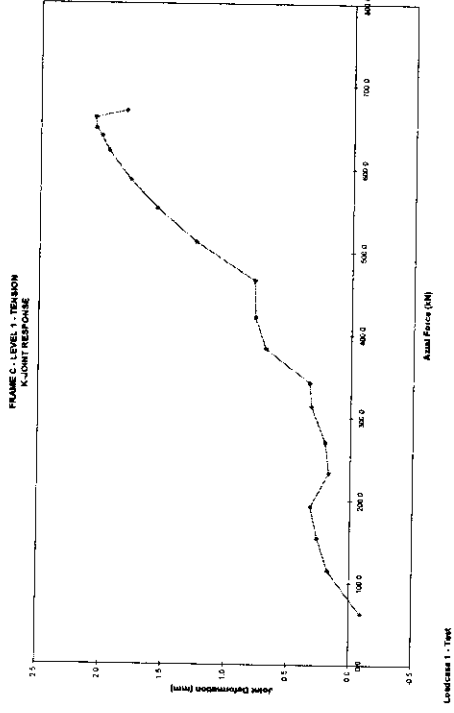


Figure 2.21 Local K joint response characteristics - Frame C intersections at 3D frame multiplanar joints



It should be noted that the unevenness in the traces is not considered to be due to physical phenomena, rather it is due to some interference within the logging system. The same 'jaggedness' can be seen in plots from displacement transducers monitoring global displacements of the frame and rig whereas it is clear from the actuator signals that the loading (and response) were smooth. The transducers were connected within the same sub-bank in the logger. Similar effects were not seen in any other test. A smoothing curve to the traces can be readily eyed in.

Figure 2.22 presents the corresponding local responses recorded at the Frame VIII K joint in the Phase II plane frame test programme. The capacities differ because of different chord properties. Nevertheless the order of magnitude of deformations and comparison between tension and compression response characteristics are similar. However, it is important to recognise that instrumentation on the 3D joints was necessarily placed on the outside face where deformations were greatest; at the 'inside' face the multiplanar braces constrained the deformations. The 'average' deformations in the 3D cases may therefore be inferred to be somewhat less than for the planar joints.

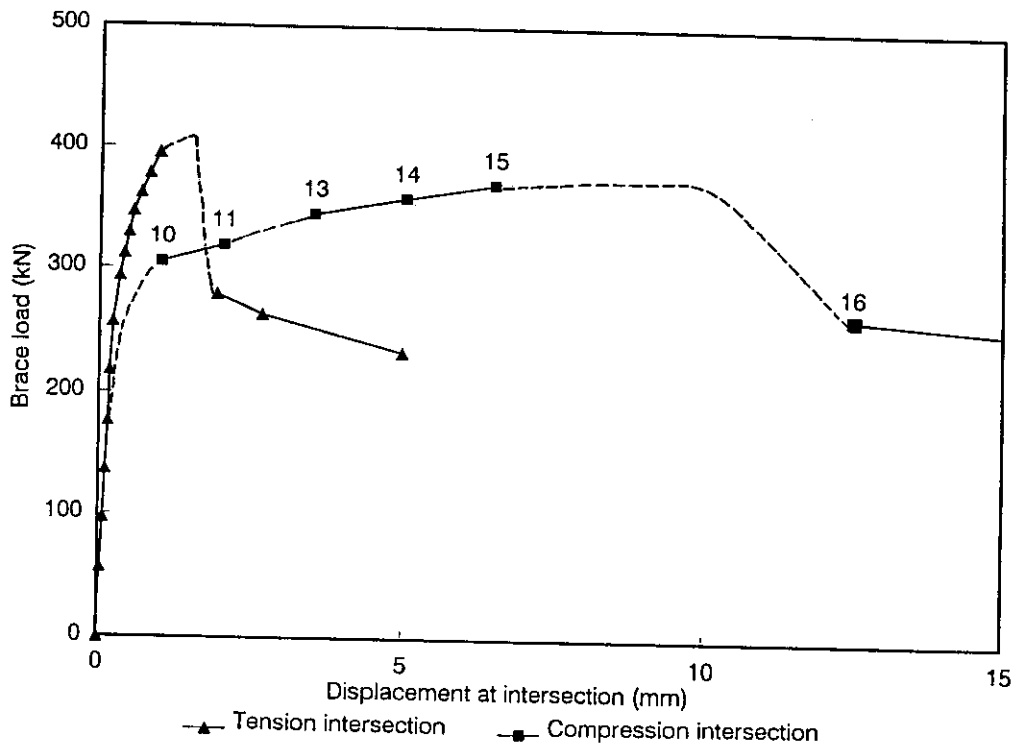


Figure 2.22 Local joint response characteristics - Phase II planar K joint in Frame VIII

### 2.2.5.2 Combined bending and axial action

Axial force and moment data from loadcells and strain gauges on the braces framing into Nodes 37 and 38 on Frame C are plotted in Figures 2.23 and 2.24. Loadcell forces are calculated using pre-calibrated values; loadcell moments and axial forces and moments at Near and Far strain gauge positions are based on nominal geometric properties. A slight discrepancy may therefore be anticipated but in general correlation is good. Braces 86 and 87 at Node 37 present an exception however which is discussed further below.

For the K braces in Frame C (Braces 61, 62, 63 and 64) the sign convention gives positive moments in-plane for bowing towards Frame B and out-of-plane for inwards curvature towards Frames D and E. Given the upward application of load to the structure towards Frame B and the greater stiffness of the chords on the inside face, it is to be expected that in-plane moments are positive in all Frame C braces and that tension braces exhibit positive out-of-plane moments whereas they are negative for the compression braces.

Within the planes of Levels 1 and 2, positive moments also indicate bowing upwards towards Frame B. Out-of-plane positive moments correspond with bowing towards Level 1 and away from Level 2 (see Figures 2.2 and 2.3 for reference). Once again the sign of the moments in the Brace 86-87 and 94-95 figures fits with physical expectations. About the axis of the joint chords, the corresponding Frame C and Level 1 or 2 tension braces bend consistently in one sense - conditions in the compression braces are consistent with each other but opposite.

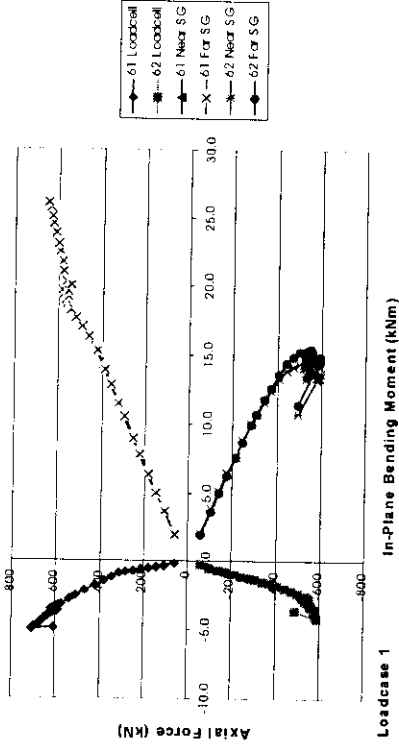
Results for a specific set are not presented (eg. 95 Near SG for out-of-plane bending in Figure 2.24), where it was found that raw values for an individual gauge were spurious due to the gauge or cable being damaged. Use is made however of the orthogonal gauge pair (to extract in-plane values in the example cited).

A number of important observations can be made regarding the secondary moments resulting from the global frame movements:

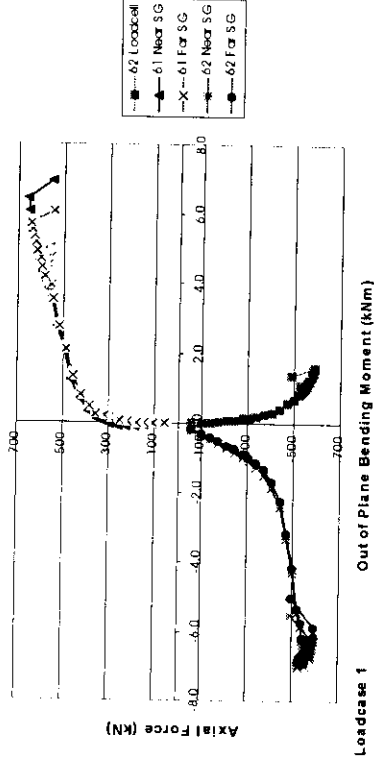
- As K joint 38 approached failure so the in-plane moment in the primary compression brace reduced (Figure 2.24) reflecting the diminishing ability of the gap region to transfer load as the crack-initiated and propagated at the tension weld toe. However bending in the tension brace continued to add to the axial effects driving crack development.

A similar characteristic can be seen developing at Node 37 (Figure 2.23) even though a peak in the axial load sustained had not been reached by the end of the test.

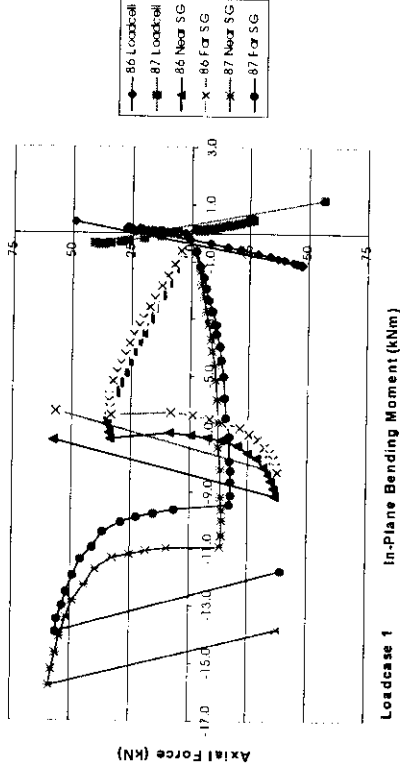
Axial Force Versus In-Plane Bending Moment (K-Joint 61&62)



Axial Force Versus Out of Plane Bending Moment (K-Joint 61&62)



Axial Force Versus In-Plane Bending Moment (K-Joint 86&87)



Axial Force Versus Out of Plane Bending Moment (K-Joint 86&87)

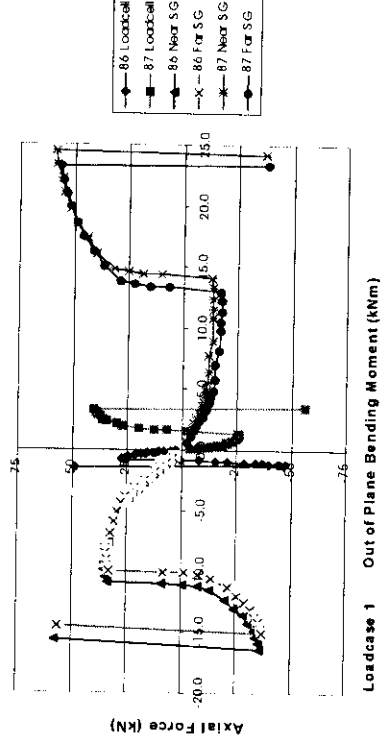
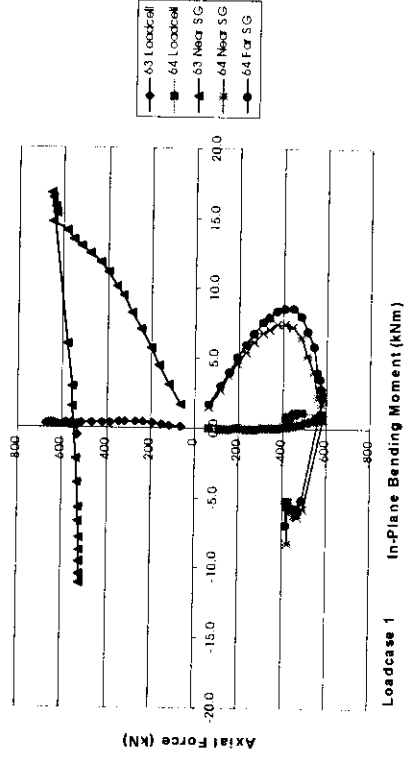


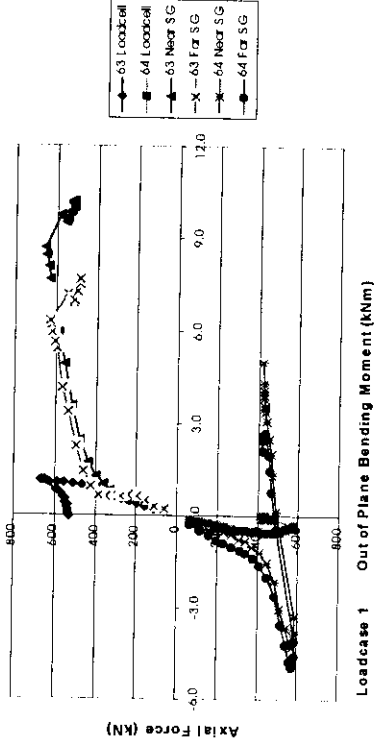
Figure 2.23 Axial force and moment combinations acting at braces intersecting Node 37

(Measurement locations - distance from brace chord intersection: Braces 61, 62 - LC 4537mm Far SG 441mm Near SG 241mm)  
 : Braces 86, 87 - LC 2844mm Far SG 484mm Near SG 284mm)

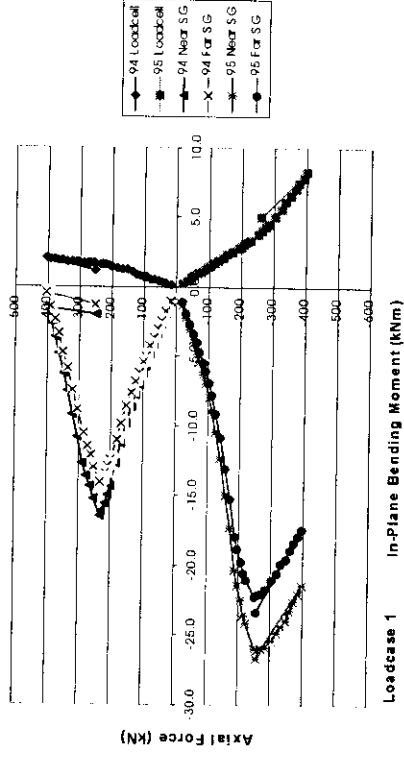
Axial Force Versus In-Plane Bending Moment (K-Joint 63&64)



Axial Force Versus Out of Plane Bending Moment (K-Joint 63&64)



Axial Force Versus In-Plane Bending Moment (K-Joint 94&95)



Axial Force Versus Out of Plane Bending Moment (K-Joint 94&95)

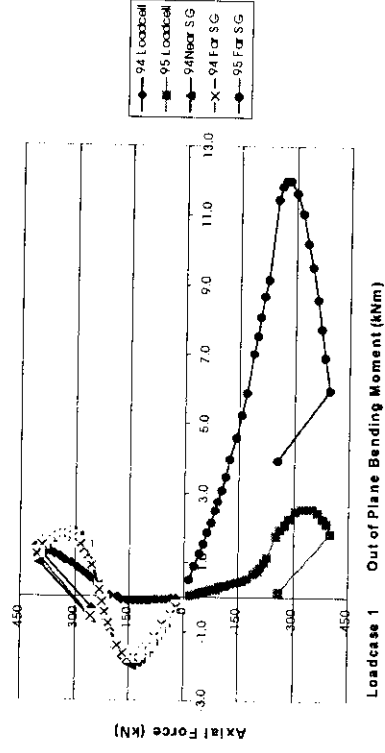


Figure 2.24 Axial force and moment combinations acting at braces intersecting Node 38

(Measurement locations - distance from brace chord intersection: Braces 63, 64 - LC 4537mm Far SG 441mm Near SG 241mm)  
 : Braces 94, 95 - LC 2844mm Far SG 484mm Near SG 284mm)



- The magnitude of the moments at Nodes 37 and 38 were comparable being somewhat higher in the former case.
- Moments at the loadcells were relatively small (as anticipated when positioning them to obtain reliable axial force measurements). The magnitude of moments close to the multiplanar K joint intersections was considerably greater and was larger at the 'Near' as opposed to 'Far' locations. The Near and Far gauges were respectively 241 (284) mm and 441 (484) mm from the brace-chord intersections and 366 (477) mm and 566 (677) mm from the chord centerline. The first figures are for the bracing in frame C; figures in brackets are for the 45° bracing in Levels 1 and 2. On this basis the acting moments can be extrapolated and combined with axial force data to assess fully the joint capacity and utilisation.
- There is evidence in the measurements for Braces 86 and 87 that distortion of the section (ovalisation) is taking place. In the absence of such ovalisation, linear gauges give an accurate measure of axial stress. As hoop strains become significant (relative to the magnitude of axial components) the fuller conversion to axial stress is required (ie. Axial stress =  $E / (1 - \nu^2) * (\text{Axial strain} + \nu * \text{Hoop strain})$ , where  $\nu$  = Poisson's ratio and E is Young's modulus).

When a fuller conversion is not used the averages from opposite pairs of linear strain gauges do not equate as hoop strains are greater at the major axis than minor. The effects can be seen in Figure 2.23 for Braces 86 and 87. There is a discrepancy between the axial forces calculated on the basis of opposite gauge pairs at loadcell and strain gauge locations precisely because hoop strains due to ovalisation are neglected. The effect is marked in this case because the net axial strains are very small. In the other cases ovalisation is also occurring but the hoop effects are minor in comparison with the very much greater levels of axial strain.

## 2.3 QUANTIFIED SUMMARY OF RESULTS

For ease of reference in the subsequent evaluation of the results, the key events and associated forces described in Section 2.2 for the Loadcase 1 test, are summarised in Table 2.3.

Table 2.3 Loadcase 1 - Key events and measured load effects in response to applied load

Scan	Event	Applied actuator load (kN)	Component capacities and associated member forces <sup>(1)</sup> (kN)				For joints - coacting chord loads				Component properties <sup>(3)</sup>			
			Brace 1 No	Force (kN) Moment (kNm) <sup>4</sup> In-/out-of-plane	Brace 2 No	Force (kN) Moment (kNm) <sup>4</sup> In-/out-of-plane	Chord 1 No	Force (kN)	Chord 2 No	Force (kN)	Yield (N/mm <sup>2</sup> )	D (mm)	T (mm)	g (mm)
20	K joint failure cracking - N38 Corresponding forces: N38 overlapped out-of-plane braces	844	63	669.6 17.7 / 11.6	64	-578.0 -1.4 / -2.3	67 <sup>(2)</sup>	-493.3	68 <sup>(2)</sup>	443.2	288.6	273.3	5.61	12
			94	235.9 -19.9 / 0.4	95	-229.4 -28.7 / 10.8								
			61	619.3 20.4 / 4.9	62	-553.8 12.0 / -7.1	65 <sup>(2)</sup>	-254.2	66 <sup>(2)</sup>	278.9	288.6	273.1	5.61	9
			86	25.7 -8.5 / -12.1	87	-25.4 -12.9 / 15.7								
32	Buckling - K brace 72 - end of test Corresponding forces: N37 in-plane K braces (pre failure) N37 out-of-plane braces N38 in-plane K braces (post-failure) N38 out-of-plane braces	1013	72	-617.5	-	-				288.3	168.6	4.58		
			61	705.7 26.1 / 7.5	62	-591.5 12.3 / -6.8	65 <sup>(2)</sup>	-232.4	66 <sup>(2)</sup>	255.4	288.6	273.1	5.61	9
			86	-46.5 -10.2 / -18.5	87	40.4 -18.2 / 26.2								
			63	531.5 -11.1 / 13.0	64	-418.2 -6.1 / 6.5	67 <sup>(2)</sup>	-442.2	68 <sup>(2)</sup>	531.0	288.6	273.3	5.61	12
94	406.2 -3.1 / 0.7	95	-401.9 -27.1 / 6.9											

- Notes:
1. Source C636\37\011w.xls
  2. From strain gauges (nominal section chord)
  3. For joints - local chord properties. For members - selected 'typical' properties from segments (C636\06\294w-b)
  4. Moments calculated at intersection from Near and Far strain gauges (Figures 2.23 and 2.24). Loadcells used when a set of strain gauges is unavailable.





### 3. COMPONENT TESTING AND ANALYSIS

#### 3.1 NORSK HYDRO FINITE ELEMENT ANALYSIS

##### 3.1.1 Background

As part of the validation studies during the design of the 3D test structure, Norsk Hydro contributed a series of finite element analyses to determine the response characteristics of multiplanar K joints being considered within the Loadcase 1 scenario<sup>(5)</sup>. The work included the development of planar and multiplanar K joint models and analysis using ANSYS. An example is shown in Figure 3.1. Alternative configurations with overlapping and non-overlapped out-of-plane braces were considered. The joints were analysed in isolation and within a beam element representation of the 3D frame (Figure 3.2). Different combinations of gap and overlap geometries were considered at the Level 1 and Level 2 K nodes in Frame C.

A number of validation checks were performed initially. The response of the 2D X-braced frame and  $\beta=1.0$  gap K joints tested in earlier phases of the Frames Project were back analysed. In the X-braced case the combination of shell and beam element modelling was validated. For the K joint, both coarse and fine mesh ANSYS analyses underpredicted the measured capacity by some 20% and 15% respectively. The discrepancy was attributed to the presence of the welds in the test which effectively reduce the actual gap between the braces compared with the nominal values used in analysis.

##### 3.1.2 Modelling

The joint configurations adopted for the analysis of the 3D frame were generally similar, but not identical to, the as-built properties in the LC1 test. External diameters and gap/overlap dimensions correspond between the analysis and test. In-plane and out-of-plane braces were 4.5mm thick in the analysis whereas in the test the Frame C K bracing thickness was 5.6mm. However, it is clear from the Norsk Hydro results that this change would have had little influence on the predicted response, as all primary deformations occurred within the chord wall at the joints. However the chord wall thickness (T) was 5.9mm in the analysis with a yield stress value ( $F_y$ ) of 250 N/mm<sup>2</sup>; in the test the corresponding properties were 5.61mm and 288.6 N/mm<sup>2</sup> as shown in Table 2.3. Joint capacity is generally accepted as being proportional to  $F_y T^{2(4)}$ . On that basis the analysis may be considered to offer a reasonable prediction  $((5.9/5.61)^2 * (250 / 288.6) = 0.96)$ .

An elastic perfectly plastic material stress strain model was adopted. The ANSYS SHELL43 Plastic Shell elements adopted are said to be well suited to model nonlinear, flat or warped, thin to moderately-thick shell structures. The element has four nodes with six degrees of freedom



at each node: translation in nodal x, y and z deformation directions and rotation about the nodal x, y and z axes. The deformation shapes are linear in both in-plane directions. For the out-of-plane motion, a mixed interpolation of tensorial components is used. The element has plasticity, creep, stress stiffening, large deflection, and large strain capabilities.

### 3.1.3 Joint Responses

Figure 3.3 provides a comparison between planar and multiplanar joint responses from isolated analyses. In the multiplanar case the relative magnitude of in- and out-of-plane brace loads was determined from a beam model analysis of the structure. It is therefore somewhat artificial in that the coacting forces do not adjust as the joint progressively deforms and becomes plastic to different degrees in different areas. Nevertheless the indication is that the multiplanar joint has greater capacity in the primary vertical plane and the tension loadpath offers greater resistance than the more ductile compression route. The responses were almost identical whether the out-of-plane braces overlapped or had a gap.

### 3.1.4 Joint / Frame Responses

To overcome the above difficulties, the joint meshes were included in the beam model as shown in Figure 3.2 at Node 38. Figure 3.4 shows the global response plot together with the trace of member forces in the primary K braces (63 and 64) and out-of-plane diamond braces at Level 1 (94 and 95). The traces were indistinguishable irrespective of the out-of-plane configuration. However, this actually encouraged further comparison through the experimental investigations as it was recognised that the analysis did not account for cracking. However it can be seen from the plots that the compression capacity reached a plateau around 300kN comparing well with the isolated analysis results (Figure 3.3(b)), whereas the load transfer via the tension load path continued to increase reaching some 400kN. The two sudden drops in the traces were associated with buckling in Frame D (first) and diamond bracing at Level 1 (second); they are therefore not significant in considering the joint responses.

### 3.1.5 Comparisons

Scaled deformations of the joints at a global frame displacement around 60mm are shown in Figure 3.5 onto which colour contours of equivalent stress are drawn. In comparison with the photographs in Section 2 it can be seen that the deformations around the compression intersection were well captured in the analysis. Similarly the effect of the out-of-plane braces constraining the chord is evident.

The loads sustained by the joints can be compared between the analysis (Figure 3.4) and test results (Figure 2.8 - two figures, top right). It is important to note that the test results are presented with respect to a zero applied load datum; some 54kN of the applied load effects (Table 2.2) in the primary Frame C Braces, 63 and 64, were reversing the self weight gravitational forces neglected in the analysis. Nevertheless with reference to Table 2.3, the peak



capacities in the test (tension =  $670 - 54 = 616\text{kN}$ ; compression =  $-578 + 54 = -524\text{kN}$ ) were significantly greater than the analytical values (tension =  $400\text{kN}$  at the point the analysis was terminated; compression =  $-300\text{kN}$ ). Table 3.1 summarises the comparison. In addition the analytical results are 'adjusted' reflecting the 15% underprediction when trial analyses were compared with the 2D test data (Section 3.1.1) and the 4% discrepancy in chord wall properties (Section 3.1.2). These values have no physical meaning nevertheless they do confirm that the multiplanar test values were significantly higher than predicted.

Table 3.1 Summary of analysis results and test comparison

Frame C K brace intersection	Forces (kN)					Comparison: test capacity / ANSYS
	3D Test Result			Analysis		
	Due to applied load	Due to gravity	Capacity	ANSYS	ANSYS adjusted ANSYS*1.15 / 0.96	
63	670	-54	616	400	479	1.29
64	-578	54	-524	-300	-359	1.46

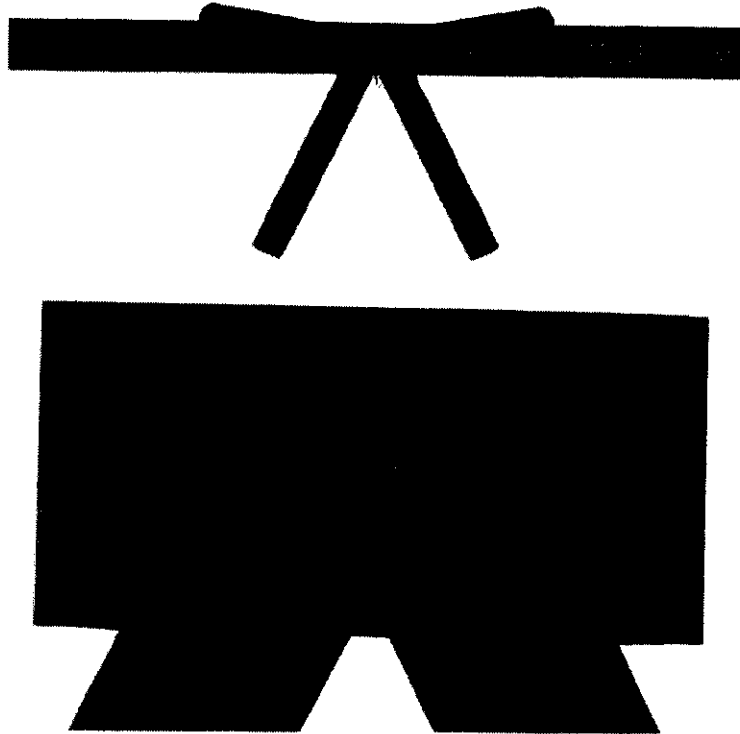


Figure 3.1 ANSYS SHELL43 model<sup>(5)</sup>

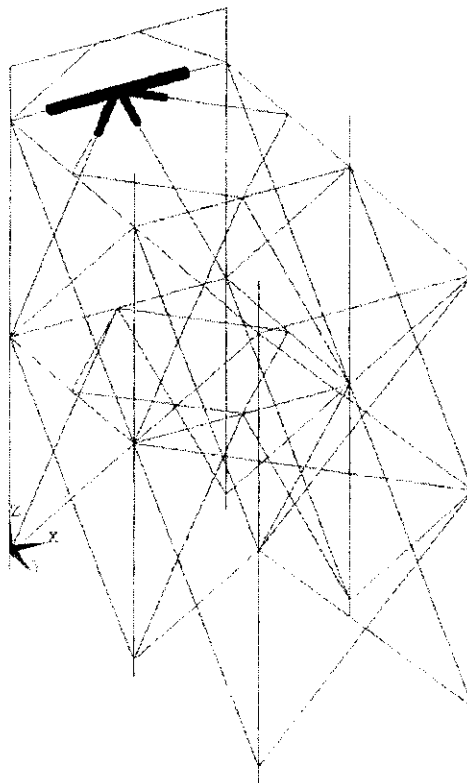
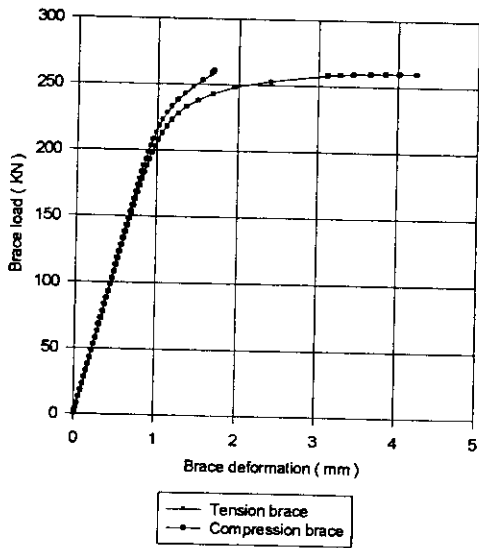
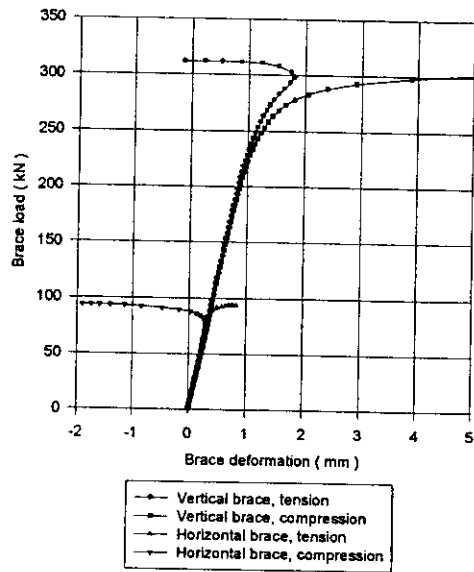


Figure 3.2 Inclusion of joint model in 3D frame<sup>(5)</sup>

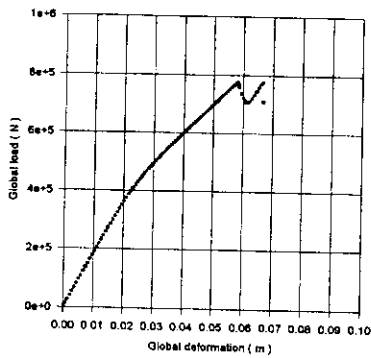


(a) Frame C planar K joint

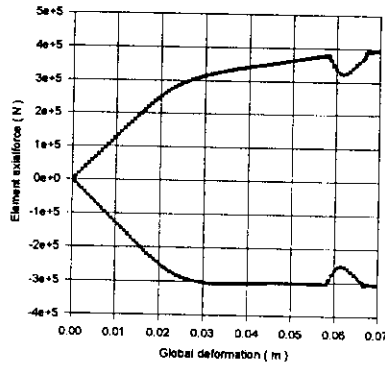


(b) Frame C - Level 2 multiplanar K joint

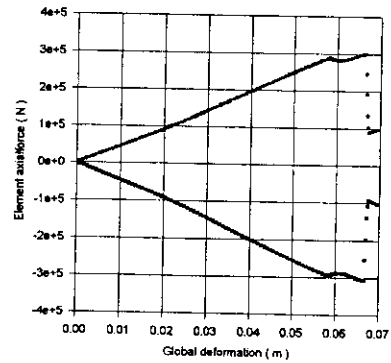
Figure 3.3 Comparison of planar and multiplanar K joint responses<sup>(5)</sup>  
 'Vertical' bracing corresponds to primary intersection in Frame C and 'Horizontal' bracing to Level 2



(a) Global

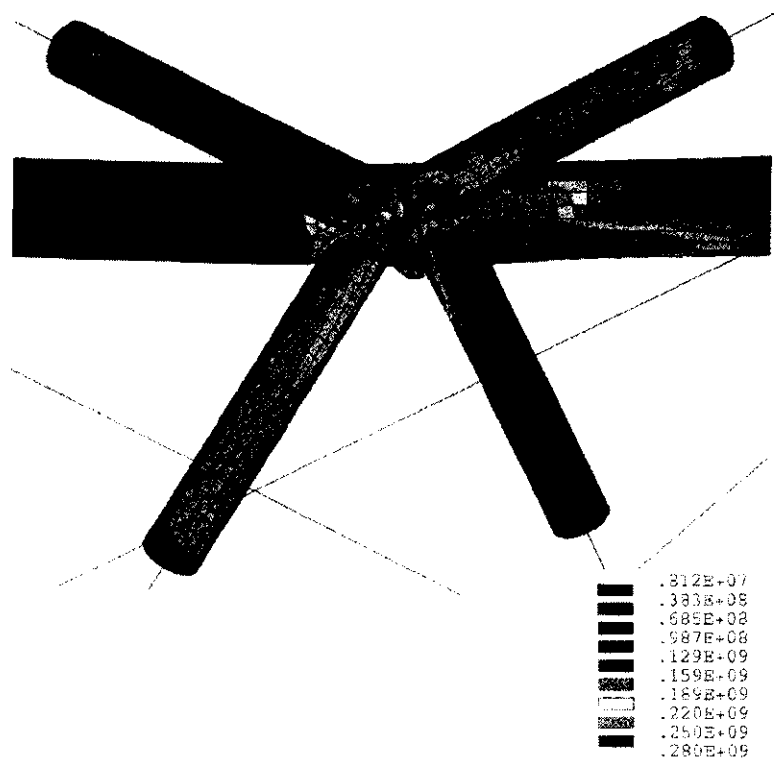


(b) Frame C bracing

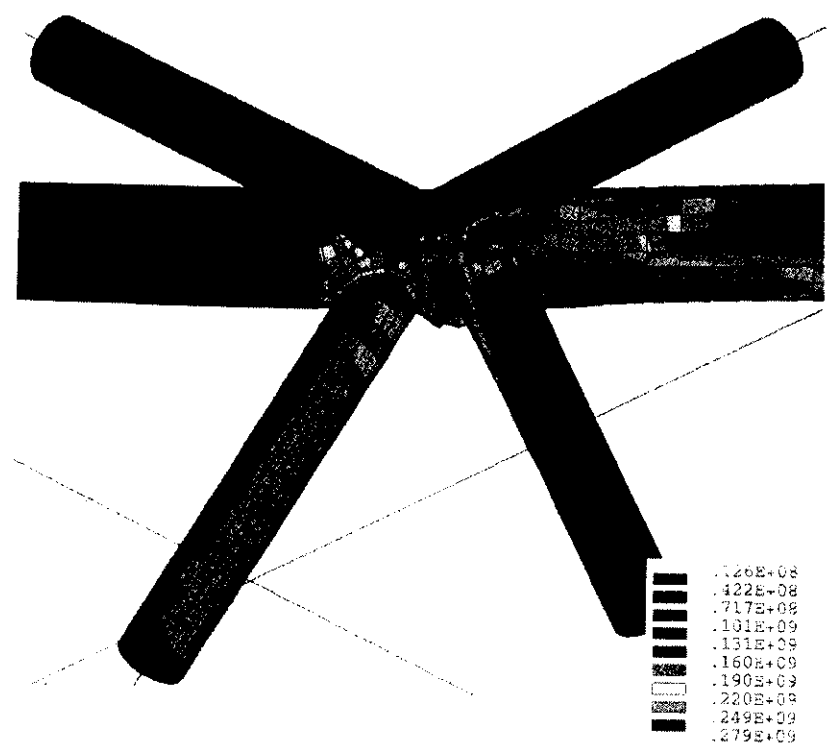


(c) Diamond bracing

Figure 3.4 3D frame response and multiplanar K joint member forces<sup>(5)</sup>



(a) Out-of-plane braces with gap



(b) Overlapped out-of-plane braces

Figure 3.5 Scaled deformations and equivalent stresses for corresponding global displacements of 0.061m<sup>(5)</sup>

## 3.2 SINTEF ISOLATED STATIC TESTS

### 3.2.1 Background

A significant aspect of the Phase III 3D Frames Project was to test the validity of static pushover analysis for assessing the ability of jacket structures to survive cycles of extreme loading in a storm. It was recognised that, although 'static' conditions are a snapshot of reality, data on the cyclic capacity of components and particularly tubular joints are sparse. In order to provide a systematic progression between a range of cyclic and static responses, planar and multiplanar effects, and component tests and frame behaviour, a programme of related investigations was devised. The interrelation is associated initially with the Loadcase 1 scenario as illustrated in Figure 3.6.

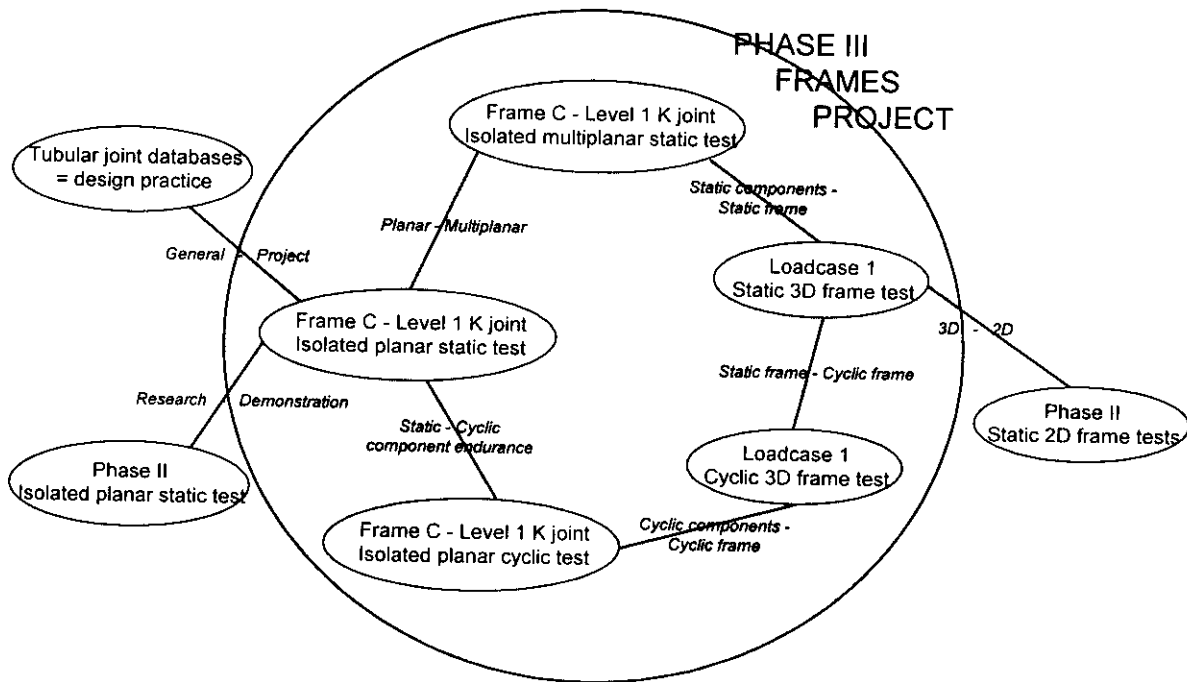


Figure 3.6 The context of Loadcase 1 and K joint investigations

All the isolated tests within the programme were undertaken by SINTEF Civil and Environmental Engineering at Trondheim in Norway. However to ensure consistency the components were fabricated by AKD Engineering Limited in the UK using materials from the same batches as used in the frame and were shipped to Norway for testing. Results from the isolated tests were reported and interpreted by SINTEF<sup>(6)</sup>. The response of the frame under cyclic loading conditions is detailed in a companion BOMEL report<sup>(12)</sup>. However in the present context of interpreting the Loadcase 1 static force response, results from the static isolated tests are particularly relevant. The connection is highlighted in Figure 3.6. This section therefore extracts relevant data from Reference 6.



### 3.2.2 Test Specimens and Procedures

Construction drawings for the joints are provided in Appendix A. As noted above the properties were nominally identical to the corresponding joints in the frame. Specific values using micrometer wall thickness readings are presented together with the capacity results in Table 3.2 at the end of this sub-section.

The test set-up is illustrated in Figure 3.7. This is a plan view and in the multiplanar case the out-of-plane overlap braces were unrestrained coming upwards. The comparison was therefore how the local effects due to the presence of the out-of-plane brace intersections and their constraint to chord ovalisation, affected the primary K joint response.

The supports were bolted to the laboratory strong floor. Both ends of the chord were fixed to reflect the continuity within a frame. The I sections between the braces ends and actuators were provided to introduce a degree of flexibility protecting the rams from large lateral loads and minimising bending effects. The actuators were slaved generating equal and opposite displacements at each brace end. This is a somewhat unusual arrangement for static testing of isolated joints. Nevertheless it provides a defensible basis for the subsequent cyclic tests and was intended to relate at the simplest level to compatibility constraints within a frame.

Figure 3.8 shows the strain gauges and transducers (LVDTs) applied to the joints. The transducer arrangement was similar in planar and multiplanar cases and all instrumentation was fixed to the floor. For the strain gauges, the 'C' series is additional in the multiplanar case. Gauges type A, B and C were 3mm single gauges; the 'ballooned' strips comprised five 1mm gauges.

### 3.2.3 Isolated Test Results

Figure 3.9 compares the tension and compression responses for the planar and multiplanar isolated specimens. Brace A was loaded in tension and B in compression in the planar test but vice versa in the multiplanar case. The forces recorded at the actuator are plotted against the axial displacements recorded by LVDTs 5 and 8. As these are floor mounted the readings may be expected to be slightly greater than associated with local deformations across the brace chord-intersection. Nevertheless the readings have the advantage of not being distorted by ovalising deformations of the chord. Furthermore output from LVDT 9 for example suggests the displacements of the chord as a whole are relatively small.

The graphs should be examined carefully as different scales have been adopted in each case. It can be seen that the multiplanar joint sustains a slightly higher tension load than the planar case. However, what appears to be more significant is the substantial increase in the compression branch capacity both up to and beyond the peak load. Table 3.2 summarises the comparison and provides details of the relevant chord properties.

Table 3.2 Isolated static K joint test results

Joint	Capacity, $P_u$ (kN)		Chord Properties			Non-dimensional capacity (absolute) $P_u / F_y T^2$	
	Tension	Compression	Yield, $F_y$ (N/mm <sup>2</sup> )	D (mm)	T (mm)	Tension	Compression
Planar	480	-375	288.5	274.1	5.65	52.1	40.7
Multiplanar	500	-430	311.4	273.4	5.70	49.4	42.5

It can be seen from the table that once the chord properties are accounted for, the non-dimensional capacities from the two tests are in fact comparable. This means that the presence of the out-of-plane braces does not influence the in-plane K joint capacity substantially. Any differences observed between isolated and frame mounted joint responses in the Loadcase 1 test must therefore be attributable to the spatial constraints imposed by the structure.

### 3.2.4 Results Update

*Having completed the first draft of this report it was recognised that this finding relied heavily on the accuracy of the measured yield and wall thickness properties for the specimens. Furthermore the chord yield for the multiplanar specimen was higher than for any other tubular in the batch<sup>(9)</sup>. BOMEL therefore commissioned two further material tests from each chord using offcuts from the specific tubulars. The contractor and procedures were identical. The results were similar and confirmed the properties to be representative and not extreme outliers. Nevertheless taking all these material tests in both cases slightly reduced the nondimensional capacity in the planar case (-3.2%) and increased the multiplanar value (+2.5%).*

The resulting planar:multiplanar capacity calculations for the tension branch are 50.5 : 50.6 and for the compression side 39.4 : 43.6. *These figures still indicate there is no substantial effect on capacity although it might be inferred that a small (10%) enhancement in the compression capacity can be attributed to the out-of-plane braces constraining ovalising deformations in the chord.*

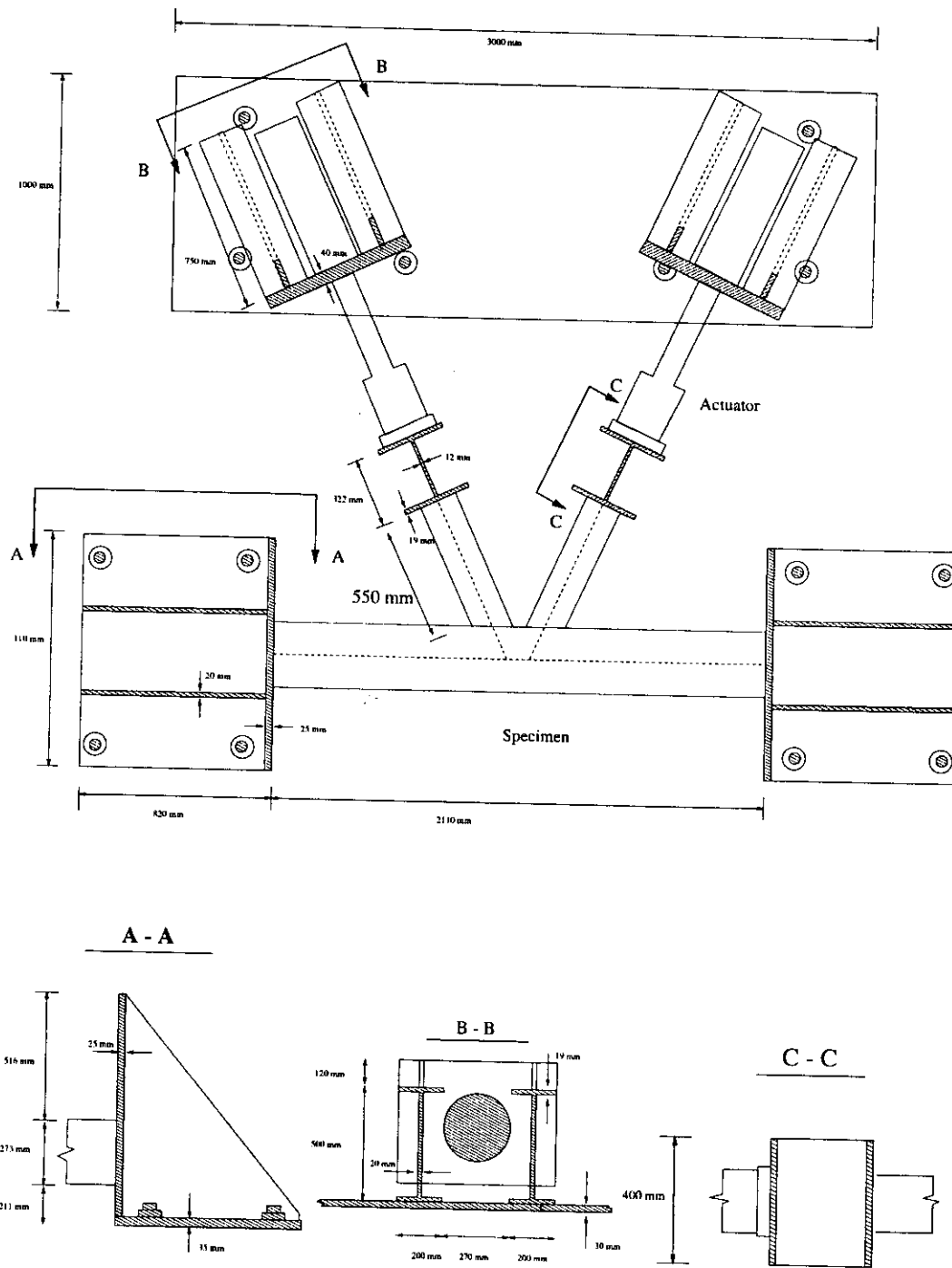
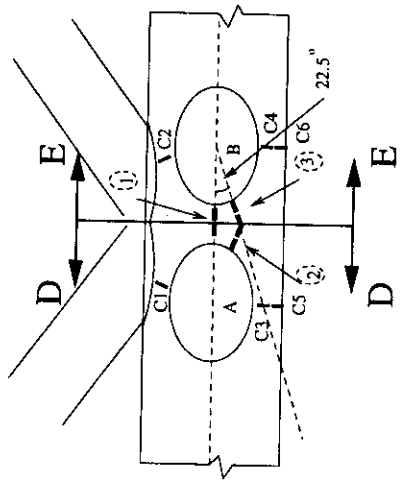
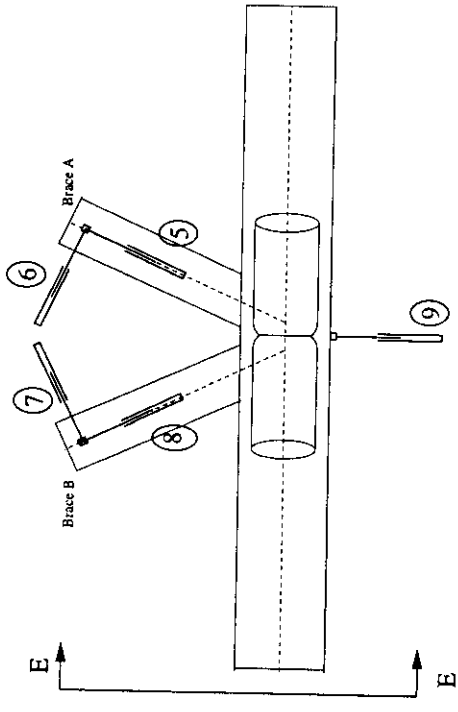


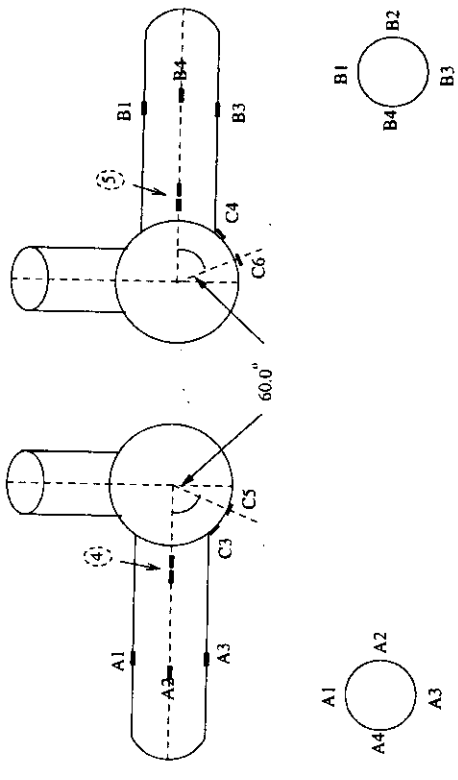
Figure 3.7 SINTEF isolated joint test set up<sup>(6)</sup>





D - D

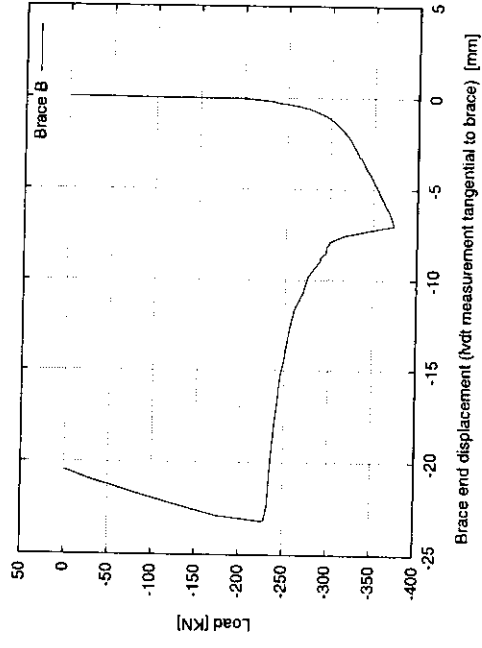
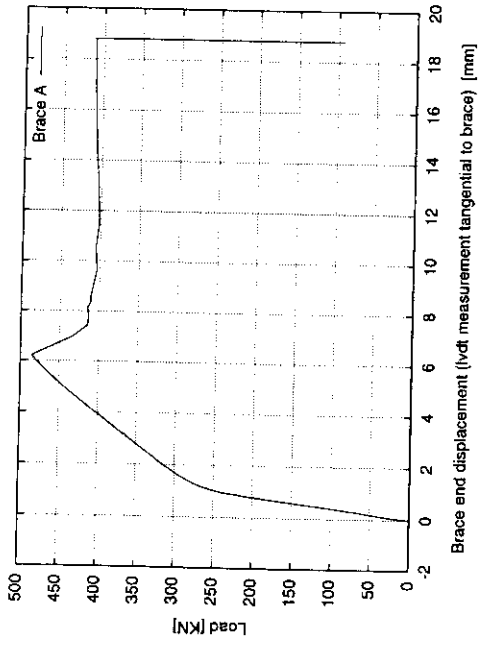
E - E



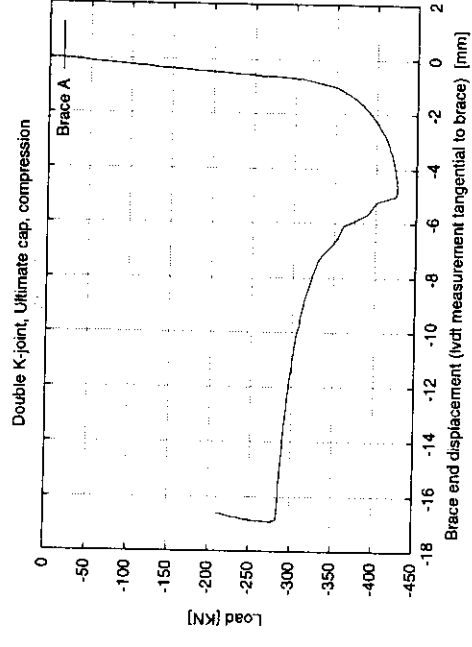
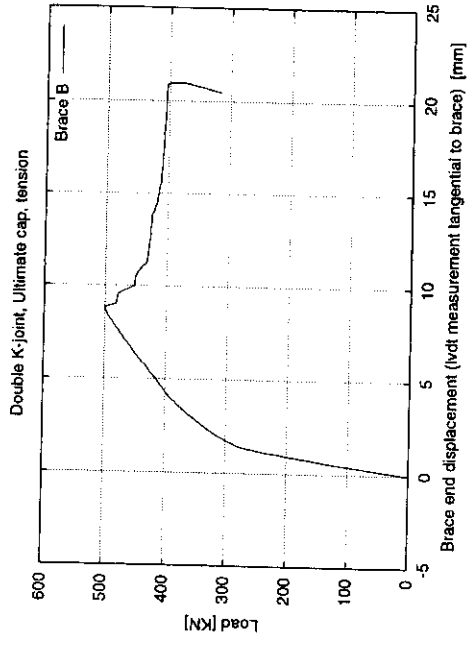
(a) Displacement transducers (LVDTs)

(b) Strain gauge layout

Figure 3.8 Isolated K joint specimen instrumentation<sup>(6)</sup>



(a) Planar joint



(b) Multiplanar joint

Figure 3.9 Isolated static joint capacities<sup>(6)</sup>



### 3.3 FRAMES PROJECT PHASE II INFORMATION

#### 3.3.1 Basis of 2D Investigations

As described in Section 1 the K-braced frame tests undertaken in Phase II of the Frames Project (see Figure 1.2) examined the ultimate capacity of gap K joints within the constraints of a planar frame<sup>(2)</sup>. A range of gap sizes and joint geometries (brace to diameter ratios) was examined and comparisons were made with isolated test data on which design practice is based. Particular attention was paid to the way in which isolated joints are tested.

Typically K joints have been tested with one end of the chord free, the two braces and one chord end providing a statically determinate reaction system. Nominally identical tests for a gap joint in the 2D frame and tested in isolation with<sup>(2)</sup> and without<sup>(13)</sup> both ends of the chord supported, indicated that the typical configuration does not represent the effects of frame constraint well and, in the  $\beta=1.0$  case examined, underestimates capacity by some 20%.

#### 3.3.2 Capacity Results

Figure 3.10 presents the Phase II plane frame joint results in comparison with the body of isolated test data which underpinned HSE Guidance<sup>(4)</sup>. The presentation is non-dimensional and the solid line indicates the effective  $Q_g$  formulation accounting for gap effects adopted by HSE<sup>(4)</sup>. Also highlighted are two results for  $\beta=0.89$  K joints which unusually were tested with both ends of the chord supported<sup>(14)</sup>. Clearly the effects of constraint are to significantly increase capacity by some 20-40% particularly for the high  $\beta$  (large brace to chord diameter) configurations.

The joint geometries in the Loadcase 1 3D frame scenario give  $\beta=0.62$  and a nominal gap to diameter ratio,  $\xi$ , of 0.1.

#### 3.3.3 Bending Moment Results

Data were also gathered during the Phase II tests about the moments developed towards the K joint intersections. Figure 3.11 compares the in-plane moments developed in the Frame VII K joint with those in the nominally identical specimen tested in isolation with both ends of the chord constrained. As might be expected the out-of-plane moments are at least an order of magnitude smaller and are not therefore considered. The brace diameter, angles and gauge positions are nominally identical to those in the Loadcase 1 Frame C primary K bracing. The chord diameters and hence  $\beta$  ratios are different and the absolute values are therefore not comparable. Qualitative comparison can however be made between the data in Figure 3.11 and Figures 2.22 and 2.23.

Focusing first on the 2D results it is clear that although the test was nominally axial, and great care was taken to ensure applied loads were concentric, the asymmetry at the intersection

causes secondary moments to develop. It is important that such effects are distinguished from primary moments when assessing the axial force-moment interactions. The graphs in Figure 3.11 do also indicate that the moments arising in the frame are 50 to 100% greater than those in the isolated test and may be attributed to primary bending.

The reduction in the moments in the compression brace of the 2D specimen, as in the 3D frame, correspond to gross chord deformations as failure approaches.

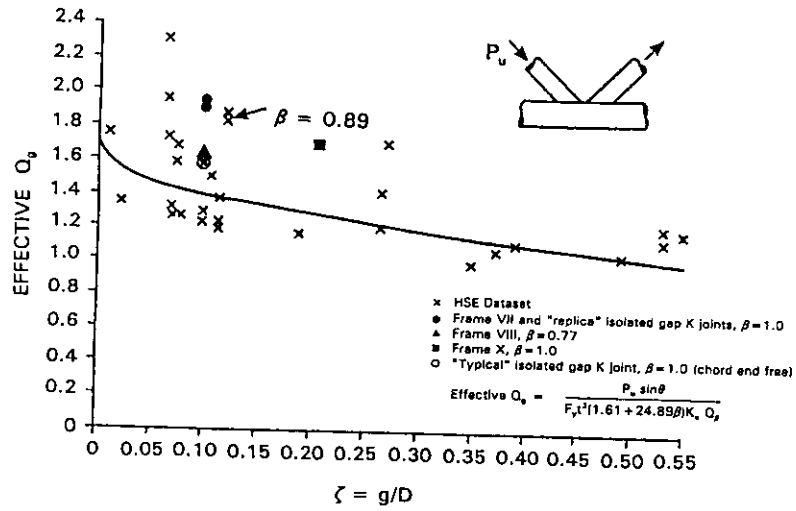


Figure 3.10 Comparison between Frames Project Phase II planar K joint data<sup>(2, 13)</sup> and HSE isolated test database<sup>(4)</sup>

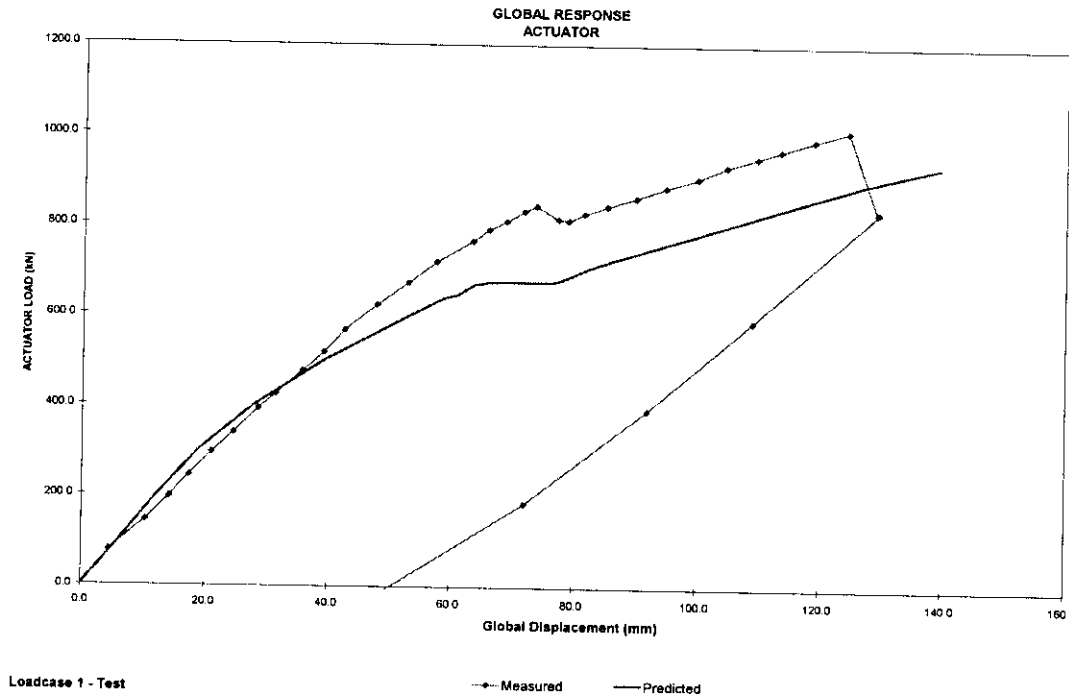
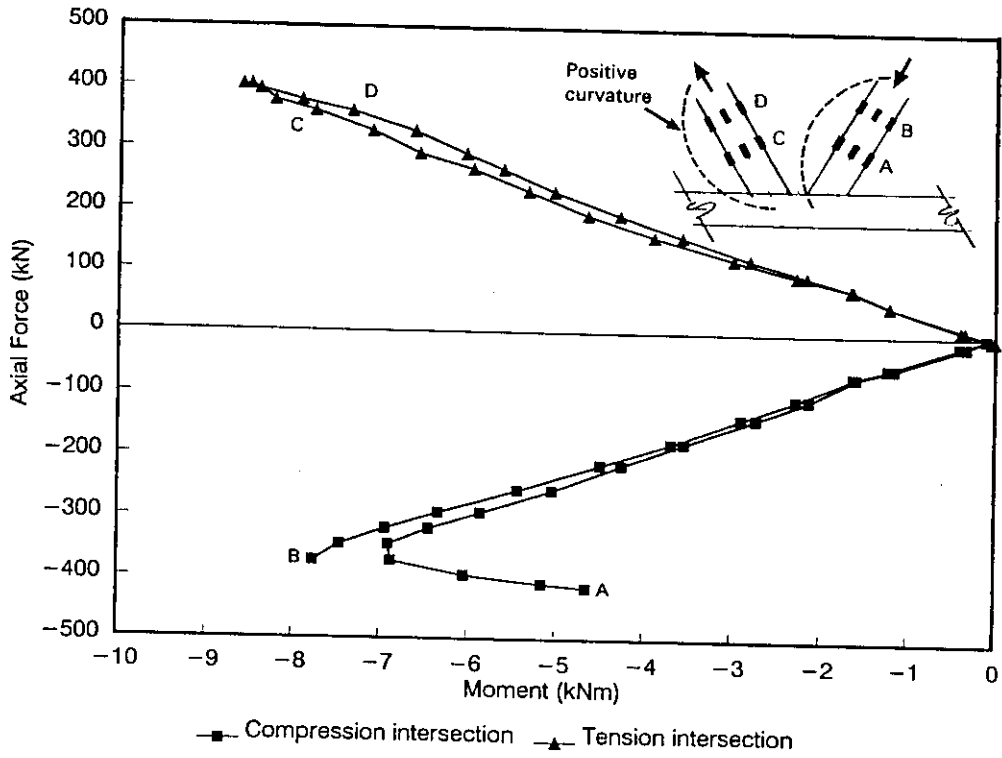
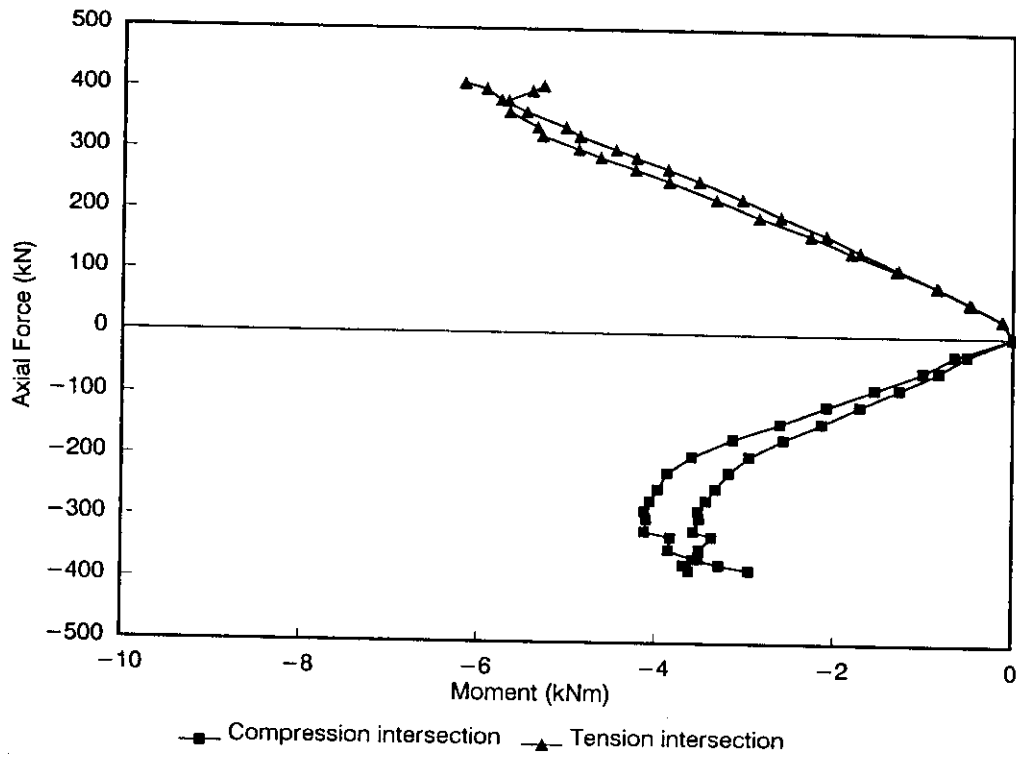


Figure 3.12 Comparison between SAFJAC predicted and measured global response for 3D frame in Loadcase 1



(a) Isolated Joint



(b) Joint in Frame VII

Figure 3.11 Comparison between bending moments detected near nominally identical K joints tested within Frame VII and in isolation<sup>(2)</sup>

## 3.4 SAFJAC FRAME RESPONSE PREDICTIONS

### 3.4.1 Background

As part of BOMEL's contribution to the 3D Frames Project, blind predictions of ultimate strength were contributed to the benchmark exercise. For the Loadcase 1 scenario, K joint response characteristics were assumed for the multiplanar connections on Frame C.

Within SAFJAC the joint response characteristics, at the time of the benchmark analysis, were based on the HSE mean capacity formulations<sup>(4)</sup> together with five-part piece-wise linear load-deflection relationships devised from the corresponding HSE isolated joint database available in the first phase of the project<sup>(15)</sup>.

The specific characteristics were based on nominal section properties but measured yield stress data. Different post-ultimate response characteristics were also assigned to each node. At Node 37, where the out-of-plane braces were separated by a gap, it was assumed they would not contribute significantly to post-ultimate capacity and the strength would fall off abruptly once tensile failure in the primary K joint in Frame C occurred. This characteristic was exhibited by the planar gap K joints in Phase II<sup>(2)</sup>. At Node 38 however, it was considered that the overlapping out-of-plane braces might help maintain integrity such that the strength might plateau. This was seen with in-plane loading of overlapping joints in the 2D tests<sup>(2)</sup>. This background data was available to all Benchmark Analysts as part of the information provided by BOMEL.

### 3.4.2 Comparison between Predicted and Measured Responses

The effect of these characteristics on the frame response predictions is shown in Figures 3.12 to 3.14, in comparison with the measured results for the Loadcase 1 test. The analysis includes the effect of gravity and is therefore directly comparable to the test result. For example for brace 63 where the peak tensile load is 310kN this is based on:  $HSE_{\text{meancapacity}} + 54$  where the latter contribution reverses the initial compression in the member due to gravity.

It is evident from the figures that the joints in the 3D frame test sustained significantly greater loads than predicted. This is discussed further in Section 5. The underprediction in the global response is due to this factor. The sudden drop in measured brace loads around 75mm displacement is associated with through thickness cracking at Node 38; the corresponding drop in the measured 'bottom bay' brace loads (Braces 61 and 62) is in response to this. With reference to Figure 3.13 it can be seen that the out-of-plane overlap braces did not prevent load being shed as had been postulated in the predictions, as the primary K joint connecting Braces 63 and 64 cracked. Nevertheless the degree of load shedding was not as rapid as it would have been had it been assumed that the restraint had not been there (see Figure 3.14 predictions compared with Figure 3.13 measurements).

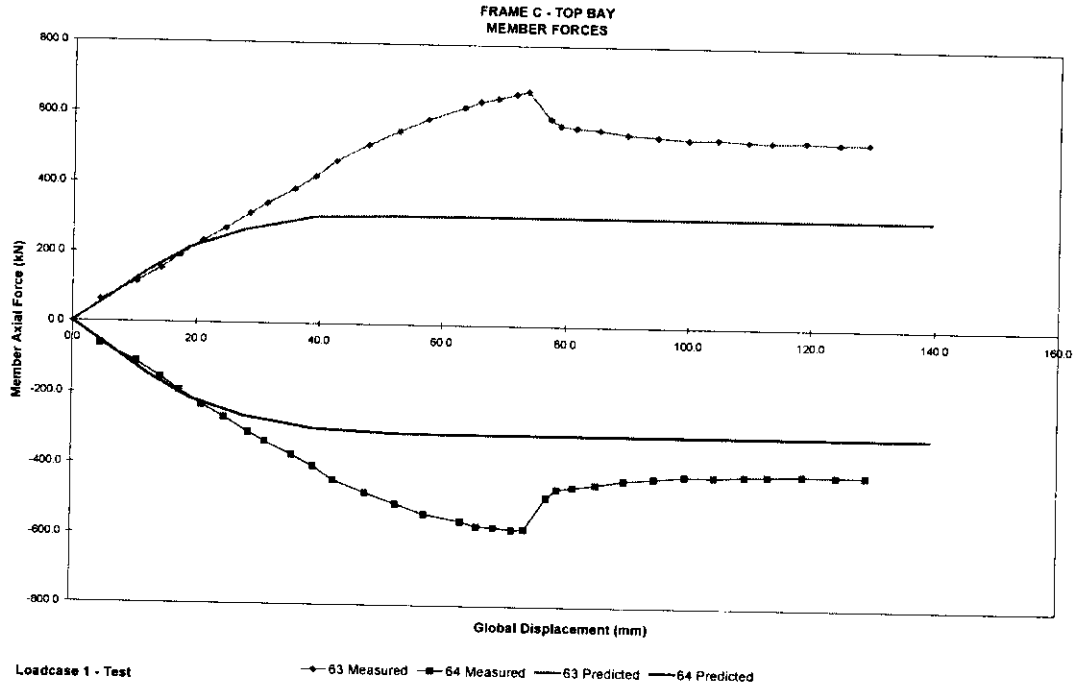


Figure 3.13 SAFJAC - Loadcase 1 - test comparison of primary brace forces through Node 38

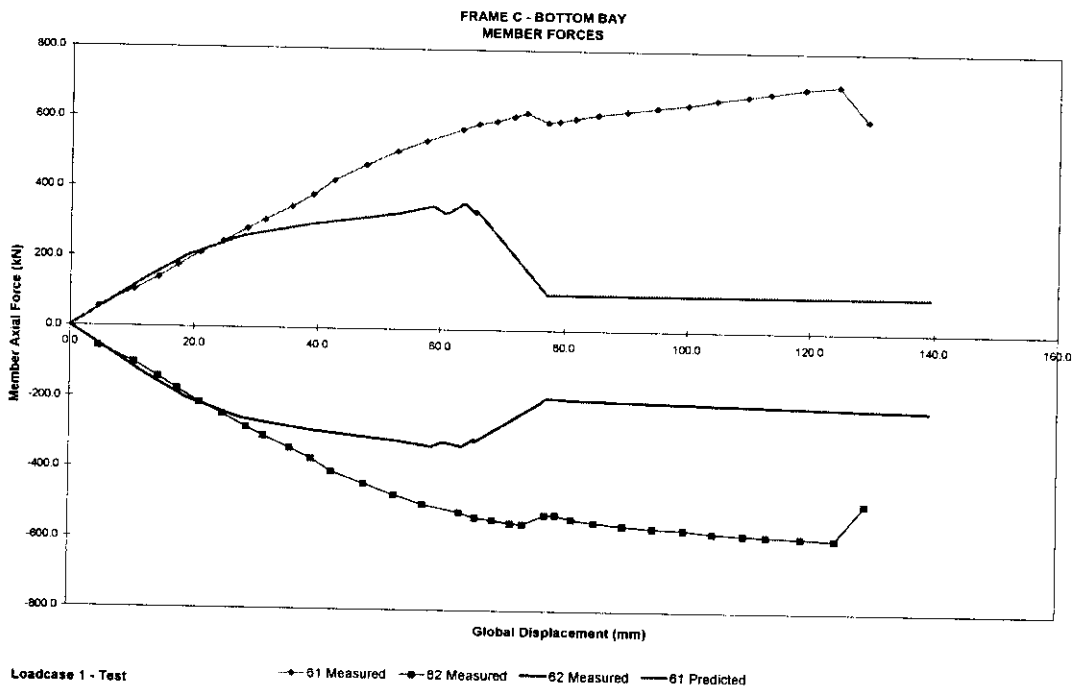


Figure 3.14 SAFJAC - Loadcase 1 - test comparison of primary brace forces through Node 37



## 4. INDUSTRY PRACTICE

### 4.1 PREAMBLE

In addition to comparative evidence from associated test programmes and analysis, an important reference base for interpreting the 3D frame tests is current engineering practice. Over the years component tests have been performed and the findings have been generalised and introduced into codes of practice. With time greater understanding of factors affecting joint behaviour has developed and databases have been rescreened and supplemented. Where necessary codes and standards have been revised.

For tubular joints many alternative formulations are available. Those particularly relevant to offshore practice include:

- API RP2A<sup>(16, 17)</sup>. The equations were developed as lower bound formulations to what is now considered to be a fairly limited database<sup>(18)</sup>. Their original introduction was in working stress design (WSD) practice but they are now also adopted in load and resistance factor design (LRFD).
- HSE<sup>(4)</sup>. An extended database was developed to determine mean and hence characteristic formulations for joint capacity. Although HSE 4th Edition Guidance is now formally withdrawn, the background document provides a useful reference base.
- BOMEL Tubular Joints Guide<sup>(19)</sup>. The remit to BOMEL's Tubular Joints Group was specifically not to develop new formulations. Improved data searches and screening criteria were to be used to develop more reliable databases against which published formulae were to be assessed. The recommendations varied with joint type but for gap K joints the 'best' offshore formulations were those from HSE Guidance<sup>(4)</sup>.
- ISO 13819-2 (Draft)<sup>(20)</sup>. The development of a harmonised international standard for fixed offshore structures took as its baseline API RP2A<sup>(17)</sup>. Wherever possible this practice was to be adopted but where necessary changes could be introduced. For tubular joints the static strength equations have been replaced in entirety. The draft standard includes characteristic capacity, bias and COV data enabling the underlying mean formulae to be deduced.

On the basis of the above the Loadcase 1 K joint results are compared against API<sup>(16)</sup>, HSE<sup>(4)</sup> and ISO<sup>(20)</sup> capacity equations which in turn are used as a basis for correlation with the body of isolated component test data.





## 4.2 PLANAR JOINT CODE CAPACITY FORMULATIONS

The capacity equations for gap K joints are reproduced in Table 4.1 below in order that the different influencing factors can be seen. However for further detail on the background, reference should be made to the source documents. In all cases the capacity equations take the form:

$$\text{Axial force: } P_u = \frac{F_y T^2}{\sin\theta} Q_u Q_f \quad (4.1)$$

$$\text{Bending: } M_u = \frac{F_y T^2 d}{\sin\theta} Q_u Q_f \quad (4.2)$$

where:	$F_y$	= chord yield stress
	$T$	= chord wall thickness
	$\theta$	= brace angle
	$Q_u$	= geometry factor in Table 4.1
	$\beta$	= brace / chord diameter ratio (d/D)
	$\gamma$	= chord slenderness (D/2T)
	$Q_\beta$	= $0.3 / \beta(1-0.833\beta)$ for $\beta > 0.6$ ; $Q_\beta = 1.0$ for $\beta \leq 0.6$
	$\xi$	= gap ratio (g/D)
	$K_a$	= relative length factor = $0.5 (1 + 1/\sin\theta)$
	$Q_f$	= chord stress factor in Table 4.1.

In all cases no distinction is made between tension and compression branch responses. In the background to the former HSE Guidance<sup>(4)</sup> K joint failure is described as a compressive failure mode and the formulae were developed in conjunction with data for compression loaded Y joints.

To assess combined load effects the interaction formulae are also compared in Table 4.1 where the suffix 'L' denotes the load effects and 'R' the calculated resistance. The inclusion of partial load or resistance factors to give design values or comparison between acting and allowable depends on the code format in use.

In all cases the codes suggest each plane within a multiplanar joint is assessed separately, with no quantitative recommendations to account for multiplanar interactions for joints as seen in the Loadcase 1 K-K configuration.

## 4.3 AS-BUILT JOINT CAPACITY PREDICTIONS

Using the as-built properties for the Loadcase 1 joints at Nodes 37 and 38 the calculated axial capacities, neglecting any degradation due to chord stresses, are given in Table 4.2. Understandably the API lower bound formulation gives significantly lower capacities than the mean ISO or HSE values. The HSE and ISO values are comparable although for axial and in-plane bending capacities the draft ISO standard gives values some 12.5% and 7.8% greater than the earlier HSE document.

Table 4.1 Code formulae for K joint capacity

Component	Reference		
	API <sup>(16)</sup> (lower bound)	HSE <sup>(4)</sup> (mean)	ISO <sup>(20)</sup> (mean)
$Q_u$ Axial	$(3.4+19\beta)Q_g$	$(2.37+23.6\beta)Q_\beta^{0.5} K_a Q_g$	$1.3(1.9+19\beta)Q_\beta^{0.5} Q_g$
$Q_g$	1.8-4g/D (for $\gamma > 20$ )	1.67 - 0.86 $\xi^{0.5}$	1.9-0.7 (2g/D) <sup>0.5</sup> (for g/T $\geq$ 2)
$Q_u$ IPB	0.8(3.4+19 $\beta$ )	(6.2 $\beta$ - 0.27) $\gamma^{0.5}$	1.243(4.5 $\beta$ $\gamma^{0.5}$ )
$Q_u$ OPB	0.8(3.4+7 $\beta$ ) $Q_\beta$	(1.88+8.64 $\beta$ ) $Q_\beta$	1.217(3.2 $\gamma^{0.5\beta^2}$ )
$Q_r$	1 if all chord stresses are tensile, or $1 - \lambda \gamma A^2$	as API	1 if all chord stresses are tensile  $1 - \lambda A^2$
$\lambda_{\text{brace ax}}$	0.03	as API	as API
$\lambda_{\text{brace ipb}}$	0.045	as API	as API
$\lambda_{\text{brace opb}}$	0.021	as API	as API
A	$\frac{(f_{ax}^2 + f_{ipb}^2 + f_{opb}^2)^{0.5}}{F_y}$	as API	$\left( C_1 \left( \frac{P_D}{P_y} \right)^2 + C_2 \left( \frac{M_D}{M_p} \right)_{ipb}^2 + C_2 \left( \frac{M_D}{M_p} \right)_{opb}^2 \right)^{0.5}$
	$f_{ax}, f_{ipb}, f_{opb}$ = chord stress components	as API	$C_1=14, C_2=43$ - K joints under balanced axial loading $C_1=25, C_2=43$ - K joints with brace moments $P_D, M_D$ - factored load effects in chord $P_y$ = yield capacity of chord $M_p$ = plastic moment capacity of chord
Interaction check ( $\leq 1.0$ )	$1 - \cos \left[ \frac{\pi}{2} \left( \frac{P_L}{P_R} \right) \right] + \left[ \left( \frac{M_L}{M_R} \right)_{ipb}^2 + \left( \frac{M_L}{M_R} \right)_{opb}^2 \right]^{0.5}$	$\left( \frac{P_L}{P_R} \right) + \left( \frac{M_L}{M_R} \right)_{ipb}^2 + \left( \frac{M_L}{M_R} \right)_{opb}$	as HSE

Table 4.2 Loadcase 1 K joint capacity 'predictions' from codes

(Nodes 37 and 38:  $D = 273.1\text{mm}$ ,  $d = 168.7\text{mm}$ ,  $T = 5.61\text{mm}$ ,  $g_{\text{nom}} = 27.3\text{mm}$ ,  $F_y = 288.6\text{ N/mm}^2$ ,  $\theta = 64.3^\circ$ )

Component	Reference		
	API (lower bound)	HSE (mean)	ISO (mean)
Absolute:			
Axial capacity (kN)	169.1	252.9	284.7
IPB capacity (kNm)	16.1	26.9	29.0
OPB capacity (kNm)	8.2	12.3	12.2
Non-dimensional:			
Axial capacity	18.6	27.8	31.3
IPB capacity	10.5	17.6	18.9
OPB capacity	5.4	8.0	8.0

The table gives absolute values for direct comparison with the test results as well as non-dimensionalised values ( $P_v/F_y T^2$  and  $M_v/F_y T^2 d$ ) to compare with isolated tests and analyses in which these parameters differ slightly.

#### 4.4 MULTIPLANAR JOINT CAPACITY FORMULATIONS

In many instances tubular joint failure is associated with ovalisation of the chord. The presence of out-of-plane braces can restrain that ovalisation but the forces within those members can act to increase or reverse ovalisation driven by loading in-plane. A number of experimental investigations have been undertaken for specific isolated joint geometries<sup>(19)</sup> but there are few generalised recommendations.

The exception is the multibrace formulation in the AWS structural welding code<sup>(21)</sup> which includes the  $\alpha$  ovalising parameter defined in Figure 4.1.

For each brace the ovalising influence of the forces in all braces at the node is accounted for. The  $\cos 2\phi$  term accounts for the out-of-plane brace forces and  $L_1$  accounts for the lesser influence the greater the separation along the chord.

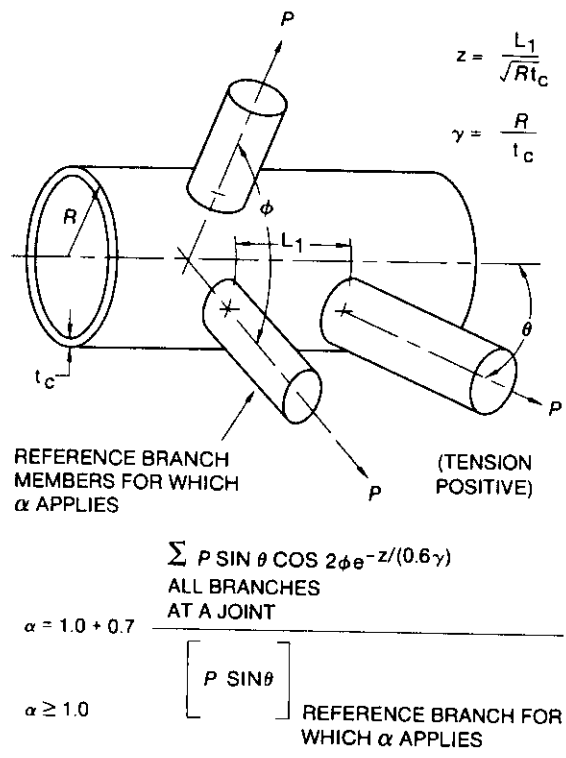


Figure 4.1 AWS multibrace ovalisation parameter  $\alpha^{(21)}$

The AWS capacity formulations themselves are cast in punching shear terms ( $V_p$ ) where:

$$V_p = Q_q Q_t \frac{F_y}{0.6\gamma} \tag{4.3}$$

For the present purposes  $Q_q$  can be considered analogous to  $Q_u$  in Equation 4.1 above.  $Q_q$  incorporates the  $\alpha$  ovalising effects and for axial loads is given by:

$$Q_q = \left( \frac{1.7}{\alpha} + \frac{0.18}{\beta} \right) Q_\beta^{0.7(\alpha-1)} \tag{4.4}$$

The reference case is for a single brace T/Y joint for which  $\alpha = 1.7$ . If  $\alpha$  is greater than 1.7 the forces in other braces are acting to reduce the capacity, whereas for  $\alpha$  between 1 and 1.7 the effects are beneficial. Specific  $\alpha$  and  $Q_q$  results for the Node 38 K joint (forces in braces 63<sup>(+)</sup>, 64<sup>(-)</sup>, 94<sup>(+)</sup> and 95<sup>(-)</sup>) are plotted in Figure 4.2 based on measured forces reached through the test. Two cases are considered: (1) the four brace multiplanar joint values; and (2) the results were only the in-plane braces (63 and 64) considered.

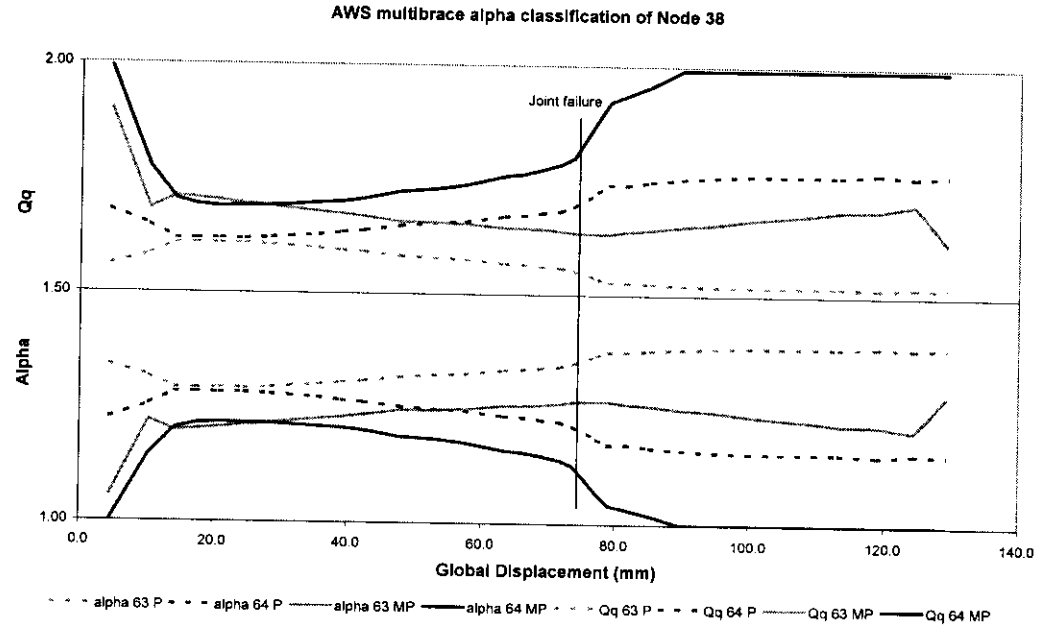


Figure 4.2 Multibrace  $\alpha$  ovalisation effects at Node 38 through the Loadcase 1 test

It can be seen from the figure that the AWS formulation indicates the loading in the (Level 1) out-of-plane braces would slightly increase the in-plane (Frame C) K joint capacity by about 5% compared to that of a corresponding planar joint.

Reference can also be made to experimental data for isolated multiplanar joints in the open literature. Experiments undertaken by Paul<sup>(22)</sup> on K-K specimens are most relevant. The joints had 60° and 90° out-of-plane angles and  $\beta$  ratios in the range 0.22 to 0.47. However, the magnitude of forces in in- and out-of-plane braces was similar, precipitating strong interaction in the gap region between planes of braces. When the  $\beta$  ratio was high the two adjacent compression braces acted together to ovalise the chord; for smaller  $\beta$  ratios the chord wall in the out-of-plane gap tended to be pinched. In the Loadcase 1 test frame, as in most jacket loading scenarios, there is a dominant plane of loading. For this reason little additional insight could be gained from the previous test data to account for multiplanar interactions for joints in the Loadcase 1 K-K configuration.



## 5. ASSESSMENT OF LOADCASE 1 COMPONENT AND SYSTEM RESPONSES

### 5.1 JOINT CAPACITY DATA ASSIMILATION

In order to assimilate the data presented in the foregoing sections, Table 5.1 brings forward the capacities and properties. The non-dimensionalised data are presented again in Figure 5.1 to give a clearer picture of the relative findings.

Table 5.1 Quantified comparison of joint data

Investigation	Source	Capacity (kN)	$F_y$ (N/mm <sup>2</sup> )	T (mm)	Capacity / $F_y T^2$
1. Loadcase 1 N38 N37 (capacity corrected for gravity)	Tables 2.2 & 2.3	+616	288.6	5.61	67.8
		-524	288.6	5.61	57.7
		> +630	288.6	5.61	69.4
		-516	288.6	5.61	56.8
2. Norsk Hydro FE Multiplanar Planar	Table 3.1	+400	250	5.9	46.0
		-300	250	5.9	34.5
		260	250	5.9	29.9
3. SINTEF isolated test Planar Multiplanar	Table 3.2 (Section 3.2.4)	+480	288.5	5.65	52.1 (50.5)
		-375	288.5	5.65	40.7 (39.4)
		+500	311.4	5.70	49.4 (50.6)
		-430	311.4	5.70	42.1 (43.6)
4. Former HSE Guidance (mean)	Table 4.2	253	288.6	5.61	27.8
5. ISO draft (mean)	Table 4.2	285	288.6	5.61	31.3
6. API (lower bound)	Table 4.2	169	288.6	5.61	18.6
7. SAFJAC (as per former HSE)	Section 3.4	256	292	5.6	28.0
8. Phase II 'enhancements'	Section 3.3	253x1.2	288.6	5.61	33.7
		to 253x1.4	288.6	5.61	39.4

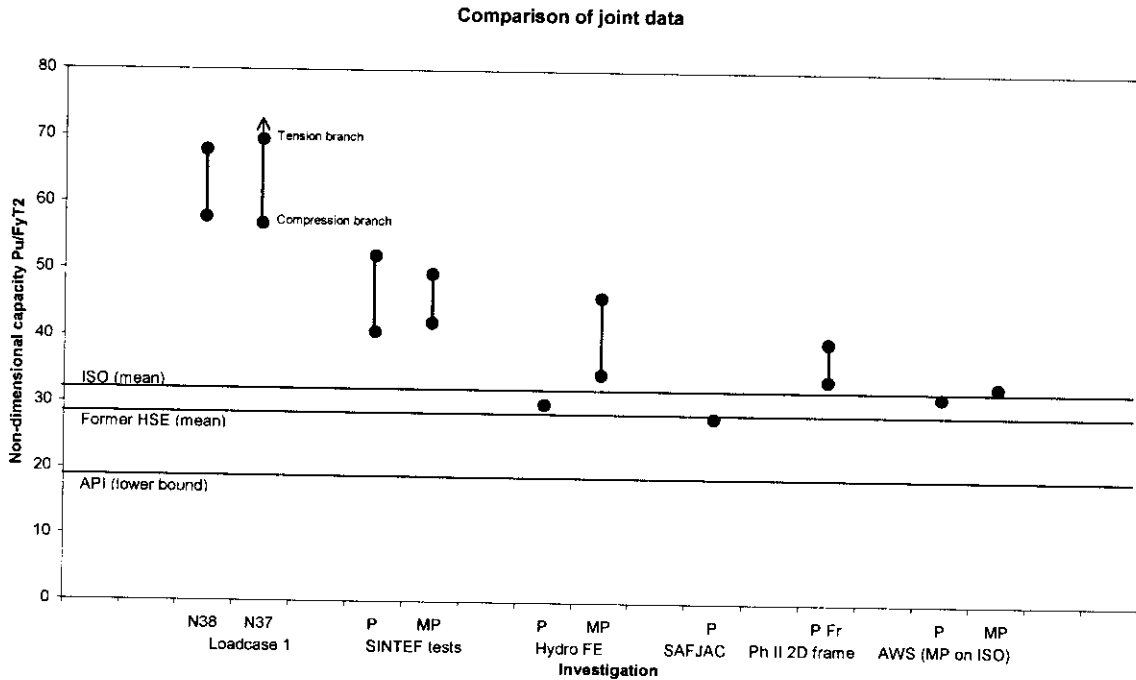


Figure 5.1 Comparison between joint capacities

The extreme range is between the tension load sustained at Node 37 in the 3D frame without failure and the API lower bound capacity assessment. The experimental result delivers a factor of 3.7 on the calculated strength.

In comparison with the isolated database, represented for example by the ISO mean capacity equation, the lower load in Node 38 at failure is still some 84% greater. Furthermore the tension brace is transmitting even greater loads. The comparison between the multiload path frame response and component behaviour is explained further in Section 5.2 below.

It is useful also to discuss the findings in the context of the interrelation between the various investigations highlighted in Figure 3.6.

- Irrespective of the isolated joint database considered<sup>(eg 4, 18, 20)</sup>, the resulting capacity equations attribute significantly lower capacity to the Frame C gap K joint tests than demonstrated in any of the analytical or numerical investigations. The ISO and former HSE capacity levels indicated on the graph represent the mean of the respective isolated joint test databases. In design, factored loads would be used in conjunction with partial resistance factors and characteristic capacity equations some 30% lower than the values shown.
- In the 2D frame and companion isolated tests it was shown that support at both ends of the chord better reflected conditions in a frame than 'typical' isolated tests with one



chord end free. The restraint to chord deformations enabled loads from 20-40% greater to be sustained.

- The effects of chord constraint were reflected in the Hydro FE analysis although the analysis strategy did not make any allowance for welds encroaching the nominal gap region between K braces. Were these to be accounted for, calibration analyses suggested some 15% greater strength might be anticipated.
- The influence of the actual gap between weld toes compared with the nominal values (12mm compared with 27mm in the Node 38 case) was explored in the code comparisons and indicated an 8% enhancement in both the ISO and former HSE formulations.
- Once the out-of-plane braces were included and the Hydro analysis was undertaken for the joint in a frame, an increase in strength of the order of 15-54% was observed. The greatest enhancement was for the tension branch and it was recognised that cracking, which was not accounted for in the analysis, might precipitate earlier failure.
- The planar joint tests at SINTEF provide a basis for comparison with the simple joint FE analysis.

However whereas the Hydro analysis showed limited deformation for the tension intersection compared with the compression side, the SINTEF tests imposed equal but opposite deformations. The minimum test capacity was some 36% greater than the initial Hydro analysis indicated - realistic 'gap' effects and the brace constraints may be expected to account for this.

- The multiplanar isolated test undertaken at SINTEF enabled the effect of the presence of overlapped out-of-plane braces stiffening the chord to be assessed. However, the effects were shown not to be significant.
- Referring back to the isolated / multiplanar joint in frame analyses conducted by Hydro, it can be inferred from the SINTEF findings that the greater capacity in the frame should be attributed to the multiplanar constraints and/or out of plane brace loads but not the local congestion in the geometry.
- The only code providing general quantitative guidance on multiplanar effects, AWS, considers only the contributions from brace loads. However this suggests that for the Loadcase 1 nodes the out-of-plane brace loads would only be slightly beneficial. It therefore appears that it is the spatial constraints to the node in the frame that





principally affect capacity.

- The relative enhancement between the Node 37 and 38 capacities in the Loadcase 1 frame tests and the SINTEF planar test are in the range 32 to 42%  $[(67.8+69.4)/2 \times 52.1 \text{ to } (57.7+56.8)/2 \times 40.1]$  and may be compared with the enhancement in the Hydro analysis between isolated and frame mounted conditions of 15-54% as noted above. There are a number of distinguishing factors, nevertheless the magnitude of the effects is comparable.

On the basis of the foregoing it appears that the significant enhancements in capacity observed in the Frames Project tests over and above indications from isolated joint databases (code formulations) are attributable to the constraints within the frame confines.

It should also be noted that the approach adopted in interpreting the results is conservative in that, in applying the code equation, no account has been taken of chord stress effects which, as shown in Section 4.2, may reduce joint capacity to a degree dependent on the level of chord and brace stresses. Furthermore, as shown in Section 2.2.5.2, the brace axial forces are accompanied by significant bending effects. The magnitude of apparent moments in the test shown in Table 2.3 can be compared with primary bending capacities underlying the codes in Section 4.2. These secondary deformation induced moments are not included in the capacity evaluations but it is notable that for example in-plane curvature in the primary tension brace is acting to increase the tensile strains acting across the chord toe intersection in the gap region. These secondary bending effects might therefore be expected to be detrimental but this is not revealed by the measured responses.

## 5.2 JOINT DEFORMATION COMPARISONS

Figure 5.2 compares the local load deflection characteristics recorded across the primary K joint intersections at Nodes 37 and 38 with the isolated results from the tests undertaken at SINTEF. In the latter case the displacement is for the brace end with respect to a fixed reference frame rather than relative to the chord. Were in-line deformations of the chord centre line extracted, the response would be stiffer. The plot shows the magnitude of brace forces so tensile and compressive responses can be compared in the same quadrant. The origin for forces in the frame is offset to account for the effects of gravity which are initially reversed by applied loads.

As noted in Section 2 there were some initial irregularities within the logger system up to Scan 12 but these have been corrected for in the figure. It should be noted that the chord properties differ slightly between specimens.

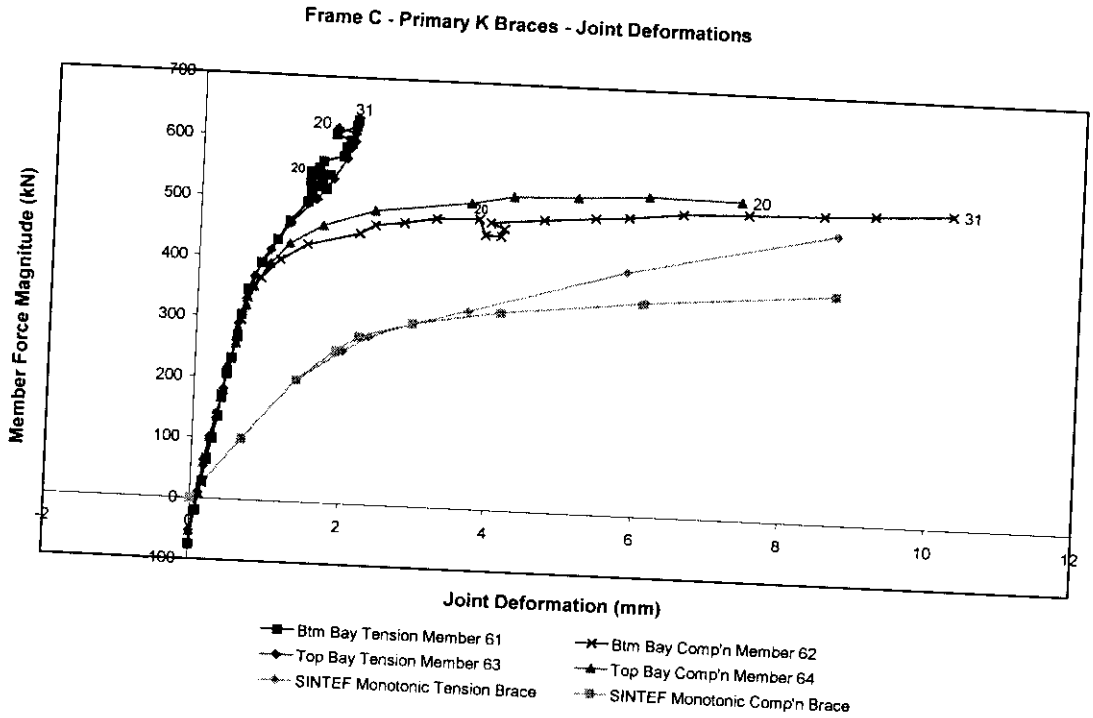


Figure 5.2 Local joint deformations in the 3D frame and in SINTEF planar test

Principal observations from the graph are:

- the remarkable consistency between the response characteristics at Nodes 37 and 38
- the stiffer response assumed by the tension loadpath for joints in the frame compared with compression.

Figure 5.3 also includes the SAFJAC assumed characteristics (assumed to be the same for tension and compression loadpaths) tied into the baseline HSE isolated test database in terms of stiffness and capacity. The figure also includes scaled predictions to reflect the enhanced strength observed in the 3D test based on an average of the maximum tension and compression branch loads sustained.

On this basis it would appear that the measured response was slightly stiffer than the 'planar' prediction but that nevertheless, once capacity is properly identified, the SAFJAC response characteristics present a reasonable representation for system response predictions.

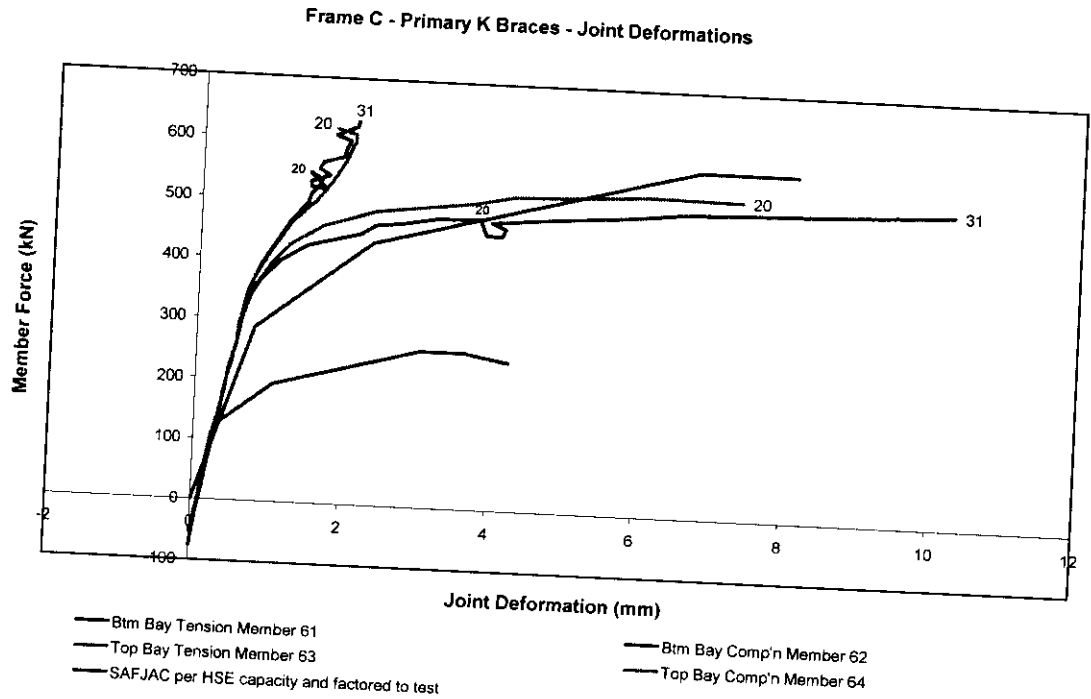


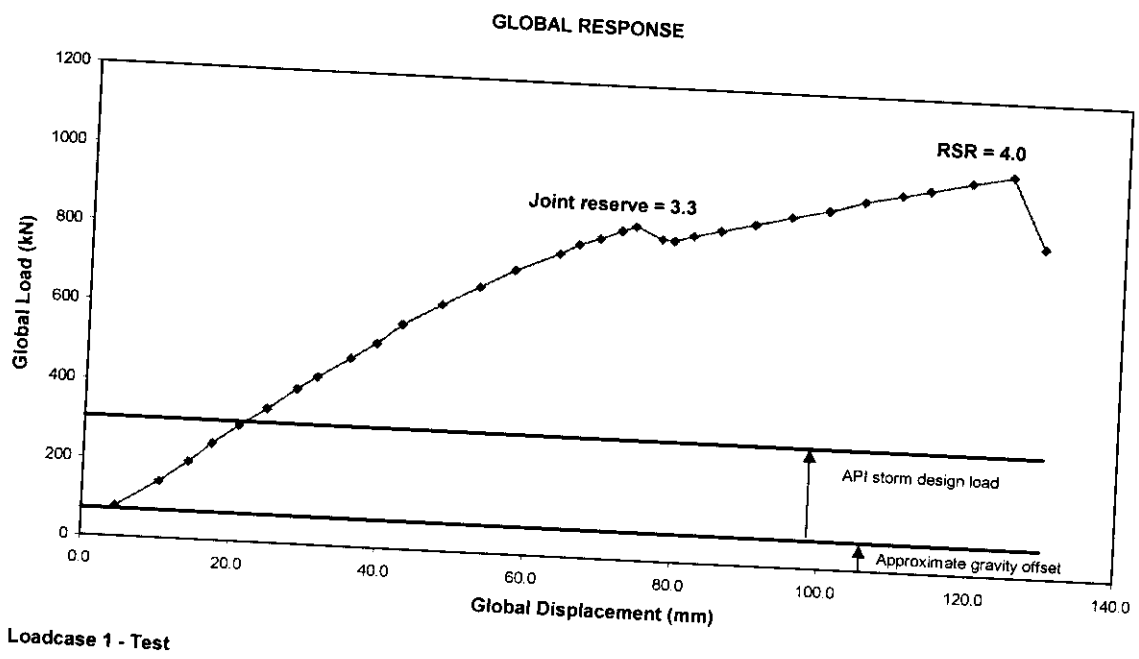
Figure 5.3 Comparison between SAFJAC and measured joint response characteristics

### 5.3 SYSTEM RESPONSE COMPARISONS

The foregoing discussion has centred on the local joint characteristics at the primary nodes influencing the Loadcase 1 response. It has been shown that the behaviour is strongly influenced by the 3D frame constraints but equally these affect the distribution of forces through the structure and the global system capacity.

From an elastic design analysis standpoint, code checking shows the Frame C K joints to be critical. Assuming an axial utilisation of unity for these nodes in a storm analysis leads to the design load levels shown against the global frame response in Figure 5.4. The graph includes an approximate gravity offset to give a basis for direct comparison of applied load effects.

The figure is annotated to show the system Reserve Strength Ratio (RSR) comparing the ultimate capacity with the design load. In terms of the overall response the peak load was actually governed by buckling in Frame D with load redistribution following joint failure in Frame C giving a massive RSR of 4.0. At that stage there was through thickness cracking at Node 38 and the global response had softened significantly, nevertheless substantial capacity to withstand the extreme load due to local and system effects was evident. With a reserve strength of 3.3 associated with the first peak and joint failure, the additional capacity (70% of the original design load) is attributable to redistribution.



Loadcase 1 - Test

Figure 5.4 System reserve strength ratio

To assess the local and global factors contributing to system strength at the point Node 38 failed, comparison with the elastic response can be made. For 100kN of applied load, forces in Braces 63 and 64 of +73 and -74kN are calculated. The global applied load at the scan prior to joint failure was 844kN. Had the local response remained elastic, the magnitude of brace forces would have been  $\pm 620$  kN ( $0.735 \times 844$ ). Interestingly the average magnitude of the forces at Node 38 (see Table 2.3) was 624 kN ( $(670 + 578) / 2$ ).

Figure 5.5 shows the tension and compression member forces in comparison with the global frame response and, although it is not obvious from this figure, the tension brace effectively stiffens to compensate for the softening compression loadpath. Given the proximity of the load application to Node 38 the behaviour is not unexpected nevertheless it demonstrates that there was negligible system contribution to strength until beyond first component failure.

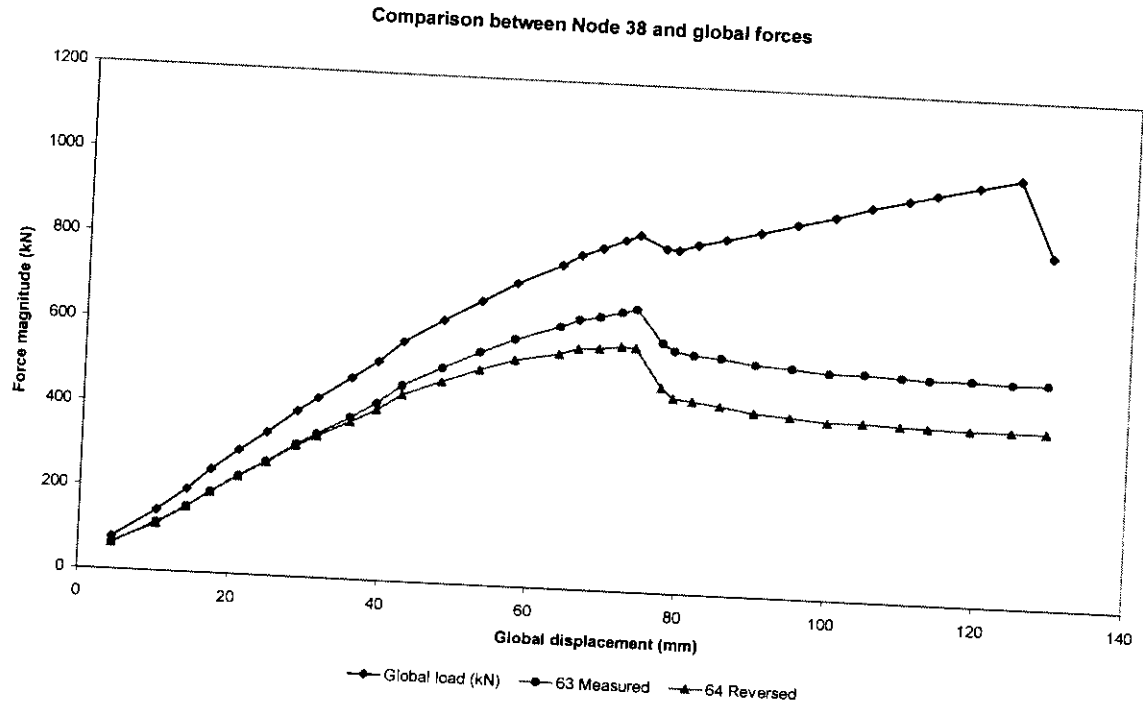


Figure 5.5 Compensating load transfer through primary Frame C braces and subsequent system reserve strength contributions



## 6. CONCLUSIONS

The Frames Project Phase III Loadcase 1 test and associated investigations have revealed significant additional capacity in multiplanar K joints than previously recognised.

Strengths as much as twice the levels indicated by isolated test databases underlying recent codes of practice have been demonstrated. The effects have been shown to be due to the in- and out-of-plane constraints on joints within a structural frame.

The inference for existing jacket structures is that multiplanar K joints similar to the configuration tested may have significant reserves of strength beyond original design load levels. Furthermore even when cracking occurs, propagation is limited by the local congestion at the node and the residual capacity is greater than for planar joints. In addition the test has demonstrated the capacity for load redistribution within the structure and has quantified corresponding system contributions to the overall reserve strength levels.

Analytical work by Norsk Hydro has suggested that some indication of the relative level of capacity enhancement can be derived by comparing isolated analyses with results for multiplanar shell nodes within a beam model of the structure. However such analyses are unable to account for the potential for cracking and there is some discrepancy in absolute strength levels.

Overall it would appear that isolated planar test data provide a poor but very conservative basis for assessing joint strength in these circumstances. Furthermore, the quantitative assessment of multibrace load effects on joint capacity given by AWS gives little indication of the effects observed.

It has been noted at all stages that the assessments of the test data have erred on the conservative side and therefore the substantial strengths observed for multiplanar K joints can be embraced in future assessment with confidence.



## 7. REFERENCES

1. BOMEL Limited. 'Joint Industry Tubular Frames Project - Phase III - Summary and Conclusions', BOMEL Reference C636\04\478R, Revision 0, August 1999.
2. BOMEL Limited. 'Joint Industry Tubular Frames Project - Phase II', Nine volume report, BOMEL Reference C556R003.50 to .58, 1992.
3. Bolt, H M. 'Results from large scale ultimate strength tests of K-braced jacket frame structures', Paper No OTC 7783, Offshore Technology Conference, Houston, May 1995.
4. Department of Energy (now HSE). 'Background to guidance on static strength of tubular joints in steel offshore structures', OTH 89 308, HMSO, 1990.
5. Norsk Hydro. 'Finite element analysis of the multiplanar K joint configurations in Frame C from Loadcase 1', NH Reference NREPLC1.sam, BOMEL Incoming reference 2659 file C636\35, August 1996.
6. SINTEF. 'Monotonic and cyclic testing of isolated K joints', SINTEF reference STF 22 F98704, BOMEL Incoming reference 14130 file C636\24, June 1999.
7. BOMEL Limited. 'Report on test frame analyses', BOMEL Reference C636\04\207R, Revision 0, August 1996.
8. BOMEL Limited. 'Benchmark Analysis - Blind predictions of ultimate strength', BOMEL Reference C636\32\002R, Revision 0, February 1998.
9. BOMEL Limited. 'Material testing report', BOMEL Reference C636\23\004R, Revision B, April 1999
10. BOMEL Limited. 'Assessment of locked-in fabrication stress', BOMEL Reference C636\21\050R, Revision 0, July 1999.
11. BOMEL Limited. 'Test frame instrumentation', BOMEL Reference C636\25\071R, Revision 0, July 1999.
12. BOMEL Limited. 'Loadcase 1 cyclic test report', BOMEL Reference C636\38\010R, Revision 0, August 1999.



13. BOMEL Limited. 'Joint Industry Tubular Frames Project - Phase IIA - Interaction between frame effects and tubular joint behaviour', BOMEL Reference C608\03\021R, Revision 0, February 1996.
14. Amoco (UK) Exploration Company. 'Final reports for the testing of K joints', ST 102/83A and ST125/83A, Wimpey Laboratories Limited, 1983.
15. 'Joint Industry Tubular Frames Project - Phase I', Nine volume report, SCI Reference SCI-RT-042, 1990.
16. American Petroleum Institute. 'Recommended practice for planning, designing and constructing fixed offshore platforms - working stress design', API RP2A-WSD, 20th edition, July 1993.
17. American Petroleum Institute. 'Recommended practice for planning, designing and constructing fixed offshore platforms - load and resistance factor design', API RP2A-LRFD, 1st edition, July 1993.
18. Yura, J et al. 'Ultimate capacity equations for tubular joints', Paper No OTC 3690, Offshore Technology Conference, Houston, May 1980.
19. BOMEL Limited. 'Guide for the design and assessment of tubular joints'. BOMEL Reference C06060R, 1999.
20. International Standards Organisation. 'Offshore structures for petroleum and natural gas industries - Part 2 - Fixed steel structures', Committee Draft ISO/CD 13819-2, May 1999.
21. American Welding Society. 'Structural Welding Code - Steel', AWS D1.1-98, ANSI/AWS, 1998.
22. Paul, J C. 'The ultimate behaviour of multiplanar TT and KK joints made of circular hollow sections', PhD Thesis, Kumamoto University, 1992.





## **APPENDIX A**

### **AS-BUILT DRAWINGS RELEVANT TO LOADCASE 1 TEST**

- General Arrangement of Test Specimen - C636\15\002D Rev G
- General Arrangement of Test Specimen - Dimensions - C636\15\003D Rev G
- Detail Drawing of Node Points 23C, 24D, 25D, 26X, 27E, 28E and 29X - C636\15\009D Revision G
- Isolated K Joints for Cyclic Tests - C636\15\015D Revision B











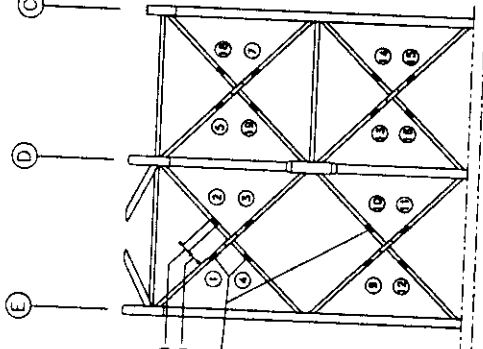
## **APPENDIX B**

### **INSTRUMENTATION LAYOUT DRAWINGS**

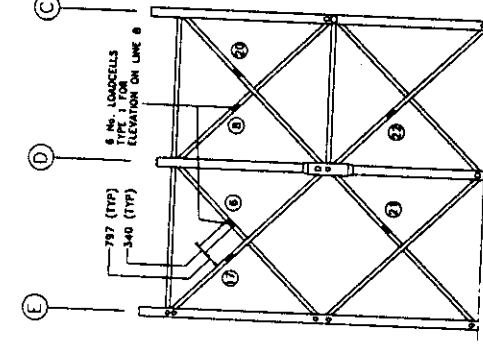
- Load Cell Details - C636\15\011D Revision D
- Strain Gauging Details - Sheet 1 of 2 - C636\15\012D Revision B
- Strain Gauging Details - Sheet 2 of 2 - C636\15\013D Revision B
- Joint Deformation Monitoring - C636\15\016D Revision 0

Drawing No. C636/15/0110

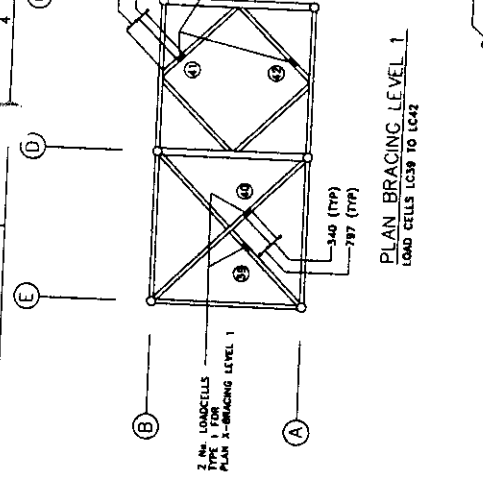
C OF 200.5 x 650 FAB. BEAM  
B (DATUM LINE)



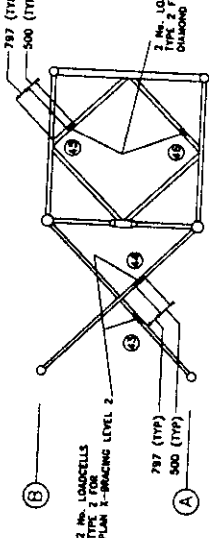
ELEVATION ON LINE A  
LOAD CELLS LC1 TO LC16 U.N.G.



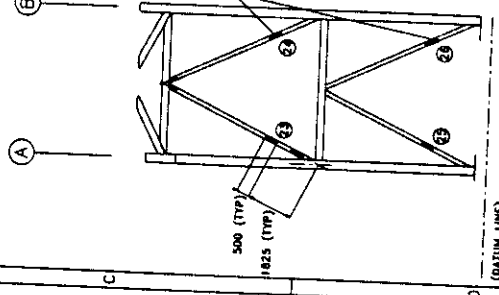
ELEVATION ON LINE B  
LOAD CELLS LC17 TO LC22 U.N.G.



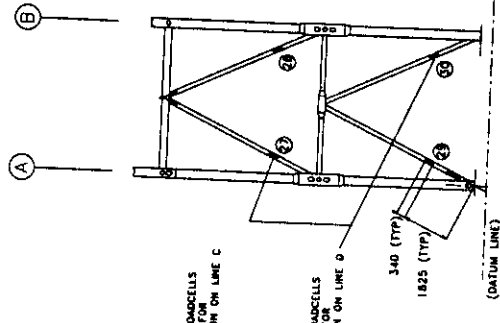
PLAN BRACING LEVEL 1  
LOAD CELLS LC39 TO LC42



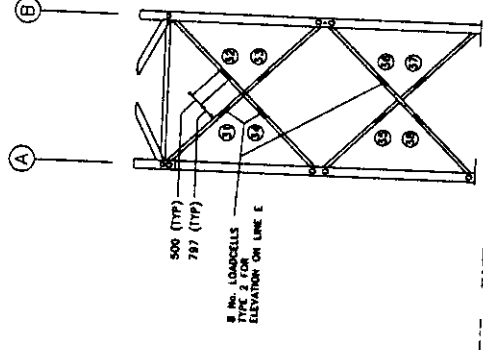
PLAN BRACING LEVEL 2  
LOAD CELLS LC43 TO LC46



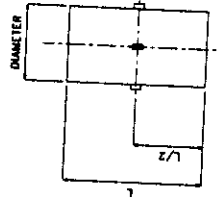
ELEVATION ON LINE C  
LOAD CELLS LC23 TO LC26



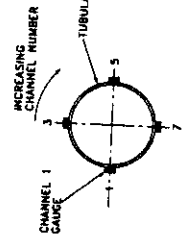
ELEVATION ON LINE D  
LOAD CELLS LC27 TO LC30



ELEVATION ON LINE E  
LOAD CELLS LC31 TO LC38



TYPICAL LOAD CELL DETAILS



CHANNEL GAUGE

NOTES

- ALL LOAD CELLS TO BE MANUFACTURED FROM HOT FINISHED HOLLOW CIRCULAR SECTION TO BS4448 PART 2 MADE FROM STEEL TO BS4360 GRADE 50C.
- ALL LOAD CELLS TO BE MANUFACTURED WITH ENDS MACHINED FLUSH AND SQUARE. END PREPARATION FOR WELDING WILL NOT TAKE PLACE UNTIL AFTER CALIBRATION.
- ALL DIMENSIONS ARE IN MM.
- ALL GAUGES TO BE APPLIED IN ACCORDANCE WITH BONEL DOCUMENT No. C636/08/2173.
- TOTAL NUMBER OF STRAIN GAUGE CHANNELS PER LOAD CELL = 4.
- LOAD CELLS TO BE CLEARLY AND PERMANENTLY IDENTIFIED AS LC1 TO LC46.
- LOAD CELL Nos. IDENTIFIED ON THIS DRAWING THUS - (1) GAUGE POSITIONS AND CHANNEL NUMBERS TO BE CLEARLY AND PERMANENTLY IDENTIFIED IN THE FOLLOWING MANNER - LC21, 21 - 24  
LC22, 21 - 24  
LC20, 201 - 204 etc  
LC20, 201 - 204 etc
- EACH LOAD CELL TO BE INSERTED IN THE TEST FRAME SUCH THAT CHANNEL NO. IDENTIFIED ON THIS DRAWING THUS - (1) GAUGE POSITIONS AND CHANNEL NUMBERS TO BE CLEARLY IDENTIFIED ON THIS DRAWING
- GAUGE POSITIONS AND CHANNEL NUMBERS TO BE CLEARLY IDENTIFIED.
- FOR GENERAL NOTES REFER TO ORG. C636/15/0020

LOAD CELL SCHEDULE

LOAD CELL	DIAMETER (mm)	WT. (mm)	LENGTH (mm)	No. OFF
TYPE 1	188.3	5.0	340	28
TYPE 2	188.3	5.0	500	18

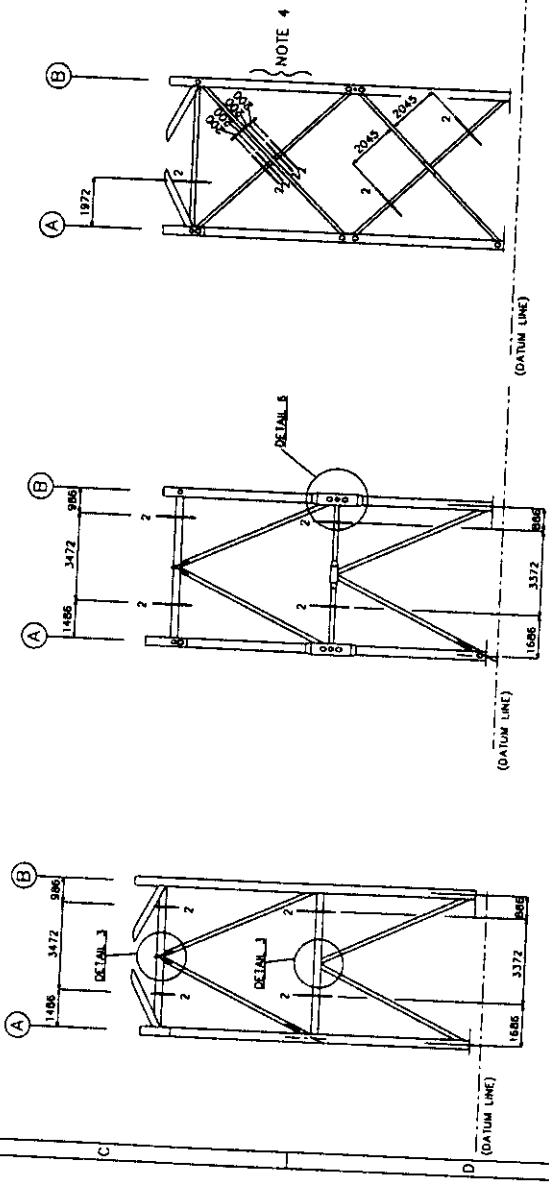
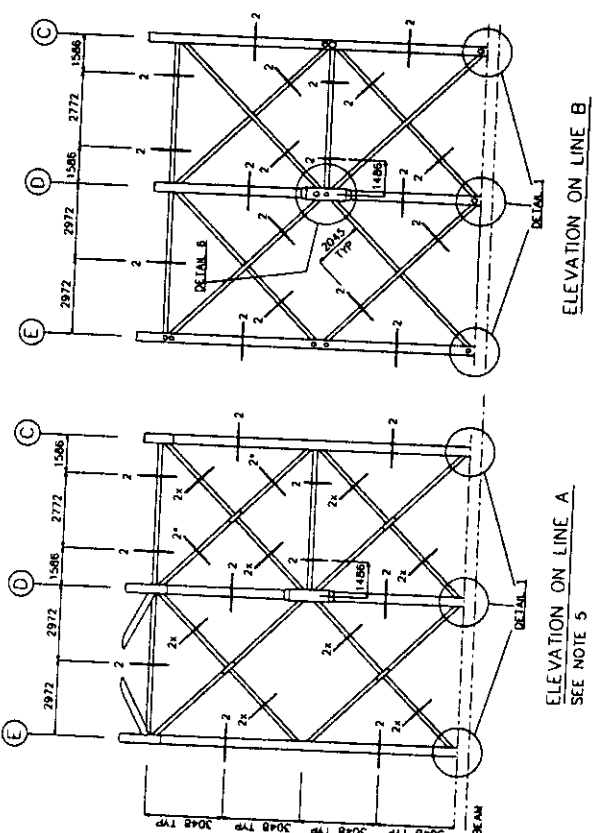
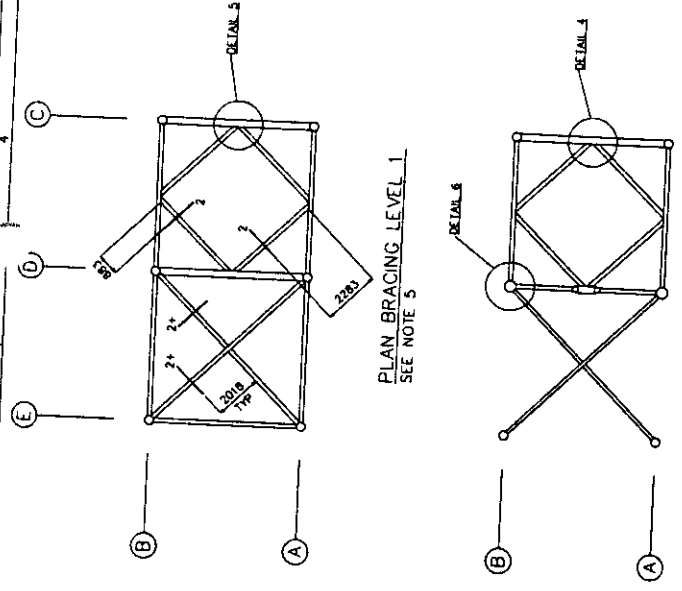
D	M/M/AS BUILT	TKG	JADC	HMB	CJB
C	LOAD CELL NUMBERS ADDED	TKG	JADC	HMB	CJB
B	APPROVED FOR CONSTRUCTION	TKG	JADC	HMB	CJB
A	LEVEL 2 & SCHEDULED LOAD CELL APPROVED	TKG	JADC	HMB	CJB
0	PRELIMINARY	TKG	JADC	HMB	CJB
WT	WEIGHT				
DATE	DATE				

BONEL CONTRACT No. C636/08/2173  
CLIENT: JOINT INDUSTRY PROJECT  
PROJECT: FRAMES PHASE III  
DRAWING TITLE: LOAD CELL DETAILS

BONEL CONSULTING  
Lodge House,  
17 Park Street,  
Birmingham, S.E. 26th,  
England.  
Tel: +44 (0)121 771707  
Fax: +44 (0)121 771707  
Drawing No. C636/15/0110

**NOTES**

1. FOR GENERAL NOTES SEE DWG. C636/15/002D
2. FOR DETAILS 1 TO 6 SEE DWG. C636/15/013D
3. \_\_\_\_\_ 2 DENOTES DETAIL 2
4. CHANGES ON LINE E CROSS BRACING TOP BAY INSTALLED FOR TESTS LC1, LC1C AND LC2 ONLY
5. \_\_\_\_\_ 2+ DENOTES DETAIL 2 INSTALLED FOR LOADCASE LC3C ONLY
- \_\_\_\_\_ 2+ DENOTES DETAIL 2 INSTALLED FOR LOADCASES LC1, LC1C, L2, LC2C, LC3 AND LC3C ONLY
- \_\_\_\_\_ 2+ DENOTES DETAIL 2 INSTALLED FOR LOADCASES LC3, LC3CA AND LC3CA ONLY



B	4" x 4"	AS BUILT - INCLUDING DETAIL 6	TKC	JADC	HMB	HMB
A	4" x 4"	AS BUILT	TKC	JADC	HMB	HMB
D	4" x 4"	SPECIFICATION	TKC	JADC	HMB	HMB
1	4" x 4"	SPECIFICATION	TKC	JADC	HMB	HMB
2	4" x 4"	SPECIFICATION	TKC	JADC	HMB	HMB
3	4" x 4"	SPECIFICATION	TKC	JADC	HMB	HMB
4	4" x 4"	SPECIFICATION	TKC	JADC	HMB	HMB
5	4" x 4"	SPECIFICATION	TKC	JADC	HMB	HMB
6	4" x 4"	SPECIFICATION	TKC	JADC	HMB	HMB

BOMEL CONTRACT NO. C08-000R  
CLIENT CONTRACT NO. \_\_\_\_\_  
CLIENT NAME JOINT INDUSTRY PROJECT  
PROJECT TITLE STRAIN GAUGING DETAILS  
Sheet 1 of 2

DATE 7/10/21  
DRAWN BY P. CALDWELL  
CHECKED BY \_\_\_\_\_  
SCALE 1:100

PROJECT JOINT INDUSTRY PROJECT

DRAWING TITLE STRAIN GAUGING DETAILS  
Sheet 1 of 2

Scale: 1:100  
Date: 7/10/21  
Project: JOINT INDUSTRY PROJECT

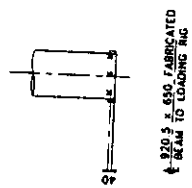
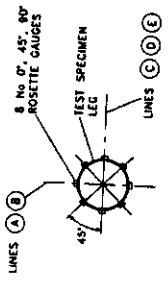
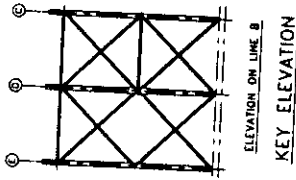
BOMEL CONSULTING  
10000 Southpark Drive  
Fifth Floor  
Atlanta, GA 30328  
Tel: +1 404 896 2720  
Fax: +1 404 896 7787

Drawing No. C636/15/012D

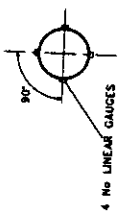


**NOTES**

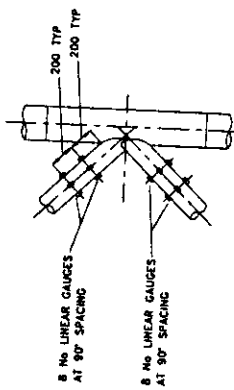
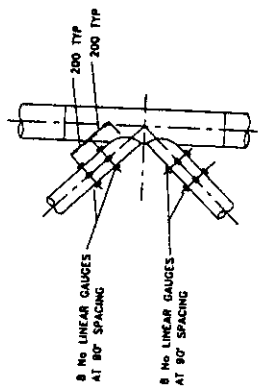
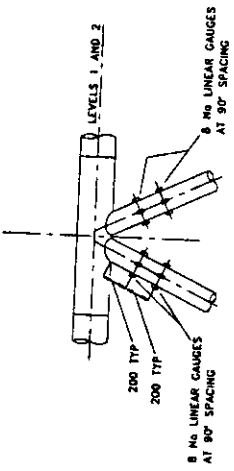
1. FOR GENERAL NOTES SEE DRG. C636/15/002D
2. FOR LOCATION OF DETAILS 1 TO 6 SEE DRG. C636/15/012D
3. DETAILS 3, 4 AND 5 - GAUGES CLOSEST TO INTERSECTION DENOTED "NEAR". OTHER SETS DENOTED "FAR".
4. \_\_\_\_\_ 2 DENOTES DETAIL 2
5. ASG 37-39 DENOTES LOGGED REFERENCE OF ADDITIONAL STRAIN GAUGES.



**DETAIL 2**



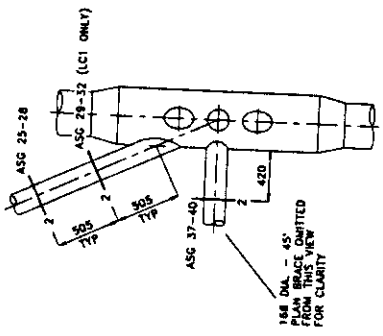
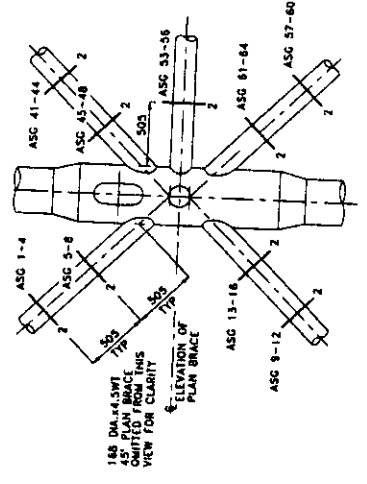
**DETAIL 1**



**DETAIL 3**

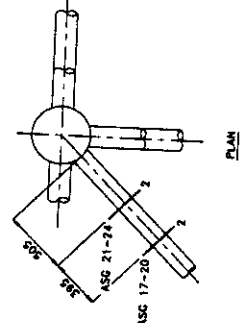
**DETAIL 4**

DETAILS 3, 4 AND 5 - NEAR AND FAR GAUGES INSTALLED FOR LOADCASES LC1 AND LC1C  
FAR GAUGES ONLY INSTALLED FOR LOADCASES LC3CA AND LC1CA

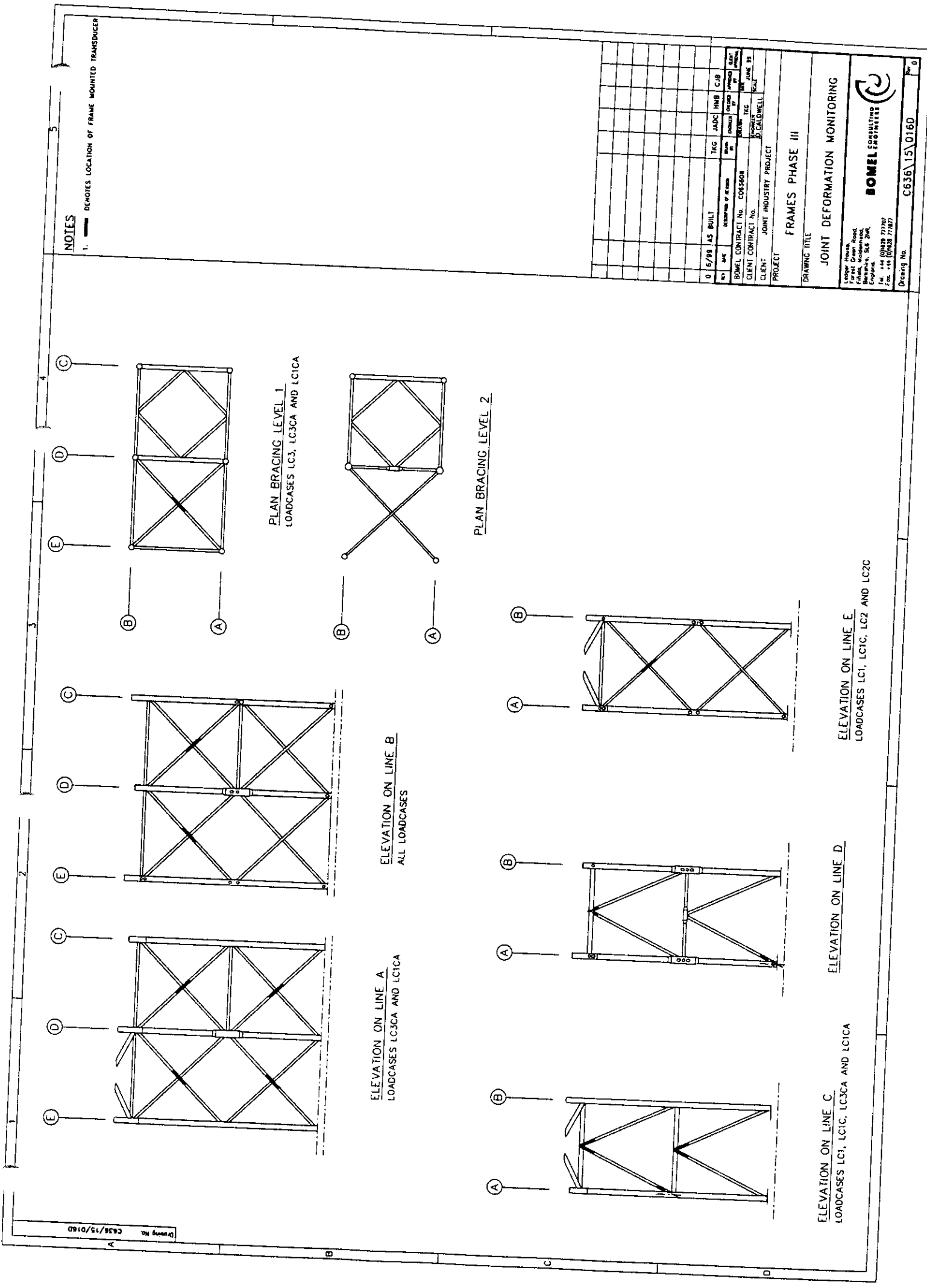


**DETAIL 5**

**DETAIL 6**



B	1/4" AS BUILT - INCLUDING	TRG	JADC	HMB	HMB
A	1/4" AS BUILT	TRG	JADC	HMB	HMB
D	1/4" AS BUILT	TRG	JADC	HMB	HMB
REV	DATE	DESCRIPTION	BY	CHECKED	DATE
BOMEL CONTRACT NO. C081508					
CLIENT CONTRACT NO. 1120					
PROJECT: JOINT INDUSTRY PROJECT					
DRAWING TITLE: STRAIN GAUGING DETAILS					
Sheet 2 of 2					
Bomel Engineering 14000 Green Road Brentwood, BC 89K England Tel: +44 (0)1823 77707 Fax: +44 (0)1823 77871					
Drawing No. C636/15/013D					



**NOTES**

1. ——— DENOTES LOCATION OF FRAME MOUNTED TRANSDUCER

NO.	DATE	DESCRIPTION OF WORK	BY	CHECKED BY	APPROVED BY	DATE
0	5/98	AS BUILT	JAC	HRB	CLB	

BUMEL CONTRACT No. C033608				DATE: JUN 98	
CLIENT: JOINT INDUSTRY PROJECT				PROJECT: SCARLETT	
CLIENT: JOINT INDUSTRY PROJECT				PROJECT: SCARLETT	
DRAWING TITLE: FRAMES PHASE III				DRAWING NO.:	
DRAWING TITLE: JOINT DEFORMATION MONITORING				DRAWING NO.:	

Drawing No. CA38/15/016D

**BOMEL ENGINEERING**  
 104-104 77707  
 1788 144 (010) 77707

Drawing No. C636/15/016D No. 0



## APPENDIX C

### FRAME RESPONSE PLOTS

Spreadsheets from C636\37\011w.xls:

- GLOBAL Scan Nos
- GLOBAL Annotated
- Sheets 1 to 5
- FrC Lev1 Tens
- FrC Lev1 Comp
- FrC Lev2 Tens
- FrC Lev2 Comp
- K joint 61-62
- K joint 63-64
- K joint 86-87
- K joint 94-95
- GLOBAL Exp&Pred
- FrC TB For Exp&Pred
- FrC BB For Exp&Pred

Spreadsheet from C636\37\012w.xls

- Loading and logger chart

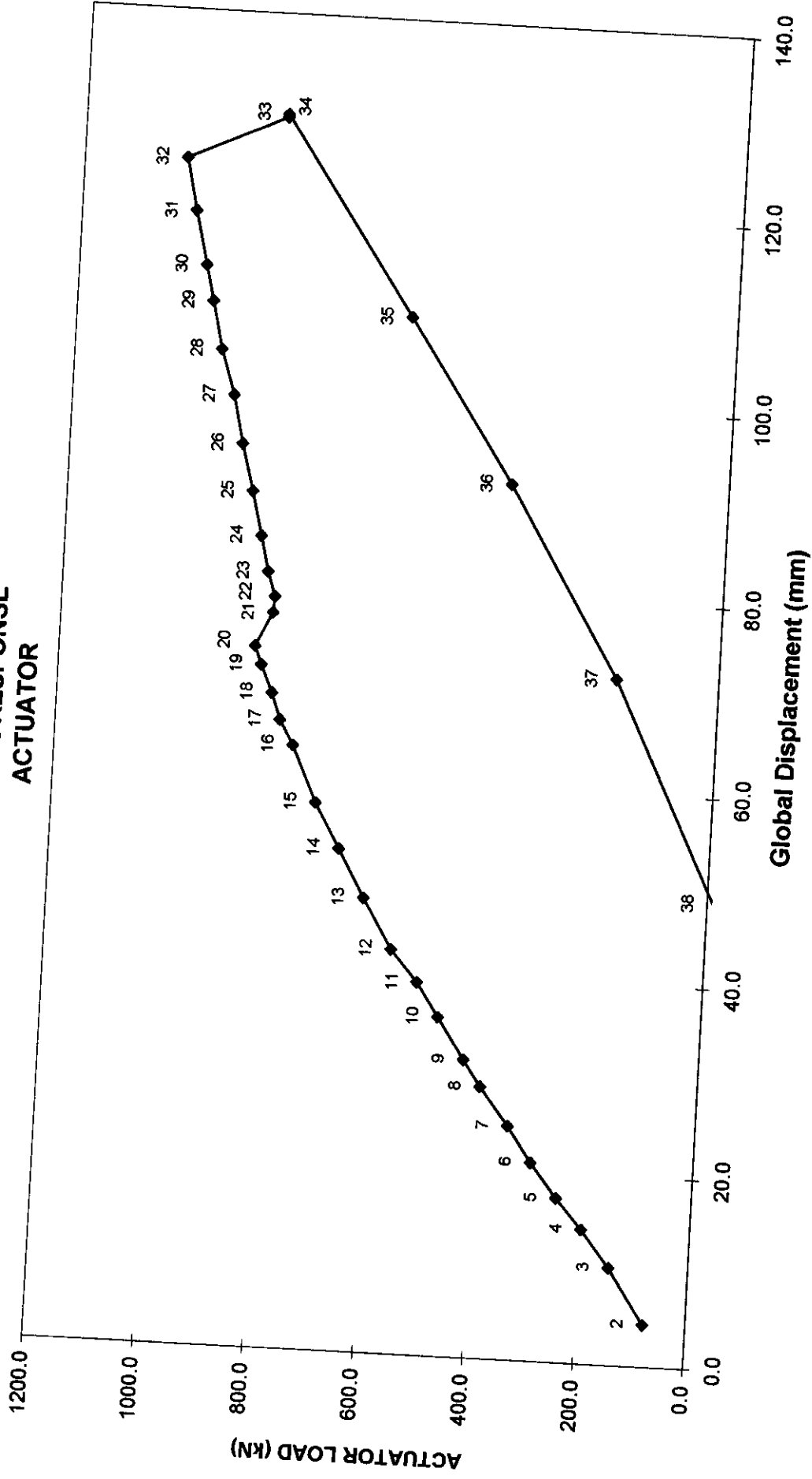
Spreadsheet from C636\24\008w-B.xls

- Corrected P- $\Delta$
- Code comparisons
- SAFJAC
- Corrected global + API
- Force comparison

Spreadsheet from C636\37\022w.xls

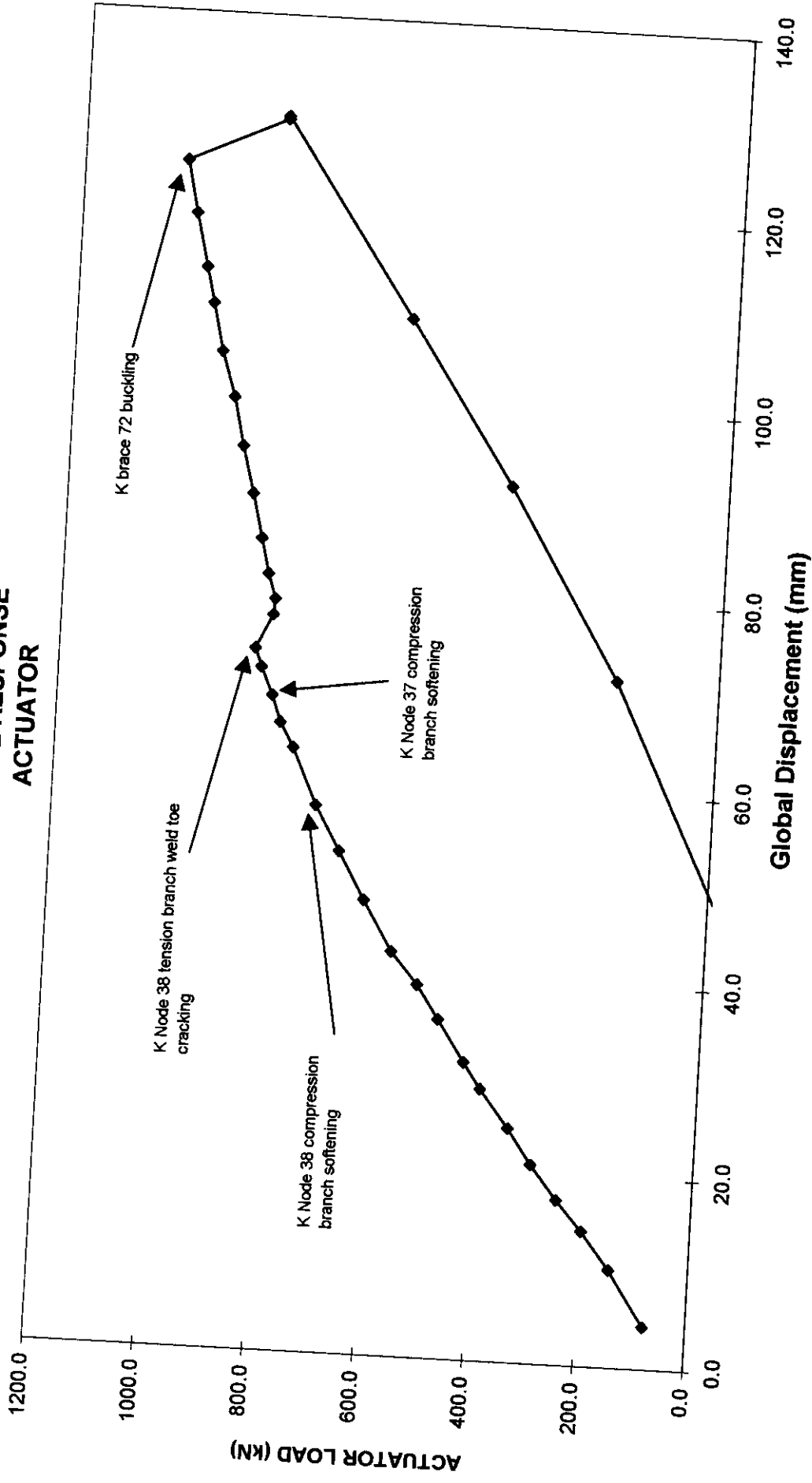
- Alpha Qq comparison

# GLOBAL RESPONSE ACTUATOR



Loadcase 1 - Test

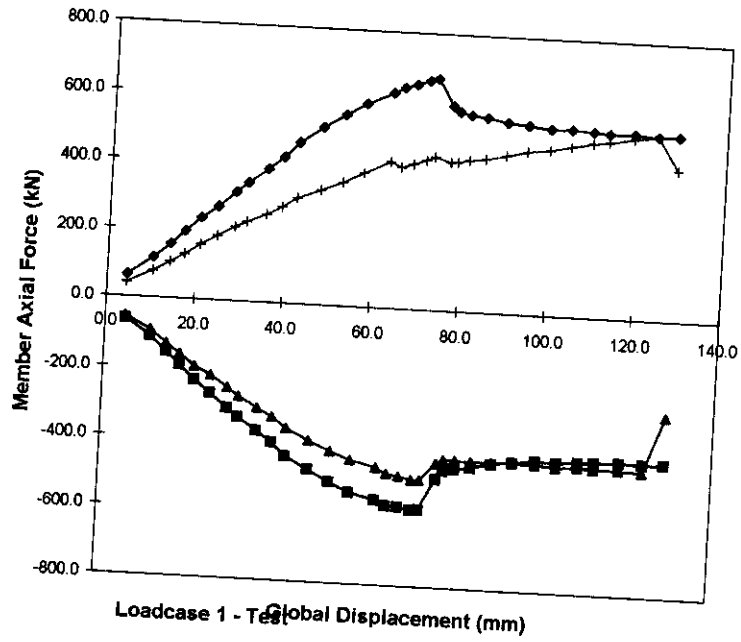
# GLOBAL RESPONSE ACTUATOR



Loadcase 1 - Test

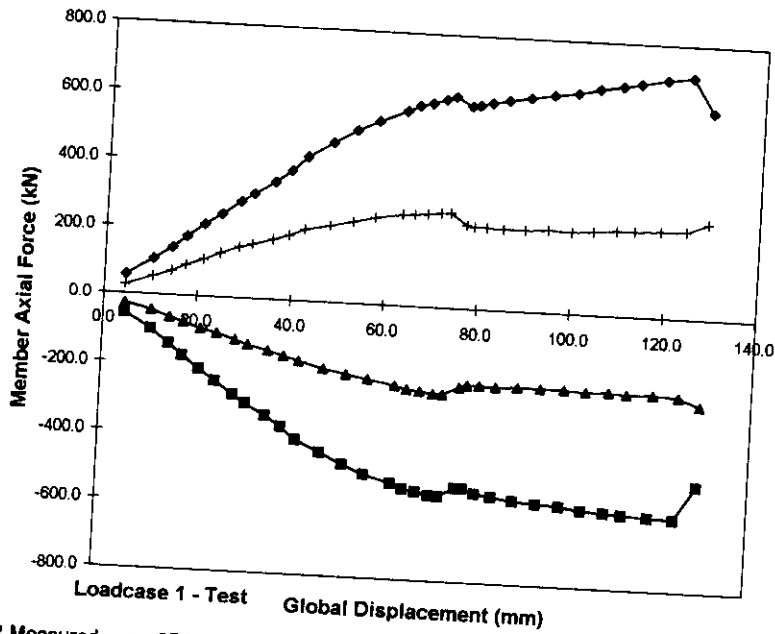
C636137\011w.xls GLOBAL Annotated 30/08/99

FRAME C - TOP BAY  
MEMBER FORCES



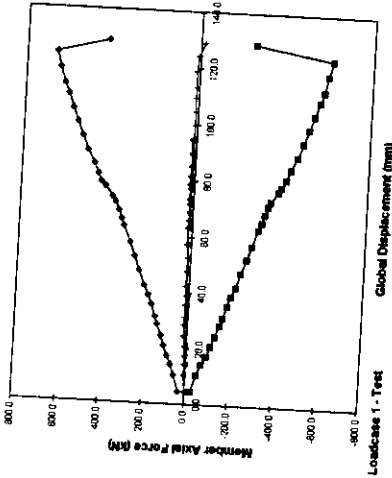
◆ 63 Measured    ■ 64 Measured    ▲ 67 Measured    + 68 Measured

FRAME C - BOTTOM BAY  
MEMBER FORCES



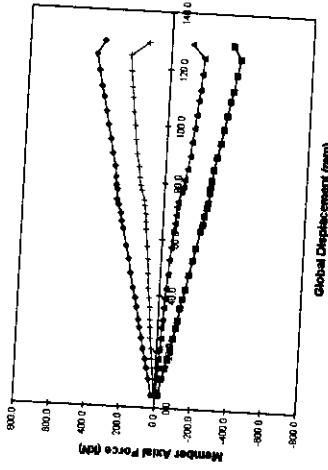
◆ 61 Measured    ■ 62 Measured    ▲ 65 Measured    + 66 Measured

FRAME D - TOP BAY MEMBER FORCES



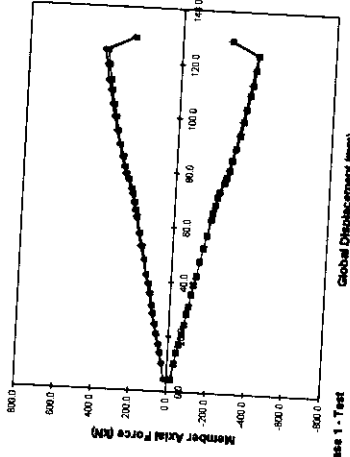
Loadcase 1 - Test  
 → 71 Measured → 72 Measured → 75 Measured → 78 Measured

FRAME D - BOTTOM BAY MEMBER FORCES



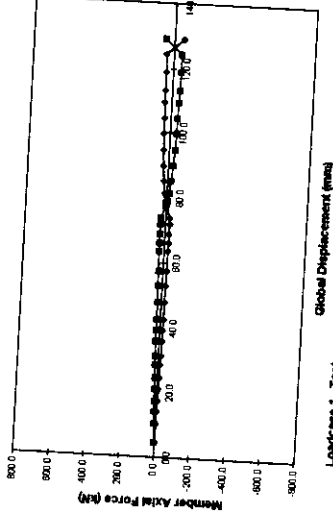
Loadcase 1 - Test  
 → 68 Measured → 70 Measured → 73 Measured → 74 Measured

LEVEL 1 - DIAMOND MEMBER FORCES



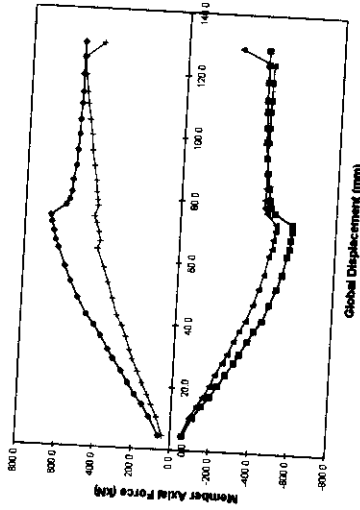
Loadcase 1 - Test  
 → 84 Measured → 85 Measured → 86 Measured → 87 Measured

LEVEL 2 - DIAMOND MEMBER FORCES



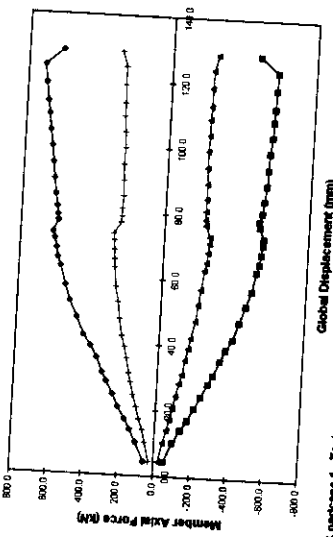
Loadcase 1 - Test  
 → 86 Measured → 87 Measured

FRAME C - TOP BAY MEMBER FORCES

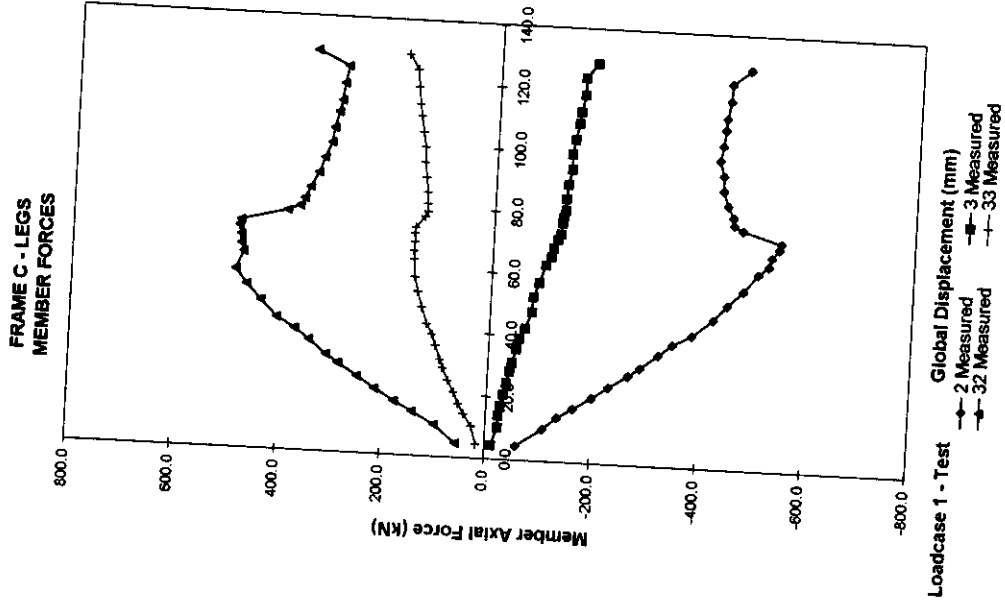
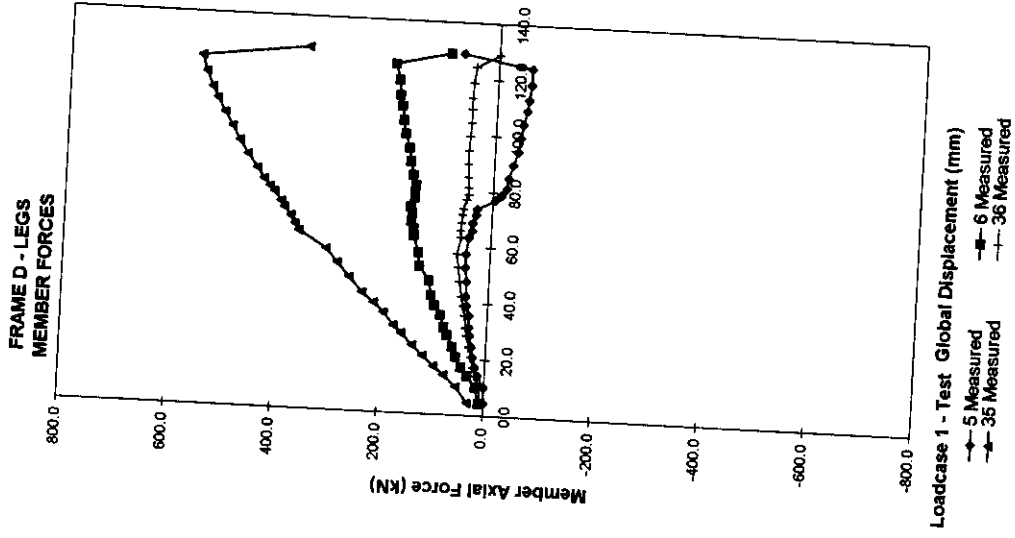
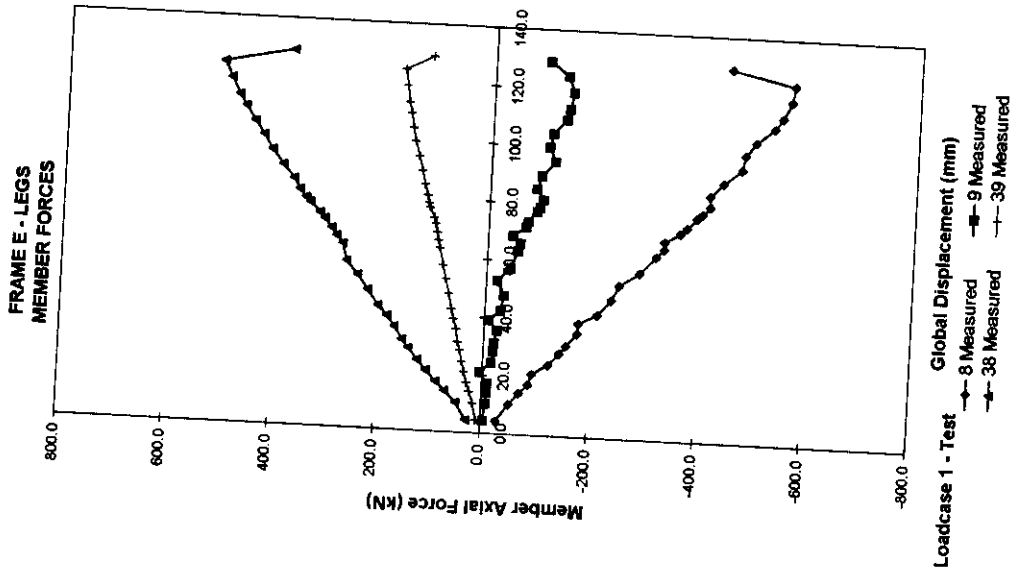


Loadcase 1 - Test  
 → 83 Measured → 87 Measured → 88 Measured

FRAME C - BOTTOM BAY MEMBER FORCES

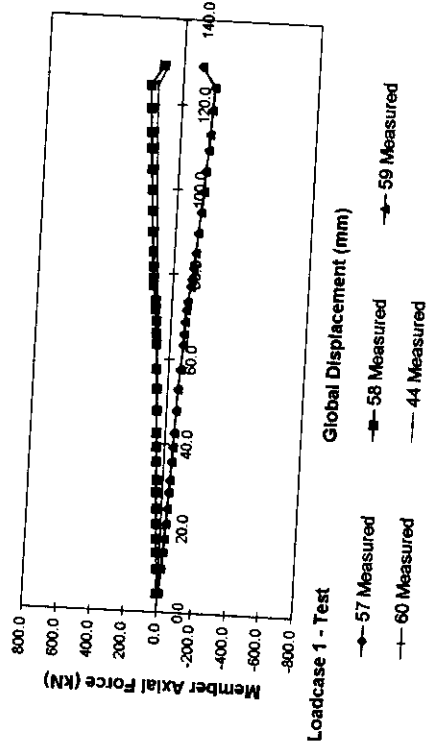


Loadcase 1 - Test  
 → 81 Measured → 82 Measured → 85 Measured → 86 Measured

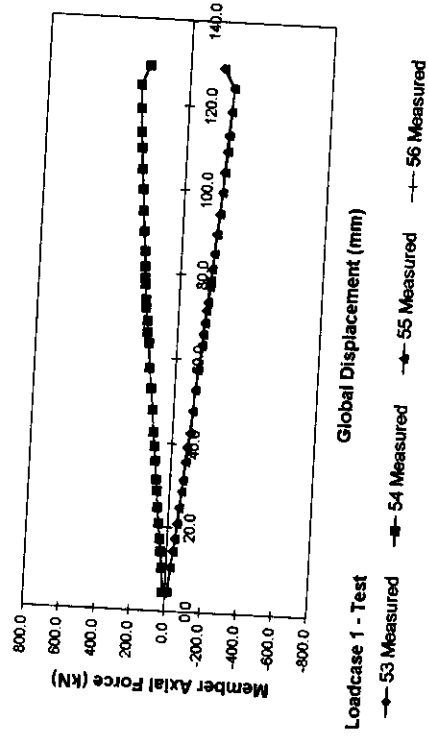




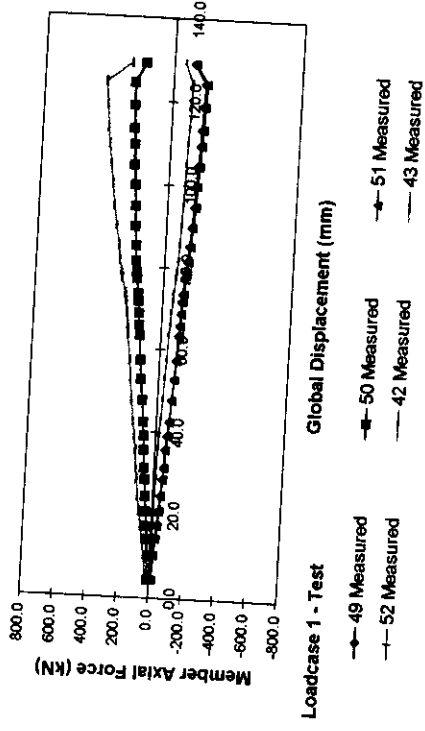
FRAME A - TOP ED  
MEMBER FORCES



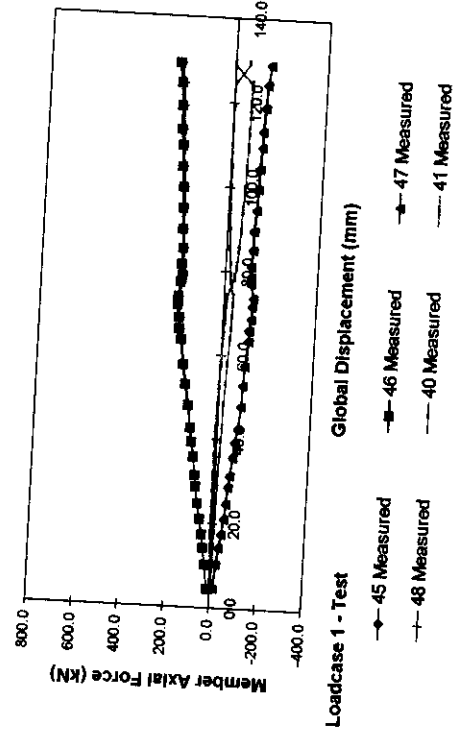
FRAME A - BOTTOM ED  
MEMBER FORCES



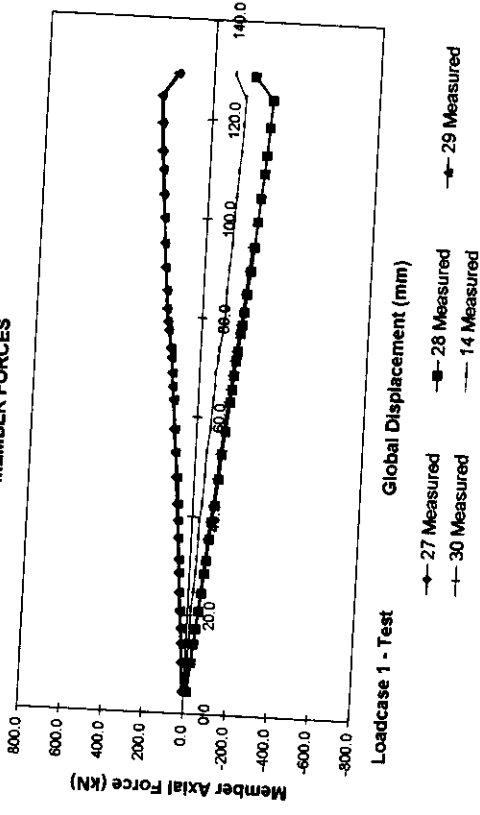
FRAME A - TOP DC  
MEMBER FORCES



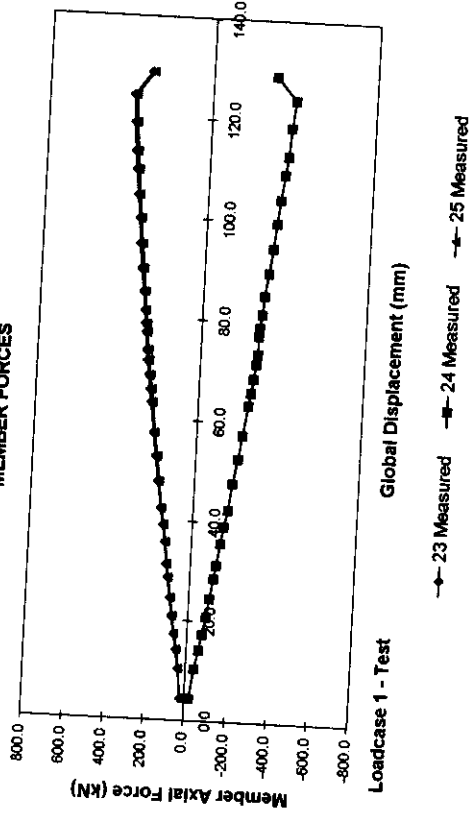
FRAME A - BOTTOM DC  
MEMBER FORCES



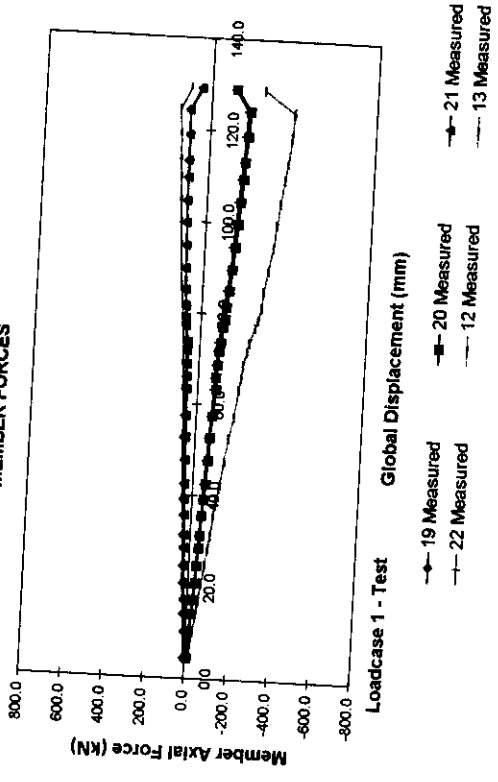
FRAME B - TOP ED  
MEMBER FORCES



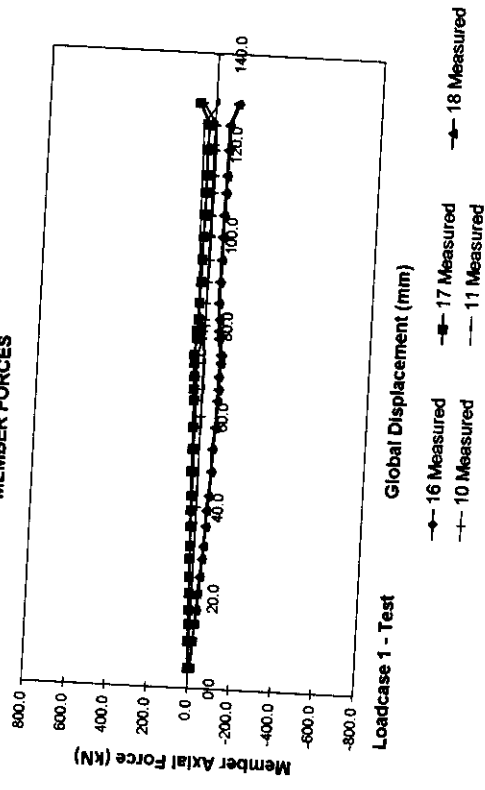
FRAME B - BOTTOM ED  
MEMBER FORCES



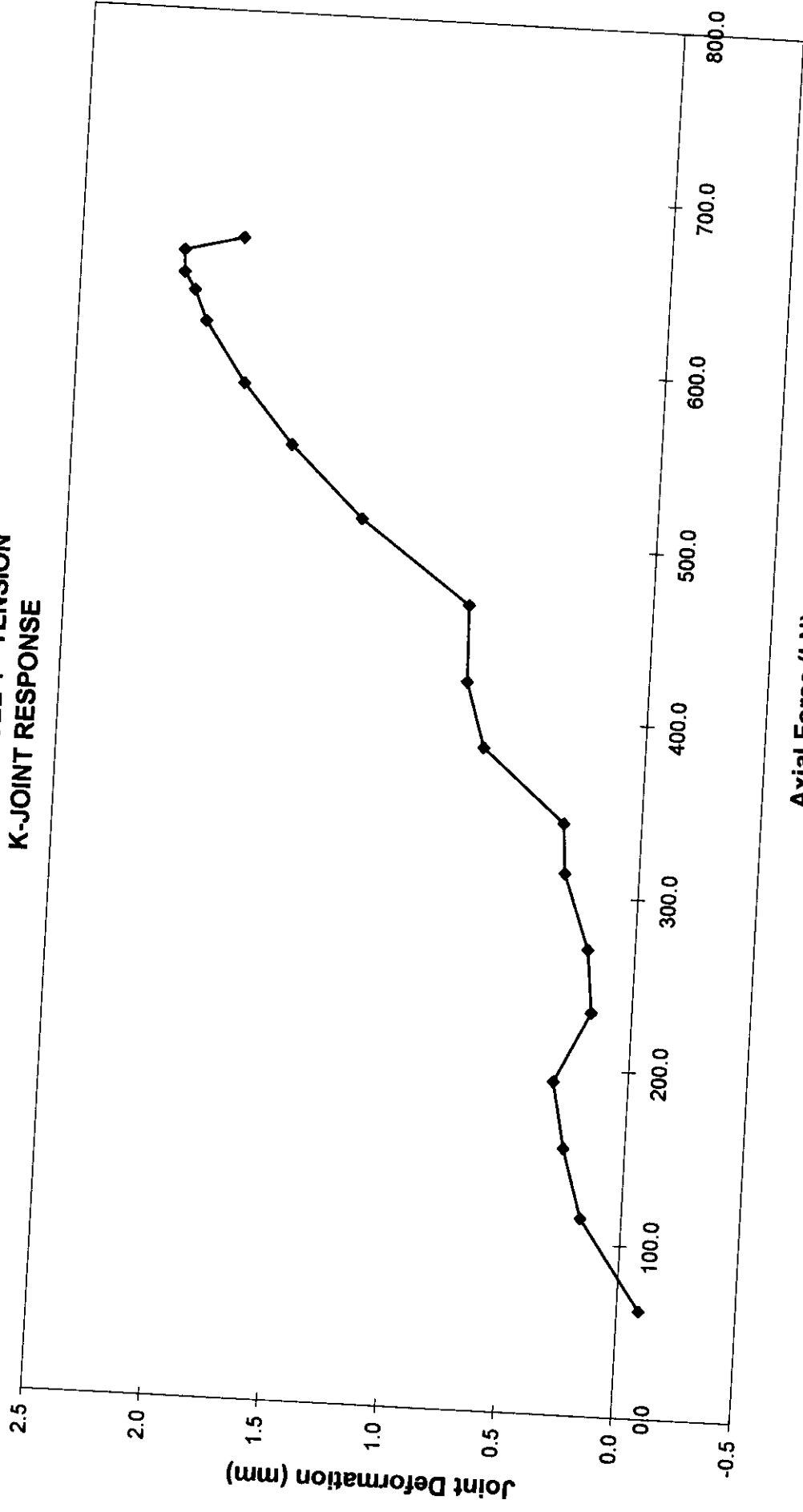
FRAME B - TOP DC  
MEMBER FORCES



FRAME B - BOTTOM DC  
MEMBER FORCES



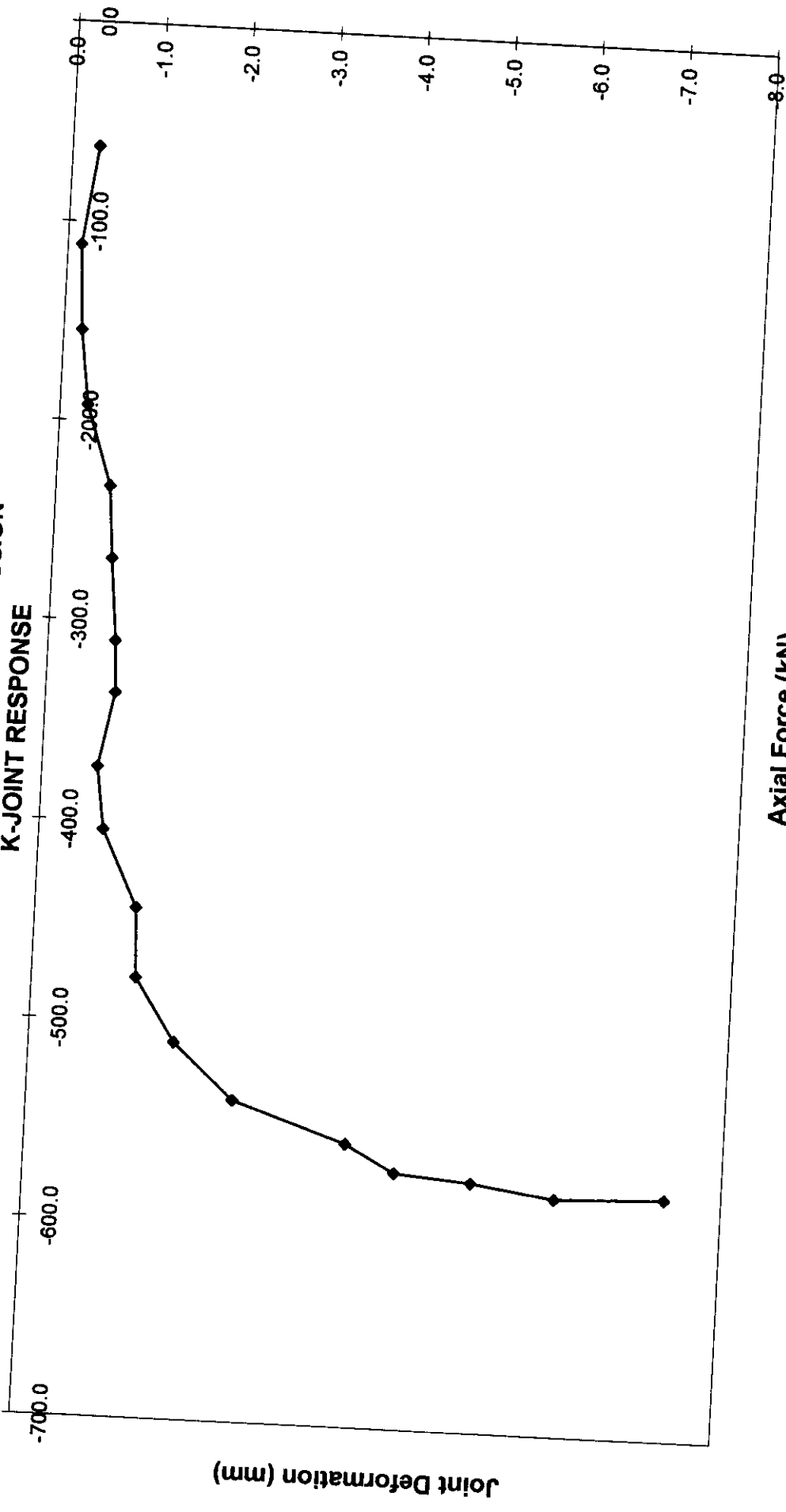
**FRAME C - LEVEL 1 - TENSION  
K-JOINT RESPONSE**



**Loadcase 1 - Test**

**Axial Force (kN)**

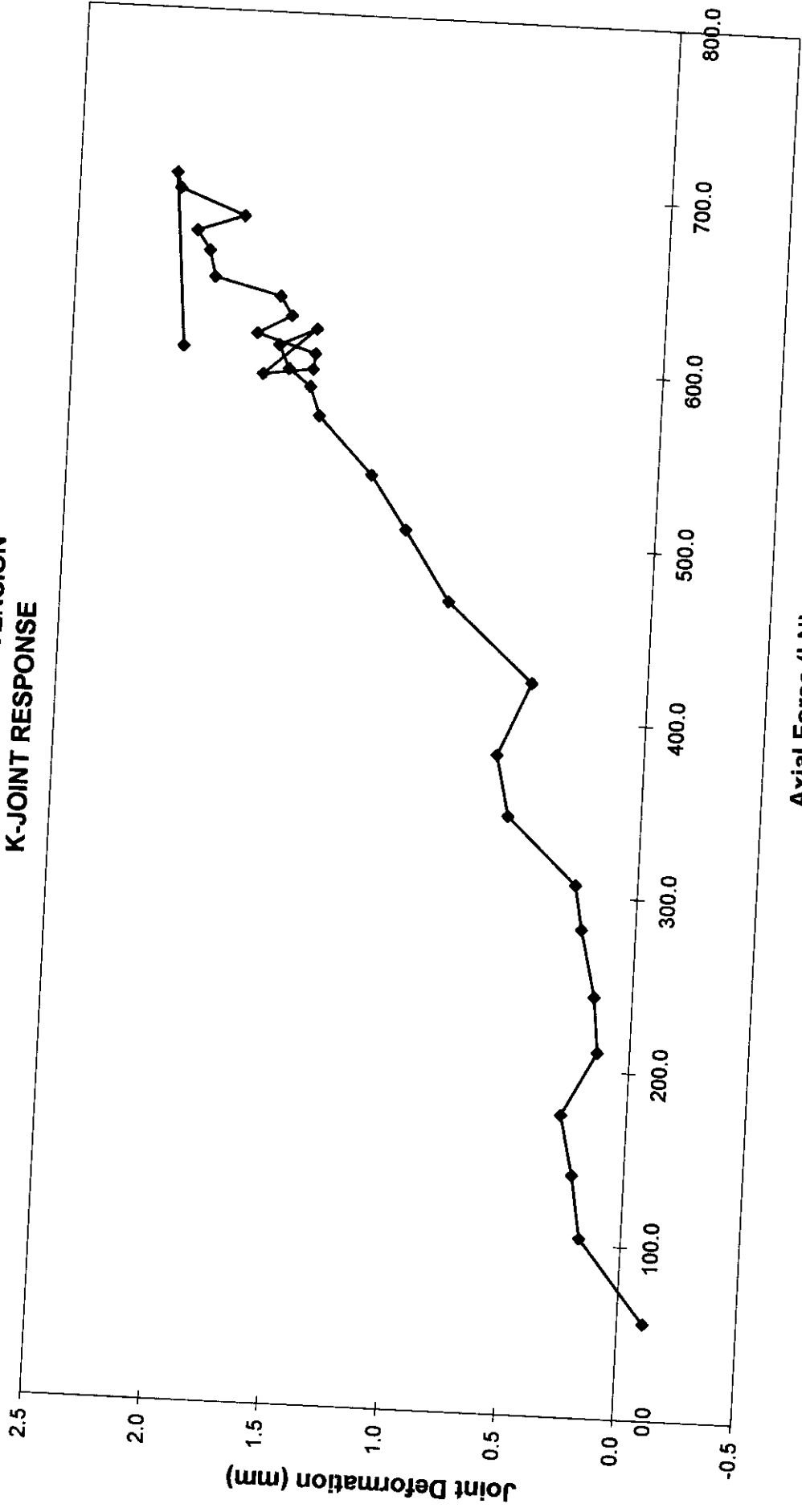
FRAME C - LEVEL 1 - COMPRESSION  
K-JOINT RESPONSE



Axial Force (kN)

Loadcase 1 - Test

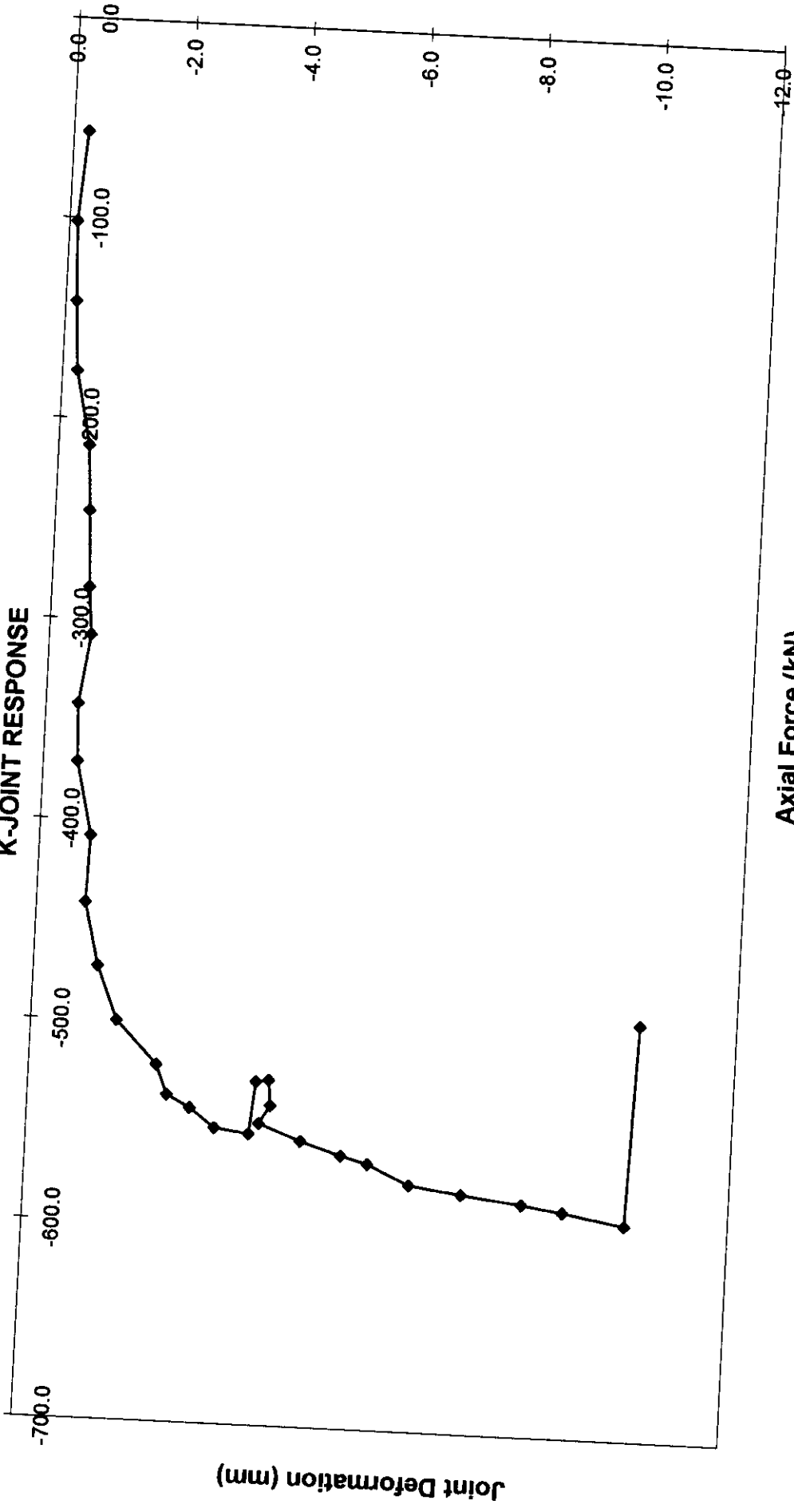
**FRAME C - LEVEL 2 - TENSION  
K-JOINT RESPONSE**



**Loadcase 1 - Test**

**Axial Force (kN)**

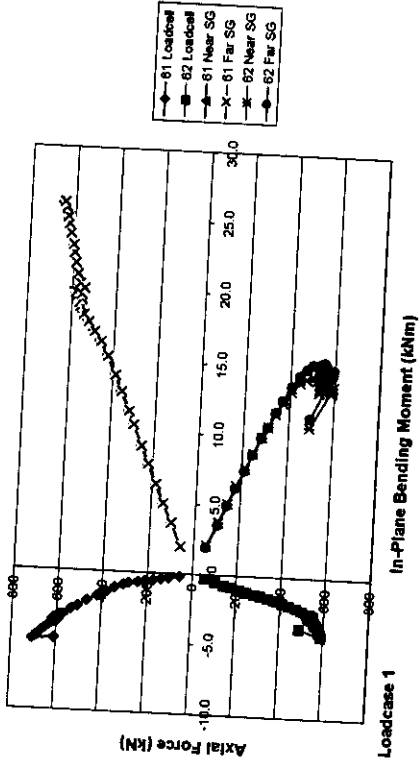
FRAME C - LEVEL 2 - COMPRESSION  
K-JOINT RESPONSE



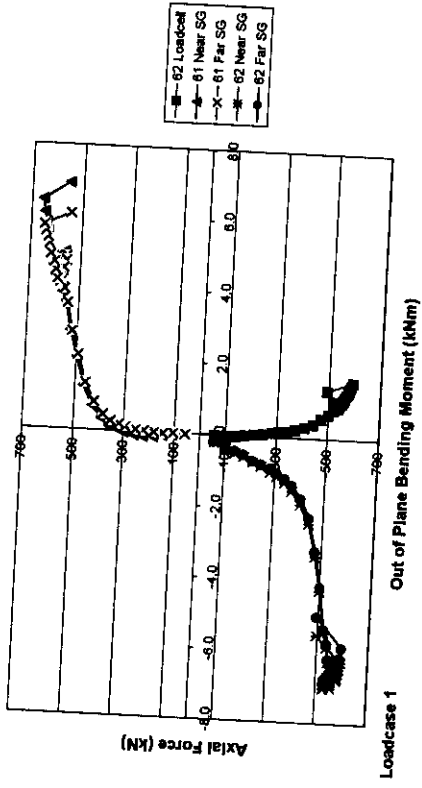
Loadcase 1 - Test

Axial Force (kN)

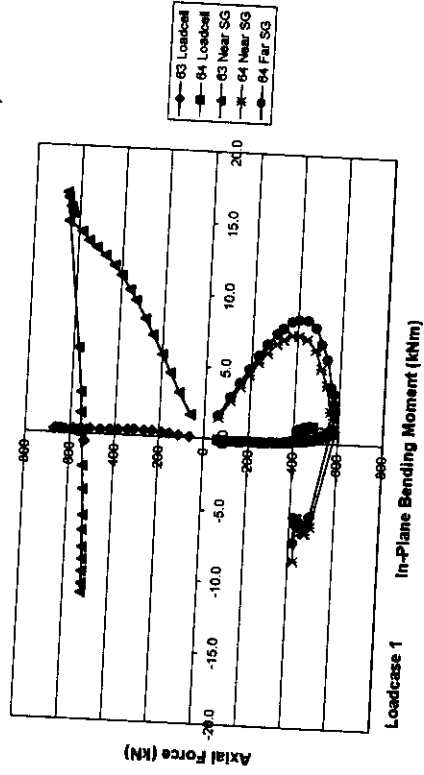
Axial Force Versus In-Plane Bending Moment (K-Joint 61&62)



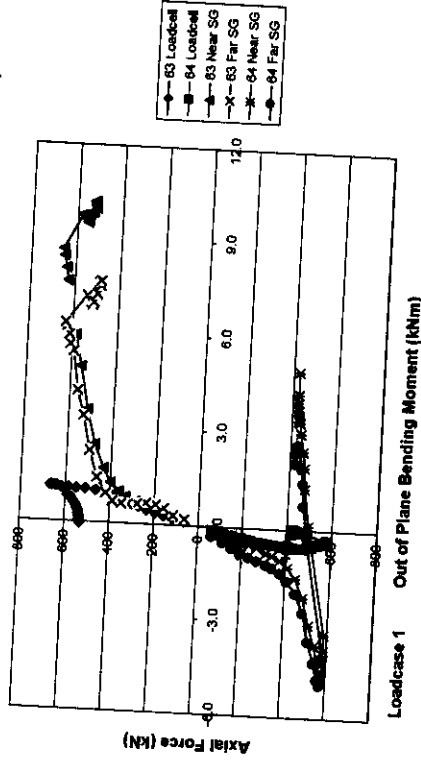
Axial Force Versus Out of Plane Bending Moment (K-Joint 61&62)



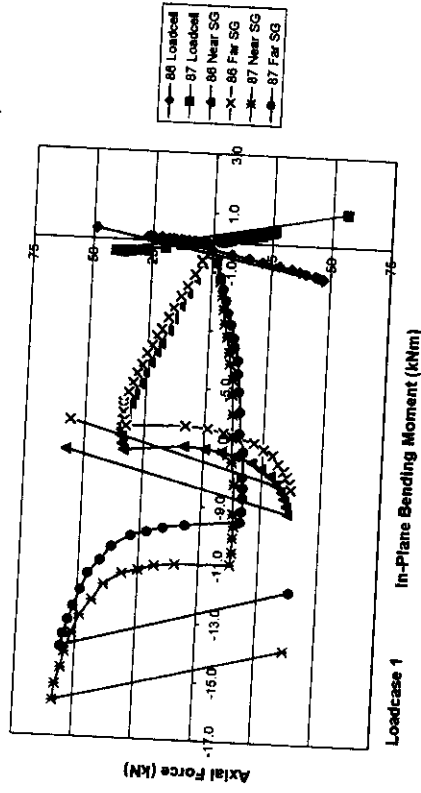
Axial Force Versus In-Plane Bending Moment (K-Joint 63&64)



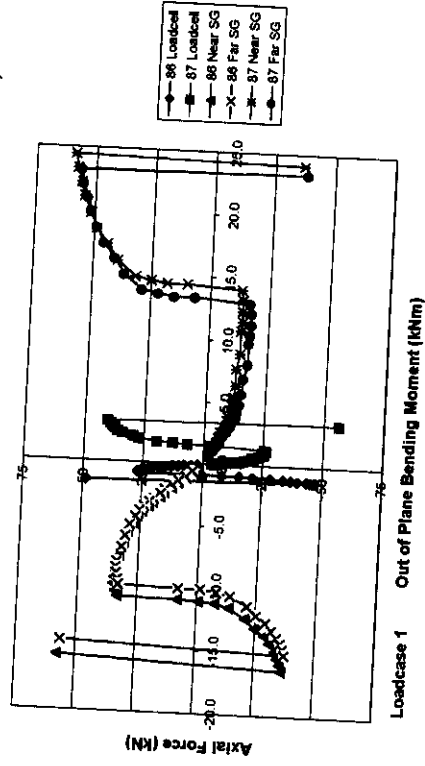
Axial Force Versus Out of Plane Bending Moment (K-Joint 63&64)



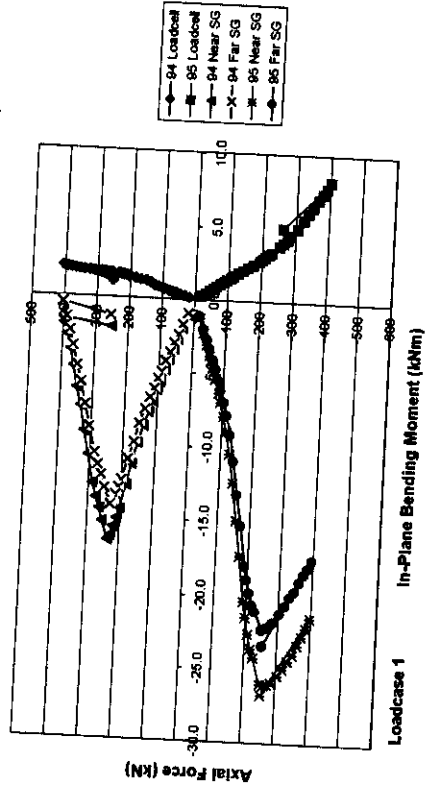
Axial Force Versus In-Plane Bending Moment (K-Joint 86&87)



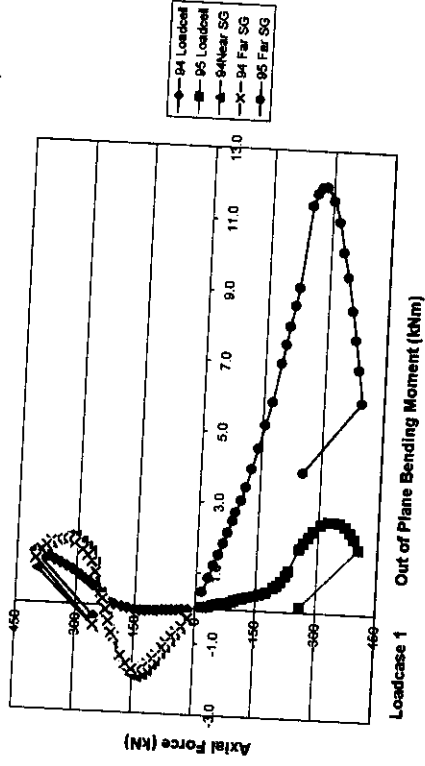
Axial Force Versus Out of Plane Bending Moment (K-Joint 86&87)



Axial Force Versus In-Plane Bending Moment (K-Joint 94&95)

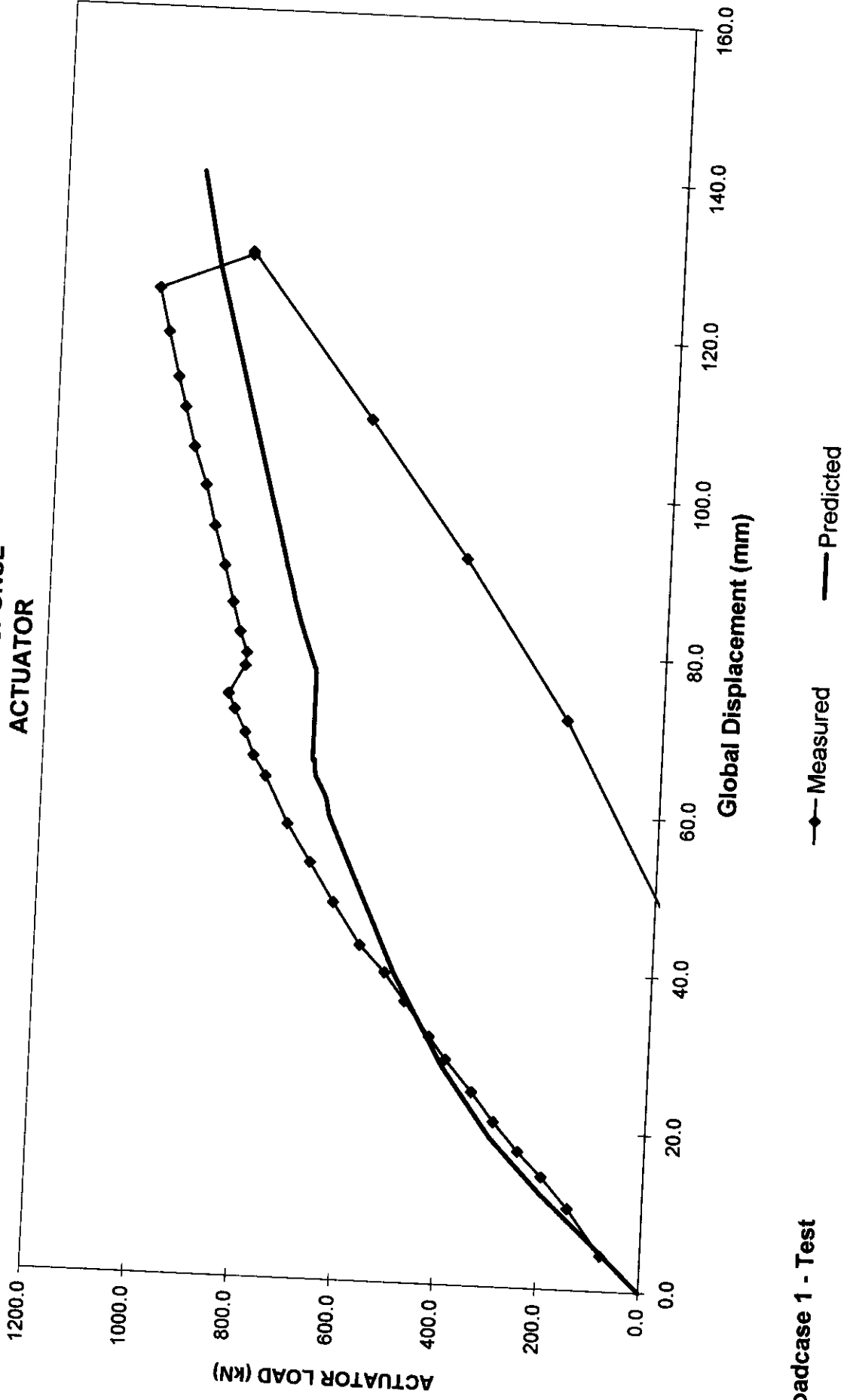


Axial Force Versus Out of Plane Bending Moment (K-Joint 94&95)



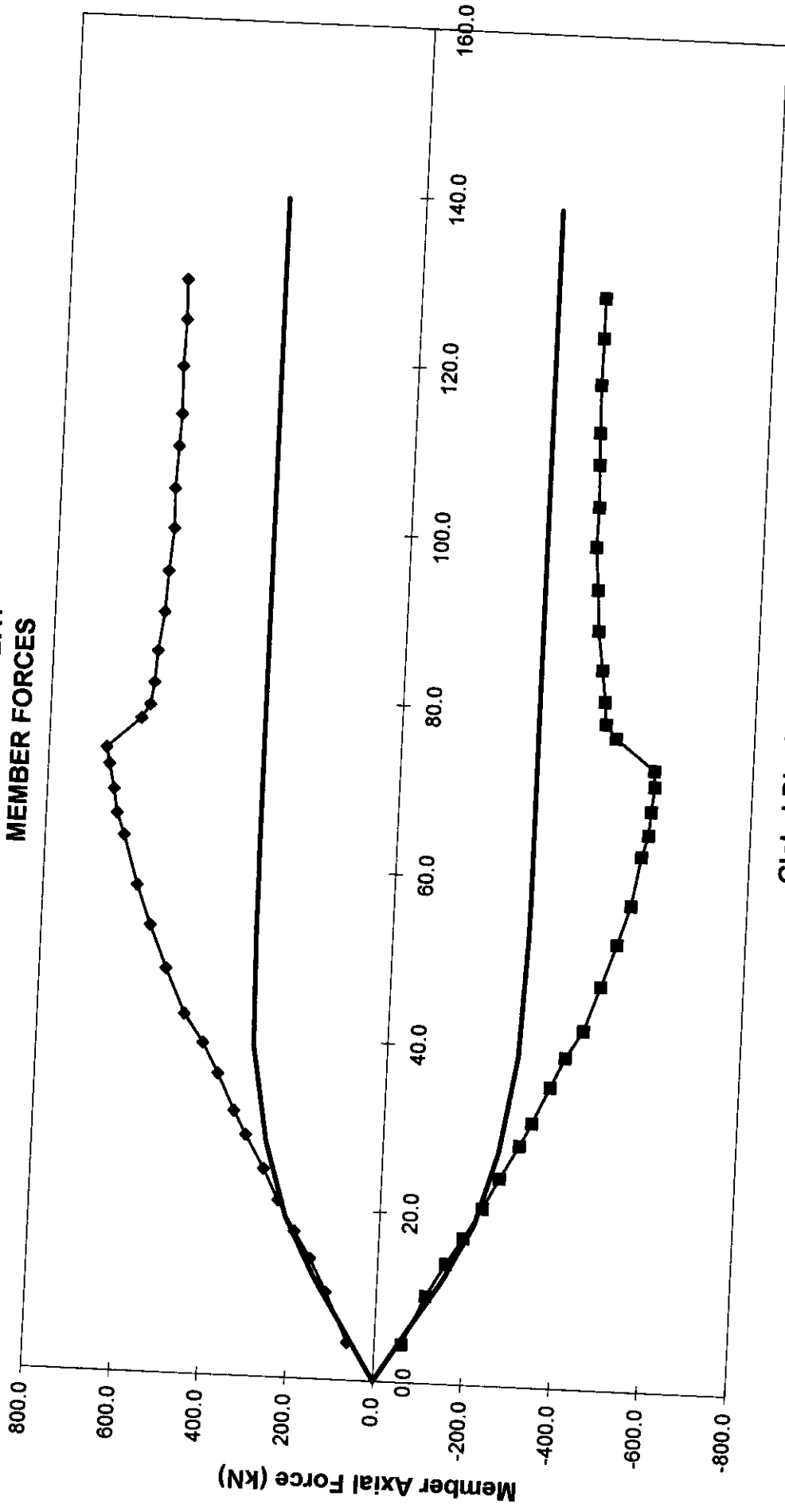


# GLOBAL RESPONSE ACTUATOR



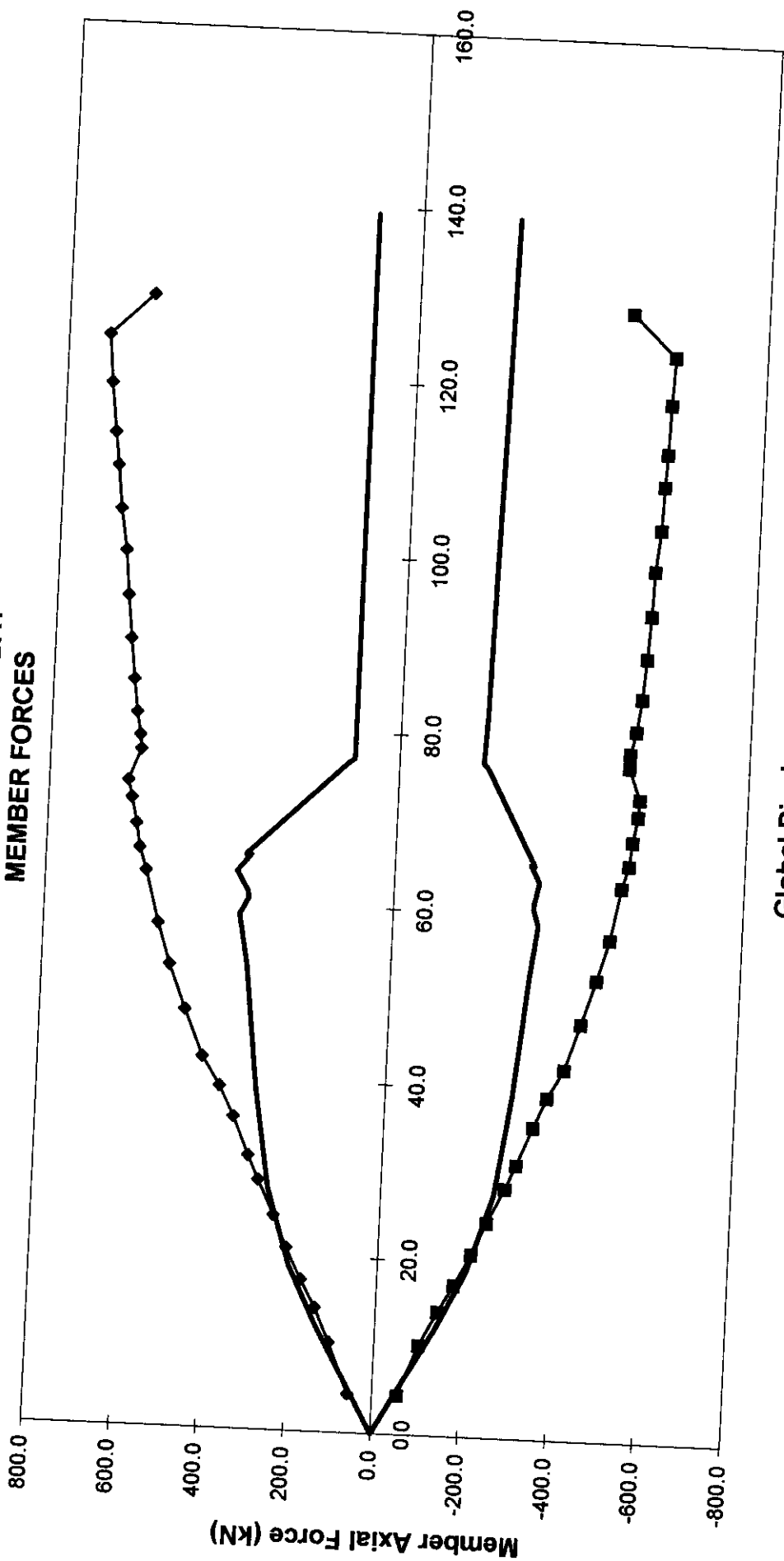
Loadcase 1 - Test

**FRAME C - TOP BAY  
MEMBER FORCES**



**Loadcase 1 - Test**    —◆— 63 Measured    —■— 64 Measured    — 63 Predicted    — 64 Predicted

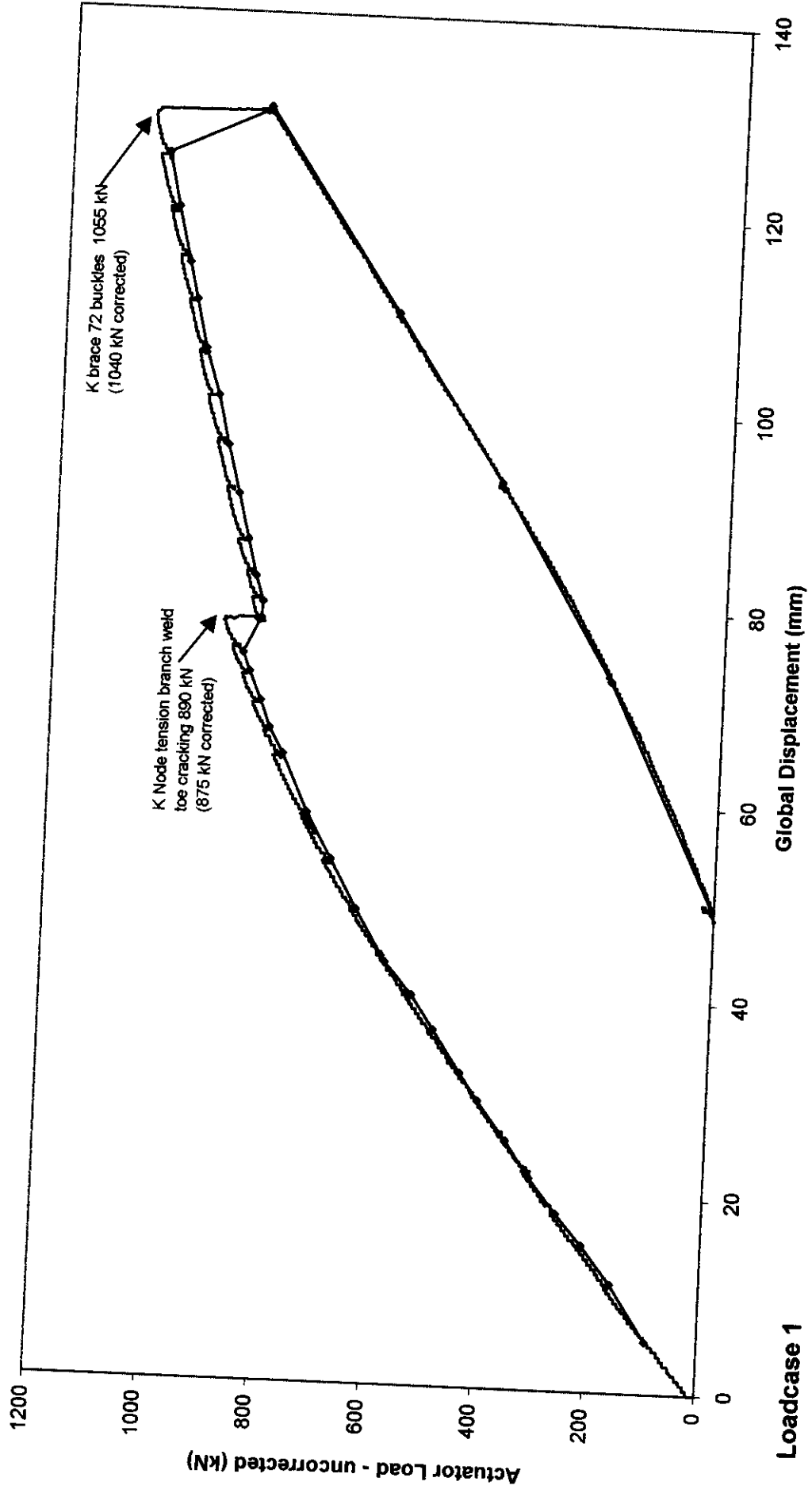
**FRAME C - BOTTOM BAY  
MEMBER FORCES**



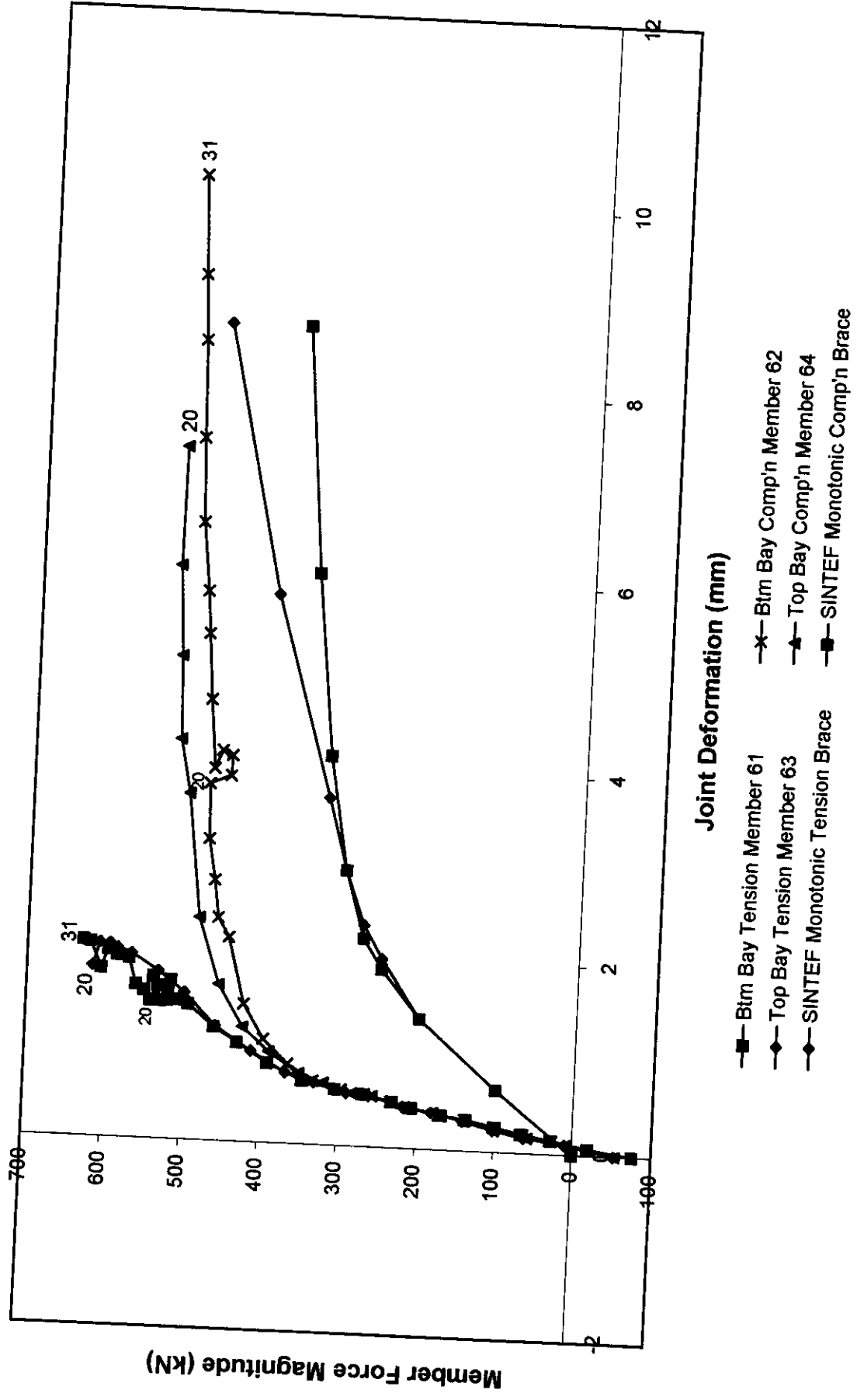
Global Displacement (mm)

Loadcase 1 - Test    ◆ 61 Measured    ■ 62 Measured    — 62 Measured    — 61 Predicted

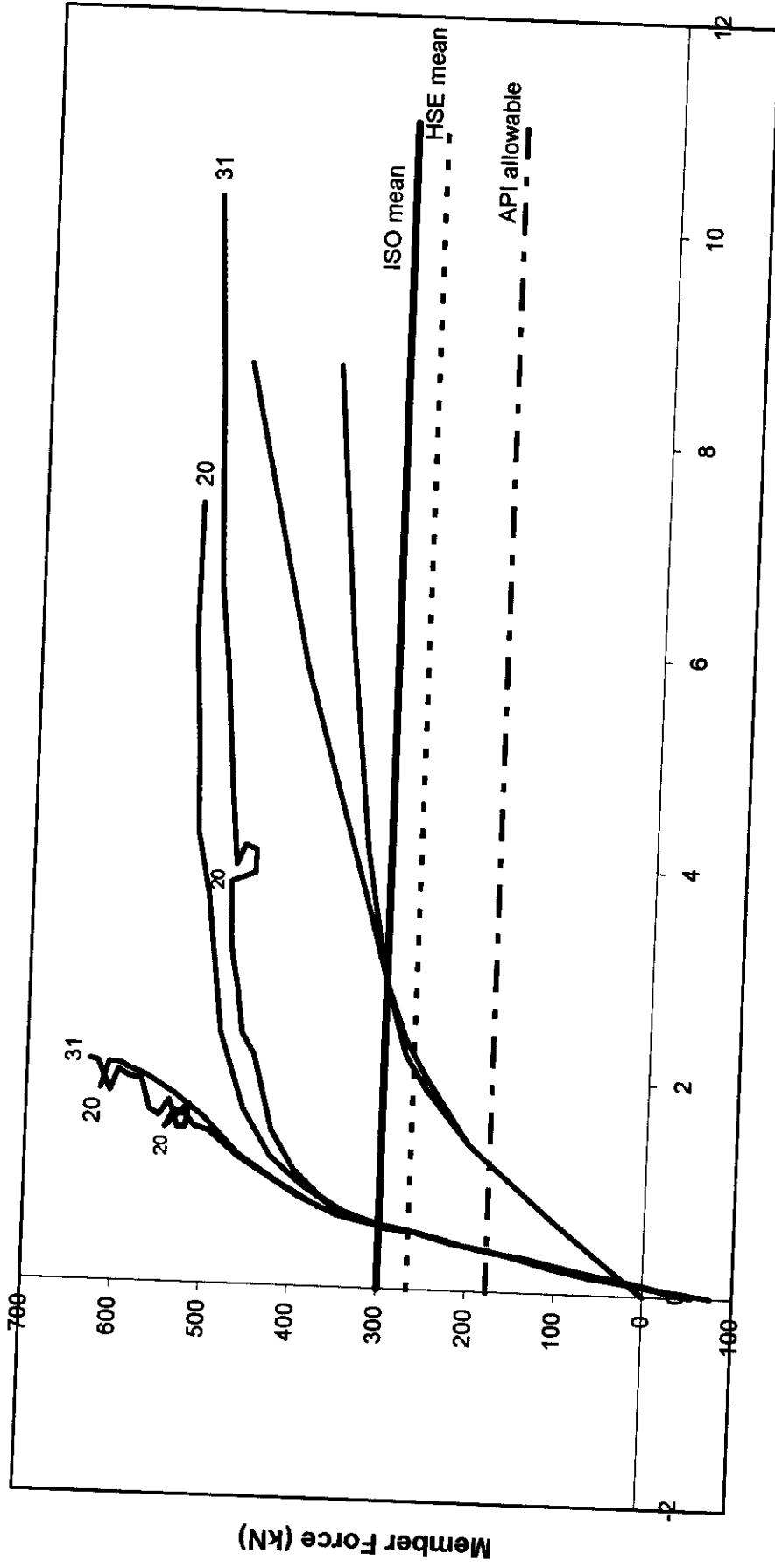
# GLOBAL RESPONSE FROM LOADING SYSTEM



Frame C - Primary K Braces - Joint Deformations



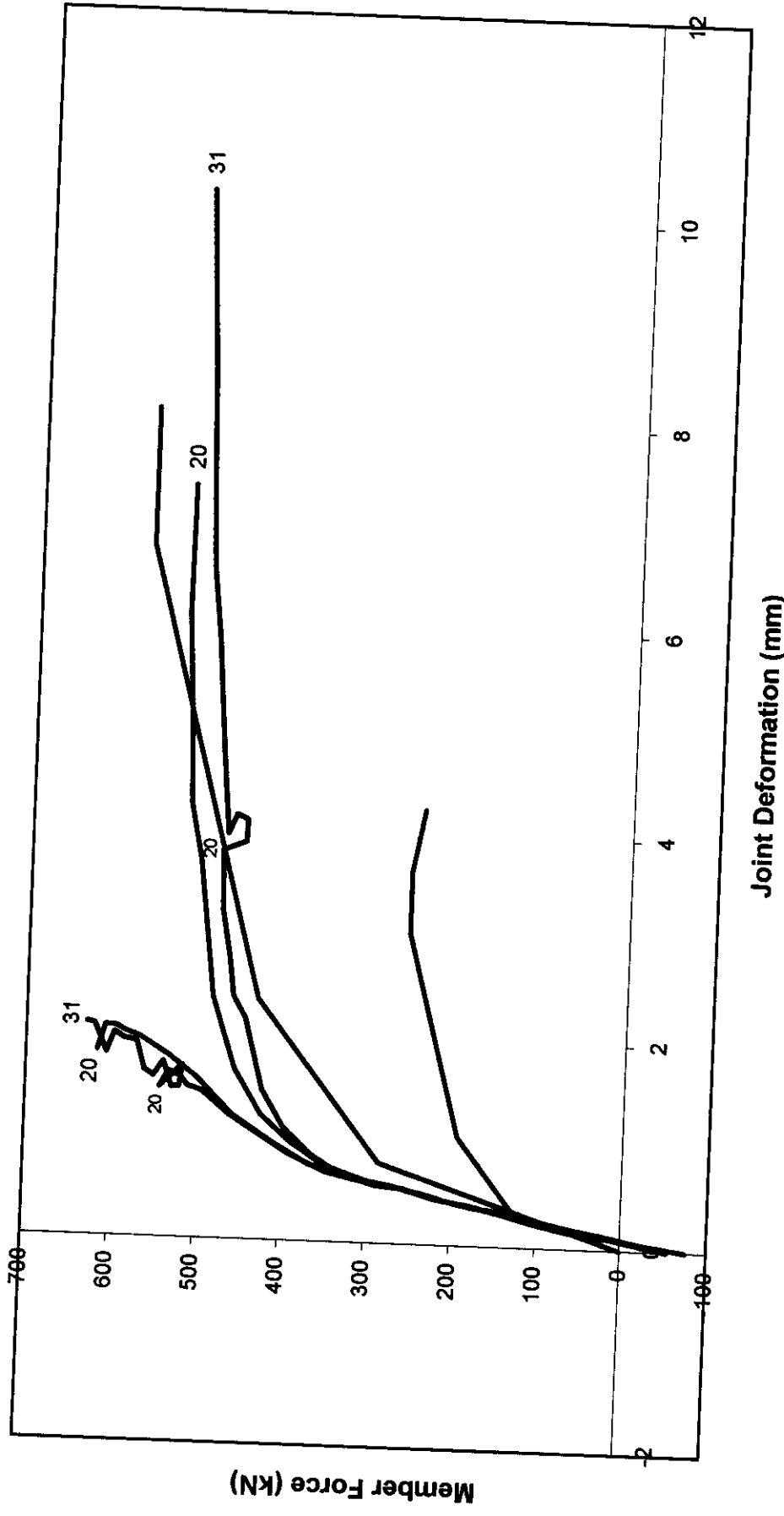
Frame C - Primary K Braces - Joint Deformations



Joint Deformation (mm)

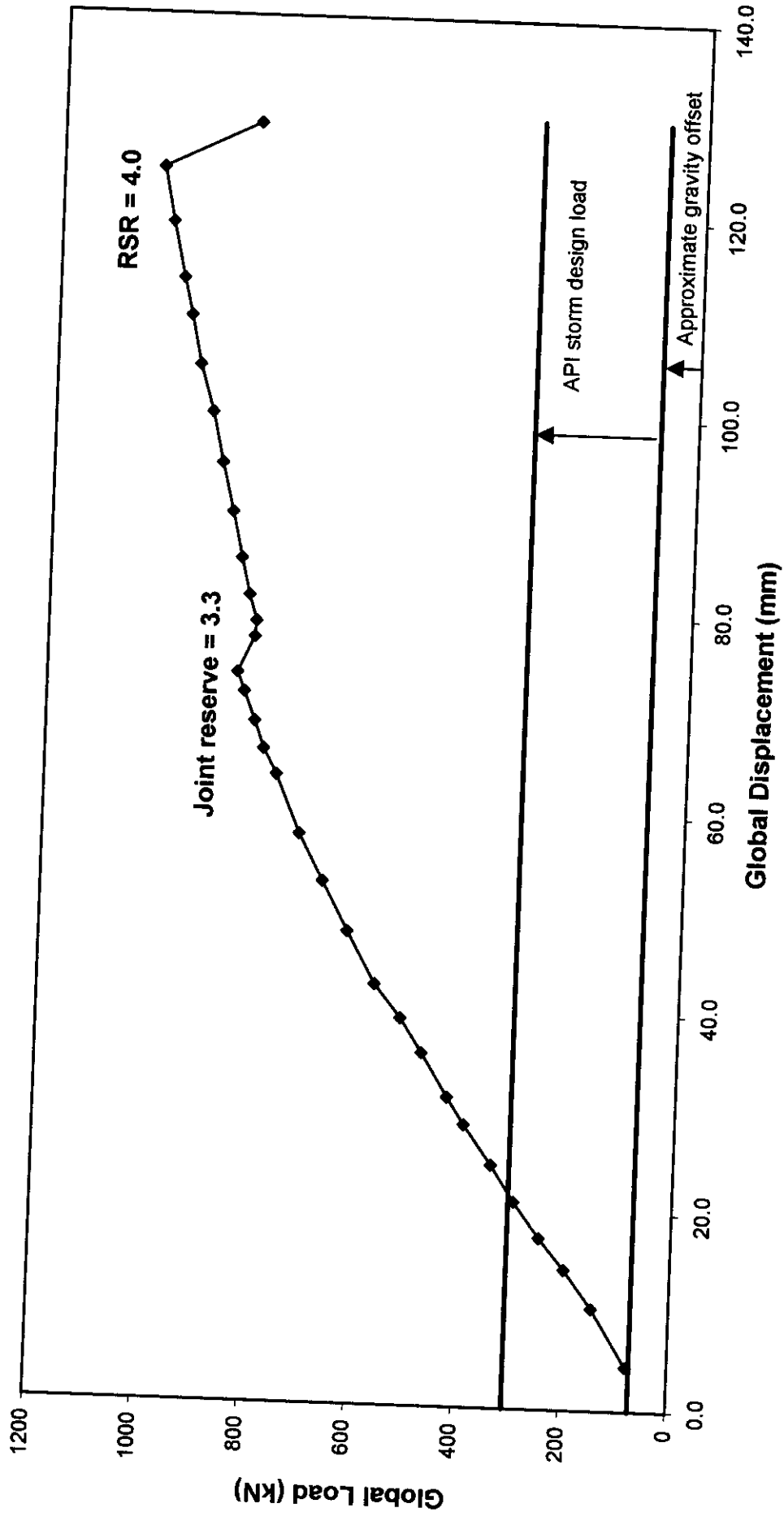
- Btm Bay Tension Member 61
- Top Bay Comp'n Member 62
- ISO mean
- Btm Bay Comp'n Member 62
- SINTEF Monotonic Tension Brace
- HSE mean
- Top Bay Tension Member 63
- SINTEF Monotonic Comp'n Brace
- API allowable (S.F.=1.28)

Frame C - Primary K Braces - Joint Deformations



- Btm Bay Tension Member 61
- Top Bay Tension Member 63
- SAFJAC per HSE capacity and factored to test
- Btm Bay Comp'n Member 62
- Top Bay Comp'n Member 64

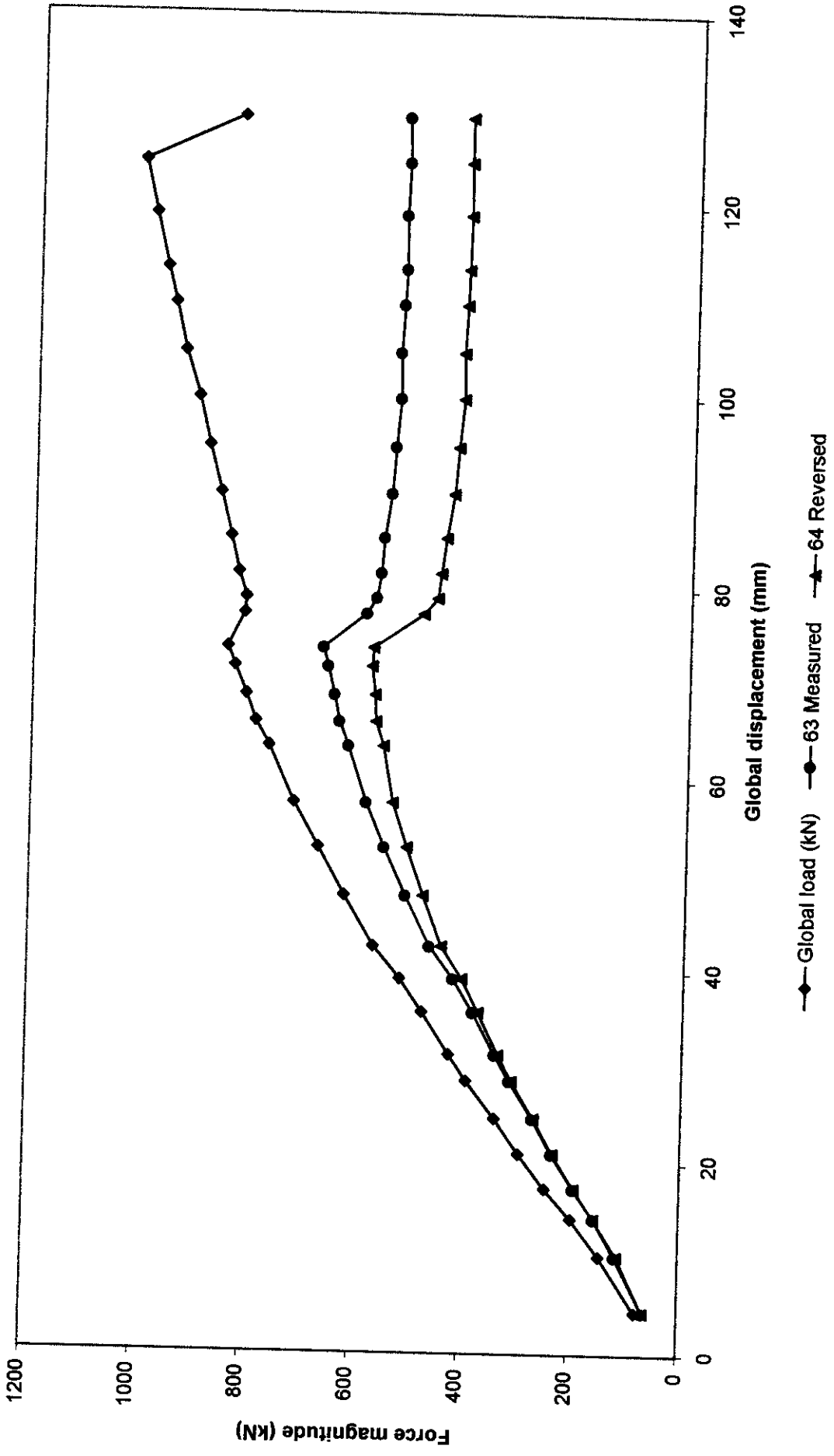
# GLOBAL RESPONSE



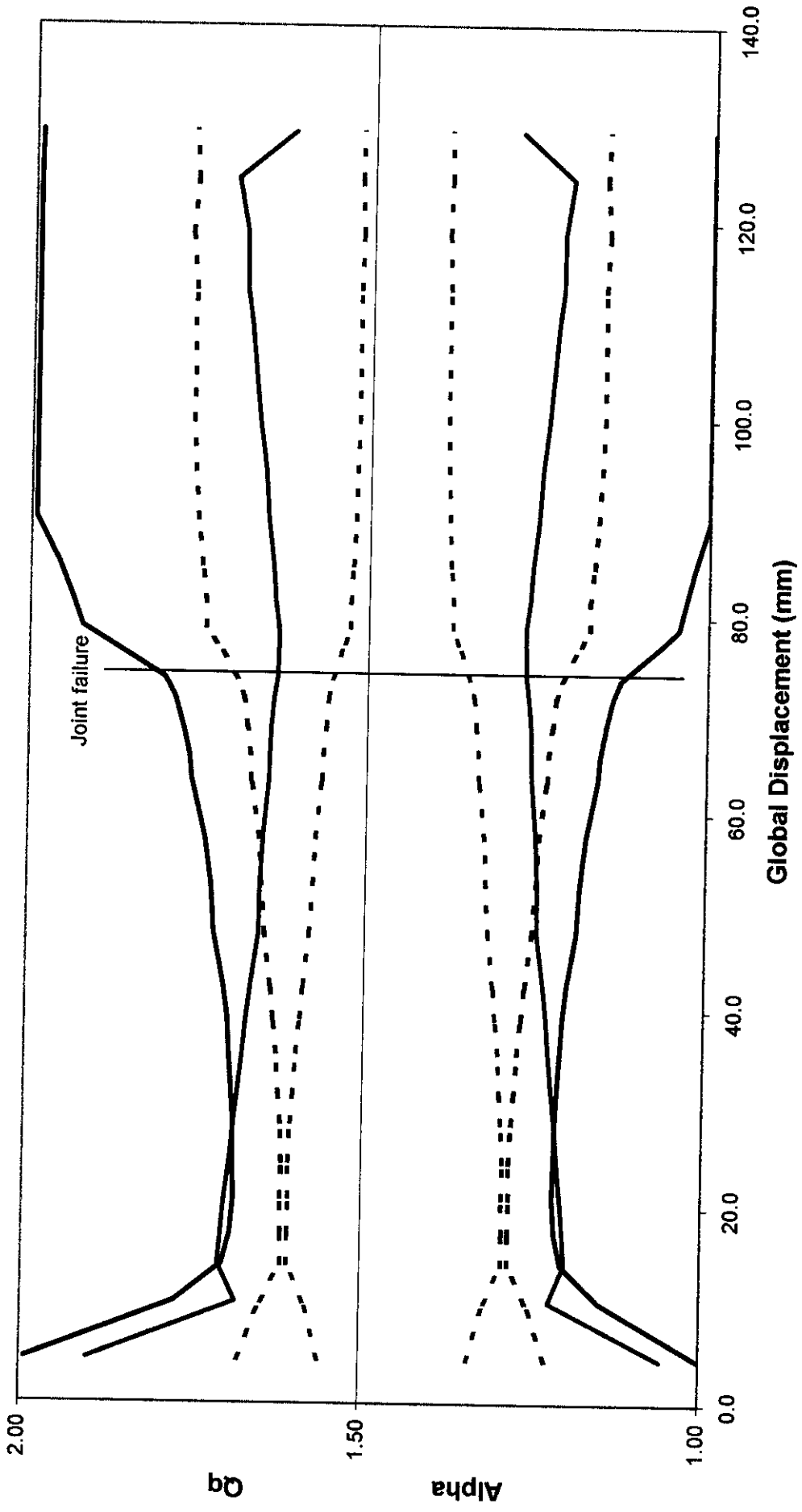
Loadcase 1 - Test



Comparison between Node 38 and global forces



AWS multibrace alpha classification of Node 38




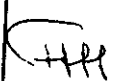
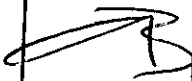
- - - alpha 63 P - - - alpha 64 P - - - alpha 63 MP - - - alpha 64 MP - - - Qq 63 P - - - Qq 64 P - - - Qq 63 MP - - - Qq 64 MP

The contents of this document are confidential to Participants of the Frames Project - Phase III, under the terms of their contract for participation in the project

**JOINT INDUSTRY TUBULAR FRAMES PROJECT -  
PHASE III**

**LOADCASE 2 TEST REPORT  
INTERACTION BETWEEN X-BRACED PLANES**

C636\39\011R REV 0 AUGUST 1999

Purpose of Issue	Rev	Date of Issue	Author	Checked	Approved
Draft for Client comment	0	August 1999	 HMB	 FHH	 CJB

Controlled Copy	10	Uncontrolled Copy	
-----------------	----	-------------------	--

**BOMEL LIMITED**  
Ledger House  
Forest Green Road, Fifield  
Maidenhead, Berkshire  
SL6 2NR, UK

Telephone +44 (0)1628 777707  
Fax +44 (0)1628 777877  
Email bomel@compuserve.com



**REVISION SHEET**

REVISION	DETAILS OF REVISION	DATE
0	Draft for Client Comment	August 1999

**FILE SHEET**

PATH AND FILENAME	DETAILS OF FILE
C636\26\frame2.pcx	Figure 1.1
C636\39\016U and 017U.pcx	Figure 1.2
C636\26\Phasel-X.pcx	Figure 1.3
C636\39\018U.pcx	Figure 1.4
C636\39\019U.pcx	Figure 1.5
C636\26\C484-23.pcx	Figure 1.6
C636\12\images\gui9.pcx	Figure 2.1
C636\12\images\gui10.pcx	Figure 2.2
C636\26\C485-2.pcx	Figure 2.3
C636\39\008w.xls sheet Global Scan Nos	Figure 2.4
C636\39\008w.xls sheet Global Annotated	Figure 2.5
C636\39\009w.xls sheet Loading & Logger Chart	Figure 2.6
C636\39\008w.xls sheet 6	Figure 2.7
C636\26\C485-12.pcx	Figure 2.8
C636\39\008W.xls Sheet Global Annotated + Joint	Figure 2.9
C636\26\C485-25.pcx	Figure 2.10
C636\26\C485-35.pcx	Figure 2.11
C636\26\C488-36.pcx	Figure 2.12(a)
C636\26\C488-26.pcx	Figure 2.12(b)



**FILE SHEET CONTINUED**

PATH AND FILENAME	DETAILS OF FILE
C636\26\C486-27.pcx	Figure 2.13
C636\26\C488-13.pcx	Figure 2.14
C636\26\C488-32.pcx	Figure 2.15
C636\26\C490-17.pcx	Figure 2.16
C636\26\C490-11.pcx	Figure 2.17
C636\39\008W.xls Sheet LC2 Fr II comparison	Figure 2.18
C636\26\Phasel-Xjt.pcx and C488-18.pcx	
C636\39\008W.xls Sheet N42 Local Forces	Figure 2.19
C636\39\008W.xls Sheets Node 42 Strains 82 and Node 42 Strains 84	Figure 2.20
C636\39\008W.xls Sheets FrE BBU Mom and FrE BBL Mom	Figure 2.21
C636\39\012U.vsd	Figure 3.1
C636\39\013U.pcx	Figure 3.2
C636\39\014U and 015U.pcx	Figure 3.3
C636\40\016W.xls Sheet Fr BTB Comp	Figure 3.4
C636\47\011W.xls Sheet Global	Figure 3.5
C636\47\011W.xls Sheet Lev2-X For	Figure 3.6
C636\47\011W.xls Sheet Fr E TB For and Fr E BB For	Figure 3.7
C636\47\011W.xls Sheet Fr D TB and Fr D BB For	Figure 3.8
C636\39\008W.xls Sheet Fr E TB Code Comparison	Figure 4.1
C636\39\008W.xls Sheet Local joint characteristics	Figure 5.1
C636\39\008W.xls Sheet Local joint characteristics	Figure 5.2
C636\39\008W.xls Sheet Global c.f API design	Figure 5.3
C636\15\002D Rev G	Appendix A
C636\15\003D Rev G	Appendix A
C636\15\009D Rev G	Appendix A
C636\15\015D Rev B	Appendix A
C636\15\011D Rev D	Appendix B
C636\15\012D Rev B	Appendix B
C636\15\013D Rev B	Appendix B
C636\15\016D Rev O	Appendix B
C636\39\008W.xls - Sheets as per Page C.1	Appendix C
C636\39\009W.xls - Sheets as per Page C.1	Appendix C
C636\47\011W.xls - Sheets as per Page C.1	Appendix C



## CONTENTS

	Page No.
<b>FOREWORD</b>	0.6
<b>EXECUTIVE SUMMARY</b>	0.9
<b>1. INTRODUCTION</b>	
1.1 BACKGROUND	1.1
1.2 LOADCASE 2 OBJECTIVES	1.1
1.3 REPORT LAYOUT	1.2
	1.8
<b>2. LOADCASE 2 TEST</b>	
2.1 CONFIGURATION	2.1
2.1.1 Reference Schemes	2.1
2.1.2 Component Properties	2.1
2.1.3 Response Data	2.1
2.1.4 Test Procedure	2.4
2.2 RESPONSE	2.5
2.2.1 Preamble	2.6
2.2.2 Global Response	2.6
2.2.3 Detailed Response	2.7
2.2.4 Comparison with Phase I 2D Results	2.11
2.2.5 Local X Joint Response	2.18
2.3 QUANTIFIED SUMMARY OF RESULTS	2.18
	2.23
<b>3. COMPONENT TESTING AND ANALYSIS</b>	
3.1 OTHER FRAMES PROJECT INFORMATION	3.1
3.1.1 Basis of 2D Investigations	3.1
3.1.2 Structural System Reserve Strength	3.1
3.1.3 X Joint Capacity Results	3.1
3.1.4 Analytical Investigations of Chord Stress Effects	3.2
3.1.5 Summary of 2D Investigations	3.3
3.1.6 Complementary Data from 3D Tests	3.4
3.2 SAFJAC FRAME RESPONSE PREDICTIONS	3.5
3.2.1 Background	3.6
3.2.2 Comparison between Predicted and Measured Responses	3.6
	3.7



## CONTENTS CONTINUED

	<b>Page No.</b>
<b>4. INDUSTRY PRACTICE</b>	
4.1 PREAMBLE	4.1
4.2 PLANAR JOINT CODE CAPACITY FORMULATIONS	4.1
4.3 AS-BUILT JOINT CAPACITY PREDICTIONS	4.2
	4.4
<b>5. ASSESSMENT OF LOADCASE 2 COMPONENT AND SYSTEM RESPONSES</b>	
5.1 JOINT CAPACITY DATA ASSIMILATION	5.1
5.2 JOINT DEFORMATION COMPARISONS	5.1
5.3 SYSTEM RESPONSE COMPARISONS	5.2
5.3.1 Reserve Strength Ratio	5.4
5.3.2 Features of Real Structures	5.5
5.3.3 The Efficacy of Plan X Bracing	5.6
	5.7
<b>6. CONCLUSIONS</b>	
	6.1
<b>7. REFERENCES</b>	
	7.1
<b>APPENDIX A AS-BUILT DRAWINGS RELEVANT TO LOADCASE 2 TEST</b>	
<b>APPENDIX B INSTRUMENTATION LAYOUT DRAWINGS</b>	
<b>APPENDIX C FRAME RESPONSE PLOTS</b>	



## FOREWORD

This report is one of a series describing different aspects of Phase III of the Joint Industry Tubular Frames Project. Each report is self contained providing detailed information in the subject area and summarising relevant data from other documents. The following table lists and briefly describes the focus of each report for cross-referencing purposes.

Report Title	Reference	Circulation
<b>Summary and Conclusions</b> Overview report describing the project and principal findings	C636\04\478R	1
<b>Background, Scope and Development</b> Scene setting report summarising previous work, identified needs and Phase III programme definition and development	C636\04\435R	1
<b>3D Test Set Up</b> Brief description of the 3D test set up and structural configuration	C636\06\313R	1
<b>Material Testing Report</b> Description of material testing procedures, test results and disposition of specific materials within test structure	C636\23\004R	1
<b>Assessment of Locked-In Fabrication Stress</b> Explanation for the build up of locked-in fabrication stresses, description of their measurement and summary of the locked-in force values in key components at the start of each test	C636\21\050R	1
<b>Test Frame Instrumentation</b> Detailed description of all instrumentation systems used in the 3D frame, accuracy, sign conventions etc. Data on CD in final report	C636\25\071R	1
<b>Loadcase 1 Test Report - Multiplanar K Joint Action</b> Detailed description of the Loadcase 1 static test response and interpretation of the results and their significance	C636\37\014R	1
<b>Loadcase 2 Test Report - Interaction Between X-Braced Planes</b> Detailed description of the Loadcase 2 static test response and interpretation of the results and their significance	C636\39\011R	1
<b>Loadcase 3 Test Report - Multiple Member Failures and 3D System Action</b> Detailed description of the Loadcase 3 static test response and interpretation of the results and their significance	C636\40\021R	1





Report Title	Reference	Circulation
<p><b>Philosophy of Cyclic Testing</b> Discussion of the background to cyclic response issues in the context of ultimate system strength and basis for specific loading scenarios</p>	C636\24\021R	1
<p><b>Loadcase 1 Cyclic Test Report</b> Detailed description of the Loadcase 1 cyclic test response and interpretation of the results and their significance. Comparison with LC1 static results</p>	C636\38\010R	1
<p><b>Monotonic and Cyclic testing of Isolated K Joints</b> Description and presentation of results from isolated component tests undertaken by SINTEF in Norway</p>	STF22 F98704 (C636\24)	1/2
<p><b>Loadcases 2 and 3 Cyclic Test Report</b> Detailed description of the Loadcases 2 and 3 cyclic test responses and interpretation of the results and their significance. Comparison with LC2 and LC3 static results</p>	C636\41\011R	2
<p><b>Loadcases 1 and 3 'Alternative' Cyclic Tests</b> Detailed description of the Loadcases 1 and 3 alternative cyclic test responses and interpretation of the results and their significance. Comparison with LC1 and LC3 static and cyclic tests</p>	C636\45\008R	3
<p><b>Multiplanar SCFs</b> Joint BG / BOMEL report describing analytical work and experimental measurements of multiplanar SCFs. Includes comparison with 'standard' empirical approaches</p>	C636\18\018R	1
<p><b>Site Testing Programme results - Report to Benchmark Analysts</b> Comprehensive report describing results for benchmark cases LC1, LC2 and LC3, including all pertinent data and providing response plots 'matching' the contributions from individual analysts</p>	C636\32\066R	4
<p><b>Benchmark Conclusions</b> Report comparing blind and post test analyses with measured responses and assimilating learnings and recommendations for future practice identified by Benchmark Analysts</p>	C636\32\084R	1



Key to circulation.

Circulation	All participants	Participants in 1st extension	Participants contributing finance/analytical results to 2nd extension	Benchmark Analysts
1	✓	-	-	
2	-	✓	-	×
3	-	-	✓	×
4	✓	-	-	✓



## JOINT INDUSTRY TUBULAR FRAMES PROJECT - PHASE III

### LOADCASE 2 TEST REPORT INTERACTION BETWEEN X-BRACED PLANES

#### EXECUTIVE SUMMARY

Phase III of the Joint Industry Tubular Frames Project involves a series of ultimate strength tests of a jacket type structure together with associated analytical and laboratory investigations. This report forms one of a series and addresses the specific results from the second, Loadcase 2, ultimate strength test of the frame.

Within the plane of loading the frame was X-braced but without an intermediate 'horizontal' between bays. However typical of recent weight saving design practice, X-braced plan framing was provided out into the 3D structure. First component failure was associated with a  $\beta=1.0$  compression X joint in the primary loading plane and the test examined the mechanisms of load redistribution and quantified the component and system capacities.

This report provides specific background to the Loadcase 2 configuration and gives a detailed description of the test. Findings from previous Frames Project research are presented together with discussion on the provisions of recent codes and standards.

The tests confirmed that, constrained within the continuity of a frame, compression X joint capacity is some 37% greater than the mean of isolated test databases underlying current design practice. Furthermore, no justification was evident for the capacity reduction factor being introduced to the draft ISO standard to account for the high levels of coacting chord tension.

The structure was shown to effectively redistribute loads via the plan X-bracing once initial component failures occurred. For the test geometry it was estimated that the global load sustained was some 50% higher than it would have been without the plan X framing. The system contribution to the global capacity was considerable and the ultimate load reached more than twice the level at which the first component (joint) failed. Had the design load been assessed to API including a storm conditions safety factor and with the considerable conservatism in the joint capacity formulations, a reserve strength ratio between the ultimate capacity and design load of 6.9 would be given. This figure is highly dependent on the (under) utilisation in surrounding parts of the structure and therefore should be considered with caution.

The ductility in the failure modes enabled gradual redistribution to take place and for multiple load paths to be utilised effectively. If the joint had had a strong joint can and first component failure had involved



member buckling, it is deduced that the system capacity would have been 25% less than recorded in the Loadcase 2 test.

An important aspect of the Loadcase 2 test was the determination of real 'imperfections' within structures and their potential effect on structural response. Factors included:

- locked-in fabrication forces having beneficial and detrimental effects on component capacity and sequence of failure
- the translation of component capacities from isolated tests to responses within the confines of a frame
- the changing constraints on components as adjacent failures occur.

This illustrated the need for ultimate strength analyses of 'perfect' structures to be assessed carefully and for the potential sensitivity to imperfections to be considered.

Despite these factors the blind SAFJAC analyses contributed to the benchmark exercise are shown to have given a good estimate of the component and system responses.



## 1. INTRODUCTION

### 1.1 BACKGROUND

Phase III of the Joint Industry Tubular Frames Project follows earlier phases of 2D frame tests and analytical investigations. These had indicated that components behave differently within the confines of a frame than in isolated tests on which engineering practice has been based. Furthermore the structural systems exhibit significant reserve of strength beyond design load levels. If these effects could be assured for jacket structures there could be important practical benefits in terms of a reduced need to strengthen existing structures and greater efficiency in future designs.

The purpose of the Frames Project Phase III was therefore to demonstrate the validity of these findings for 3D jacket type structures and in so doing to examine aspects absent from the earlier plane frame tests. The specific objectives were:

- To establish the effects of nonlinear joint/member behaviour on three-dimensional frame behaviour and collapse mechanisms.
- To quantify the reserve and residual strength of three-dimensional frames and to investigate redundancy and load shedding characteristics.
- To investigate the static performance of members and joints within three-dimensional frames and to develop procedures for the exploitation of available component data.
- To carry out comparative isolated joint tests.
- To measure locked-in stresses introduced during construction of three-dimensional frames.
- To calibrate and apply a nonlinear numerical procedure, SAFJAC, to the collapse analysis of the test frame and to provide data for the calibration of other software with similar stated capabilities.
- To benchmark the capabilities of existing 3D nonlinear analysis software.

These objectives have been fulfilled with the conduct of a series of static and cyclic tests of a three dimensional jacket type structure under different loading scenarios denoted Loadcase 1,



Loadcase 2 and Loadcase 3 (LC1, LC2 and LC3). Figure 1.1 shows the test set up and scenarios.

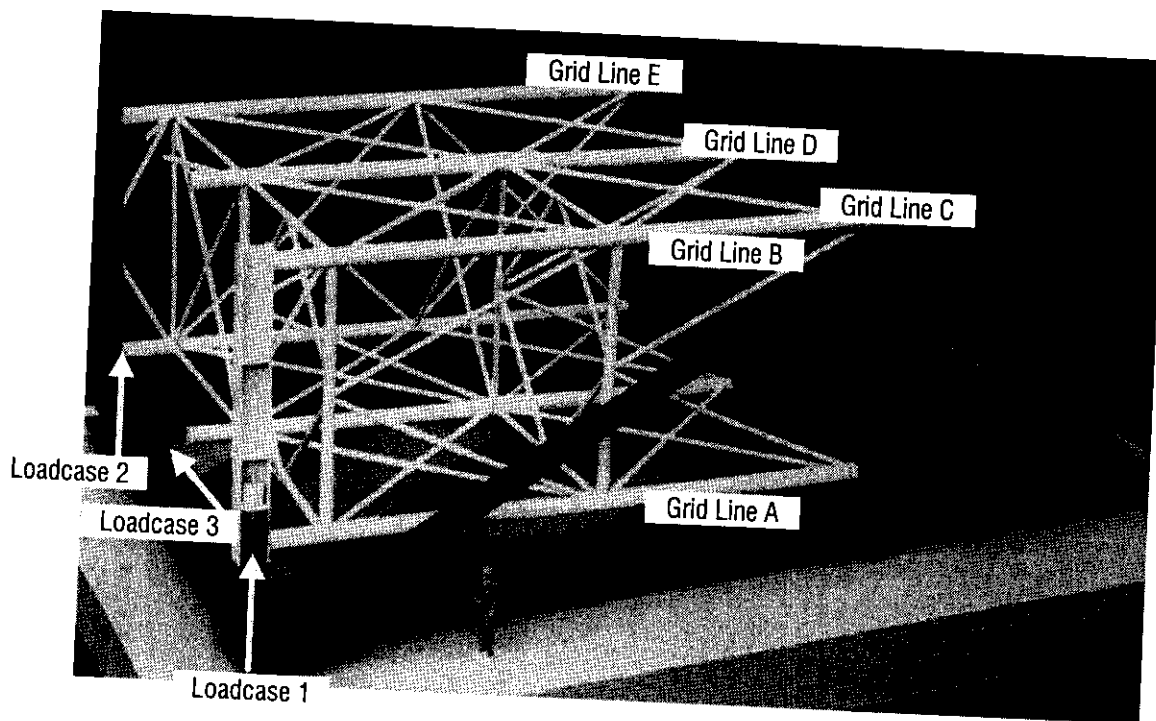


Figure 1.1 3D frame loading configuration

Reference 1 describes in detail how the test structure was designed in the context of the Phase III programme and the range of features embraced. This report focuses on the specific conduct of, and findings from, the Loadcase 2 static test. Appendix A provides structural drawings for the frame pertinent to the LC2 response.

## 1.2 LOADCASE 2 OBJECTIVES

An increasingly common feature of modern jacket design is the use of X-bracing but without horizontal members in the face frames. Instead, X or diamond plan bracing is provided between bays or at the mid-bay level. Examples are illustrated in Figure 1.2.

In elastic design, face frame horizontals carry low levels of axial load and therefore the alternative designs appear to be efficient offering weight and cost savings. However if failure occurs in a primary X-brace, the horizontal provides an important loadpath to help distribute loads through lower bracing to the foundation. In plane frame tests undertaken within Phase I of the Frames Project<sup>(2)</sup>, it was shown that without a mid-height horizontal a sequence of X brace failures rapidly propagated down through the structure. The 2D X-braced frame test set up is shown in Figure 1.3.

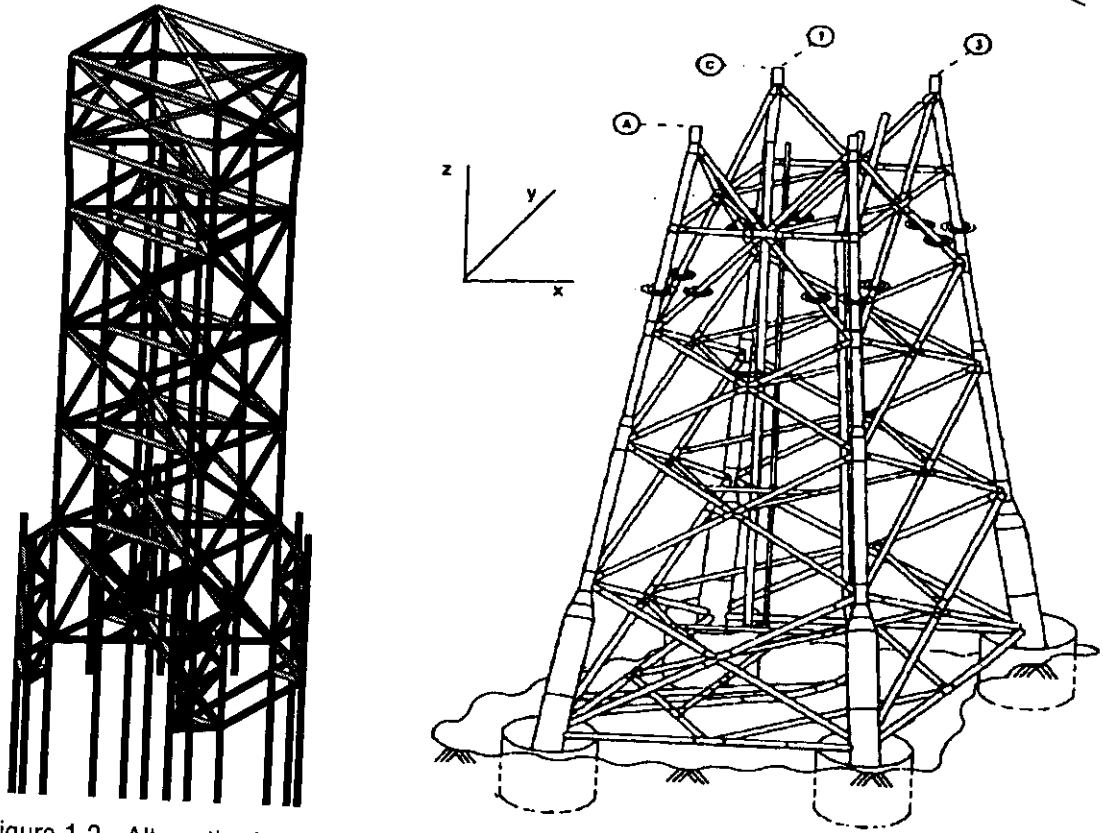


Figure 1.2 Alternative X-braced jacket configurations without face frame horizontals

Figure 1.4 compares the global load deflection responses for nominally identical test frames with and without the mid-height horizontal. After the initial buckling in the 'top' bay closest to the camera and fall off in load in Frame I, the load carrying capacity was beginning to increase at the point the test was stopped. However the forces in the bottom X-braced bay of Frame I were only some 70% of those at the corresponding point in the Frame III test (around 150mm global displacement). The low residual capacity is evident from the figure following the lower bay buckling in Frame III.

A further observation is that imperfections arising during fabrication were more significant for the structure without the mid-height horizontal. Initial placement of the horizontals minimises the distortion of the frame legs as the X braces are welded in; conversely without horizontals mechanical restraints may be needed to prevent distortion but which, when released, can result in significant forces being locked-in to structural members<sup>(3)</sup>.

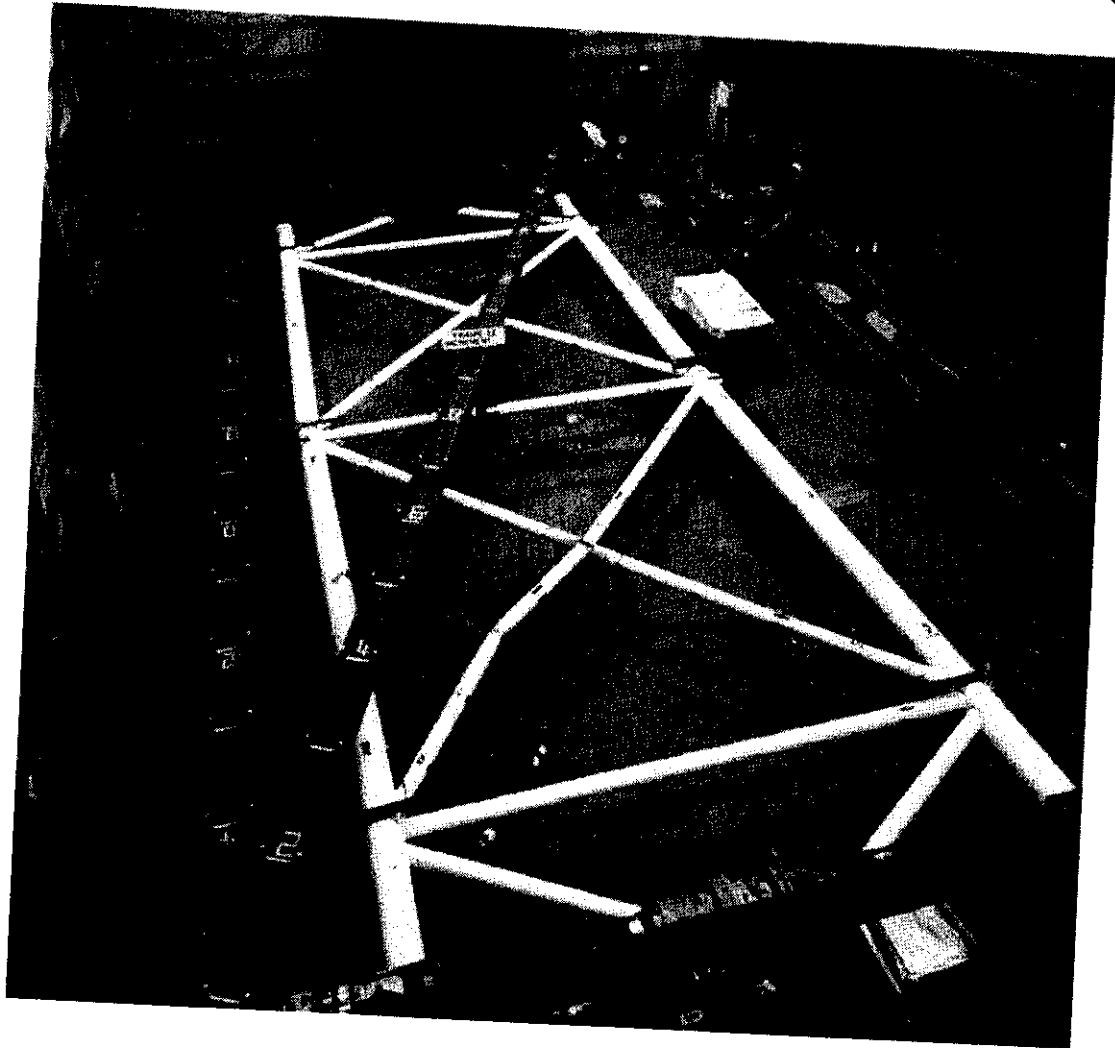


Figure 1.3 Frames Project Phase I X-braced frame tests

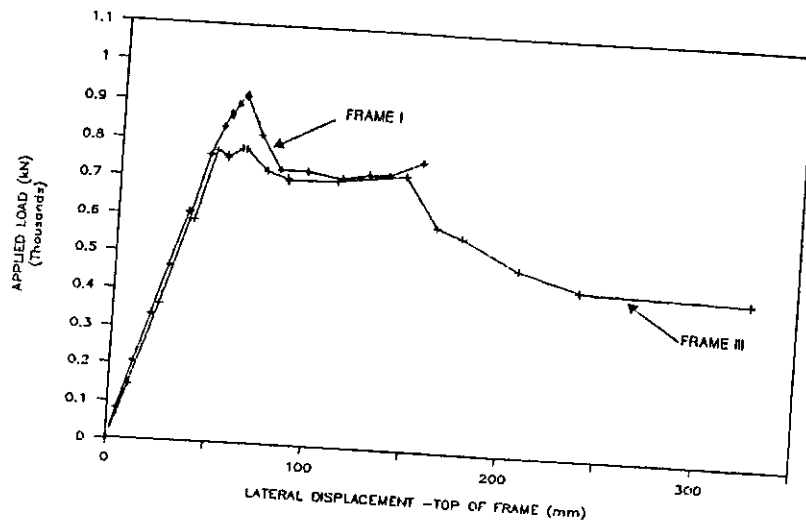


Figure 1.4 Comparison of 2D X-braced frame responses with (Frame I) and without (Frame III) a mid-height horizontal<sup>(2)</sup>





However in assessing the Phase I 2D frame test results, it was recognised that in reality jacket structures are three dimensional and that out-of-plane braces offer the potential to transfer loads.

Therefore, in the 3D demonstration phase of the Project one of the Loadcase 2 objectives was:

- to investigate the efficacy of inter-bay plan X bracing in distributing loads from the face frame as components fail into other parts of the structure.

A second objective was:

- to demonstrate the significance of compression X joint failure on the ultimate strength of a 3D structural frame.

This latter objective also followed from earlier Frames Project research<sup>(3, 4, 5)</sup> in which the failure modes of joints without cans, typical of older offshore design practice, were examined within the confines of a frame. A very ductile response was exhibited by X joints in compression as the chord ovalised and flattened (see Figure 1.3) restoring a stiff loadpath through the X-braced bay. Furthermore as compression response across the joint softened, so the alternative tension loadpath along the chord took a higher proportion of the applied load. As a result, the structure as a whole was able to sustain continually increasing global loads contributing to a very high reserve strength in comparison with the design load. Another factor was the fact that the initial failure load of the X joint itself was some 25-40% higher than evidence from isolated test databases would suggest. The frame tests had therefore been extremely important in providing realistic conditions of constraint to the joint and appropriate coacting chord loads, neither of which have been replicated in the idealised tests on which design practice has been based. These aspects were investigated analytically in Phase IIA of the project<sup>(6)</sup>.

As shown in Figure 1.3, the X-braced frame in which joint failure occurred included a mid-height horizontal. However it was recognised based on the Frame I / Frame III redundancy comparison<sup>(5)</sup>, that had the member been omitted the system response could have been quite different.

Figure 1.5 shows comparisons from SAFJAC nonlinear collapse analyses of 2D frame structures comparable to the configurations in the Frames Project Phase I tests<sup>(5)</sup>.

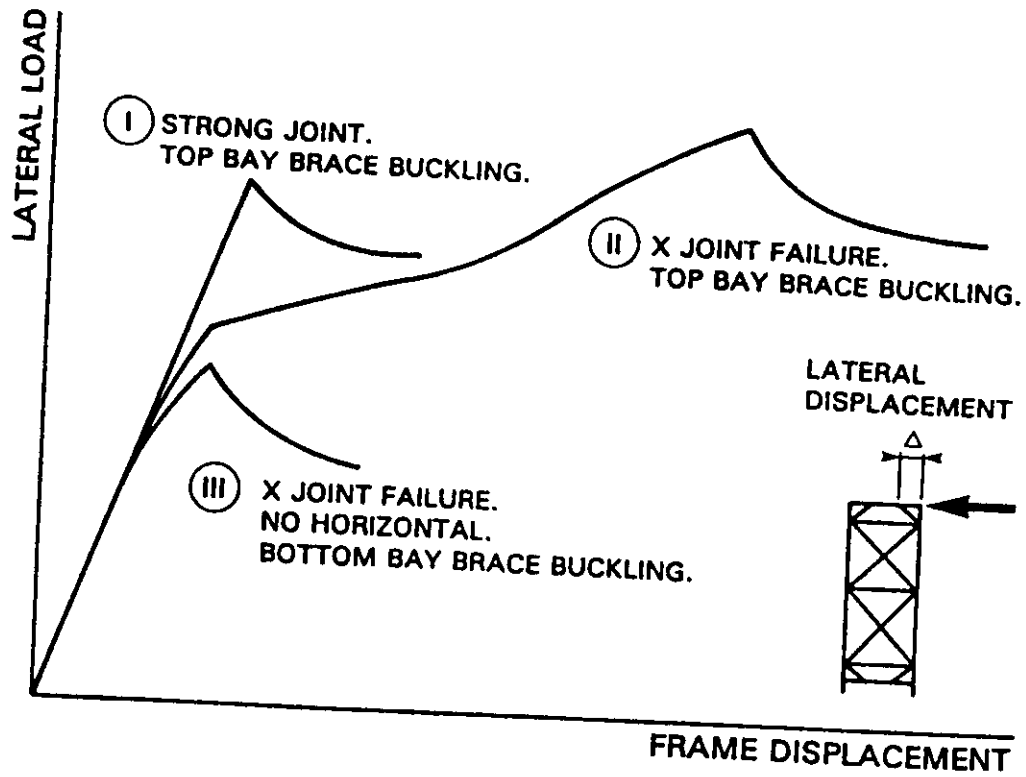


Figure 1.5 Frame responses for different combinations of joint strength and redundancy<sup>(5)</sup>

The three scenarios are as follows:

- I 2D X-braced frame with strong joint can and mid-height horizontal. Compression brace buckling failure in top bay limits system capacity.
- II 2D X-braced frame without strong joint can but with mid-height horizontal. Compression X joint in top bay softens, alternative tension loadpath and horizontal distribute applied load into bottom bay, portal action in legs develops. X joint compresses flat restoring stiff loadpath and compression brace buckling failure in top bay then limits system capacity.
- III 2D X-braced frame without strong joint can or mid-height horizontal. Compression X joint in top bay softens, alternative tension loadpath transmits applied load into bottom bay compression brace precipitating buckling and defining system capacity.

This example served to illustrate the importance of structural redundancy to redistribute loading effectively in a collapse scenario and furthermore highlighted that the benefits of the X joint ductility cannot always be realised within a structure (Case III compared with Case II in Figure 1.5).

The Loadcase 2 test scenario therefore draws on these previous research findings to provide a realistic demonstration of the response characteristics in a 3D jacket type structure. The test setup is shown in Figure 1.6 with the actuator mounted on the X-braced Frame E, pushing the structure upwards (see also Figure 1.1). The two X-braced bays without the mid-level brace can be seen to the left hand side of Figure 1.6 in the primary plane of loading, with the out-of-plane X bracing coming out across into the 3D structure.

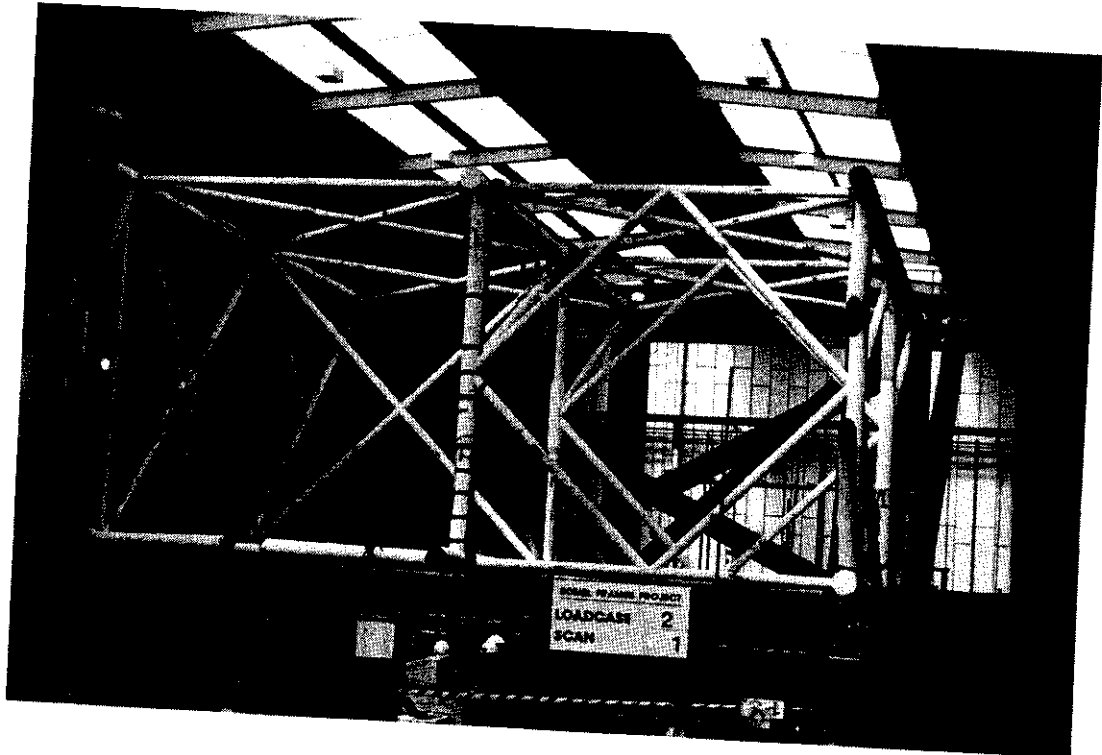


Figure 1.6 Loadcase 2 configuration - start of test

The Loadcase 2 configuration was designed to provide a direct basis for comparison with the experimental and analytical investigations from earlier phases of the Frames Project as outlined above. The section sizes and material grades were nominally identical and these, in non-dimensional terms, were representative of offshore practice.

In addition to the earlier Frames Project investigations which provide an important basis for interpreting the static Loadcase 2 results, the test was repeated after the structure had been repaired to assess the response under cyclic applied loads. Reference 7 provides a comparative reference.



### 1.3 REPORT LAYOUT

Having established the purpose of the Loadcase 2 test, Section 2 describes the structural response. Section 3 provides a corresponding factual description of the other analytical and experimental studies contributing to the understanding of the frame behaviour. In Section 4 reference is made to recent codes and standards and, by inference, isolated tubular joint databases. All these aspects are then assimilated in Section 5 leading to conclusions in Section 6.

As noted in the Foreword, this report is one of a series describing the Frames Project Phase III results. It assembles data relevant to the interpretation of the Loadcase 2 static test results. More detailed information, for example on the instrumentation or materials, can be found in the companion reports. The draft report is printed in black and white with key plots reproduced in colour in the appendices. Final and electronic issues will be in full colour.



## 2. LOADCASE 2 TEST

### 2.1 CONFIGURATION

#### 2.1.1 Reference Schemes

Figure 1.6 shows the 3D test structure at the start of the Loadcase 2 (LC2) test. The loading beam and actuator are positioned on Frame E applying positive load upwards in displacement control. The datum position (zero applied load) corresponds to the condition in which the tubular frame cantilevers under its self weight from the reaction rig; the weight of the actuator system is taken directly to ground. A consistent numbering scheme for every member and node within the frame was adopted by all parties and for all aspects of the work. This is shown in Figures 2.1 and 2.2 as it applies for Loadcase 2. The global axis system is also shown.

For internal member axial forces the convention: positive = tension, negative = compression is adopted. A left hand rule defines moment orientations; however, these are also described within the local context.

#### 2.1.2 Component Properties

Appendix A contains as-built structural drawings for the 3D frame. Reference 8 provides information on the disposition of material throughout the structure, together with diameter (D) and wall thickness (T) measurements from surveys for every member segment within each member and at key nodes. Results are developed from static tensile coupon tests giving yield properties ( $F_y$ ) corresponding to the rate of structural testing. Reference 9 explains the build up of locked-in fabrication forces within the frame. Measured values are presented and combined with calculated member forces due to self weight to give the net force in every component at the start of each test (zero applied load).

For this report, properties for key components in the Loadcase 2 test scenario have been extracted and are presented below. Table 2.1 details the geometric properties and parameters in comparison with nominal and assumed values at the design stage. Table 2.2 shows the contributions to the initial distribution of forces in the structure at the start of the Loadcase 2 test. The test followed the Loadcase 1 and Loadcase 1 cyclic investigations when the structure was loaded on Line C. Neither test caused any damage in the vicinity of Frame E and those components that were damaged were cut out and repaired prior to the LC2 test. The loading assembly was also disconnected from Frame C and relocated on Frame E. The frame properties take full account of the changes that occurred and fully reflect the condition at the start of the Loadcase 2 test.

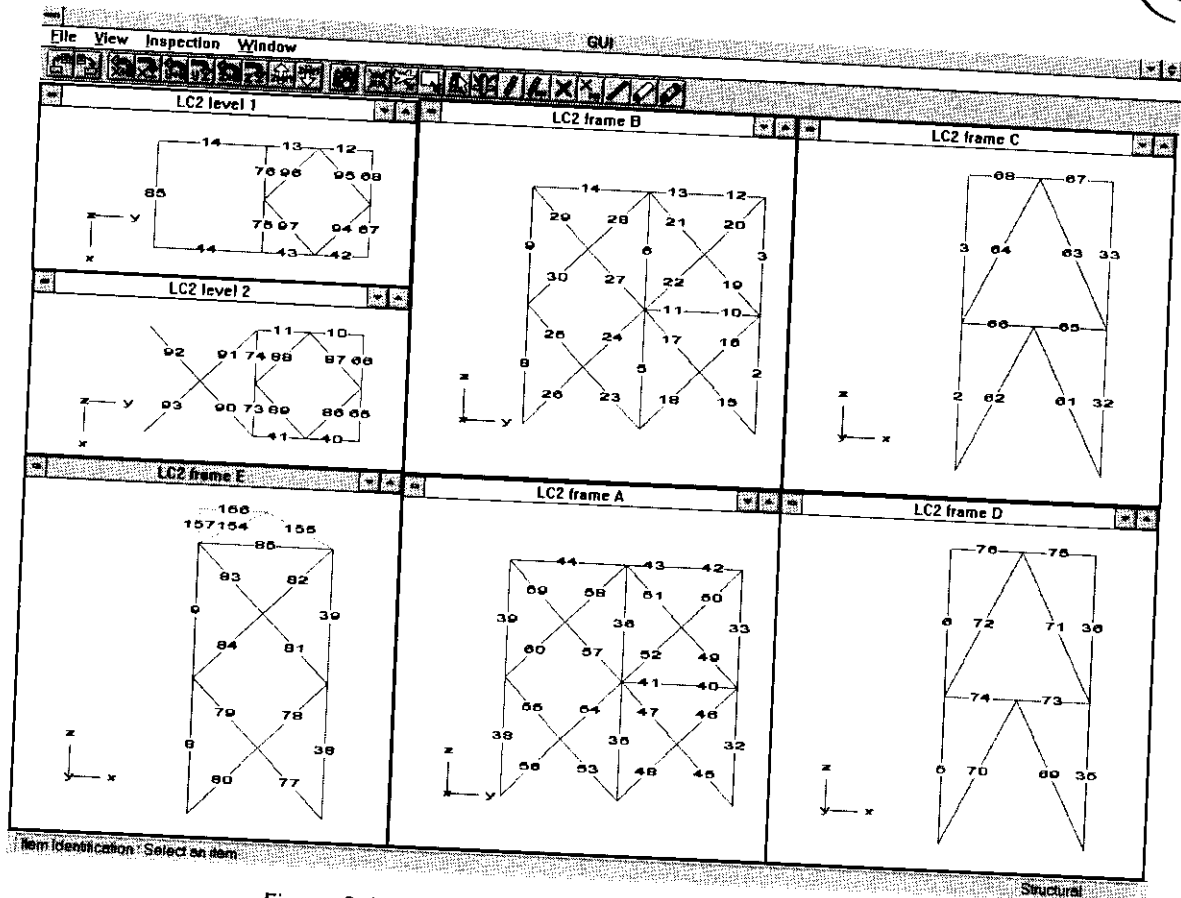


Figure 2.1 Member numbering system Loadcase 2

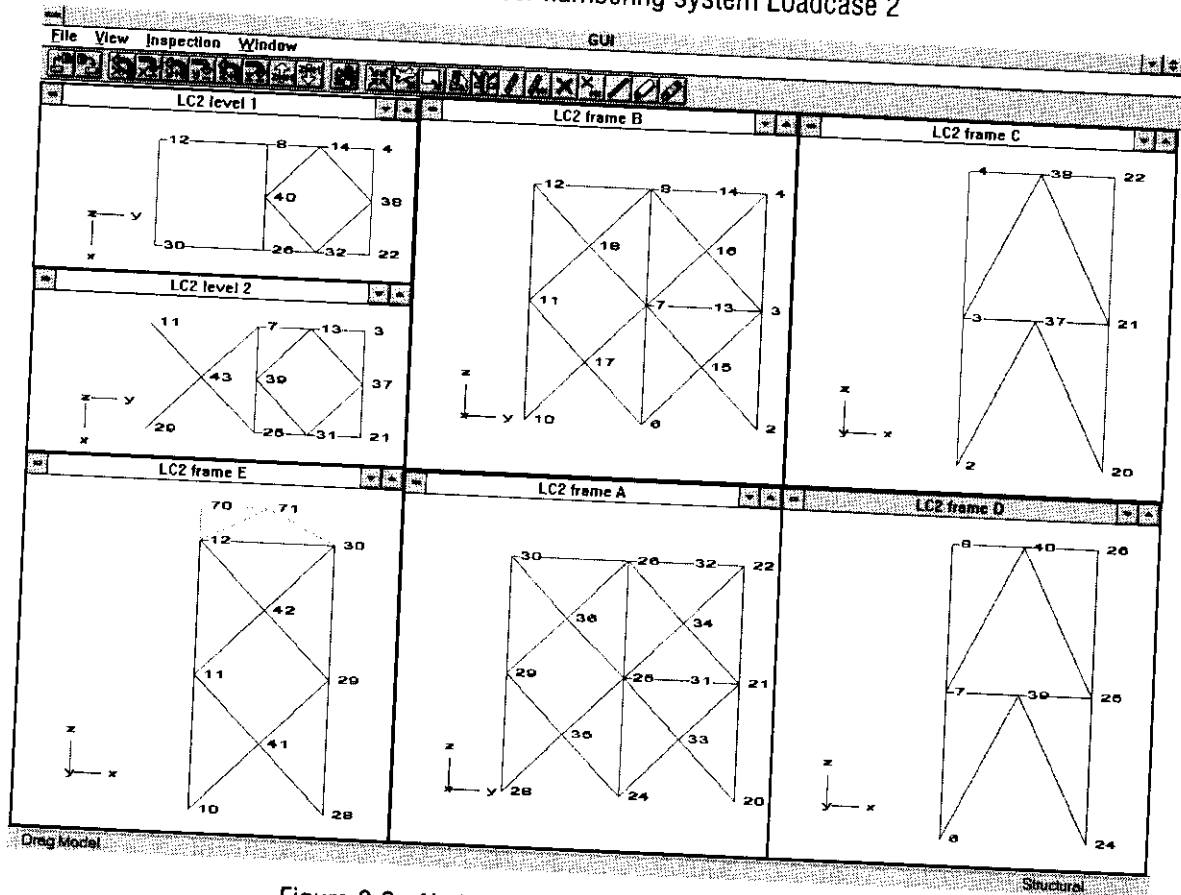


Figure 2.2 Node numbering system Loadcase 2

Table 2.1 Loadcase 2 - Actual compared with nominal component properties

Component	Braces - nominal				Chord - nominal				Chord - actual				
	Member	$\theta$	d (mm)	t (mm)	D (mm)	T (mm)	$F_y$ (N/mm <sup>2</sup> )	D (mm)	T (mm)	$F_y$ (N/mm <sup>2</sup> )	D (mm)	T (mm)	$F_y$ (N/mm <sup>2</sup> )
N42 /	82	90°	168.3	4.5	168.3	4.5	250	168.6	4.42	279.5			
Frame E	84	90°	168.3	4.5	168.3	4.5	250	168.6	4.42	279.5			

Component	Brace - nominal				Brace - actual				Chord - nominal				Chord - actual			
	$\theta$	d (mm)	t (mm)	$F_y$ (N/mm <sup>2</sup> )	d (mm)	t (mm)	$F_y$ (N/mm <sup>2</sup> )	Imperfection (mm)	d (mm)	T (mm)	$F_y$ (N/mm <sup>2</sup> )	D (mm)	T (mm)	$F_y$ (N/mm <sup>2</sup> )	Imperfection (mm)	
Member 81	90°	168.3	4.5	250	168.6	4.41	270.1	-	168.6	4.5	250	168.6	4.5	250		
Member 83	90°	168.3	4.5	250	168.7	4.41	270.1	-	168.7	4.5	250	168.3	4.5	250		
Member 82	90°	168.3	4.5	250	168.7	4.60	295.1	In-plane 0mm Out-of-plane 2mm	168.7	4.60	295.1	168.3	4.5	250		
Member 84	90°	168.3	4.5	250	168.8	4.60	295.1	In-plane 2mm Out-of-plane 2mm	168.8	4.60	295.1	168.3	4.5	250		
Member 77	90°	168.3	4.5	250	168.6	4.50	261.0	-	168.6	4.50	261.0	168.3	4.5	250		
Member 79	90°	168.3	4.5	250	168.5	4.50	261.0	-	168.5	4.50	261.0	168.3	4.5	250		
Member 78	90°	168.3	4.5	250	168.6	4.36	282.8	In-plane 2mm Out-of-plane 1mm	168.6	4.36	282.8	168.3	4.5	250		
Member 80	90°	168.3	4.5	250	168.6	4.36	282.8	In-plane 0mm Out-of-plane 0mm	168.6	4.36	282.8	168.3	4.5	250		

Sources:

D, d, T, t and  $F_y$  - C636\06\294w-b.xls  
Imperfection data - C636\06\307w-a.xls



Table 2.2 Loadcase 2 - Initial forces at zero applied load

Member	Forces (kN)		
	Locked-in fabrication force	Forces due to gravity and 15kN load cell offset	Net force at start of LC2 test
77*	-33	-60	-93
79*	-33	-59	-92
78	-54	63	9
80	-54	63	9
81	64	-52	12
83	64	-51	13
82	83	41	124
84	83	43	127

Source: Reference 9 Tables 5.12 and 5.3

Notes:

1. Figures rounded to 0 d.p.
2. Measured force values based on force released when members cut out at end of test recorded by load cell instrumentation. \*based on initial build DEMEC readings
3. Forces due to gravity and load cell offset calculated from SAFJAC linear analysis

### 2.1.3 Response Data

All data for member forces, moments and displacements are taken from the instrumentation installed and monitored on site by AV Technology Limited. Appendix B presents drawings showing the location of instrumentation within the frame. The 880 data channel system includes:

- Integral pre-calibrated load cells welded into the structure during fabrication. These are exceptionally accurate and are relied upon wherever possible. Four gauges (two opposite pairs) provide redundancy in the axial force calculation.
- Site installed surface mounted linear strain gauges to provide supplementary data on forces and moments (using nominal or local measurements of section properties). Four gauges (two opposite pairs) provide redundancy in the axial force calculation although care is needed in interpreting axial forces when sections distort and hoop strains become significant.





- Displacement transducers record deformations at key nodes and displacements of the frame and reaction rig.

Reference 10 provides a detailed description of the instrumentation techniques and data acquisition and reduction systems. Monitoring of the instrumentation was command activated (ie. not continuous). The raw data were processed online in an Excel spreadsheet programmed by BOMEL and AVT for this purpose. During and after the tests the data were validated and cross-checked wherever possible. Faulty gauges were replaced and/or formulae were altered to eliminate any erroneous values. The need for such corrections was rare and in general the quality and consistency of the data were shown to be excellent.

The final datafile provided by AVT for the Loadcase 2 test was:

LC2a\_test.xls

The updated spreadsheet incorporating BOMEL modifications as detailed on the spreadsheet revision sheet is:

C636\39\008w.xls

Copies of the datafiles are provided with Reference 10. This report presents the load effects determined from the raw data using these spreadsheet systems.

#### 2.1.4 Test Procedure

Prior to the test commencing a number of cycles of load were applied up to 100kN in stages, in order that the functionality of all systems could be checked and the take-up of load in the structure could be compared with predictions. On satisfactory completion of the trial, the actuator ram was withdrawn to leave the structure hanging at the datum position (zero applied load) relative to which all forces and moments were measured.

Throughout the test the following steps and procedures were followed:

- A datum scan of the instrumentation was taken (Scan 1) as the Scan number was displayed on the master board (see Figure 1.6). The scan number associated with each set of measurements uniquely defined the point in the test.
- An increment of load was applied under displacement control at the direction of BOMEL. Once complete, the actuator was locked-off in position. An on-screen trace of actuator load with time was monitored; a flat trace indicated a state of static equilibrium had been achieved. This was almost instantaneous when the structure was elastic but took a couple of minutes to reach once there was extensive plasticity.



- The scan number on the master board was incremented by one.
- The instrumentation system was scanned and backed up. Dial gauges were read manually.
- Throughout, all parties maintained independent logs with respect to Scan number and clock time of key events (eg. physical observations, checks on spurious gauge readings, ramp rate changes, movements in camera position, etc).
- Results within the data acquisition spreadsheet were reviewed by BOMEL. Graphs were generated automatically, plotting incremental measured values against BOMEL predictions. Built-in checks on maximum and minimum strains and functionality were monitored. Based on a review of the data the appropriate value for the next load / displacement increment was determined.

The sequence was repeated until the ultimate capacity of the structure had been attained and the pattern and level of post-peak loading capacity had been determined. The extent of post-peak deformation was limited to ensure extensive plasticity was not generated in distant parts of the structural frame.

- The applied load was then reduced in three or four decrements with scans of the instrumentation and record keeping at each stage as before.

## 2.2 RESPONSE

### 2.2.1 Preamble

The test set up for Loadcase 2 is shown in Figure 1.6. The member and node numbering schemes are shown in Figures 2.1 and 2.2. The datum position corresponds to the structure cantilevered from the reaction rig under its self weight with no actuator load.

Load was applied in displacement control on Line E, positive load pushing the frame upwards. Frame E was X-braced. The  $90^\circ \beta=1.0$  X joint between Levels 1 and 2 (Node 42 - closest to the actuator) had no thick-walled joint can. In the more distant bay the X joint between Level 2 and the reaction rig at Level 3 (Node 41), a high yield, thick-walled joint can was present.

Node 42 was the most highly utilised component in an elastic design level evaluation. Figure 2.3 shows a close up view of the node pre-test. The gap between the saddle weld toes is some 46mm.

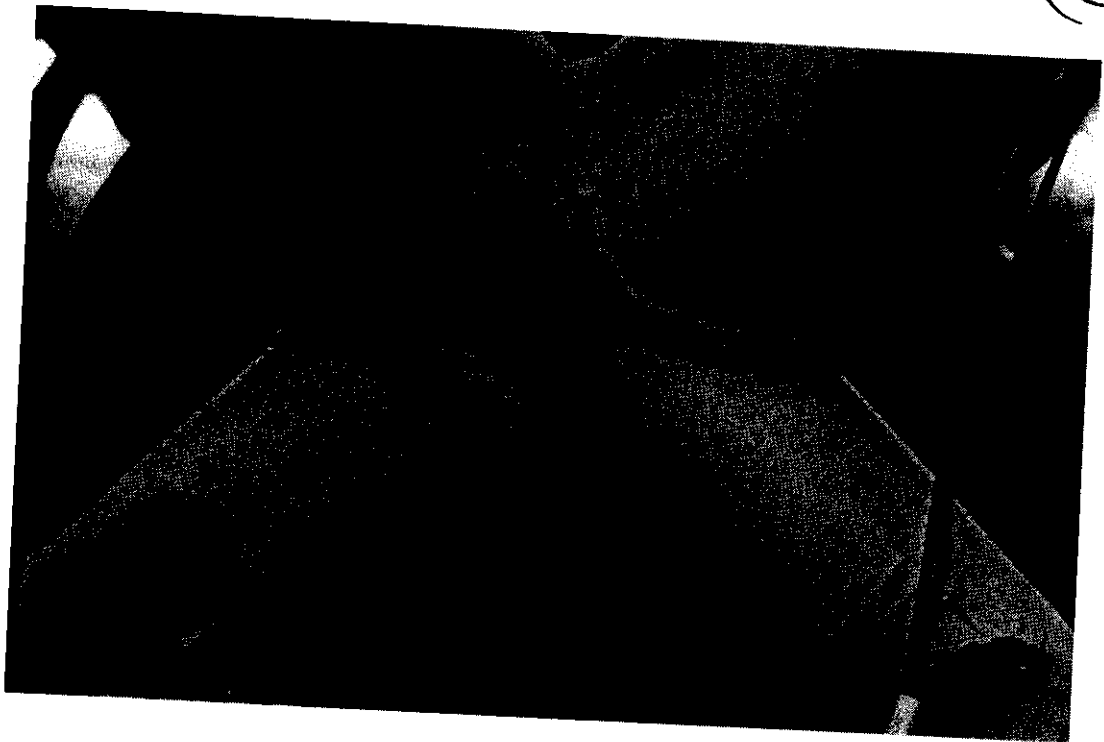
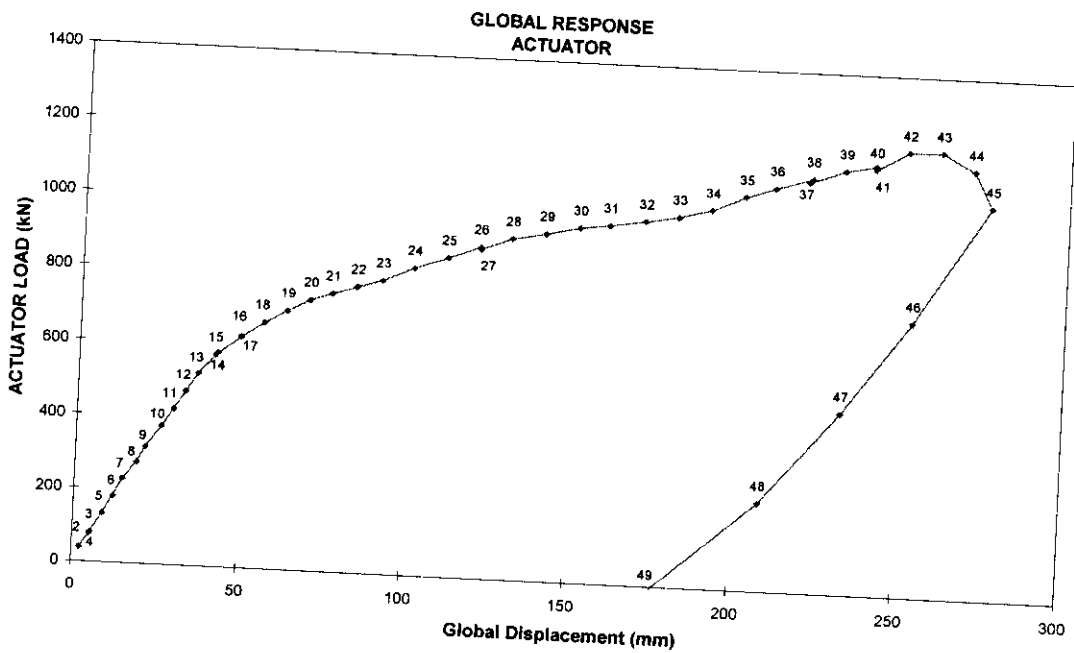


Figure 2.3 Node 42 pre-test

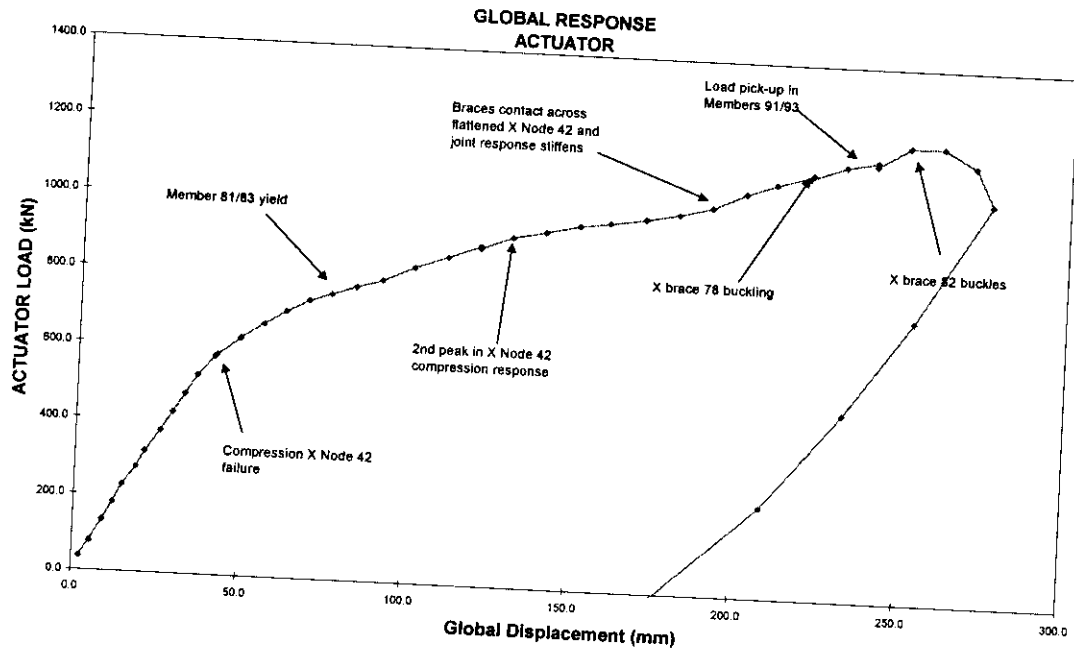
### 2.2.2 Global Response

Figures 2.4 and 2.5 show the loading and unloading trace for the full test. Figure 2.4 is annotated with the scan numbers to which reference will be made. Figure 2.5 highlights key events in the test described in further detail below.



Loadcase 2 - Test

Figure 2.4 Loadcase 2 - Scan numbers through test



Loadcase 2 - Test

Figure 2.5 Loadcase 2 - Key events through test

As described previously these traces correspond to the state of the structure after load has been applied, the actuator has been locked-off and the internal forces have equilibrated. The actuator control system supplied by Bodycote Limited independently recorded the applied load and displacement of the point of load application at one second intervals throughout. Figure 2.6 plots the loads applied by the actuator with those recorded by the logger once the system had equilibrated. The degree of 'relaxation' later in the test as the structure became plastic is evident. Furthermore the actuator system also provides evidence of the peak system capacity in instances where failure occurred as load was being applied between scans.

These global response plots are reproduced in colour in Appendix C. Corresponding plots for the member forces in different areas of the structure are also provided and will be referred to in the test descriptions which follow. The main text includes a compilation plot (Figure 2.7) from which the pattern and relative magnitude of forces in primary bracing of interest in the Loadcase 2 test can be seen.

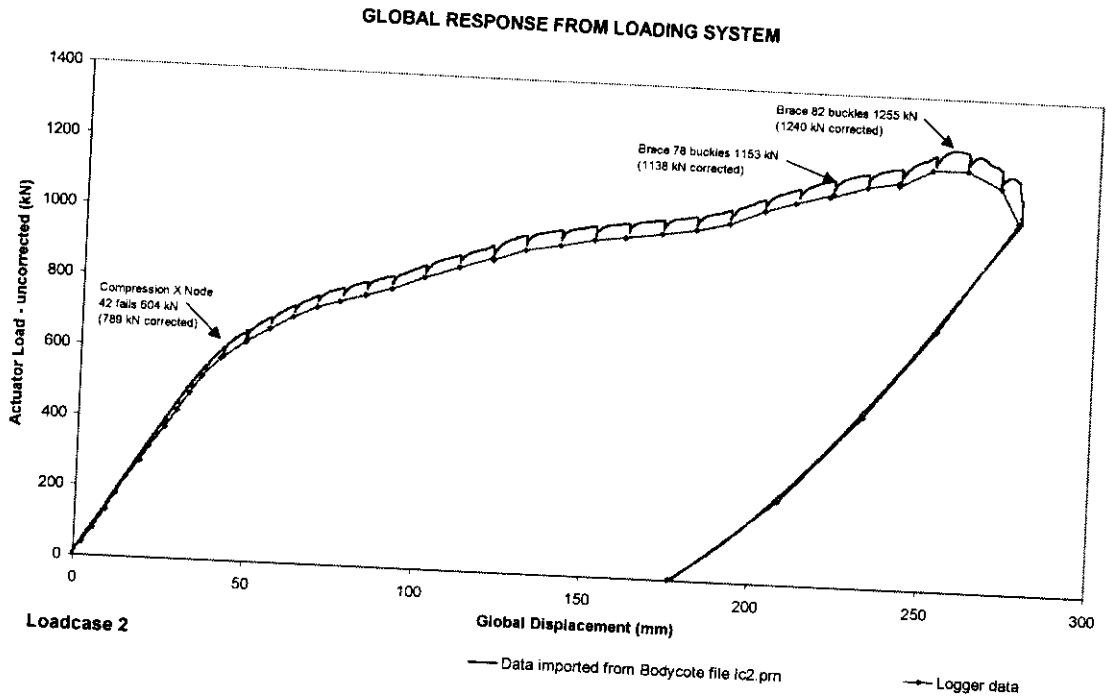


Figure 2.6 Applied actuator loads in comparison with equilibrated forces recorded at each scan

Note: The data in this plot include a 15kN positive load offset due to the self weight of the hinge unit and load cell. In all other plots and data reported in this document the appropriate correction has been made.

The plots are arranged as if looking at the structure from the viewpoint in Figure 1.6. The top diagrams relate to the bays closest to the viewer. Those on the left correspond to the loaded Frame E and those to the right give results for Frame D; the intermediate diagram are for the interconnecting X bracing at Level 2. All plots are to the same scale to enable direct comparisons to be made. The member forces are plotted with respect to the incremental displacements through the test. Graphs giving a record of the loading in other parts of the structure are included in Appendix C.

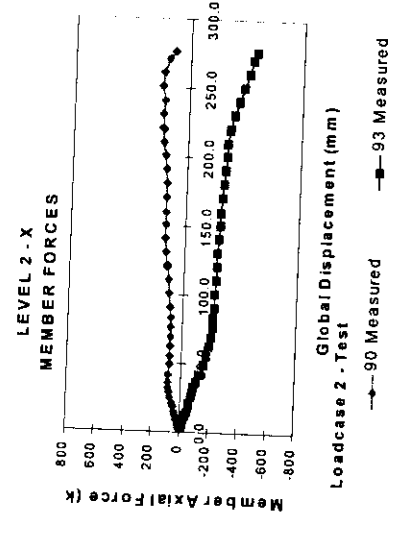
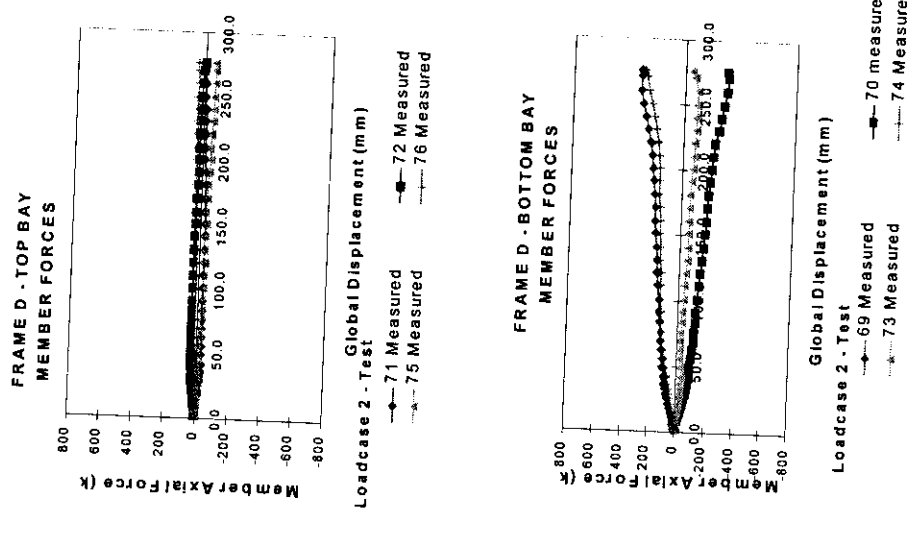
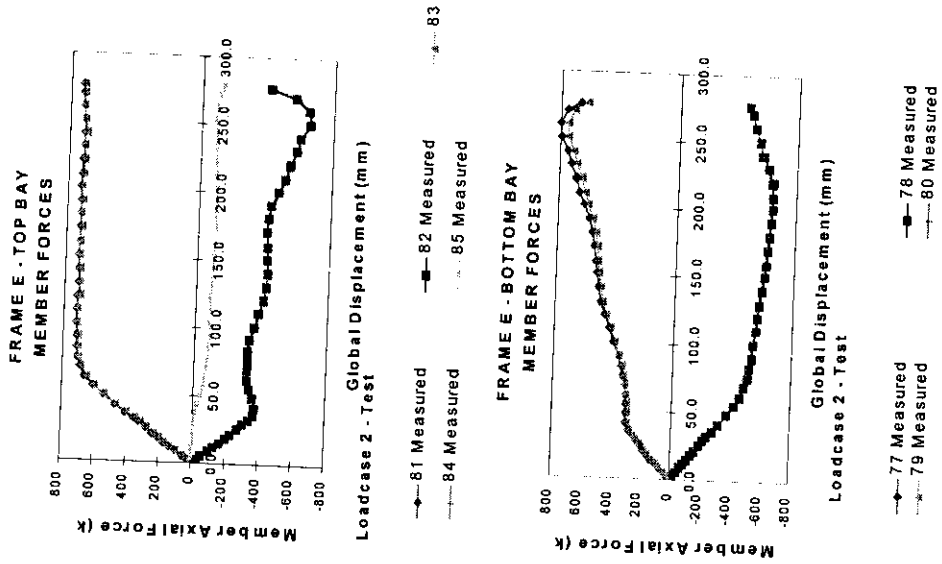


Figure 2.7 Member forces in key braces through the Loadcase 2 test



### 2.2.3 Detailed Response

During the initial stages of loading the global response was linear and there was negligible relaxation as the actuator was locked-off for each scan (Figure 2.7). However by about Scan 9 some local arching of the Node 42 chord had become visible. Figure 2.8 shows how deformation of the chord wall is actually constrained by the welds in the saddle region and the degree of ovalisation was slightly greater to either side. A corresponding view onto the face of the joint is barely distinguishable from Figure 2.3. It is also at about this stage that a degree of relaxation began to occur once actuator loading was complete and before a scan of the instrumentation was taken (see Figure 2.7).

Nevertheless, the system response remained reasonably linear until, with Scans 14 and 15, a peak in the load transmitted via the compression X joint was reached. Figure 2.9 traces the applied load and compression force across Node 42 throughout the test. The initial peak and correlation with the softening of the global response can be seen clearly.

The peak compression force recorded across the joint at Scan 15 in response to the applied loads was -373kN. The coacting force along the chord was some 469kN demonstrating how the tension loadpath had become significantly stiffer, and therefore attracted a high proportion of the applied load, than the compression route at the point failure occurred. *When considering the absolute capacity of the components in the Loadcase 2 tests, it is important to remember that the applied load effects are recorded with reference to a zero datum. Self-weight and locked-in fabrication effects are additional. For example for braces 81/83 and 82/84, the forces already present in the members at the start of the test were some +12kN and 125kN respectively (see Table 2.2). The net force across the compression X joint at Scan 15 was therefore -248kN (-373+125) with a coacting chord load of 481kN (469+12) which is almost twice as great. The measured capacities will be compared with response predictions below.*

The load sustained by the joint fell away significantly as the chord continued to deform in the saddle region. Figure 2.10 shows the joint just beyond the peak at Scan 16 and Figure 2.11 gives a wider view of the deformation at Scan 18. Nevertheless the tension chord continued to transmit increasing proportions of the applied load until at Scan 21 the members began to yield and a plateau in the local capacity was reached. The average member force in response to the actuator loading was 706kN (716kN net).

Figure 2.7 shows some evidence of the loads being transmitted by the Level 2 X-bracing across the 3D structure into Frame D. Although the force levels are not particularly high, there is evidence that the contribution is sufficient to provide some protection to the lower bay bracing. As the force in the top bay chord members 81 and 83 increased to yield at over 700kN, so that force in the out-of-plane compression Brace 93 exceeded -200kN with some -500kN being transmitted directly into the Frame E bottom bay compression Members 78 and 80. In the absence of the out-of-plane bracing the force would have been more nearly equal (but opposite)



to the 81/83 force level and buckling in the bottom bay members would have been precipitated even before the top bay chord had yielded - just as postulated in Figure 1.5.

It was not until Scan 37, at a global load some 50% greater than when yielding in the top bay occurred, that Brace 78 finally buckled in the lower bay of Frame E. Out across in the Level 2 X bracing the load carried by Member 93 then increased rapidly confirming the contribution of the out-of-plane bracing to maintaining 3D system capacity. The recorded buckling load in Brace 78 was -639kN which requires only a +9kN correction to account for compensating factors due to gravity preload and locked-in fabrication forces (net capacity -630kN).

Figure 2.12 (a) and (b) show the in and out-of-plane deformations of Brace 78 at Scan 37 just after buckling. The deflections are relatively small and buckling under the displacement control of the test was quite gradual. Nevertheless it can be seen from the load deflection traces in Figure 2.7, that the component capacity declines significantly thereafter.

However returning to the response of the Node 42 X joint and the combined plot in Figure 2.9, it can be seen that beyond the initial peak at Scan 15 the load fell away. It then increased again, firstly as the weld toes appeared to contact through the chord (Figure 2.13) and then again as the chord completely flattened (Figure 2.14) providing a new stiff loadpath through the structure.

The response was not entirely symmetric as it has been in previous 2D frame tests<sup>(2)</sup> and the slight twisting of the chord led to cracks propagating around one weld toe on either face of the joint (Figure 2.15). Nevertheless the direct loadpath between the compression braces through the flattened chord still enabled the global load to increase. The ultimate capacity was reached when Brace 82 in the top bay, buckled as shown in Figure 2.16 under an applied brace force of -639kN (-514kN net). Buckling of the brace seems to have been influenced significantly by the 'rotation' at the X Node 42. This served to increase the effective buckling length and introduced a pre-disposition or effective imperfection promoting buckling. The initial loss of component capacity was therefore quite gradual and a global load of some 1198kN was sustained for Scans 42 and 43. Thereafter the load bearing capacity of the brace decayed very rapidly (see Figure 2.7) as the joint provided little restraint to increasing rotations.

One final point with reference to Figure 2.7 is that the lower bay tension brace appeared to sustain an average load of 775kN but the presence of high gravitational and locked-in fabrication pre-compression forces (see Table 2.2) prevented yielding occurring. Indeed there was no evidence of yield in the response data or visible in the paint system on the structural members.

Figure 2.17 shows the deformation in the 3D structure and particularly Frame E at the point of maximum deflection at the end of the test. The global movement can be seen both with reference to the actuator and the portal action in the Frame B / E leg at the top of the picture. Buckling of the compression braces (both running bottom left to centre right of their respective bays as viewed in the figure) can be seen, as can the deformation of the Node 42 X joint chord.





Figure 2.8 Node 42 - Scan 9 - initial signs of chord ovalisation

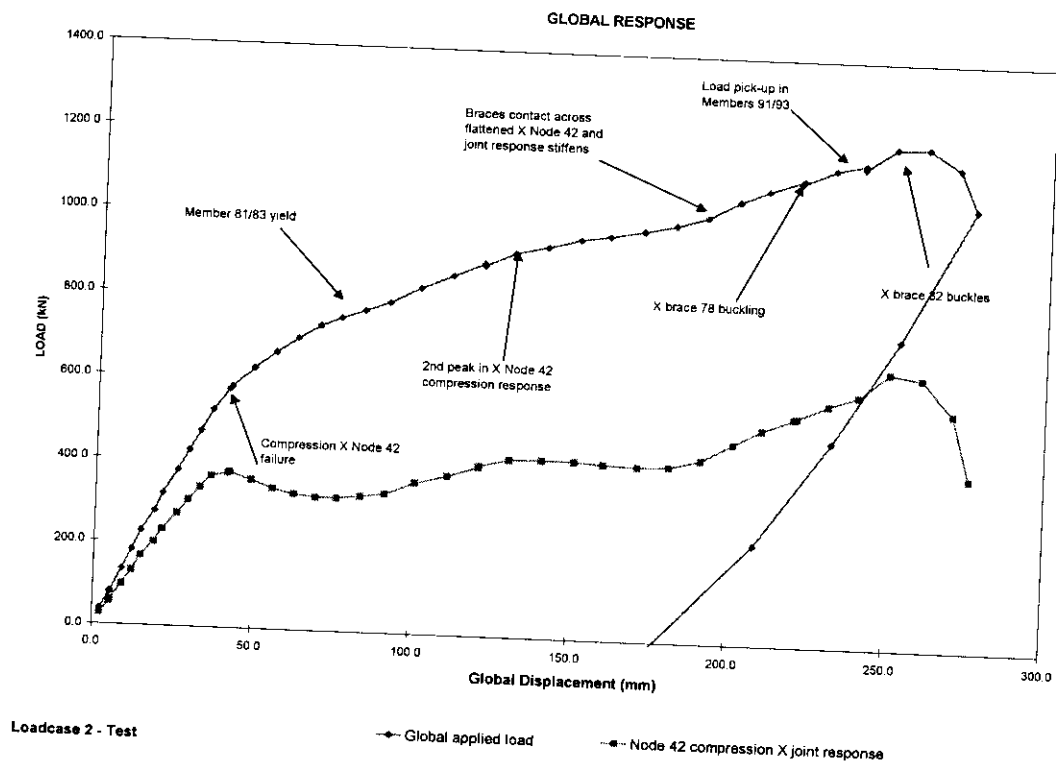


Figure 2.9 Frame E top bay compression X joint response



Figure 2.10 Node 42 - Scan 16 - chord deformation just beyond initial peak in capacity

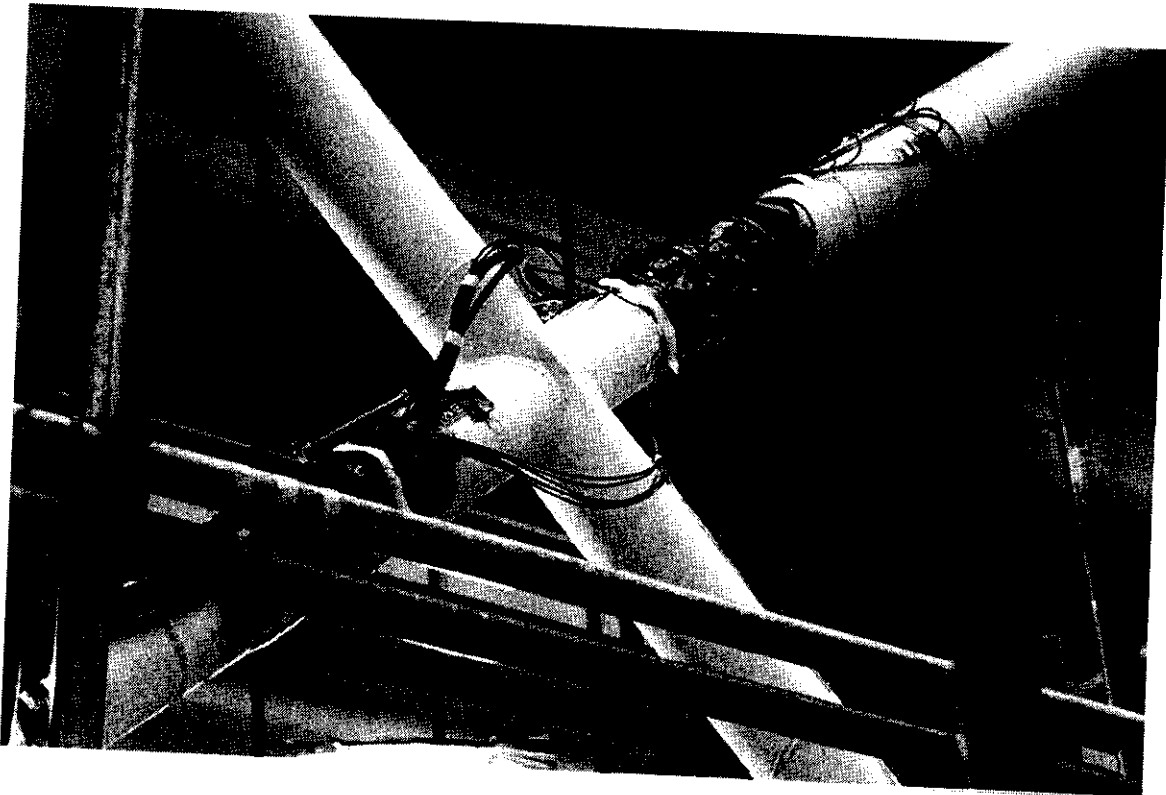


Figure 2.11 Node 42 - Scan 18 - X joint deformation



Figure 2.12(a) Brace 78 - Scan 39 - out-of-plane buckling view along Frames A/E leg from Level 2 to Level 3

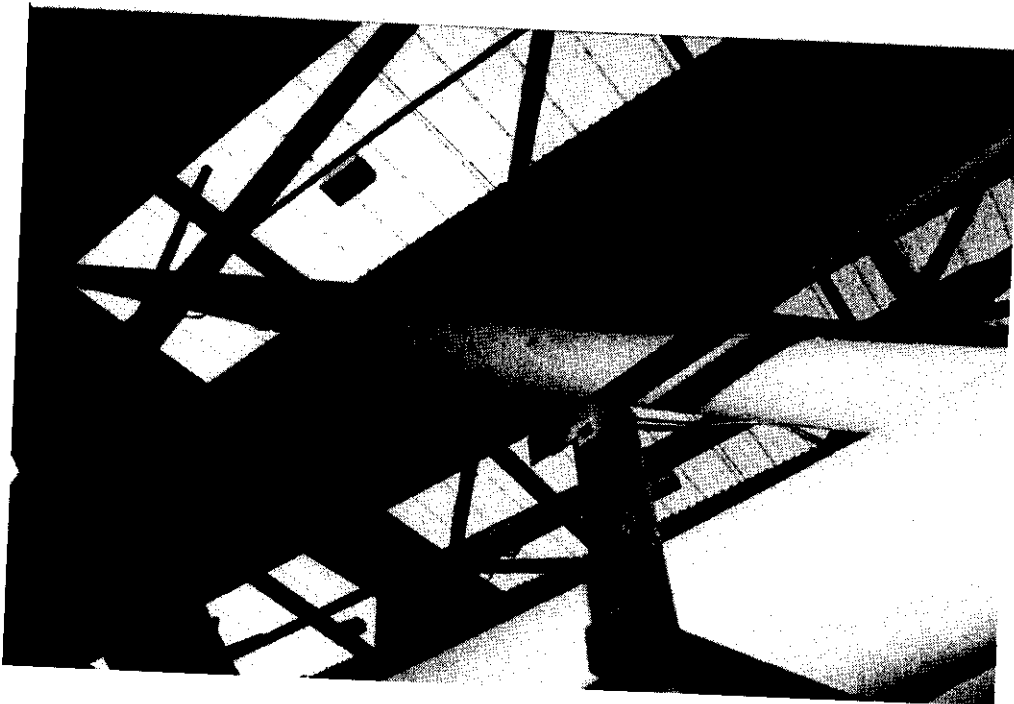


Figure 2.12(b) Brace 78 - Scan 37 - in-plane buckling - view from Frame A to Frame B



Figure 2.13 Node 42 - Scan 24 - initial contact of weld toes through chord corresponding to an increase in load transfer capacity

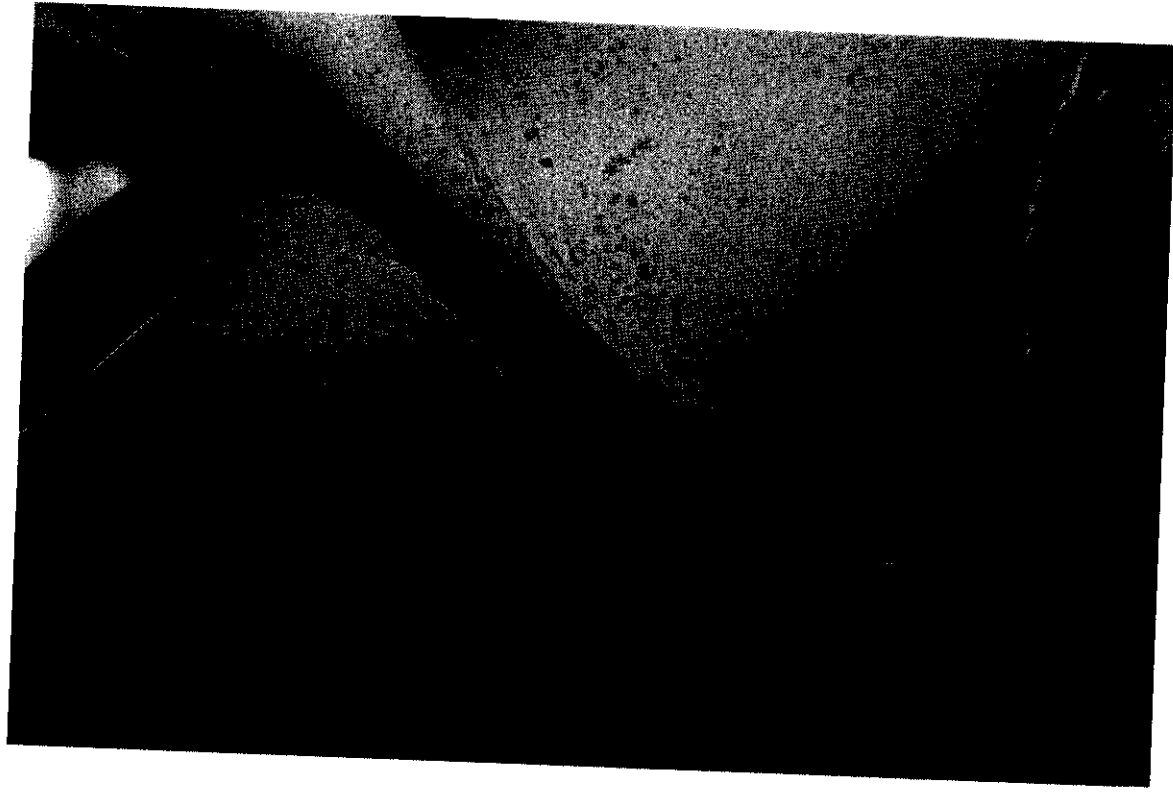


Figure 2.14 Node 42 - Scan 33 - flattening of the chord and significant increase in stiffness



Figure 2.15 Node 42 - Scan 39 - twisting at the joint precipitated growth of through thickness cracks



Figure 2.16 Brace 82 - Scan 45 - view up buckled member to flattened chord of Node 42 X joint

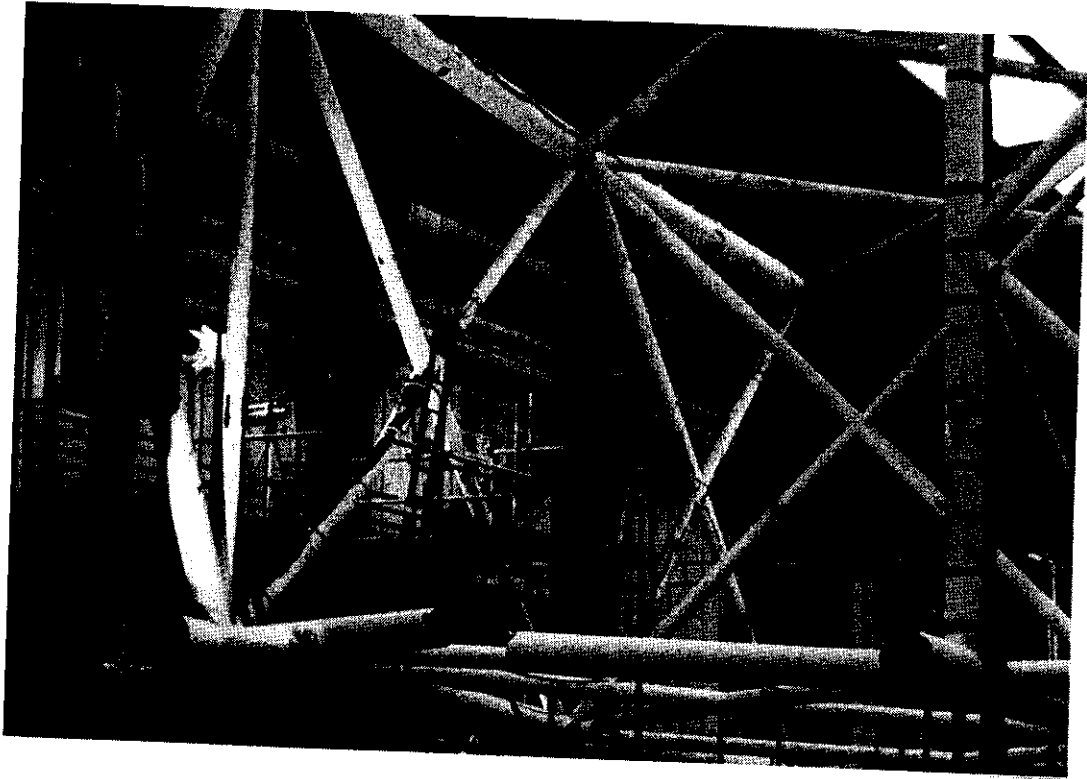


Figure 2.17 Loadcase 2 - Scan 45 - end of test

#### 2.2.4 Comparison with Phase I 2D Results

A principal consideration in configuring the Loadcase 2 test scenario was the need to provide continuity from earlier research on isolated components and 2D frames, in order that 3D system effects could be clearly distinguished. In general this objective was achieved as illustrated in Figure 2.18 which shows the global and critical component responses for the 3D Loadcase 2 test and Phase I Frame II 2D test scenario<sup>(2)</sup>. The test setups are shown in Figures 1.6 and 1.3. The absolute values displayed on the graphs cannot be compared directly because of differences in material and due to gravity, but Section 3.1 provides a detailed non-dimensional comparison. However, although the overall characteristics appear similar there are distinct differences in the mechanisms of load redistribution beyond first component failure and these are discussed further in Section 5.

#### 2.2.5 Local X Joint Response

The primary X joint in Frame E was heavily instrumented to provide complete information on the local response characteristics. Layout drawings in Appendix B show the position of sets of four site installed strain gauges on the braces to either side of the joint. Those closest to the joint are denoted 'Near', the second set 'far'. In addition, a displacement transducer straddled the chord attached along the centreline axis of the compression braces, 82 and 84. Load cells provide accurate data on the coacting axial forces in the brace and chord members.

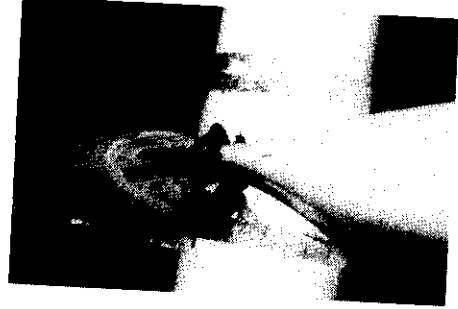
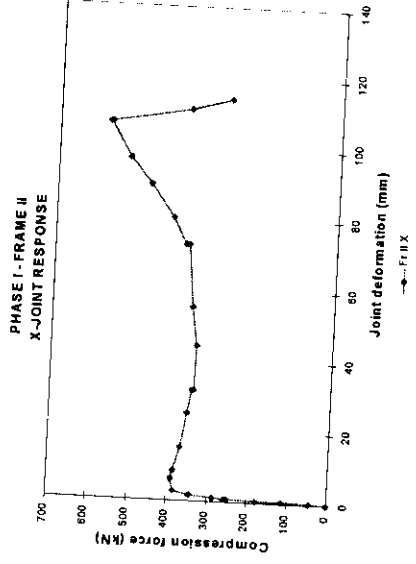
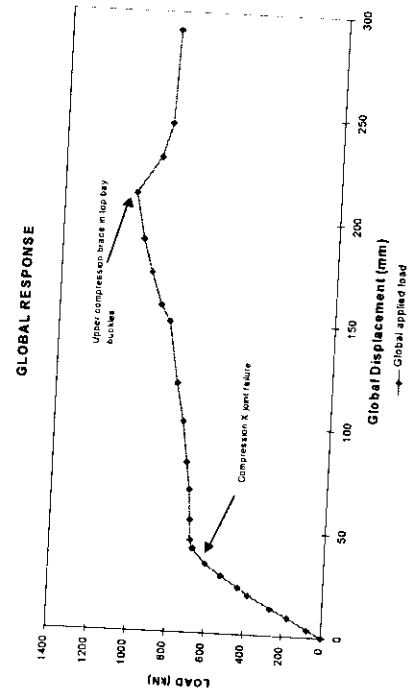
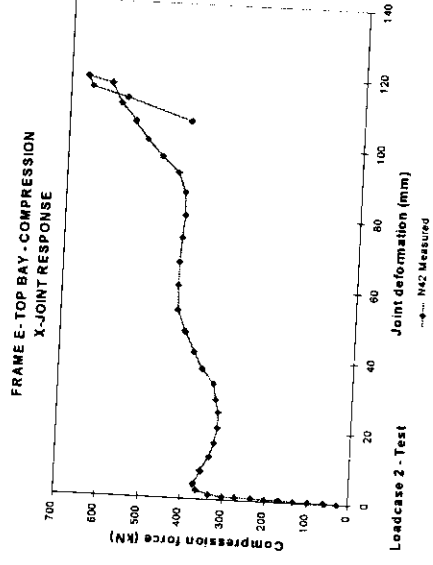
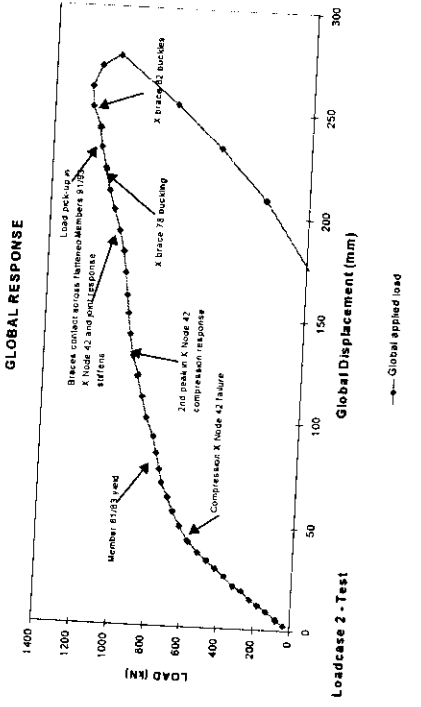


Figure 2.18 Comparison of 2D and 3D ultimate frame responses following primary X joint failure



#### 2.2.5.1 Load deformation response

The top central graph in Figure 2.18 presents the load deformation response for the compression X joint. As described in Section 2.2.3, the load carrying capacity fell away initially as the ligament in the chord wall arched, increasing again as the weld sections came into contact through the chord but then declining as the footprints rolled against each other. Once the chord sections were fully flattened the strength then increased and load transfer only ceased when the buckling capacity of the incoming braces was reached.

The corresponding response in the earlier 2D frame tests is shown in the lower diagram of Figure 2.18. The local undulations in the response were not seen in that test, and flattening of the chord was a gradual but continuous process. Nevertheless, for practical purposes in terms of providing input to system strength analysis, the response characteristics may be considered comparable.

Certainly in comparison with the chord diameter ( $D$ ) there is reasonable corroboration that the initial peak in capacity is attained when the deformation is some 2-3%  $D$ , and that with deformations around 50%  $D$  there is a substantial pick up in stiffness as the outer regions of the brace footprints contact through the chord. In terms of capacity however, the comparison between the graphs in Figure 2.18 is purely qualitative - the chord wall properties and levels of gravitational forces acting differ significantly between the two tests.

#### 2.2.5.2 Combined bending and axial action

The site installed strain gauges enable the pattern of local load transfer through the primary X joint to be examined. Figure 2.19 plots the axial forces determined in the braces throughout the tests based on the measured load cell values and the averaged readings from the four sets of site installed strain gauges. The load cells were pre-calibrated with known loads prior to being built into the structure, whereas the site installed strain gauges are used in conjunction with nominal section properties to determine the force. The conclusions from Figure 2.19 are that all the gauges appear to work satisfactorily throughout the test, that the actual section properties are comparable with the nominal values, and that irrespective of section distortions, the averaging of four orthogonal gauges is valid in determining axial effects.

Figure 2.20 then plots the individual strains recorded at each gauge within the four sets installed 200mm (near - N) and 400mm (far - F) from the chord face on Braces 82 and 84. These figures show immediately that the pattern of load transfer became quite uneven through the joint as it distorted.

For detailed examination of the figures the designation '1', '3', '5' and '7' requires clarification. Throughout the instrumentation system<sup>(10)</sup> in-plane gauges were placed in positions 1 and 5, and out-of-plane gauges were denoted 3 and 7. For the X bracing in Frame E the orientation is:



- 1 in-plane on the side of members towards Frame B
- 3 out-of-plane on the outside face of the structure
- 5 in-plane on the side of members towards Frame A
- 7 out-of-plane on the inside face of the structure, ie. towards Frame D.

If loads were being transferred purely axially, the recorded strains at all four positions would be equal. If load transfer were even but with a degree of bending, the average of in-plane and out-of-plane gauge pairs would be equal.

As initial failure of the joint is approached, the graphs in Figure 2.20 indicate that the strain (force) distribution is reasonably even but with a slight tendency for greater transfer along the in-plane axis (square symbols) rather than across the saddle region. Indeed as the joint deforms beyond the initial peak, the effect becomes more marked. In particular for Brace 84 it can be seen that strains at gauges on the outside face of the member (Gauge position 3 - diamond symbols) reduce significantly indicating a growing out-of-plane bending action.

A similar effect can be seen on the inside face of Brace 82. With references to Figure 2.18 (top right photo) and Figure 2.15, it can be confirmed that the reduction in load transfer capability is associated with the crack formation and greater flexibility at these locations around the intersection. The locations of the cracks, uneven load transfer, and twisting of the node, induce bending within the brace members. The eventual buckling of Brace 82 followed the sense of bending induced by the rotation at the node and the low buckling capacity is attributable to the reduced constraint. Where Brace 82 buckled under a net load of 537kN a nominally identical brace in the other bay of Frame E buckled at 630kN.

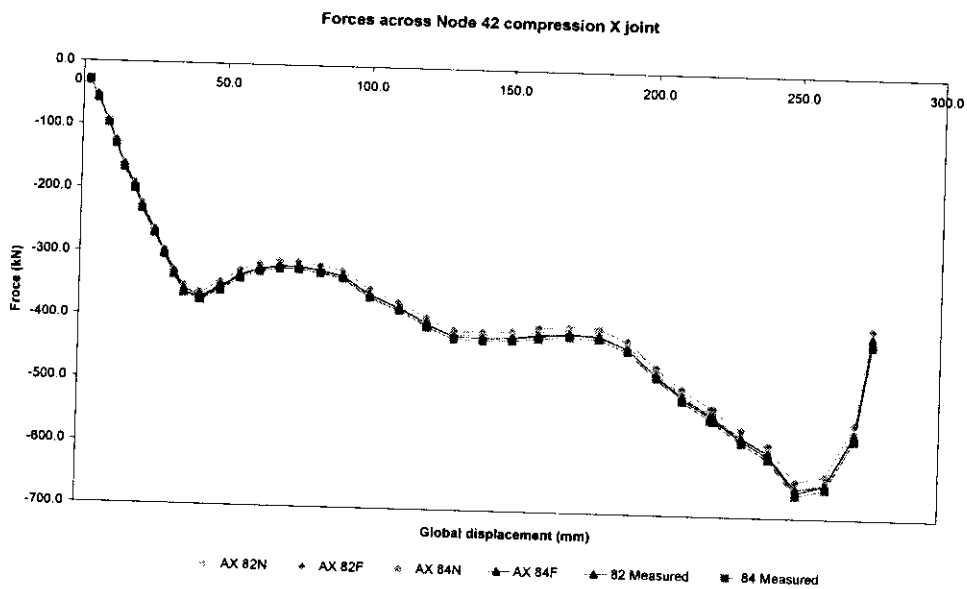
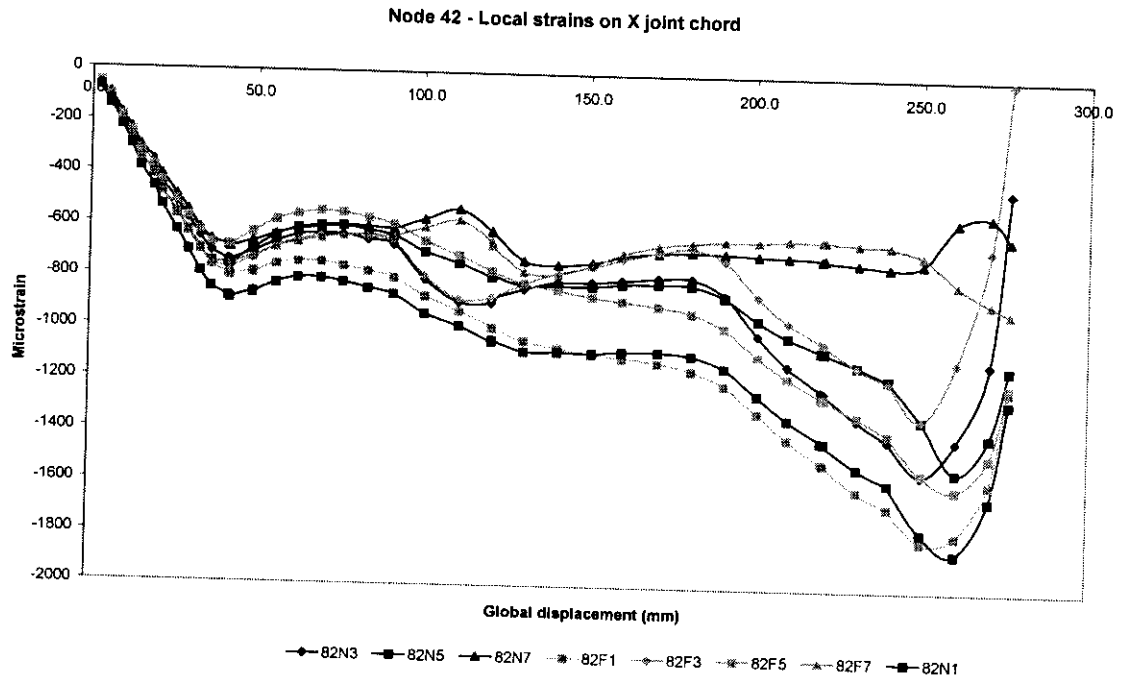
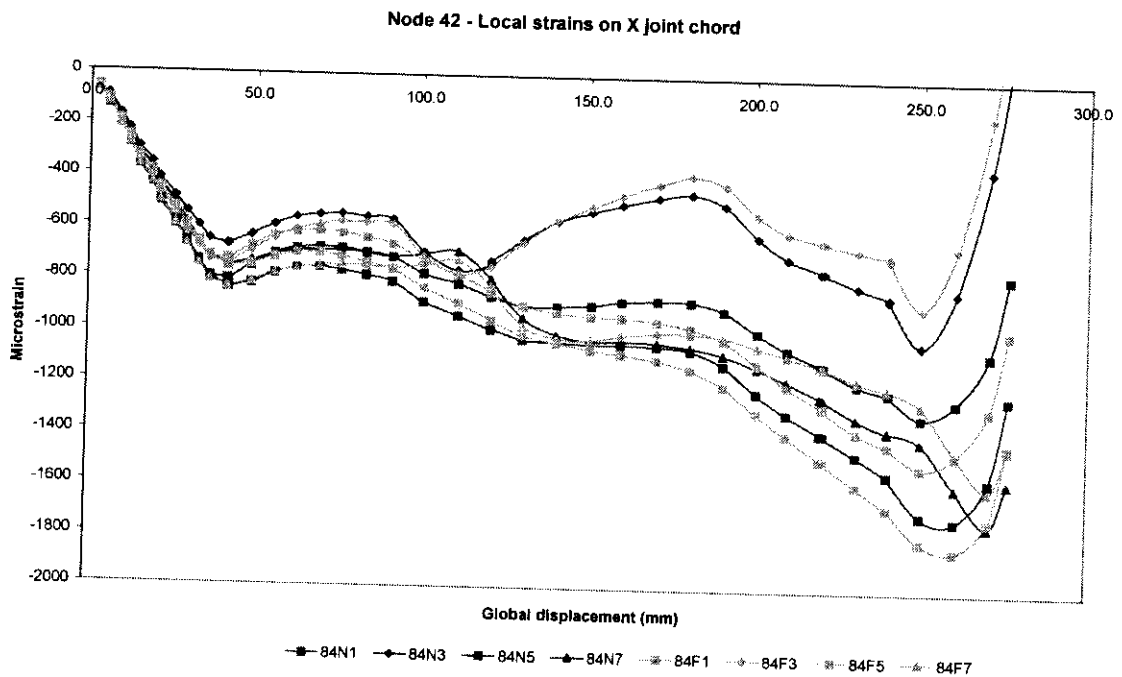


Figure 2.19 Correlation between axial forces in Braces 82 and 84 determined from strain gauges and load cells



(a) Brace 82



(b) Brace 84

Figure 2.20 In- (1, 5) and out-of-plane (3, 7) strains from gauges at near (N) and far (F) positions on braces at X joint Node 42



### 2.2.5.3 Buckling response

Detailed instrumentation was also provided on compression Braces 78 and 80 in Frame E to monitor the growth of in- and out-of-plane moments where buckling was anticipated. As shown in the drawings in Appendix B, the load cells were supplemented with four site installed strain gauges at orthogonal positions at the centre of each member.

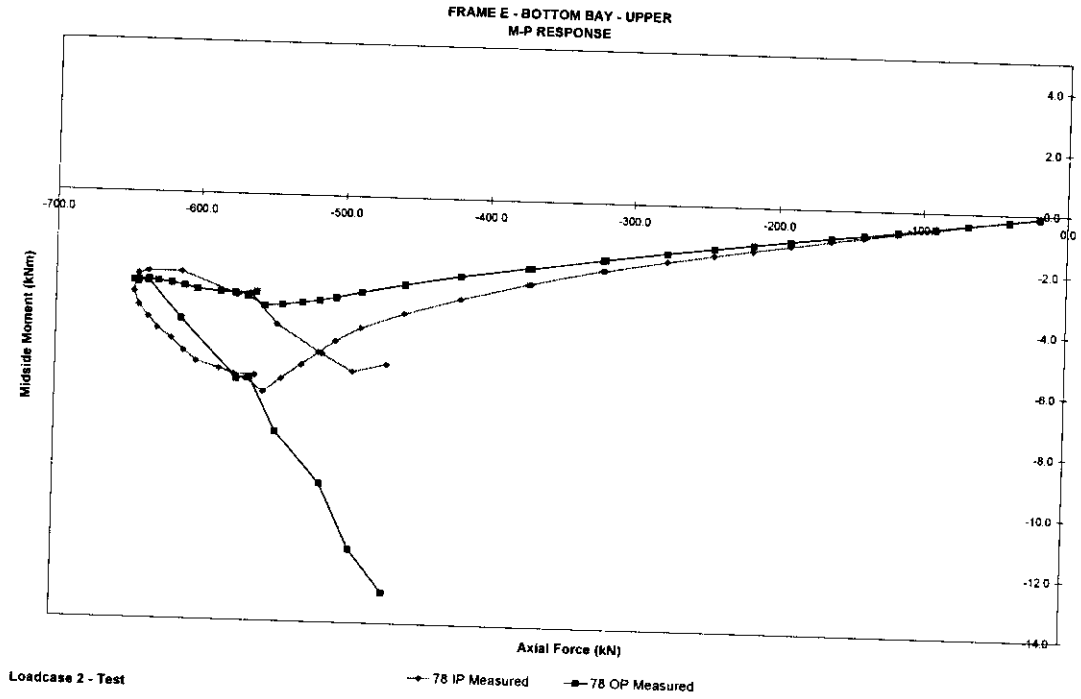
The axial moment relationships recorded in the Loadcase 2 test are plotted in Figure 2.21. In line with the sign convention described in Section 2.2.5.2, positive in-plane curvature corresponds to arching of the member towards Frame B and out-of-plane arching to the outside of the structure is positive.

It can be seen that from the outset of the test bending effects were greater in Brace 78 than 80 and indeed at Scan 37 Brace 78 buckled inwards and towards Frame A (see Figure 2.12). As buckling is approached the traces in Figure 2.21 show how the bending moment reduces slightly.

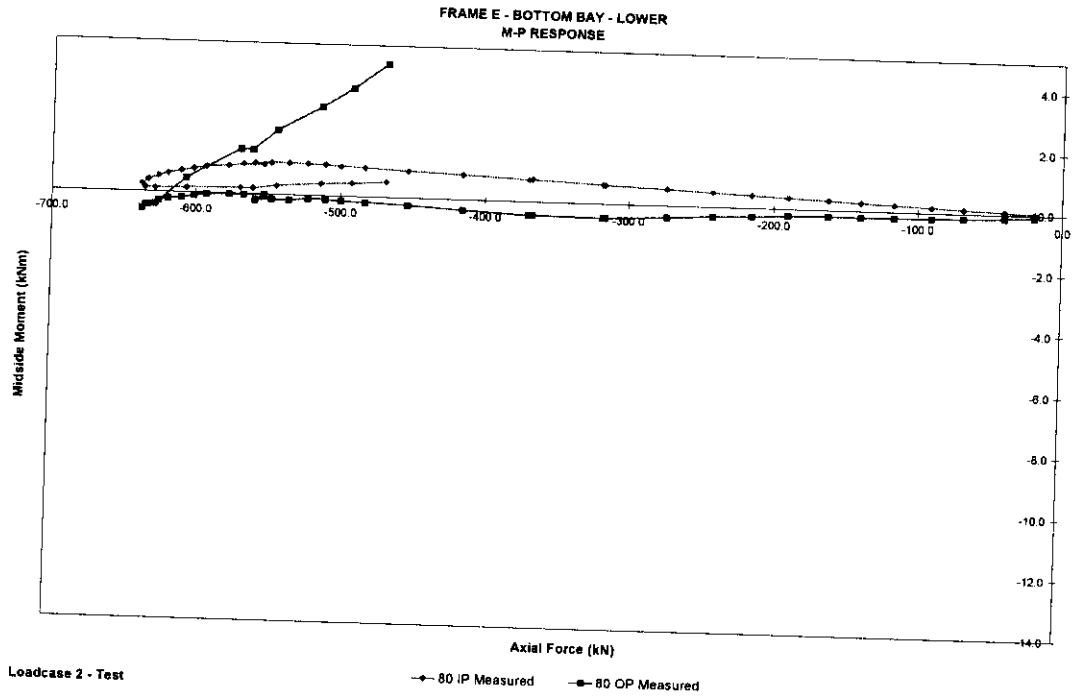
More detailed examination of buckling capacities and response characteristics is reported in the companion report on the Loadcase 3 test (see Foreword) in which multiple member failures were generated.

## 2.3 QUANTIFIED SUMMARY OF RESULTS

For ease of reference in the subsequent evaluation of the results, the key event and associated forces described in Section 2.2 for the Loadcase 2 test, are summarised in Table 2.3.



(a) Brace 78



(b) Brace 80

Figure 2.21 Axial-moment relationships in Frame E compression braces

Table 2.3 Loadcase 2 - Key events and measured load effects in response to applied load (see Note 1)

Scan	Event	Averaged capacity (kN)	Applied actuator load (kN)	Backup to component capacity <sup>(2)</sup>				For joints - coacting chord loads				Component properties <sup>(3)</sup>			Chord stress (N/mm <sup>2</sup> )
				Brace 1 No	Force (kN)	Brace 2 No	Force (kN)	Chord 1 No	Force (kN)	Chord 2 No	Force (kN)	Yield (N/mm <sup>2</sup> )	D (mm)	T (mm)	
15	Compression X Joint 42 - initial peak load	-373 -248	577	82	-372.0 -248	84	-374.5 -248	81	471.6	83	465.7	168.6	4.42	205.5 211	
21	Yield - X braces 81 / 83	706 718	748	81	709.4 721	83	701.9 715					168.6	4.41		
28	Compression X Joint 42 - second peak load	-426 -300	917	82	-423.9 -300	84	-427.9 -301	81	715.9	83	708.9	168.6	4.42	312.5 318	
37	Buckling - X brace 78	-639 -630	1114	78	-642.8 -634	80	-635.1 -626					168.6	4.36		
42	Buckling - X brace 82	-662 -537	1197	82	-659.3 -535	84	-664.6 -538					168.7	4.60		

Notes:

1. Forces recorded by load cells in response to applied load presented in roman type. Net member forces, corrected for gravitational offset and locked-in fabrication forces using Table 2.2 shown in italics
2. Source C636\39\008w.xls
3. For joints local chord properties  
For members - selected 'typical' properties from segments (C636\06\294W-b)

### 3. COMPONENT TESTING AND ANALYSIS

#### 3.1 OTHER FRAMES PROJECT INFORMATION

##### 3.1.1 Basis of 2D Investigations

Phases I and II of the Frames Project<sup>(2, 4)</sup> provided important results bridging the gap between isolated test databases of components and their real performance in the context of a three dimensional structure as demonstrated in the Phase III tests. Figure 3.1 provides a schematic representation of the interrelation.

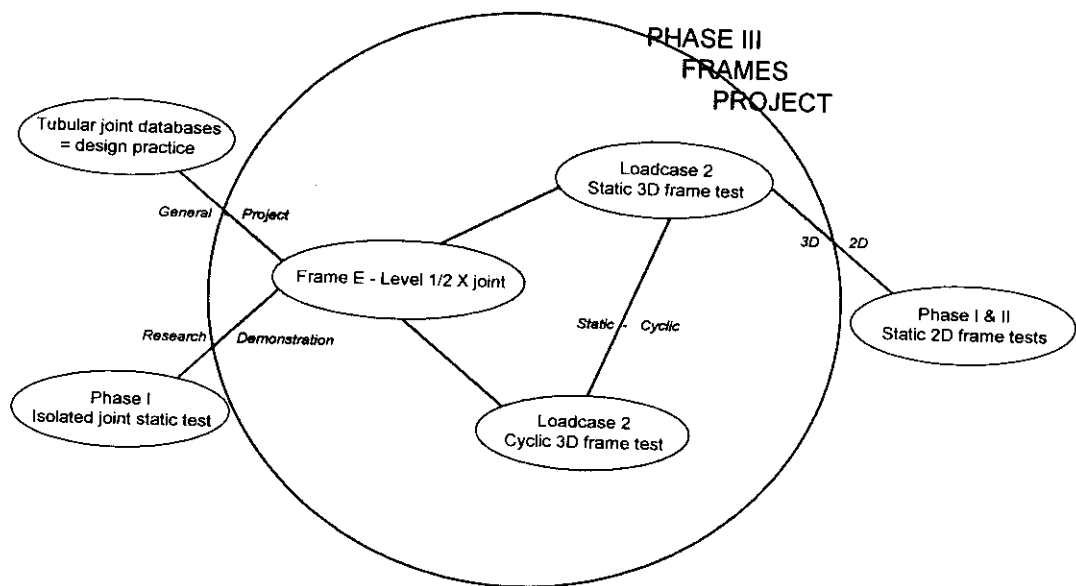


Figure 3.1 The context of Loadcase 2 and X joint investigations

The so-called 'Frame II' test shown in Figure 1.3 was particularly significant as, for the first time, a frame was tested to collapse in which a joint was the most highly utilised component in the context of current design practice<sup>(eq. 14)</sup>. The absence of a joint can within an X joint is typical of many older style jacket structures. At the time the experimental results were unexpected in that, although the limiting capacity of the joint was reached, the ductility and potential for redistribution were such that the structure as a whole continued to sustain increasing levels of applied load.

##### 3.1.2 Structural System Reserve Strength

The ultimate system strength achieved was some 3.9 times the design load level although the utility of this capacity in a cyclic storm scenario was questioned given the gross deformations (see joint photograph in Figure 2.18). A number of factors contributed to this strength:



1. the known 'safety factors' in determining the design capacity
2. the known bias in the characteristic capacity equations
3. the mobilisation of alternative loadpaths in a configuration and with levels of utilisation to absorb these loads
4. The higher than anticipated capacity of the critical X joint.

The first two points are a necessary and appropriate part of engineering practice. The third point is important in the context of the present tests as discussed in Section 1.2. In the 2D frame there was a mid-height horizontal between the two X-braced bays. In one bay there was a relatively weak X joint. In the other bay the braces were heavier walled. These factors gave adequate capacity for redistribution. In the Loadcase 2 3D test, both bays of bracing in Frame E have nominally identical properties. There is no horizontal in-plane but X bracing out into the 3D structure offer the potential for redistribution. Comparisons are made in Section 5.

### 3.1.3 X Joint Capacity Results

The final point, 4, will be investigated further here with reference to the accumulated evidence from the Frames Project research to date. Particular elements include:

- Frame II test in which a  $\beta=1.0$  compression X joint was the critical component<sup>(2)</sup>
- Frame IV test, nominally identical to Frame II but with a pre-fatigued crack at the X joint weld toe<sup>(2)</sup>
- Results from a nominally identical joint tested in isolation with brace and chord loads<sup>(2)</sup>
- Frame V test in which initial failure of a  $\beta=1.0$  compression X joint was generated<sup>(4)</sup>
- FE analysis undertaken by van der Valk<sup>(11)</sup> to investigate the influence of chord loads on compression X joint capacity
- Supplementary FE analysis by BOMEL in Phase IIA of the Frames project<sup>(6)</sup>.

Quantitative results from the four experimental programmes are summarised in Table 3.1. The results are presented in non-dimensional terms to allow for the different wall thicknesses and material types used. In each case comments are made concerning the validity of the results and applicability to jacket structures.

It will be shown in Section 4.2 that the mean X joint capacity underlying the then current HSE Guidance<sup>(17)</sup>, in non-dimensional terms, was 33.1. Not only does this reflect current engineering practice but it is also a direct output from isolated test results embodied in the database. In comparison with Table 3.1 it would therefore appear that the isolated test was typical of results in the wider body of data in the open literature. However the test observation was that failure was unsymmetric as the joint moved out of plane facilitated by the pinned constraints at the brace and chord supports. In contrast the joint in the frame stayed completely within the plane and compression of the chord wall was symmetric.



Table 3.1 Non-dimensional X joint capacity from earlier Frames Project studies<sup>(2, 4)</sup>

Investigation	First peak capacity $P_u / F_y T^2$	Notes
Frame II	46.1	No measure of locked-in fabrication forces. Symmetric failure, pickup in load once braces contacted
Frame IV	42.0	Joint cracked. No measure of locked-in fabrication forces. Symmetric failure. Pickup in load once braces contacted
Isolated Test	34.0	Chord tension = brace compression - in other tests chord tension > brace compression. Joint failed out-of-plane because of limited constraint at chord supports
Frame V	41.4	Locked-in fabrication forces measured and allowed for. Test intentionally stopped before gross deformation occurred.

As noted in Table 3.1 the potential significance of locked-in fabrication forces on structural performance had not been fully recognised at the time of the early frame tests and so the Frame II and IV data are likely to require some (downward) adjustment to account for these. Therefore taking the Frame V result as the most reliable indication of the capacity of a  $\beta=1.0$  compression X joint in a frame, suggests that the strength may be some 25% higher than the mean of the isolated test database.

For the purposes of re-assessing an existing structure such additional capacity may be extremely important and may help form the basis for continued operations without the need for strengthening.

### 3.1.4 Analytical Investigations of Chord Stress Effects

Analytical investigations therefore proceeded to try and explore the sources of additional strength. Key factors distinguishing the condition of the joint in a frame from typical isolated test conditions, were the framing continuity and high levels of coacting tension in the chord.

A project sponsor<sup>(11)</sup> performed finite element (FE) analyses to investigate the influence of chord load on the joint capacity. The results were compared with API and other design recommendations in which it is considered that compressive stresses in the chord reduce the available joint capacity whereas chord tensile stresses have no effect. The FE results are plotted in Figure 3.2 together with subsequent BOMEL analyses<sup>(6)</sup>.



The analyses were conclusive in suggesting that the compression capacity of a  $\beta=1.0$  X joint would actually reduce in the presence of chord tensile loads. This finding has apparently influenced the introduction of a chord stress capacity reduction factor in the ISO draft standard<sup>(19)</sup> but runs contrary to the experimental evidence from the frame.

However baseline analyses in the BOMEL investigations<sup>(6)</sup>, gave a non-dimensional capacity for the joint without chord load of 36.0 which is comparable to the results of tests in the database undertaken in similar conditions. Furthermore when the joint was analysed within the frame the response characteristic was comparable to the test results. Figure 3.3 shows how an initial peak in the capacity is reached followed by a degree of load shedding and subsequent stiffening. The load deflection response and degree of deformation can be compared with the test data in the central diagrams within Figure 2.18.

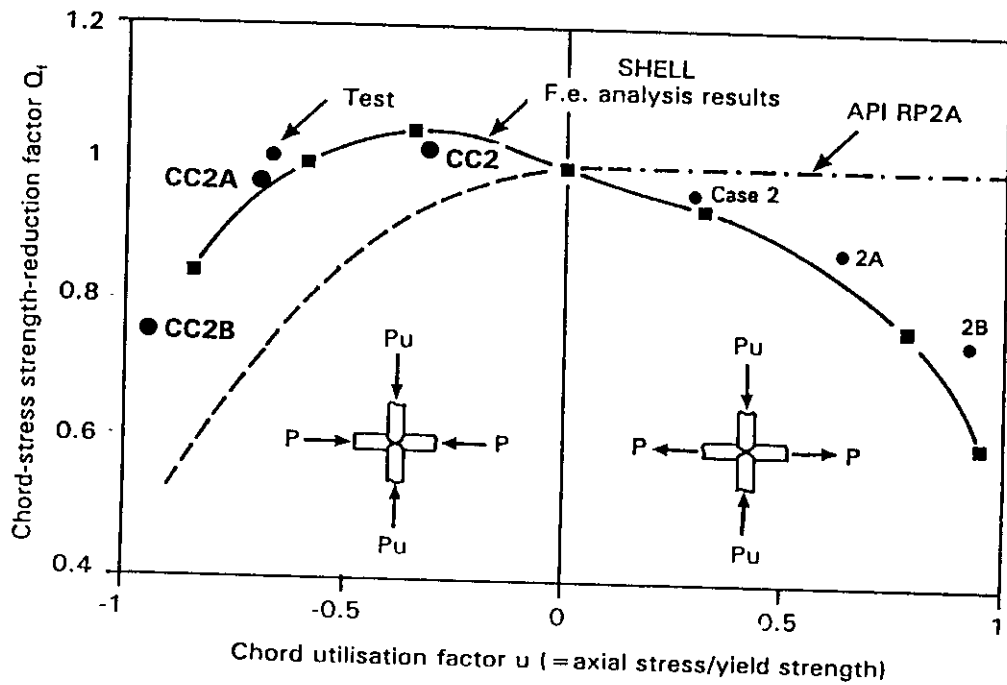


Figure 3.2 Comparison between API provisions<sup>(14)</sup> and analytical results<sup>(6,11)</sup> concerning the effects of chord load on  $\beta=1.0$  compression X joint capacity

### 3.1.5 Summary of 2D Investigations

In summary the strong evidence from the Frames project tests was that  $\beta=1.0$  compression X joint in a frame may be some 25% stronger than isolated databases indicate. However although the constraints of the surrounding frame are beneficial in enforcing a degree of symmetry supporting explanations for the enhanced capacity could not be found through analysis. In fact, to the contrary the analyses indicated that the presence of chord load would be reducing the joint capacity suggesting that in the absence of chord loads the capacities would have been even higher.

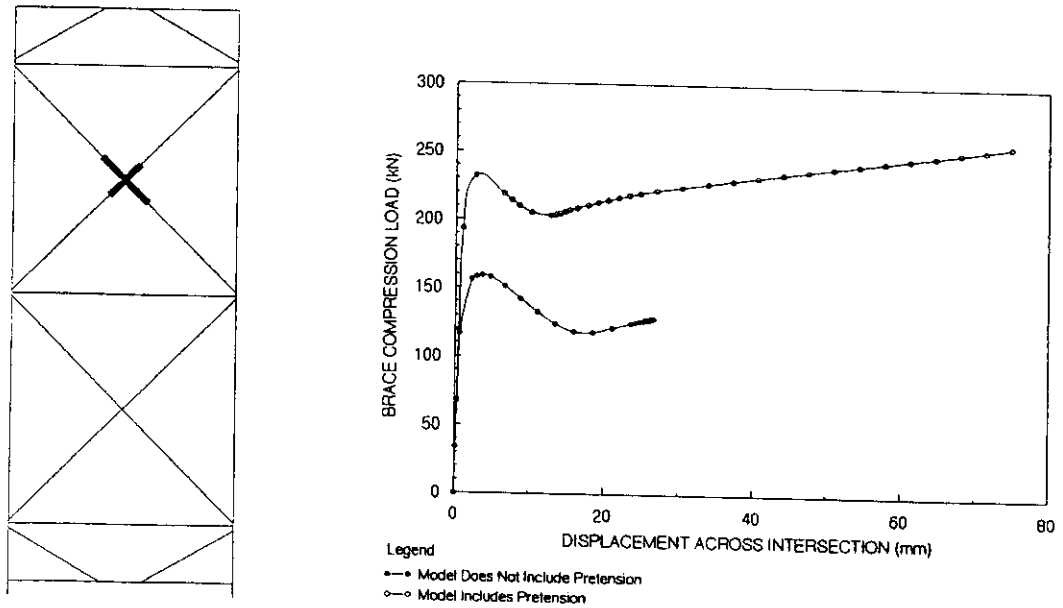


Figure 3.3 Analytical prediction of load deflection response for  $\beta=1.0$  compression X joint in frame<sup>(6)</sup>

### 3.1.6 Complementary Data from 3D Tests

As shown in the structural drawings in Appendix A, in addition to Node 42 three other X joints in the 3D structure were fabricated without joint cans. Node 18 in the Frame B X bracing (see Figure 2.2) experienced significant compressive forces in the Loadcase 3 scenario (see Figure 1.1) such that a peak in the capacity was reached. The load deflection data recorded by load cells and a displacement transducer straddling the joint are plotted in Figure 3.4. The rapid load shedding just beyond the peak is precipitated by buckling in a transverse plane which reduced the load transferred into Frame B.

The full details of the Loadcase 3 test response are provided in a companion report (see Foreword) but the X joint results are extracted here to provide further evidence for the in-frame capacity. Specific parameters for the Node 18 joint in the Loadcase 3 test are as follows:

- Chord diameter,  $D = 168.8\text{mm}$
- Chord thickness,  $T = 4.52\text{mm}$
- Chord yield,  $F_y = 289.4\text{ N/mm}^2$
- Peak measured capacity,  $P_u = -321.3\text{ kN}$
- Locked-in fabrication force = 53 kN (see Table 5.12, Reference 9)
- Gravity = +1 kN (see Table 3.1, Reference 9)

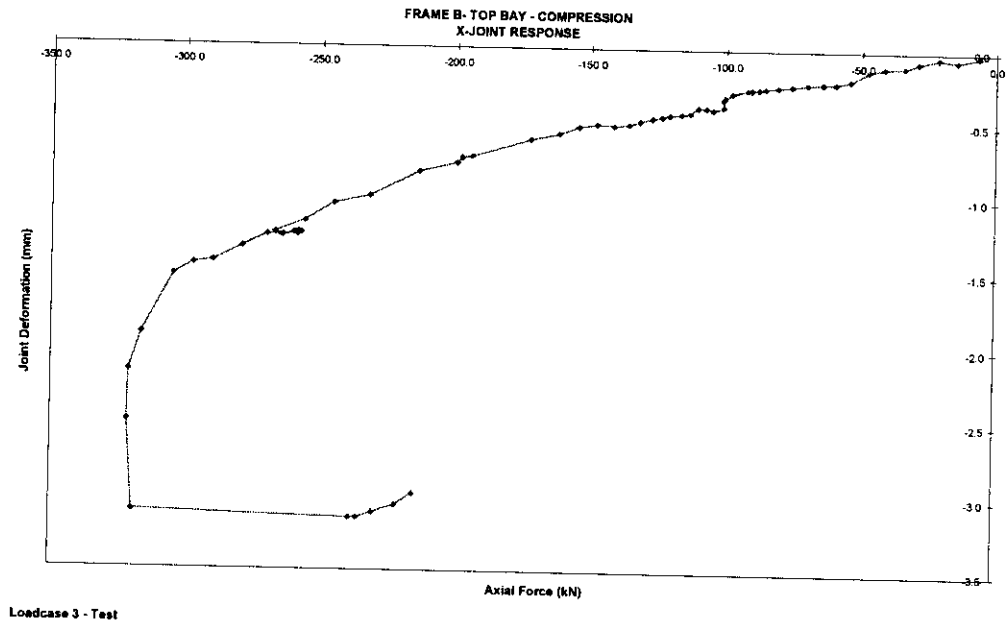


Figure 3.4 Loadcase 3 - Node 18 - compression X joint response

The initial pretensions in the member serve to reduce the net compression at the point of failure to -267 kN which give a non-dimensional capacity ( $P_u / F_y T^2$ ) of 45.2 some 37% greater than the HSE database mean.

This result together with the earlier findings are carried forward to the discussion in Section 5.1.

## 3.2 SAFJAC FRAME RESPONSE PREDICTIONS

### 3.2.1 Background

As part of BOMEL's contribution to the 3D Frames Project, blind predictions of ultimate strength were submitted to the benchmark exercise. For the Loadcase 2 scenario X joint response characteristics were assumed for the connection between Levels 1 and 2 on Frame E.

Within SAFJAC the joint response characteristics, at the time of the benchmark analysis, were based on the HSE mean capacity formulations<sup>(17)</sup> together with five-part piece-wise linear load-deflection relationships devised from the corresponding HSE isolated joint database available in the first phase of the project<sup>(2)</sup>.

The specific characteristics were based on nominal section properties but measured yield stress data. No enhancement to the HSE mean was allowed for by the analyst even though there was evidence from the background data available to all Benchmark Analysts that the capacity in the 2D frames had been some 25% higher than anticipated.



### 3.2.2 Comparison between Predicted and Measured Responses

The effect of these characteristics on the frame response predictions is shown in Figures 3.5 to 3.8, in comparison with the measured results for the Loadcase 2 test. These prediction data were provided to the instrumentation contractor prior to testing and were used as a basis for on-line comparisons throughout the Loadcase 2 test.

The analysis output has been adjusted to give a datum at the point the structure is hanging under gravity but with zero applied load. For example, for Braces 82 and 84 through the compression X joint (Figure 3.7), the capacity was based on the HSE mean of -183kN but given an initial pre-tension of 33kN due to gravity at the start of the test the apparent failure load is some -216kN. The effects of any locked-in fabrication forces were not allowed for, but in the case of braces 82 and 84 were significant, contributing 83kN to the discrepancy between predicted and measured values.

In general the correlation between predicted and measured response characteristics is good even though the actual capacity of the primary X joint was higher than anticipated. However with reference to Table 2.1, it can be seen that the locked-in fabrication stresses influenced the sequence of failures. Furthermore the presence of locked-in tension in Brace 82 served to delay the buckling failure despite the reduced rotational constraint at Node 42 which was acting to precipitate an earlier failure. Indeed the close correlation between the predicted and measured responses is, to a degree, a fortuitous consequence of the practical influences affecting the real structure performance compensating for each other.

In many circumstances, despite all the imperfections being detected in the tests, their influence will cancel out. However the sense of locked-in fabrication forces is generally not controlled and depends on the sequence of fabrication. It is therefore important that future analyses allow for imperfections in a rational manner.

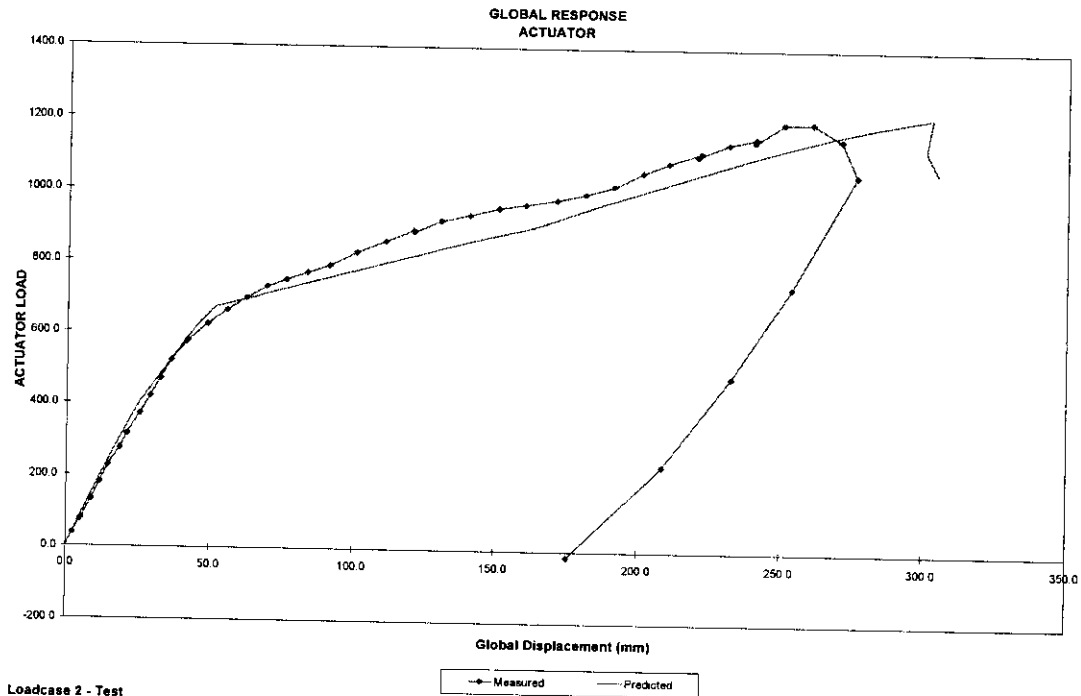


Figure 3.5 Comparison between SAFJAC predicted and measured global response for 3D frame in Loadcase 2

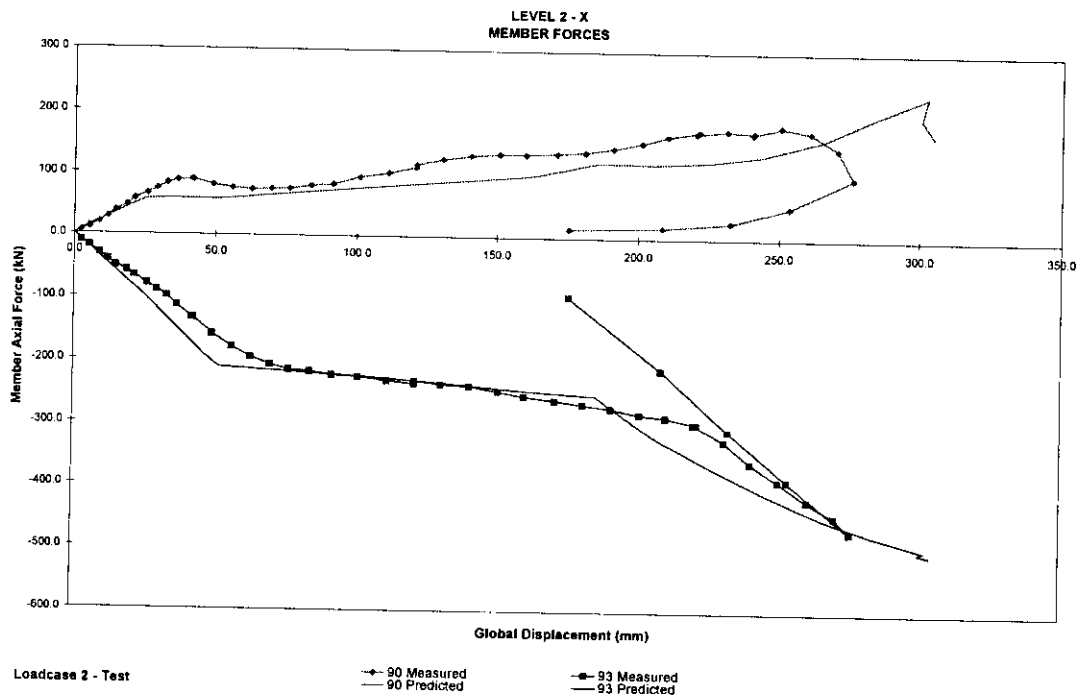


Figure 3.6 SAFJAC - Loadcase 2 - test comparison of 3D load distribution through Level 2 X bracing

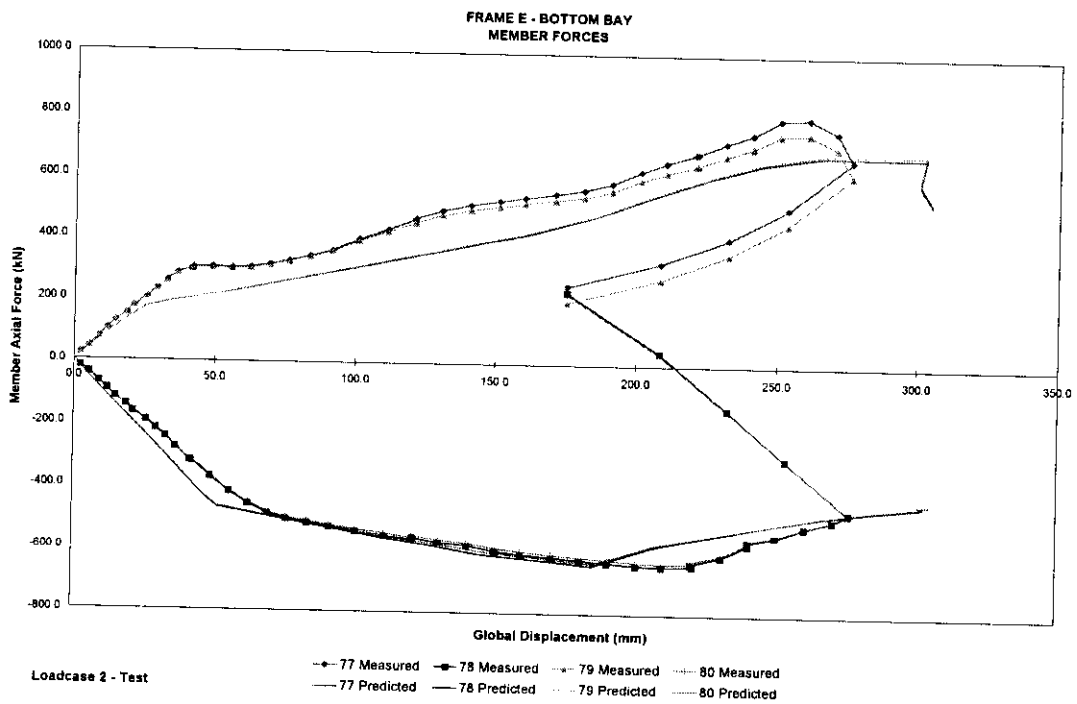
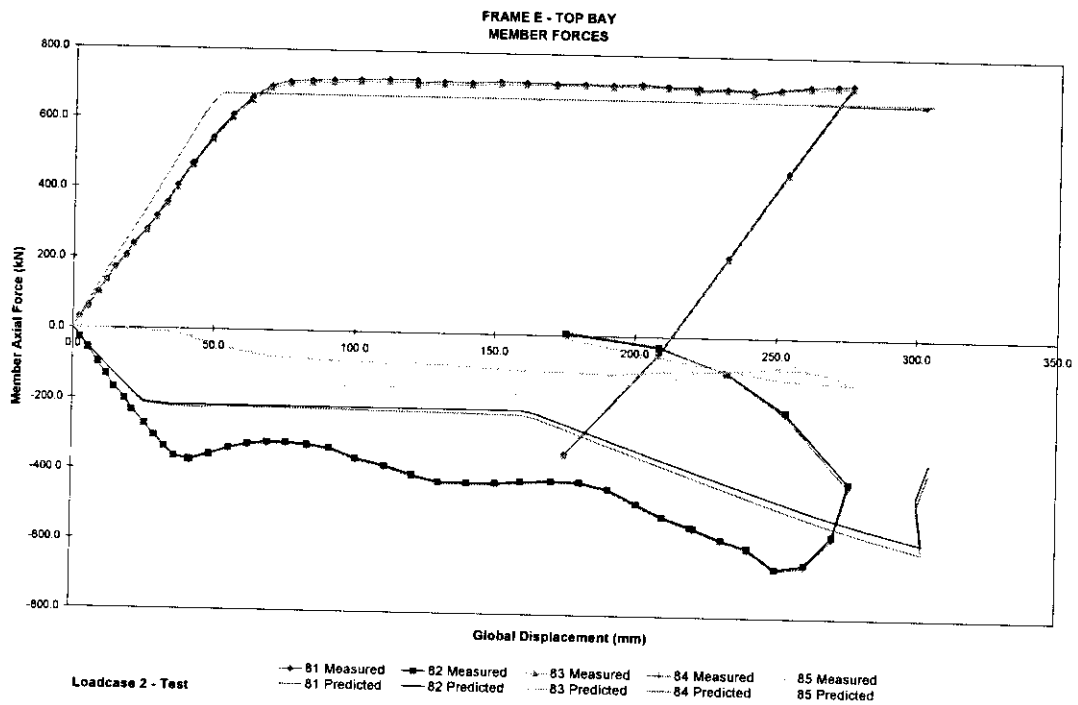


Figure 3.7 SAFJAC - Loadcase 2 - test comparison of primary brace forces through Frame E

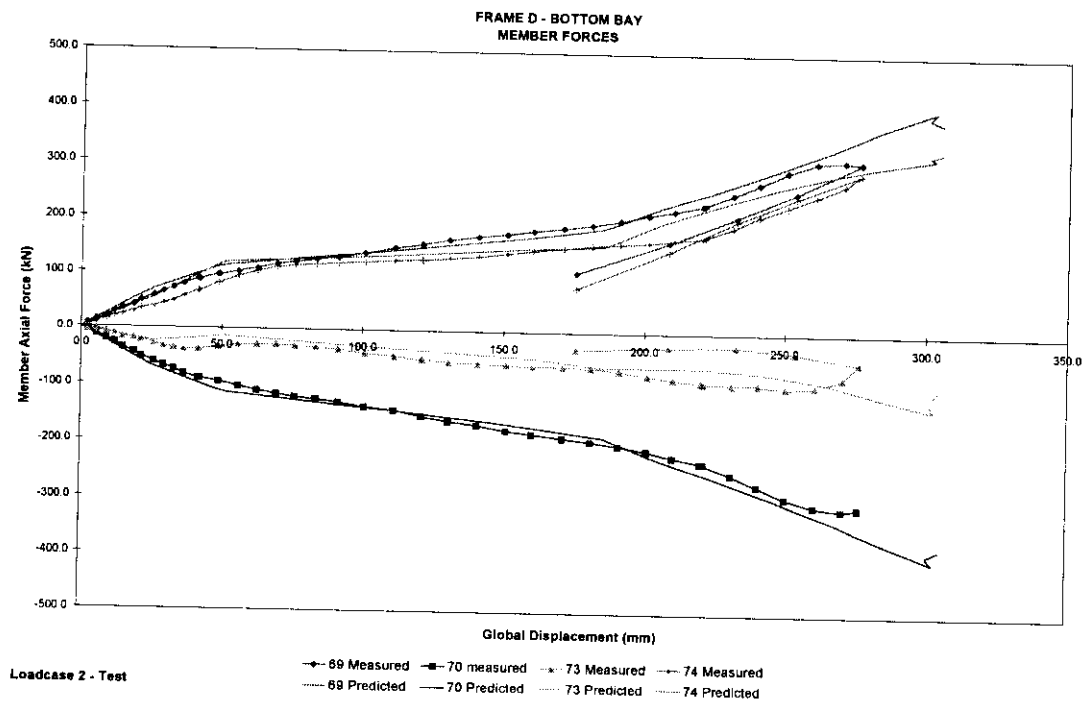
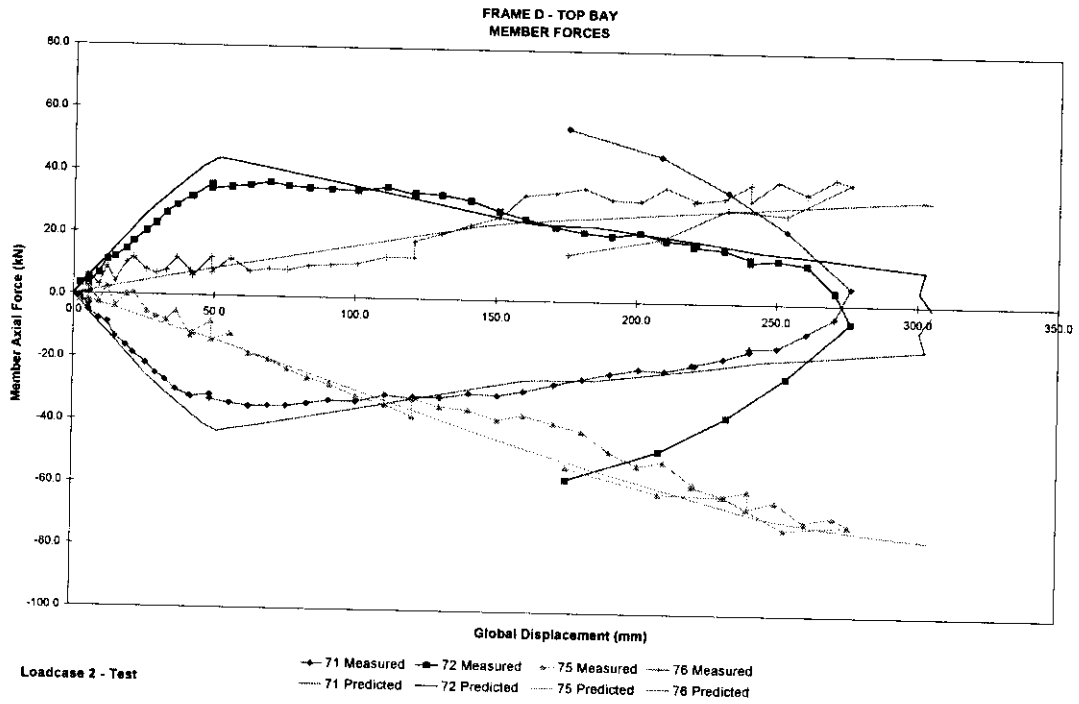


Figure 3.8 SAFJAC - Loadcase 2 - test comparison of primary brace forces through Frame D



## 4. INDUSTRY PRACTICE

### 4.1 PREAMBLE

In addition to comparative evidence from associated test programmes and analysis, an important reference base for interpreting the 3D frame tests is current engineering practice. Over the years component tests have been performed and the findings have been generalised and introduced into codes of practice. With time greater understanding of factors affecting joint behaviour has developed and databases have been rescreened and supplemented. Where necessary codes and standards have been revised.

For tubular joints many alternative formulations are available. Those particularly relevant to offshore practice include:

- API RP2A<sup>(14, 15)</sup>. The equations were developed as lower bound formulations to what is now considered to be a fairly limited database<sup>(16)</sup>. Their original introduction was in working stress design (WSD) practice but they are now also adopted in load and resistance factor design (LRFD).
- HSE<sup>(17)</sup>. An extended database was developed to determine mean and hence characteristic formulations for joint capacity. Although HSE 4th Edition Guidance is now formally withdrawn, the background document provides a useful reference base.
- BOMEL Tubular Joints Guide<sup>(18)</sup>. The remit to BOMEL's Tubular Joints Group was specifically not to develop new formulations. Improved data searches and screening criteria were to be used to develop more reliable databases against which published formulae were to be assessed. The recommendations varied with joint type but for DT/X joints in compression the 'best' offshore formulations were those from HSE Guidance<sup>(17)</sup>.
- ISO 13819-2 (Draft)<sup>(19)</sup>. The development of a harmonised international standard for fixed offshore structures took as its baseline API RP2A<sup>(15)</sup>. Wherever possible this practice was to be adopted but where necessary changes could be introduced. For tubular joints the static strength equations have been replaced in entirety. The draft standard includes characteristic capacity, bias and COV data enabling the underlying mean formulae to be deduced.

On the basis of the above, the Loadcase 2 X joint results are compared against API<sup>(14)</sup>, HSE<sup>(17)</sup> and ISO<sup>(19)</sup> capacity equations which in turn are used as a basis for correlation with the body of isolated component test data.





## 4.2 PLANAR JOINT CODE CAPACITY FORMULATIONS

The capacity equations for X joints in compression are reproduced in Table 4.1 below in order that the different influencing factors can be seen. However for further detail on the background, reference should be made to the source documents. In all cases the capacity equations take the form:

$$\text{Axial force: } P_u = \frac{F_y T^2}{\sin\theta} Q_u Q_f \quad (4.1)$$

$$\text{Moment: } M_u = \frac{F_y T^2 d}{\sin\theta} Q_u Q_f \quad (4.2)$$

where:	$F_y$	= chord yield stress
	$T$	= chord wall thickness
	$\theta$	= brace angle
	$Q_u$	= geometry factor in Table 4.1
	$\beta$	= brace / chord diameter ratio ( $d/D$ )
	$\gamma$	= chord slenderness ( $D/2T$ )
	$Q_\beta$	= $0.3 / \beta(1-0.833\beta)$ for $\beta > 0.6$ ; $Q_\beta = 1.0$ for $\beta \leq 0.6$
	$\xi$	= gap ratio ( $g/D$ )
	$K_s$	= relative length factor = $0.5 (1 + 1/\sin\theta)$
	$Q_f$	= chord stress factor in Table 4.1.

To assess combined load effects the interaction formulae are also compared in Table 4.1 where the suffix 'L' denotes the load effects and 'R' the calculated resistance. The inclusion of partial load or resistance factors to give design values or comparison between acting and allowable depends on the code format in use.

Table 4.1 Code formulae for compression X joint capacity

Component	Reference		
	API <sup>(14)</sup> (lower bound)	HSE <sup>(17)</sup> (mean)	ISO <sup>(19)</sup> (mean)
Q <sub>u</sub> Axial	$(3.4+13\beta)Q_\beta$	$(2.98+15.45\beta)Q_\beta$	$1.158(2.8+(12+0.1\gamma)\beta)Q_\beta$
Q <sub>u</sub> IPB	$3.4+19\beta$	$(6.2\beta - 0.27) \gamma^{0.5}$	$1.235(4.5\beta \gamma^{0.5})$
Q <sub>u</sub> OPB	$(3.4+7\beta)Q_\beta$	$(1.88+8.64\beta) Q_\beta^{0.5}$	$1.139(3.2\gamma^{(0.5\beta^2)})$
Q <sub>t</sub>	<p>1 if all chord stresses are tensile</p> <p><math>1 - \lambda \gamma A^2</math></p> <p><math>\lambda_{\text{brace ax}} = 0.03</math></p> <p><math>\lambda_{\text{brace ipb}} = 0.045</math></p> <p><math>\lambda_{\text{brace opb}} = 0.021</math></p> <p><math>A = \frac{(f_{ax}^2 + f_{ipb}^2 + f_{opb}^2)^{0.5}}{F_y}</math></p> <p><math>f_{ax}, f_{ipb}, f_{opb} =</math> chord stress components</p>	<p>as API</p> <p>as API</p> <p>as API</p> <p>as API</p> <p>as API</p> <p>as API</p>	<p>1 if <math>\beta \leq 0.9</math> and all chord stresses are tensile</p> <p><math>1 - \lambda A^2</math></p> <p>as API</p> <p>as API</p> <p>as API</p> <p><math>\left( C_1 \left( \frac{P_D}{P_y} \right)^2 + C_2 \left( \frac{M_D}{M_p} \right)_{ipb}^2 + C_2 \left( \frac{M_D}{M_p} \right)_{opb}^2 \right)^{0.5}</math></p> <p><math>C_1=25, C_2=43</math> - all DT/X joints</p> <p><math>P_D, M_D</math> - factored load effects in chord</p> <p><math>P_y</math> = yield capacity of chord</p> <p><math>M_p</math> = plastic moment capacity of chord</p>
Interaction check ( $\leq 1.0$ )	$1 - \cos \left[ \frac{\pi}{2} \left( \frac{P_L}{P_R} \right) \right] + \left[ \left( \frac{M_L}{M_R} \right)_{ipb}^2 + \left( \frac{M_L}{M_R} \right)_{opb}^2 \right]^{0.5}$	$\left( \frac{P_L}{P_R} \right) + \left( \frac{M_L}{M_R} \right)_{ipb}^2 + \left  \frac{M_L}{M_R} \right _{opb}$	as HSE

### 4.3 AS-BUILT JOINT CAPACITY PREDICTIONS

Using the as-built properties for the Loadcase 2 joint at Node 42 the calculated axial capacities, neglecting any degradation due to chord stresses, are given in Table 4.2. Understandably the API lower bound formulation gives significantly lower capacities than the mean ISO or HSE values. The HSE and ISO values are comparable, with the axial capacity from the draft ISO standard being just 5% greater than the earlier HSE document.

However, it is important to note that no account has been taken of the chord stress reduction factor  $Q_r$ . In API and HSE practices  $Q_r$  is set to unity if all chord stresses are tensile. In the new ISO standard (see Table 4.1) the factor is retained in the case of DT/X joints with  $\beta > 0.9$ . Given the level of stress at Node 42 in the Loadcase 2 test, this would imply the axial capacity was only 58% of the strength without chord load. As discussed in Section 5 the measured capacity far exceeds code predictions and certainly does not suggest that  $\beta = 1.0$  compression X joint capacity is undermined by a high level of tension in the chord. The more conservative approach is to neglect  $Q_r$  in the data reduction. Further comments are made in Section 5.

Table 4.2 Loadcase 2 X joint capacity predictions from codes  
(Nodes 42:  $D = 168.6\text{mm}$ ,  $d = 168.6\text{mm}$ ,  $T = 4.42\text{mm}$ ,  $F_y = 279.5\text{ N/mm}^2$ ,  $\theta = 90^\circ$ )

Format	Reference		
	API (lower bound)	HSE (mean)	ISO (mean)
Axial capacity (kN)	-125.8	-181.0	-190.0
Non-dimensional Axial capacity	23.0	33.1	34.8

Figure 4.1 presents the strength predictions underlying the HSE and ISO documents together with API design values in comparison with the measured joint response data. It can be seen that the as-recorded data are corrected to account for both the initial pre-tension across the joint due to gravity effects and the locked-in fabrication force. Clearly the measured capacity was significantly greater than the databases underlying current engineering practice would suggest.

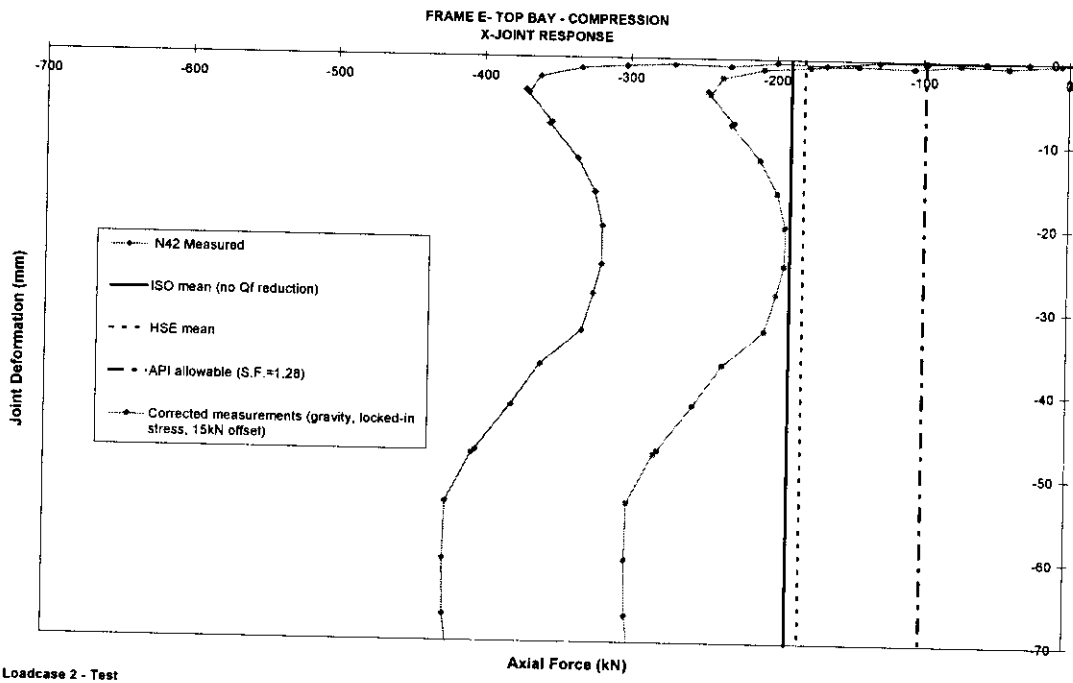


Figure 4.1 Comparison between measured and corrected joint capacities with predictions from databases / code of practice



## 5. ASSESSMENT OF LOADCASE 2 COMPONENT AND SYSTEM RESPONSES

### 5.1 JOINT CAPACITY DATA ASSIMILATION

In order to assimilate the data presented in the foregoing sections for the response of the  $\beta=1.0$  compression X joint, Table 5.1 brings forward the capacities and properties.

Table 5.1 Quantified comparison of joint data

Investigation	Source	Capacity (kN)	$F_y$ (N/mm <sup>2</sup> )	T (mm)	Capacity / $F_y T^2$
Loadcase 2 N42	Tables 2.2 & 2.3	-248	279.5	4.42	45.4
Loadcase 3 N18	Section 3.1	-267	289.4	4.52	45.2
Frames Project Ph I Frame II *	Table 3.1, Reference 6	-390	325	5.1	46.1
Ph I Frame IV (cracked) *		-396	393	4.9	42.0
Ph I Isolated X		-224	325	5.1	34.0
Ph II Frame V		-218	260	4.5	41.4
Former HSE Guidance (mean)	Table 4.2	-181	279.5	4.42	33.1
ISO draft (mean)	Table 4.2	-190	279.5	4.42	34.8
API (lower bound)	Table 4.2	-126	279.5	4.42	23.1
Note: * Potential for locked-in fabrication forces to influence the results. Effects measured and accounted for in all other cases					

The immediate observation is that the 3D demonstration structure has confirmed that the capacity of  $\beta=1.0$  compression X joints is significantly greater than the mean of databases underlying modern design practices would suggest. In comparison with form HSE Guidance<sup>(4)</sup> the measured strengths are some 37% greater, being reasonably comparable to the 25% strength enhancement in the 2D test of Frame V.

A number of factors arising from the previous sections should be noted as they all ensure that the assessment of strength enhancement is conservative:



- In all three cases noted above the effects of initial locked-in fabrication tensions have been accounted for and the apparent capacities reduced accordingly.
- Only the initial peak in the response has been considered. Where the joint subsequently distorted and carried extra load as the braces contacted through the chord, the higher strength has been neglected.
- No allowance for the presence of bending moments reducing the available axial capacity has been taken.
- The ISO code evaluation has neglected the detrimental effects of chord tension contained in the Draft provisions. Similarly although FE analyses have indicated the high chord tensions would reduce capacity this has been discounted.

On that basis the Phase III results confirm that the capacity of these joints is at least 25% greater than the mean of isolated test databases on which current design practice is based.

Furthermore the results call into question the validity of the chord stress reduction factor despite the analytical indications. The comparison with the Phase I isolated test, suggests that the frame constraints keeping the joint within the plane are a powerful influence on capacity within a structure. FE shell analyses have been shown to correlate well with the isolated results but symmetry is enforced in the analyses and it is therefore possible that this is masking a strength underprediction in the basic modelling, for example, due to the substantial weld effects around the intersections.

## 5.2 JOINT DEFORMATION COMPARISONS

Figure 5.1 compares the local load deflection characteristics recorded at Nodes 42 and 18 in the 3D frame with the original Phase I Frame II joint response. Given the different properties the capacities (with gravitational and locked-in stress effects accounted for), are plotted in non-dimensionalised terms. A suitable deformation non-dimensionalisation would be with respect to diameter which is the same in all cases.



Compression X joint - Load deformation responses

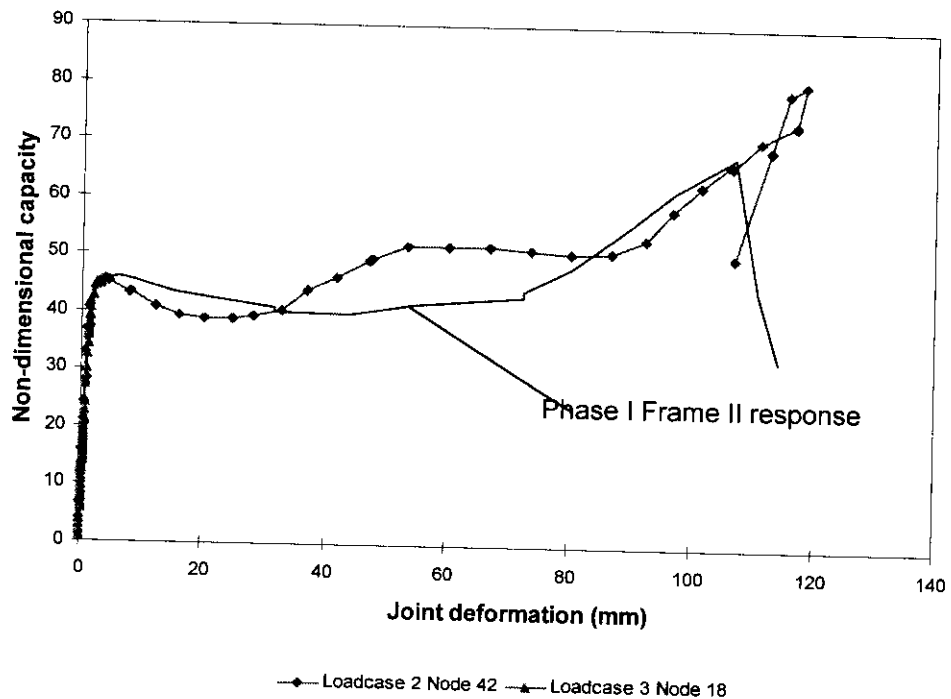


Figure 5.1 Local compression X joint response characteristics

There is strong confirmation that the response characteristics are typical of these  $\beta=1.0$  X joints which are a common feature of many existing offshore structures.

In Figure 5.2 comparison is made with the response characteristics embodied within the Frames Project ultimate strength analysis software SAFJAC. The piecewise linear response is defined in terms of the initial capacity of the joint, the incoming brace capacity, and deformations scaled in relation to the chord diameter.

The lower trace was that adopted in the benchmark analysis in which capacity was based on the former HSE<sup>(4)</sup> database. Although the general characteristic is reasonably well captured the initial capacity was underestimated. However accepting the 37% strength enhancement found in the frame tests and substituting this in the SAFJAC formulation generates a characteristic which matches the experimental results extremely well.

An alternative might be considered in which the load shedding beyond the initial peak is captured. However, as the tests have shown, this depends on whether the chord ligament between the saddle weld toes arches gently (as in Frame II) or bends with a more sudden instability (see Loadcase 2 response). Clearly the relative size of the ligament and the profile of the welds themselves will influence the response. The intersection of tubulars of nominally identical diameter is particularly difficult and the degree of cut back etc., may vary somewhat particularly in older structures. On that basis the representation of the joint characteristics with a plateau is reasonable in the context of an ultimate strength analysis of the structural system.

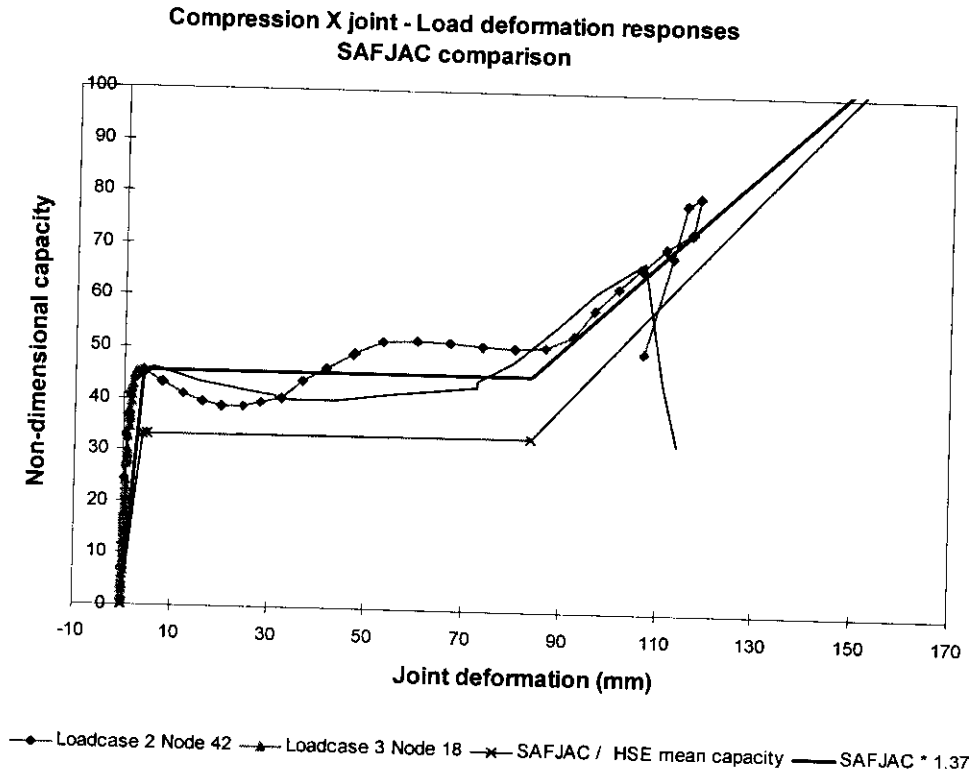


Figure 5.2 Comparison between SAFJAC and measured joint response characteristics

### 5.3 SYSTEM RESPONSE COMPARISONS

The foregoing discussion has centred on the local joint characteristics at the primary X node influencing the Loadcase 2 response. It has been confirmed that the behaviour is influenced by the frame constraints which then affect the distribution of forces through the structure and the global system capacity.

From an elastic design analysis standpoint, code checking shows the Frame E X joint to be critical. Assuming an API axial utilisation of unity for these nodes in a storm analysis, leads to the design load levels shown against the global frame response in Figure 5.3. The graph includes an approximate gravity offset to give a basis for direct comparison of applied load effects. Applying an actuator load of 57kN induces a force across the primary X joint approximately offsetting self-weight gravitational effects. Of course the same force does not negate the effects in other members exactly, nevertheless it serves as a sensible approximation.



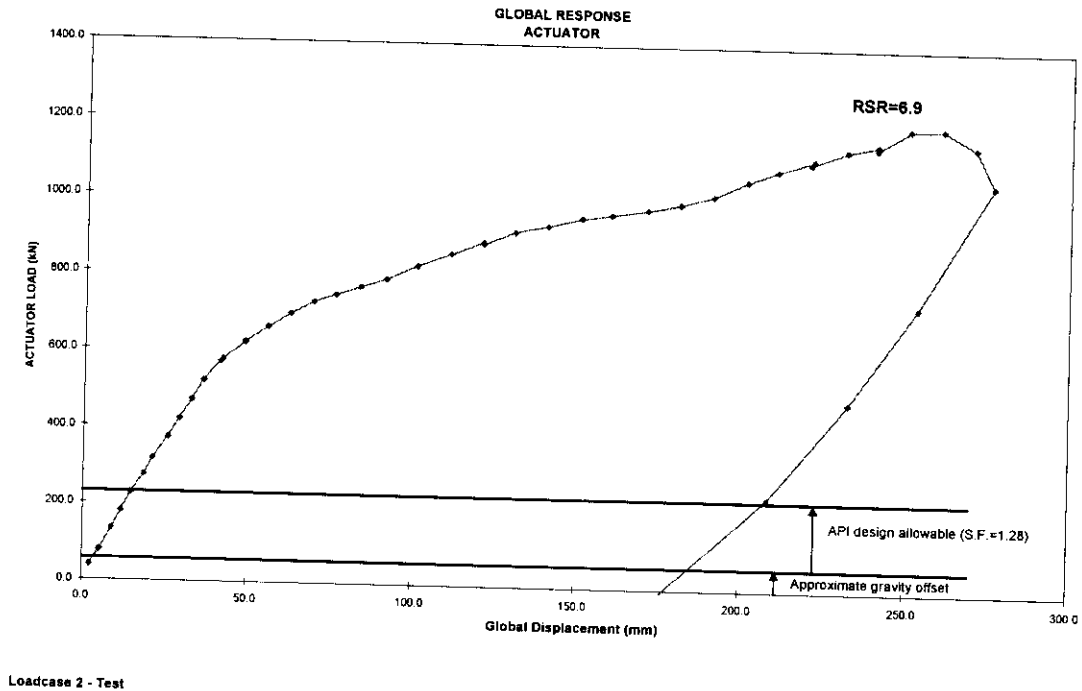


Figure 5.3 System reserve strength ratio

### 5.3.1 Reserve Strength Ratio

The figure is annotated to show the system Reserve Strength Ratio (RSR) comparing the ultimate capacity with the design load. In terms of the overall response the peak load was actually governed by buckling within Frame E with load redistribution following joint failure giving a massive RSR of 6.9.

Of course the reserve strength is dependent on the level of unused capacity in the surrounding structure. The 3D frame has been tested under a point load, in the Loadcase 2 test on Line E, and the surrounding structure is therefore able to accommodate significant levels of force redistribution. The absolute RSR values should be used with caution and an alternative interpretation provides better insight to the component and system contributions to system strength.

The RSR embodies within it intended conservatism in terms of safety factors and lower bound / characteristic interpretations of component data. To give a measure of the system contribution to ultimate capacity, an instructive comparison is with the global load at first member failure. This not only excludes intended conservatism but also what might be called an 'ignorance factor' due to the discrepancy between the actual component capacity and mean estimates from isolated test databases:



- Ultimate global capacity: 1198kN
- Global load at initial X joint failure: 577kN
- Approximate gravitational offset: 57kN
- 'System' contribution to ultimate capacity beyond first component failure  
 $= (1198-577) / (577-57) = 1.2$

If there were no system contribution the factor would be zero. The structure therefore sustain 2.2 times the global load at the point the joint failed. The system contribution was clearly substantial.

The limiting capacity was governed by buckling within an X brace to the primary compression joint in the Frame E bay adjacent to the loading beam. Once the capacity of that bay was reached the mechanism for applied load to pass into the structure was undermined. The ductility of the X joint failure mode and the remaining tension chord capacity meant that the bay was not compromised in the early stages of the test. However it is interesting to postulate the scenario in which the primary joint had a strong joint can and therefore first component failure would be triggered by buckling in the bay. Extrapolating the initial linear responses measured, it can be inferred that member failure would have occurred at a global load of some 950kN. The actual load sustained at the end of the Loadcase 2 test was 25% greater. In this fictitious scenario other loadpaths in the structure would have been relatively lowly utilised at the point buckling occurred, whereas the ductility and redistribution following joint failure in the test enabled other loadpaths to be mobilised.

### 5.3.2 Features of Real Structures

The system response of the 3D structure in the Loadcase 2 test was well predicted in blind ultimate strength analyses. This observation is almost *despite* the imperfections inherent in real structures which can influence the response. Examples include:

- the underlying response characteristic of the  $\beta=1.0$  compression X joint as it deformed, which may be attributed to the weld geometry in the saddle region
- the presence of significant tensile and compressive locked-in forces remaining from fabrication affecting the sequence and applied load level of failures
- the uncertainty in actual capacities of components in the constraints of a frame
- the early buckling of the brace framing into the primary X joint precipitated by the reducing rotational constraint as the joint failed increasing the effective length.

The Loadcase 2 test has provided particular insight to these factors none of which is automatically accounted for in any nonlinear analysis software. Although the factors in the present case appear to have compensated for each other and the global response characteristic has been robust in the face of these imperfections, it is clear that in the more general case the



analyst needs to think very carefully about the physics of the situation being modelled. The validity of analyses for 'perfect' structures needs to be tested with due regard to 'real' factors which may influence performance.

### 5.3.3 The Efficacy of Plan X Bracing

A principal driver behind the Loadcase 2 scenario was interest in relatively modern X-braced jacket design without horizontal bracing in the primary face frames but with X bracing in plan.

The scenario in Figure 1.5, based on previous 2D findings, suggested that once X joint failure occurred and additional load passed through the tension chord the corresponding brace in the next bay would buckle limiting the system capacity. The sequence and load level clearly depends on relative properties but for the current example considering the Frame E bracing, buckling and yield may be expected within about 10% of each other.

With reference to the Loadcase 2 test results, it can therefore be inferred that, were the Level 2 X bracing ineffective compression buckling in the bottom bay would occur at around the load level at which the top bay bracing yielded. This event would define system capacity. With reference to Figure 2.5 it can be seen that yielding in Braces 81/83 occurred at a global load of some 750kN. The global load continued to increase and it was not until around 1100kN applied load that buckling occurred. The difference, some 360kN, can be attributed to the redistribution of loads from Frame E via the Level 2 X bracing out into the 3D structure. This effect alone contributed some 50% additional capacity beyond the point of yielding in the one bay.

By that stage in the test the compression X joint had assumed renewed strength and stiffness which in turn contributed to additional system capacity. The transfer of load via the 'plan' Level 2 X bracing was therefore effective and, by delaying the sequence of failures between bays, enabled additional sources of strength to be mobilised.



## 6. CONCLUSIONS

The Frames Project Phase III Loadcase 2 test has provided important insight to the ultimate response of 3D structural systems.

It has been demonstrated that plan X bracing can be effective in redistributing loads from face framing out into the 3D structure. The configuration is a popular weight/cost saving feature in modern jacket design. The bracing is able to protect adjacent bays from a sequence of failures propagating through a structure. The extent is dependent on relative section properties but in the Loadcase 2 test the global load sustained was more than 50% greater than it would have been without the plan bracing.

The test has confirmed, with two consistent results, that  $\beta=1.0$  X joints failing in compression are some 37% stronger than isolated test databases underlying current design practices suggest. Furthermore there is no evidence of a reduction in capacity due to the presence of chord tension although this has been indicated by previous analyses and is being introduced as a capacity reduction factor in the draft ISO standard. It should be noted that at all stages the assessment of the test data has erred on the conservative side and locked-in stress effects which reduce the measured capacities have been accounted for. Taken in conjunction with earlier Frames Project findings, there is compelling evidence that a 25% increase in  $\beta=1.0$  compression X joint capacity may be exploited in the assessment of older platforms where such connections are prevalent.

The test has provided an important opportunity to benchmark nonlinear system strength analysis practice. The blind SAFJAC predictions presented in this report gave excellent correlation both at system and component levels. This was despite a number of practical features of real 3D structures being manifested in the test which were not accounted for in the analyses. These included:

- joint capacities being different from mean estimates from isolated test database
- presence of tensile and compressive locked-in fabrication forces affecting sequence and apparent capacity of component failures
- changing fixity at brace ends due to joint failure and release of rotational constraint.

In the Loadcase 2 test the factors appeared to compensate for each other but for more general cases it is clearly important that analysis output is scrutinised carefully and the sensitivity to physical imperfections such as these assessed.



Overall the Loadcase 2 test has provided good news regarding the strength of structural components and systems and the validity of ultimate strength analysis. Nevertheless it has underlined the fact that real structures are 'imperfect' and the interpretation of idealised models needs to proceed with caution appropriate to the level of analysis and use to which the results are to be put.



## 7. REFERENCES

1. BOMEL Limited. 'Joint Industry Tubular Frames Project - Phase III - Summary and Conclusions', BOMEL Reference C636\04\478R, Revision 0, August 1999.
2. 'Joint Industry Tubular Frames Project - Phase I', Nine volume report, SCI Reference SCI-RT-042, 1990.
3. Bolt, H M and Smith, J K. 'The influence of locked-in fabrication stresses on structural performance', Offshore Mechanics and Arctic Engineering Conference, Copenhagen, 1995.
4. BOMEL Limited. 'Joint Industry Tubular Frames Project - Phase II', Nine volume report, BOMEL Reference C556R003.50 to .58, 1992.
5. Bolt, H M et al. 'Results from large scale ultimate strength tests of X-braced jacket frame structures', Paper No OTC 7451, Offshore Technology Conference, Houston, May 1994.
6. BOMEL Limited. 'Joint Industry Tubular Frames Project - Phase IIA - Interaction between frame effects and tubular joint behaviour', BOMEL Reference C608\03\021R, Revision 0, February 1996.
7. BOMEL Limited. 'Loadcases 2 and 3 cyclic test report', BOMEL Reference C636\04\011R, Revision 0, September 1999.
8. BOMEL Limited. 'Material testing report', BOMEL Reference C636\23\004R, Revision B, April 1999
9. BOMEL Limited. 'Assessment of locked-in fabrication stress', BOMEL Reference C636\21\050R, Revision 0, July 1999.
10. BOMEL Limited. 'Test frame instrumentation', BOMEL Reference C636\25\071R, Revision 0, July 1999.
11. Van der Valk, C A C. 'New aspects related to the ultimate strength of tubular K and X joints', Offshore Mechanics and Arctic Engineering Conference, Stavanger, 1991.



12. Pecknold, D A et al. Minutes of meeting of the Offshore Tubular Joints Research Centre, Houston, August 1999.
13. BOMEL Limited. 'Benchmark Analysis - Blind predictions of ultimate strength', BOMEL Reference C636\32\002R, Revision 0, February 1998.
14. American Petroleum Institute. 'Recommended practice for planning, designing and constructing fixed offshore platforms - working stress design', API RP2A-WSD, 20th edition, July 1993.
15. American Petroleum Institute. 'Recommended practice for planning, designing and constructing fixed offshore platforms - load and resistance factor design', API RP2A-LRFD, 1st edition, July 1993.
16. Yura, J et al. 'Ultimate capacity equations for tubular joints', Paper No OTC 3690, Offshore Technology Conference, Houston, May 1980.
17. Department of Energy (now HSE). 'Background to guidance on static strength of tubular joints in steel offshore structures', OTH 89 308, HMSO, 1990.
18. BOMEL Limited. 'Guide for the design and assessment of tubular joints'. BOMEL Reference C06060R, 1999.
19. International Standards Organisation. 'Offshore structures for petroleum and natural gas industries - Part 2 - Fixed steel structures', Committee Draft ISO/CD 13819-2, May 1999.



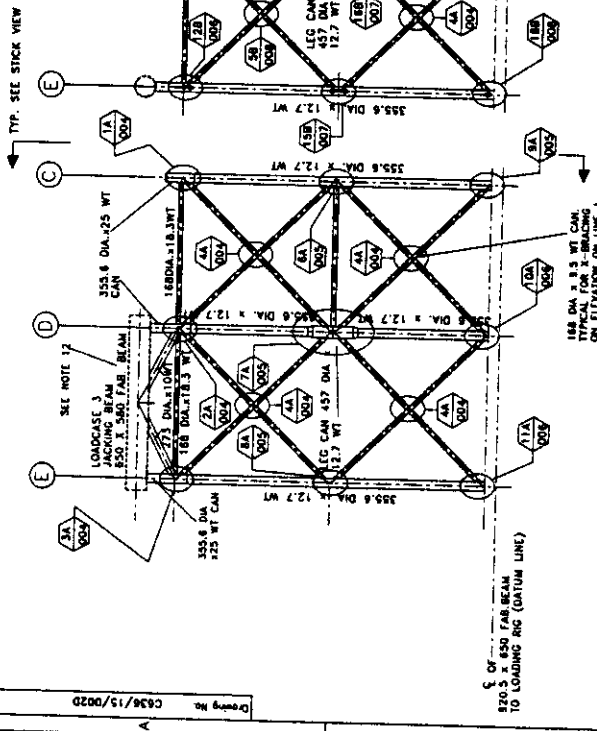
## **APPENDIX A**

### **AS-BUILT DRAWINGS RELEVANT TO LOADCASE 2 TEST**

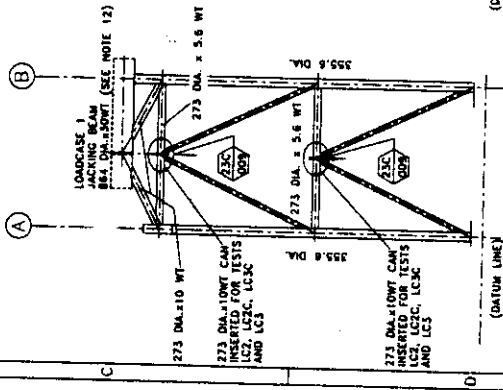
General Arrangement of Test Specimen - C636\15\002D Rev G  
General Arrangement of Test Specimen - Dimensions - C636\15\003D Rev G  
Detail Drawing of Node Points 6A, 7A, 8A and 9A - C636\15\005D Rev F  
Detail Drawing of Node Points 23C, 24D, 25D, 26X, 27E, 28E and 29X - C63615\009D  
Revision G



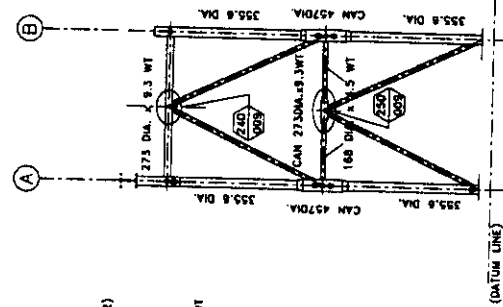
Drawing No. C636/15/0020



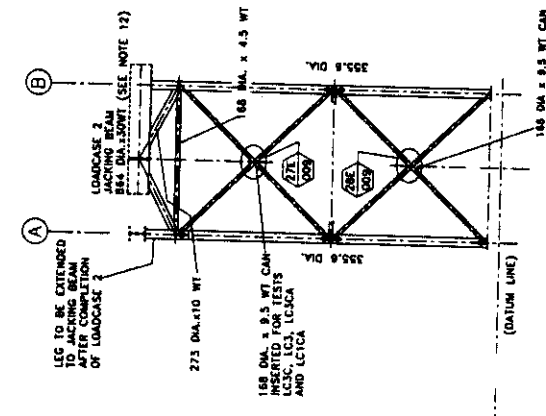
ELEVATION ON LINE A



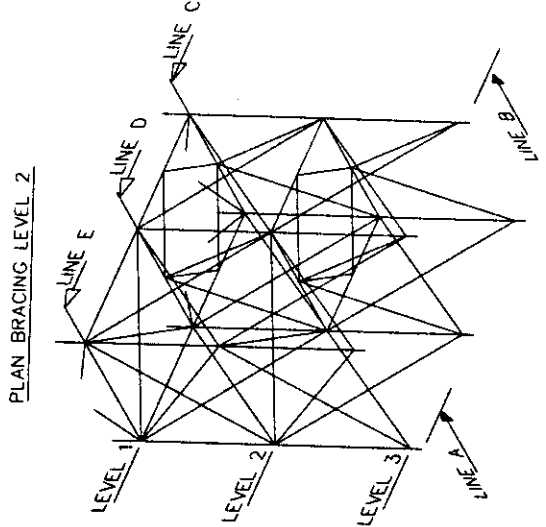
ELEVATION ON LINE C



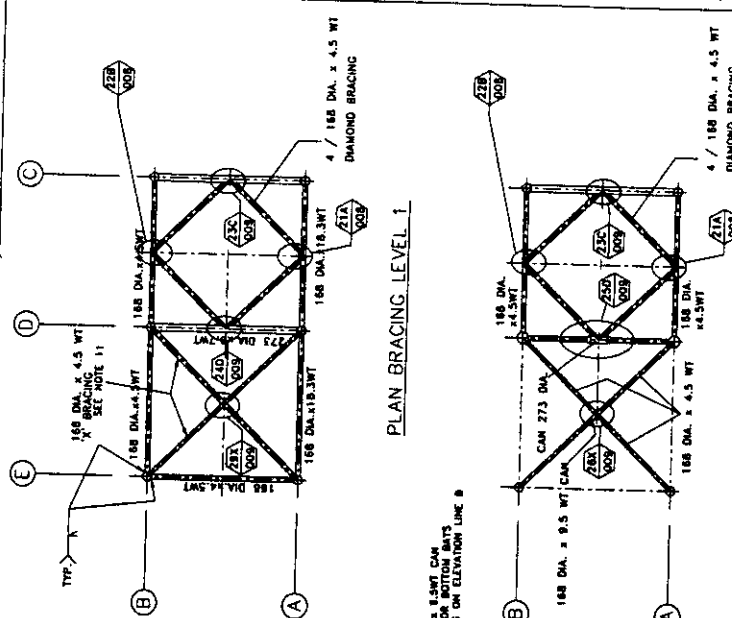
ELEVATION ON LINE D



ELEVATION ON LINE B



3D STICK VIEW OF TEST SPECIMEN  
SHOWING ELEVATIONS TAKEN



PLAN BRACING LEVEL 1

PLAN BRACING LEVEL 2

SIZE	SPECIFICATION
168 DIA x 4.5 WT	BS 3602 ERW
273 DIA x 5.6 WT	API 5L X52 GR B
273 DIA x 11.0 WT	API 5L X52
355.8 DIA x 12.7 WT	API 5L X52
457 DIA x 12.7 WT	API 5L X52
168 DIA x 18.3 WT	API 5L X52
168 DIA x 9.5 WT	API 5L X52
168 DIA x 5.6 WT	BS 3602 ERW
355 DIA x 23.4 WT	API 5L X52

**NOTES**

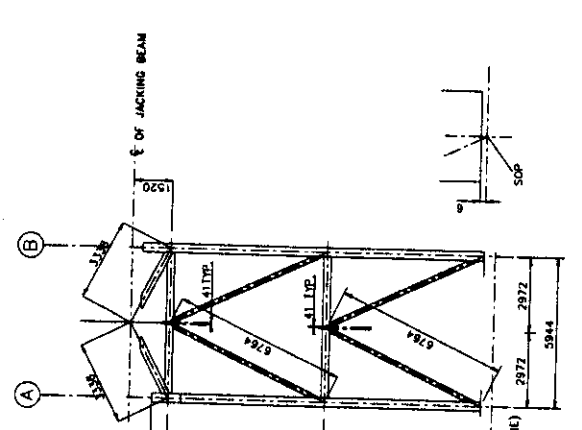
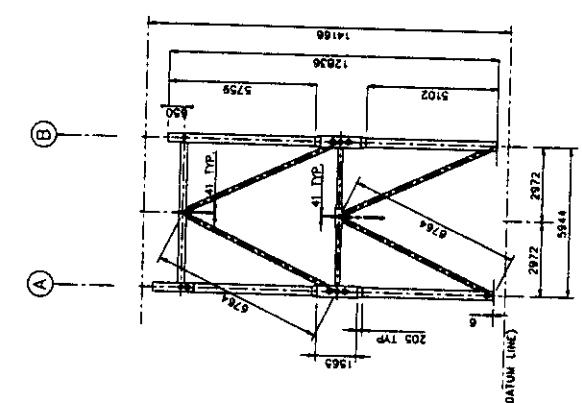
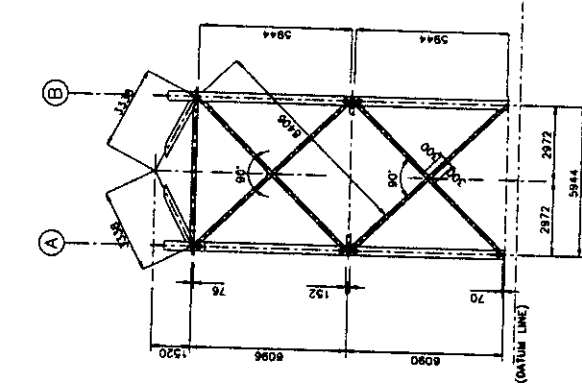
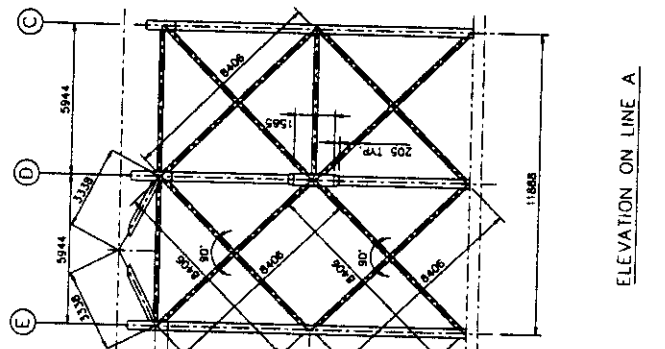
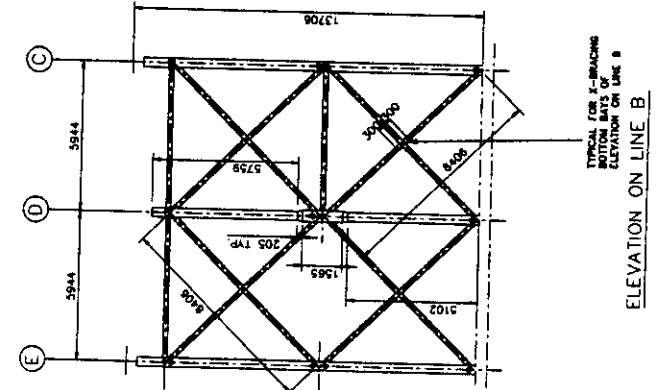
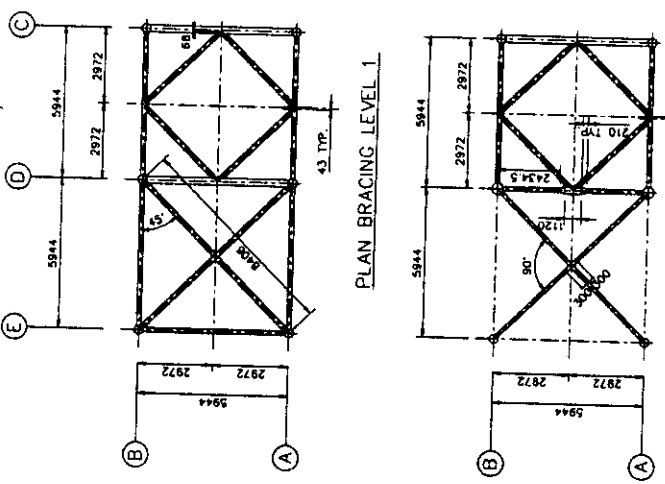
1. ALL DIMENSIONS ARE IN MILLIMETRES.
2. TUBULARS TO BE SUPPLIED AS PER TABLE.
3. ALL PLATES AND STIFFENERS TO BE BS3602 1986 GRADE 43 U.N.O.
4. HOT ROLLED SECTIONS TO BE SUPPLIED TO THE DIMENSIONS AND TOLERANCES GIVEN IN BS4 PART 1:1993. MATERIAL PROPERTIES SHALL COMPLY WITH TABLE 14 AND 15 OF BS3602:1986.
5. ALL MATERIAL SHALL BE SUPPLIED WITH AUTHENTIC TRACEABLE MILL CERTIFICATES.
6. ALL FABRICATION SHALL COMPLY WITH THE LATEST EDITION OF CEENIA 1984 AND ALL DIMENSIONS SHALL BE IN ACCORDANCE WITH THESE TOLERANCES UNLESS NOTED OTHERWISE.
7. WELD STICKERS ARE IN ACCORDANCE WITH BS599 PART 2:1980.
8. ALL WELDS SHALL BE FULL STRENGTH FULL PENETRATION SINGLE SIDED U.N.O.
9. ALL WELDS SHALL BE INSPECTED BY VISUAL EXAMINATION FOR COMPLIANCE WITH THE FABRICATION SPECIFICATION (NOTE 6).
10. ALL FULL PENETRATION WELDS SHALL BE SUBJECT TO 100% VISUAL INSPECTION AND 10% ULTRASONIC INSPECTION U.N.O.
11. LEVEL 1 X-BRACING TO BE ADDED AS MODIFICATION AFTER LOAD CASE 3 CYCLIC TEST. PRESENT FOR LC3, LC3CA AND LC3CA TESTS ONLY.
12. FOR DETAILS OF JACKING BEAMS SEE DRC. G636/15/0100

C	1/99	AS BUILT	THE	JADC	HMB	CJB
F	18/07/02	APPROVED FOR CONSTRUCTION	THE	JADC	HMB	CJB
E	17/07/02	ISSUED AS PER DRAWING	THE	JADC	HMB	HMB
D	17/07/02	JACKING BEAM AND WELDS	THE	JADC	HMB	HMB
C	17/07/02	COLUMNS MODIFIED	THE	JADC	HMB	HMB
B	17/07/02	LEVEL 1 X-BRACING BEAM AND WELDS	THE	HMB	JADC	JADC
A	17/07/02	WELDED TO ANALYSIS	THE	PC	JADC	JADC
D	17/07/02	PRELIMINARY	HPS	PC		
REV		DATE	BY	CHKD	APPD	CLTD

BOMEL CONTRACT NO. C636/08  
 CLIENT CONTRACT NO. JOINT INDUSTRY PROJECT  
 CLIENT JOINT INDUSTRY PROJECT  
 DRAWING TITLE: FRAMES PHASE III  
 GENERAL ARRANGEMENT OF TEST SPECIMEN  
 BOMEL ENGINEERING  
 111 GLENVIEW ROAD, WILLOWBROOK, VICTORIA 3103  
 TEL: +61 (0)3 9528 7770  
 FAX: +61 (0)3 9528 7787  
 Drawing No. C636/15/0020

**NOTES**

1. FOR GENERAL NOTES REFER TO DRG-- C636/15/003D



C	7/76	1st BUILT	TRG	JADC	HMB	CJB			
F	14/7/76	APPROVED FOR CONSTRUCTION	TRG	JADC	HMB	CJB			
E	12/7/76	ISSUES RELATED FOR FRAME 1	TRG	JADC	HMB	CJB			
D	27/7/76	COLUMNS, J-BEAM BRACING AND DIMENSIONS MODIFIED	TRG	JADC	HMB	CJB			
C	20/7/76	ON LINE A MOVED	TRG	JADC	HMB	CJB			
B	20/7/76	REVISIONS	TRG	JADC	HMB	CJB			
A	13/7/76	INCORPORATED TO ANALYSIS	TRG	JADC	HMB	CJB			
D	10/7/76	PRELIMINARY	TRG	JADC	HMB	CJB			
B	10/7/76	PRELIMINARY	TRG	JADC	HMB	CJB			
BOMEL CONTRACT NO.	BOMEL CONTRACT NO. C083608								
CLIENT CONTRACT NO.	CLIENT CONTRACT NO. C083608								
CLIENT	JOINT INDUSTRY PROJECT								
PROJECT	FRAMES PHASE III								
DRAWING TITLE	GENERAL ARRANGEMENT OF TEST SPECIMEN - DIMENSIONS								
LEADER	L. GARDNER								
DESIGNER	L. GARDNER								
CHECKED BY	L. GARDNER								
DATE	15/03/2015								
SCALE	1:100								
DRAWING NO.	C636/15/003D								



**BOMEL CONSULTING**  
 Level 10, 100, 101, 102, 103, 104, 105, 106, 107, 108, 109, 110, 111, 112, 113, 114, 115, 116, 117, 118, 119, 120, 121, 122, 123, 124, 125, 126, 127, 128, 129, 130, 131, 132, 133, 134, 135, 136, 137, 138, 139, 140, 141, 142, 143, 144, 145, 146, 147, 148, 149, 150, 151, 152, 153, 154, 155, 156, 157, 158, 159, 160, 161, 162, 163, 164, 165, 166, 167, 168, 169, 170, 171, 172, 173, 174, 175, 176, 177, 178, 179, 180, 181, 182, 183, 184, 185, 186, 187, 188, 189, 190, 191, 192, 193, 194, 195, 196, 197, 198, 199, 200, 201, 202, 203, 204, 205, 206, 207, 208, 209, 210, 211, 212, 213, 214, 215, 216, 217, 218, 219, 220, 221, 222, 223, 224, 225, 226, 227, 228, 229, 230, 231, 232, 233, 234, 235, 236, 237, 238, 239, 240, 241, 242, 243, 244, 245, 246, 247, 248, 249, 250, 251, 252, 253, 254, 255, 256, 257, 258, 259, 260, 261, 262, 263, 264, 265, 266, 267, 268, 269, 270, 271, 272, 273, 274, 275, 276, 277, 278, 279, 280, 281, 282, 283, 284, 285, 286, 287, 288, 289, 290, 291, 292, 293, 294, 295, 296, 297, 298, 299, 300, 301, 302, 303, 304, 305, 306, 307, 308, 309, 310, 311, 312, 313, 314, 315, 316, 317, 318, 319, 320, 321, 322, 323, 324, 325, 326, 327, 328, 329, 330, 331, 332, 333, 334, 335, 336, 337, 338, 339, 340, 341, 342, 343, 344, 345, 346, 347, 348, 349, 350, 351, 352, 353, 354, 355, 356, 357, 358, 359, 360, 361, 362, 363, 364, 365, 366, 367, 368, 369, 370, 371, 372, 373, 374, 375, 376, 377, 378, 379, 380, 381, 382, 383, 384, 385, 386, 387, 388, 389, 390, 391, 392, 393, 394, 395, 396, 397, 398, 399, 400, 401, 402, 403, 404, 405, 406, 407, 408, 409, 410, 411, 412, 413, 414, 415, 416, 417, 418, 419, 420, 421, 422, 423, 424, 425, 426, 427, 428, 429, 430, 431, 432, 433, 434, 435, 436, 437, 438, 439, 440, 441, 442, 443, 444, 445, 446, 447, 448, 449, 450, 451, 452, 453, 454, 455, 456, 457, 458, 459, 460, 461, 462, 463, 464, 465, 466, 467, 468, 469, 470, 471, 472, 473, 474, 475, 476, 477, 478, 479, 480, 481, 482, 483, 484, 485, 486, 487, 488, 489, 490, 491, 492, 493, 494, 495, 496, 497, 498, 499, 500, 501, 502, 503, 504, 505, 506, 507, 508, 509, 510, 511, 512, 513, 514, 515, 516, 517, 518, 519, 520, 521, 522, 523, 524, 525, 526, 527, 528, 529, 530, 531, 532, 533, 534, 535, 536, 537, 538, 539, 540, 541, 542, 543, 544, 545, 546, 547, 548, 549, 550, 551, 552, 553, 554, 555, 556, 557, 558, 559, 560, 561, 562, 563, 564, 565, 566, 567, 568, 569, 570, 571, 572, 573, 574, 575, 576, 577, 578, 579, 580, 581, 582, 583, 584, 585, 586, 587, 588, 589, 590, 591, 592, 593, 594, 595, 596, 597, 598, 599, 600, 601, 602, 603, 604, 605, 606, 607, 608, 609, 610, 611, 612, 613, 614, 615, 616, 617, 618, 619, 620, 621, 622, 623, 624, 625, 626, 627, 628, 629, 630, 631, 632, 633, 634, 635, 636, 637, 638, 639, 640, 641, 642, 643, 644, 645, 646, 647, 648, 649, 650, 651, 652, 653, 654, 655, 656, 657, 658, 659, 660, 661, 662, 663, 664, 665, 666, 667, 668, 669, 670, 671, 672, 673, 674, 675, 676, 677, 678, 679, 680, 681, 682, 683, 684, 685, 686, 687, 688, 689, 690, 691, 692, 693, 694, 695, 696, 697, 698, 699, 700, 701, 702, 703, 704, 705, 706, 707, 708, 709, 710, 711, 712, 713, 714, 715, 716, 717, 718, 719, 720, 721, 722, 723, 724, 725, 726, 727, 728, 729, 730, 731, 732, 733, 734, 735, 736, 737, 738, 739, 740, 741, 742, 743, 744, 745, 746, 747, 748, 749, 750, 751, 752, 753, 754, 755, 756, 757, 758, 759, 760, 761, 762, 763, 764, 765, 766, 767, 768, 769, 770, 771, 772, 773, 774, 775, 776, 777, 778, 779, 780, 781, 782, 783, 784, 785, 786, 787, 788, 789, 790, 791, 792, 793, 794, 795, 796, 797, 798, 799, 800, 801, 802, 803, 804, 805, 806, 807, 808, 809, 810, 811, 812, 813, 814, 815, 816, 817, 818, 819, 820, 821, 822, 823, 824, 825, 826, 827, 828, 829, 830, 831, 832, 833, 834, 835, 836, 837, 838, 839, 840, 841, 842, 843, 844, 845, 846, 847, 848, 849, 850, 851, 852, 853, 854, 855, 856, 857, 858, 859, 860, 861, 862, 863, 864, 865, 866, 867, 868, 869, 870, 871, 872, 873, 874, 875, 876, 877, 878, 879, 880, 881, 882, 883, 884, 885, 886, 887, 888, 889, 890, 891, 892, 893, 894, 895, 896, 897, 898, 899, 900, 901, 902, 903, 904, 905, 906, 907, 908, 909, 910, 911, 912, 913, 914, 915, 916, 917, 918, 919, 920, 921, 922, 923, 924, 925, 926, 927, 928, 929, 930, 931, 932, 933, 934, 935, 936, 937, 938, 939, 940, 941, 942, 943, 944, 945, 946, 947, 948, 949, 950, 951, 952, 953, 954, 955, 956, 957, 958, 959, 960, 961, 962, 963, 964, 965, 966, 967, 968, 969, 970, 971, 972, 973, 974, 975, 976, 977, 978, 979, 980, 981, 982, 983, 984, 985, 986, 987, 988, 989, 990, 991, 992, 993, 994, 995, 996, 997, 998, 999, 1000

**NOTES**

1. FOR GENERAL NOTES REFER TO DRG:- C636/15/005D

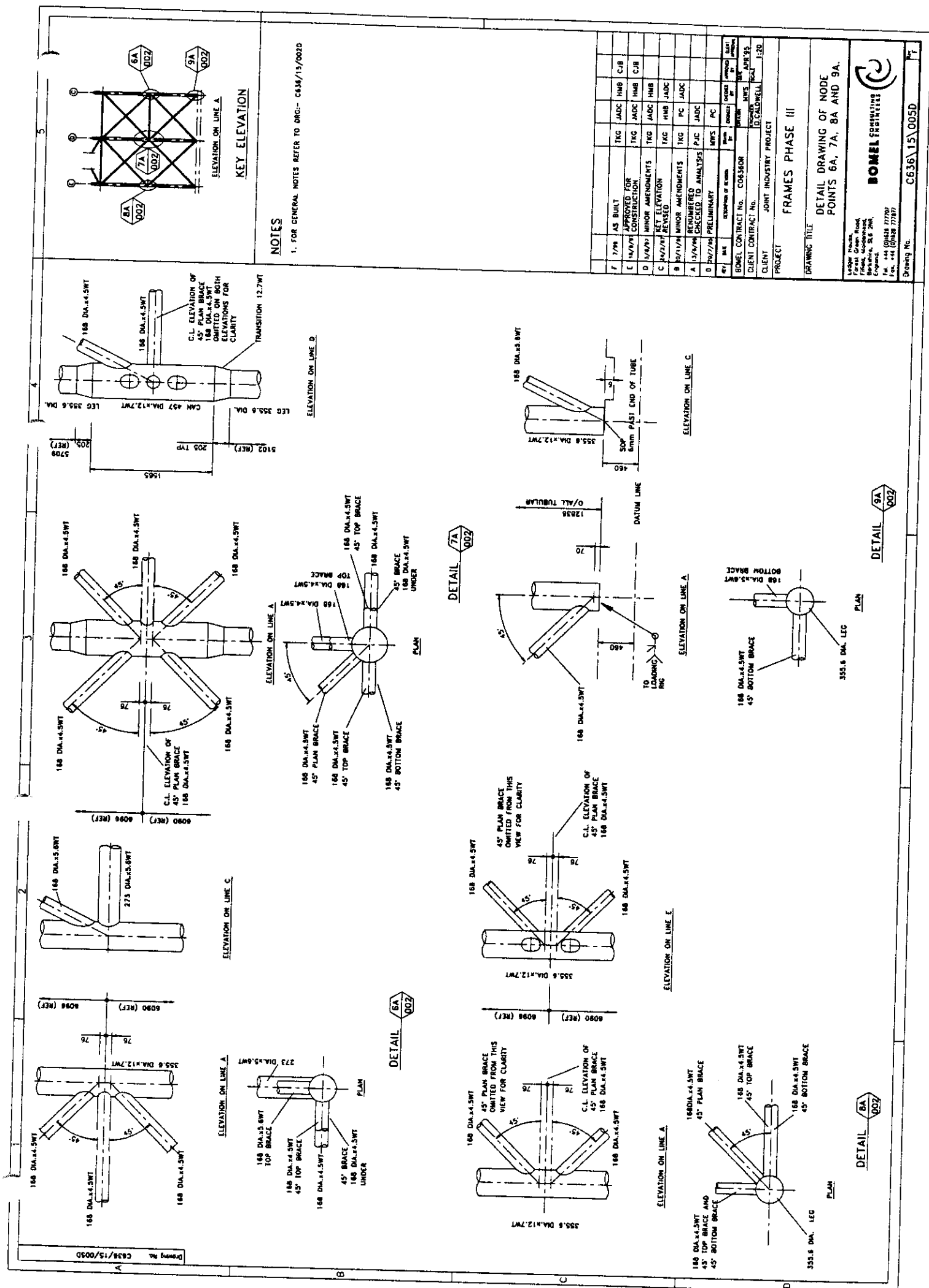
F	1/76	AS BUILT	TNG	JADC	HMB	CJB
C	14/9/97	APPROVED FOR CONSTRUCTION	TNG	JADC	HMB	CJB
D	14/9/97	MINOR AMENDMENTS	TNG	JADC	HMB	CJB
C	24/2/97	REVISION ELEVATION	TNG	HMB	JADC	
B	30/1/94	MINOR AMENDMENTS	TNG	PC	JADC	
A	13/9/94	RENUMBERED CHECKED TO ANALYSIS	P.C	JADC		
D	20/7/94	PRELIMINARY	MWS	PC		

REV	DATE	DESCRIPTION OF REVISION	BY	CHECKED BY
BOMEL CONTRACT NO. C06340R				
CLIENT CONTRACT NO. 120				
CLIENT D. CALDWELL				
PROJECT JOINT INDUSTRY PROJECT				
DRAWING TITLE				
FRAMES PHASE III				
DETAIL DRAWING OF NODE				
POINTS 6A, 7A, 8A AND 9A.				

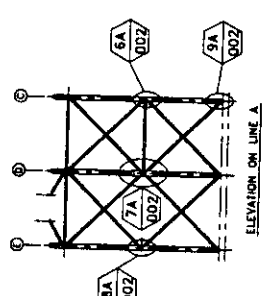


**BOMEL ENGINEERS**  
 LEGGIE HOUSE,  
 FIRST FLOOR,  
 BRISTOL ROAD,  
 BRISTOL, S.G. 2NH,  
 ENGLAND.  
 TEL: 0117 928 7770  
 FAX: 0117 928 7787

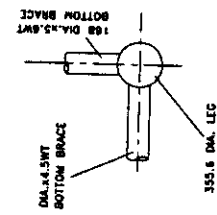
Sheet No. C636/15/005D



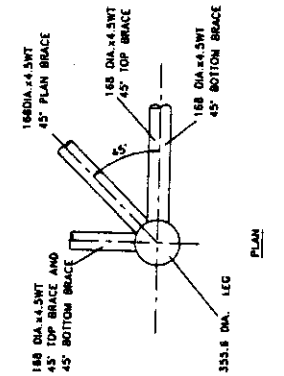
**KEY ELEVATION**



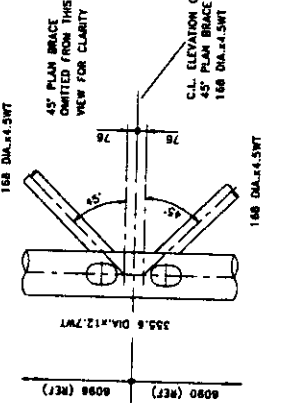
**DETAIL 9A**



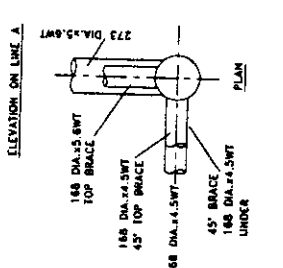
**DETAIL 8A**

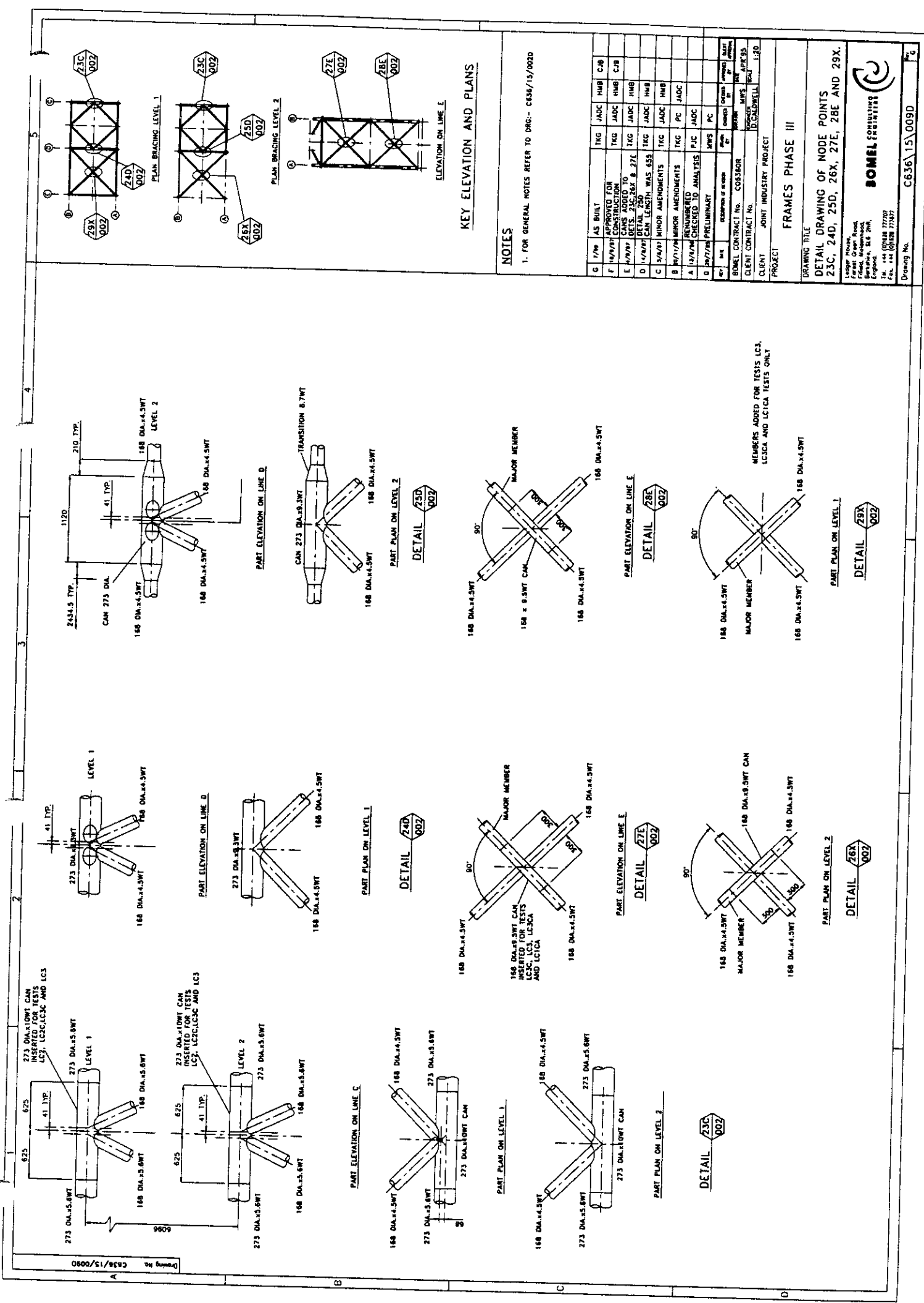


**DETAIL 7A**



**DETAIL 6A**





**KEY ELEVATION AND PLANS**

**NOTES**

1. FOR GENERAL NOTES REFER TO DRG- C636/15/0020

G	1/76	AS BUILT	TKG	JADC	HMB	CJB
F	10/7/77	APPROVED FOR CONSTRUCTION	TKG	JADC	HMB	CJB
E	8/7/77	CANS ADDED TO BEAMS 235, 26X & 27E	TKG	JADC	HMB	HMB
D	1/7/77	BEAM 235, 26X & 27E CAN LENGTH WAS 453	TKG	JADC	HMB	HMB
C	5/4/77	MINOR AMENDMENTS	TKG	JADC	HMB	HMB
B	1/4/77	MINOR AMENDMENTS	TKG	PC	JADC	JADC
A	1/4/77	RENUMBERED CHECKED TO ANALYSIS	PJC	JADC	JADC	JADC
D	20/7/76	PRELIMINARY	MWS	PC	PC	PC

DESIGNED BY	DATE	CHECKED BY	DATE
APPROVED BY	DATE	APPROVED BY	DATE
CLIENT CONTRACT NO.	COR-316308	CLIENT CONTRACT NO.	COR-316308
PROJECT	JOINT INDUSTRY PROJECT	PROJECT	JOINT INDUSTRY PROJECT
DRAWING TITLE	FRAMES PHASE III	DRAWING TITLE	FRAMES PHASE III

**DETAIL DRAWING OF NODE POINTS**  
 23C, 24D, 25D, 26X, 27E, 28E AND 29X.

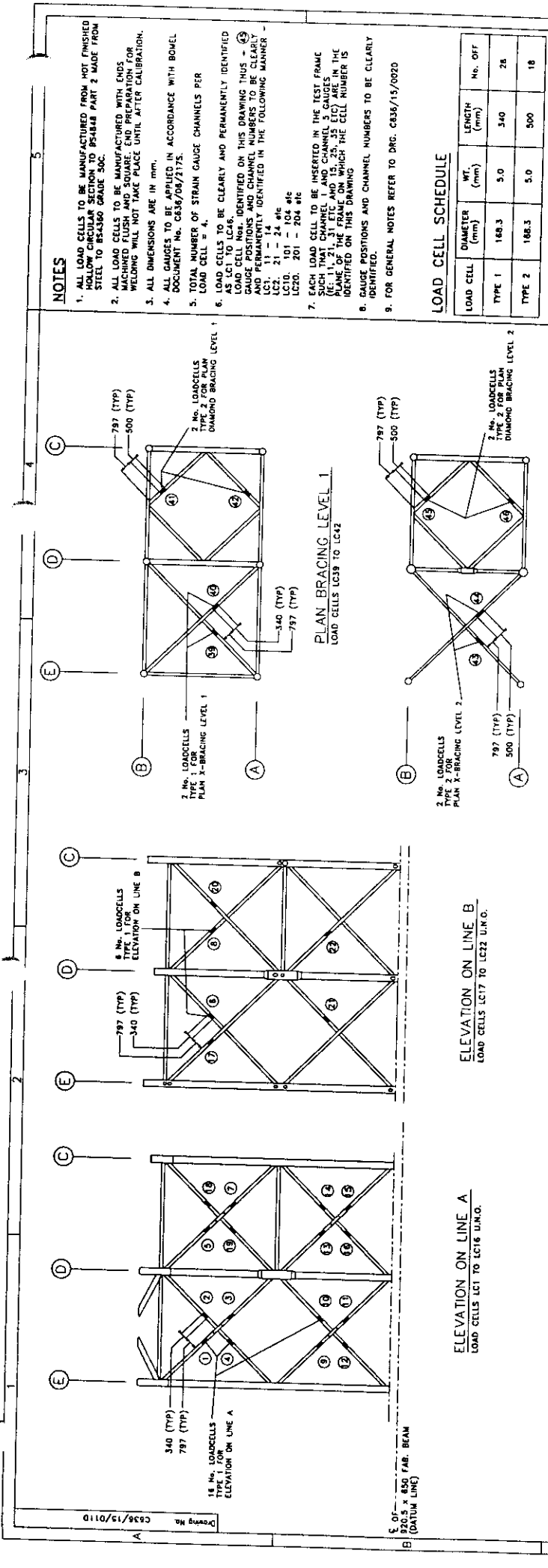
**BOMEL ENGINEERING**  
 100, 101, 102, 103, 104, 105, 106, 107, 108, 109, 110, 111, 112, 113, 114, 115, 116, 117, 118, 119, 120, 121, 122, 123, 124, 125, 126, 127, 128, 129, 130, 131, 132, 133, 134, 135, 136, 137, 138, 139, 140, 141, 142, 143, 144, 145, 146, 147, 148, 149, 150, 151, 152, 153, 154, 155, 156, 157, 158, 159, 160, 161, 162, 163, 164, 165, 166, 167, 168, 169, 170, 171, 172, 173, 174, 175, 176, 177, 178, 179, 180, 181, 182, 183, 184, 185, 186, 187, 188, 189, 190, 191, 192, 193, 194, 195, 196, 197, 198, 199, 200, 201, 202, 203, 204, 205, 206, 207, 208, 209, 210, 211, 212, 213, 214, 215, 216, 217, 218, 219, 220, 221, 222, 223, 224, 225, 226, 227, 228, 229, 230, 231, 232, 233, 234, 235, 236, 237, 238, 239, 240, 241, 242, 243, 244, 245, 246, 247, 248, 249, 250, 251, 252, 253, 254, 255, 256, 257, 258, 259, 260, 261, 262, 263, 264, 265, 266, 267, 268, 269, 270, 271, 272, 273, 274, 275, 276, 277, 278, 279, 280, 281, 282, 283, 284, 285, 286, 287, 288, 289, 290, 291, 292, 293, 294, 295, 296, 297, 298, 299, 300



## **APPENDIX B**

### **INSTRUMENTATION LAYOUT DRAWINGS**

Load Cell Details - C636\15\011D Revision D  
Strain Gauging Details - Sheet 1 of 2 - C636\15\012D Revision B  
Strain Gauging Details - Sheet 2 of 2 - C636\15\013D Revision B  
Joint Deformation Monitoring - C636\15\016D Revision 0

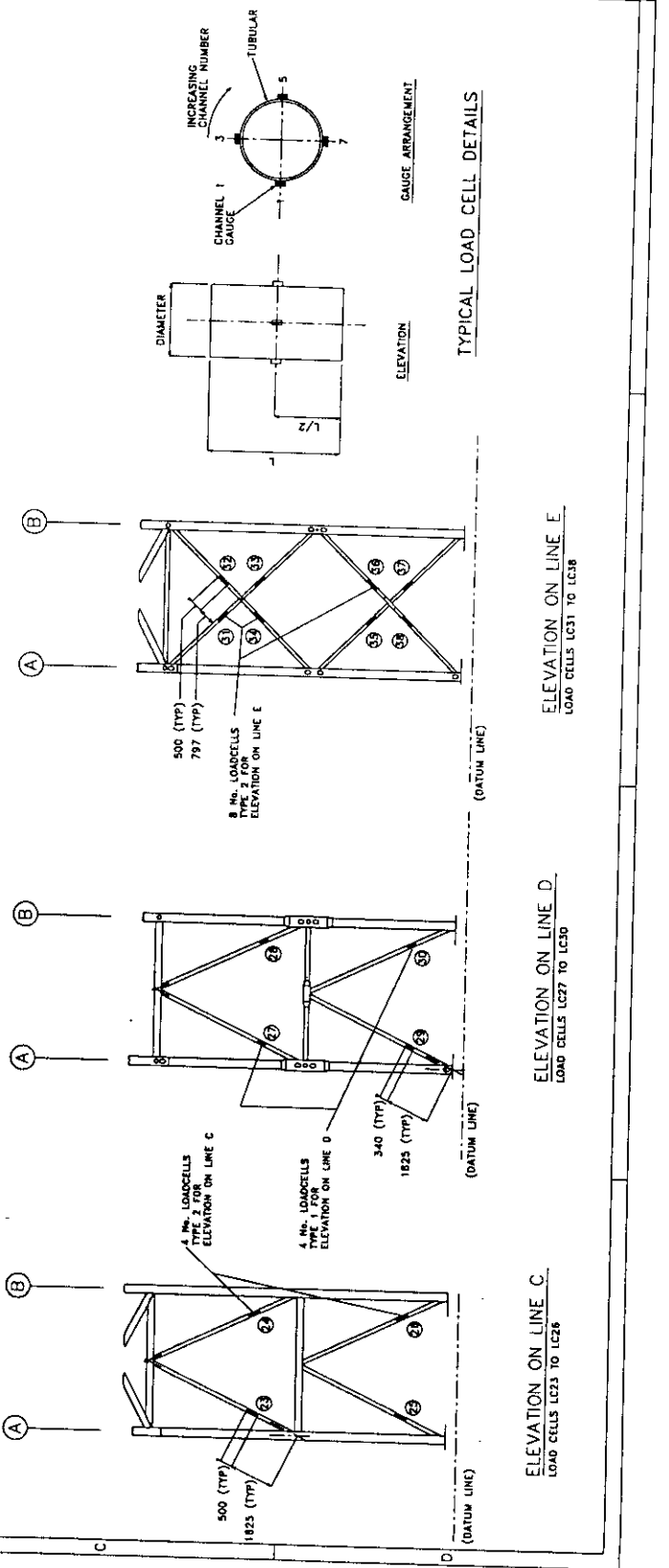


**LOAD CELL SCHEDULE**

LOAD CELL	DIAMETER (mm)	WT. (mm)	LENGTH (mm)	No. OFF
TYPE 1	168.3	5.0	540	28
TYPE 2	168.3	5.0	500	18

**NOTES**

- ALL LOAD CELLS TO BE MANUFACTURED FROM HOT FINISHED RINGED CHANNEL SECTION TO BS4848 PART 2 MADE FROM STEEL TO BS595 GRADE 30C.
- ALL LOAD CELLS TO BE MANUFACTURED WITH ENDS ALL BEVELLED AND SQUARE. END PREPARATION FOR WELDING WILL NOT TAKE PLACE UNTIL AFTER CALIBRATION.
- ALL DIMENSIONS ARE IN MM.
- ALL GAUGES TO BE APPLIED IN ACCORDANCE WITH BOMEL DOCUMENT No. C636/08/2175.
- TOTAL NUMBER OF STRAIN GAUGE CHANNELS PER LOAD CELL = 4.
- LOAD CELLS TO BE CLEARLY AND PERMANENTLY IDENTIFIED AS LCG TO LCG46.
- LOAD CELL Nos. IDENTIFIED ON THIS DRAWING THUS - (1) GAUGE POSITIONS AND CHANNEL NUMBERS TO BE CLEARLY AND PERMANENTLY IDENTIFIED IN THE FOLLOWING MANNER - LCG 1 - 24 #16 LCG 2 - 21 - 24 #16 LCG 10 - 101 - 104 #16 LCG 20 - 201 - 204 #16
- EACH LOAD CELL TO BE INSERTED IN THE TEST FRAME SUCH THAT CHANNEL 1 AND CHANNEL 3 GAUGES (IN PLANE 1, 2, 3, 4, 5, 6, 7, 8, 9, 10, 11, 12, 13, 14, 15, 16, 17, 18, 19, 20, 21, 22, 23, 24) ARE IN THE PLANE OF THE CHANNEL WHICH THE CELL NUMBER IS IDENTIFIED ON THIS DRAWING.
- GAUGE POSITIONS AND CHANNEL NUMBERS TO BE CLEARLY IDENTIFIED.
- FOR GENERAL NOTES REFER TO DRG. C636/15/0020



Drawing No. C636/15/0110

PROJECT: JOINT INDUSTRY PROJECT

CLIENT: BOMEL CONTRACT No. C083508

DATE: 7/8/97

DESIGNED BY: D. CALDWELL

PROJECT: JOINT INDUSTRY PROJECT

FRAMES PHASE III

LOAD CELL DETAILS

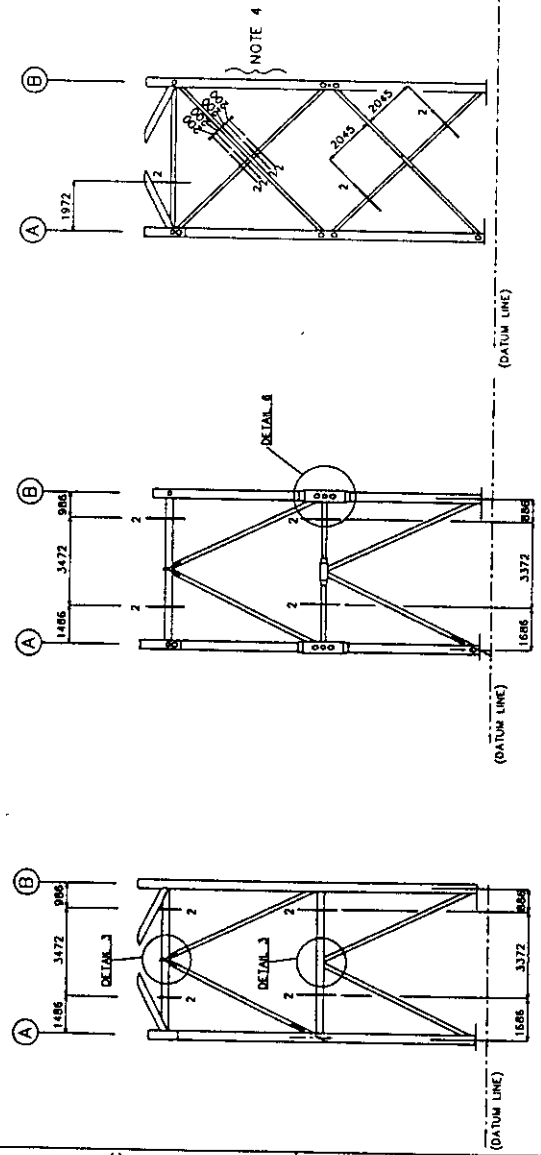
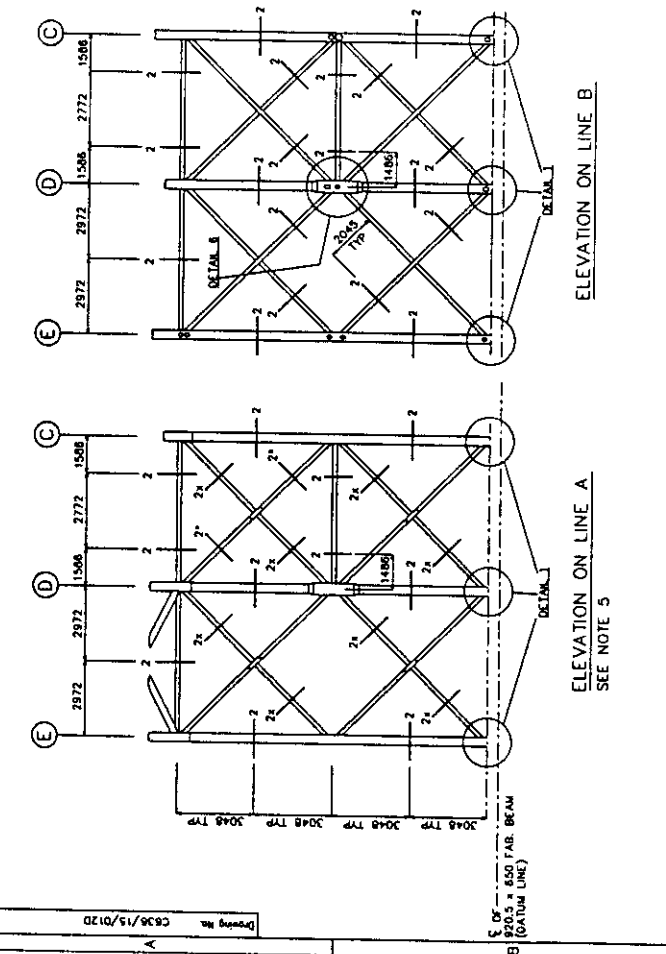
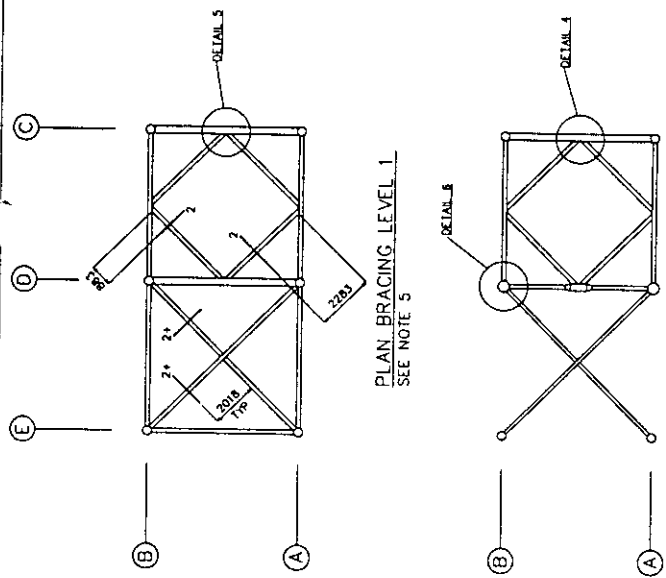
**BOMEL ENGINEERING**

Leigh Road, Forest Green Road, Macclesfield, Cheshire, England.

Tel. +44 (0)1625 777977 Fax. +44 (0)1625 77877

**NOTES**

1. FOR GENERAL NOTES SEE DWG. C636/15/0120
2. FOR DETAILS 1 TO 6 SEE DWG. C636/15/0130
3. \_\_\_\_\_ 2 DENOTES DETAIL 2  
INSTALLED FOR ALL TESTS U.N.O.
4. CANGES ON LINE E CROSS BRACING TOP BAY  
INSTALLED FOR TESTS LC1, LC1C AND LC2 ONLY
5. \_\_\_\_\_ 2\* DENOTES DETAIL 2\* INSTALLED FOR  
LOADCASE LC3C ONLY
6. \_\_\_\_\_ 2# DENOTES DETAIL 2# INSTALLED FOR  
LOADCASES LC1, LC1C, L2, LC2C, LC3 AND LC3C ONLY
7. \_\_\_\_\_ 2# DENOTES DETAIL 2# INSTALLED FOR  
LOADCASES LC1, LC2CA AND LC2CA ONLY



ITEM	DESCRIPTION	UNIT	QUANTITY
B	AS BUILT - INCLUDING DETAIL 6	TKG JADC HMB HMB	
A	AS BUILT	TKG JADC HMB HMB	
D	SPECIFICATION	TKG JADC HMB HMB	
REV	DESCRIPTION	DATE	BY
1	ISSUED FOR PERMIT	7/10/97	...
2	ISSUED FOR PERMIT	7/10/97	...
3	ISSUED FOR PERMIT	7/10/97	...
4	ISSUED FOR PERMIT	7/10/97	...
5	ISSUED FOR PERMIT	7/10/97	...
6	ISSUED FOR PERMIT	7/10/97	...
7	ISSUED FOR PERMIT	7/10/97	...
8	ISSUED FOR PERMIT	7/10/97	...
9	ISSUED FOR PERMIT	7/10/97	...
10	ISSUED FOR PERMIT	7/10/97	...

BOMEL CONTRACT No. C063609  
CLIENT: JOINT INDUSTRY PROJECT  
PROJECT: FRAMES PHASE III  
DRAWING TITLE: STRAIN GAUGING DETAILS  
Sheet 1 of 2

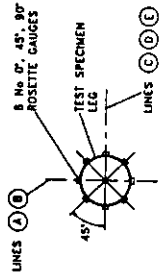
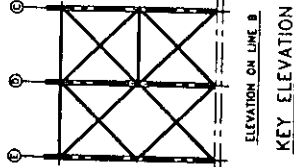
Legend:   
 1. 200.5 x 850 PAR. BEAM  
 2. 200.5 x 850 PAR. BEAM  
 3. 200.5 x 850 PAR. BEAM  
 4. 200.5 x 850 PAR. BEAM  
 5. 200.5 x 850 PAR. BEAM  
 6. 200.5 x 850 PAR. BEAM  
 7. 200.5 x 850 PAR. BEAM  
 8. 200.5 x 850 PAR. BEAM  
 9. 200.5 x 850 PAR. BEAM  
 10. 200.5 x 850 PAR. BEAM

**BOMEL ENGINEERING**  
 14000 Valley Road  
 Forest Green, Wiltshire  
 England, SN6 2HR  
 Tel: +44 (0)1458 77780  
 Fax: +44 (0)1458 77877

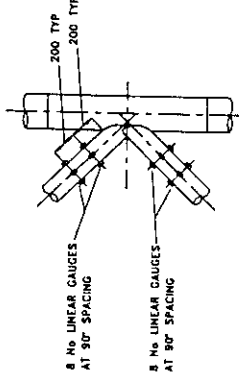
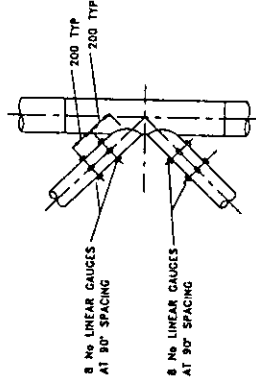
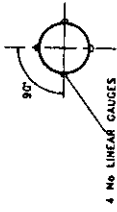
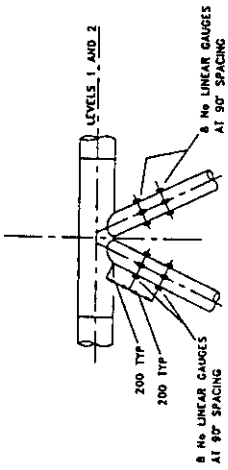
Drawing No. C636/15/0120

**NOTES**

1. FOR GENERAL NOTES SEE DRG. C636/15/0130
2. FOR LOCATION OF DETAILS 1 TO 6 SEE DRG. C636/15/0130
3. DETAILS 3, 4 AND 5 - GAUGES CLOSEST TO INTERSECTION DEMOTED 'NEAR' OTHER SETS DEMOTED 'FAR'.
4. \_\_\_\_\_ 2 DENOTES DETAIL 2
5. ASG 37-39 DENOTES LOGGER REFERENCE OF ADDITIONAL STRAIN GAUGES.



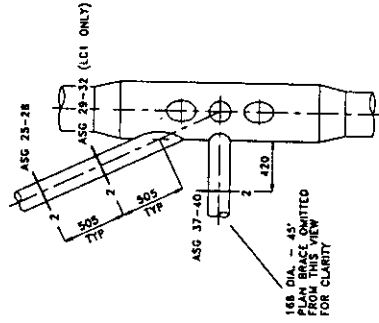
DETAIL 1  
ELEVATION



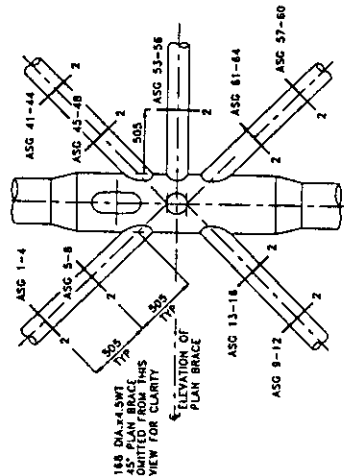
DETAIL 3  
ELEVATION ON LINE B

DETAILS 3, 4 AND 5 - NEAR AND FAR GAUGES INSTALLED FOR LOADCASES LC1 AND LC1C  
FAR GAUGES ONLY INSTALLED FOR LOADCASES LC3CA AND LC1CA

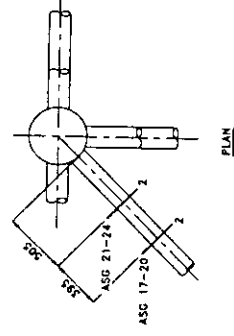
DETAIL 4  
ELEVATION ON LINE D



DETAIL 4  
ELEVATION ON LINE D



DETAIL 5  
ELEVATION



DETAIL 6  
PLAN

NO.	ITEM DESCRIPTION	QTY	UNIT	PRICE	TOTAL
1	ASB				
2	ASB				
3	ASB				
4	ASB				
5	ASB				
6	ASB				
7	ASB				
8	ASB				
9	ASB				
10	ASB				
11	ASB				
12	ASB				
13	ASB				
14	ASB				
15	ASB				
16	ASB				
17	ASB				
18	ASB				
19	ASB				
20	ASB				
21	ASB				
22	ASB				
23	ASB				
24	ASB				
25	ASB				
26	ASB				
27	ASB				
28	ASB				
29	ASB				
30	ASB				
31	ASB				
32	ASB				
33	ASB				
34	ASB				
35	ASB				
36	ASB				
37	ASB				
38	ASB				
39	ASB				
40	ASB				
41	ASB				
42	ASB				
43	ASB				
44	ASB				
45	ASB				
46	ASB				
47	ASB				
48	ASB				
49	ASB				
50	ASB				
51	ASB				
52	ASB				
53	ASB				
54	ASB				
55	ASB				
56	ASB				
57	ASB				
58	ASB				
59	ASB				
60	ASB				
61	ASB				
62	ASB				
63	ASB				
64	ASB				
65	ASB				
66	ASB				
67	ASB				
68	ASB				
69	ASB				
70	ASB				
71	ASB				
72	ASB				
73	ASB				
74	ASB				
75	ASB				
76	ASB				
77	ASB				
78	ASB				
79	ASB				
80	ASB				
81	ASB				
82	ASB				
83	ASB				
84	ASB				
85	ASB				
86	ASB				
87	ASB				
88	ASB				
89	ASB				
90	ASB				
91	ASB				
92	ASB				
93	ASB				
94	ASB				
95	ASB				
96	ASB				
97	ASB				
98	ASB				
99	ASB				
100	ASB				

**BOMEL CONSULTING ENGINEERS**

Level 10, 110, The Arcade, 110, Market Street, Singapore, S.S. 238  
 Tel: (65) 434 2710  
 Fax: (65) 434 2717

PROJECT: JOINT INDUSTRY PROJECT  
 DRAWING TITLE: STRAIN GAUGING DETAILS  
 Sheet 2 of 2

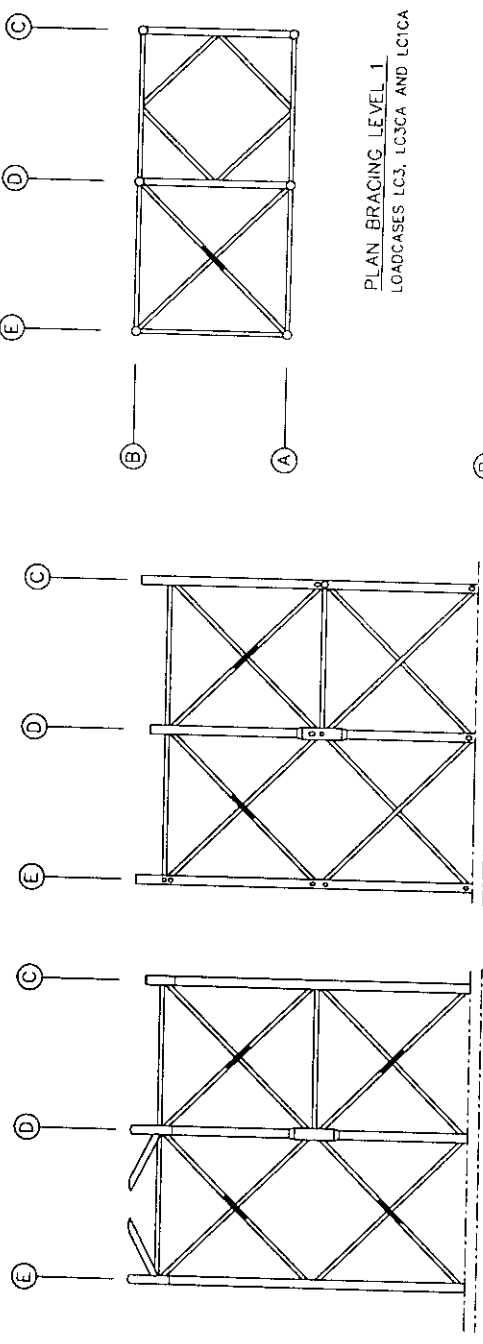
Drawing No. C636/15/0130



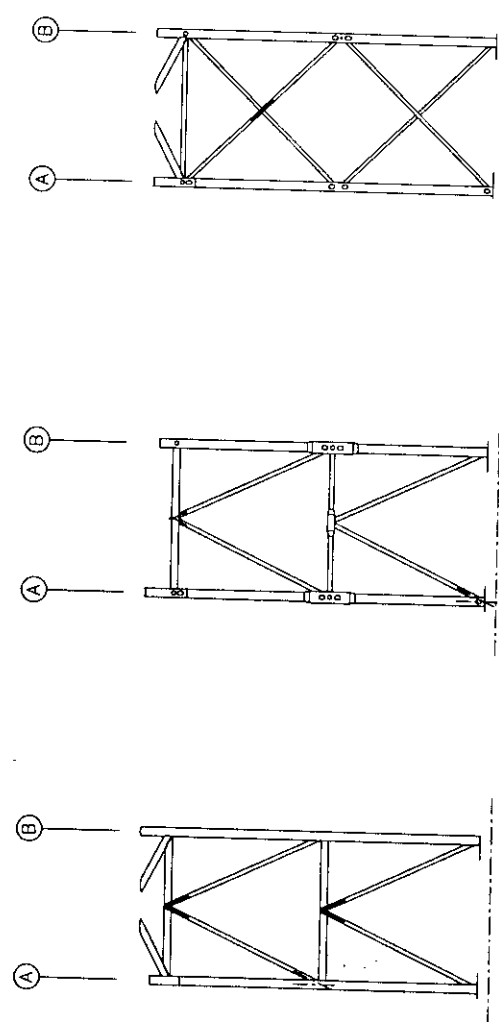
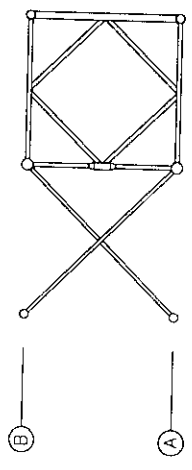
Drawing No. C636/15/016D

**NOTES**

1. ——— DENOTES LOCATION OF FRAME MOUNTED TRANSDUCER



**PLAN BRACING LEVEL 1**  
LOADCASES LC3, LC3CA AND LC1CA



REV	DATE	DESCRIPTION OF REVISION	TKG	JADC	HME	CJB
0	16/98	AS BUILT				

PROJECT: JOINT INDUSTRY PROJECT  
 DRAWING TITLE: FRAMES PHASE III

PROJECT: JOINT INDUSTRY PROJECT  
 DRAWING TITLE: FRAMES PHASE III

Legend Tower,  
 Leeger Green Road,  
 Park Road,  
 Birmingham, B15 2YR,  
 England.  
 Tel: +44 (0)121 77727  
 Fax: +44 (0)121 77727

**BOMEL CONSULTING**

Drawing No. C636/15/016D



## **APPENDIX C**

### **FRAME RESPONSE PLOTS**

Spreadsheets from C636\39\008w.xls:

- GLOBAL Scan Nos
- GLOBAL Annotated
- GLOBAL Annotated + joint
- Sheets 3 to 6
- Fr E TB Comp code comparison
- N42 Local forces
- Node 42 strains 82
- Node 42 strains 84
- Fr E BBU Mom
- Fr E BBL Mom
- Local joint characteristics

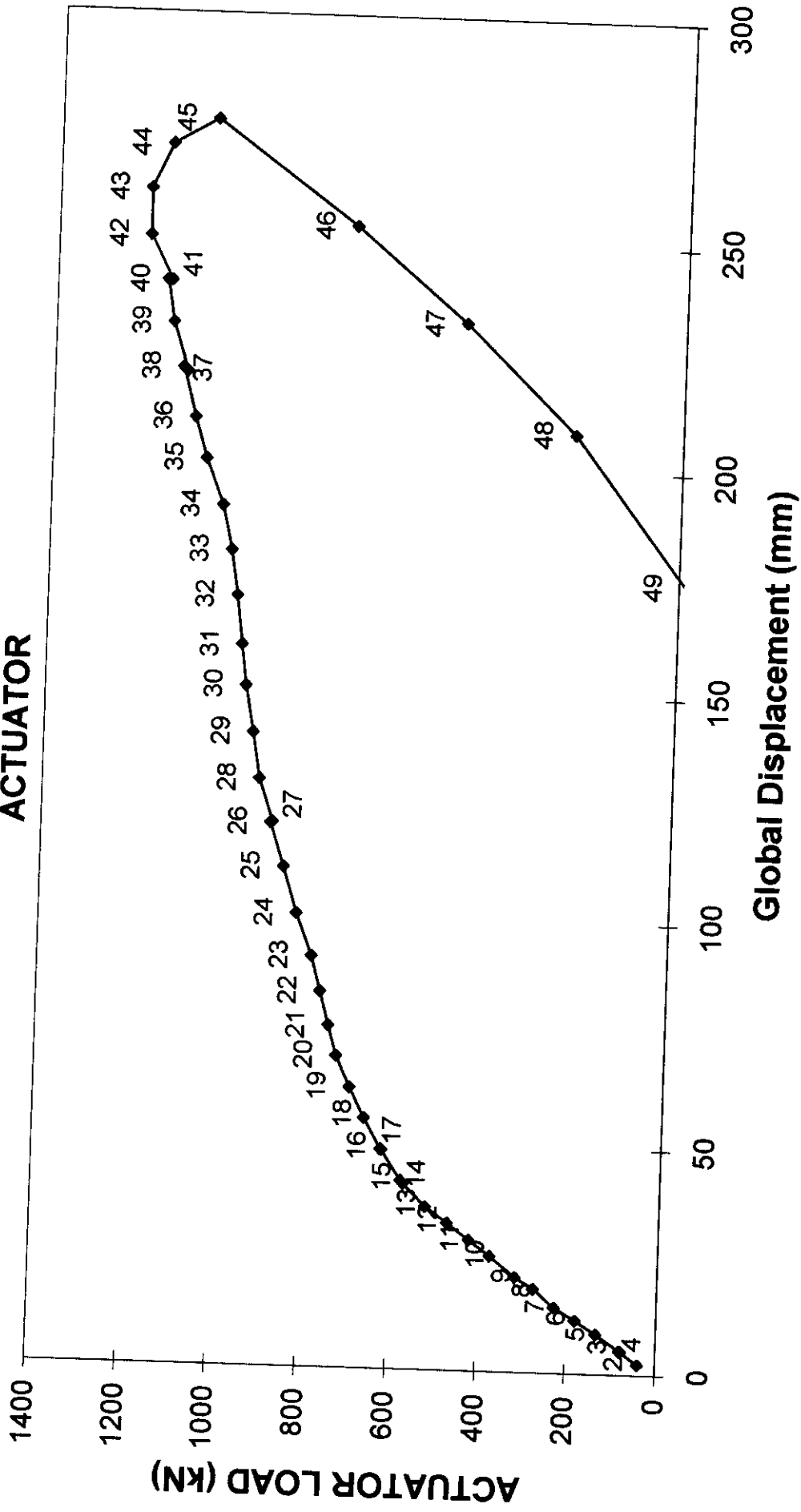
Spreadsheet from C636\39\009w.xls

- Loading and logger chart

Spreadsheet from C636\47\011w.xls

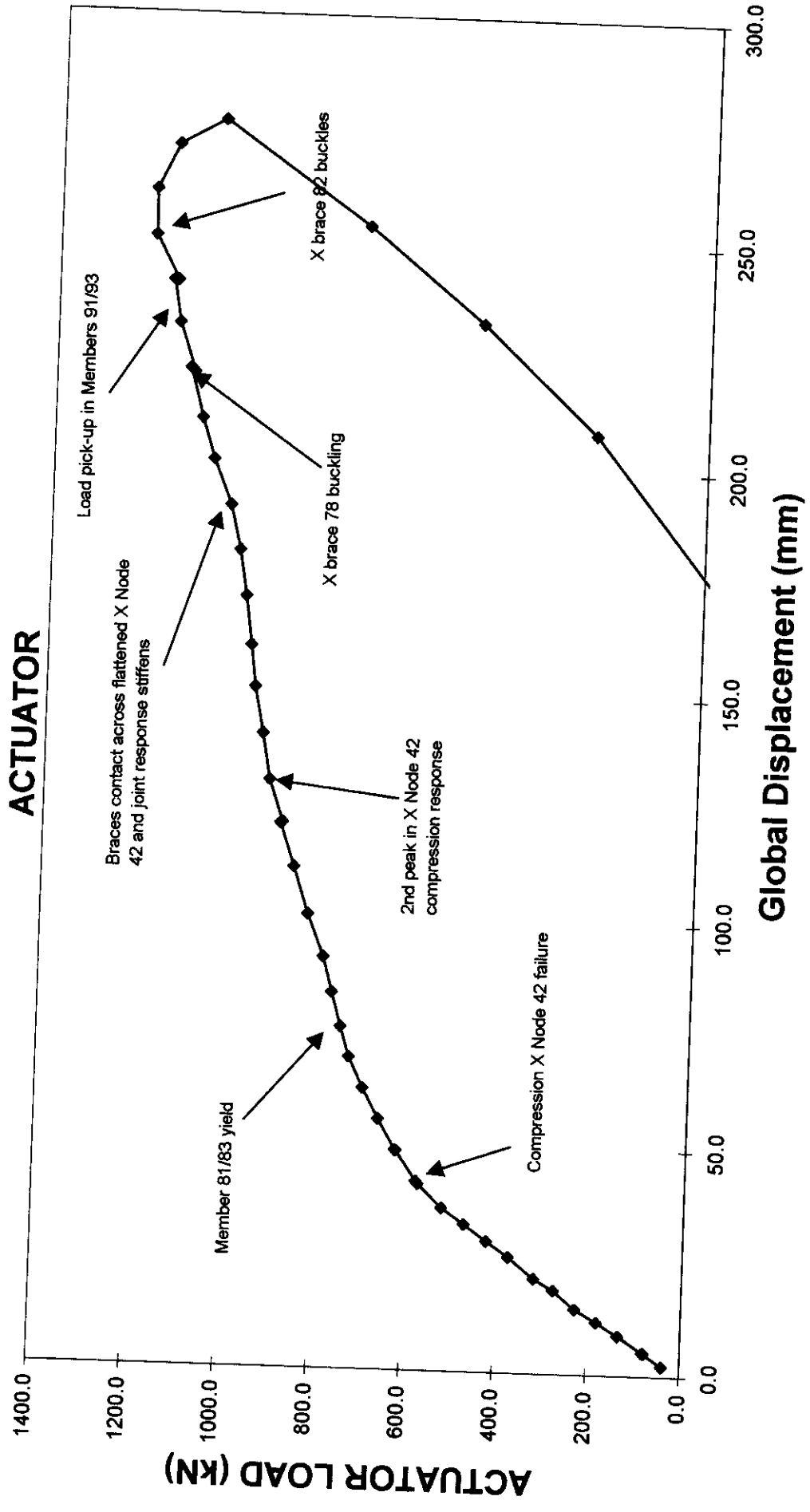
- Global
- Fr E TB For
- Fr E BB For
- Fr D TB For
- Fr D BB For
- Fr E Leg For
- Level 2-X For

# GLOBAL RESPONSE ACTUATOR



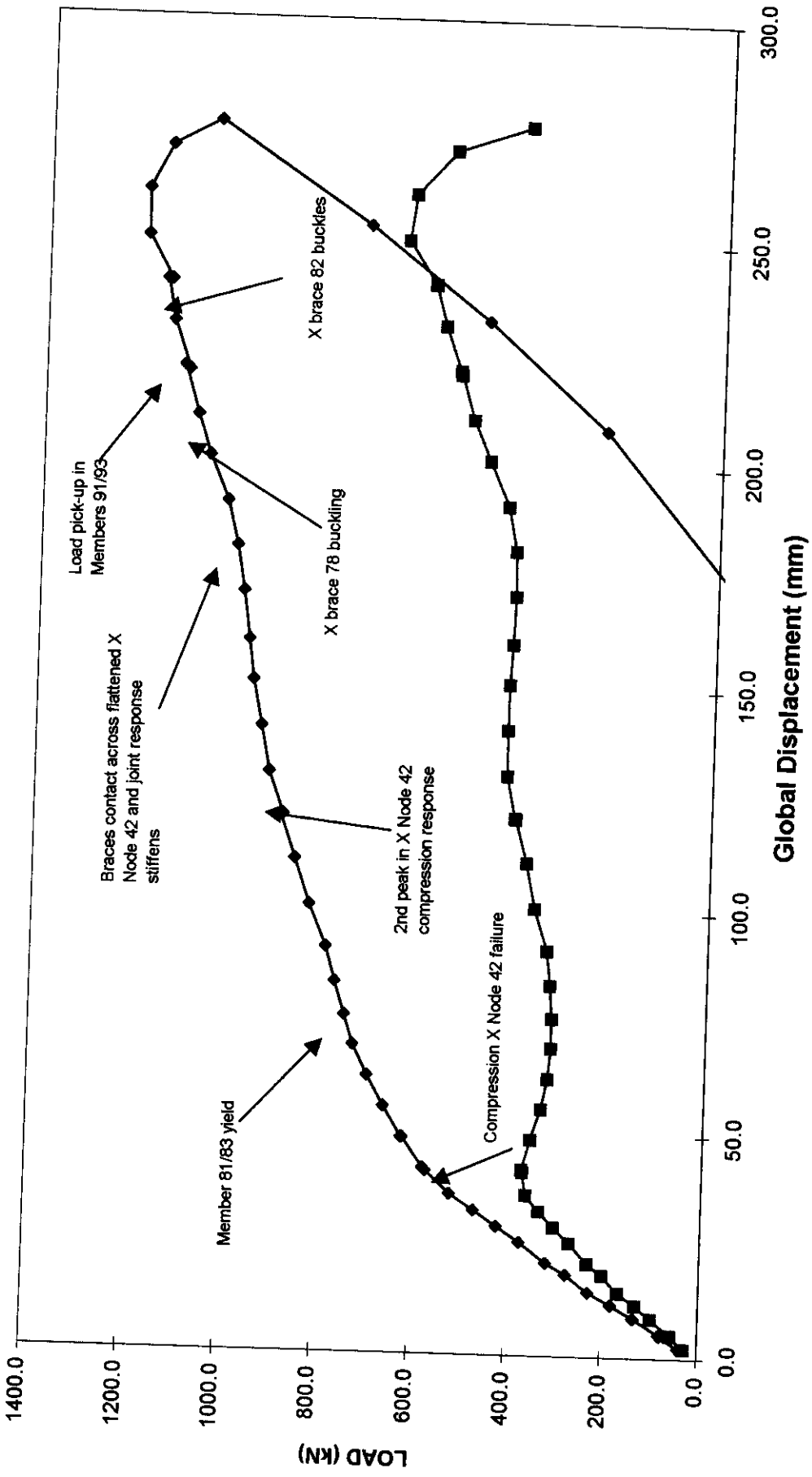
Loadcase 2 - Test

# GLOBAL RESPONSE ACTUATOR



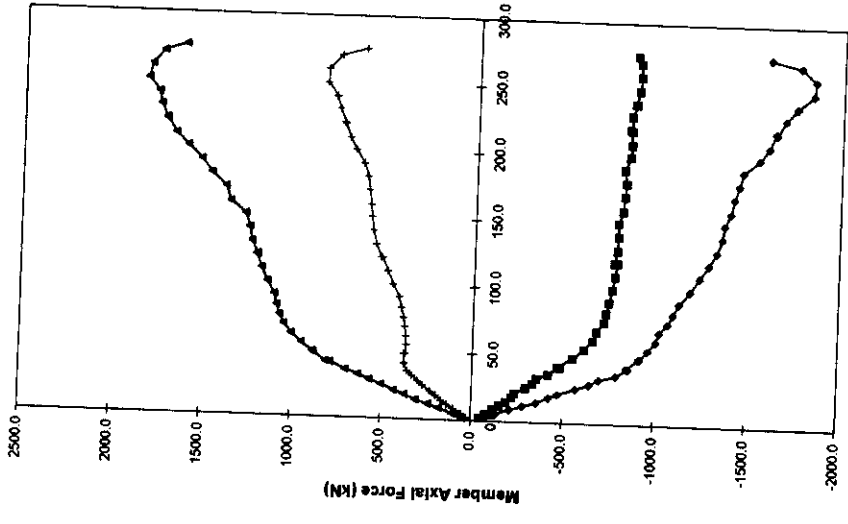
## Loadcase 2 - Test

# GLOBAL RESPONSE



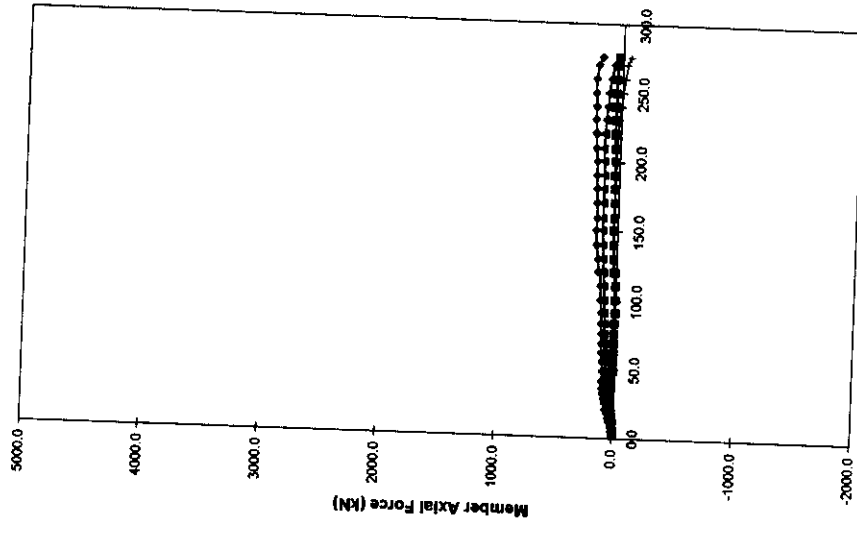
Loadcase 2 - Test      ◆ Global applied load      ■ Node 42 compression X joint response

FRAME E - LEGS  
MEMBER FORCES



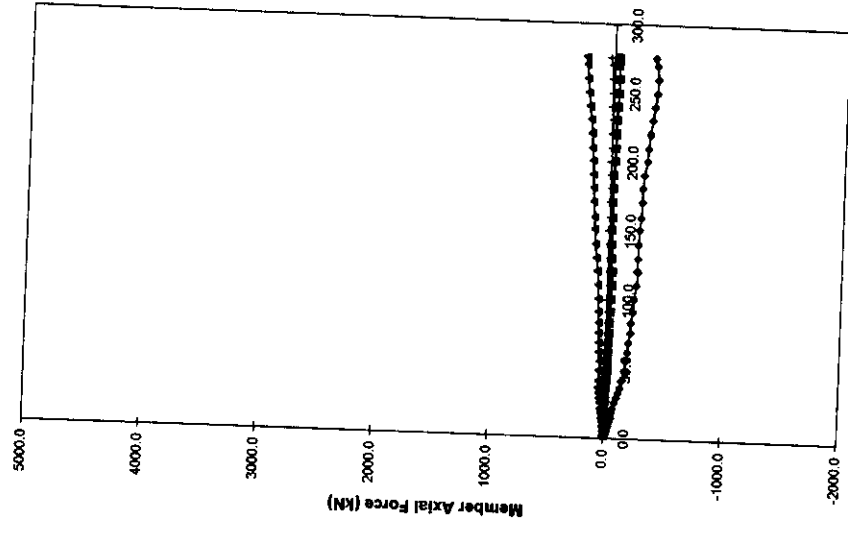
Global Displacement (mm)  
Loadcase 2 - Test  
8 Measured 38 Measured  
9 Measured 39 Measured

FRAME D - LEGS  
MEMBER FORCES



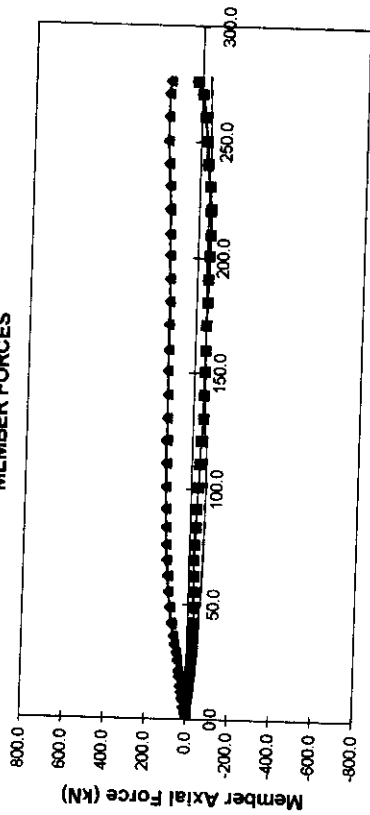
Global Displacement (mm)  
Loadcase 2 - Test  
5 Measured 35 Measured  
6 Measured 36 Measured

FRAME C - LEGS  
MEMBER FORCES



Global Displacement (mm)  
Loadcase 2 - Test  
2 Measured 32 Measured  
3 Measured 33 Measured

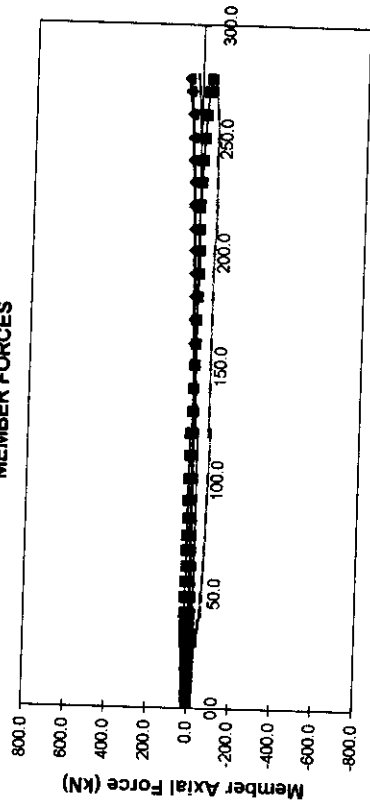
FRAME A - TOP ED  
MEMBER FORCES



Loadcase 2 - Test

◆ 57 Measured    ■ 58 Measured    ▲ 59 Measured  
+ 60 Measured

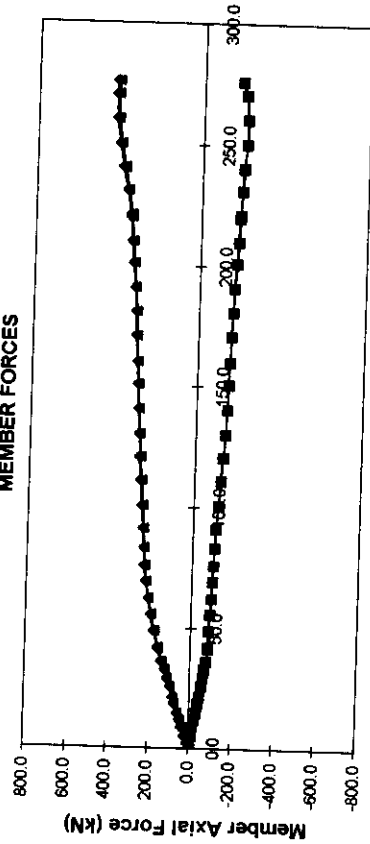
FRAME A - TOP DC  
MEMBER FORCES



Loadcase 2 - Test

◆ 49 Measured    ■ 50 Measured    ▲ 51 Measured  
+ 52 Measured    - 42 Measured    - 43 Measured

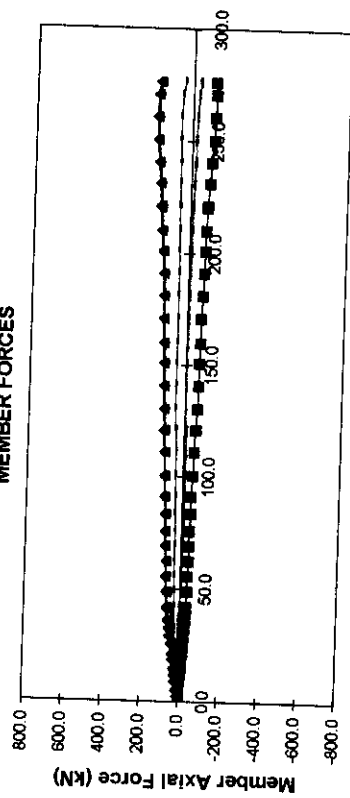
FRAME A - BOTTOM ED  
MEMBER FORCES



Loadcase 2 - Test

◆ 53 Measured    ■ 54 Measured    ▲ 55 Measured    + 56 Measured

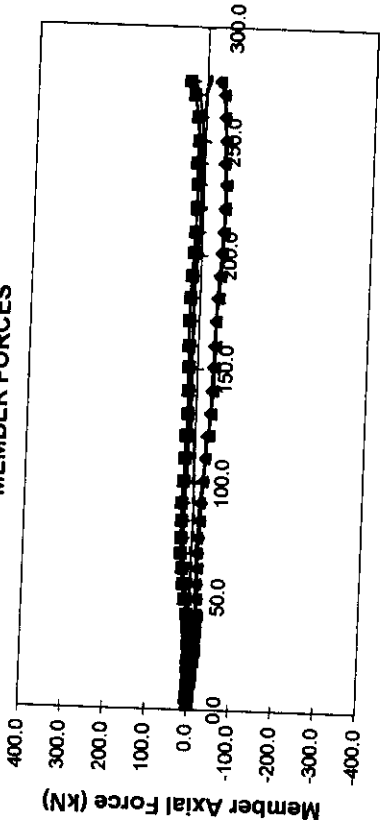
FRAME A - BOTTOM DC  
MEMBER FORCES



Loadcase 2 - Test

◆ 45 Measured    ■ 46 Measured    ▲ 47 Measured  
+ 48 Measured    - 40 Measured    - 41 Measured

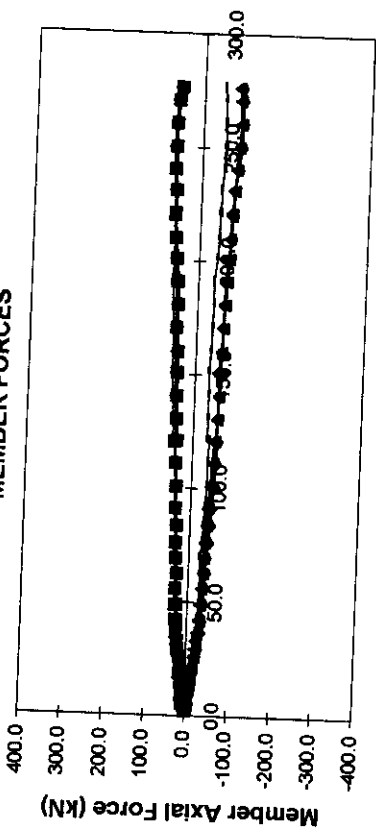
FRAME B - TOP ED  
MEMBER FORCES



Loadcase 2 - Test Global Displacement (mm)

- ◆ 27 Measured
- ◆ 28 Measured
- ◆ 30 Measured
- ◆ 14 Measured
- ◆ 29 Measured

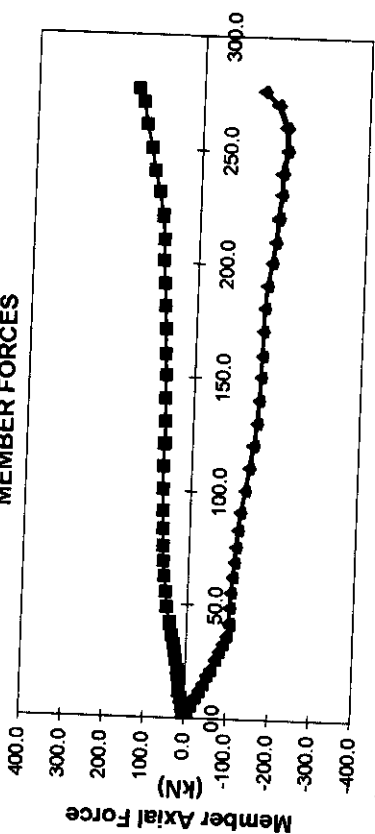
FRAME B - TOP DC  
MEMBER FORCES



Loadcase 2 - Test Global Displacement (mm)

- ◆ 19 Measured
- ◆ 20 Measured
- ◆ 22 Measured
- ◆ 12 Measured
- ◆ 21 Measured
- ◆ 13 Measured

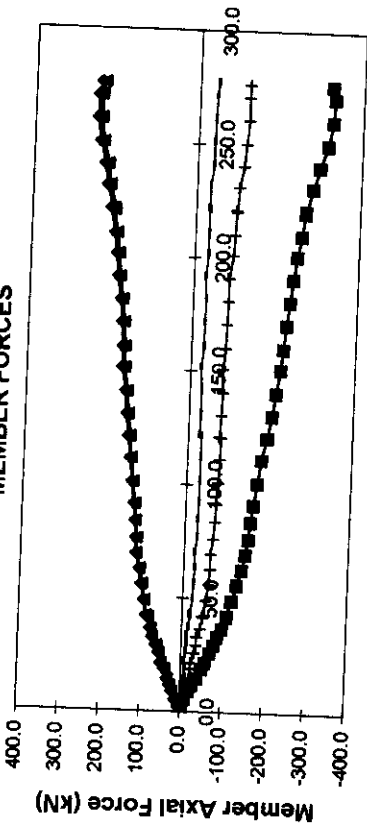
FRAME B - BOTTOM ED  
MEMBER FORCES



Loadcase 2 - Test Global Displacement (mm)

- ◆ 23 Measured
- ◆ 24 Measured
- ◆ 25 Measured

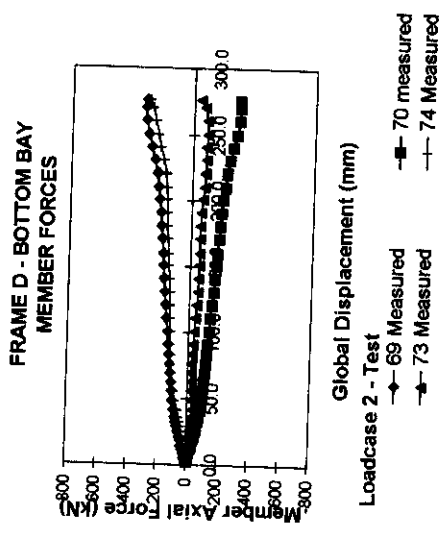
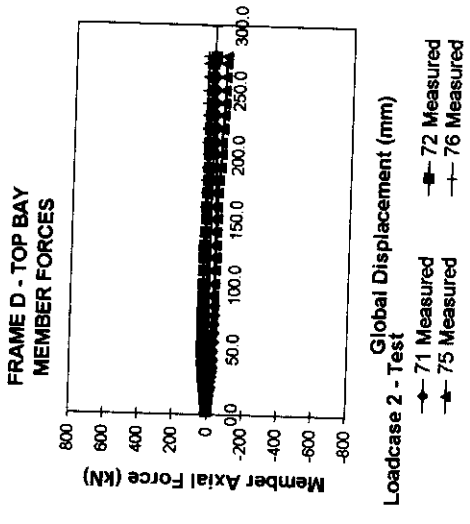
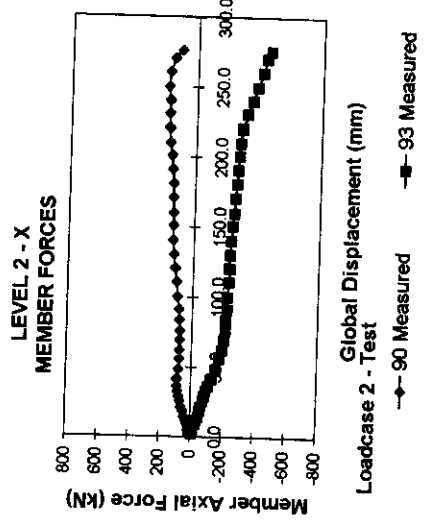
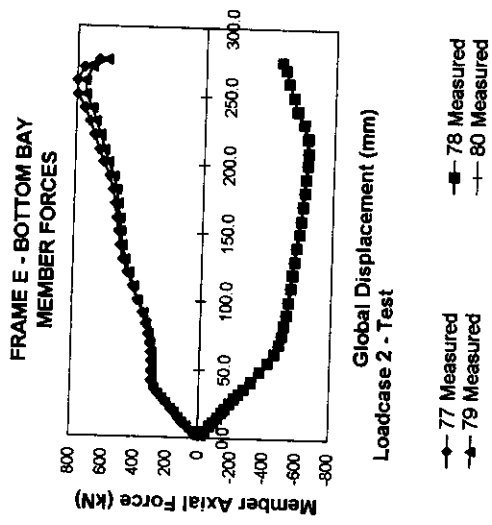
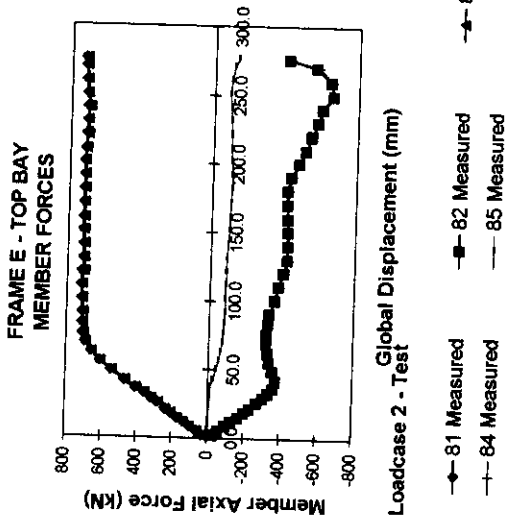
FRAME B - BOTTOM DC  
MEMBER FORCES



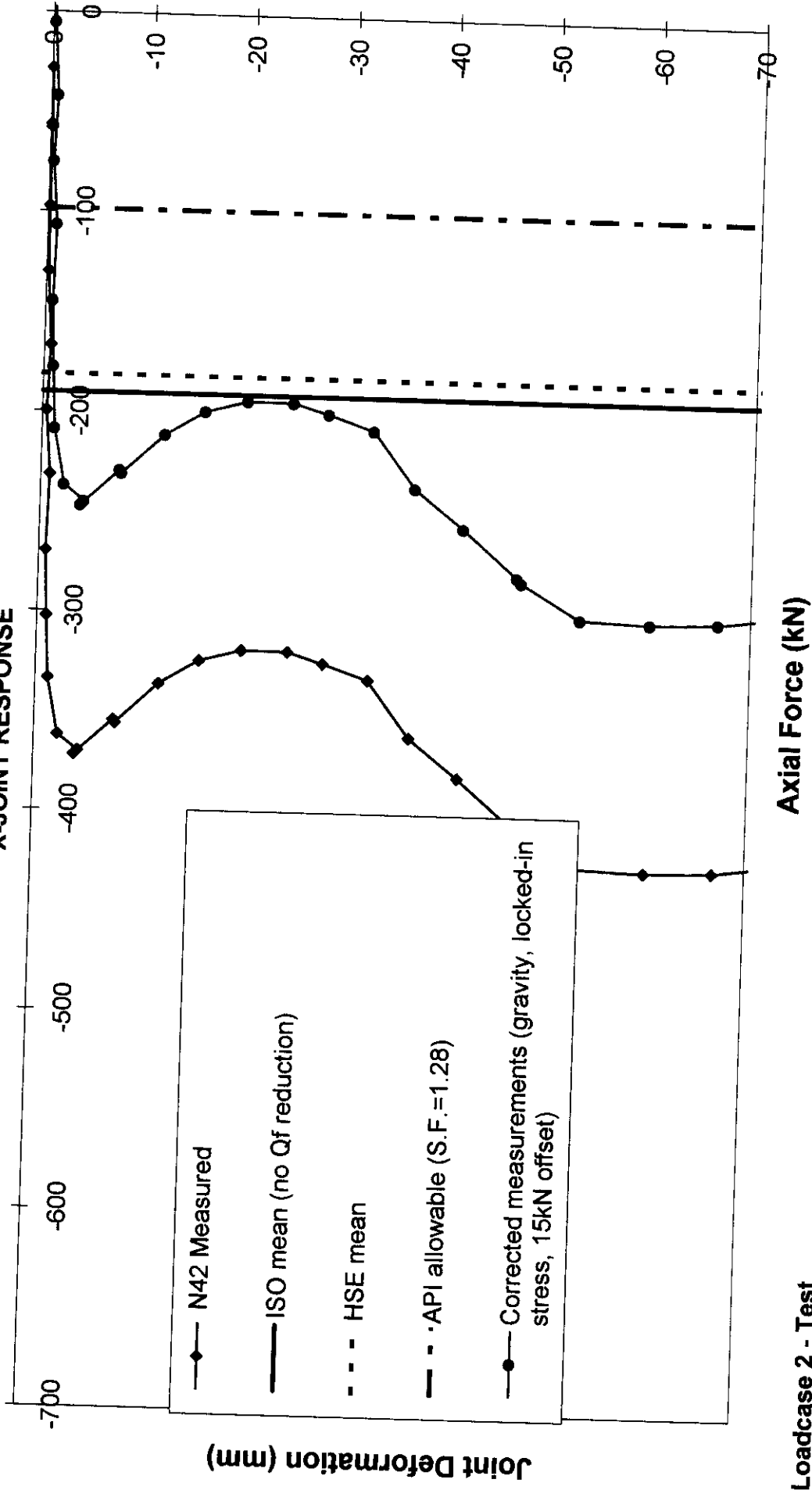
Loadcase 2 - Test Global Displacement (mm)

- ◆ 16 Measured
- ◆ 17 Measured
- ◆ 10 Measured
- ◆ 11 Measured
- ◆ 18 Measured



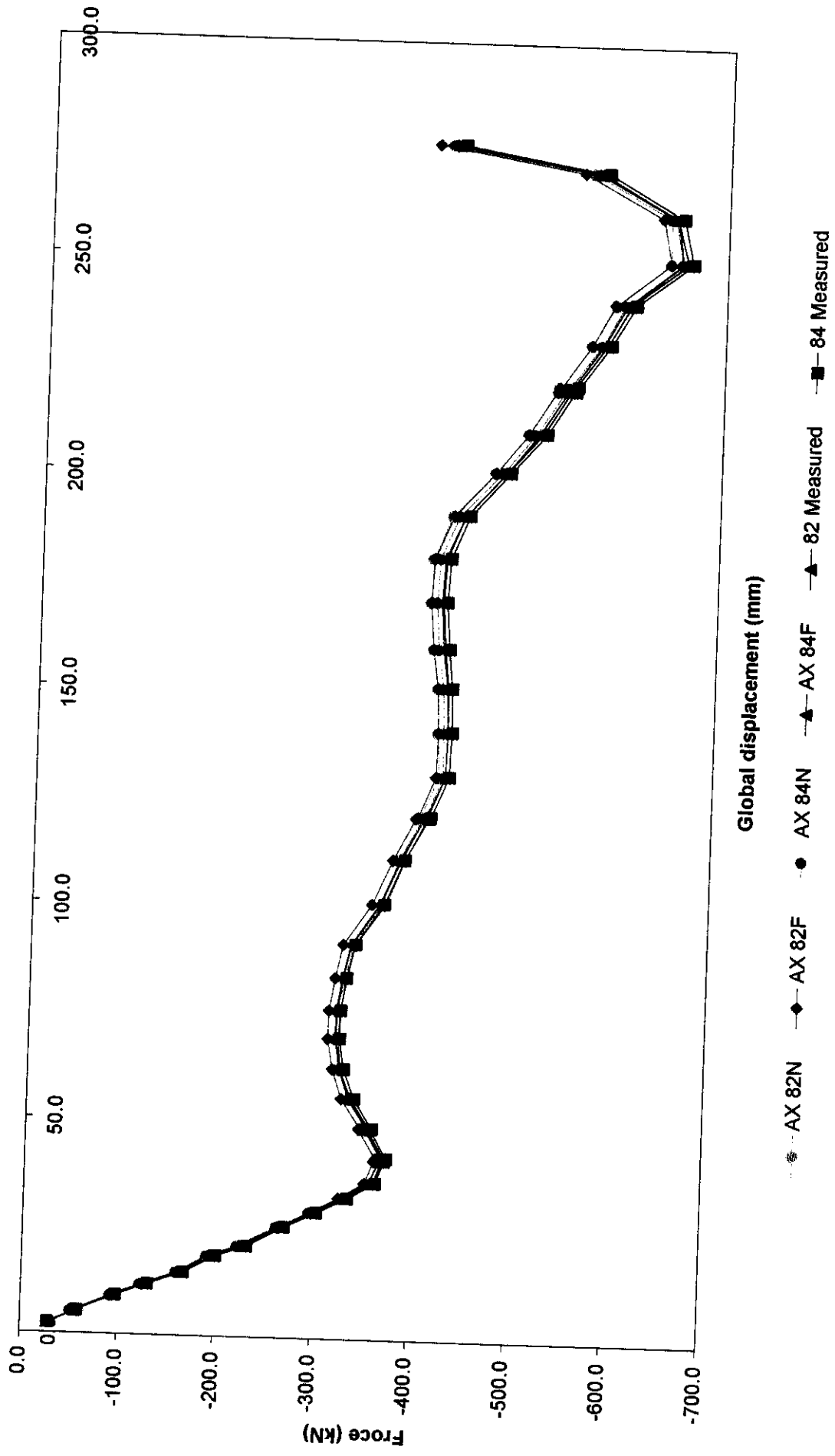


FRAME E- TOP BAY - COMPRESSION  
X-JOINT RESPONSE

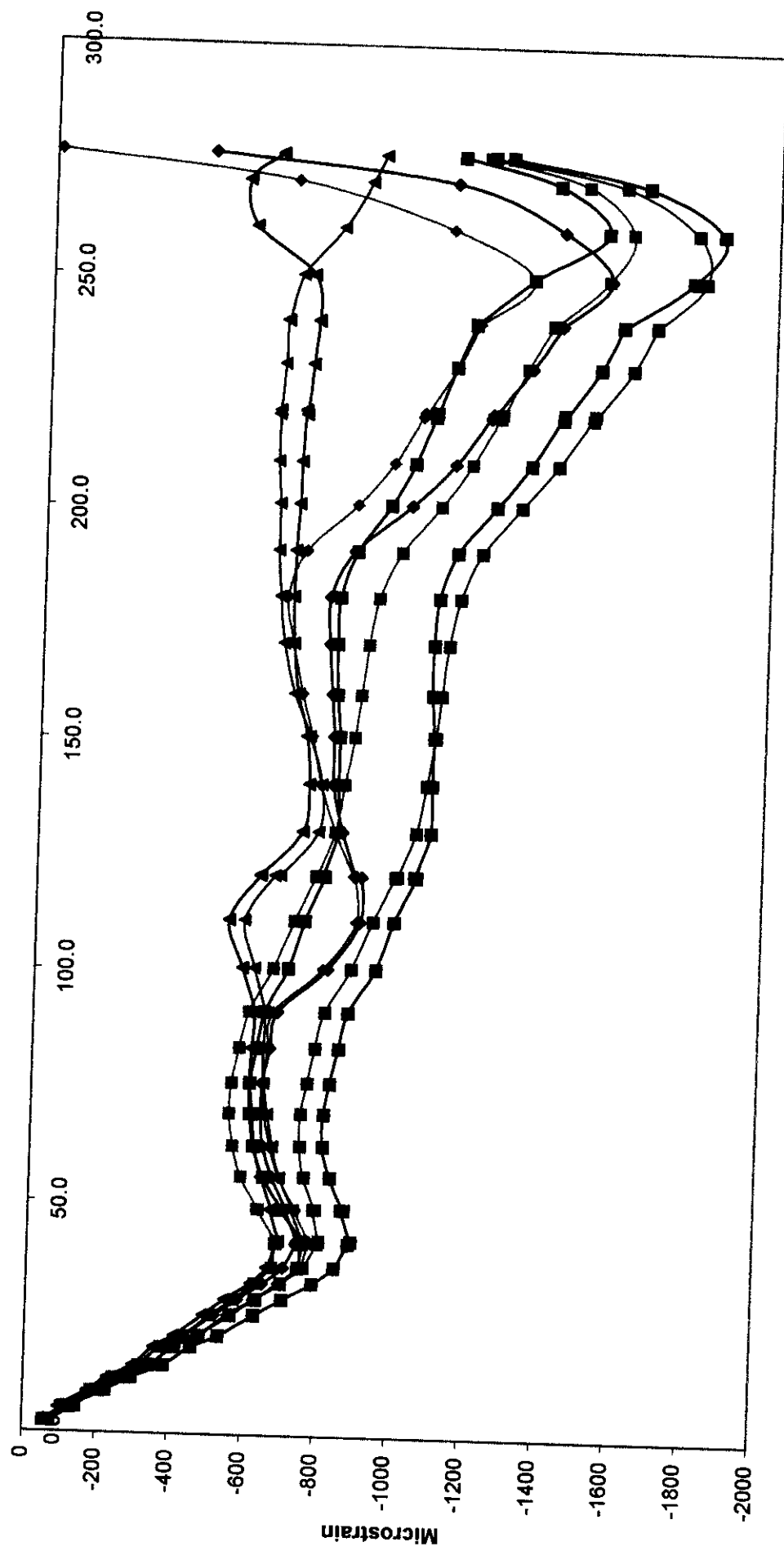


Loadcase 2 - Test

Forces across Node 42 compression X joint



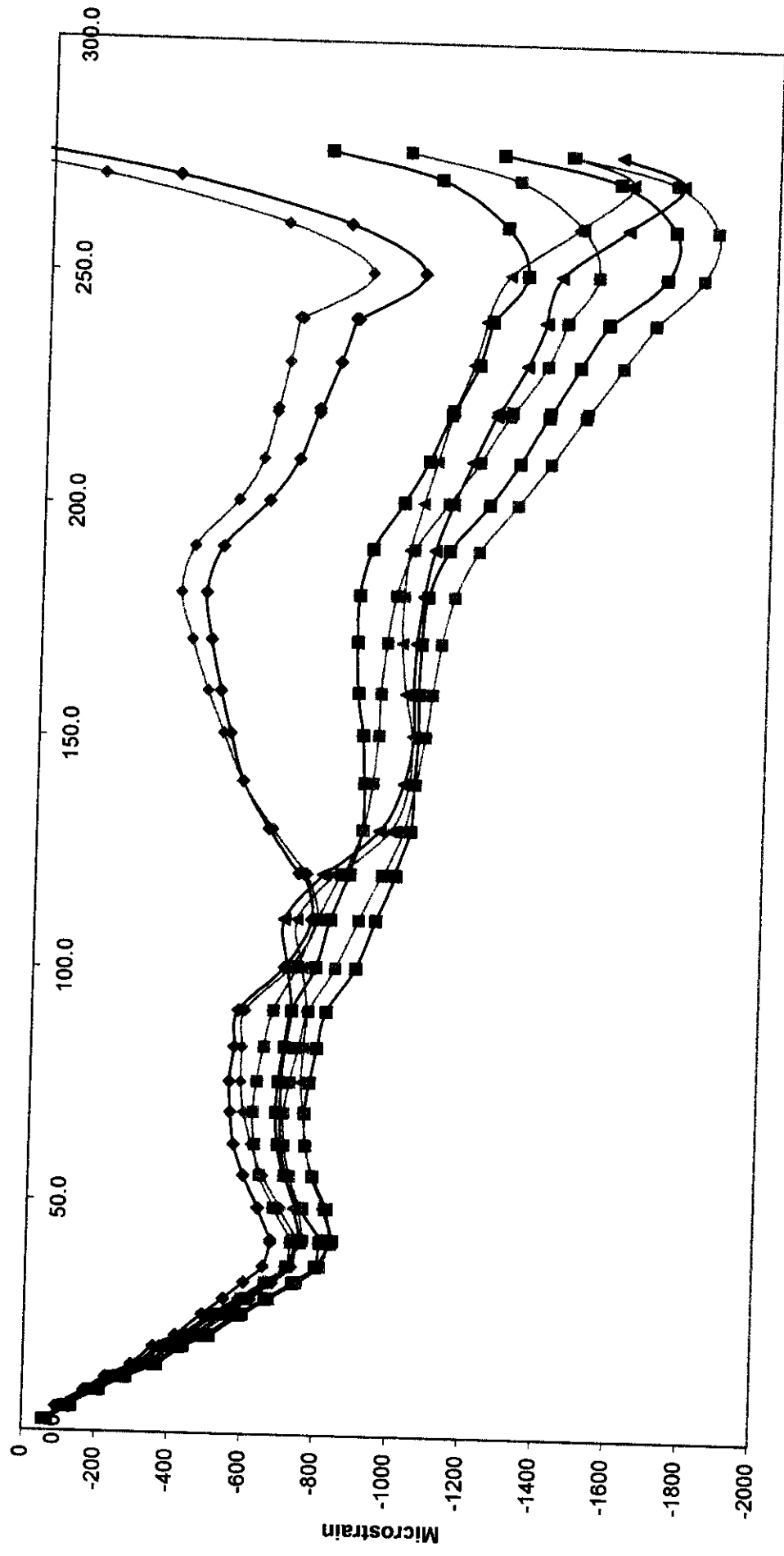
### Node 42 - Local strains on X joint chord



Global displacement (mm)

—◆— 82N3 —■— 82N5 —▲— 82N7 —■— 82F1 —◆— 82F3 —■— 82F5 —▲— 82F7 —■— 82N1

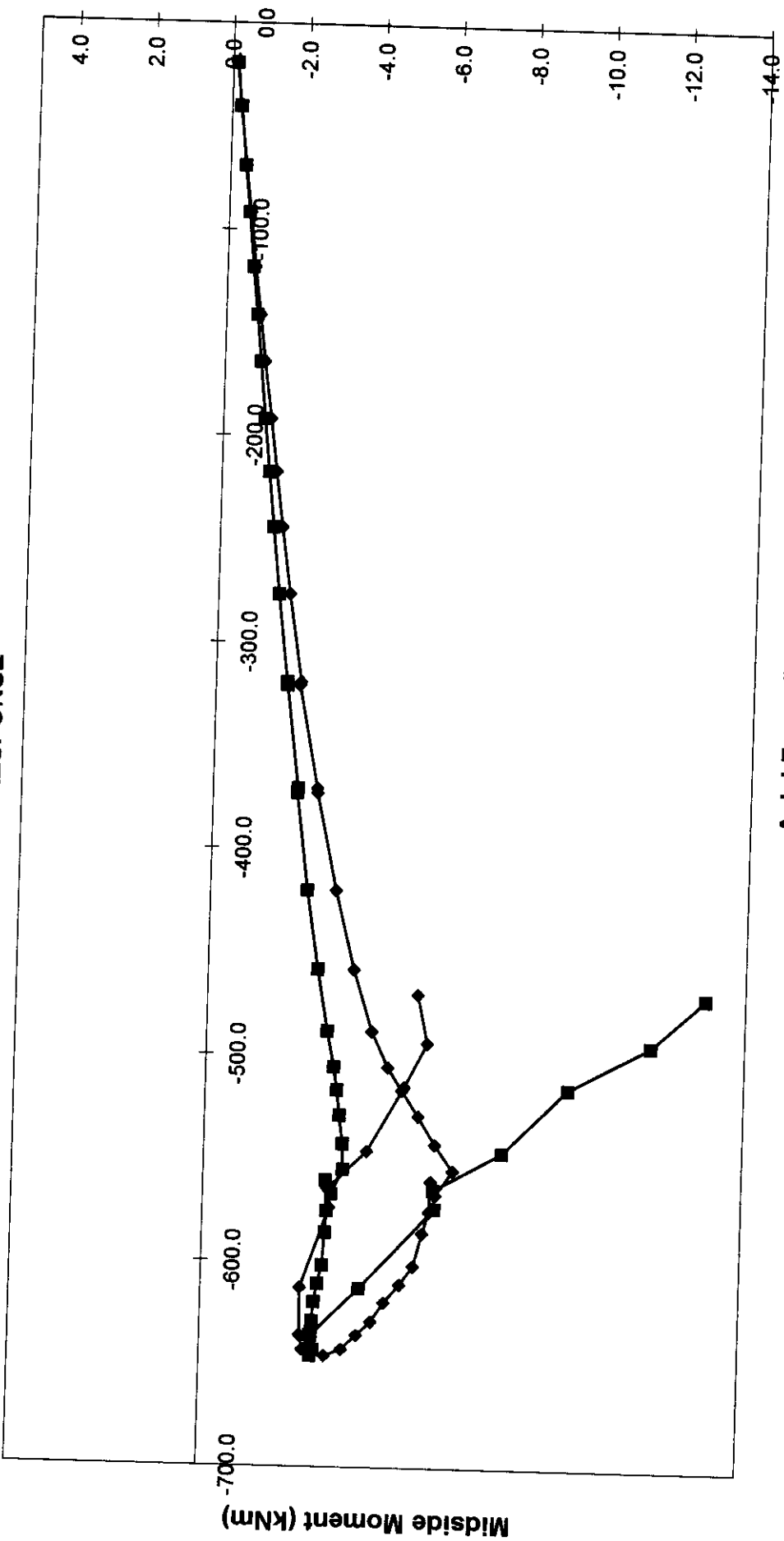
### Node 42 - Local strains on X joint chord



Global displacement (mm)

- 84N1
- 84N3
- 84N5
- 84N7
- 84F1
- 84F3
- 84F5
- 84F7

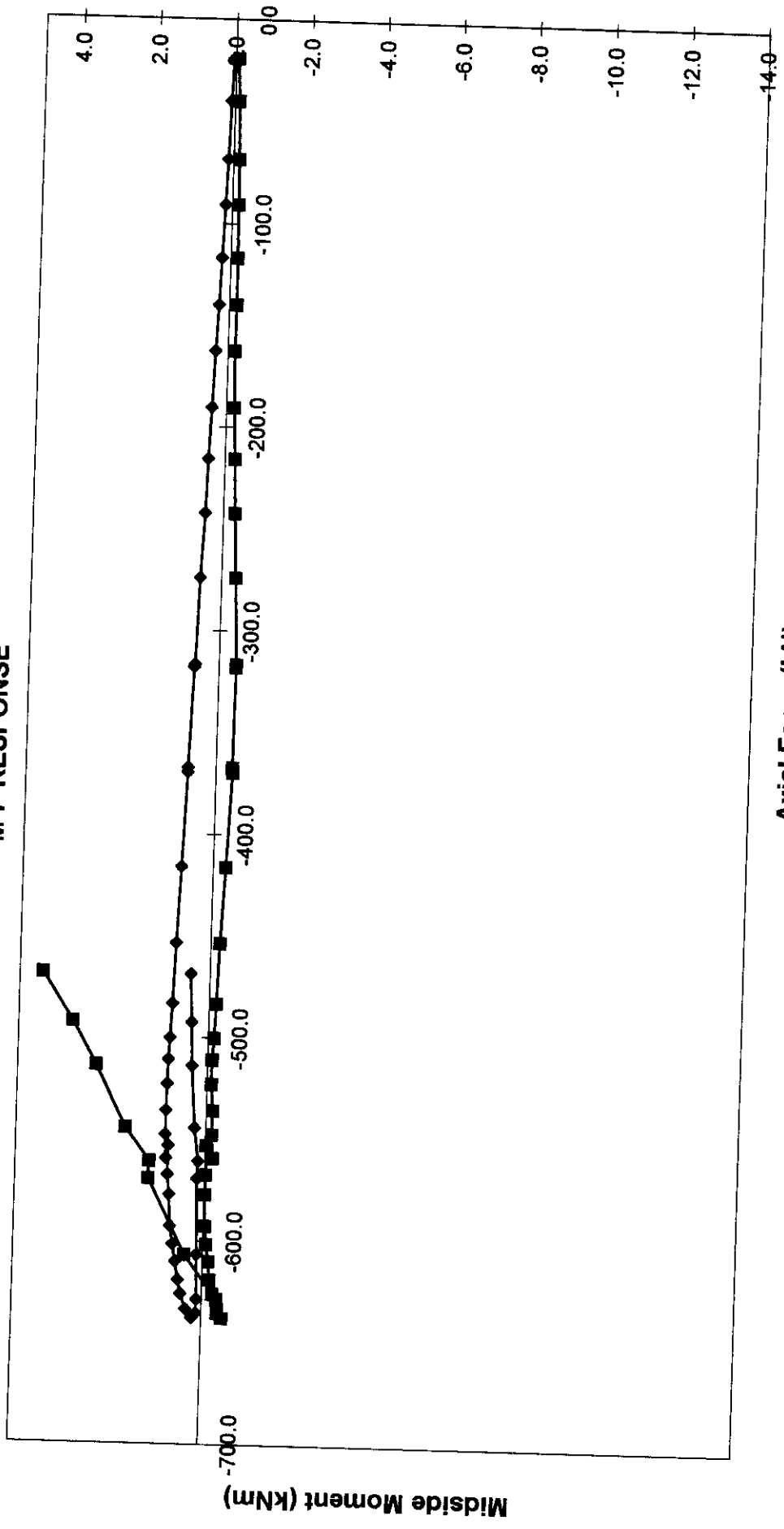
**FRAME E - BOTTOM BAY - UPPER  
M-P RESPONSE**



Loadcase 2 - Test

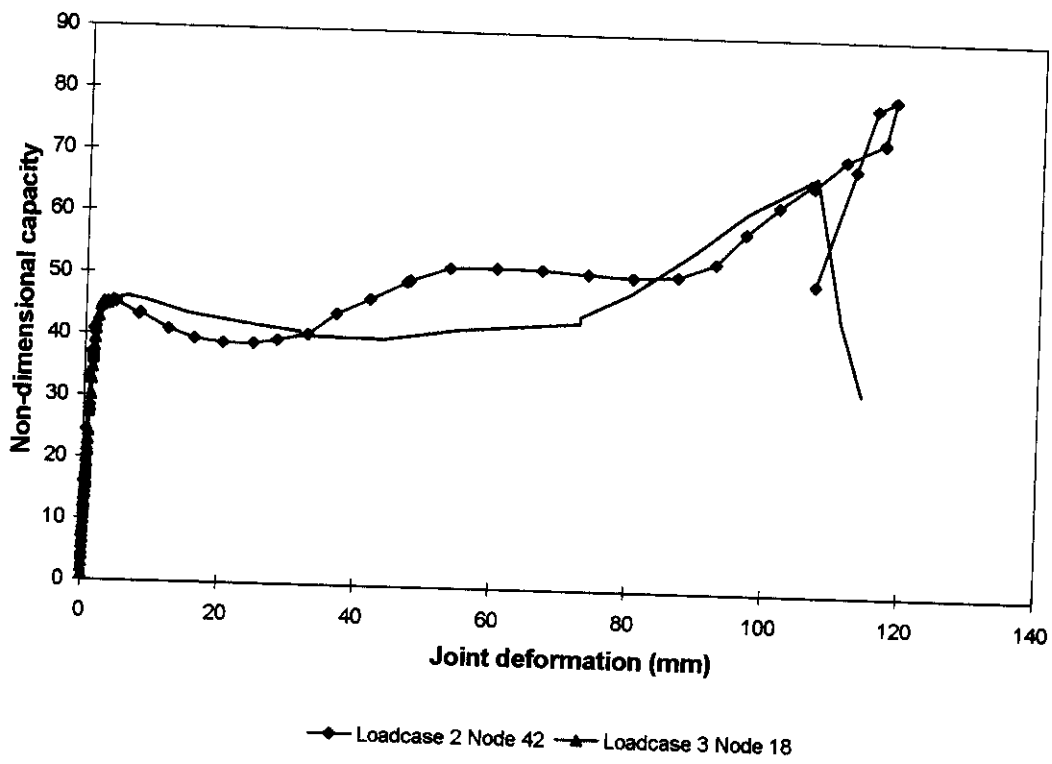
78 IP Measured    78 OP Measured

**FRAME E - BOTTOM BAY - LOWER  
M-P RESPONSE**

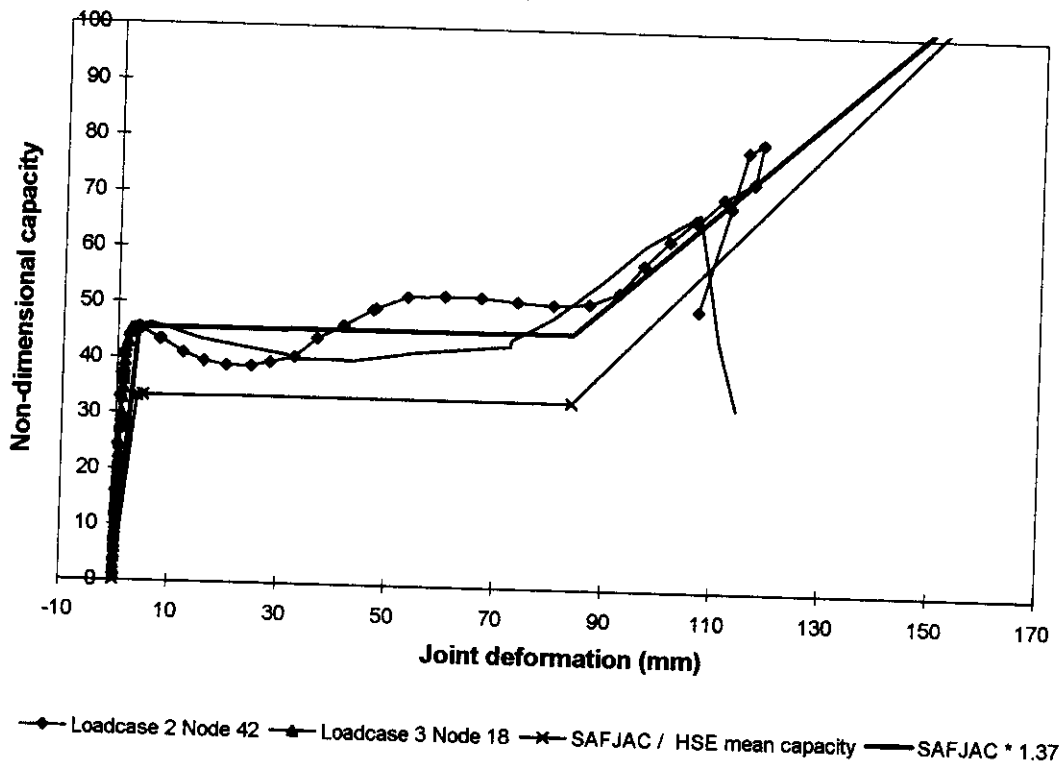


**Loadcase 2 - Test**      **Axial Force (kN)**  
 —◆— 80 IP Measured      —■— 80 OP Measured

Compression X joint - Load deformation responses

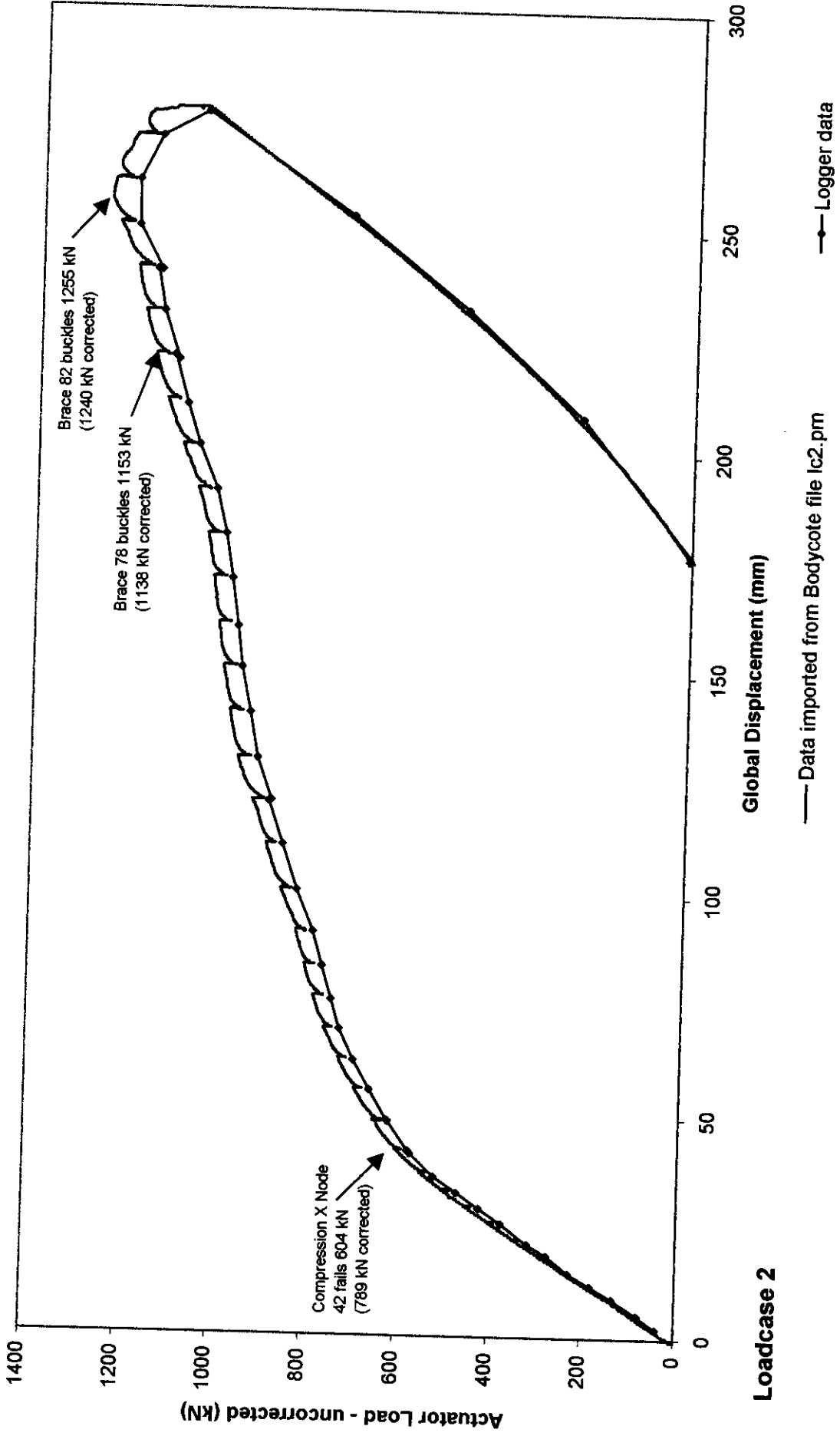


Compression X joint - Load deformation responses  
SAFJAC comparison

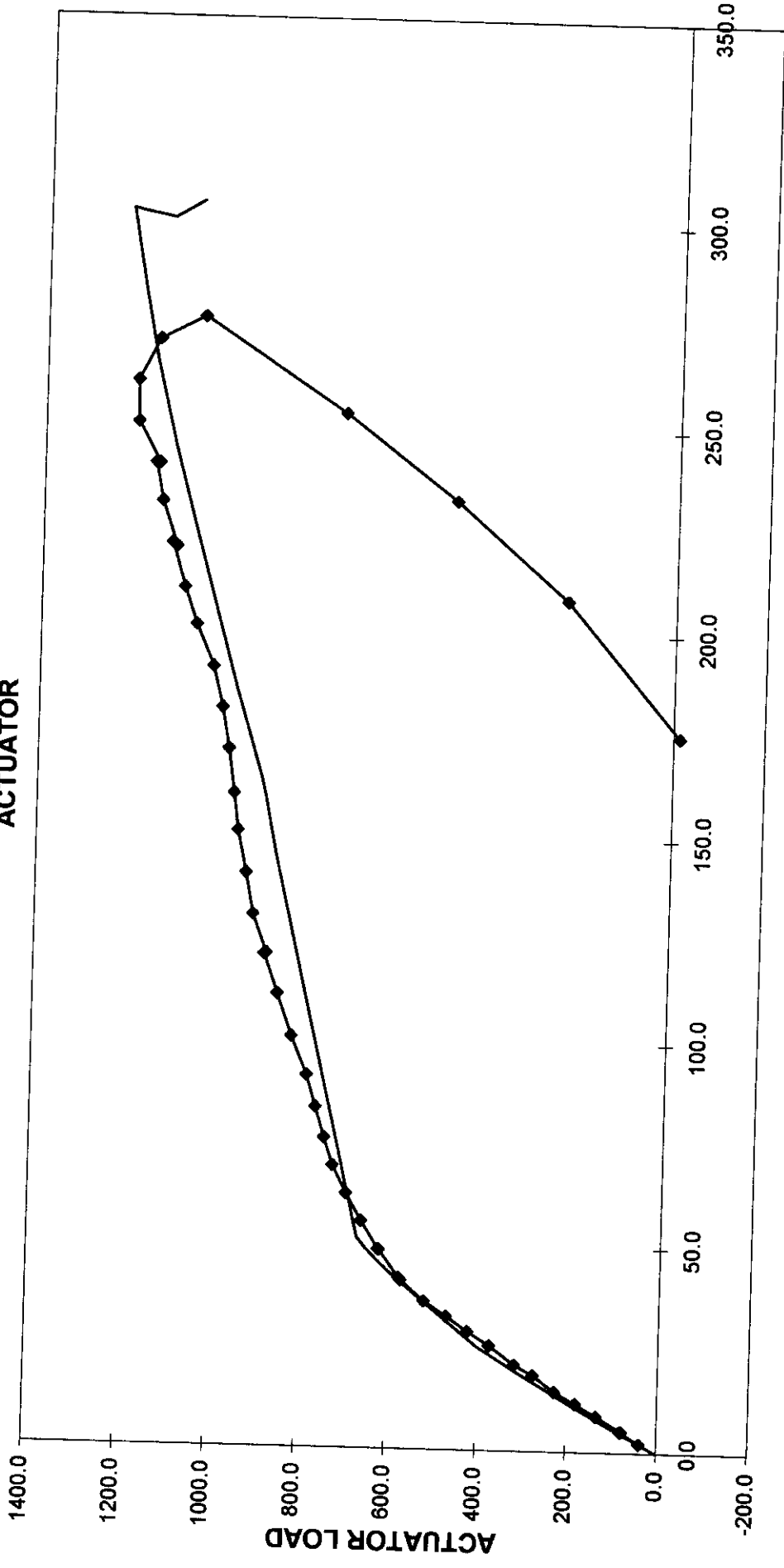




# GLOBAL RESPONSE FROM LOADING SYSTEM



# GLOBAL RESPONSE ACTUATOR



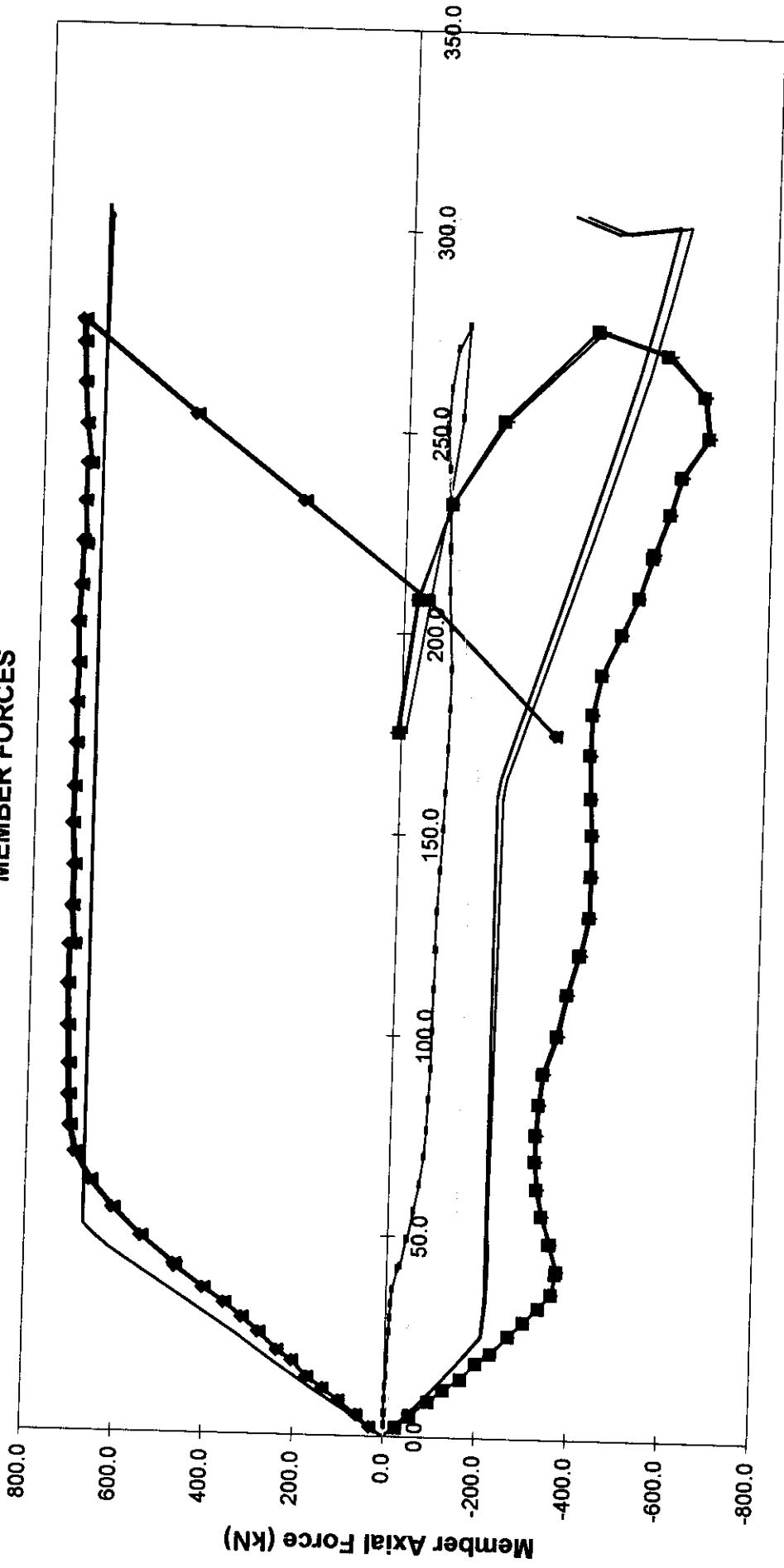
Global Displacement (mm)

◆ Measured  
— Predicted

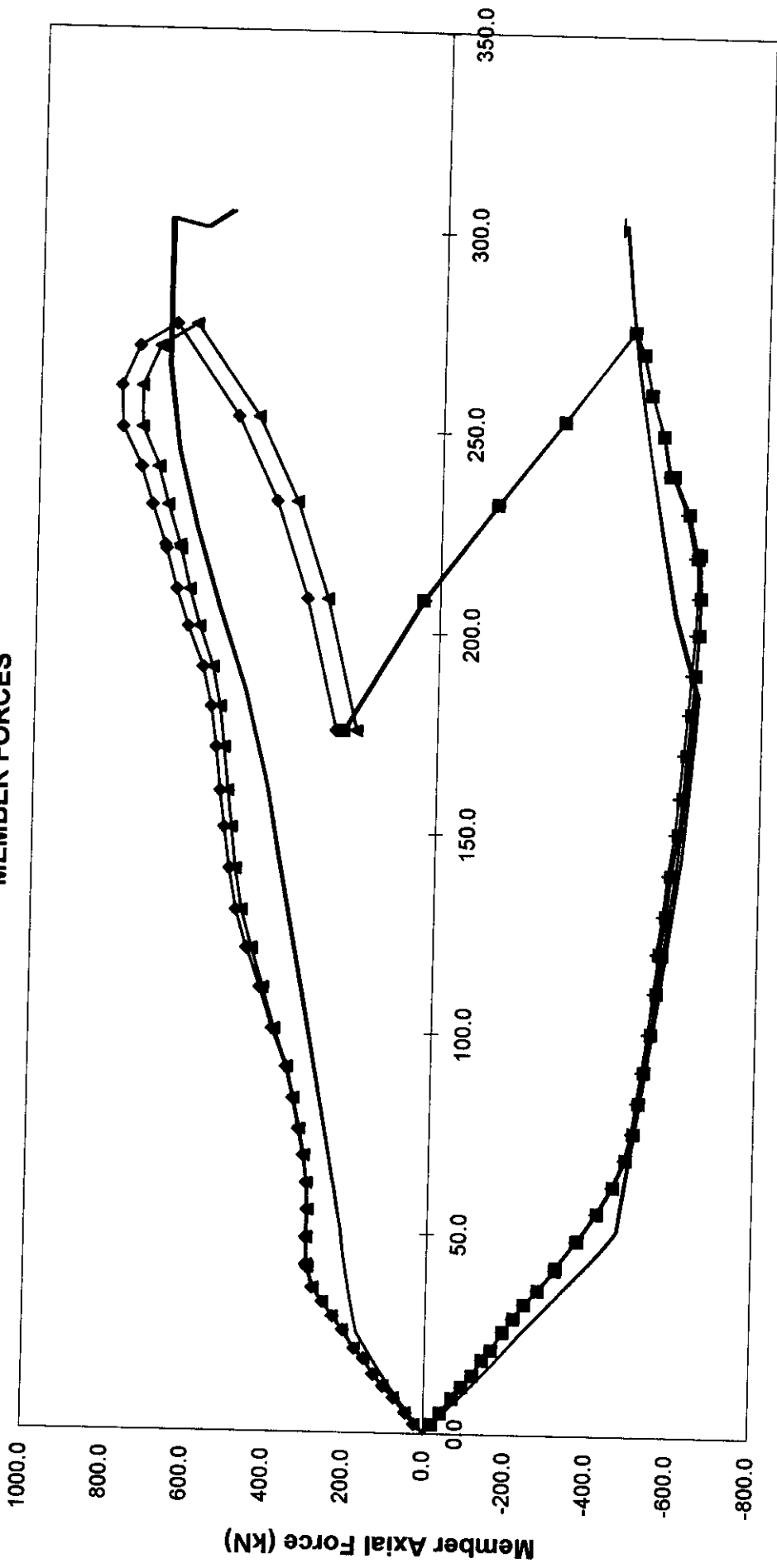
Loadcase 2 - Test

011w\_copy of LC2a\_Test with 15kN corm.xls GLOBAL 02/09/99

FRAME E - TOP BAY  
MEMBER FORCES



**FRAME E - BOTTOM BAY  
MEMBER FORCES**

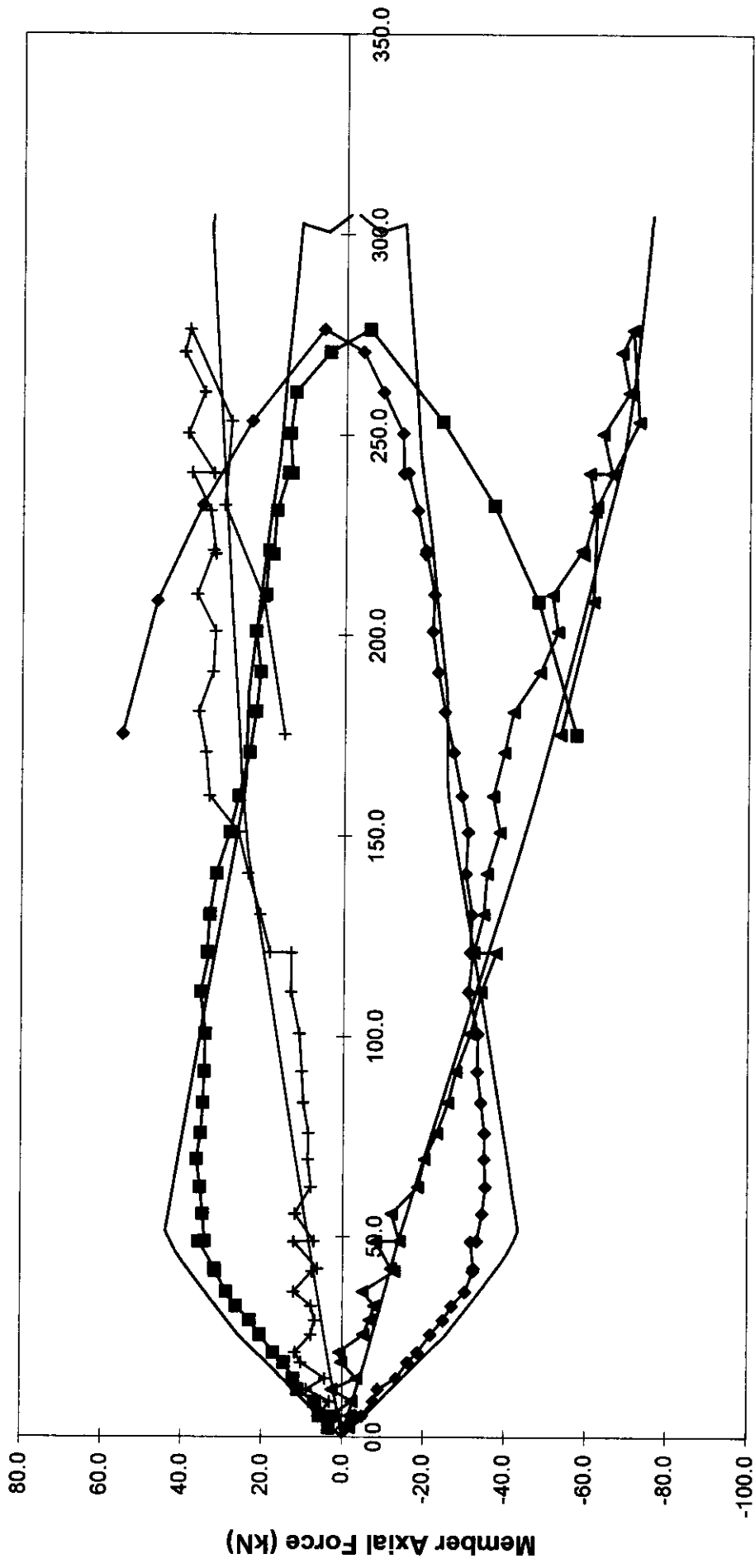


**Loadcase 2 - Test**

◆ 77 Measured    ■ 78 Measured    ▲ 79 Measured    + 80 Measured  
 — 77 Predicted    — 78 Predicted    — 79 Predicted    — 80 Predicted

**Global Displacement (mm)**

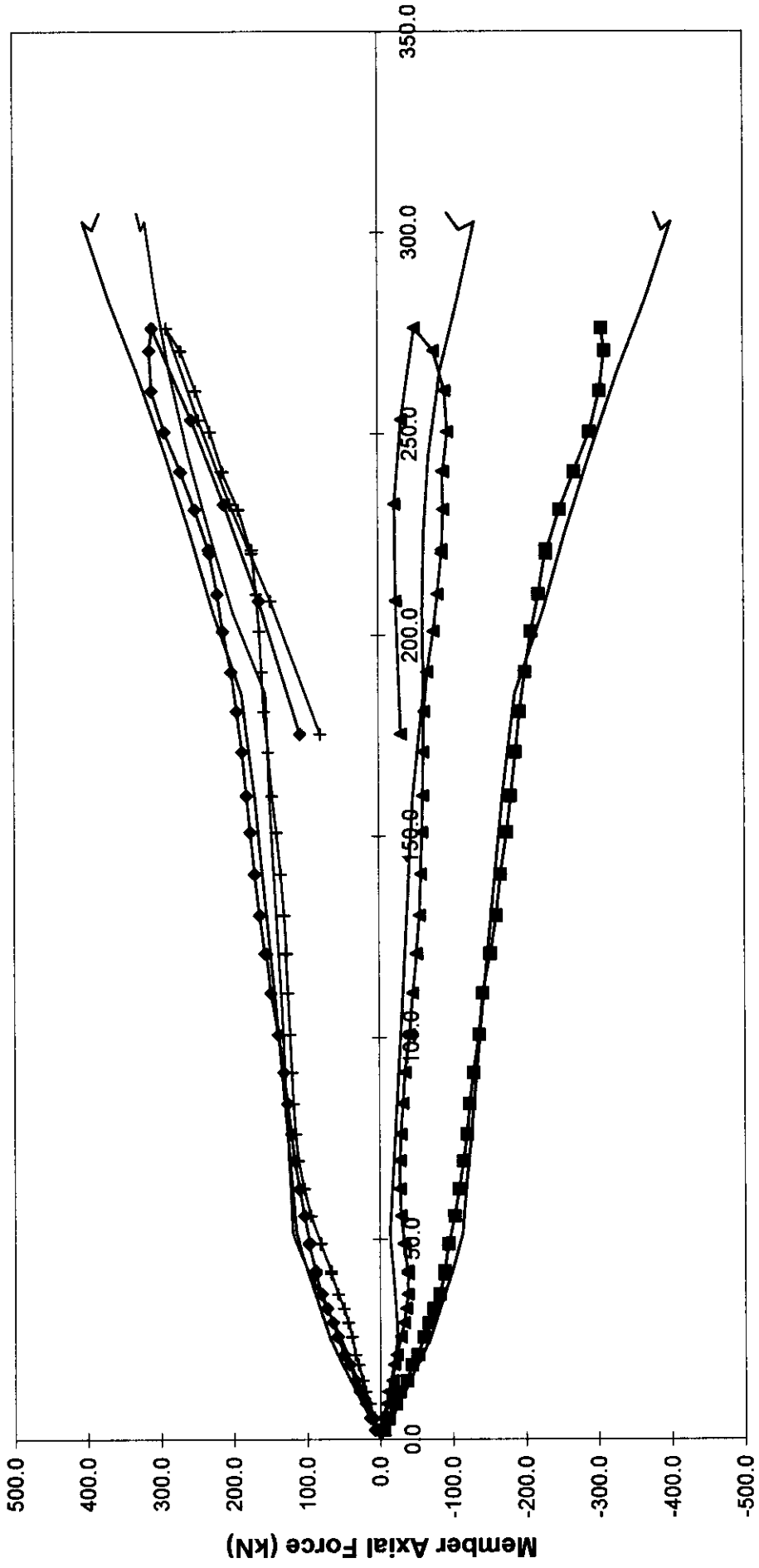
**FRAME D - TOP BAY  
MEMBER FORCES**



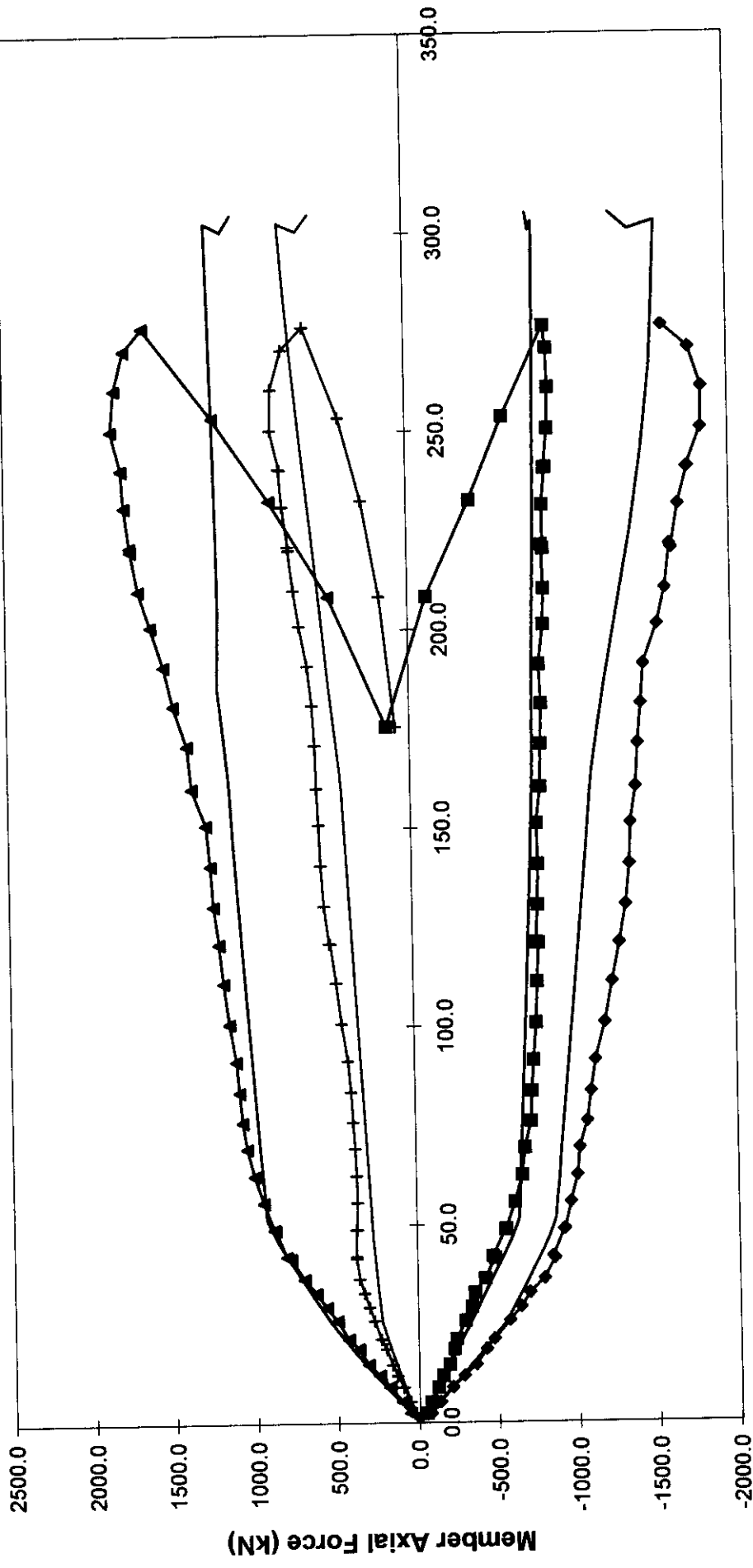
**Global Displacement (mm)**

- Loadcase 2 - Test**
- ◆— 71 Measured
  - 72 Measured
  - ▲— 75 Measured
  - +— 76 Measured
  - 71 Predicted
  - 72 Predicted
  - 75 Predicted
  - 76 Predicted

**FRAME D - BOTTOM BAY  
MEMBER FORCES**



**FRAME E - LEGS  
MEMBER FORCES**

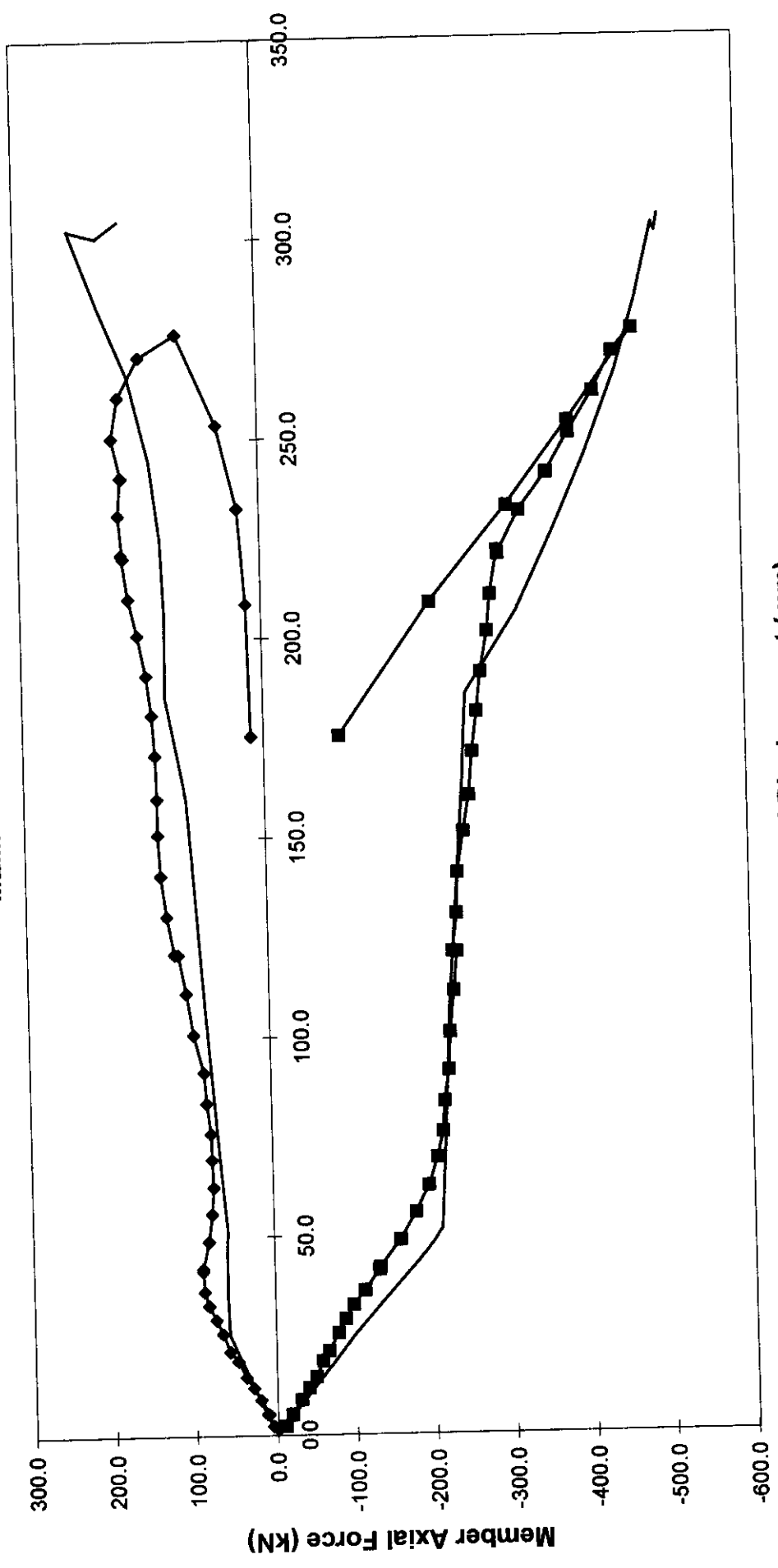


**Loadcase 2 - Test**

**Global Displacement (mm)**

- ◆ 8 Measured
- 9 Measured
- ▲ 38 Measured
- + 39 Measured
- 8 Predicted
- 9 Predicted
- 38 Predicted
- 39 Predicted

**LEVEL 2 - X  
MEMBER FORCES**



**Global Displacement (mm)**

◆ 90 Measured  
 ◆ 93 Measured  
 — 90 Predicted  
 — 93 Predicted

**Loadcase 2 - Test**



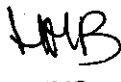




*The contents of this document are confidential to Participants of the Frames Project - Phase III, under the terms of their contract for participation in the project*

**JOINT INDUSTRY TUBULAR FRAMES PROJECT -  
PHASE III**

**SITE TESTING PROGRAMME RESULTS  
REPORT TO BENCHMARK ANALYSTS**

C636\32\066R REV A AUGUST 1999

Purpose of Issue	Rev	Date of Issue	Author	Checked	Approved
For implementation by Benchmark Analysts	0	July 1999	HMB	RCH	CJB
For review by Participants	A	August 1999	 HMB	 RCH	 CJB

Controlled Copy	24	Uncontrolled Copy	
-----------------	----	-------------------	--

**BOMEL LIMITED**

Ledger House  
Forest Green Road, Fifield  
Maidenhead, Berkshire  
SL6 2NR, UK

Telephone +44 (0)1628 777707  
Fax +44 (0)1628 777877  
Email bomel@compuserve.com



**REVISION SHEET**

REVISION	DETAILS OF REVISION	DATE
0	For implementation by Benchmark Analysts	July 1999
A	For review by Project Participants. Revision 0 updated to include Foreword and minor typographical corrections	August 1999

**FILE SHEET**

PATH AND FILENAME	DETAILS OF FILE
C636\26\frame2.pcx	Figure 2.1
C636\26\C476-7.pcx	Figure 2.2(a)
C636\26\C484-23.pcx	Figure 2.2(b)
C636\26\C514-7.pcx	Figure 2.2(c)
C636\12\images\gui7.pcx to gui12.pcx	Figures 2.3 to 2.8
C636\46\001W-a.xls	Figure 3.1
C636\06\307W-a.xls	Figure 3.2
C636\32\005W-B.xls	Figure 4.1
C636\37\011W.xls sheet GLOBAL Scan Nos	Figure 4.2
C636\37\011W sheet GLOBAL Annotated	Figure 4.3
C636\26\C476-30.pcx	Figure 4.4
C636\26\C476-35.pcx	Figure 4.5
C636\26\C476-34.pcx	Figure 4.6
C636\26\C476-25.pcx	Figure 4.7
C636\26\C476-28.pcx	Figure 4.8
C636\32\007W-B.xls	Figure 4.9
C636\39\008W.xls sheet GLOBAL Scan Nos	Figure 4.10
C636\39\008W.xls sheet GLOBAL Annotated	Figure 4.11
C636\26\C486-2.pcx	Figure 4.12
C636\26\C488-4.pcx	Figure 4.13
C636\26\C488-36.pcx	Figure 4.14



**FILE SHEET CONTINUED**

PATH AND FILENAME	DETAILS OF FILE
C636\26\C490-17.pcx	Figure 4.15
C636\26\C490-11.pcx	Figure 4.16
C636\32\009W-C.xls	Figure 4.17
C636\40\016W.xls sheet GLOBAL Scan Nos	Figure 4.18
C636\40\016W.xls sheet GLOBAL Annotated	Figure 4.19
C636\26\515-11.pcx	Figure 4.20
C636\26\515-33.pcx	Figure 4.21
C636\26\C518-3.pcx	Figure 4.22
C636\26\C516-12.pcx	Figure 4.23
C636\26\C518-9.pcx	Figure 4.24
C636\12\006S-B.wpd	Appendix A
C636\25\063W.xls	Appendix B
C636\32\046U.doc	Appendix B
C636\32\058U-A.doc	Appendix B
C636\15\011D-D	Appendix C
C636\15\012D-B	Appendix C
C636\15\013D-B	Appendix C
C636\15\016D	Appendix C
C636\25\075D	Appendix C
C636\06\294W-B.xls sheets: Initial Build, 2nd	Appendix D
Repair, 5th Repair	Loadcase 1 Plots in Appendix E
C636\37\011W.xls	Loadcase 2 Plots in Appendix F
C636\39\008W.xls	Loadcase 3 Plots in Appendix G
C636\40\016W.xls	Summary tables for Appendicse E, F and G
C636\32\064W.xls	Appendix H
C636\32\082U.doc	



## CONTENTS

	Page No.
<b>FOREWORD</b>	0.6
<b>EXECUTIVE SUMMARY</b>	0.9
<b>1. INTRODUCTION</b>	1.1
1.1 BACKGROUND TO TESTING PROGRAMME	1.1
1.2 OBJECTIVES OF THE BENCHMARK	1.2
1.3 BENCHMARK REQUIREMENTS AND STATUS	1.2
1.3.1 Blind Predictions	1.2
1.3.2 Test Programme and Report Structure	1.3
1.3.3 Remaining Benchmark Activities	1.3
<b>2. 3D FRAME TEST PROGRAMME</b>	2.1
2.1 TEST FRAME AND REACTION RIG	2.1
2.2 LOADCASES	2.2
2.3 EXECUTION OF TEST PROGRAMME	2.7
2.3.1 Fabrication	2.7
2.3.2 Instrumentation	2.8
2.3.3 Conduct of Tests	2.10
<b>3. 3D TEST FRAME CONSTRUCTION</b>	3.1
3.1 MATERIAL AND SECTION PROPERTIES	3.1
3.2 MEMBER SURVEYS	3.4
3.3 LOCKED-IN FABRICATION FORCES	3.6
<b>4. DESCRIPTION AND RESULTS OF SITE TESTS</b>	4.1
4.1 LOADCASE 1	4.1
4.2 LOADCASE 2	4.6
4.3 LOADCASE 3	4.13
4.4 PRESENTATION OF RESULTS	4.21
4.5 BENCHMARK ACTIONS	4.21
<b>5. REFERENCES</b>	5.1



## **CONTENTS CONTINUED**

<b>APPENDIX A</b>	<b>BENCHMARK SCOPE OF WORK</b>
<b>APPENDIX B</b>	<b>INTERIM SUMMARIES OF TEST RESULTS</b>
<b>APPENDIX C</b>	<b>INSTRUMENTATION LAYOUT DRAWINGS</b>
<b>APPENDIX D</b>	<b>MEASURED MATERIAL AND SECTION PROPERTIES</b>
<b>APPENDIX E</b>	<b>LOADCASE 1 RESULTS</b>
<b>APPENDIX F</b>	<b>LOADCASE 2 RESULTS</b>
<b>APPENDIX G</b>	<b>LOADCASE 3 RESULTS</b>
<b>APPENDIX H</b>	<b>BENCHMARK ANALYSTS' RESPONSE PRO-FORMA</b>



## FOREWORD

This report is one of a series describing different aspects of Phase III of the Joint Industry Tubular Frames Project. Each report is self contained providing detailed information in the subject area and summarising relevant data from other documents. The following table lists and briefly describes the focus of each report for cross-referencing purposes.

Report Title	Reference	Circulation
<b>Summary and Conclusions</b> Overview report describing the project and principal findings	C636\04\478R	1
<b>Background, Scope and Development</b> Scene setting report summarising previous work, identified needs and Phase III programme definition and development	C636\04\435R	1
<b>3D Test Set Up</b> Brief description of the 3D test set up and structural configuration	C636\06\313R	1
<b>Material Testing Report</b> Description of material testing procedures, test results and disposition of specific materials within test structure	C636\23\004R	1
<b>Assessment of Locked-In Fabrication Stress</b> Explanation for the build up of locked-in fabrication stresses, description of their measurement and summary of the locked-in force values in key components at the start of each test	C636\21\050R	1
<b>Test Frame Instrumentation</b> Detailed description of all instrumentation systems used in the 3D frame, accuracy, sign conventions etc. Data on CD in final report	C636\25\071R	1
<b>Loadcase 1 Test Report - Multiplanar K Joint Action</b> Detailed description of the Loadcase 1 static test response and interpretation of the results and their significance	C636\37\014R	1
<b>Loadcase 2 Test Report - Interaction Between X-Braced Planes</b> Detailed description of the Loadcase 2 static test response and interpretation of the results and their significance	C636\39\011R	1
<b>Loadcase 3 Test Report - Multiple Member Failures and 3D System Action</b> Detailed description of the Loadcase 3 static test response and interpretation of the results and their significance	C636\40\021R	1



Report Title	Reference	Circulation
<p><b>Philosophy of Cyclic Testing</b> Discussion of the background to cyclic response issues in the context of ultimate system strength and basis for specific loading scenarios</p>	C636\24\021R	1
<p><b>Loadcase 1 Cyclic Test Report</b> Detailed description of the Loadcase 1 cyclic test response and interpretation of the results and their significance. Comparison with LC1 static results</p>	C636\38\010R	1
<p><b>Monotonic and Cyclic testing of Isolated K Joints</b> Description and presentation of results from isolated component tests undertaken by SINTEF in Norway</p>	STF22 F98704 (C636\24)	1/2
<p><b>Loadcases 2 and 3 Cyclic Test Report</b> Detailed description of the Loadcases 2 and 3 cyclic test responses and interpretation of the results and their significance. Comparison with LC2 and LC3 static results</p>	C636\41\011R	2
<p><b>Loadcases 1 and 3 'Alternative' Cyclic Tests</b> Detailed description of the Loadcases 1 and 3 alternative cyclic test responses and interpretation of the results and their significance. Comparison with LC1 and LC3 static and cyclic tests</p>	C636\45\008R	3
<p><b>Multipanar SCFs</b> Joint BG / BOMEL report describing analytical work and experimental measurements of multipanar SCFs. Includes comparison with 'standard' empirical approaches</p>	C636\18\018R	1
<p><b>Site Testing Programme results - Report to Benchmark Analysts</b> Comprehensive report describing results for benchmark cases LC1, LC2 and LC3, including all pertinent data and providing response plots 'matching' the contributions from individual analysts</p>	C636\32\066R	4
<p><b>Benchmark Conclusions</b> Report comparing blind and post test analyses with measured responses and assimilating learnings and recommendations for future practice identified by Benchmark Analysts</p>	C636\32\084R	1



Key to circulation.

Circulation	All participants	Participants in 1st extension	Participants contributing finance/analytical results to 2nd extension	Benchmark Analysts
1	✓	-	-	×
2	-	✓	-	×
3	-	-	✓	×
4	✓	-	-	✓





## **JOINT INDUSTRY TUBULAR FRAMES PROJECT - PHASE III**

### **SITE TESTING PROGRAMME RESULTS REPORT TO BENCHMARK ANALYSTS**

#### **EXECUTIVE SUMMARY**

This report to Benchmark Analysts describes the Frames Phase III site tests and presents results from Loadcases 1, 2 and 3 carried out between April and September 1998 at AKD Engineering, Lowestoft.

In all, thirteen organisations took part in the benchmarking exercise and submitted predictions for the behaviour of the test frame structure under the three scenarios, using a variety of analytical software tools. The extent of investigation varied and, in accordance with the Agreement, this report is customised to provide like for like feedback to each analyst.

The testing programme was carried out successfully under the overall project management of BOMEL. A number of sponsors and benchmark analysts attended the tests. All systems worked well throughout the tests and a high degree of confidence is placed in the accuracy of the measured responses.

The purpose of the report is to enable each Benchmark Analyst to gain insight to the structural behaviour and to update pre-test predictions in light of the as-built properties and measured responses. In consultation with BOMEL and industry sponsors, the Project will then deliver best practice recommendations for future ultimate strength analyses.



## 1. INTRODUCTION

This report to Benchmark Analysts presents the site test results from the Phase III demonstration phase of the Joint Industry Funded Frames Project being managed by BOMEL Limited. The premise for the benchmark activity, together with a description of the test programme and the scope of work to be undertaken, was presented in the Benchmark Analysis Project Work Plan<sup>(1)</sup>, which was issued to Benchmark Analysts as Exhibit A of the Benchmark Analysts Participation Agreement (C636\12\004C).

### 1.1 BACKGROUND TO TESTING PROGRAMME

The testing programme was established in response to industry's interest in applying nonlinear pushover analytical techniques to the assessment and design of offshore jacket structures. Their use may be either to demonstrate that existing installations can be operated safely beyond their intended service life without expensive modifications, or to provide efficient designs for challenging environments by exploiting the reserves of strength within a three dimensional structural system. The nonlinear interactions due to material and geometric factors are complex to model and considerable validation is therefore required to ensure that the software is applied correctly and appropriately to predict the ultimate response of 3D jacket structures.

These tests provided an important opportunity to demonstrate the validity of the techniques and their application for a series of representative 3D collapse scenarios and to that end the project encompassed an open benchmarking activity. The successful outcome of the project will be an increased level of confidence in the use of pushover analysis techniques in the assessment and design of offshore structures.

Three tests were selected to form the basis of the benchmark. These tests involved different loading scenarios and were expected to demonstrate different modes of structural response.

The tests were extremely successful and in the event the schedule was extended to encompass a number of additional tests examining influences of a cyclic loading environment on ultimate system performance. Global response summaries were issued to analysts after each benchmark test as detailed in Section 1.3.2 below. However, confirmatory data relevant to the interpretation of the benchmark tests could only be extracted once the frame was finally cut up and the test facility dismantled (for example, concerning the level of locked-in fabrication forces and instrumentation conversion factors). Issue of this detailed report to Benchmark Analysts therefore follows the conclusion of the test programme.



## 1.2 OBJECTIVES OF THE BENCHMARK

The objectives for including the benchmark exercise within the Frames Project Phase III activity were:

- To enable industry practice in ultimate strength analysis to benefit as soon as possible from the findings of the 3D collapse tests.
- To demonstrate industry capability and provide assurance in the application of nonlinear analysis techniques in the ultimate strength assessment of jacket structures.

The objectives are being achieved through the dissemination of information to Benchmark Analysts in return for their contribution and evaluation of the response predictions.

## 1.3 BENCHMARK REQUIREMENTS AND STATUS

### 1.3.1 Blind Predictions

The benchmark activity was established with the premise that Benchmark Analysts should actively participate in the work undertaking their own evaluation of the comparisons between test results and analysis, and determining lessons for future practice. With active participation of the analysts, factual accuracy is to be assured and misinterpretation avoided. It was stated in the Agreement that there would not be any discrediting of organisations or software as a result of this benchmark<sup>(1)</sup>. The objectives are firmly to distil positive recommendations for good practice. The full scope of work from Reference 1 is reproduced in Appendix A.

Thirteen Benchmark Analysts submitted blind predictions prior to the deadline (23 July 1998). Two late submissions were received on 26 January and 6 February. A sixteenth contribution was received on 23 September 1998 (after the tests were complete). The comparisons presented to date use only the qualifying submissions. However benefit will be taken from all the analyses in identifying lessons to be learned in terms of future good practice.

It should be noted that pre-test predictions were made on an equal basis by all parties with no knowledge of the outcome of the tests, thus reflecting the circumstances under which ultimate strength analyses of offshore structures are conducted.

A report compiling the initially predictions was issued to industry sponsors and all Benchmark Analysts in February 1998<sup>(2)</sup>. Two analysts submitted 'corrected' predictions having examined the comparisons. Three analysts supplied additional information.



Initial materials information provided in the Project Work Plan was supplemented with additional static yield tests once the disposition of the supplied tubulars within the test frame was known. The material testing report was updated<sup>(3)</sup> and information was supplied to Benchmark Analysts in March 1998. Three Analysts submitted additional predictions utilising the as-built material data. One commented that significant effects were not expected and the results would not be repeated.

### **1.3.2 Test Programme and Report Structure**

The Loadcase 1 test took place on 25 and 26 April 1998. Based on the nature of the response it was not anticipated the findings would influence other test predictions. The Loadcase 2 test took place on 20 June 1998. BOMEL prepared a summary report describing the measured responses<sup>(5)</sup>. The Loadcase 3 test followed on 28 and 29 August and results were presented in a summary report to Benchmark Analysts<sup>(6)</sup>. These reports are reproduced here as Appendix B. On the strength of these reports two Analysts volunteered updated evaluations for Loadcase 3.

This report provides Benchmark Analysts with more comprehensive insight to the as-built condition of the test frame at the start of each test. The test set up and test procedures are summarised in Section 2. Information is provided on the material properties (static yield stress), geometry (diameter, thickness, out-of-straightness), and initial forces (locked-in fabrication effects) (see Section 3 of this report). Information about component capacities and the distribution of forces throughout the structure is provided in Section 4. This is supplemented by appendices giving response plots corresponding to the level of detail reported by each Analyst in the respective predictions. A complete description of the physical response of the structure is also provided in conjunction with a global load-displacement plot.

### **1.3.3 Remaining Benchmark Activities**

The remaining requirements under the terms of the Agreement is for Benchmark Analysts to review the contents of this report and update and rerun the ultimate strength analyses. These 'best estimate' analyses shall then be reported indicating the basis of any changes from the original prediction and their manner of implementation.

The analysts shall attempt to explain any remaining discrepancies, which may be attributable to aspects of the tests and or analysis. To help structure the responses, a pro-forma is presented in Appendix H. Completion of the pro-forma is requested by 27 August 1999 but analysis reports will be accepted up to 17 September. Points of clarification may be raised with BOMEL at any stage. A collation report will then be finalised by BOMEL and issued to all Benchmark Analysts and Participants for review and comment.



A final presentation meeting will be held with Project Participants on 4/5 October. Benchmark Analysts are invited to attend on Tuesday 5 October when the benchmark analysis and particularly the future recommendations for good practice in ultimate strength analysis will be discussed.

## 2. 3D FRAME TEST PROGRAMME

### 2.1 TEST FRAME AND REACTION RIG

Full details of the test frame and reaction rig were included within the Project Work Plan<sup>(1)</sup>. A summary follows.

A model of the test frame and reaction rig used in the 3D frame test programme is shown in Figure 2.1, with the three loadcases indicated by arrows. The reaction rig consisted of both fabricated and rolled sections. Connections within the reaction rig were heavily stiffened and could be considered rigid. The reaction rig was designed to remain within code throughout the tests.

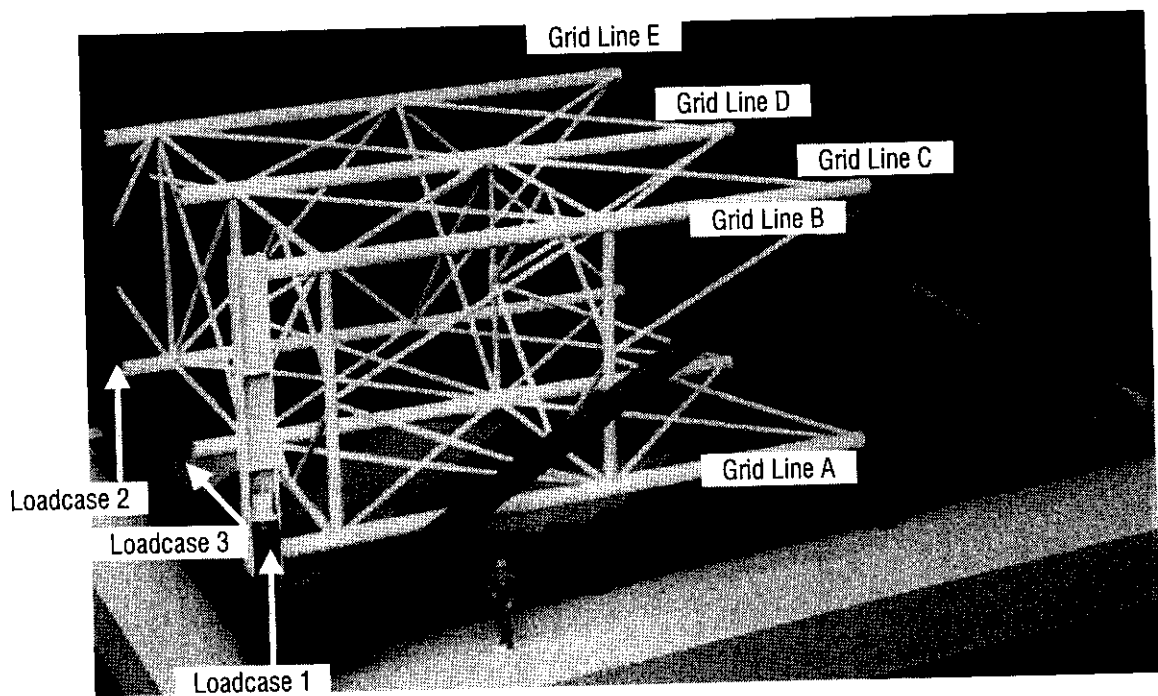


Figure 2.1 Test frame and reaction rig model

The 'upright' sections were inclined to the back of the rig through 2.02°, away from the tubular frame. The bearings on the rig supports generally provided for lateral movement and sliding. The exception is at the rear corner of the rig on frame Grid Line E where full in plane fixity was provided. No supports provided restraint against uplift.



The legs of the test frame were fully welded to the 'upright' sections of the reaction rig. Plan X bracing was only provided at Level 1 within the frame for Loadcase 3. Changes to the joint details were introduced in Frames C and E in the course of repairs following Loadcases 1 and 2 respectively. However the raking members of the rig to either side of the frame were left in-situ for the Loadcase 3 test and were not removed. Benchmark Analysts were advised of this change to the Project Work Plan<sup>(1)</sup> prior to the test and were given the opportunity to assess the potential implications.

Load was applied by a single high capacity, long stroke, double-acting actuator operating under displacement control. Load was applied to a stiff jacking beam from which short stub diagonals distributed loading into the remainder of the structure in framing action. Two jacking beams were provided, one of which was used for Loadcases 1 and 2 (repositioned between tests), the other was used for Loadcase 3. Figure 2.2 shows the configuration of the frame prior to each test.

## 2.2 LOADCASES

A brief description of each of the three benchmark loadcases under investigation is provided below (refer to Figures 2.1 and 2.2). The datum point for all tests is when the test frame is effectively cantilevered from the reaction rig with zero applied load from the actuator.

### **Loadcase 1**

Load was applied upwards, inside the jacking beam and at the centreline of Frame C, in displacement control.

### **Loadcase 2**

Load was applied upwards, inside the jacking beam and at the centreline of Frame E, in displacement control.

### **Loadcase 3**

Load was applied in displacement control to the jacking beam on Frame A pushing the structure 'from' Gridline C 'towards' Gridline E. Additional X bracing was provided at Level 1 between Gridlines D and E (above the jacking beam) as intended prior to the Loadcase 3 test. However, the long raking members of the reaction rig frame were not removed.

Figures 2.3 to 2.8 reproduce the member and node numbering scheme adopted for the three benchmark tests. The scheme remains unchanged from the Project Work Plan<sup>(1)</sup> and was used consistently by all parties involved with the test programme.

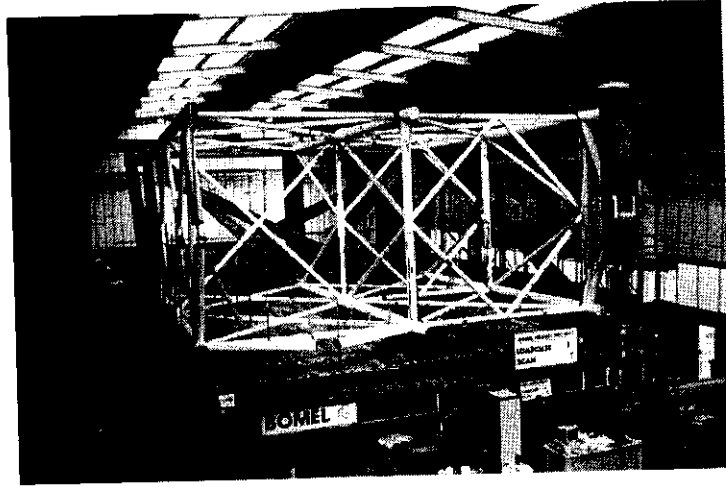


Figure 2.2(a) Loadcase 1 test configuration (LC1)

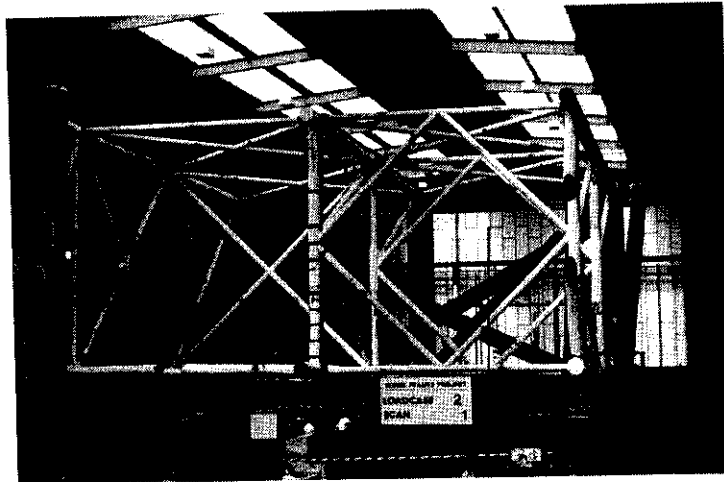


Figure 2.2(b) Loadcase 2 test configuration (LC2)

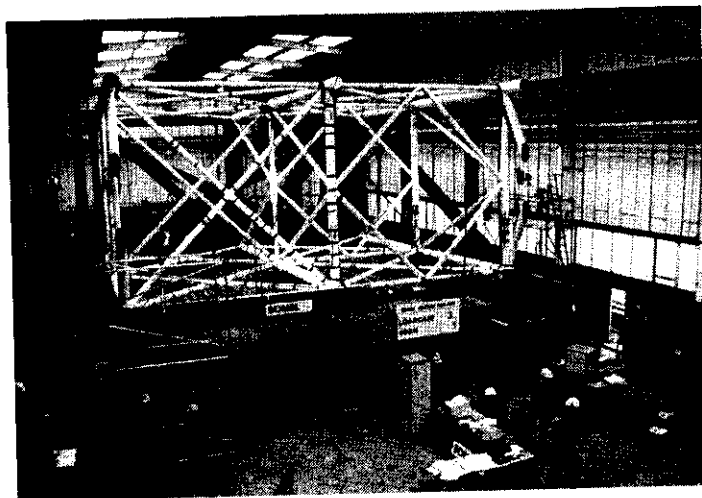


Figure 2.2(c) Loadcase 3 test configurations (LC3)



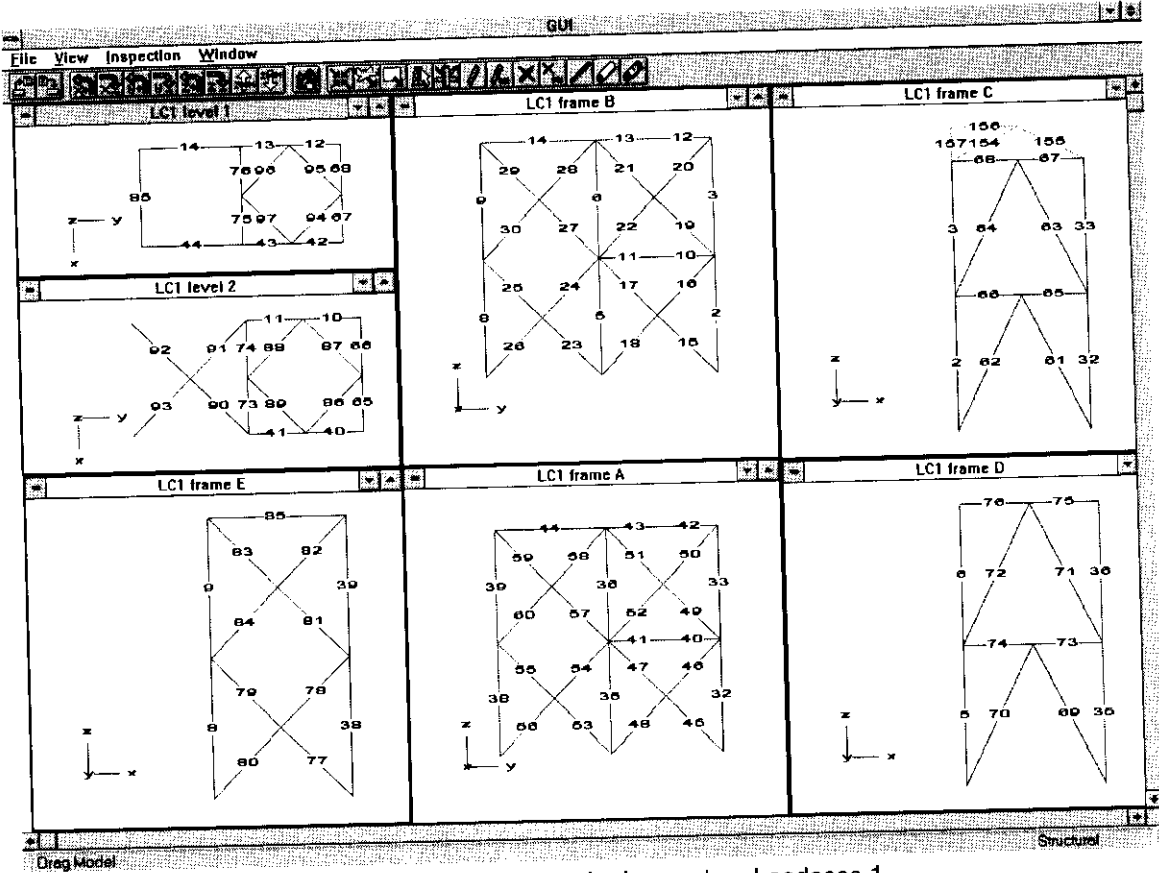


Figure 2.3 Member numbering system Loadcase 1

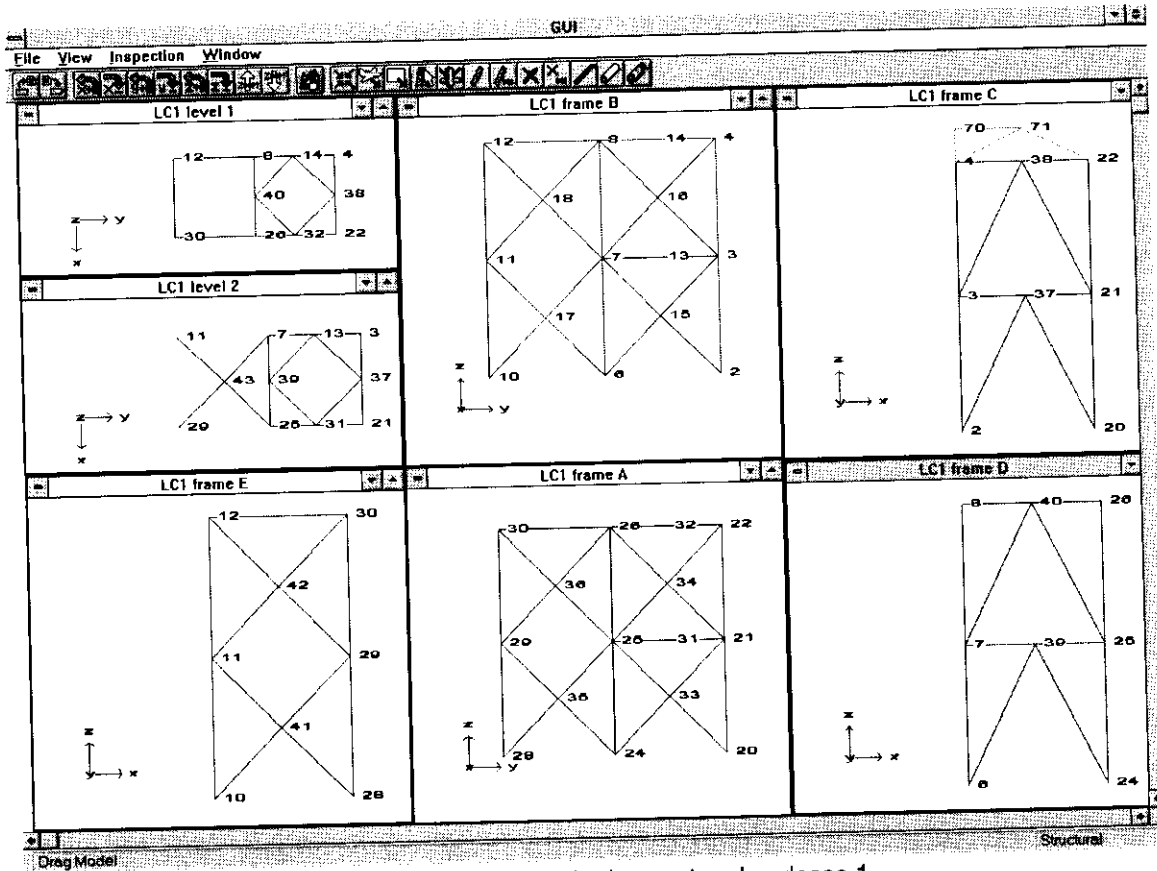


Figure 2.4 Node numbering system Loadcase 1

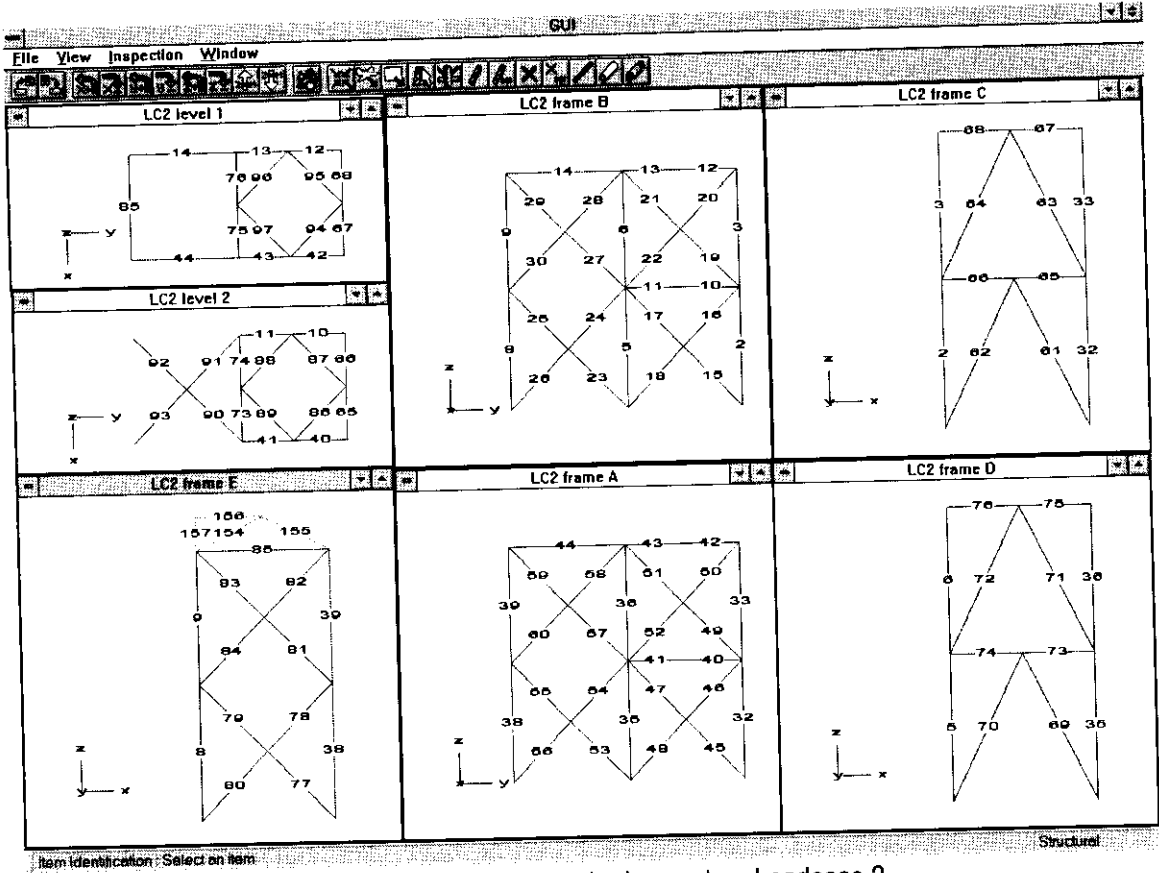


Figure 2.5 Member numbering system Loadcase 2

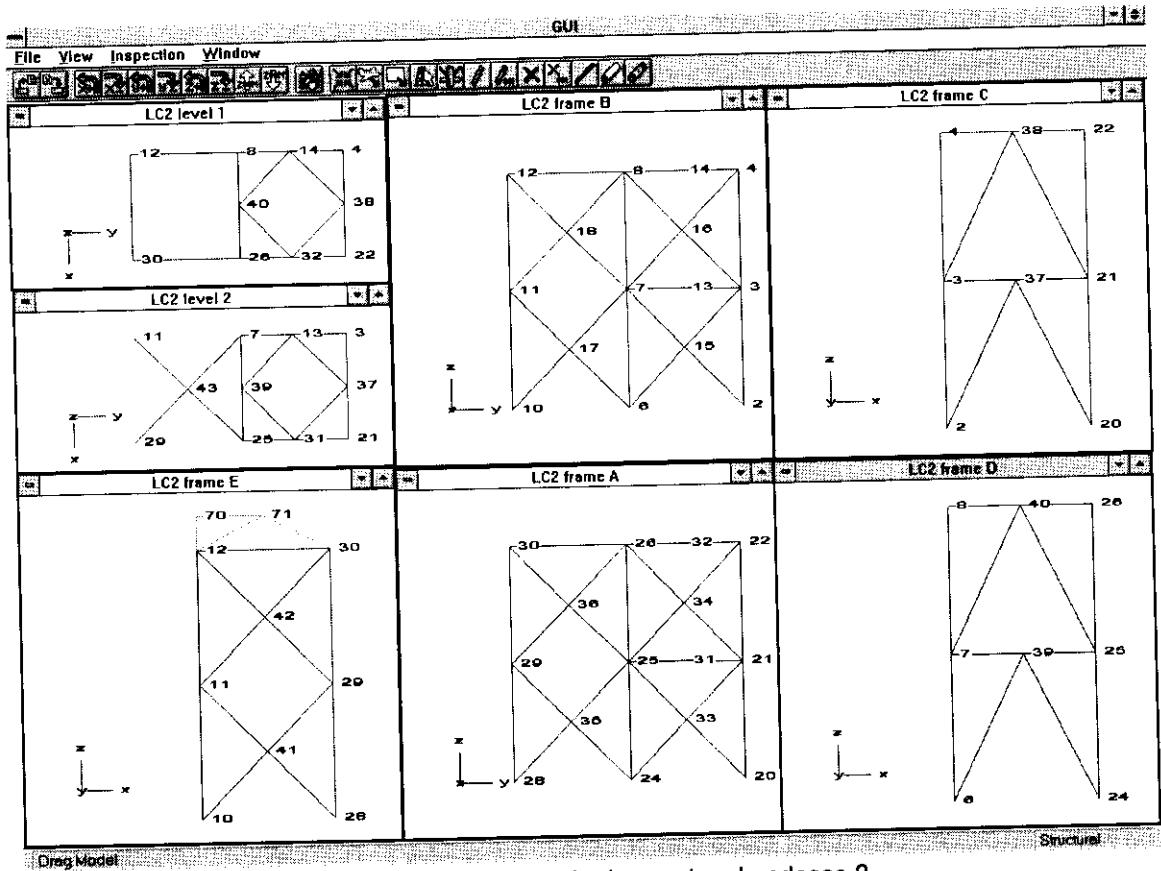


Figure 2.6 Node numbering system Loadcase 2

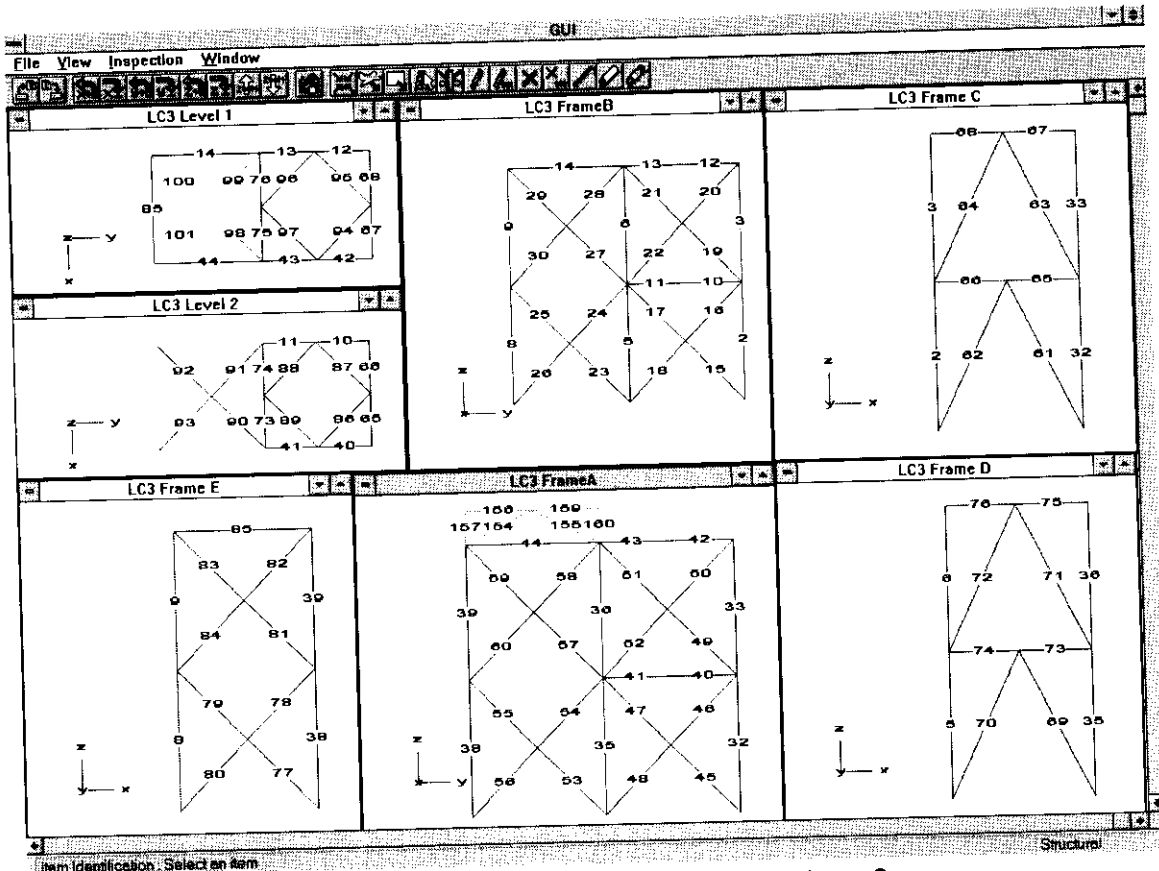


Figure 2.7 Member numbering system Loadcase 3

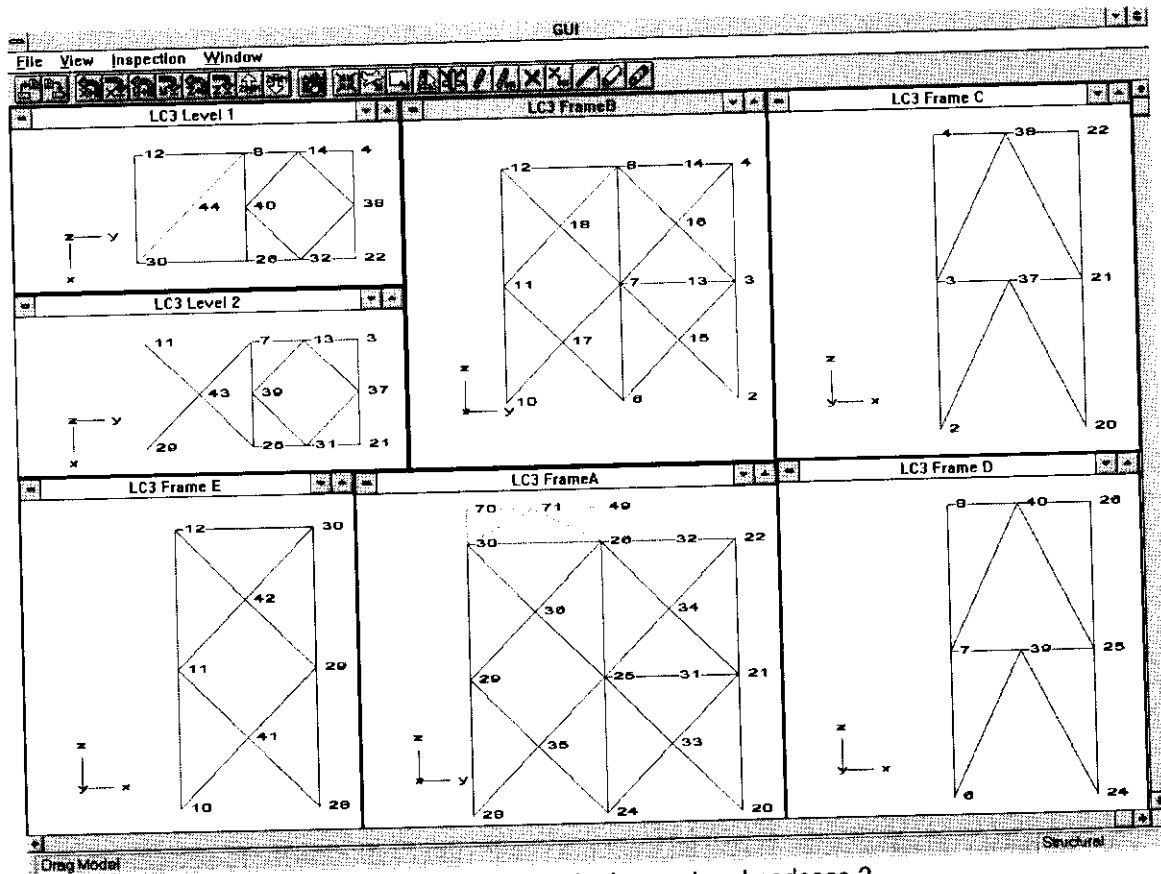


Figure 2.8 Node numbering system Loadcase 3



## 2.3 EXECUTION OF TEST PROGRAMME

### 2.3.1 Fabrication

A number of steps were taken when constructing the test structure to provide detailed information on the basis of which the measured responses could be interpreted. In particular every length of tubular supplied was given a unique reference number (eg. P27) and markers were placed at one metre intervals. The information collected is described below. Quantitative results are given in Section 3.

#### Material Properties

Static tensile coupon tests were performed by Materials Engineering Limited in Aberdeen for representative samples from each type of tubular (material specification / batch) and for specific tubulars used at critical locations in the structure where plasticity occurred. The rate of testing was representative of conditions in the frame tests. An initial set of sample tests was performed and supplemented once the material disposition in the initial build was known<sup>(3)</sup>. A further set of tests was performed once the frame testing programme was complete<sup>(7)</sup>.

Previous stub column tests of material to the same specification as the primary bracing confirmed a Young's Modulus value of  $207 \times 10^3 \text{ N/mm}^2$ .

#### Section Properties

Prior to cutting, diametrically opposed measurements of diameter and thickness (using calipers and UT) were recorded at one metre interval members on each tubular by the fabricator AKD Engineering Limited<sup>(9)</sup>. As the frame members were cut and prepared the tubular identifier and interval marks were noted. Where a member extends across several markers average values are used.

At tubular joints without joint cans additional sets of thickness measurements were recorded (in millimetres to two decimal places) for the chord. Four orthogonal measurements were taken at seven sections 100mm apart straddling the centreline of the node.

#### Out of Straightness

Checks were performed by AKD to ensure that the structure geometry was within specified tolerances (based on accepted offshore industry practice) in terms of local ovalisation, member out-of-straightness and set-out dimensions.

In addition, for members which might be anticipated to buckle during the tests, specific measurements of in- and out-of-plane curvature were recorded.



### Initial State of Stress

In a statically indeterminate fabrication there is a build up of initial forces in components as the welds cool and shrinkage is restrained by the surrounding structure. These locked-in fabrication forces are present in the frame together with self-weight gravitational forces at the start of each test (zero applied actuator load). A mechanical system of strain measurement (DEMEC) was used to record the changes as members were fabricated into the structure<sup>(10)</sup>. Subsequent changes were monitored with the system of electrical instrumentation described in Section 2.3.2. A number of cross-checks were performed to confirm the validity of the system for this purpose. In addition the electrical instrumentation was used to record the force released in critical members as they were cut following each test. This provided an additional means to back calculate the initial state of stress within the frame at the start of each test.

### 2.3.2 Instrumentation

A comprehensive set of instrumentation was installed on the test frame by AV Technology Limited to measure axial forces, bending moments, stress concentration factors and displacements<sup>(11)</sup>. The system comprised:

- 46 pre-calibrated loadcells (184 gauges)
- ~ 400 site installed linear strain gauges
- ~ 300 site installed rosette strain gauges
- 30 displacement transducers
- 22 km of cabling
- 8 multi-day tests
- ~ 1600 complete scans of all 880 data channels
- 166 Mb of Excel spreadsheet data capture files.

The system was to a high specification providing full temperature compensation for strain gauges and with repeated sampling to eliminate fluctuations through an alternating current cycle. Data acquisition was complete across all 880 channels within seconds providing consistent and, to all practical purposes, instantaneous information on the condition through the structure even in the plastic regime. The raw voltage values were written directly to a Microsoft Excel spreadsheet which provided an immediate conversion to engineering units and calculation and graphing of forces, deflections etc. It is very important to note that the system was only initialised once (ie. when it was first switched on). For subsequential tests the same datum was used and incremental changes throughout the whole programme could be monitored. Of course, for any gauges that had to be replaced or had wires reconnected a new datum was established.

Specific features of the instrumentation relevant to the benchmark are highlighted below. As-built layout drawings are reproduced in Appendix C.



### **Load Cells**

Load cells were installed in all primary bracing to give accurate information on member forces (see drawing C636\15\011D in Appendix C). The load cells were higher yield and slightly thicker walled than the members to ensure elastic interpretation of readings was valid even as failures occurred. They were positioned at potential points of contraflexure to minimise their influence on member buckling characteristics.

Each load cell was instrumented with four linear strain gauges at 90° intervals. Two opposite gauges would be sufficient to determine axial force; four provided redundancy. The load cells were pre-calibrated by applying known loads in the laboratory and monitoring changes in strain. A conversion factor from measured strains to axial force for each load cell could then be determined without reliance on wall thickness measurements. The gauges were protected during fabrication and none was affected by the welding process.

The load cells therefore gave an accurate measure of axial force.

### **Site Installed Strain Gauges**

Sets of four linear strain gauges were installed on the fabricated structure on site. Drawings C636\15\012D and 013D provide layout details. The gauges were provided with full temperature compensation but calculation of axial forces and moments must be based either on nominal section properties or averaged measured values for the local section (see Section 2.3.1). The gauges were positioned to provide supplementary information on the distribution of member forces and on bending effects close to critical joints or in members prone to buckling.

### **Joint Deformations**

Displacement transducers were positioned along the axis of un-reinforced joints to monitor any nonlinear deformations. Drawing C636\15\016D in Appendix C shows their location throughout the structure.

### **Global Displacements**

Sets of three orthogonal transducers were attached between nodal points on Frame A and the ground. These were resolved to track the spatial movement of the structure in the x, y and z planes of the coordinate system. As noted in Section 2.1 the reaction rig rested on supports. Displacement transducers monitored the 3D movements at the supports at the front of the structure (as seen in Figure 2.2). Dial gauges were positioned to monitor whether uplift occurred at other rig support points around the perimeter (see Drawing C636\25\075D in Appendix C).

### **Applied Loads**

The actuator system was provided and controlled by Bodycote Limited. It contained a pre-calibrated loadcell and transducer to monitor the force transmitted and extension of the actuator



ram. For Loadcases 1 and 2 this provides a direct measure of the displacement of the point of load application. For Loadcase 3 the reaction stub (see Figure 2.2(a)) experiences a few millimetres deformation. This was monitored during the test and subtracted from the actuator displacements to give a true measure of the displacement of the frame at the point of load application. The signals were fed to the logging system to give simultaneous capture of global load-displacement values with data for member force calculations etc. In addition the actuator control system logged the data at one second intervals providing a complete trace of the loading history.

### **General**

The above systems provide the data on the frame responses reported in Section 4 and supplementary Appendices. In addition spalling of the paint system gave reliable information on the locations of large strains and plasticity. Close monitoring of critical joints through the relayed video system (provided by Eastern Associates) enabled key events to be defined.

### **2.3.3 Conduct of Tests**

In order for the measured data to be interpreted correctly, it is important that the sequence of activities through each test is understood.

During the initial build the geometric properties and locked-in fabrication forces were measured as described in Section 2.3.1. Instrumentation was installed and thoroughly checked out as described in Section 2.3.2. The actuator was positioned on Frame C as shown in Figure 2.2(a). All temporary supports to the frame were removed and the actuator was withdrawn to set the frame in the datum position, ie. hanging under self-weight, with no applied load from the actuator.

### **Trial**

Prior to each test a few cycles of load were applied within the elastic range of structural response. The purpose was to check all personnel were familiar with the procedures to be followed, that all systems were bedded in and functioning properly, and that the initial response of the frame was as anticipated.

### **Test**

Throughout each test the following steps and procedures were followed:

- All test personnel were given a safety briefing and information was circulated on the predicted test responses and corresponding sequence of controls.
- The frame was set at the datum position (zero applied load) relative to which all forces and movements are measured. Watches were synchronised.



- A datum scan of the instrumentation was taken (Scan 1) as the Scan number was displayed on the master board (see Figure 2.2).
- An increment of load was applied under displacement control at the direction of BOMEL. Once complete, the actuator was locked-off in position. The on-screen trace of actuator load with time was monitored; a flat trace indicated a state of static equilibrium had been achieved. This was almost instantaneous when the structure was elastic but took a couple of minutes to reach once there was extensive plasticity.
- The scan number on the master board was incremented by one.
- The instrumentation system was scanned and backed up. Dial gauges were read manually.
- Throughout, all parties (BOMEL, AVT, Bodycote and Eastern Associates) maintained independent logs with respect to Scan number and clock time of key events (eg. physical observations, checks on spurious gauge readings, ramp rate changes, movements in camera position).
- Results within the data acquisition spreadsheet were reviewed by BOMEL. Graphs were generated automatically, plotting incremental measured values against BOMEL predictions. Built-in checks on maximum and minimum strains and functionality were monitored. Based on a review of the data the appropriate value for the next load / displacement increment was determined.

The cycle was repeated until the ultimate capacity of the structure for the given loading configuration had been attained and the pattern and level of post-peak loading capacity had been determined. The extent of post-peak deformation was limited to ensure extensive plasticity was not generated in distant parts of the structural frame.

- The applied load was then reduced in three or four decrements with scans of the instrumentation and record keeping at each stage as before. In all cases there was a displacement offset due to the plastic deformations within the structure when the applied load was reduced to zero.

### **Cut Out**

After each test areas of the structure were cut out. For Loadcases 2 and 3 this was undertaken with the control and monitoring of the actuator and instrumentation systems, as follows:



- Actuator loads were applied to minimise the force in a damaged component to minimise springback as it was cut. The global position was locked.
- Instrumentation was scanned.
- The component was cut.
- Instrumentation was scanned.

The cycle was repeated until all necessary members were cut. The applied load was then reduced to zero and a final scan of the instrumentation taken.

### **Repairs**

The extent of repairs / component replacement was determined after each test with reference to the physical condition of the structure and the measured data. All zones of damage and plasticity were removed and reinstated. The same measures for material traceability, dimensional records and determination of initial forces were adopted during repairs as for the initial build. Based on detailed examination of the records for each test it is considered that the strategy was entirely successful and no zones of residual damage influenced subsequent tests.

### **Benchmark Feedback**

Measured data from the test in its raw state were transferred at intervals to the compilation spreadsheet of benchmark predictions. Benchmark Analysts present were able to monitor the global behaviour and make comparison with their individual response predictions.

### **Post Test Data Reduction**

The raw data gathered on site were examined and consolidated by AVT who provided a preliminary and final issue of the Excel spreadsheet files to BOMEL. The final files include a (small) number of corrections and modifications to eliminate the use of faulty gauges and account for re-assigned data channels. Further (minor) modifications have been made by BOMEL in post-processing to account for a 15 kN global load offset (weight of hinge unit and load cell) in Loadcases 1 and 2 and movement of the actuator stub support in Loadcase 3.

Wherever possible cross-checks were made to validate all aspects of the test data during post-processing. Details are not presented here but are contained in background reports to the project sponsors. However it can be stated that the consistency and stability in the data mean that a high degree of confidence can be placed in the measured results.

### **3. 3D TEST FRAME CONSTRUCTION**

This Section presents as-built data for the test frame relevant to the measured responses in the Loadcase 1, 2 and 3 tests. These data update and/or expand on the information provided in the benchmark project work plan. Figure 3.1 presents a summary of all eight tests.

Importantly, it shows the sequencing of the benchmark cases within the overall programme. The extent of prior repairs can be seen. In addition, although a detailed description of each test is presented in Section 4, Figure 3.1 presents an initial summary of the components which 'failed' in each test.

The member and node referencing scheme was presented in Figures 2.3 to 2.8.

Pertinent data for the LC1, LC2 and LC3 benchmark tests are presented below.

#### **3.1 MATERIAL AND SECTION PROPERTIES**

The Benchmark Work Plan<sup>(1)</sup> provided structural drawings showing the disposition of material types in the 3D test frame together with anticipated yield properties. The use of material types within the structure was as intended.

Table 3.1 presents an updated summary of the static yield stress values by material type in comparison with the original assumptions.

It can be seen from Figure 3.1 that several components were removed and replaced after the initial build and before the Loadcase 2 and 3 tests. Table 3.2 summarises key areas within the structure where the nominal properties of the replacement components differ from the initial build. All these are exactly as intended and set down in the Benchmark Work Plan.

Test	Date	Recording Time (24hr)	AVT Filename	Scan Numbers	BOMEL Working File C6361	Member Failures (Scan No)	Members Cut
LC1 *	T 25/04/98	17:25-23:05	LC1a_inal	1 to 18			
	T 26/04/98	09:30-10:44	LC1a_test	19 to 29	37\011w.xls	K38 (20), 72b (32) & K37 (softening)	61, 62, 63, 64, 66, 67, 94, 95 & 72
	T 26/04/98	10:44-16:45	LC1a_test	1 to 36			
LC1C	T 29/05/98	09:15-14:40	LC1Ca_inal	1 to 26			
	T 30/05/98	13:45-21:18	LC1Ca_test	1 to 185	38\009w.xls	K38 (158) & K37 (184)	61, 62, 63, 64, 66, 67, 94 & 95
	T 31/05/98	08:20-23:28	LC1Ca_test	1 to 15			
LC2 *	T 19/06/98	14:20-16:32	LC2n_T1	1 to 15			
	T 20/06/98	10:27-20:03	LC2a_test	1 to 49	39\008w.xls	X42 (15), 81/83y (21), 70b (37) & 82b (42)	78, 81 & 82
	T 20/06/98	20:03-22:34	LC2a_cut	50 to 59			
LC2C	T 19/07/98	17:30-18:44	LC2Ca_inal	1 to 9			
	T 20/07/98	08:47-09:40	LC2Ca_test1	1 to 143	41\008w.xls	X42 (116) & 81/83y (134)	
	T 20/07/98	09:41-21:13	LC2Ca_test2	144 to 292	41\009w.xls		81, 82 & 84
LC3	T 21/07/98	08:52-20:44	LC3Ca_test	144 to 292			
	T 21/07/98	20:44-21:42	LC3Ca_cut	293 to 300			
	T 04/08/98	19:56-23:47	LC3Ca_inal	1 to 35			
LC3C	T 05/08/98	09:40-10:47	LC3Ca_test1	1 to 33			
	T 05/08/98	13:14-21:45	LC3Ca_test2	1 to 133	42\013w.xls	51b (125), 57b (127), 50/52y (126), 54/56y (125) & 46/48y (126)	
	T 06/08/98	08:25-18:18	LC3Ca_test3	334 to 252	42\014w.xls		49, 51, 52, 57, 59 & 60
LC3CA	T 06/08/98	18:18-20:19	LC3Ca_cut	253 to 265			
	T 28/08/98	14:45-17:42	LC3a_inal	1 to 29			
	T 29/08/98	09:34-20:47	LC3a_test	1 to 73	40\016w.xls	49/51y (19), 45/47y (32), 57/59y (33), 53/55y (37), 50b (37), 60b (38), 46b (41), 54b (44), X16 (55), X44 (59), X18 (61) & 61b (62)	45, 46, 47, 49, 50, 51, 53, 54, 55, 57, 58, 59 & 61
LC3CA	T 31/10/98	10:15-16:32	LC3a_cut	1 to 41			
	T 10/09/98	10:38-11:32	LC3Cab_inal	1 to 25			
	T 24/10/98	12:12-21:07	LC3Cab_test	1 to 205	44\010w.xls	X36comp (90), X35comp (154), 59/57y (164), X33ten (165), X34ten (165) with possible 50/52y (165) & 46/48y (165)	
LC3CA	T 09/11/98	09:28-10:33	LC3Cab_test	1 to 22			
	T 09/11/98	10:46-22:00	LC3Cab_test	1 to 168	45\007w.xls	K37 (69), K38 (125), 72b (140), 70b (146) & K38 severed (162)	57, 80, 54, 55, 46, 51, 47, 50, 61, 63, 69, 71, 98 & 101
	T 10/11/98	08:15-09:56	LC3Cab_cut	169 to 174			

KEY:  
 \*: Benchmark case  
 T: Loadcase trial  
 c: Loadcase cut  
 K: Joint number  
 X: X joint number  
 b: Member buckled  
 y: Member yielded  
 Material has been tested  
 eg X42 = X Node 42 failed  
 81y = Member 81 yielded

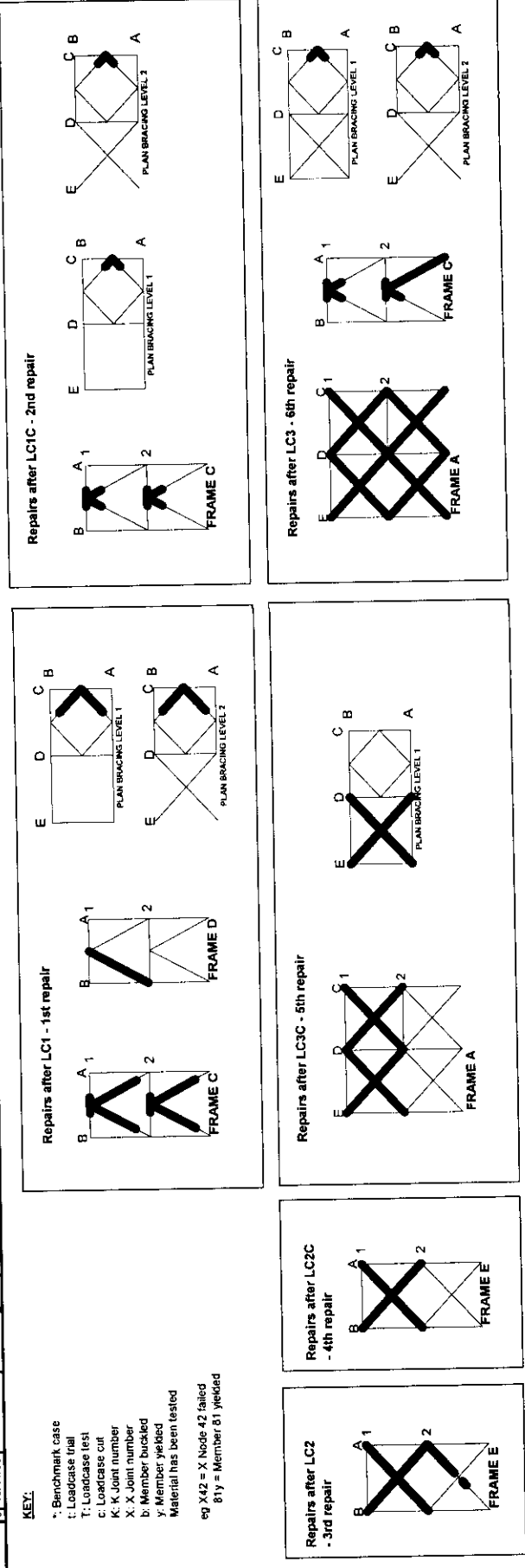


Figure 3.1 Frames Project Phase III summary of member failures, cuts and repairs through test programme



Table 3.1 Material properties based on static coupon tests (averaged)

Product	Minimum Specified Yield (N/mm <sup>2</sup> )			Total No. of Static Coupon Tests
	Original Assumptions	Preliminary Tests	Updated after All Tests	
<b>RIG SECTIONS</b>				
TMCP plate - fabricated sections*	420	420	-	0
Rolled Sections*	355	330	-	0
<b>SPECIMEN TUBULARS</b>				
168.3 DIA x 4.5 WT BS 3602 ERW	250	273	278	52
273.0 DIA x 5.6 WT API 5L GRADE B	240	292	-	5
273.0 DIA x 9.3 WT API 5L X52 *	358	354	-	0
273.0 DIA x 10.0 WT API 5L X52 *	358	371	-	0
355.6 DIA x 12.7 WT API 5L X52	358	325	327	6
457.2 DIA x 12.7 WT API 5L X52	358	355	-	1
168.3 DIA x 18.3 WT API 5L X52 *	358	324	-	0
168.3 DIA x 9.5 WT API 5L X52 *	358	335	-	0
168.3 DIA x 5.6 WT BS 3602 ERW	250	273	274	6
355.6 DIA x 25.4 WT API 5L X52 *	358	422	-	0
Notes:				
* Static yield properties ('preliminary tests') based on average or single values as available from 'standard' tests on certificates with a 12% reduction (ref dynamic/static yield ratios <sup>(7)</sup> ).				

Table 3.2 Principal frame changes between tests

Test	Location		
	Frame C K Joints	Frame E Level 1-2 X Joint	Level 1 Frames D-E X bracing
Initial build/ Loadcase 1	No joint cans 5.6mm WT	No joint can 4.5mm WT	None
Loadcase 2	Joint can 10mm WT	No joint can 4.5mm WT	None
Loadcase 3	Joint can 10mm WT	Joint can 9.5mm WT	Present



Details of the actual diameter, thickness and static yield stress values for each member are tabulated in Appendix D. Some explanation of the table contents is warranted:

- Information is provided for every member in the structure. The member numbering scheme is as shown in Figures 2.3 to 2.8. Details are also provided for joint cans and for the local properties at key nodes without joint cans.
- The information covers the fabricator's tubular reference number, the associated yield stress value, the diameter and thickness, together with calculated values of the cross-sectional area, axial yield load, section bending modulus and yield moment.
- In some cases, as in a jacket structure, a member comprises several parts. The properties for each segment are listed with the longest first. Comparison of maximum and minimum yield loads for multiple segments is provided in the final columns.
- Whether measured local, measured batch or nominal properties are presented depends on the significance of the component in the overall response, e.g.:
  - if a component 'failed' or was anticipated to 'fail', local properties were measured;
  - if a component was over specified to remain elastic (e.g. 168.3 x 9.5mm WT joint cans) no measurements were taken and nominal properties were accepted (italicised);
  - in other cases geometric properties were measured, yield values may be available from other component tests otherwise average values for batches to that specification are presented.
- Where measured geometries for members are provided these come from the 1m interval readings. The thickness measurements at nodes without joint cans are based on seven sets of four orthogonal measurements at 100mm intervals symmetrically disposed about the centreline.
- Each table presents the full listing for every member at the start of each test. However, those components which have been replaced are distinguished with an asterisk.

### 3.2 MEMBER SURVEYS

The tubular frame and reaction rig were fabricated in accordance with a specification based on accepted offshore standards<sup>(12)</sup>. The positioning of nodal points on the reaction rig was to within

a sphere of error of 6mm and for the test specimen 3mm. However, relative work point positions at a node were to be achieved within 1mm (e.g. alignment of X bracing or gap dimensions for K joints).

The overall tolerance on member straightness was set a L/1000. After fabrication and repairs key components were surveyed to record the level of 'imperfections'. In all cases the fabrication was within the specified tolerances. Measured values for key components in the benchmark tests are summarised in Figure 3.2.

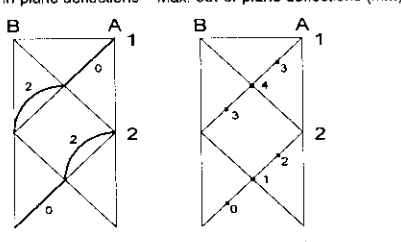
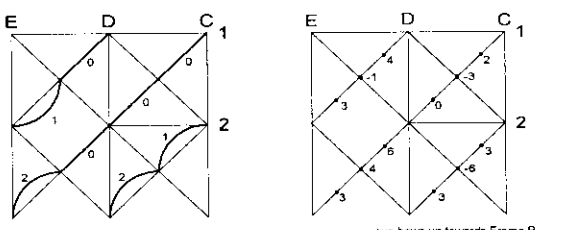
Relevant Test	Component	Survey results
Loadcase 1	Frame C 60 multiplanar gap K node 38 Level 1 Frame C 60 multiplanar gap K node 37 Level 2 Frame D K brace 72	Nominal gap tubular surfaces: 26mm. Gap between weld toes: 12mm Nominal gap tubular surfaces: 26mm. Gap between weld toes: 9mm Maximum in-plane curvature towards leg member 6: 2mm. No discernable out-of-plane curvature
Loadcase 2	Frame E X node 42 Levels 1 to 2  Frame E X braces	Gap between weld toes outside face: 36mm Gap between weld toes inside face (towards Frame D): 46mm Max. in-plane deflections    Max. out-of-plane deflections (mm)  +ve bows outwards
Loadcase 3	Frame B X node 16 Levels 1 to 2  Frame B X node 18 Levels 1 to 2  Level 1 X node Frame A X braces	Gap between weld toes outside face: 37mm Gap between weld toes inside face (towards Frame A): 44mm Gap between weld toes outside face: 33mm Gap between weld toes inside face (towards Frame A): 30mm No gap measurements Maximum in-plane deflections (mm)    Maximum out-of-plane deflections (mm)  +ve bows up towards Frame B

Figure 3.2 Key component surveys

Out-of-straightness values are based on maximum offsets from a taut wire run node to node for each component. Joint geometry details are based on caliper readings prior to welding and casts of joint intersections post-welding.

It can be seen that the out-of-straightness values are generally small. As may be anticipated, the degree of out-of-plane restraint for a bracing panel is somewhat less than in-plane, and the

out-of-straightness values are somewhat higher. It can be noted that detailed comparison of the test results with initial curvatures is not consistent. This suggests that initial imperfections have not had a significant influence on the ultimate structural responses.

### 3.3 LOCKED-IN FABRICATION FORCES

As a structure is fabricated and the welds cool, the shrinkage is restrained by the surrounding structure. Depending on the sequence of fabrication, individual members may be left with a residual tensile or compressive force 'locked-in'. In general analyses these forces will not be known but previous BOMEL studies associated with the Frames Project and full scale jacket measurements have shown that the effects on ultimate structural performance may be significant<sup>(13)</sup>. Therefore, to ensure the 3D experimental results were interpreted appropriately, measurements were taken to determine the locked-in forces within structural members at the start of each test<sup>(10)</sup>.

Results for key components in each of the benchmark test cases are presented in Table 3.3. It is important to note that the mechanical DEMEC system used is somewhat coarse in comparison with load cell/strain gauge readings. Nevertheless, DEMEC values have been back-checked against strain gauge readings and validated with equilibrium checks. A maximum error range of  $\pm 10\text{kN}$  has been determined for primary brace sections with readings generally very much more accurate. When considering the influence of these locked-in forces on component capacities this error range is tolerable, particularly in comparison with the high levels of locked-in forces recorded. Note: the notional axial yield capacity of a 168.3mm  $\phi$  by 4.5mm WT tubular (average yield 278 N/mm<sup>2</sup>) is 644kN.

In determining the locked-in fabrication forces, allowance has been made for self weight gravitational forces. The figures in Tables 3.3 are purely due to fabrication shrinkage effects. Components of force due to gravity are additional, as are forces due to applied actuator loads.

Table 3.3 Summary of locked-in fabrication forces for key members at the start of each test (kN - positive-tension)

Loadcase	Member (see Figures 2.3 to 2.8)	Force (kN)
1	Frame C 61	-5
	62	54
	63	-25
	64	40
2	Frame E 77/79	-33
	78/80	-54
	81/83	64
	82/84	83
3	Frame B 19/21	83
	20/22	78
	27/29	65
	28/30	53
	Frame A 45/47	2
	46/48	13
	49/51	166
	50/52	180
	53/55	31
	54/56	68
	57/59	110
	58/60	48
	Level 1 98/100	177
	99/101	156
Frame C 61	67	



## 4. DESCRIPTION AND RESULTS OF SITE TESTS

This section presents a general description of the frame behaviour in each of the three benchmark tests. Reference is made to the global load deflection responses, physical observations and component capacities. Graphical data are presented in Appendices E to G, with the level of detail corresponding to the extent of information submitted by each Benchmark Analyst.

### 4.1 LOADCASE 1

The test set up for Loadcase 1 is shown in Figure 2.2(a). The member and node numbering schemes are shown in Figures 2.3 and 2.4. The datum position corresponds to the structure cantilevered from the reaction rig under its self weight with no actuator load.

Load was applied in displacement control on Line C, positive load pushing the frame upwards. Frame C was K-braced. The  $64^\circ \beta=0.6$  K joints at Level 1 (Node 38) and Level 2 (Node 37) have a nominal gap ratio ( $\xi=g/D$ ) of 0.1. Typical of jacket structures, the K nodes form part of a multiplanar connection. In both cases the out-of-plane K joints have  $45^\circ$  brace angles. At Node 37 the configuration is non-overlapping but at Node 38, closest to the loading beam, the brace intersections overlap.

Figure 4.1 shows the global response of the frame in the Loadcase 1 test in comparison with the original Benchmark Analysts' predictions.

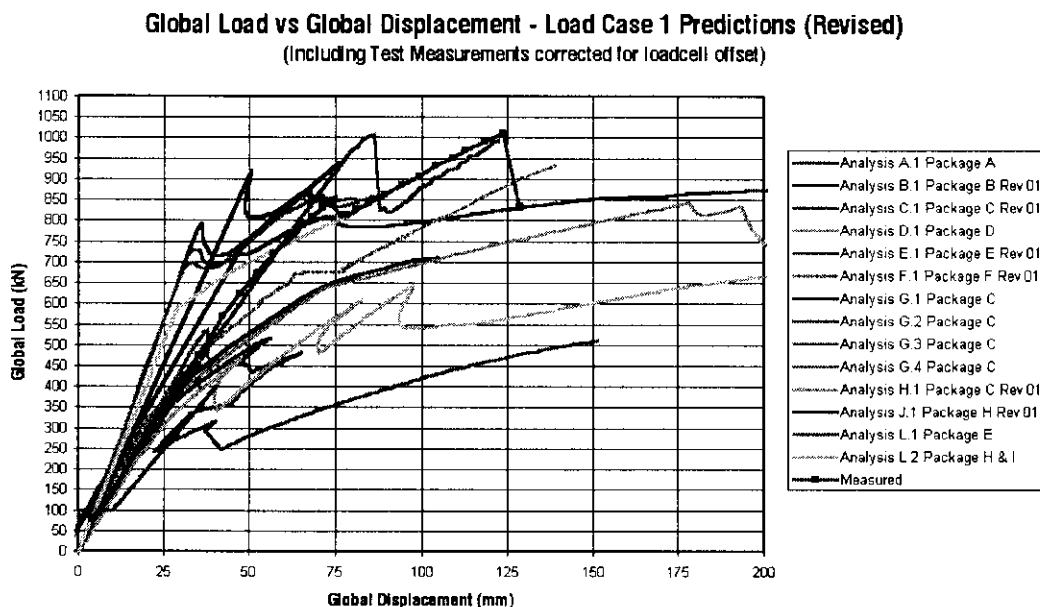
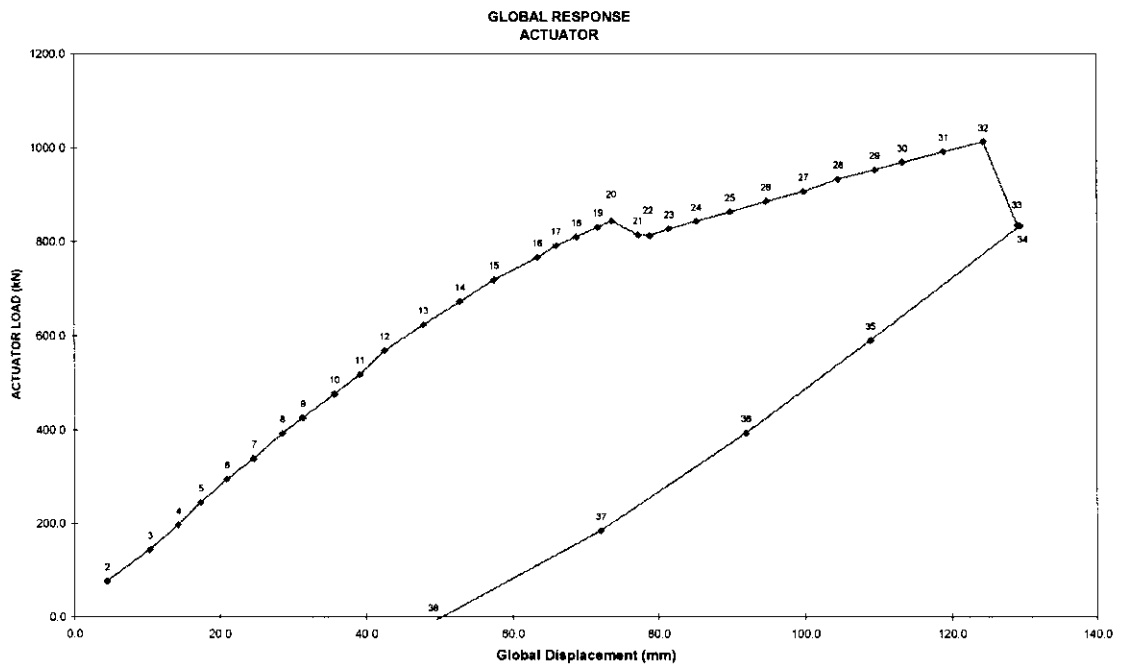


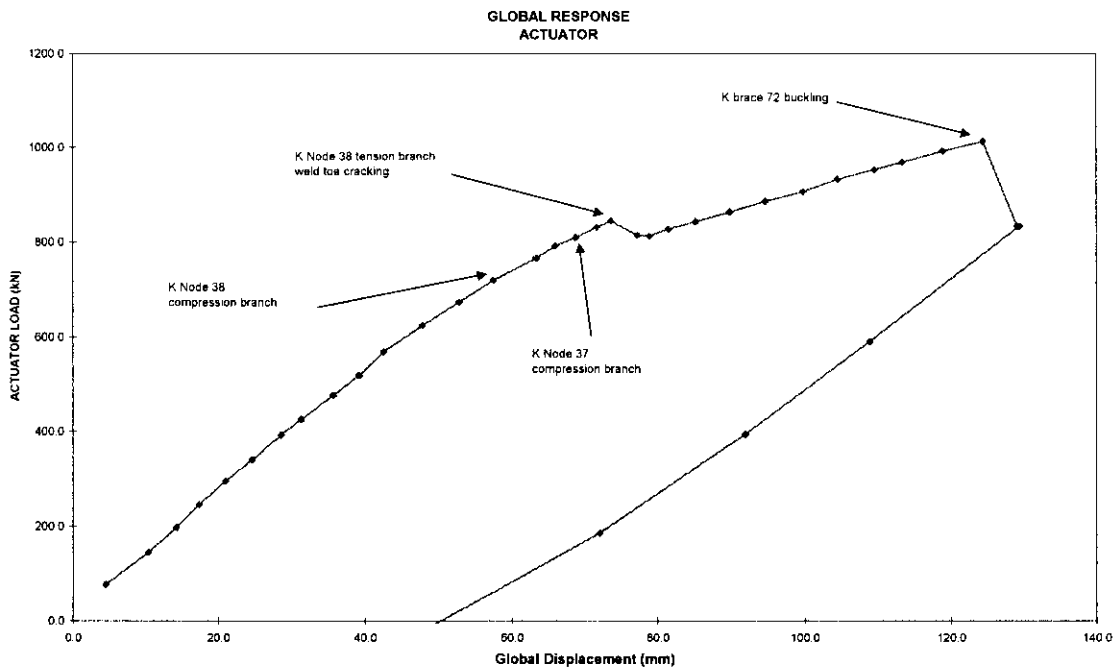
Figure 4.1 Loadcase 1 test result and benchmark predictions

Figures 4.2 and 4.3 show the loading and unloading trace for the full test. Figure 4.2 is annotated with the scan numbers to which reference will be made. Figure 4.3 highlights key events in the test.



Loadcase 1 - Test

Figure 4.2 Loadcase 1 - Scan numbers through test



Loadcase 1 - Test

Figure 4.3 Loadcase 1 - key events through test



During the initial stages of loading the global response was linear and there was negligible relaxation as the actuator was locked-off for each scan. It was not until Scan 16 (see Figure 4.2) that any signs of distress were visible. Initially distortion of the chord around the compression intersections of K Nodes 37 and 38 could be seen, then close-up video shots of Node 38 revealed evidence of surface cracking at the tension weld toe in the gap region.

During the early stages of the test the tension and compression K braces 61/62 and 63/64 in the Frame C plane sustained equal and opposite forces for each increment of applied load. However, as the K nodes began to distort the compression loadpaths softened and the relative magnitude of the forces in the tension braces, 61 and 63, increased. A slight softening in the global response was also evident until, as the load was increased beyond Scan 20, the crack at Node 38 went through thickness and the global load fell to the equilibrium position recorded at Scan 21. Logging at one second intervals from the actuator system indicates a load of 875kN was being applied at the point failure occurred.

Instrumentation output for the equilibrium condition at Scan 20 indicates maximum tension and compression forces in the braces at Node 38 of 670kN (Brace 63) and -578kN (Brace 64). Corresponding values at Node 37, which remained uncracked, were 619kN and -554kN. *When considering the absolute capacities of the components it is important to remember that the applied load effects are recorded with reference to a zero datum. Self weight effects are additional. For example, self weight forces in Braces 63 and 64 at Node 38 oppose the applied loads and are calculated to be -53 and +54kN. Neglecting locked-in fabrication force effects in the illustration the net forces acting at Scan 20 just prior to failure are therefore +617kN (670-53) and -524kN (-578+54).*

Once the structure had re-equilibrated at Scan 21 additional actuator loads were sustained by the structure with a greater transfer of applied load through the diamond bracing at Level 1 across into the 3D structure and Frame D. Load transfer through K Node 37 at Level 2 in Frame C also continued.

Having applied a global load of 1040kN the actuator system was locked off for Scan 33. However, as the structure equilibrated Brace 72 slowly buckled in-plane and the pressure in the hydraulic system fell to 834kN for the same global displacement. The Loadcase 1 test was terminated at this point.

In the original scheme it had only been intended to investigate failures in Frame C and establish the pattern of subsequent load redistribution. In the event the test was continued significantly beyond that point giving information on the subsequent failure modes and specific data on K braced member buckling which had not been covered in the earlier Frames Project investigations. It was necessary to stop at this point to limit the degree of damage and extent (cost) of repairs

in view of the subsequent tests to be performed.

Figures 4.4 to 4.8 show the condition of the structure at the end of the test. Figures 4.4 and 4.5 show the condition of Node 38: deformation around the compression intersection, cracking in the gap region and overall deformation of the chord. Despite the damage, the load transferred by the primary K joint had fallen less the 25% below the failure load. At Scan 32 the measured brace forces were still 531 and -418kN. Node 37 (Figure 4.6) remained intact despite surface cracking and chord distortions, sustaining tension/compression brace loads of 706kN / -592kN under the applied actuator load at the end of the tests. (630/-516kN when corrected for initial gravitational effects of  $\pm 76$ kN).

Brace 72 can be seen in its buckled state in Figure 4.7. The axial force recorded at Scan 32 prior to the load increment causing failure was -618kN (-584kN corrected for gravity).

Figure 4.8 shows the structure subsequent to unloading at Scan 38.

Throughout the test uplift of the rig from the support stools was monitored. The reactions were taken out beneath the actuator and at supports to the rear of the rig. However, at the remainder of the supports the rig lifted up by as much as 7mm.

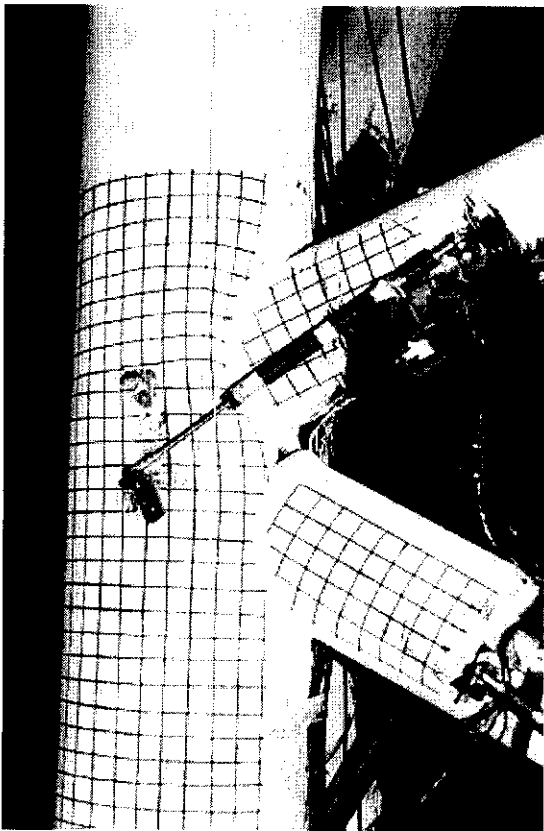


Figure 4.4 Node 38 post failure

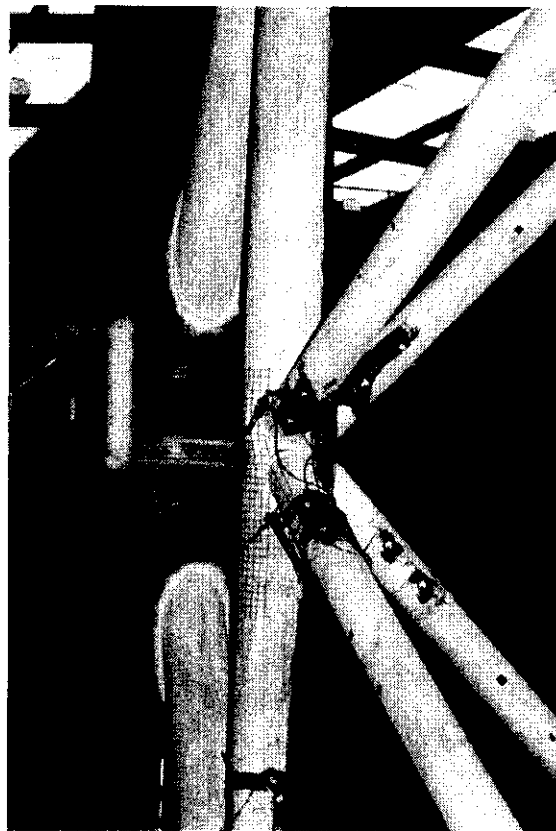


Figure 4.5 Node 38 deformation

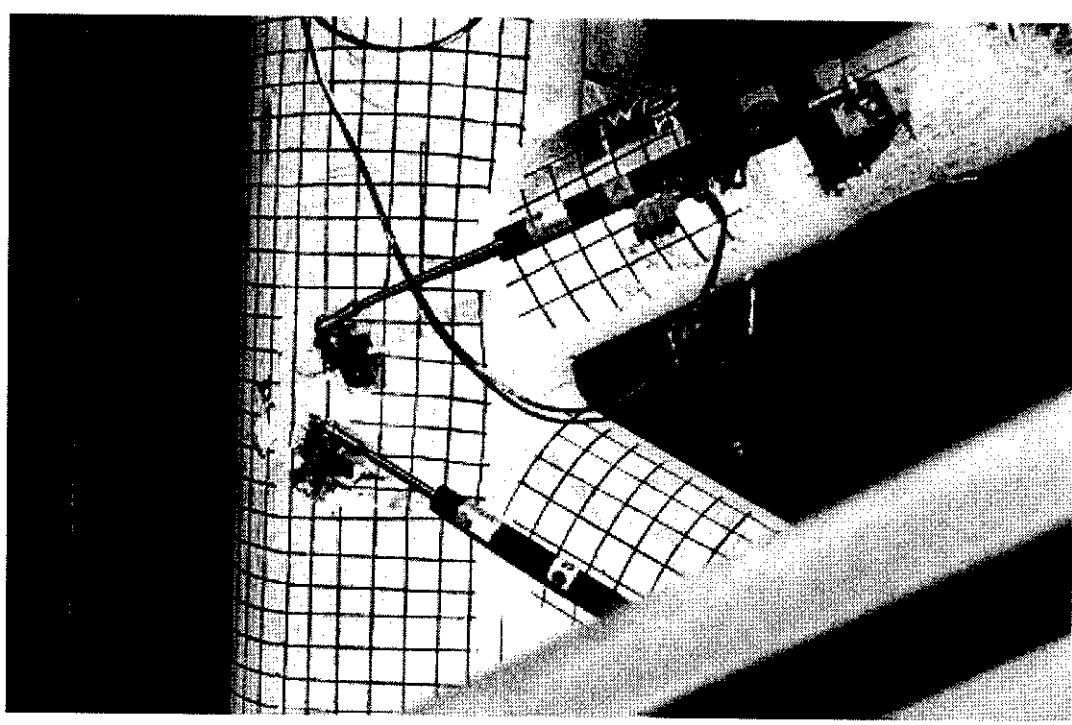


Figure 4.6 Node 37 - local chord deformation and surface cracking



Figure 4.7 Brace 72 - buckled

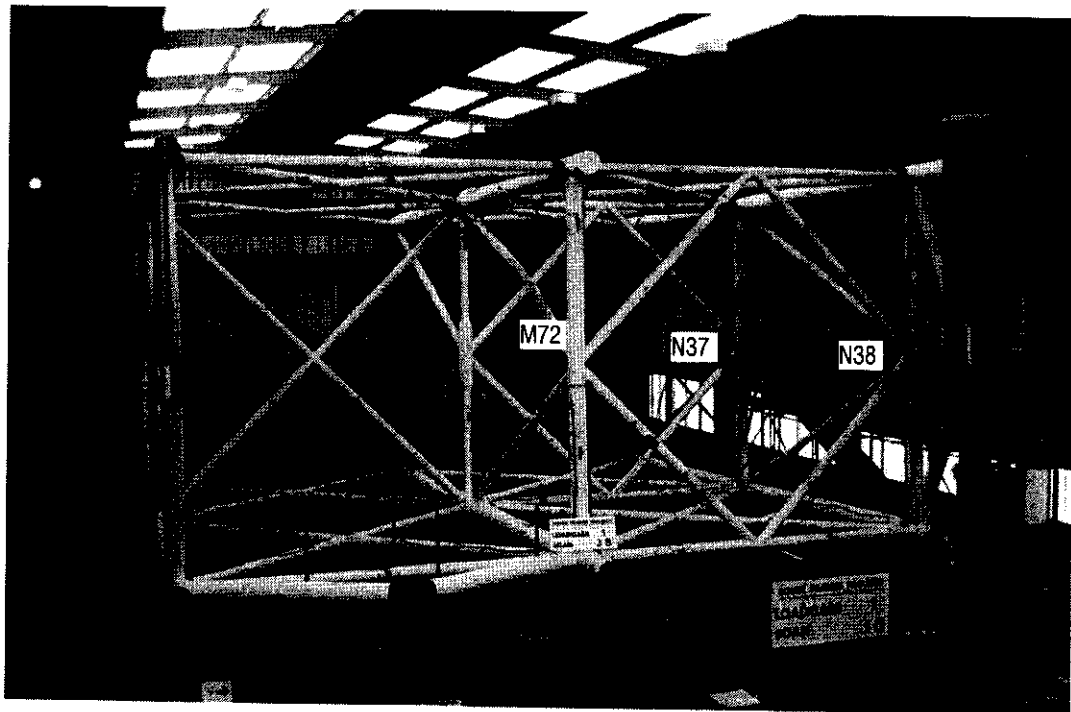


Figure 4.8 3D test from after Loadcase 1 test (NB Brace 72 buckled in Frame D)

## 4.2 LOADCASE 2

The test set up for Loadcase 2 is shown in Figure 2.2(b). The member and node numbering schemes are shown in Figures 2.5 and 2.6. The repairs carried out on the 3D structure prior to the test are shown in Figure 3.1. All the bracing participating in the Loadcase 2 failure sequence remain from the initial build. The loading beam and actuator system previously on Line C were removed and installed prior to the Loadcase 2 test on Line E.

Load was applied in displacement control, positive load pushing the frame upwards. Frame E was X-braced. The  $90^\circ \beta=1.0$  X joint (Node 42) between Levels 1 and 2 did not have a joint can and was load in compression. In the bay distant from the actuator there was a thick walled high yield joint can (Node 41). There was no mid height horizontal within the plane of Frame E but the out-of-plane bracing at Level 2 is typical of recent configurations in jacket structures.

Figure 4.9 shows the global response of the frame in the Loadcase 2 test in comparison with the original Benchmark Analysts' predictions.

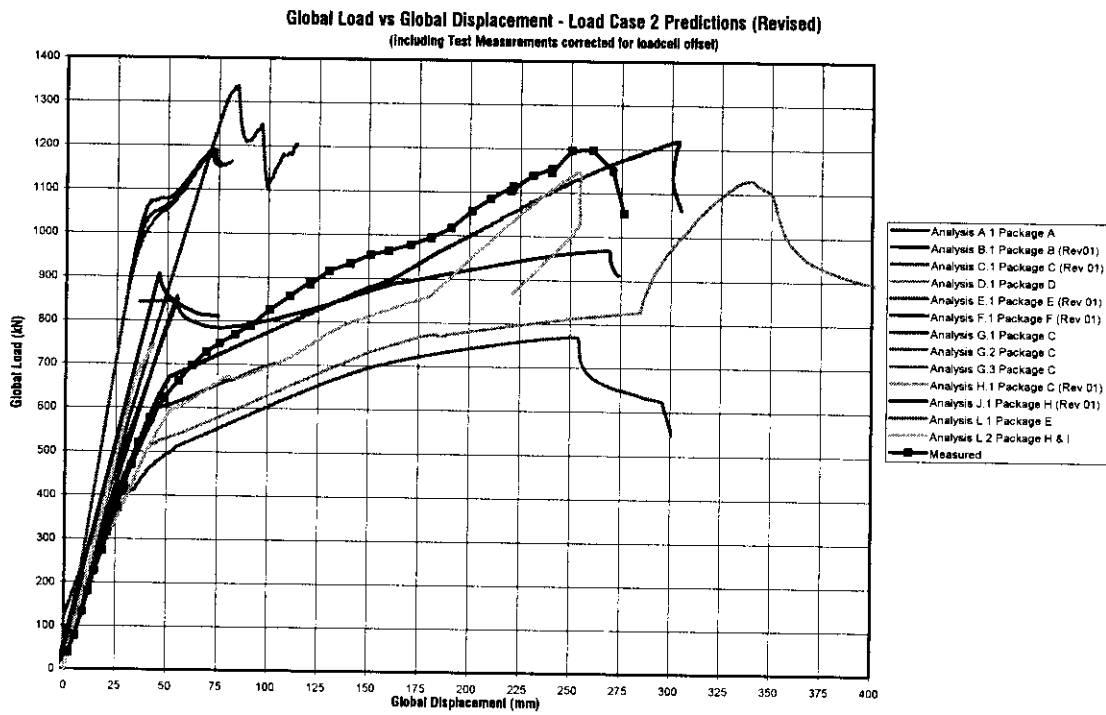
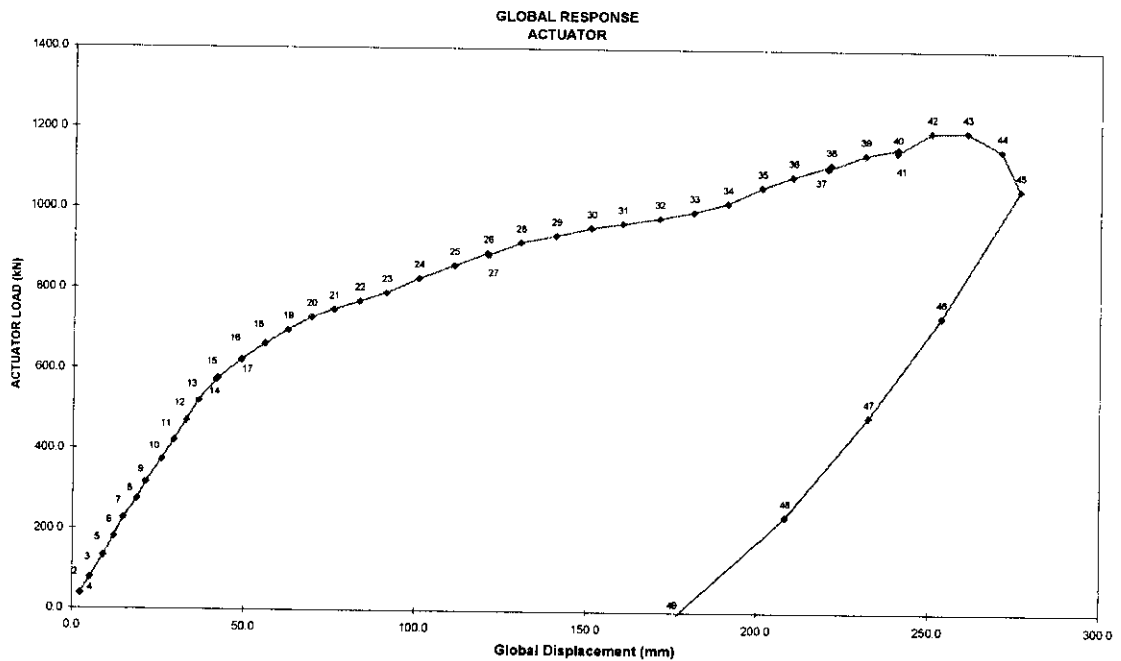


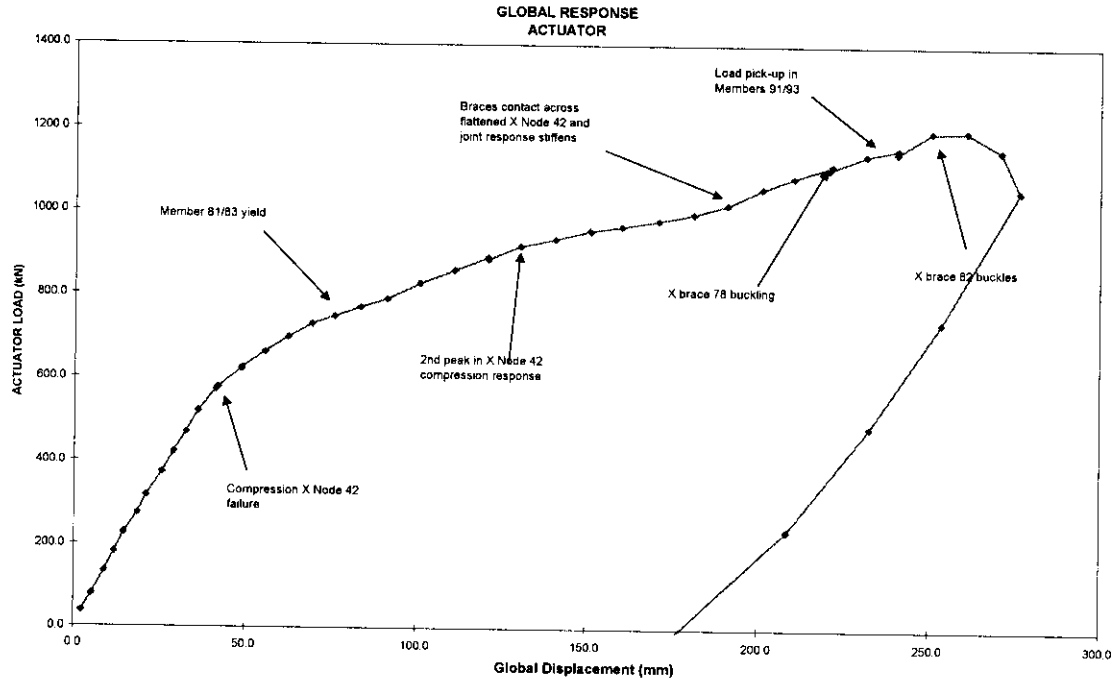
Figure 4.9 Loadcase 2 test results and benchmark predictions

Figures 4.10 and 4.11 show the loading and unloading trace for the full test. Figure 4.10 is annotated with the scan numbers to which reference will be made. Figure 4.11 highlights key events in the test.



Loadcase 2 - Test

Figure 4.10 Loadcase 2 - scan numbers through test



Loadcase 2 - Test

Figure 4.11 Loadcase 2 - key events through test

During the initial stages of loading the global response was linear as was the load take-up through the X bracing in Frame E. Tension and compression brace forces were all but equal and opposite.

From Scan 9 some distortion of the chord ligament between the X brace weld toes at Node 42 became evident, but it was not until Scan 13 that any softening in the local or global responses could be discerned. As the actuator load was increased beyond Scan 13 there was negligible increase in the forces transmitted through the Node 42 compression loadpath and beyond Scan 15 the capacity reduced. The peak force across the joint in response to the applied load (of 577kN) was -372kN. Accounting for the initial tension in the braces due to self weight gravitational effects (~33kN), the absolute force would be -339kN. However, the effects of locked-in fabrication forces also need to be considered as shown in Table 4.1 at the end of this subsection.

As the global load was increased and the structure continued to be pushed upwards, the X joint continued to deform (primarily on the inside face of the joint) with arching of the chord in the saddle region as shown in Figure 4.12 (Scan 18). Within the X-braced bay a greater proportion of the applied load was carried by the chord in tension until it began to yield with a recorded capacity of 706kN at Scan 21 (Braces 81 and 83). The net force allowing only for gravity would be ~660kN.



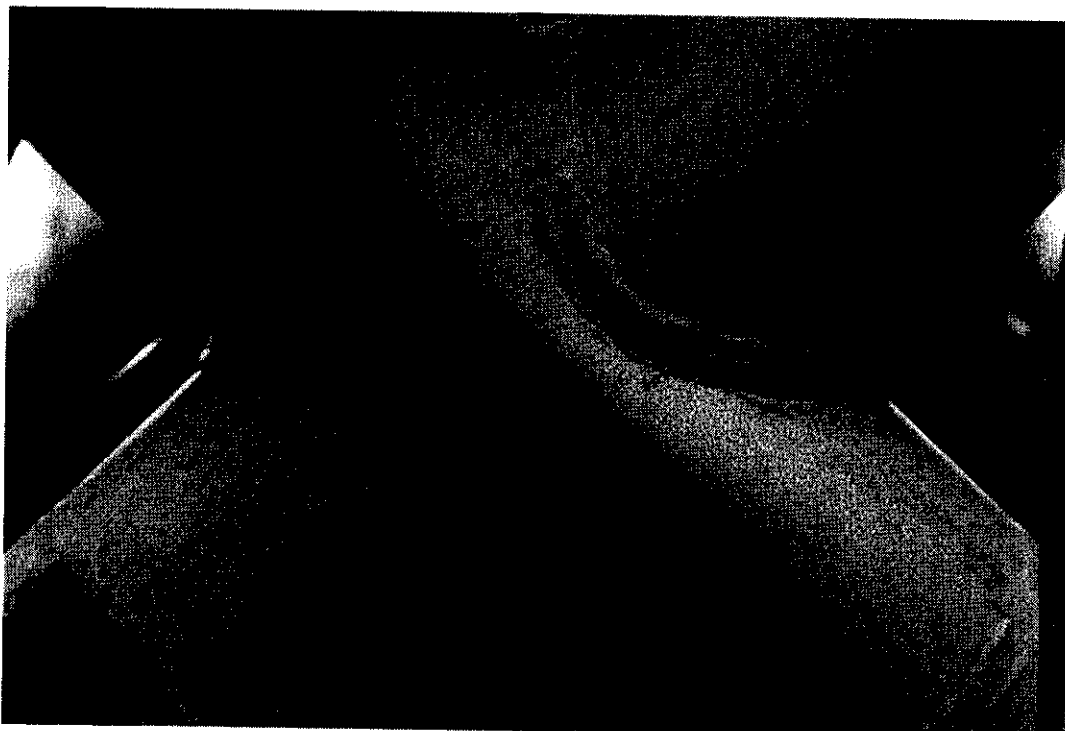


Figure 4.12 Deformation of X Node 42 - Scan 18

Despite the component failures in the X-braced bay the structure still sustained increasing global load (see Figures 4.10 and 4.11). There were a number of contributory factors.

From Scan 23 the strength of the compression X joint increased as the weld toes come into contact through the weld generating a new stiffer loadpath through the intersection. A second peak in the local joint response occurred at Scan 28 but by Scan 33 the load had again reached a higher value. Figure 4.13 shows the condition of the joint at that stage.

The overall increase in load carrying capacity was also being sustained by load transfer through the 3D structure (particularly the Level 2 X bracing) with increasing member forces in X-braced panels of Frames A and B and the distant bay in Frame E. At Scan 37 Brace 78 gradually buckled as seen in Figure 4.14, looking from Level 2 along Leg 38 to the connection with the reaction rig.

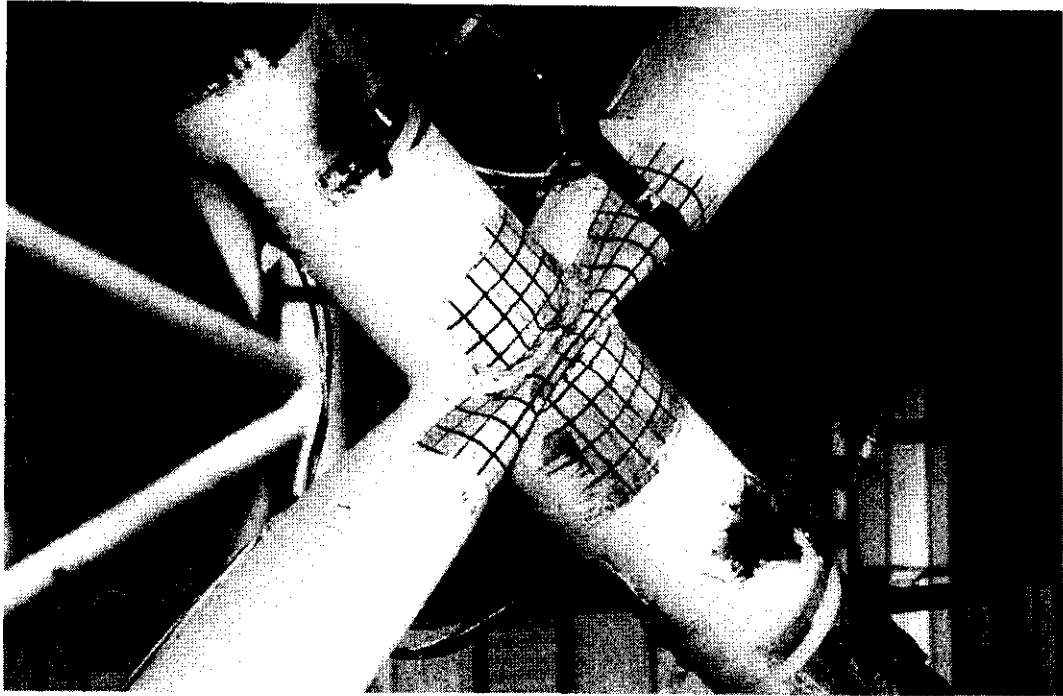


Figure 4.13 Deformation of X Node 42 - Scan 33

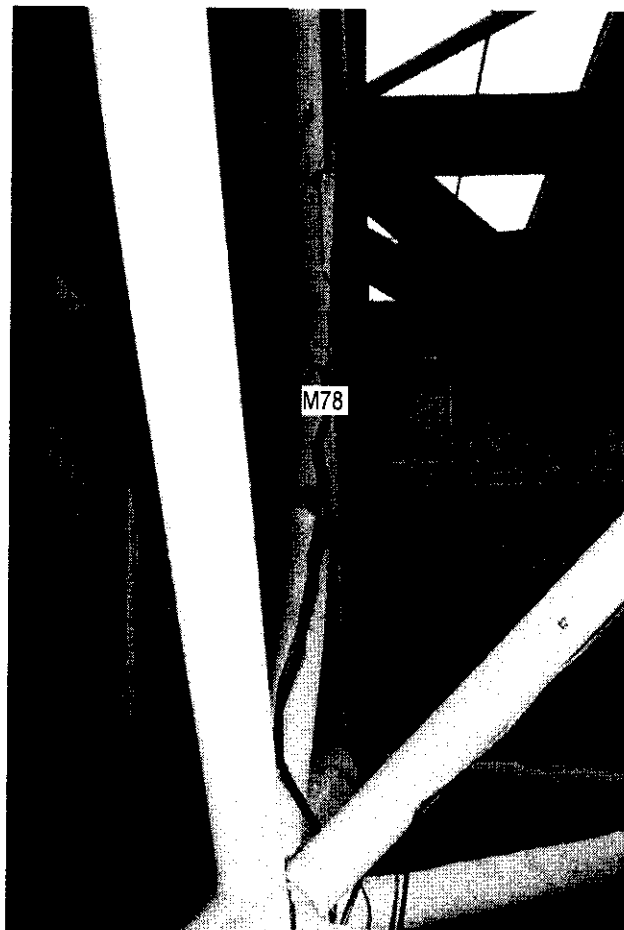


Figure 4.14 Buckling of Brace 78 - seen at Scan 39

The maximum compression load reached in Member 78 in response to the applied loads was some -642kN. Considering gravitational contributions (~54kN) the net force would be only -588kN. However, as shown in Table 3.3, the braces in this bay (Braces 77-80) did have a significant initial pre-compression from locked-in fabrication forces. Where Brace 78 apparently buckled at a low load the tension braces recorded a peak force of some 770kN significantly beyond the nominal yield value.

Load shedding from the buckled brace (Brace 78) was only gradual but there was a significant increase in the load transferred by Brace 93 within the Level 2 X bracing into the rest of the structure.

Overall the global load continued to increase exhibiting a reasonably consistent system stiffness despite the extensive plasticity and multiple nonlinear events at the detailed component level. However, the system capacity was defined around Scans 42 to 43 as X Brace 82 buckled. The peak load recorded at the actuator during the load application was 1240kN settling to 1198kN in the equilibrated scan.

The measured force acting in the brace (and across X Node 42 which had exhibited an initial peak of -372kN - see above) was -665kN. Figure 4.15 shows Brace 82 in the buckled condition; the gross deformation of the flattened chord at Node 42 can also be seen.



Figure 4.15 Brace 82 buckled and Node 42 distorted at Scan 45

From that point the 3D frame was unable to sustain further load and the actuator load fell with increasing ram displacement. At Scan 45 it was decided to terminate the test; the test objectives had been achieved and further deformation could have prejudiced subsequent tests.

Figure 4.16 shows a side view on to Frame E at the end of the test. The two buckled members run bottom left to top right and are in the lower parts of the frame as viewed. In both cases the deformations were largely out-of-plane bowing to the inside of the 3D structure.

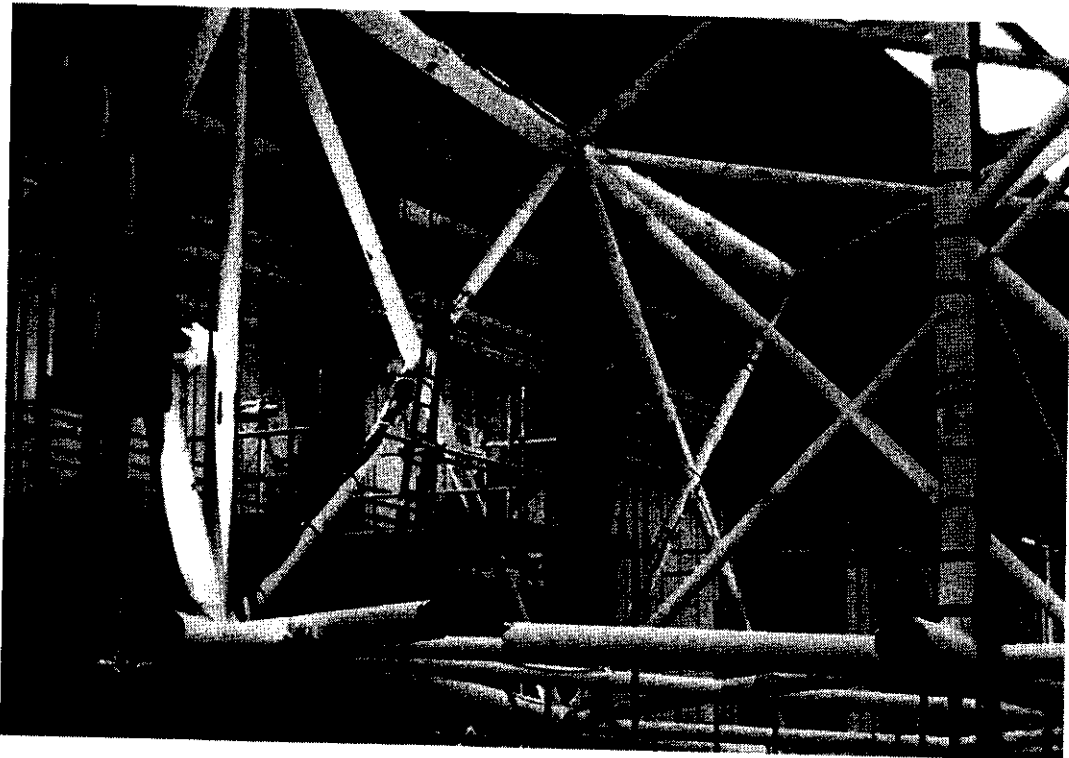


Figure 4.16 Maximum Frame E deformation - Scan 45

The degree of uplift of the rig from the support stools was limited with no deflection exceeding 3mm. However, the degree of uplift increased with increasing load and the reactions were largely taken out under the actuator and at the distant supports to the rig.

In the foregoing discussion distinction has been drawn between measured load effects and the net forces when initial self weight and fabrication force components are accounted for. For clarity the data are collated in Table 4.1 as they apply to key components in the Loadcase 2 test.

Table 4.1 Loadcase 2 net forces in key components (kN)

Members	Component capacity (measured) (C636\39\008W) a	Gravity (Calculated) b	Locked-in force (Table 3.1) c	Net force at failure a+b+c
Frame E 77/79	* 774	-53	-33	* 688
78/80	-642	54	-54	-642
81/83	706	-40	64	730
82/84	+ -372	33	83	+ -256
82/84	-665	33	83	-549

Notes:  
 + Joint failure  
 \* Component did not reach peak capacity

### 4.3 LOADCASE 3

The test set up for Loadcase 3 is shown in Figure 2.2(c). The member and node numbering schemes are shown in Figures 2.7 and 2.8. The repairs carried out to the 3D structure prior to the test are shown in Figure 3.1. The tubular loading beam formerly on Line E was removed and a new stiffer beam was installed on Line A as shown in Figure 2.2(c). The actuator applied load to the end of the beam on Line D and was reacted by a stiff stub beam on the reaction rig between Grid Lines C and D as shown.

Load was applied in displacement control, positive load pushing the structure from Grid Line C to E (right to left as viewed). Members in the loaded face, Frame A, were X-braced. At each of the 90° X nodes there was a thick walled high yield joint can. Similarly all the nodes in the transverse frames (C, D and E) had all been reinstated with 'strong' joints. This is typical of most modern structures. In Frame B however, X nodes 16 and 18 did not have joint cans. Under positive frame loads Node 16 was loaded in tension and Node 18 in compression. In addition the newly installed X bracing at Level 1 was governed by the tension capacity of Node 44.

The Loadcase 3 test was performed with the long ties of the reaction rig, to either side of the tubular frame specimen, in place.

Figure 4.17 shows the global response of the Frame in the Loadcase 3 test in comparison with the original Benchmark Analysts' predictions. In all the results presentations the global deflections have been corrected for the deformation of the reaction stub to which the actuator was connected. This reduces the displacements recorded at the actuator by 1 mm per 500kN applied load to give the true frame displacement.

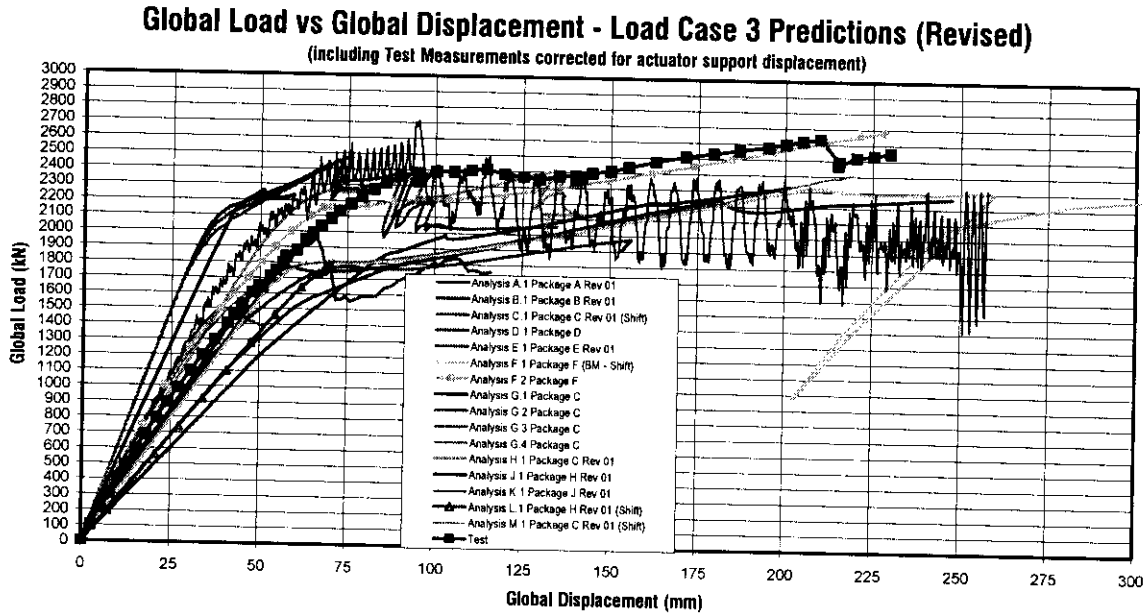
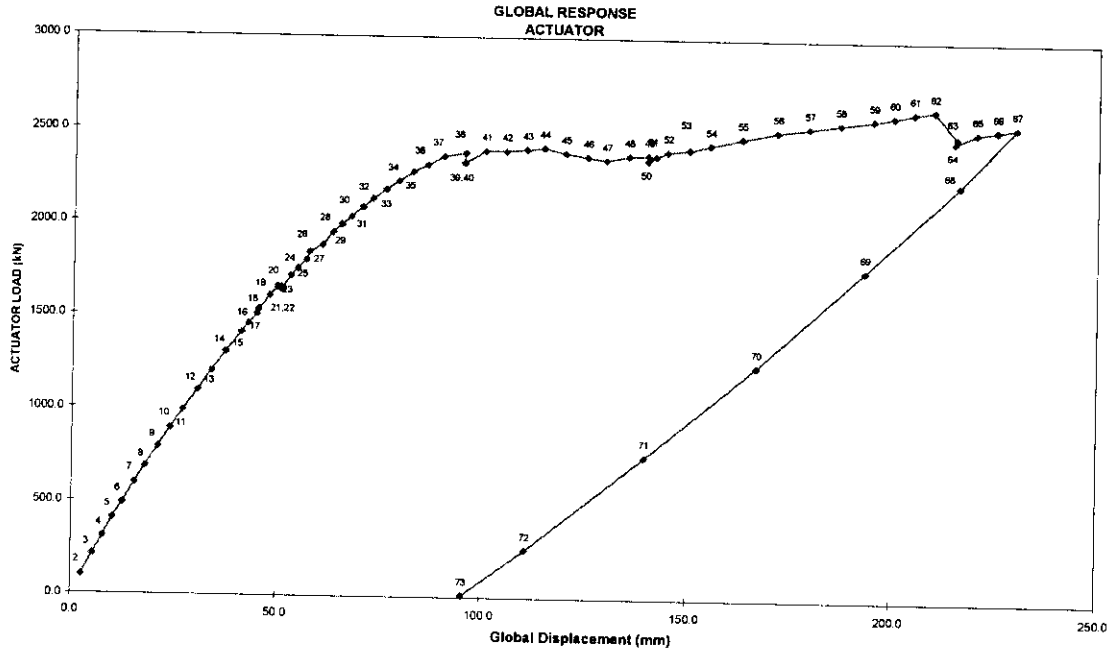


Figure 4.17 Loadcase 3 test results and benchmark predictions

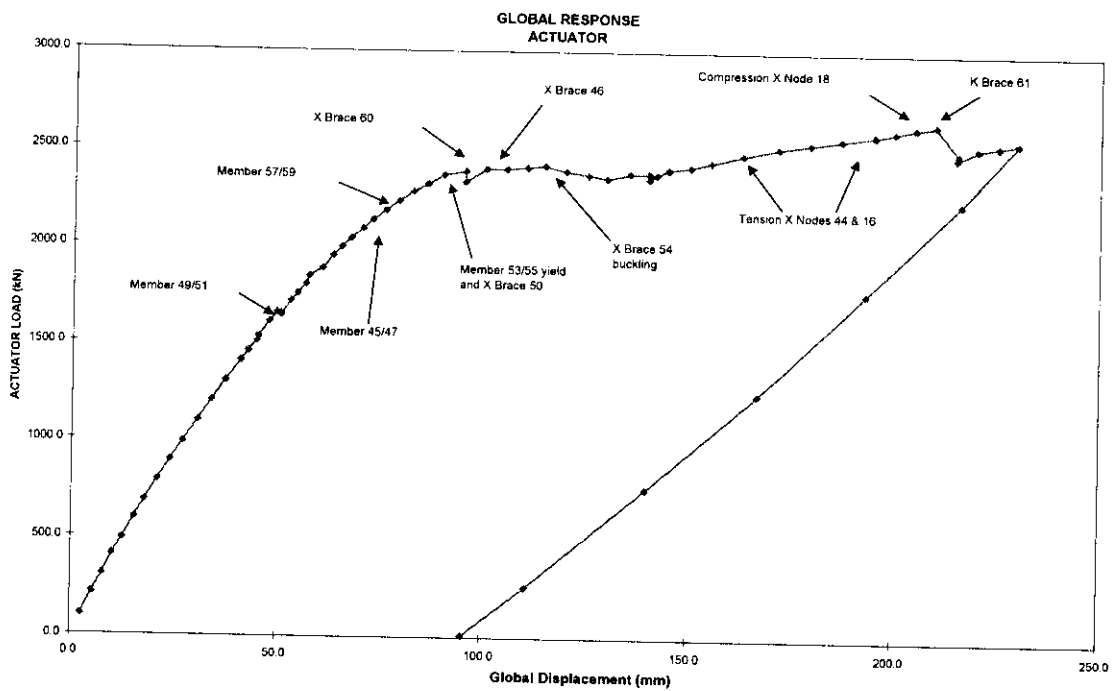
Figures 4.18 and 4.19 show the loading and unloading trace for the full test. Figure 4.18 is annotated with the scan numbers to which reference will be made. Figure 4.19 highlights key events in the test.

As indicated in Figure 4.19, there was no nonlinearity in the 3D tubular frame until Scan 19 when yielding was observed in Braces 49 and 51 in Frame A. However, the global response is not completely linear due to changing conditions at the reaction rig supports (see Drawing C636\25\075D in Appendix C). From Scan 9 onwards Node 48 at the front of the rig along Line E began to lift off, followed by Node 52 and subsequent nodes towards the back of the rig (Node 56 ~Scan 25; Node 58 ~Scan 42 etc). The degree of uplift was considerable approaching 100mm at the front of the structure on Line E.



Loadcase 3 - Test

Figure 4.18 Loadcase 3 - scan numbers through test



Loadcase 3 - Test

Figure 4.19 Loadcase 3 - key events through test

As the global load increased first component failures occurred in the bracing in Frame A. Tensile yield in the brace members preceded buckling in compression braces. This was due in part to the high load passing into Braces 49 and 51, for example, from the loading beam. However, an additional factor was the level of locked in fabrication forces which in Frame A were tensile and served to precipitate earlier yield whilst delaying buckling in response to applied loads. Table 4.2 summarises the details and contributions.

Table 4.2 Loadcase 3 Net forces in key components (kN)

Members	Component capacity (measured) (C636\40\016W)	Gravity (calculated)	Locked-in force (Table 3.1)	Net force at failure
	a	b	c	a+b+c
Frame B 19/21	+ 462	5	83	+* 550
20/22	* -633	-10	78	*-565
27/29	* 586	-5	65	* 646
28/30	+ -321	1	53	+ -267
Frame A 45/47	750	-9	2	743
46/48	-711	3	13	-695
49/51	588	-2	166	752
50/51	-859	3	180	-676
53/55	689	3	31	723
54/56	-767	-7	68	-706
57/59	647	0	110	757
58/60	-720	4	48	-668
Level 1 98/100	+ 418	15	177	+ 610
99/101	* -640	-10	156	*-494
Frame C 61	-671	-73	-	-744

Notes:  
 + Joint failure  
 \* Component did not reach peak capacity

Figure 4.20 shows the typical pattern of yield, here seen for Brace 51 at Scan 38.



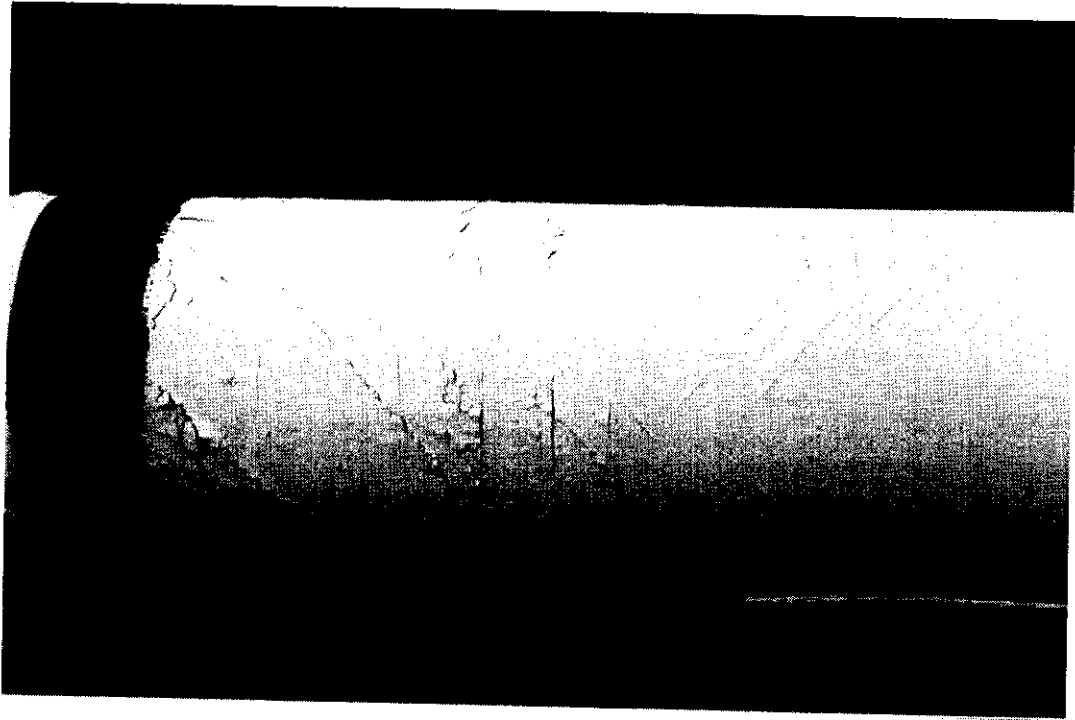


Figure 4.20 Yield in Frame A tensile members

The global response softened continually as each tensile load path yielded. Then, at Scan 37, Brace 50 buckled having sustained an applied load effect of  $-859\text{kN}$  (albeit with a locked-in fabrication force of some  $180\text{kN}$  - see Table 4.2). The initial deformation was almost entirely out-of-plane bowing to the inside of the structure towards Frame B. In contrast, Brace 60 then buckled in-plane at Scan 38 bowing outwards towards the leg on Line E as seen in Figure 4.24. The local load carrying capacity fell off abruptly but the structure re-equilibrated and the global response reattained the plateau level. Brace 46 also buckled in-plane (at Scan 41) bowing outwards to the Frame C leg. Figure 4.21 shows the physical 'hinge' formed.

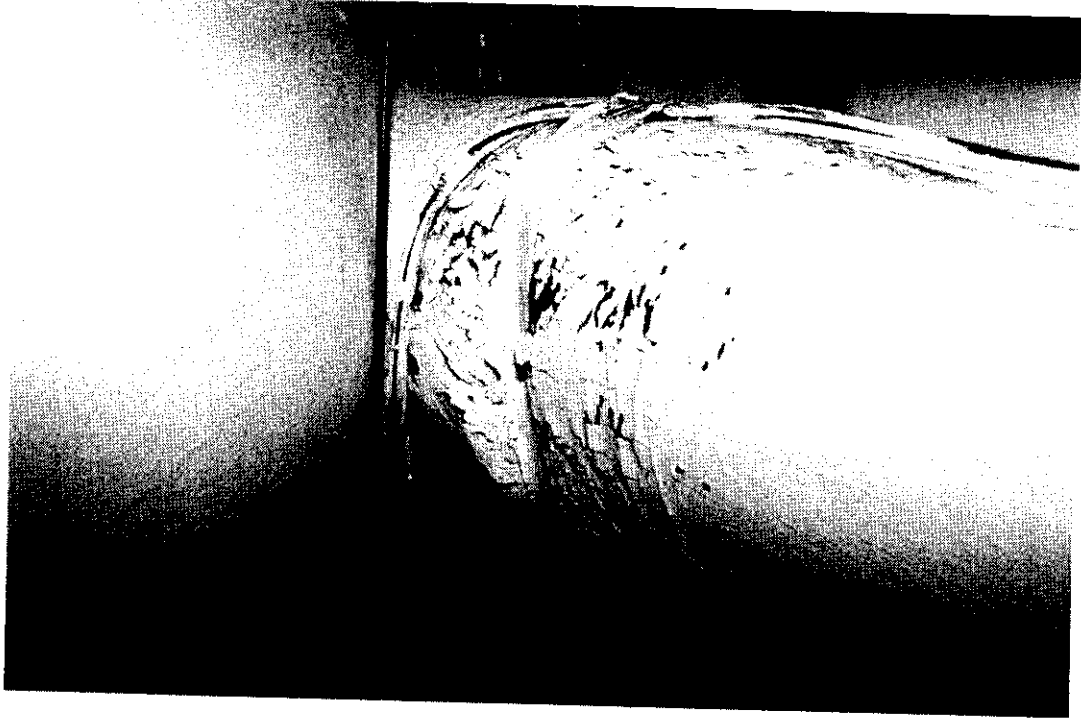


Figure 4.21 Hinge formation in buckled compression brace

Finally, Brace 54 buckled at Scan 44, deforming upwards towards Frame B.

Throughout this sequence of compression brace failures as the load carry capacity of Frame A was reached, the global load sustained was remarkably constant, at around 2440kN. It can be seen from the local traces that the failures in Frame A were being offset by an increasing take-up of applied load through the transverse frames (C, D and E) and the Level 1 X bracing.

However, with increasing global deformation the rate at which the buckled Frame A braces were shedding load was initially too great for additional applied loads to be sustained. By about Scan 52 the global capacity started to increase and significant force levels were being recorded in the remote Frame B X bracing. Clear evidence of softening in the tensile load paths through Nodes 44 and 16 (without joint cans) became evident at Scans 55 and 58 respectively. Figure 4.22 shows the typical flattening of the joint and cracking within the paint, although in both cases the joints remained intact.

As the Level 1 X bracing loadpath softened, so the K bracing on Line C transferred greater proportions of the applied load.

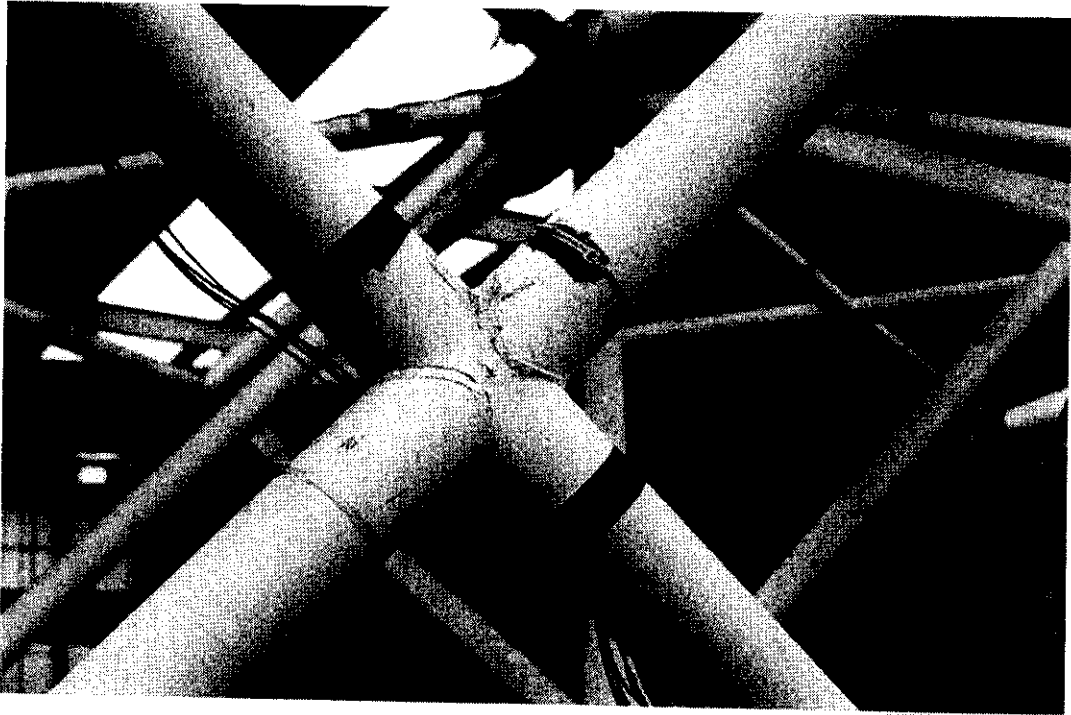


Figure 4.22 Tensile X joint failure at Node 44

At Scan 61 a peak in the load transmitted by the compression X joint (Node 18) in Frame B was recorded. Very shortly afterwards, as the actuator was powered beyond Scan 62, the K brace 61 in Frame C buckled. The maximum applied load recorded within the actuator system was 2659kN but fell sharply as the structure equilibrated. Figure 4.23 presents a view looking up the Frame C leg with the long buckled brace 61 in the foreground. The member bowed slightly out-of-plane to the outside of the 3D frame but principally in-plane towards the Frame C leg. Also visible in Figure 4.23 is Brace 50 buckling out-of-plane contrasting with the in-plane buckling of Brace 46 in the foreground.

With continued actuator load there was considerably greater load transfer across the structure via Frame D than previously. However, the rate of take-up of load was very gradual and it was clear that massive deformations would be required to precipitate additional component failure. Having established the pattern of force redistribution and anticipating additional tests of the structure, Loadcase 3 was terminated. Figure 4.24 shows the deformation within the Frame A X-braced bays at the end of the test.

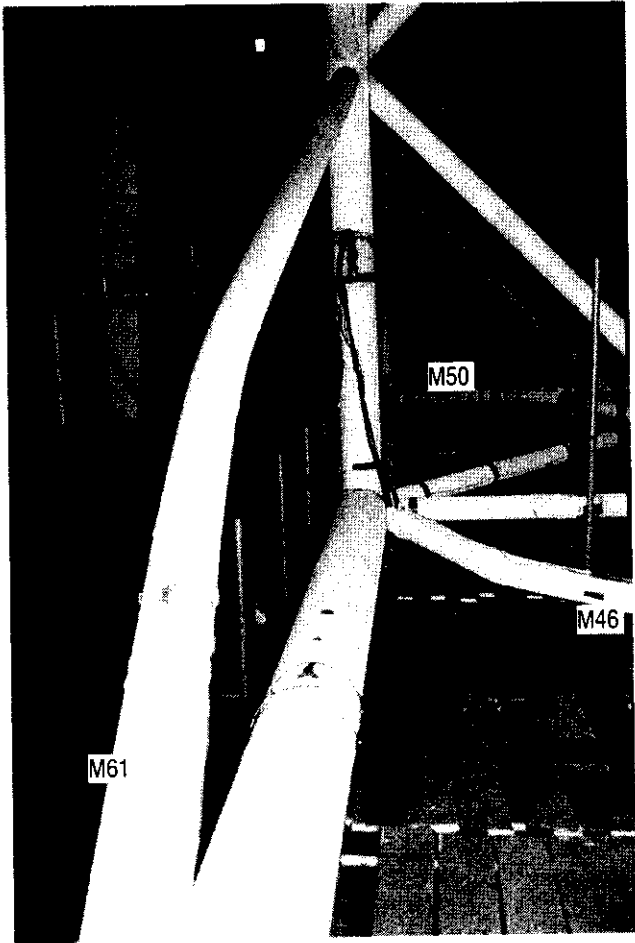


Figure 4.23 Brace buckling in Loadcase 3 test

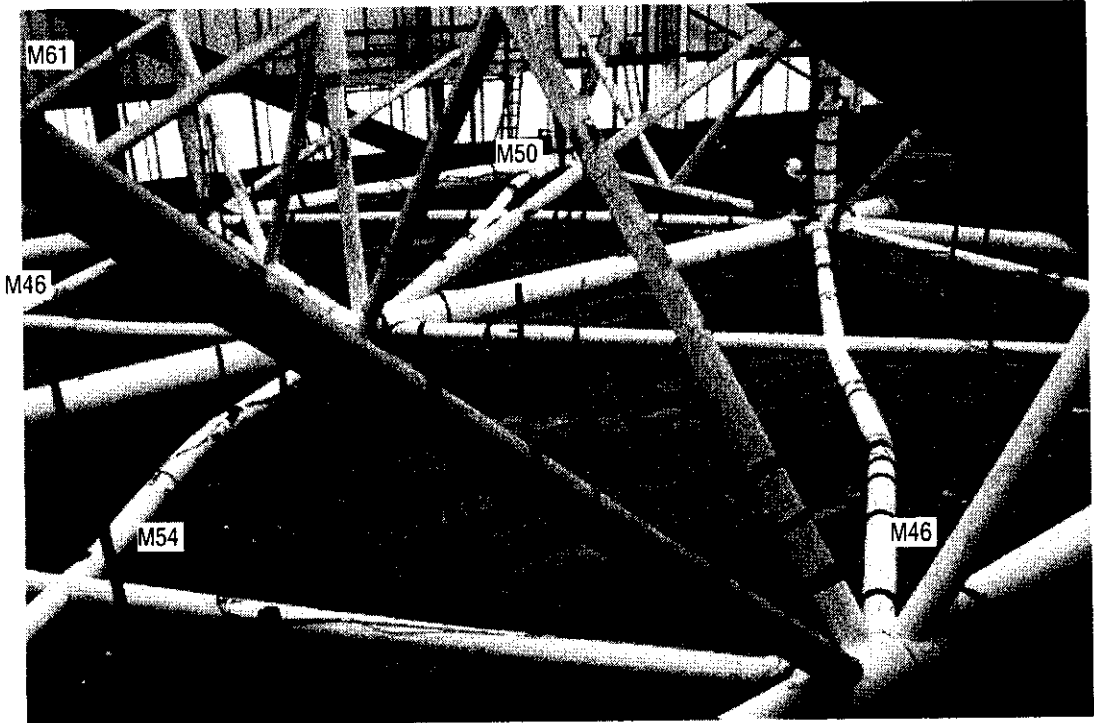


Figure 4.24 Member failures in Loadcase 3 post test



#### 4.4 PRESENTATION OF RESULTS

The foregoing sections have described the physical response of the 3D test frame and key components through each of the benchmark analysis tests. Within the Work Programme<sup>(1)</sup> the level of detail provided with the response predictions was left to the discretion of the Analyst. The basis for this was that corresponding detail would be provided by BOMEL in the results package. On this basis Appendices E, F and G provide bespoke details of the rig support conditions, local joint deformation and member forces respectively. Where data are not presented it is believed they were not supplied in the benchmark submission.

#### 4.5 BENCHMARK ACTIONS

The action remaining for Benchmark Analyst to perform are detailed in Section 1.3.3. A proforma to help structure and provide for complementary feedback is presented in Appendix H.

Clarification of any of the information provided can be obtained from BOMEL at any stage.



## 5. REFERENCES

All references supplied to Benchmark Analysts, unless noted otherwise.

- \* Indicates relevant data extracted and reproduced in this report.
- 1. BOMEL Limited. 'Benchmark Analysis - Project Work Plan', BOMEL reference C636\21\006S, Revision B, September 1997.
- 2. BOMEL Limited. 'Benchmark Analysis - Blind predictions of Ultimate strength', BOMEL reference C636\32\002R, Revision 0, February 1998.
- 3. BOMEL Limited 'Material testing report', BOMEL reference C636\23\004R, Revision A, March 1998 (see Reference 4).
- 4. BOMEL Limited. Fax to Benchmark Analysts with summary table from Reference 3 and sketches indicating disposition of tubulars within 3D Frame. BOMEL reference C636\32\022F, 27 March 1998.
- 5. BOMEL Limited. 'Interim summary of Loadcase 1 and 2 test results', BOMEL reference C636\32\046U, Revision 0, August 1998.
- 6. BOMEL Limited. 'Interim summary of Loadcase 3 test results', BOMEL reference C636\32\058U, Revision A, October 1998.
- 7.\* BOMEL Limited. 'Material testing report', BOMEL reference C636\23\004R, Revision B, April 1999.
- 8.\* 'Joint Industry Tubular Frames Project - Phase I', Nine Volume Report, SCI Reference SCI-RT-042, 1990.
- 9.\* AKD Engineering Limited. 'Test specimen documentation package', AKD Reference 4065/4413-2/4570. BOMEL Incoming Document 11900, File C636\31, November 1998.
- 10.\* BOMEL Limited. 'Assessment of locked-in fabrication stress', BOMEL reference C636\21\050R, Revision 0, July 1999.
- 11.\* BOMEL Limited. 'Test frame instrumentation', BOMEL reference C636\25\071R, Revision 0, July 1999.



- 12.\* BOMEL Limited. 'Joint Industry Tubular Frames Project - Phase III - Fabrication specification - supplement to EEMUA publication No 158', BOMEL reference C636\06\007S, Revision C, March 1997.
13. Bolt, H M and Smith, J K. 'The influence of locked-in fabrication stresses on structural performance', Offshore Mechanics and Arctic Engineering Conference, Copenhagen, 1995.

**APPENDIX A**  
**BENCHMARK SCOPE OF WORK**

(Reproduced from Reference 1)





## APPENDIX A BENCHMARK SCOPE OF WORK

The scope of work to be undertaken by Benchmark Analysts is detailed below. Those items **emboldened** are essential to fulfilling the base scope. *Italicised* items are optional. Roman text provides supplementary information.

1. **Model and analyse the test specimen and reaction rig as described in [Section 3 and Appendix A] to predict the ultimate response of the specimen under the three static Load Cases prescribed.**

**Prepare and submit report to BOMEL on or before [23 January 1998] covering:**

- **Software package used and version**
- **Element modelling options selected**
  - **type and characterisation.**
- **Material modelling assumptions**
- **Boundary conditions**
- **Any variations in modelling from Load Case to Load Case**
- **Any account of physical imperfections outwith the specification in [Appendix A]**
- **For each Load Case:**
  - **plot applied load versus displacement of the point of load application annotated with sequence of component 'failures'/ nonlinear 'events'.**
  - **plot key component loads against displacement for components sustaining significant loads before and after the system capacity is reached.**
  - **produce diagram of test specimen indicating sequence and location of yielding and / or component failures.**
  - **plot vertical support reactions between test rig and support stools against applied frame load**
  - **Provide data in spreadsheet format (compatible with Lotus 123 Version 4) for applied load, displacement and corresponding component forces/ moments and reactions, using the reference scheme in [Appendix A].**

(Test results provided to Benchmark Analysts will reciprocate the extent of reporting in their individual submissions)
- **Indication of benchmark constraints/ qualifications.**
  - **experience of personnel (with software and typical applications to date).**
  - **manhours dedicated to the work.**
  - **note of any funding.**
  - **analysis time (including computer speed/ specification).**

Actual material yield values will be made available in the course of the analyses. ***Actual yield values may be accounted for in place of the minimum specified values provided at the outset***



*in an additional set of analyses.*

*An additional set of analyses may be performed and reported for the tubular frame specimen only, without the reaction rig and assuming the structure to be fixed at its base.* Verification analyses have been performed by BOMEL and SINTEF on this basis and this configuration will therefore provide a further basis for comparison.

All clarification requests raised with BOMEL will be documented and all responses will be conveyed by fax within three working days to all Benchmark Analysts and the Participants' Review Panel.

An opportunity for Benchmark Analysts to view the fabrication will be provided in late November and will be combined with an interim meeting for any further queries to be raised. ***Benchmark Analysts as well as members of the Participants' Review Panel will be invited to attend the meeting.*** The proceedings will be fully recorded and presentation material, questions and answers will be circulated to Benchmark Analysts unable, or who do not wish, to attend.

2. BOMEL will collate the response predictions identifying each contribution solely by alphabetical letter (A, B, C etc) and circulate the compendium to all Benchmark Analysts and project Participants prior to the tests. No reference to software will be included in this initial distribution.
3. BOMEL and its test sub-contractors will undertake the Load Case 1 static test. Within ten days, BOMEL will provide to Benchmark Analysts, a description of the structural response together with graphical results of loads and deflections corresponding to the input data provided by the Benchmark Analyst.

***Benchmark Analysts will have the opportunity to witness one of the collapse tests during the course of the test programme.*** Due notice of the precise test dates will be given.

4. ***The Benchmark Analyst may review the Load Case 1 results and update its response predictions for the Load Case 2 and 3 tests, if appropriate. Such updated results should be reported prior to the next test in accordance with the required breakdown under Activity 1, including a description of the extent of changes from the original submission and their basis.***
5. BOMEL and its sub-contractors will undertake the Load Case 2 tests and provide results to Benchmark Analysts as under Activity 3. The schedule may not permit repeat analyses prior to Loadcase 3.
6. BOMEL and its sub-contractors will undertake the Load Case 3 test. BOMEL will then prepare an as-built update to the data package provided in [Appendix A] together with a description /



critique of the tests, noting particular physical features which may be a source of discrepancy with respect to analysis predictions.

7. **Benchmark Analysts shall receive and review the results package and test critique. The original analyses shall be repeated and the best estimate analysis reported for the three loadcases in accordance with the brief in Activity 1. The report shall describe the basis of any changes and their manner of implementation. An attempt shall be made to explain any remaining discrepancies (which may be attributable to aspects of the tests and / or analysis).**
8. BOMEL will compile the results retaining the alphabetical anonymity. The combined results and overall lessons learned will form a summary from which publications may be developed in accordance with the terms set down in the Benchmark Analysts' Participation Agreement. **During the course of preparation, Benchmark Analysts shall cooperate with BOMEL to ensure accuracy and consistency.** BOMEL will circulate the draft collation report to the Participants' Review Panel and the **Benchmark Analysts who shall review and comment.** BOMEL will update the draft report reflecting comments received and distribute this to all Benchmark Analysts and project Participants. A meeting will be held with the project sponsors. ***Attendance at the meeting is not mandatory as part of the full scope but will be encouraged.***

## **APPENDIX B**

### **INTERIM SUMMARIES OF TEST RESULTS**

(Reproduced from References 5 and 6)

# FRAMES PROJECT PHASE III

## INTERIM SUMMARY OF LOADCASE 1 AND 2 TEST RESULTS

### INTRODUCTION

This brief report presents the global response data for the Loadcase 1 and 2 tests. Detailed results will be provided to benchmark analysts on an individual basis once post-processing of the data is complete. The frame test facility is shown in Figure 1 prior to the Loadcase 1 test. Figure 2 presents the framing details as given in the benchmark specification.

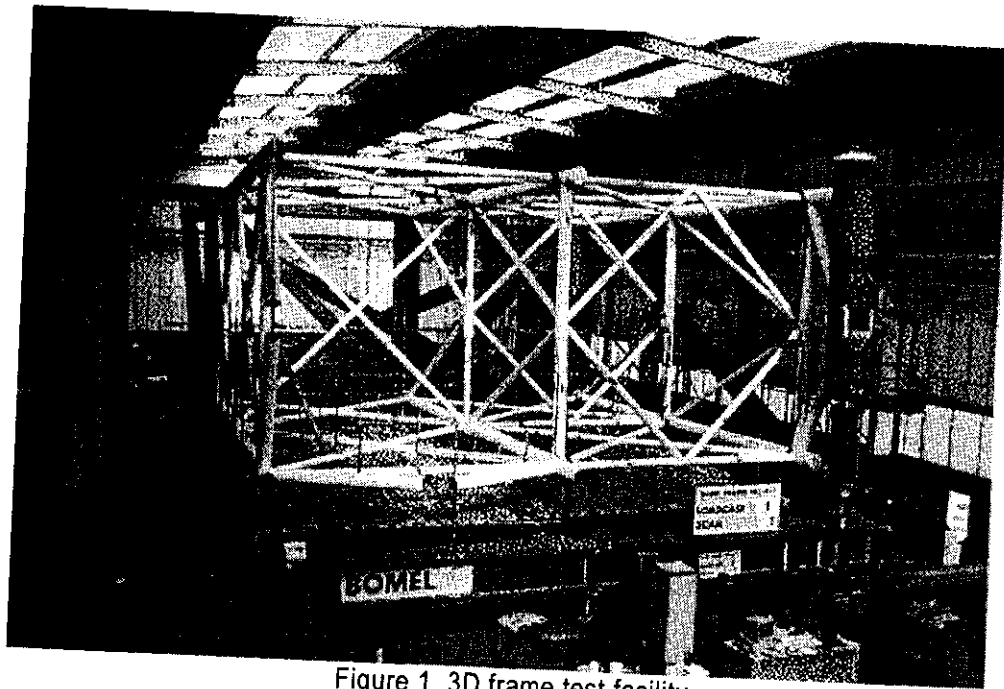


Figure 1 3D frame test facility

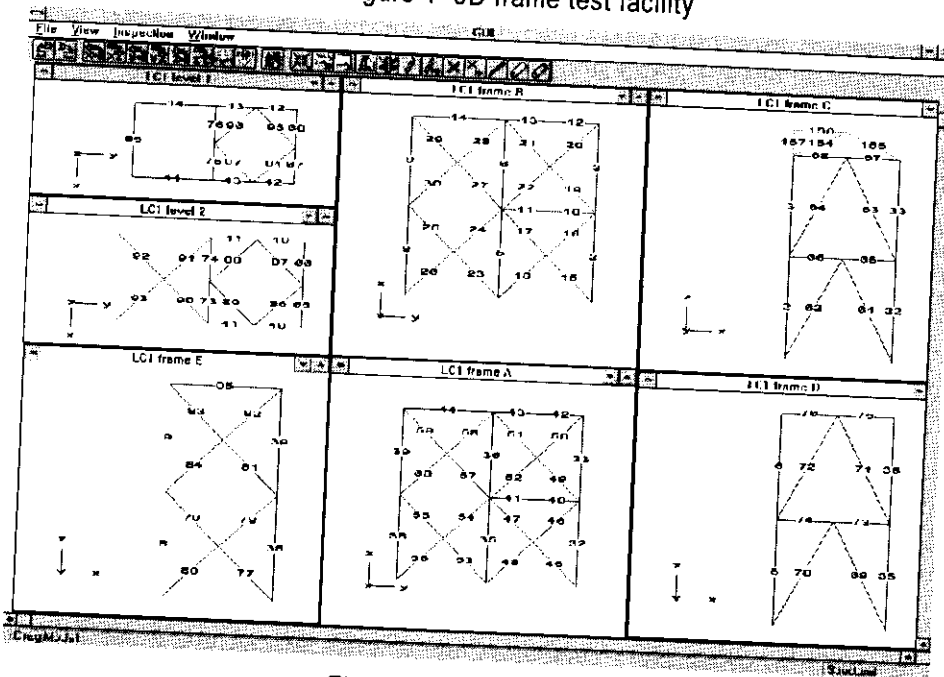


Figure 2 3D Framing



## FRAME TEST RESULTS

### LOADCASE 1

#### Configuration

The  $\beta = 0.6$  K joints at Levels 1 and 2 on the loaded end transverse frame C are gapped.

Out-of-plane, the K configuration is overlapped at Level 1 and gapped at Level 2.

#### Response (see Figure 3)

Following initial deformation around the compression intersection of the Frame C K joint at Level 1, tensile cracking in the gap region limited joint capacity.

With increasing global load, redistribution occurred across the Level 1 diamond bracing into Frame D and loads continued to increase through the Level 2 K joint on Frame C. This joint sustained increasing loads without failure and ultimate system strength was governed by compression brace buckling in Frame D.

The capacity of the first multiplanar joint was some 50% greater than the isolated planar K joint tested by SINTEF (nominally identical to those in Frame C). The strength was more than twice the mean capacity of isolated test data on which current design formulae are based. This compares with an enhancement of 15-35% attributed to boundary restraints seen in the 2D frames in Phase II.

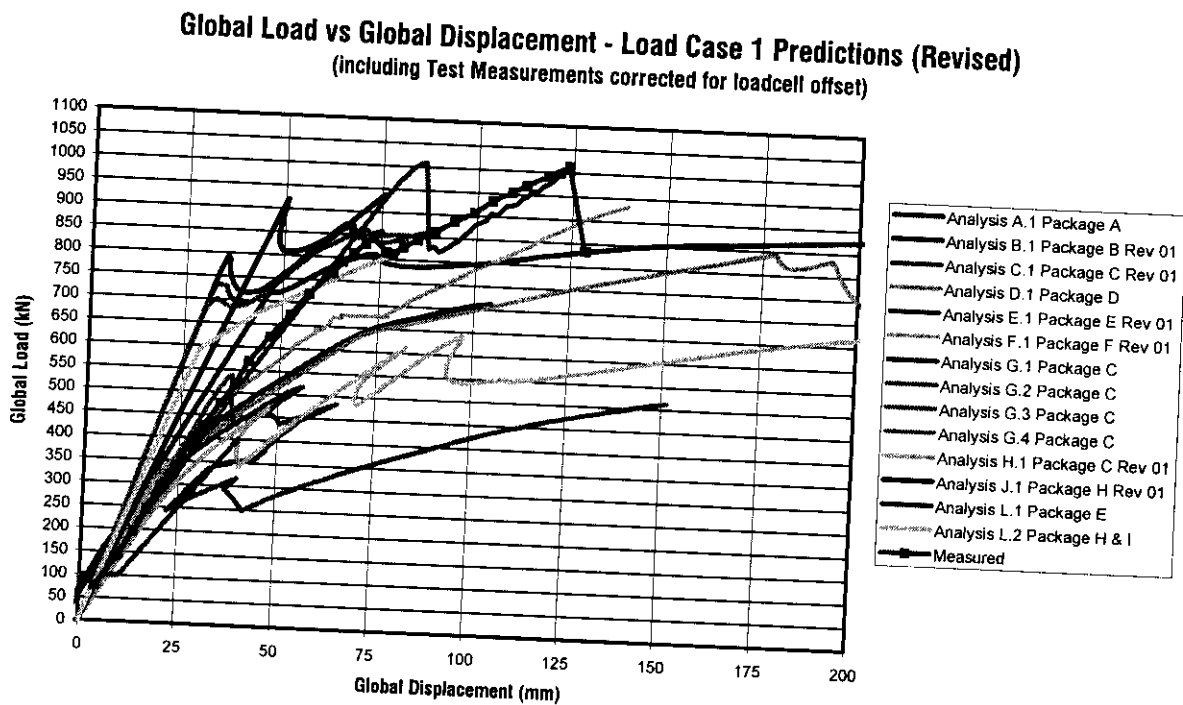


Figure 3 Loadcase 1 test result and benchmark predictions (C636\32\005W-B)



## LOADCASE 2

### Configuration

The  $\beta = 1.0$  X joint between Levels 1 and 2 on Line E has no joint can and is loaded in compression. In the lower bay, the X joint has a thick walled high yield can. There is no mid-height horizontal in Frame E and the ability of the Level 2 X bracing to distribute loads in frame action is being explored.

### Response (see Figure 4)

The upper X joint response began to soften as the global load was increased. A sudden drop in the load carrying capacity of the joint was exhibited as the saddle region arched. Once the weld toes came into contact across the chord, the response stiffened but then softened again as the braces ovalised the chord in compression.

Because of the reduced stiffness in the compression loadpath in the top X bay, greater proportions of the applied load were carried by the tension chord. The forces were then transmitted in part by the Level 2 X bracing out into the 3D structure, initially protecting the bottom bay bracing from overload despite the absence of a mid-height horizontal in the plane of loading. Nevertheless as the top bay chord yielded extensively in tension and the global deformation increased, buckling in the lower bay occurred. The alternative loadpath through the Level 2 X bracing however ensured the structure as a whole continued to sustain increasing load.

Eventually the braces fully contacted through the upper X joint chord developing a stiff load path. The through loads then increased sufficiently for one of the top bay compression branches to buckle. This event defined a peak in the global load.

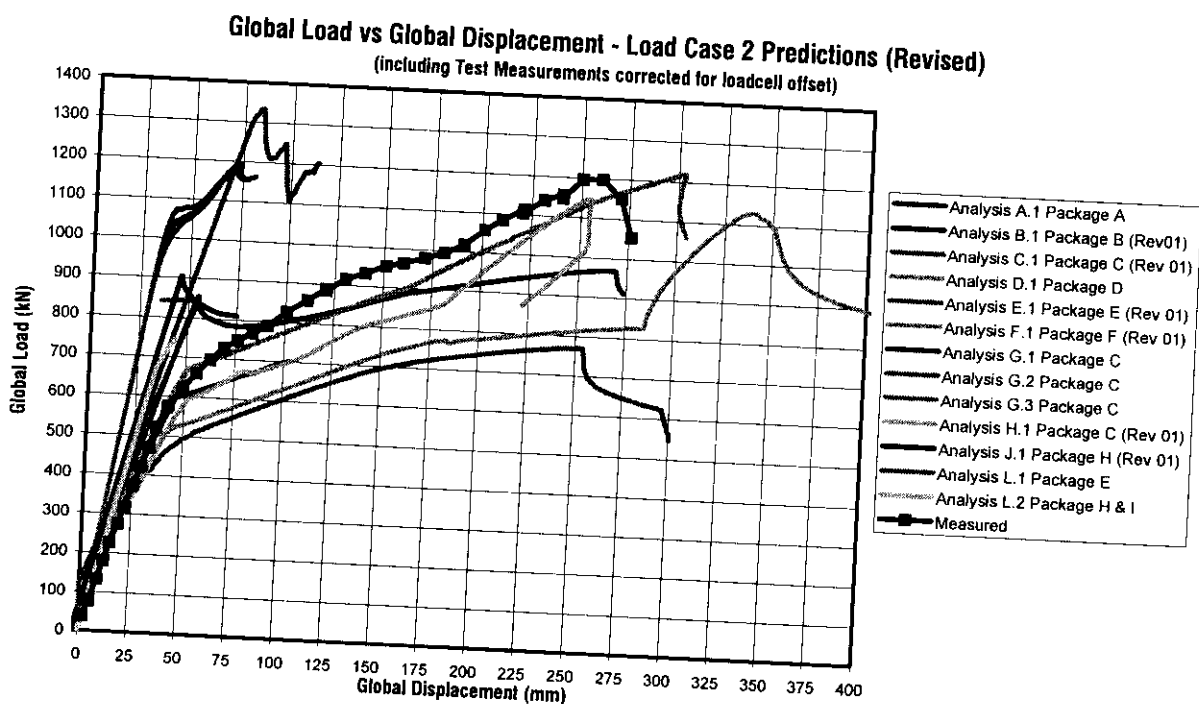


Figure 4 Loadcase 2 test result and benchmark predictions (C636\32\007W-B)



# FRAMES PROJECT PHASE III

## INTERIM SUMMARY OF LOADCASE 3 TEST RESULTS

### INTRODUCTION

This brief report presents the global response data for the Loadcase 3 test. Corresponding information and general arrangement details were provided in BOMEL document C636\32\046U distributed August 1998.

More detailed results are being prepared for circulation to benchmark analysts.

### LOADCASE 3

#### Configuration

Load is applied longitudinally on Line A. The Frame A X-bracing has thick walled joint cans whereas Nodes 16 and 18 in Frame B have no strengthening of the chord. Similarly the X-bracing introduced between lines D and E at Level 1 has a relatively weak X joint (Node 44). The multiplanar K joints on Line C were reinstated with strong joint cans following the Loadcase 1 tests.

The Loadcase 3 test was performed with the long ties of the reaction rig in place.

#### Response (see Figure 1)

As the global load was increased first component failures occurred in the bracing in Frame A. On account of high locked-in tensile forces remaining from fabrication, chord yield preceded brace buckling. The tensile capacity of Chord 49/51 was reached first at a global displacement of ~50mm. The sequence of yielding and brace buckling proceeded in Frame A until, at a global displacement of 120mm, compression braces 46, 50, 54 and 60 had all buckled and a peak in the global response can be observed. With the softening in the Frame A response there was then a significant increase in the loads transferred across the structure through the transverse framing and Level 1 and 2 X- and diamond-bracing.

Gradually the X joints at Nodes 44 (Level 1) and 16 (Frame B) began to deform and their responses softened in tension. At a global displacement of 200mm the limiting capacity of the compression X joint at Node 18 (Frame B) was reached.

Finally buckling of Member 61 in the transverse frame on line C precipitated a sharp full off in load determining the ultimate system strength at ~220mm global deflection.





### Global Load vs Global Displacement - Load Case 3 Predictions (Revised) (including Test Measurements)

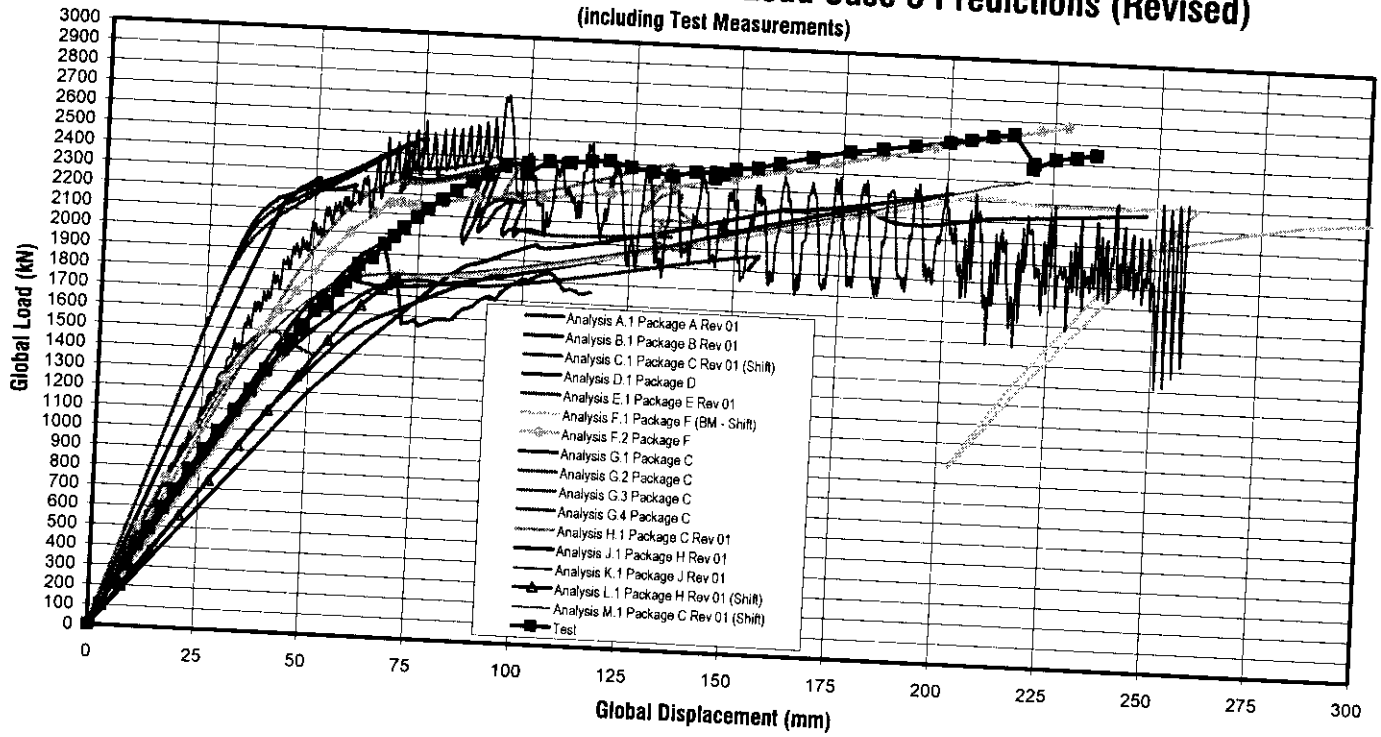


Figure 1 Loadcase 3 test result and benchmark predictions (C6361321009W-B)



## **APPENDIX C**

### **INSTRUMENTATION LAYOUT DRAWINGS**

- Load cell details - C636\15\011D Revision D
- Strain gauging details (Sheet 1 of 2) - C636\15\012D Revision B
- Strain gauging details (Sheet 2 of 2) - C636\15\013D Revision B
- Joint deformation monitoring - C636\15\016D Revision 0
- Rig node displacement monitoring - C636\25\075D

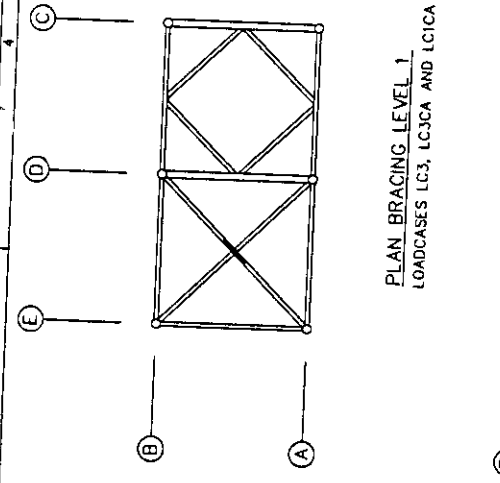




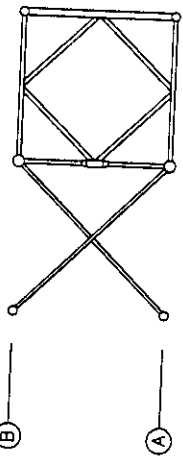


**NOTES**

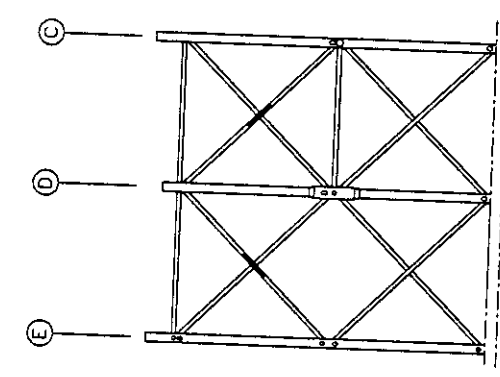
1. ——— DENOTES LOCATION OF FRAME MOUNTED TRANSDUCER



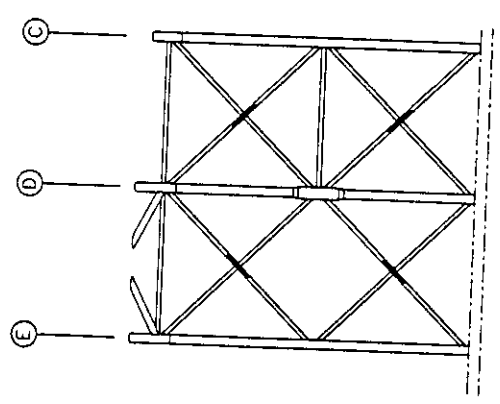
**PLAN BRACING LEVEL 1**  
LOADCASES LC3, LC3CA AND LC1CA



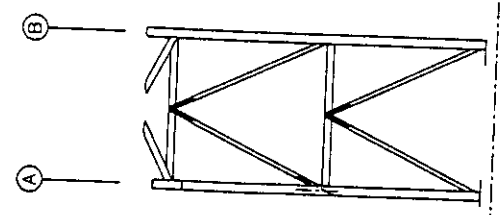
**PLAN BRACING LEVEL 2**



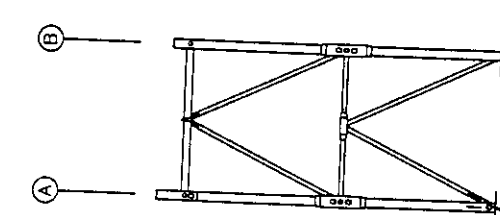
**ELEVATION ON LINE A**  
LOADCASES LC3CA AND LC1CA



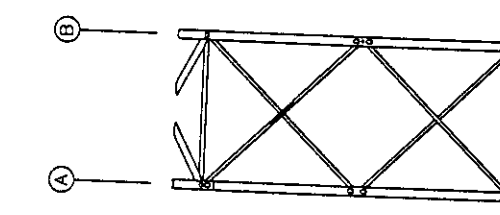
**ELEVATION ON LINE B**  
ALL LOADCASES



**ELEVATION ON LINE C**  
LOADCASES LC1, LC1C, LC3CA AND LC1CA



**ELEVATION ON LINE D**



**ELEVATION ON LINE E**  
LOADCASES LC1, LC1C, LC2 AND LC2C

REV	DATE	DESCRIPTION OF CHANGE	PREPARED BY	CHECKED BY	DATE
0	8/98	AS BUILT	JADC	NHB	CJB

BOMEL CONTRACT No.	0003608
CLIENT CONTRACT No.	0003608
CLIENT	JOINT INDUSTRY PROJECT
PROJECT	FRAMES PHASE III
DRAWING TITLE	JOINT DEFORMATION MONITORING

DATE	15/01/80
DRAWING No.	0160

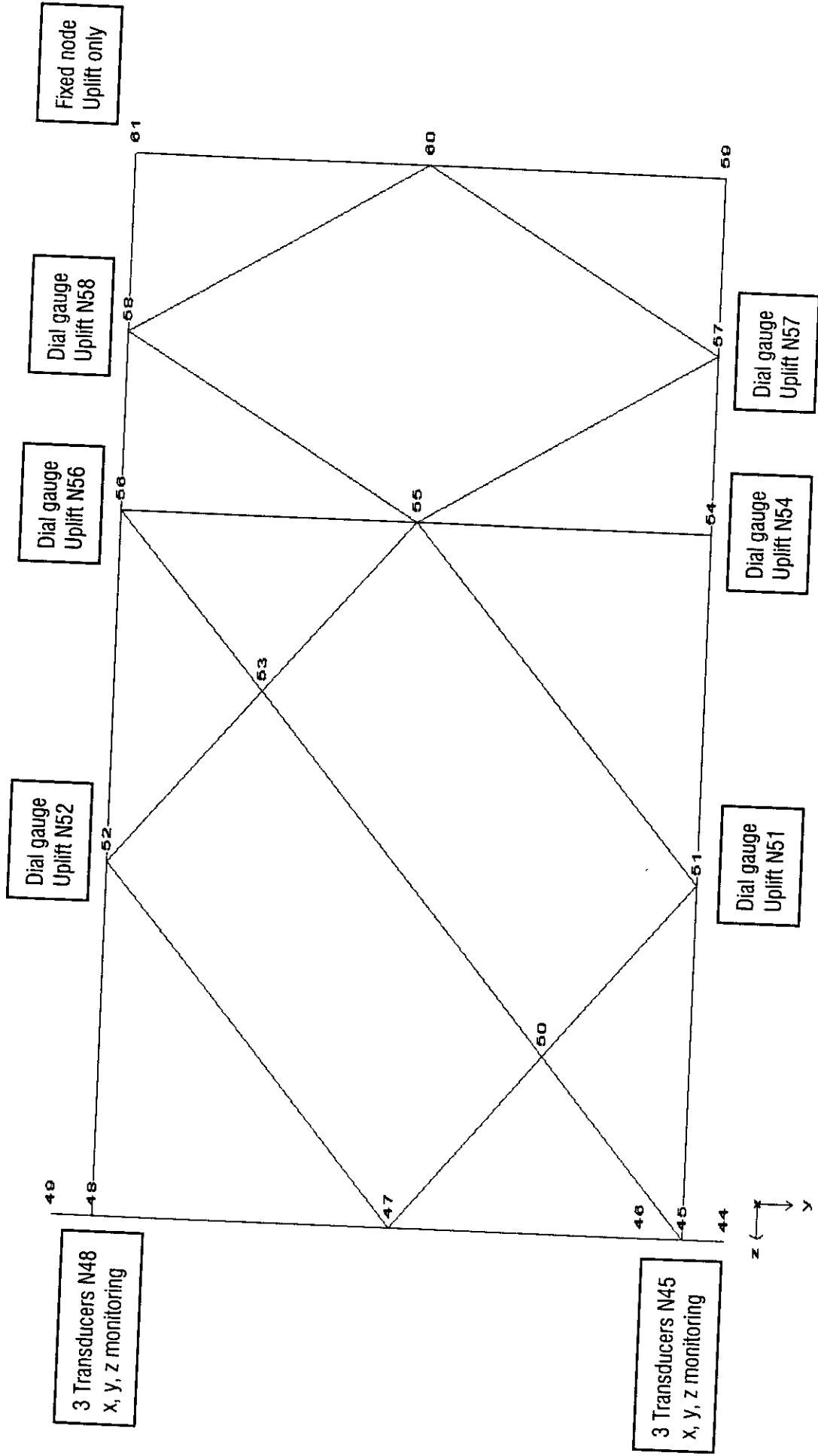


**BOMEL ENGINEERS**  
 14, +44 (0)1528 77720  
 Fax: +44 (0)1528 77787

Drawing No. **0160**

Drawing No. **0160**

**RIG NODE DISPLACEMENT MONITORING - PLAN ON BASE OF RIG**





## **APPENDIX D**

### **MEASURED MATERIAL AND SECTION PROPERTIES**

(C636\06\294W-b.xls - 6 pages)

















## APPENDIX E LOADCASE 1 RESULTS

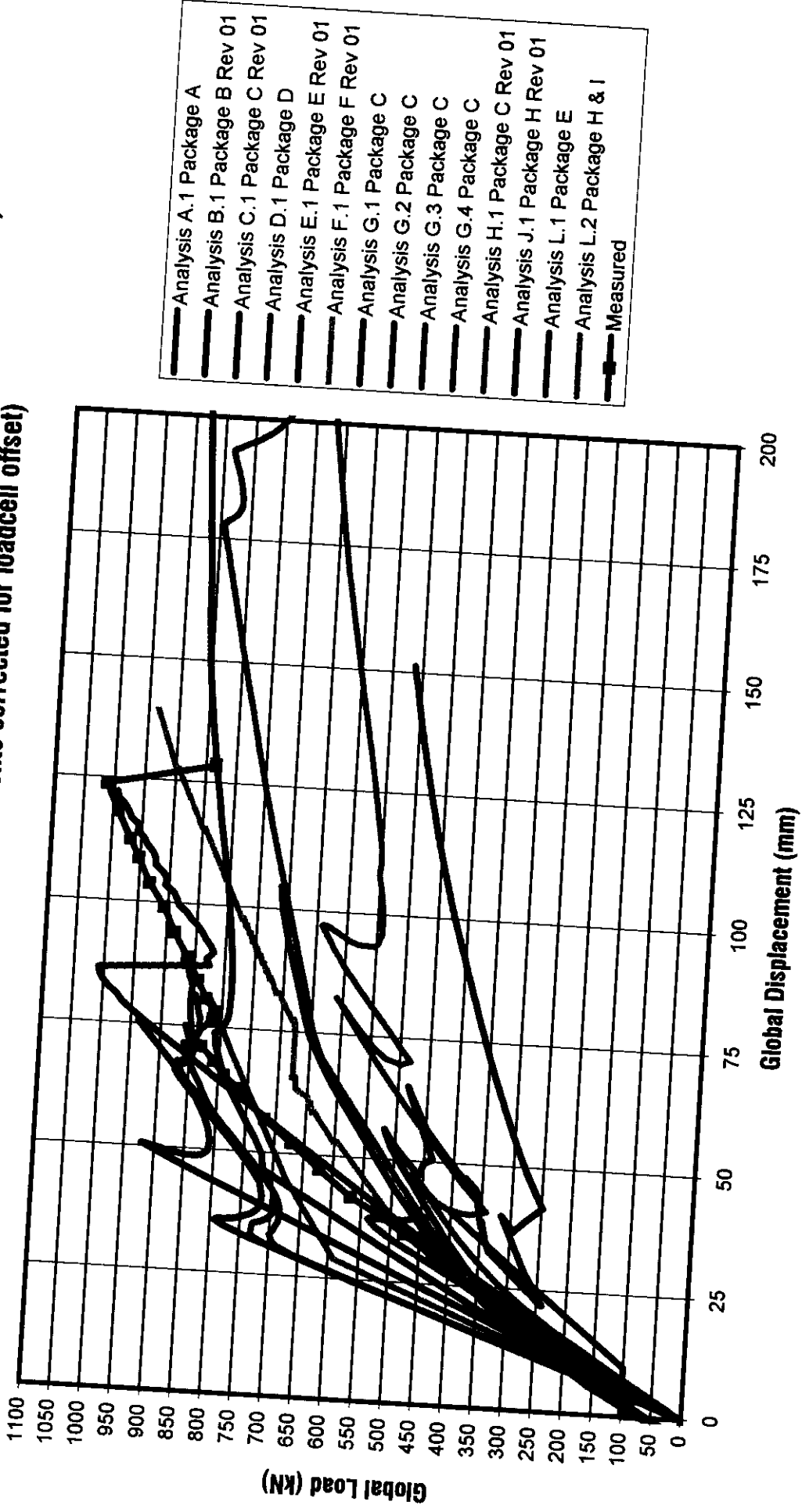
Plot	Sheet name	Plots / data provided by and supplied to Benchmark Analyst:													
		*	A	B	C	D	E	F	G	H	J	K	L	M	N
<b>Global response</b>															
Pre-test benchmark collation	ALL LC1Chart (test)	X	X	X	X	X	X	X	X	X	X	X	X	X	X
Global response with scan nos	Global Scan Nos	X	X	X	X	X	X	X	X	X	X	X	X	X	X
Global response with failures	Global Annotated	X	X	X	X	X	X	X	X	X	X	X	X	X	X
<b>Displacements</b>															
Rig node uplift c.f.global response	Combined Chart 1	X	X	X	X		X	X		X			X	X	
Spatial disp. of 3D frame nodes	**	X		X		X		X	X				X	X	
<b>Local joint characteristics:</b>															
Frame A K Node 37 tension	FrC Lev2 Tens	X	X		X			X							
Frame A K Node 37 compression	FrC Lev2 Comp	X	X		X			X							X
Frame A K Node 38 tension	FrC Lev1 Tens	X	X		X			X							X
Frame A K Node 38 compression	FrC Lev1 Comp	X	X		X			X							X
Frame E X Node 42 compression	FrE TB Comp				X			X							X
Frame B X Node 16 compression	FrB TB Comp														
Frame B X Node 18 tension	FrB TB Tens														
Level 1 X Node 44 tension	Lev1-LC3X Tens														
<b>Member Forces</b>															
Frame A X braces L1-L2 FrC-FrD	FrA TDC For														
Frame A X braces L1-L2 FrD-FrE	FrA TED For														
Frame A X braces L2-L3 FrC-FrD	FrA BDC For														
Frame A X braces L2-L3 FrD-FrE	FrA BED For														
Frame B X braces L1-L2 FrC-FrD	FrB TDC For														
Frame B X braces L1-L2 FrD-FrE	FrB TED For	X	X												
Frame B X braces L2-L3 FrC-FrD	FrB BDC For														
Frame B X braces L2-L3 FrD-FrE	FrB BED For														
Frame C K braces L1-L2	FrC TB For	X	X	X	X	X	X	X	X	X	X		X	X	X
Frame C K braces L2-L3	FrC BB For	X	X	X	X	X	X	X	X	X			X	X	X
Frame D K braces L1-L2	FrD TB For	X	X	X				X	X	X			X	X	X
Frame D K braces L2-L3	FrD BB For	X		X				X	X	X					X
Frame E X braces L1-L2	FrE TB For														X
Frame E X braces L2-L3	FrE BB For														
Level 2 X braces FrD-FrE	Lev 2-X For	X													
Level 2 diamond braces FrC-FrD	Lev 2-Dia For	X													X
Level 1 X braces FrD-FrE	Lev 1-LC3X For							X							X
Level 1 diamond braces FrC-FrD	Lev 1-Dia For	X	X		X	X		X							X
Frame C legs	Fr C Leg For														
Frame D legs	Fr D Leg For														
Frame E legs	Fr E Leg For														
All frame legs at connection to rig	Fr Feet	X						X	X	X					
<b>Bending moments</b>															
Frame A compression braces	FrA.... Mom (8)														

Reference Files:  
 Rig displacements C636\25\063W  
 Loadcase 1 global and force plots C636\37\011W  
 Loadcase 1 benchmark comparison C636\32\005W-B

\* Information provided to project sponsors  
 \*\* N21, N22, N25, N26, N29 and N30 Disp

TUBULAR FRAMES PROJECT PHASE III

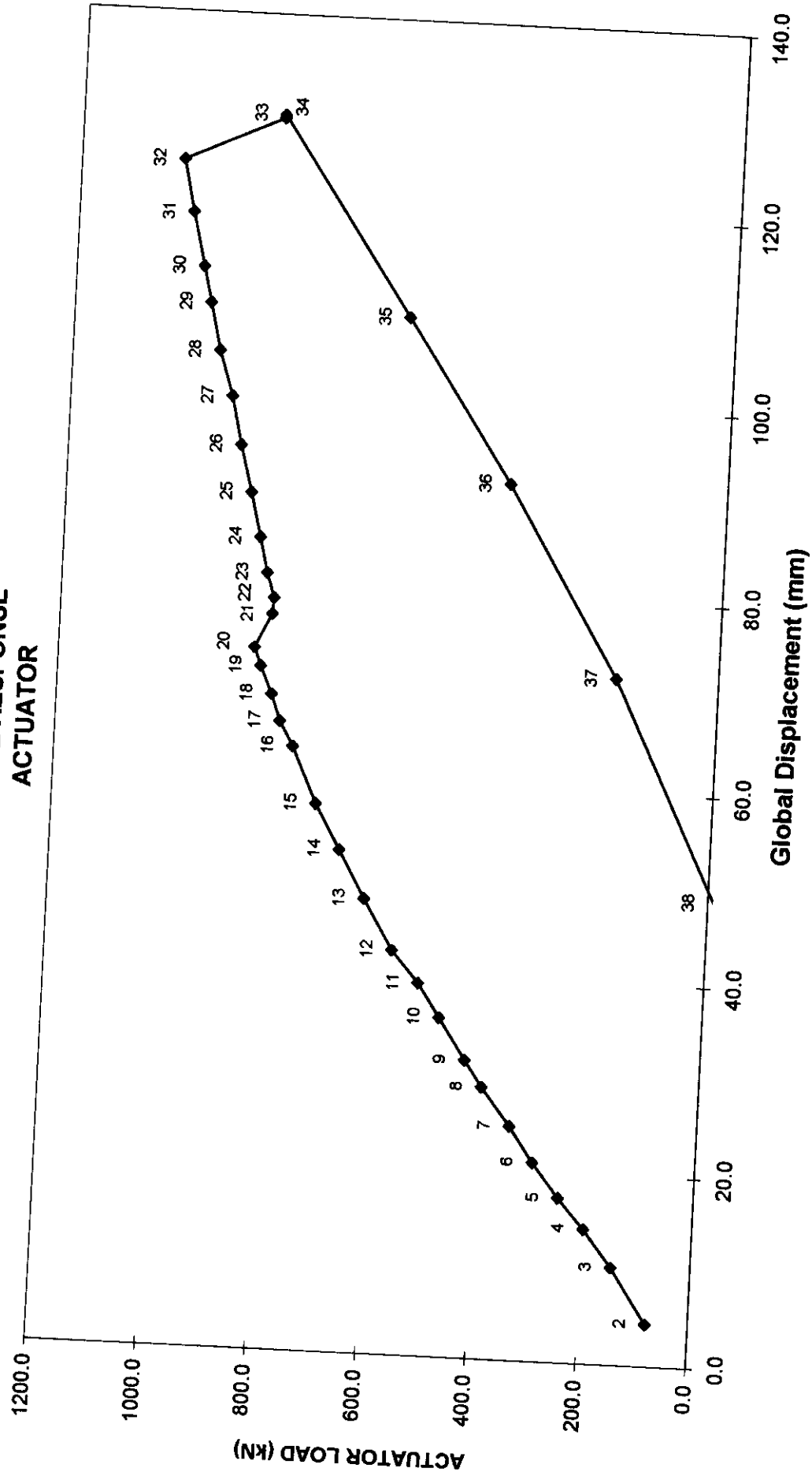
**Global Load vs Global Displacement - Load Case 1 Predictions (Revised)**  
 (including Test Measurements corrected for loadcell offset)



- Analysis A.1 Package A
- Analysis B.1 Package B Rev 01
- Analysis C.1 Package C Rev 01
- Analysis D.1 Package D
- Analysis E.1 Package E Rev 01
- Analysis F.1 Package F Rev 01
- Analysis G.1 Package C
- Analysis G.2 Package C
- Analysis G.3 Package C
- Analysis G.4 Package C
- Analysis H.1 Package C Rev 01
- Analysis J.1 Package H Rev 01
- Analysis L.1 Package E
- Analysis L.2 Package H & I
- Measured

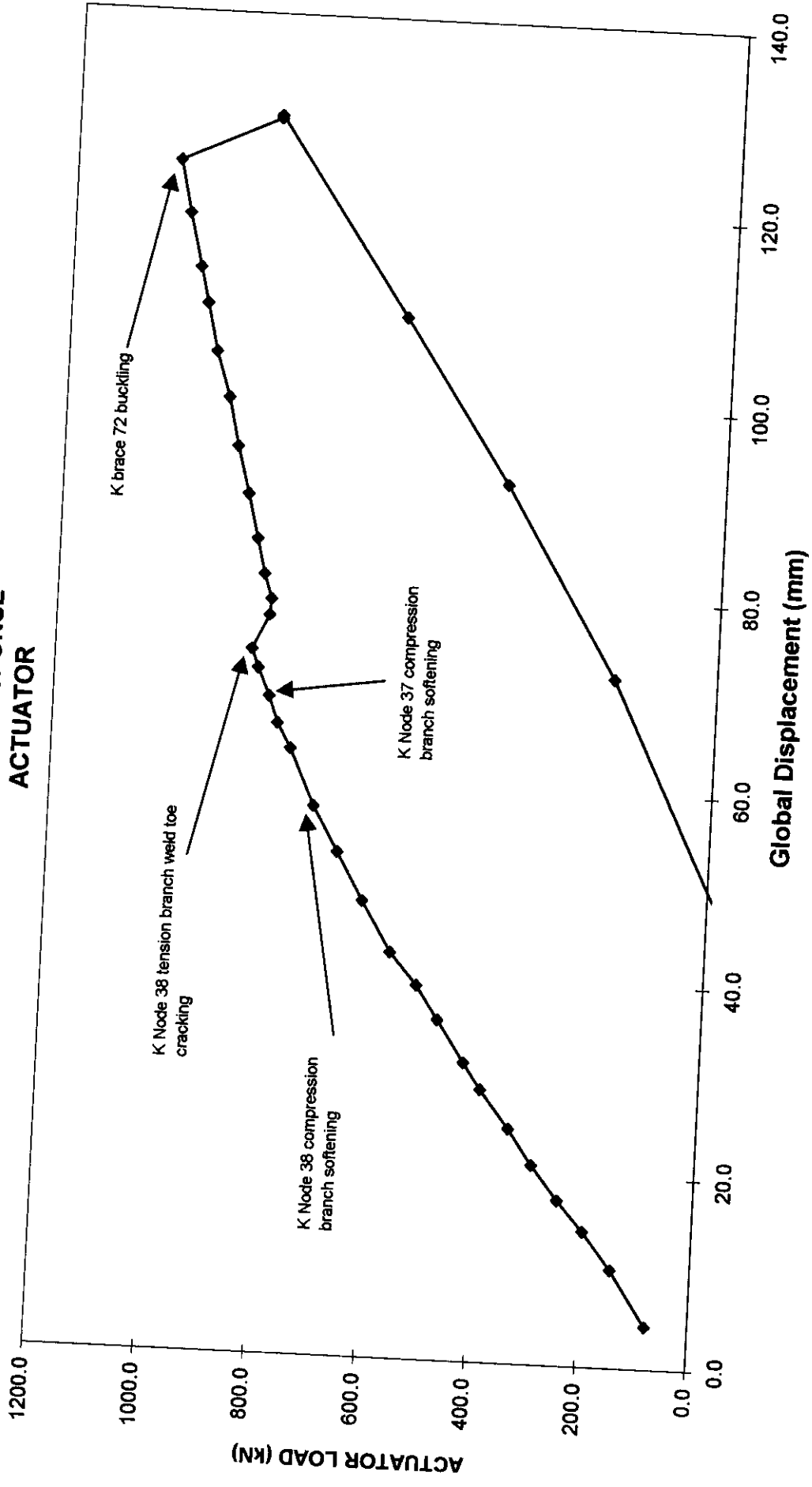


# GLOBAL RESPONSE ACTUATOR



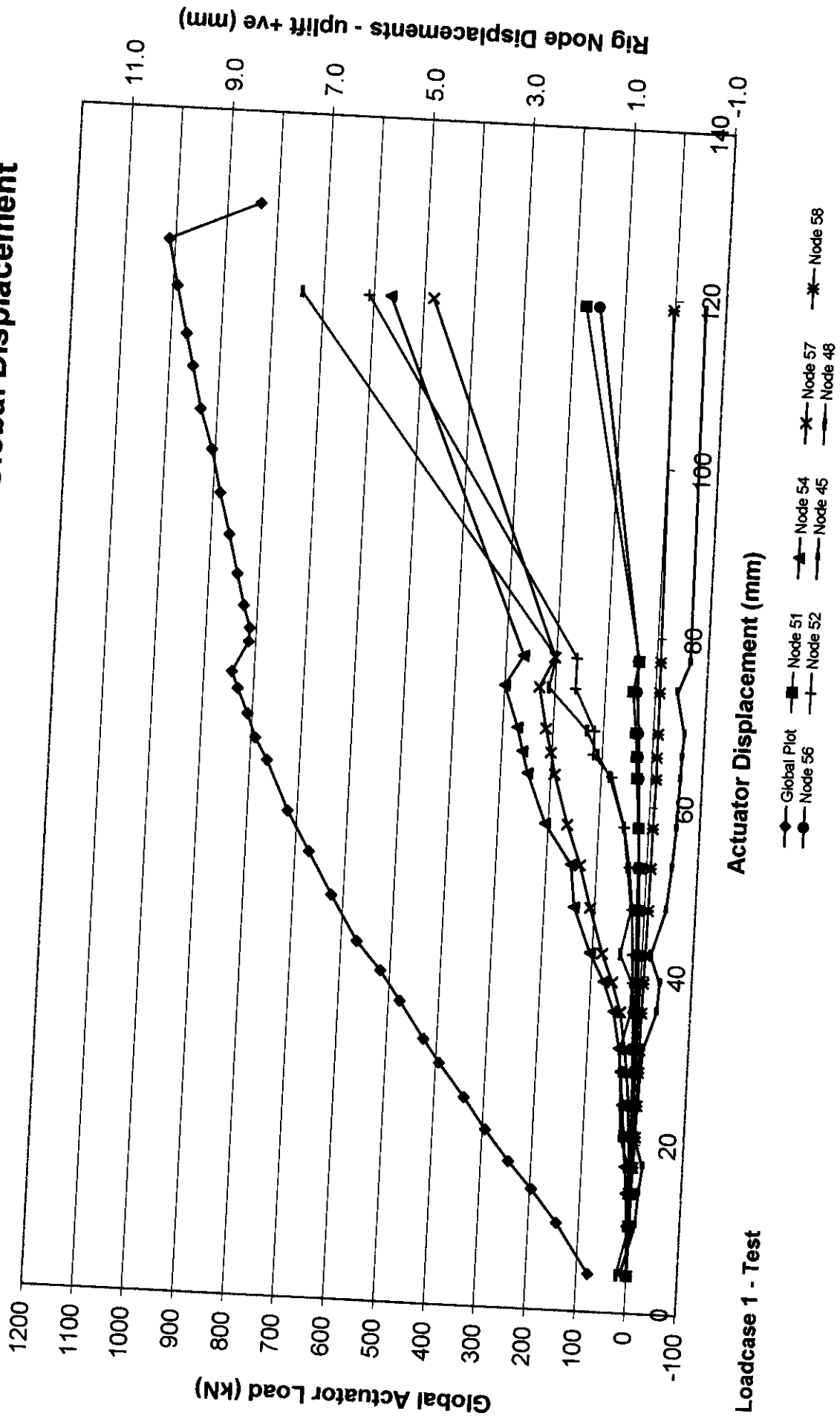
Loadcase 1 - Test

# GLOBAL RESPONSE ACTUATOR



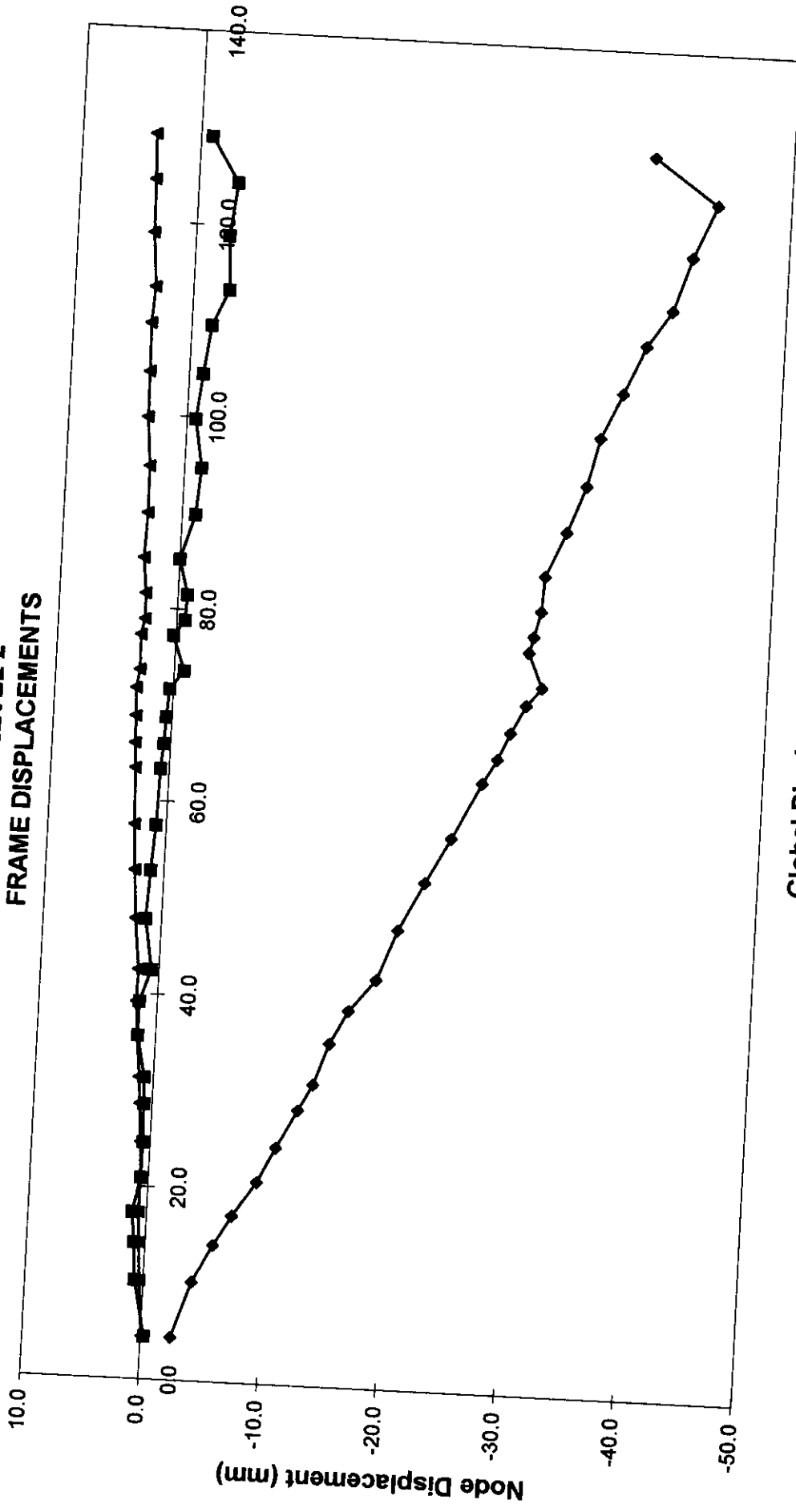
Loadcase 1 - Test

# Nodal Displacements and Global Load versus Global Displacement



Loadcase 1 - Test

LEG AC LEVEL 2  
FRAME DISPLACEMENTS



Global Displacement (mm)

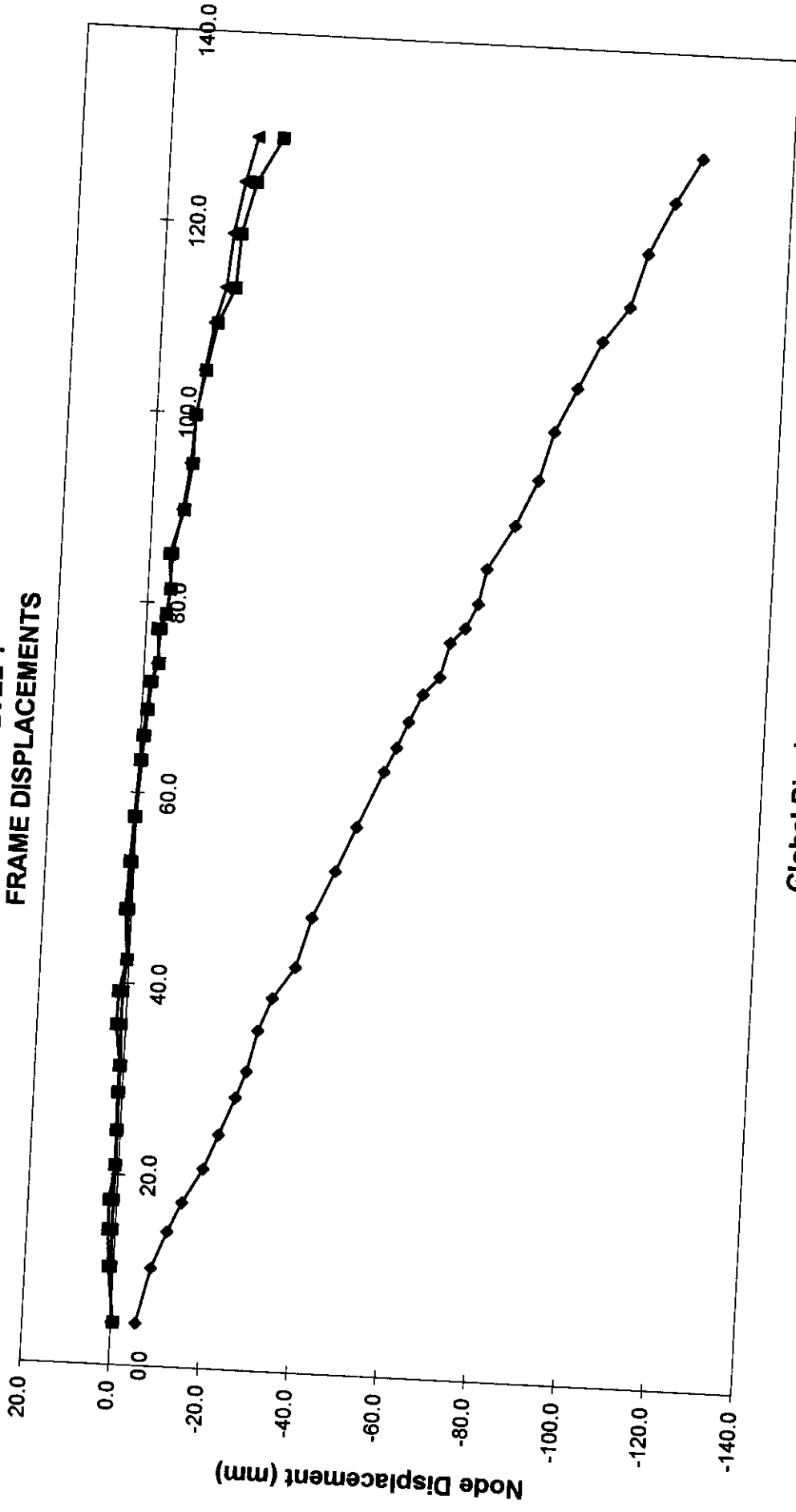
Loadcase 1 - Test

◆ X Measured

■ Y Measured

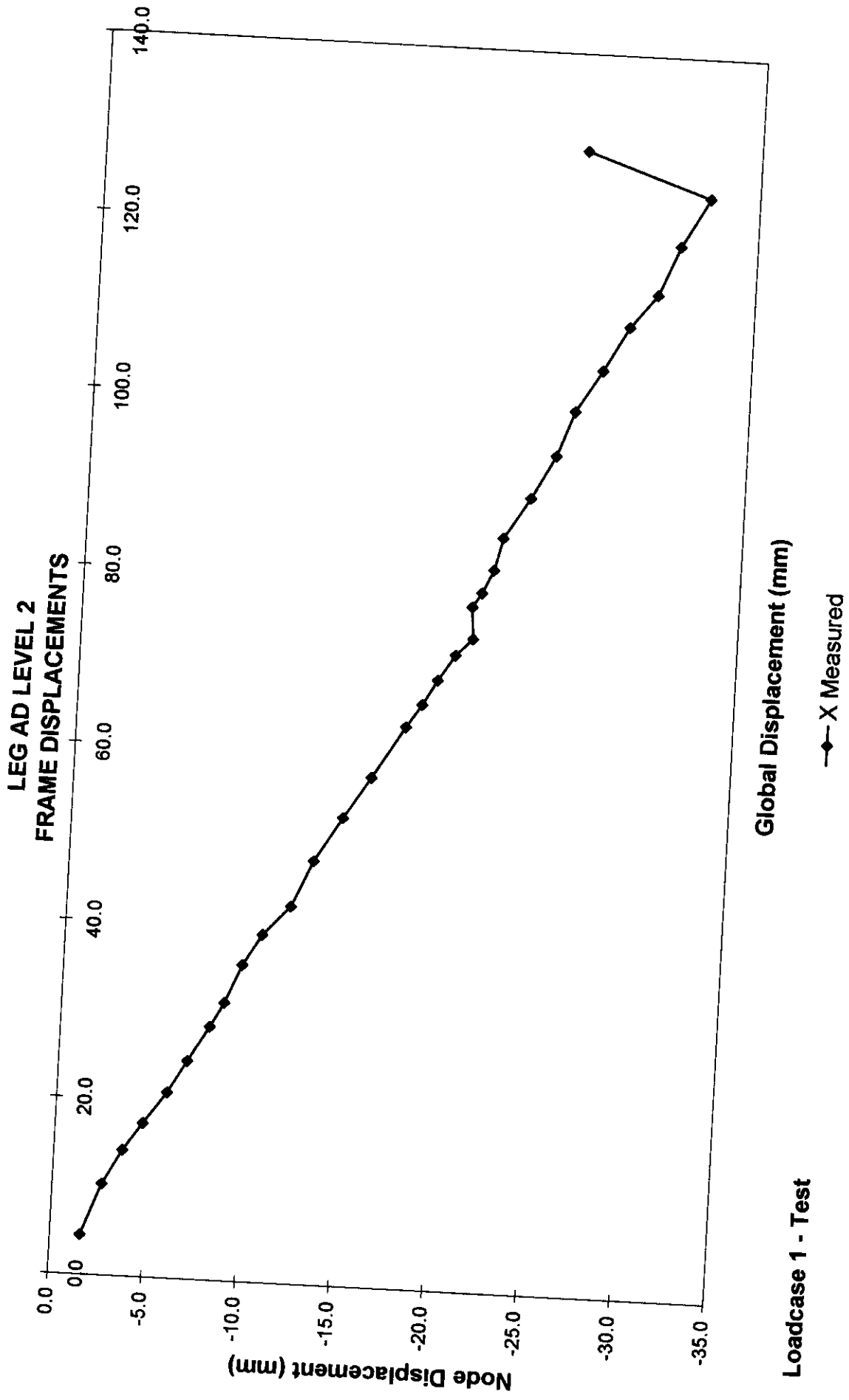
▲ Z Measured

**LEG AC LEVEL 1  
FRAME DISPLACEMENTS**

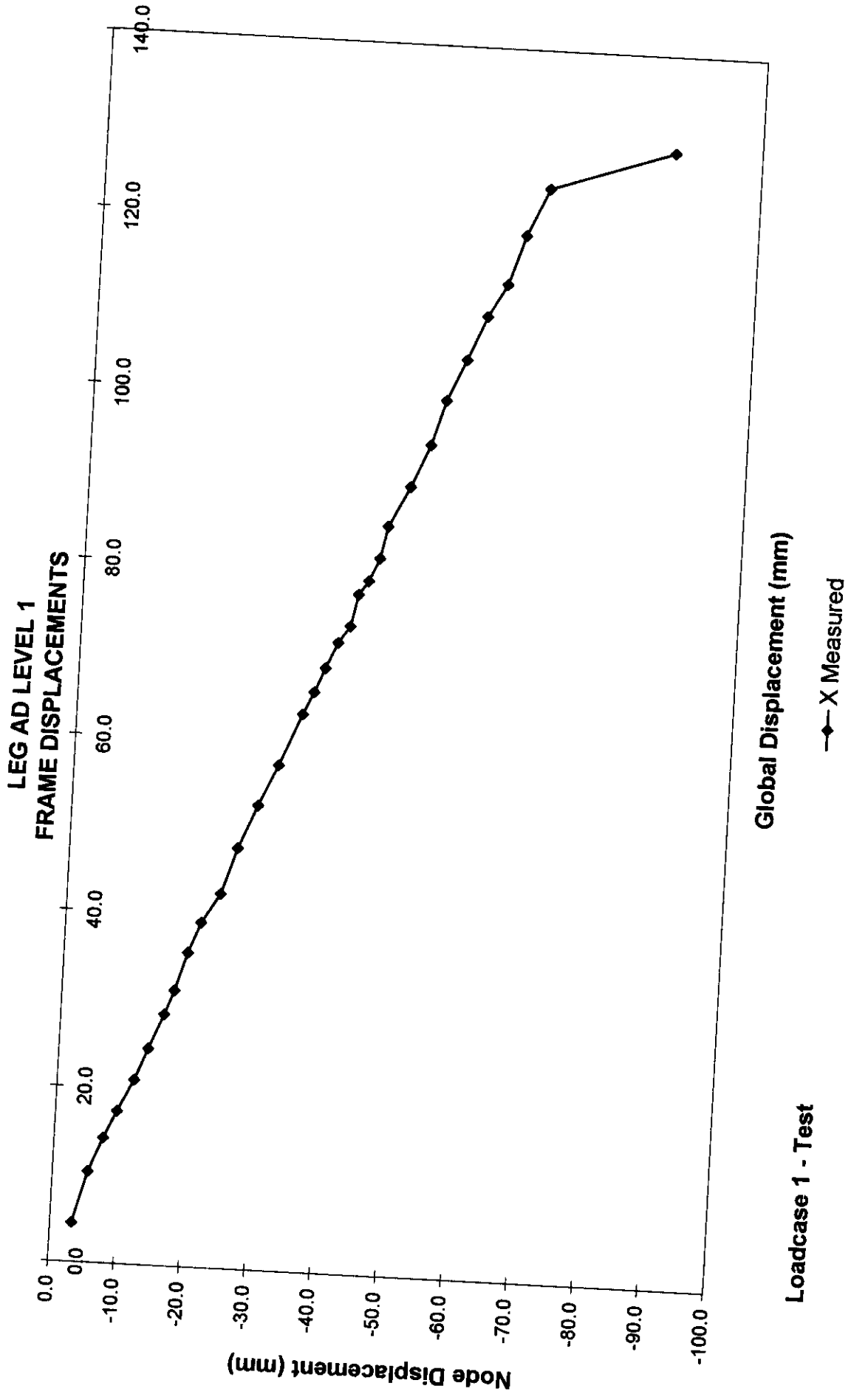


**Global Displacement (mm)**

**Loadcase 1 - Test**      **X Measured**      **Y Measured**      **Z Measured**

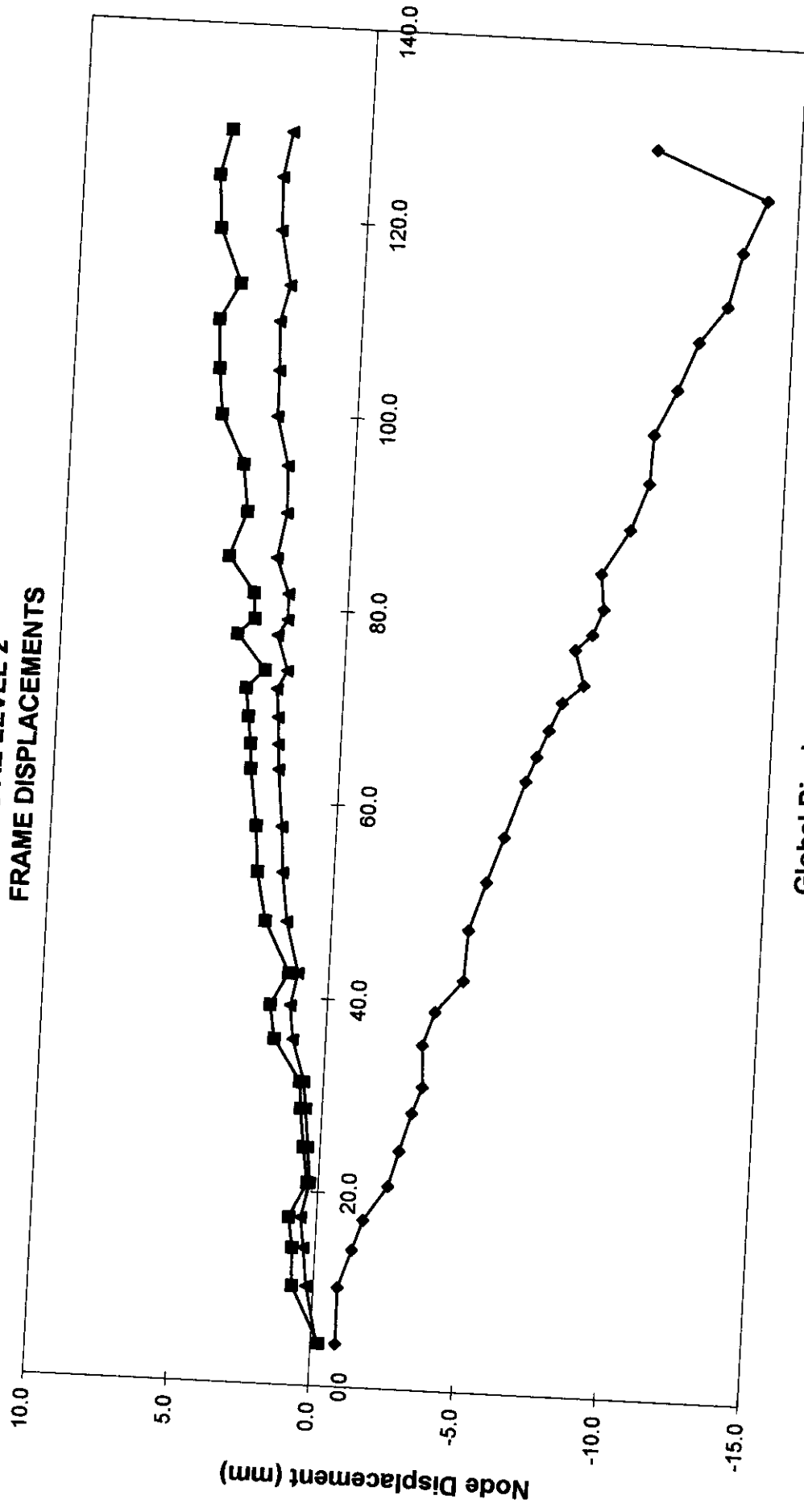


**Loadcase 1 - Test**



**Loadcase 1 - Test**

**LEG AE LEVEL 2  
FRAME DISPLACEMENTS**



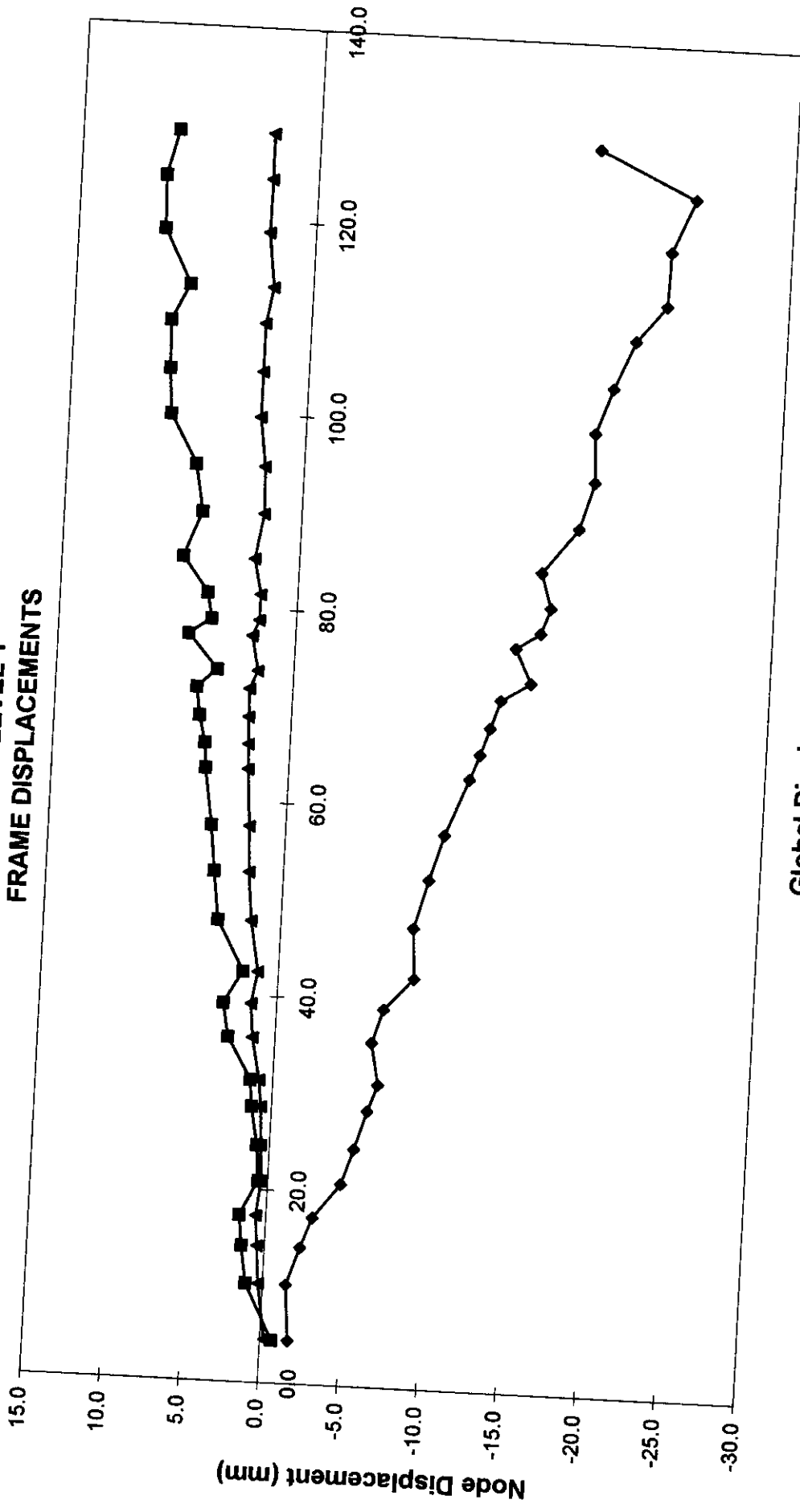
**Global Displacement (mm)**

**Loadcase 1 - Test**

◆ X Measured    ■ Y Measured    ▲ Z Measured



**LEG AE LEVEL 1  
FRAME DISPLACEMENTS**



**Global Displacement (mm)**

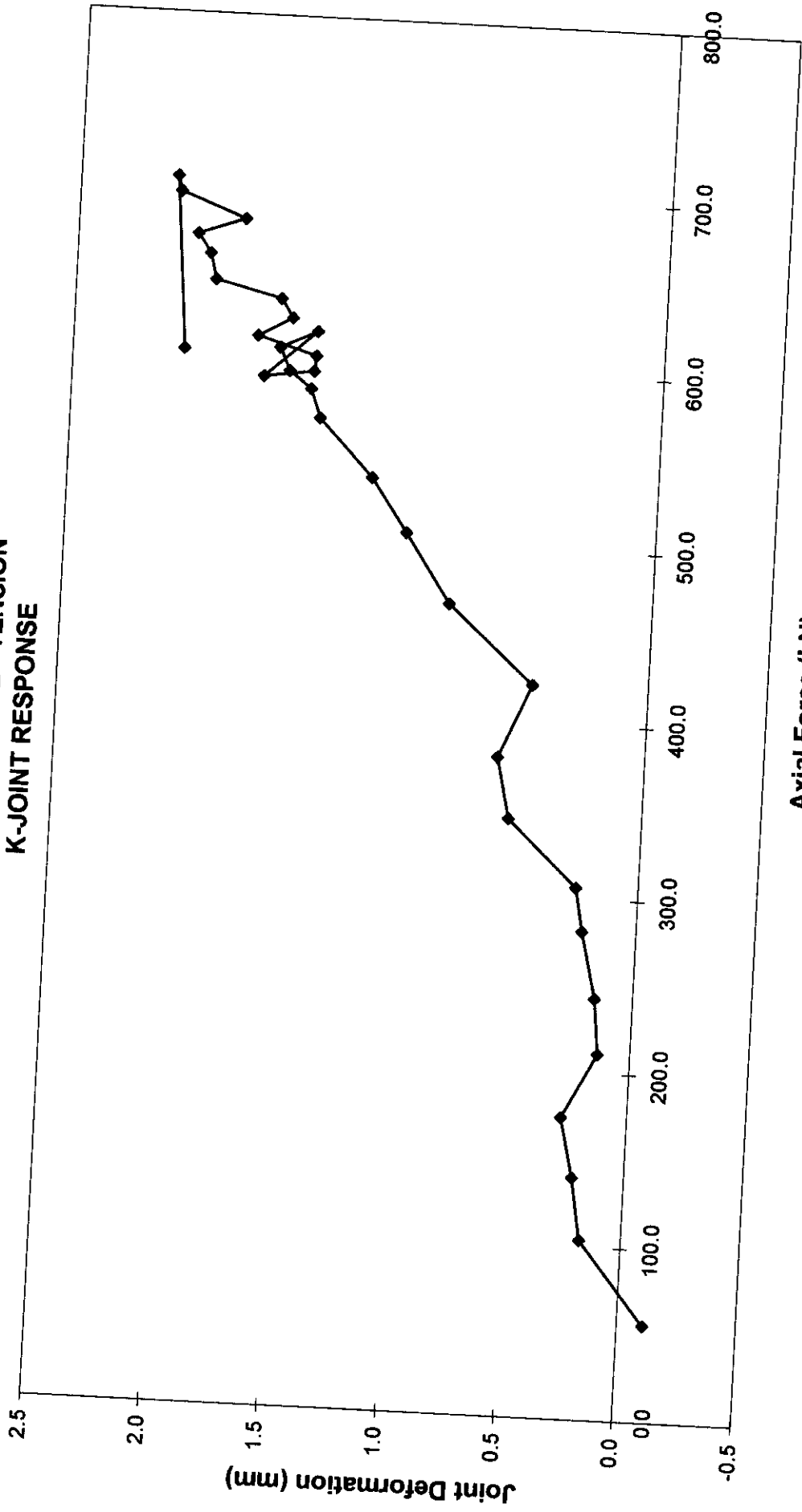
**Loadcase 1 - Test**

◆ X Measured

■ Y Measured

▲ Z Measured

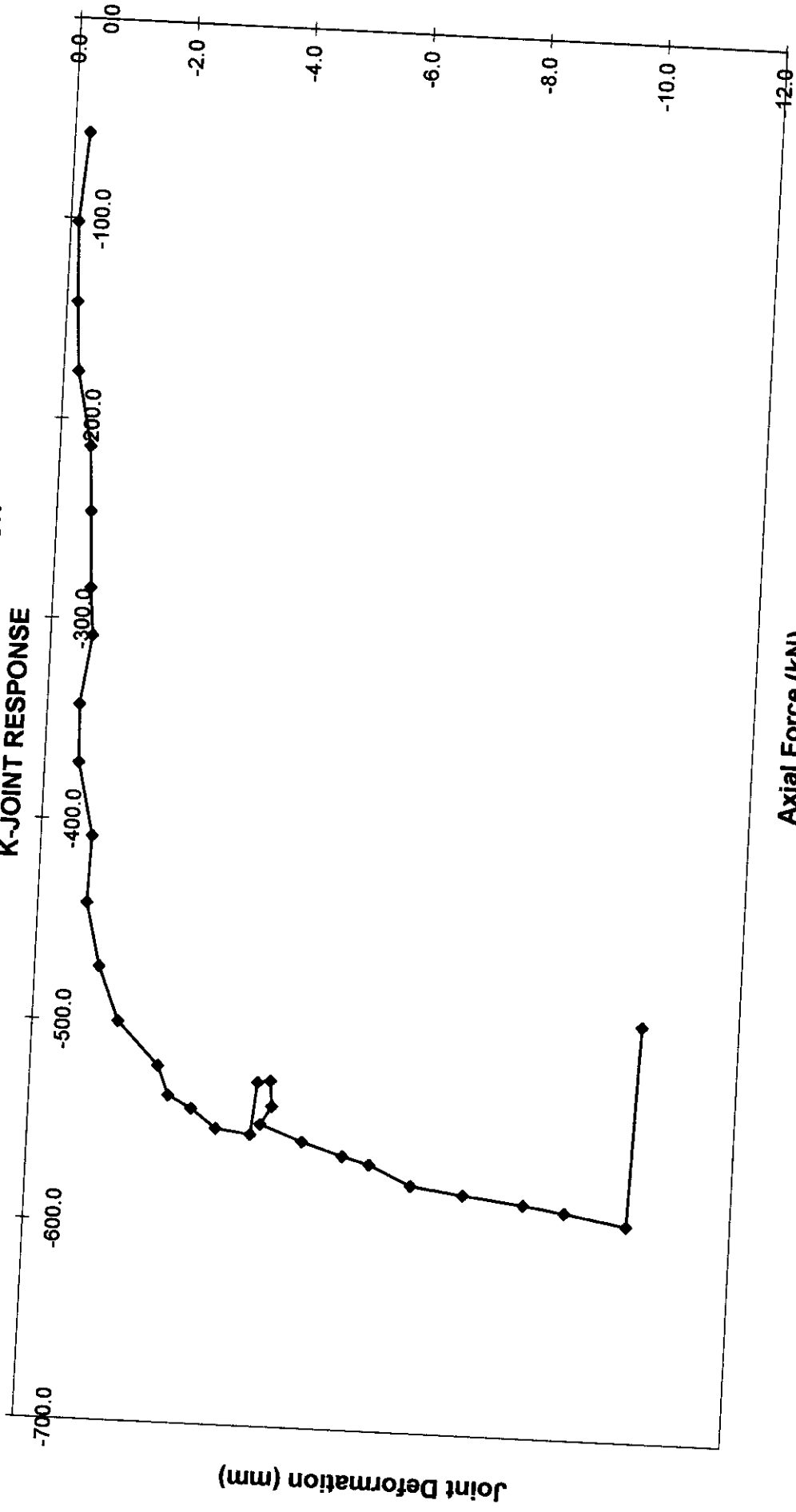
FRAME C - LEVEL 2 - TENSION  
K-JOINT RESPONSE



Axial Force (kN)

Loadcase 1 - Test

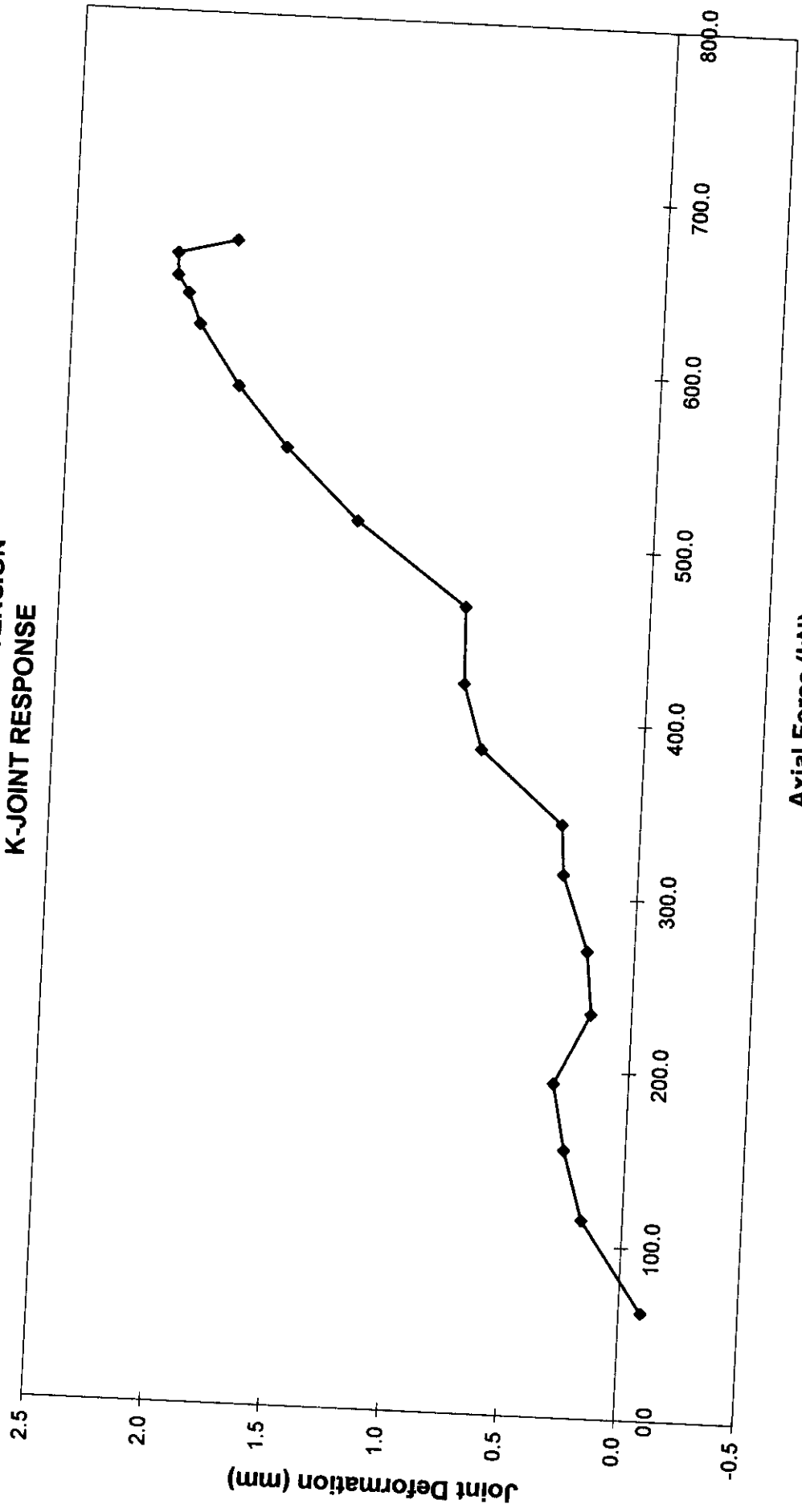
FRAME C - LEVEL 2 - COMPRESSION  
K-JOINT RESPONSE



Loadcase 1 - Test

Axial Force (kN)

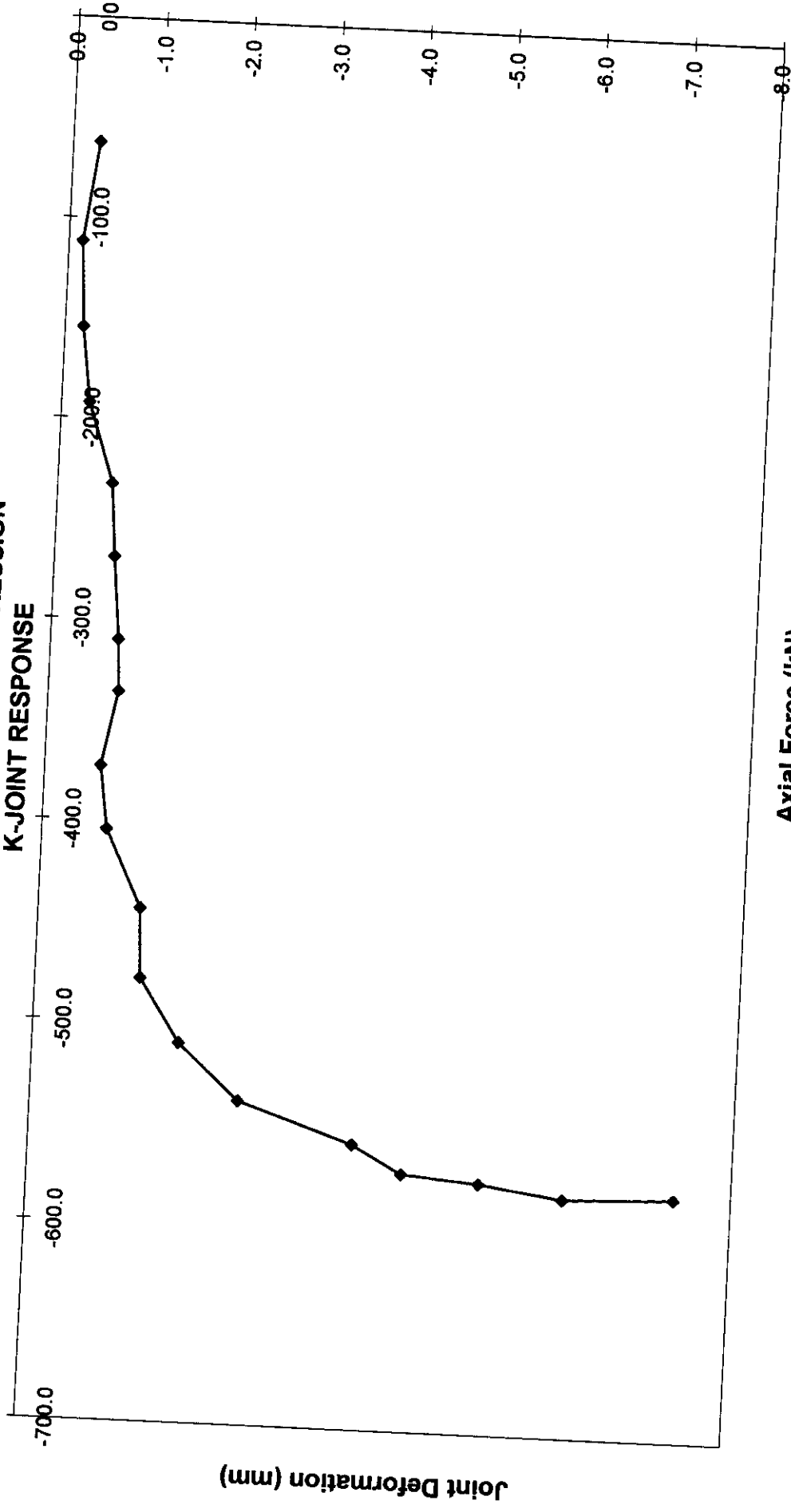
**FRAME C - LEVEL 1 - TENSION  
K-JOINT RESPONSE**



**Loadcase 1 - Test**

**Axial Force (kN)**

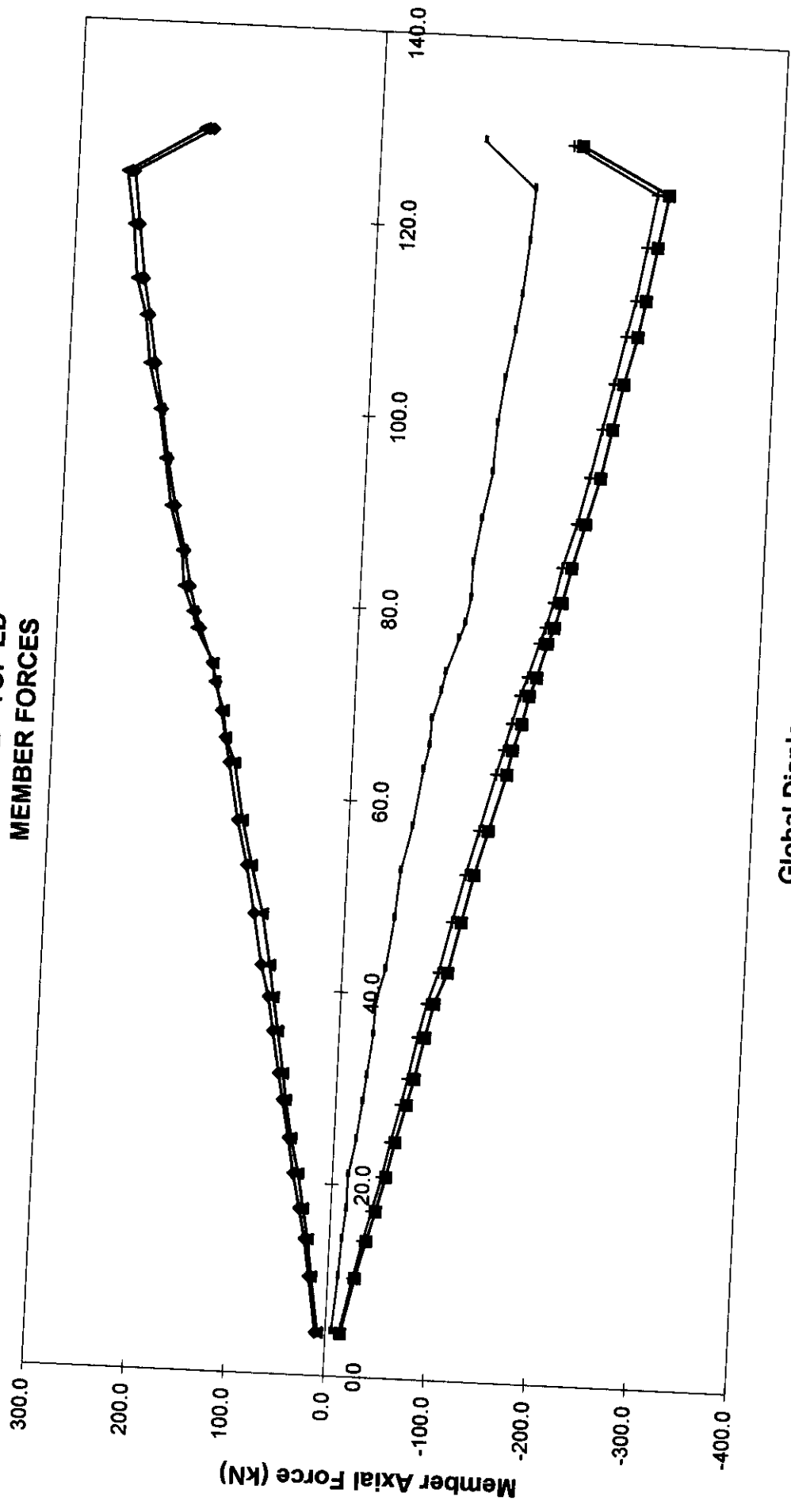
FRAME C - LEVEL 1 - COMPRESSION  
K-JOINT RESPONSE



Axial Force (kN)

Loadcase 1 - Test

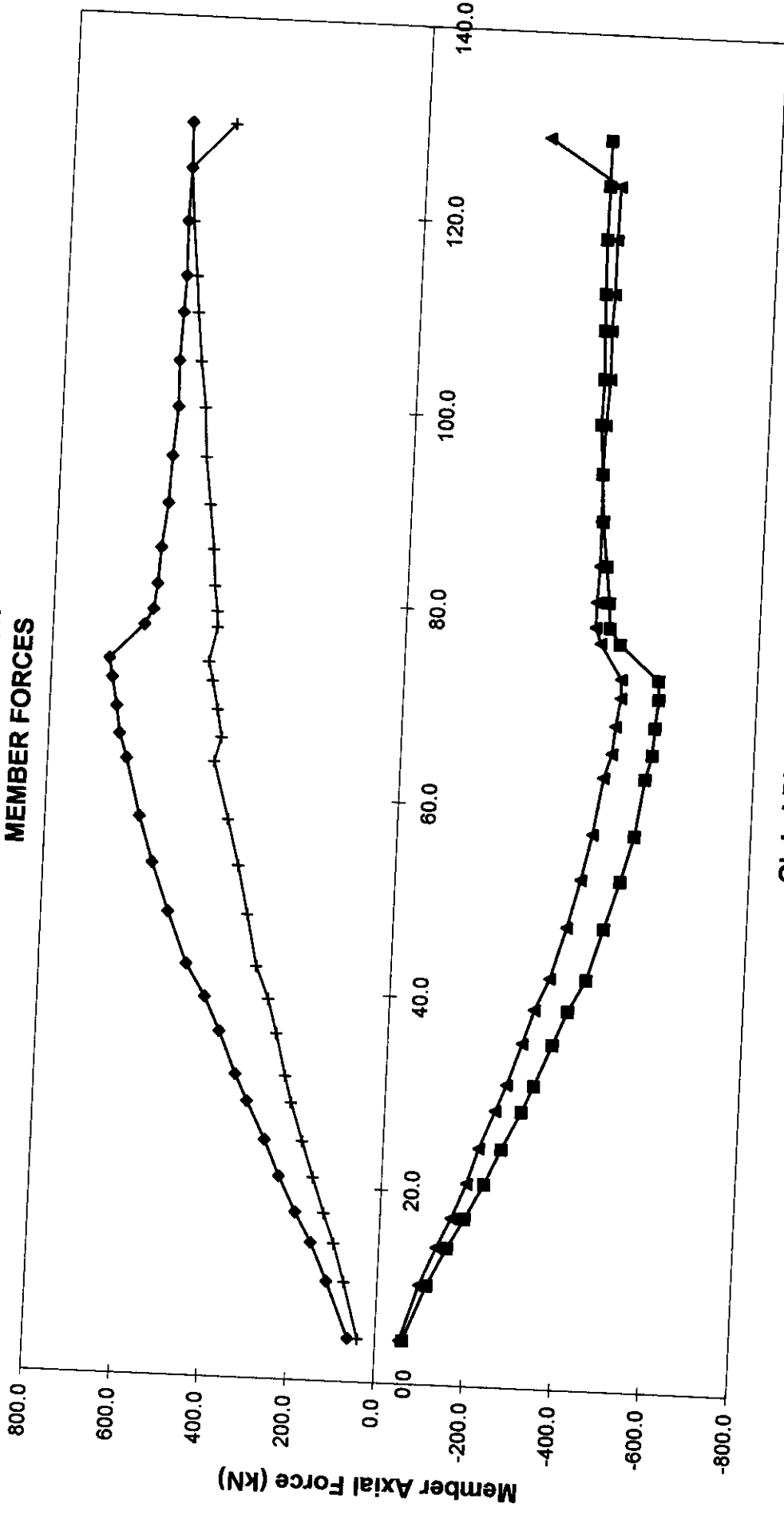
**FRAME B - TOP ED  
MEMBER FORCES**



**Global Displacement (mm)**

**Loadcase 1 - Test**    ◆ 27 Measured    ■ 28 Measured    ▲ 29 Measured    + 30 Measured    — 14 Measured

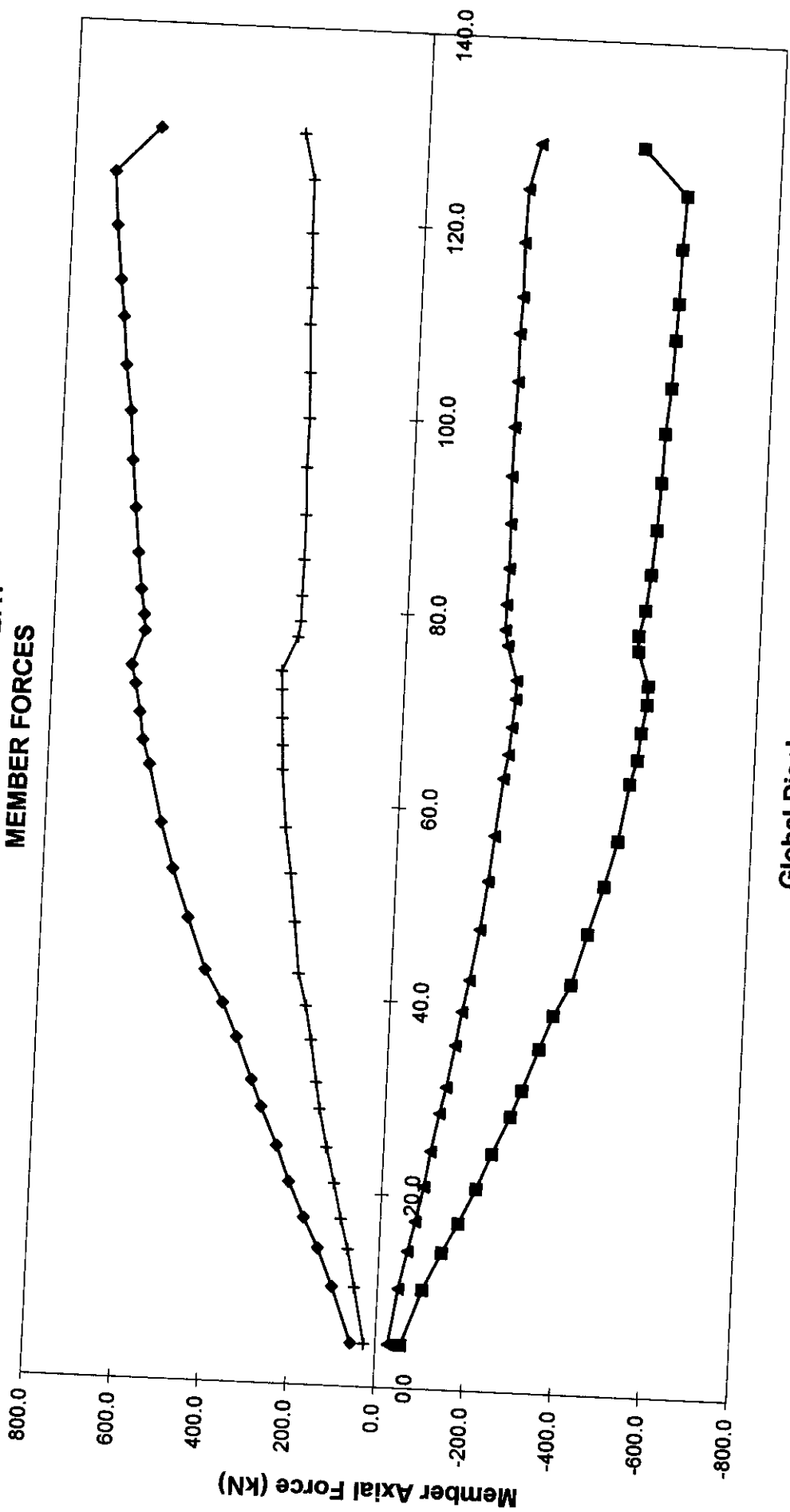
**FRAME C - TOP BAY  
MEMBER FORCES**



Global Displacement (mm)

Loadcase 1 - Test    ◆—63 Measured    ■—64 Measured    ▲—67 Measured    +—68 Measured

**FRAME C - BOTTOM BAY  
MEMBER FORCES**

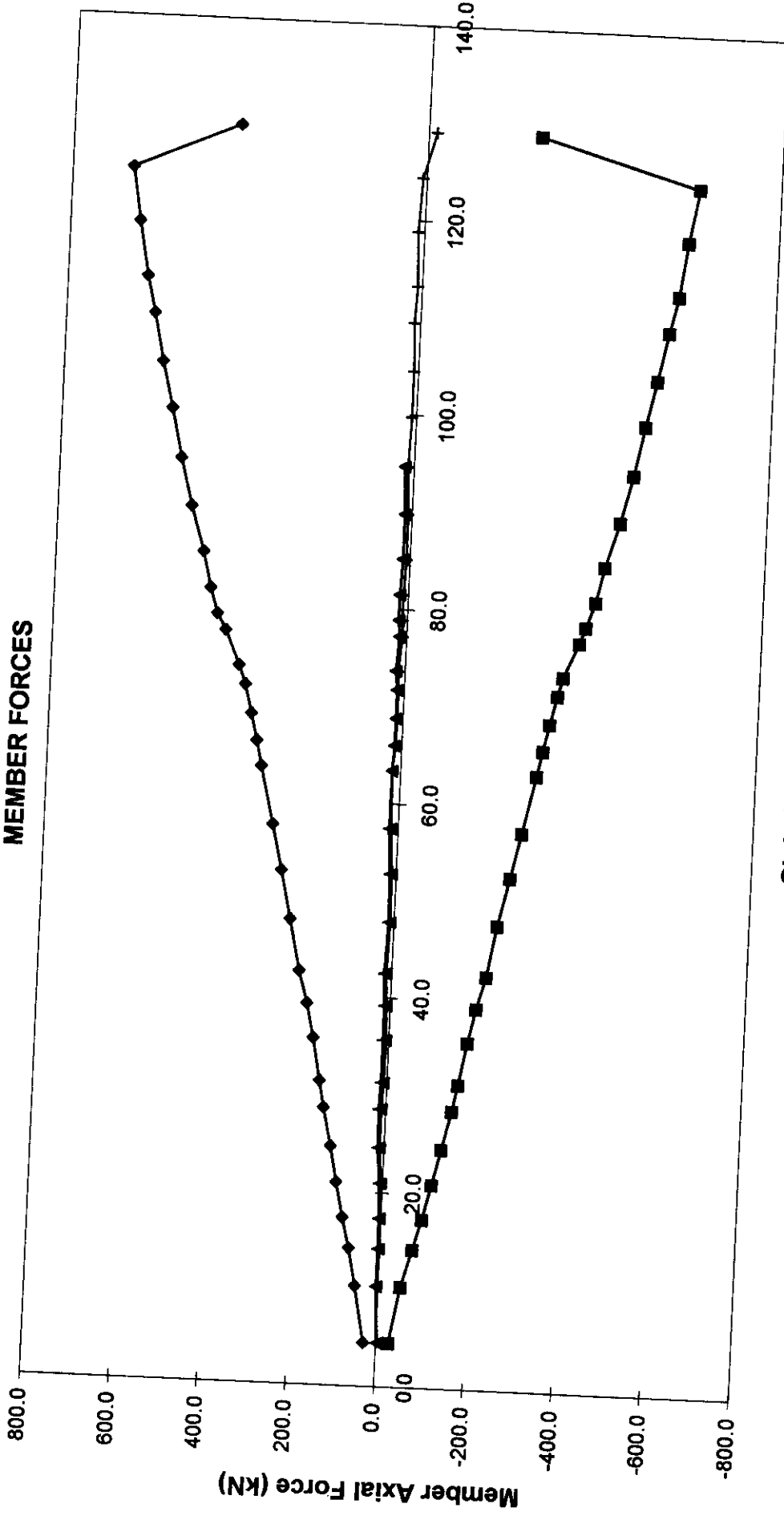


Global Displacement (mm)

Loadcase 1 - Test    ◆ 61 Measured    ■ 62 Measured    ▲ 65 Measured    + 66 Measured



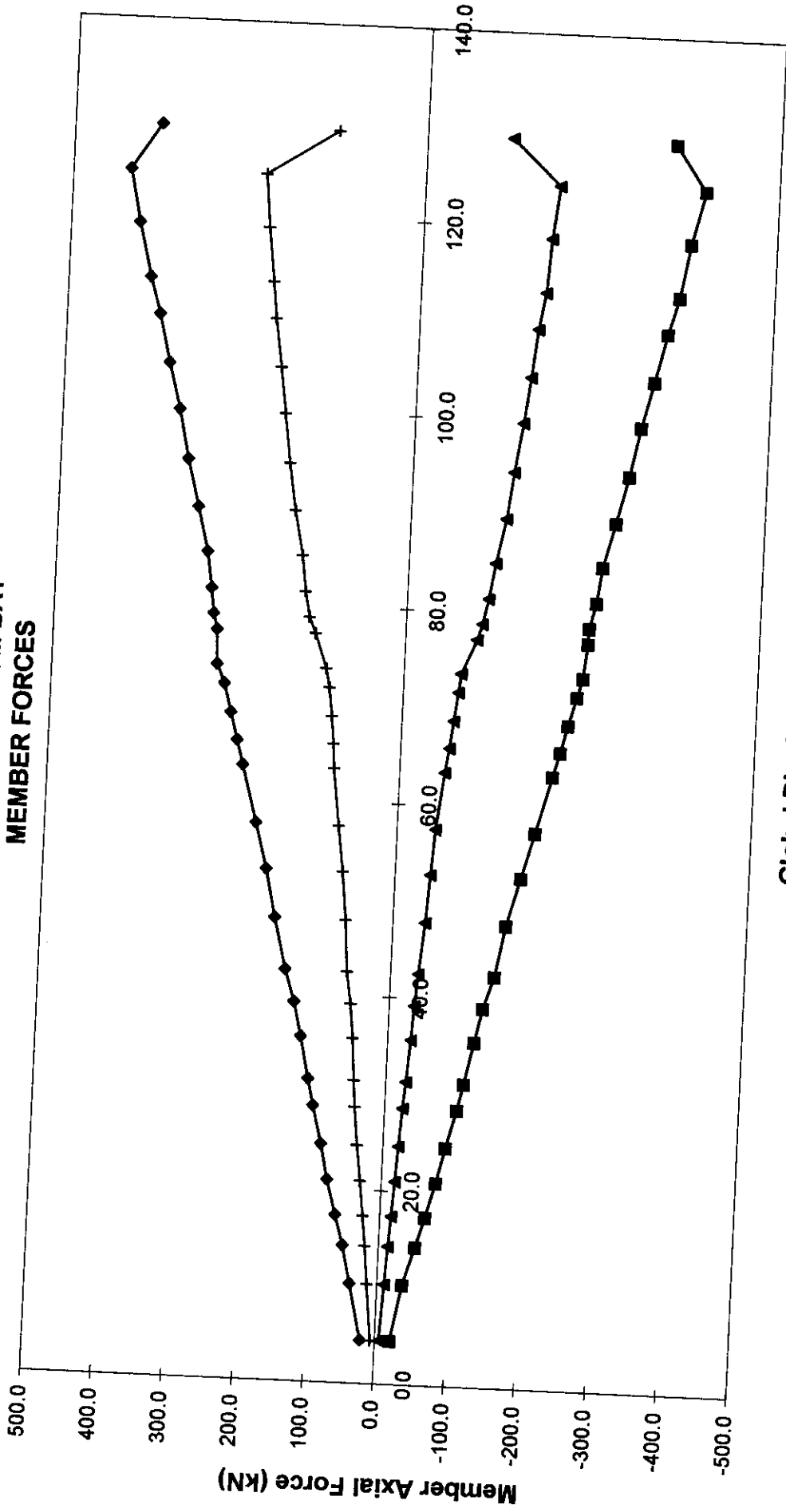
**FRAME D - TOP BAY  
MEMBER FORCES**



**Global Displacement (mm)**

**Loadcase 1 - Test**    ◆—71 Measured    ■—72 Measured    ▲—75 Measured    +—76 Measured

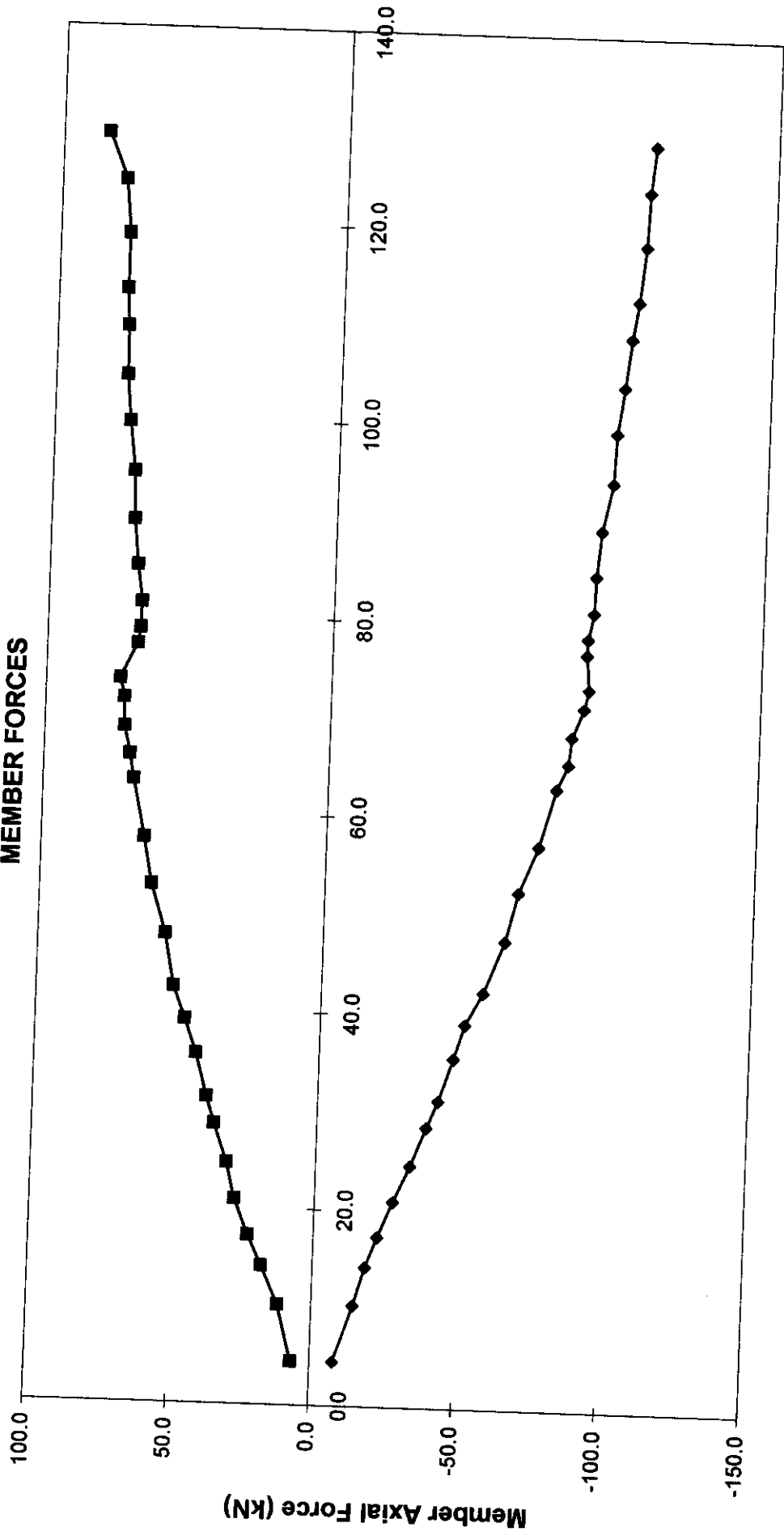
**FRAME D - BOTTOM BAY  
MEMBER FORCES**



**Global Displacement (mm)**

**Loadcase 1 - Test**    —◆— 69 Measured    —■— 70 Measured    —▲— 73 Measured    —+— 74 Measured

LEVEL 2 - X  
MEMBER FORCES



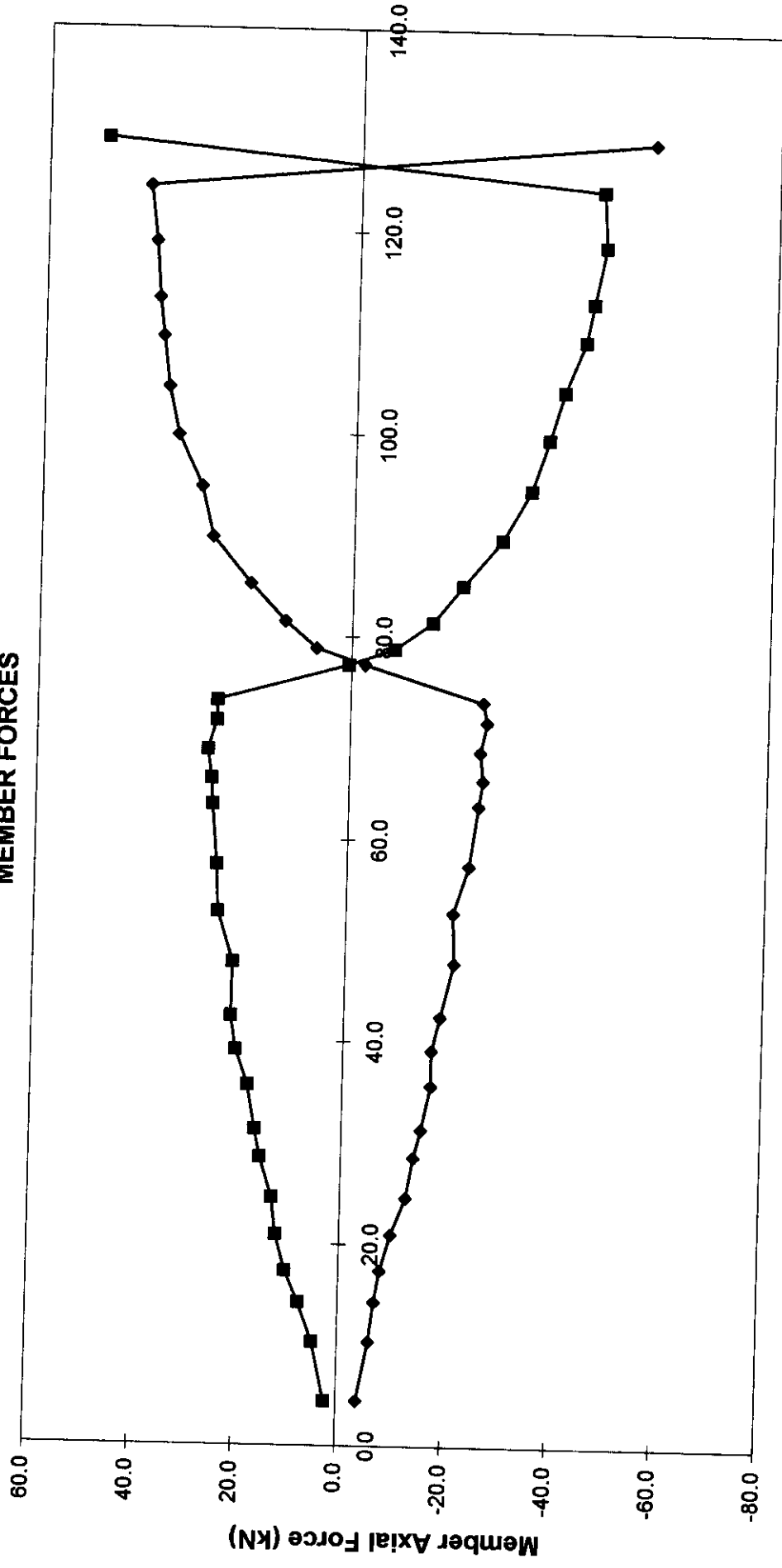
Loadcase 1 - Test

◆ 90 Measured

■ 93 Measured

Global Displacement (mm)

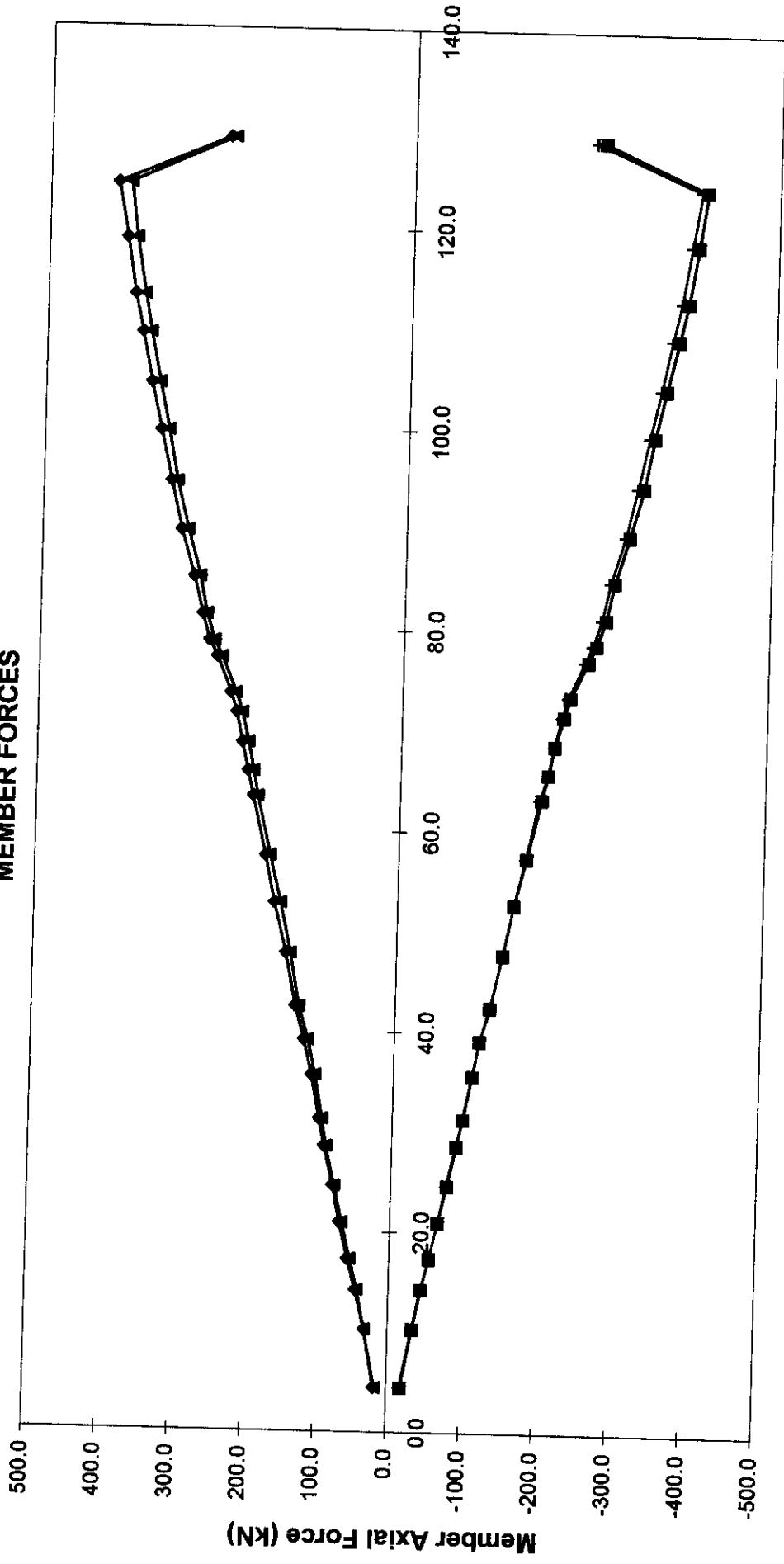
**LEVEL 2 - DIAMOND  
MEMBER FORCES**



Global Displacement (mm)

Loadcase 1 - Test      ■ 86 Measured      ◆ 87 Measured

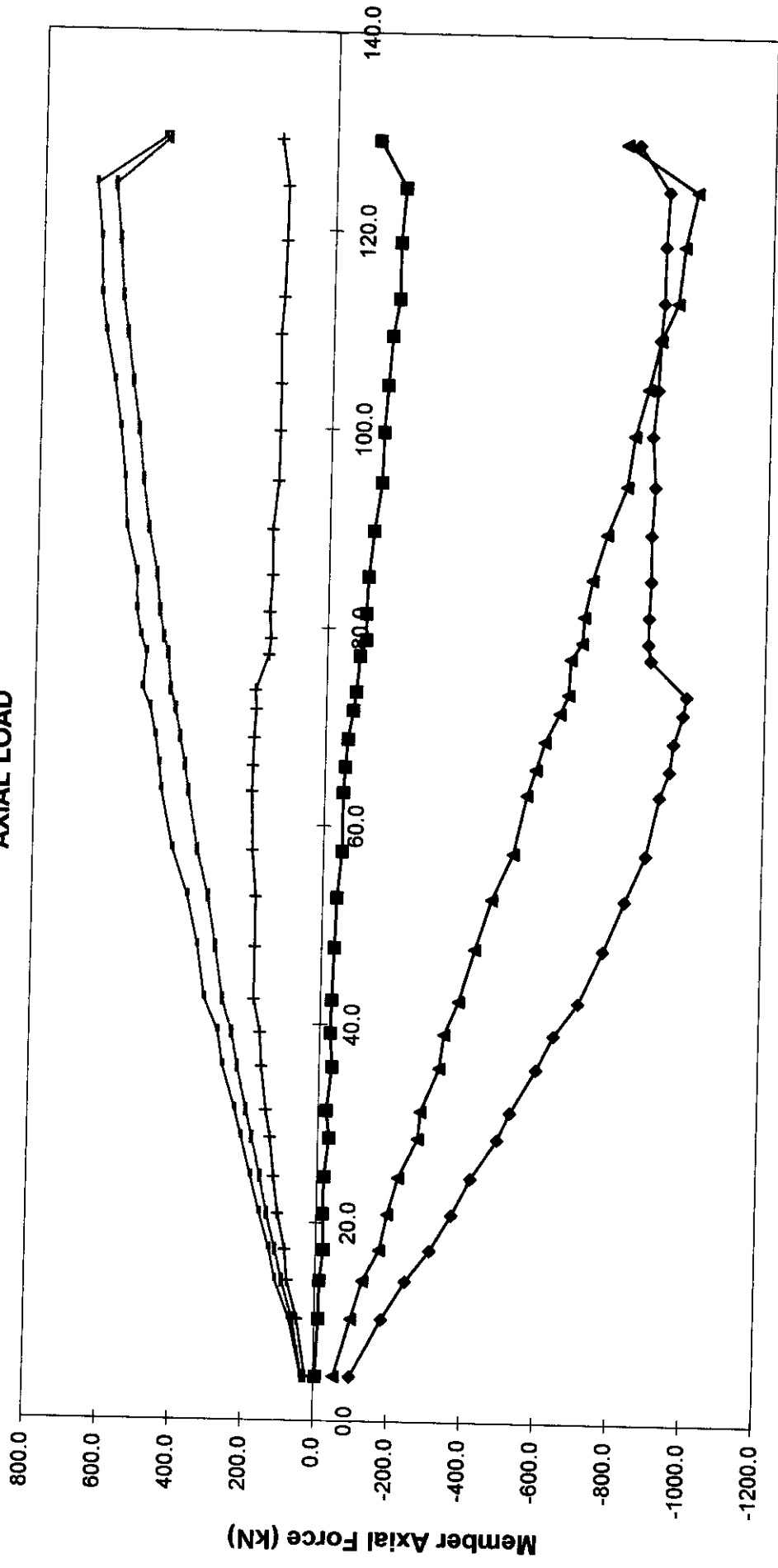
**LEVEL 1 - DIAMOND  
MEMBER FORCES**



Global Displacement (mm)

Loadcase 1 - Test    ◆ 94 Measured    ■ 95 Measured    ▲ 96 Measured    + 97 Measured

**FRAME FEET  
AXIAL LOAD**



**Global Displacement (mm)**

- ◆ 2 Measured
- 5 Measured
- ▲ 8 Measured
- + 32 Measured
- 35 Measured
- 38 Measured

**Loadcase 1 - Test**

## APPENDIX F LOADCASE 2 RESULTS

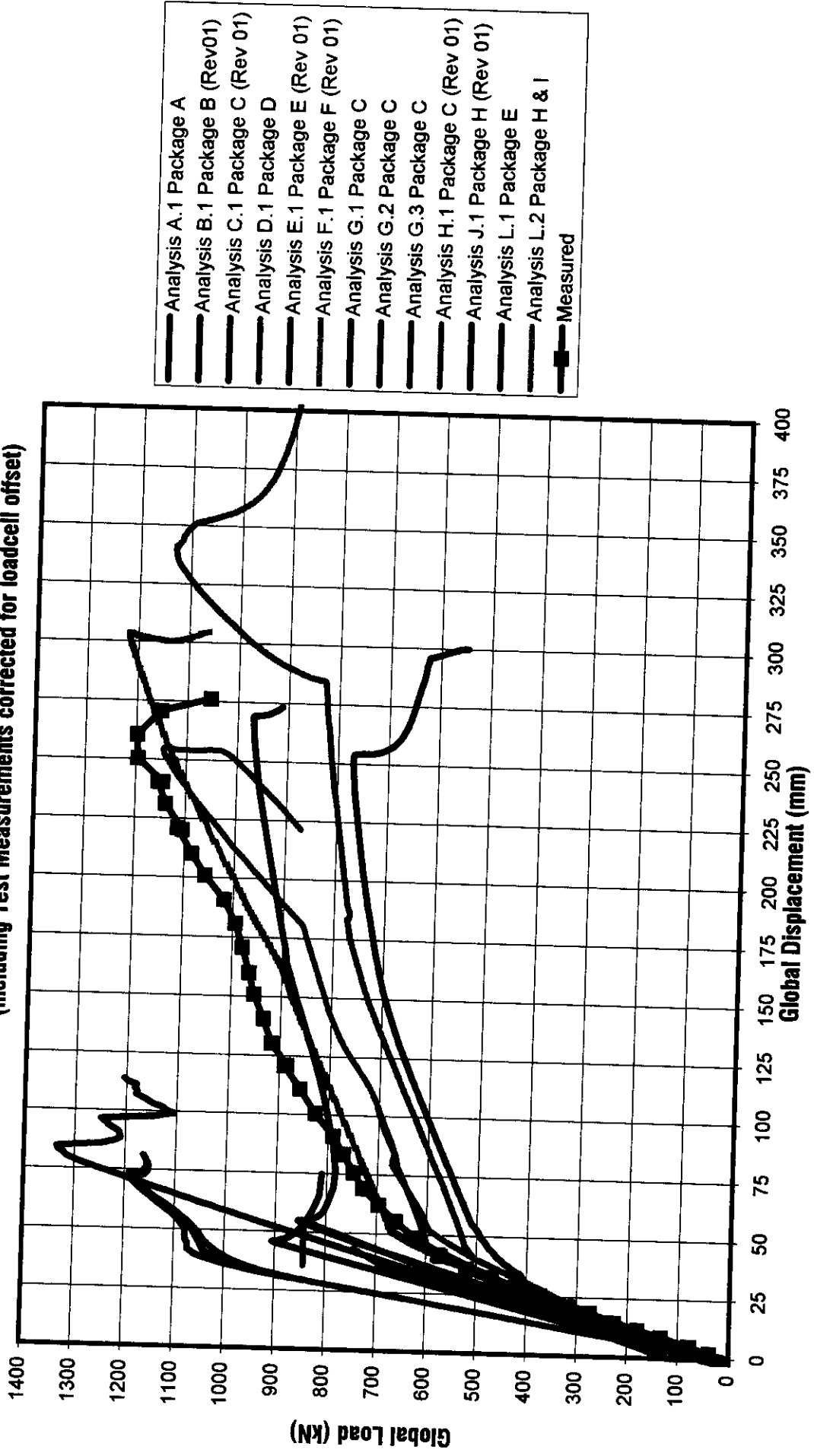
Plot	Sheet name	Plots / data provided by and supplied to Benchmark Analyst:													
		*	A	B	C	D	E	F	G	H	J	K	L	M	N
<b>Global response</b>															
Pre-test benchmark collation	ALL LC2 Chart (test)	X	X	X	X	X	X	X	X	X	X	X	X	X	X
Global response with scan nos	Global Scan Nos	X	X	X	X	X	X	X	X	X	X	X	X	X	X
Global response with failures	Global Annotated	X	X	X	X	X	X	X	X	X	X	X	X	X	X
<b>Displacements</b>															
Rig node uplift c.f.global response	Combined Chart 2	X	X	X	X		X	X		X		X	X		
Spatial disp. of 3D frame nodes	**	X		X		X		X	X						
<b>Local joint characteristics:</b>															
Frame A K Node 37 tension	FrC Lev2 Tens														
Frame A K Node 37 compression	FrC Lev2 Comp														
Frame A K Node 38 tension	FrC Lev1 Tens														
Frame A K Node 38 compression	FrC Lev1 Comp														
Frame E X Node 42 compression	FrE TB Comp	X	X		X			X		X					
Frame B X Node 16 compression	FrB TB Comp														X
Frame B X Node 18 tension	FrB TB Tens														
Level 1 X Node 44 tension	Lev1-LC3X Tens														
<b>Member Forces</b>															
Frame A X braces L1-L2 FrC-FrD	FrA TDC For														
Frame A X braces L1-L2 FrD-FrE	FrA TED For														
Frame A X braces L2-L3 FrC-FrD	FrA BDC For														
Frame A X braces L2-L3 FrD-FrE	FrA BED For														
Frame B X braces L1-L2 FrC-FrD	FrB TDC For														
Frame B X braces L1-L2 FrD-FrE	FrB TED For														
Frame B X braces L2-L3 FrC-FrD	FrB BDC For														
Frame B X braces L2-L3 FrD-FrE	FrB BED For														
Frame C K braces L1-L2	FrC TB For														
Frame C K braces L2-L3	FrC BB For														
Frame D K braces L1-L2	FrD TB For	X							X						
Frame D K braces L2-L3	FrD BB For														
Frame E X braces L1-L2	FrE TB For	X	X	X	X		X	X	X	X	X		X		X
Frame E X braces L2-L3	FrE BB For	X		X	X		X	X	X	X	X		X		X
Level 2 X braces FrD-FrE	Lev 2-X For	X			X			X							
Level 2 diamond braces FrC-FrD	Lev 2-Dia For														X
Level 1 X braces FrD-FrE	Lev 1-LC3X For														
Level 1 diamond braces FrC-FrD	Lev 1-Dia For														
Frame C legs	Fr C Leg For														
Frame D legs	Fr D Leg For														
Frame E legs	Fr E Leg For														
All frame legs at connection to rig	Fr Feet	X						X	X	X					
<b>Bending moments</b>															
Frame A compression braces	FrA... Mom (8)														

Reference Files:  
 Rig displacements C636\25\063W  
 Loadcase 2 member force plots C636\39\008W  
 Loadcase 2 benchmark comparison C636\32\007W-B

\* Information provided to project sponsors  
 \*\* N21, N22, N25, N26, N29 and N30 Disp

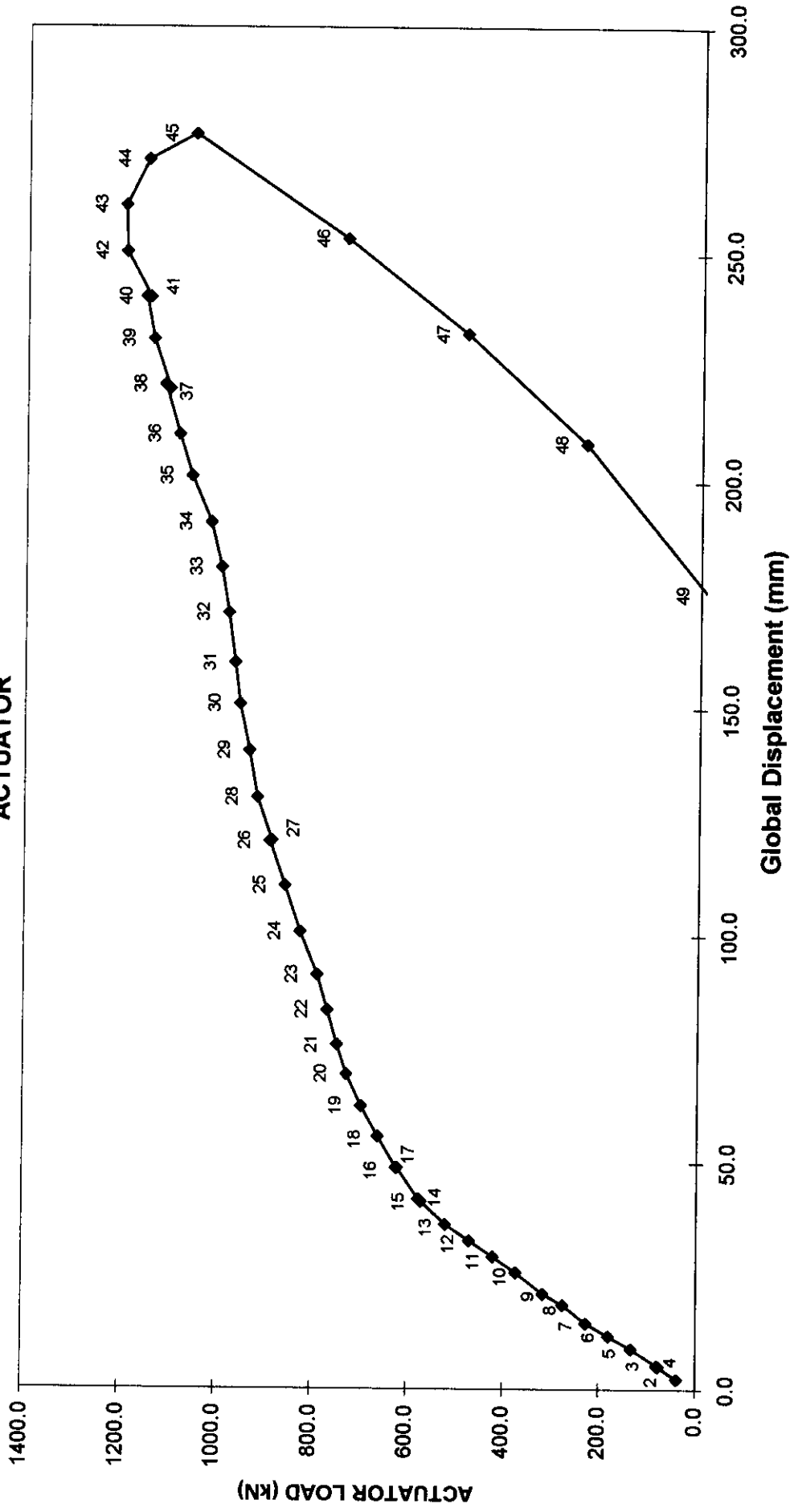
TUBULAR FRAMES PROJECT PHASE III

**Global Load vs Global Displacement - Load Case 2 Predictions (Revised)**  
 (including Test Measurements corrected for loadcell offset)



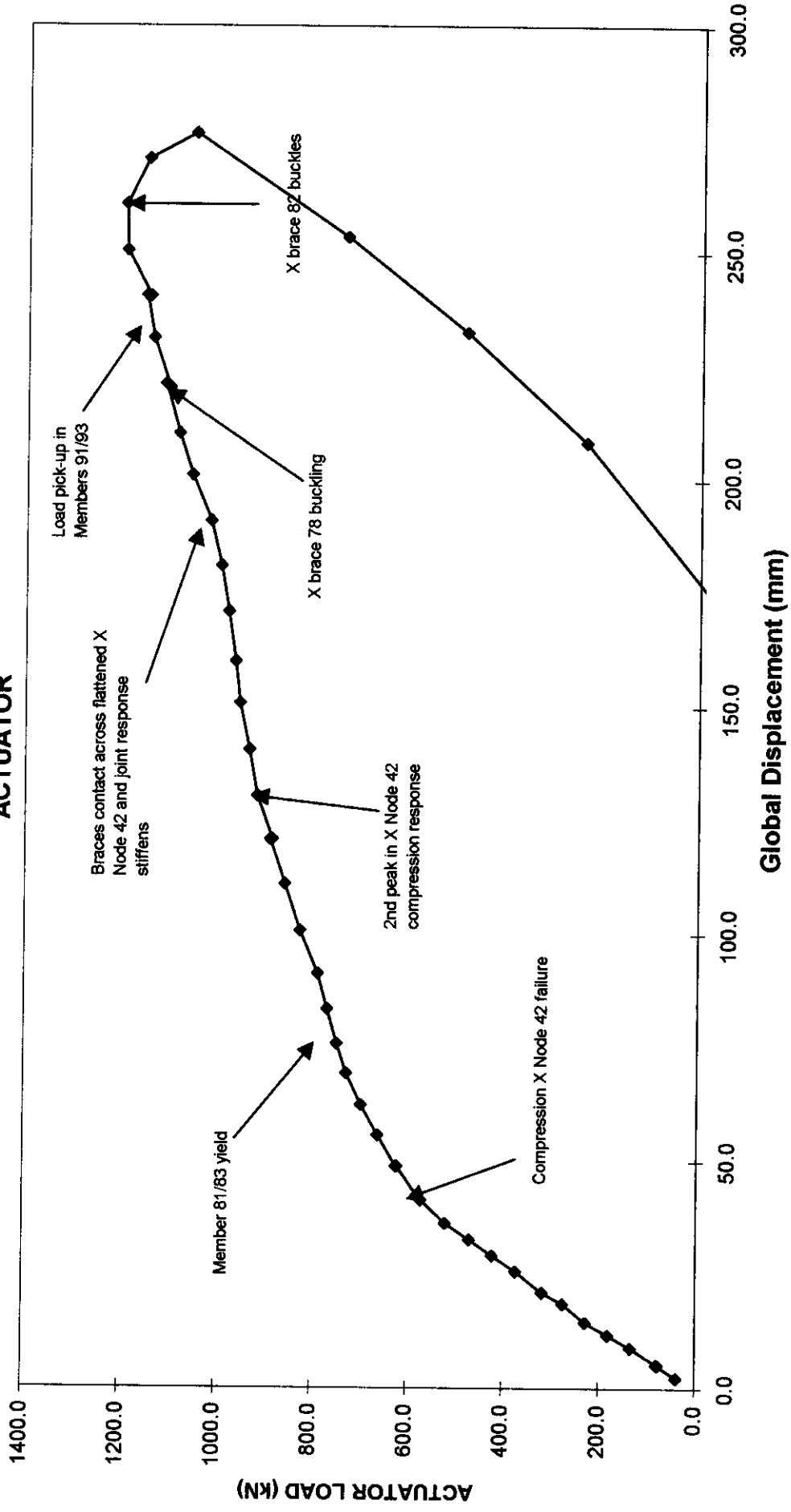


# GLOBAL RESPONSE ACTUATOR



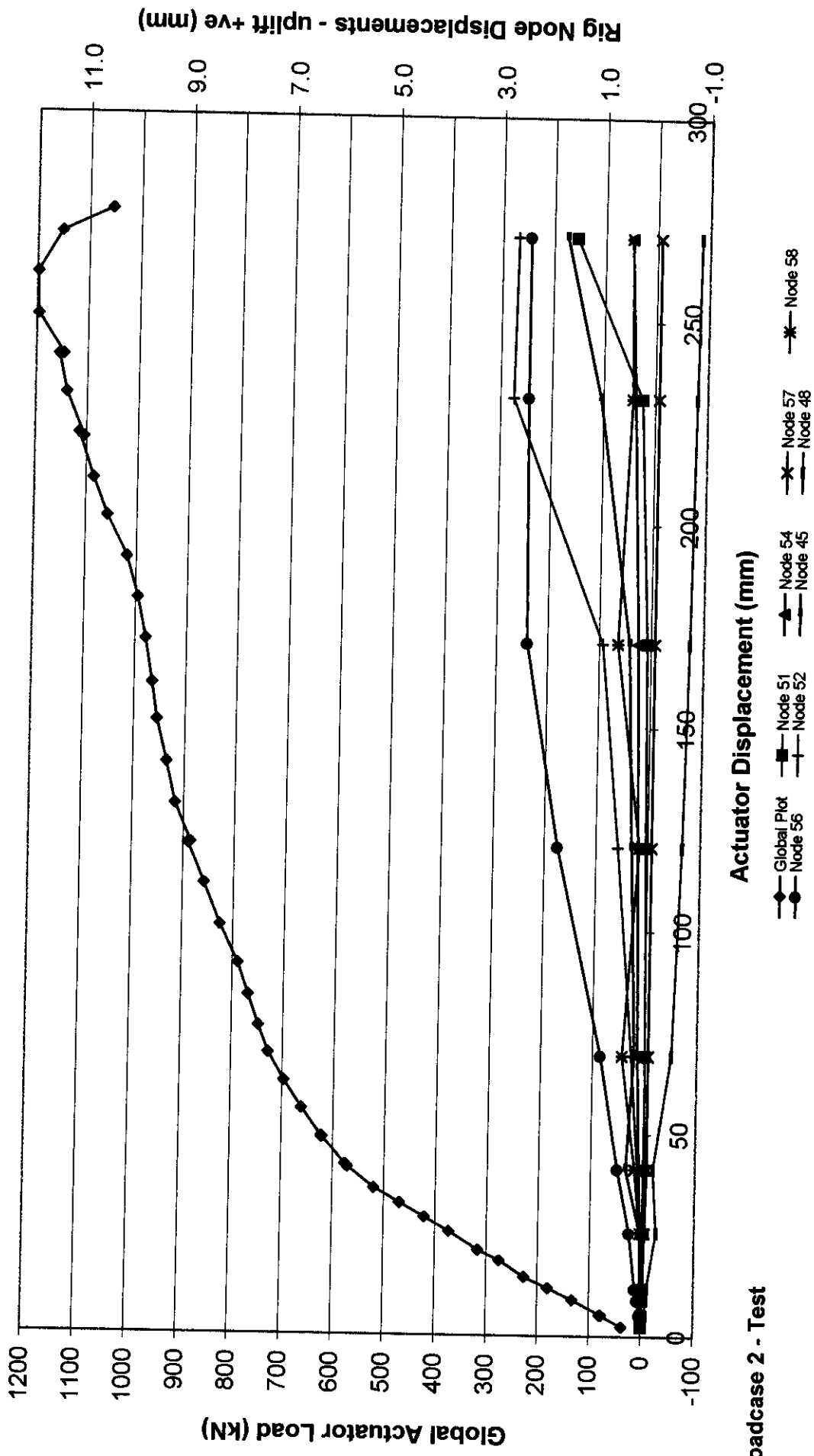
Loadcase 2 - Test

# GLOBAL RESPONSE ACTUATOR



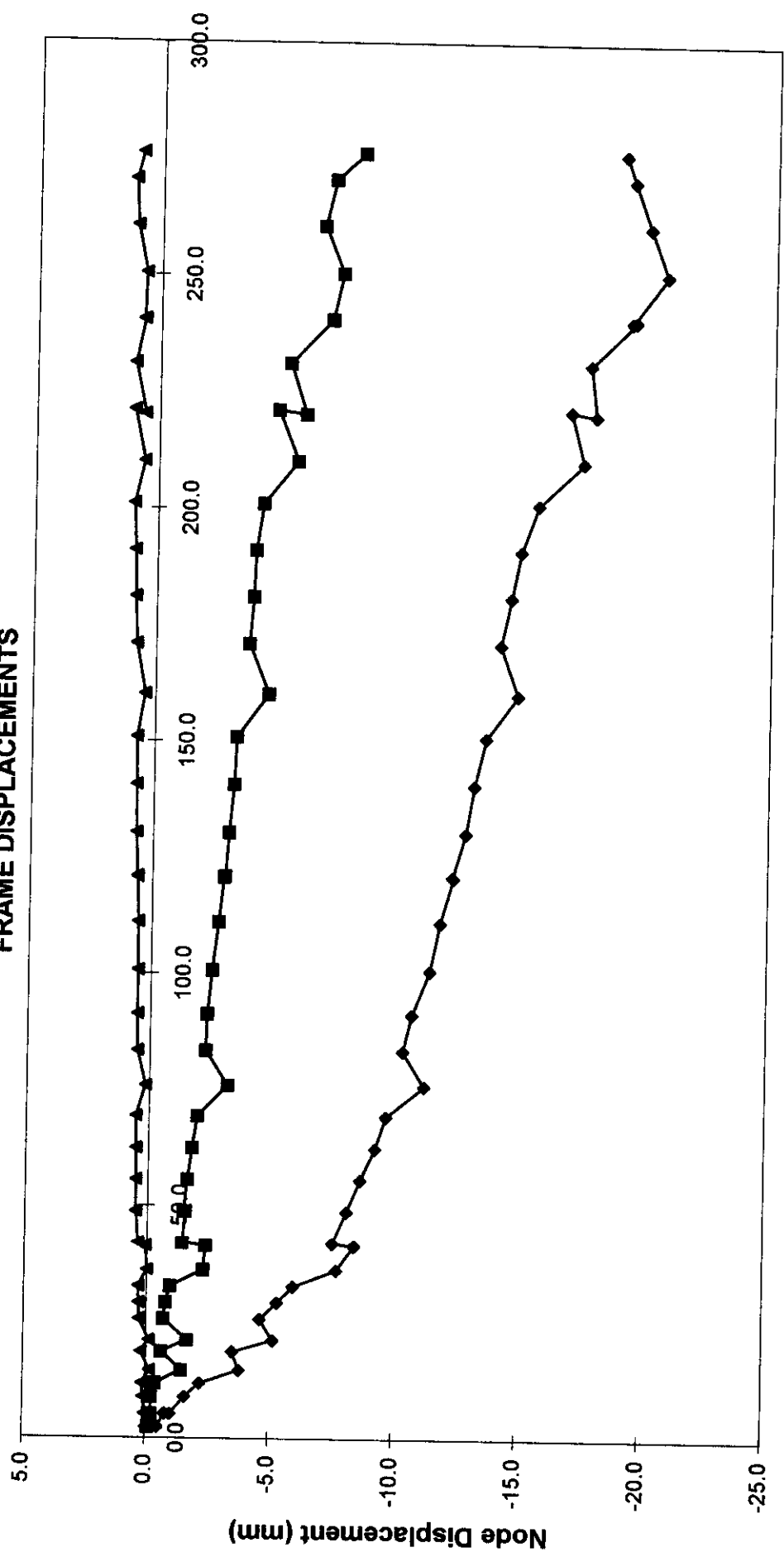
Loadcase 2 - Test

# Nodal Displacements and Global Load versus Global Displacement



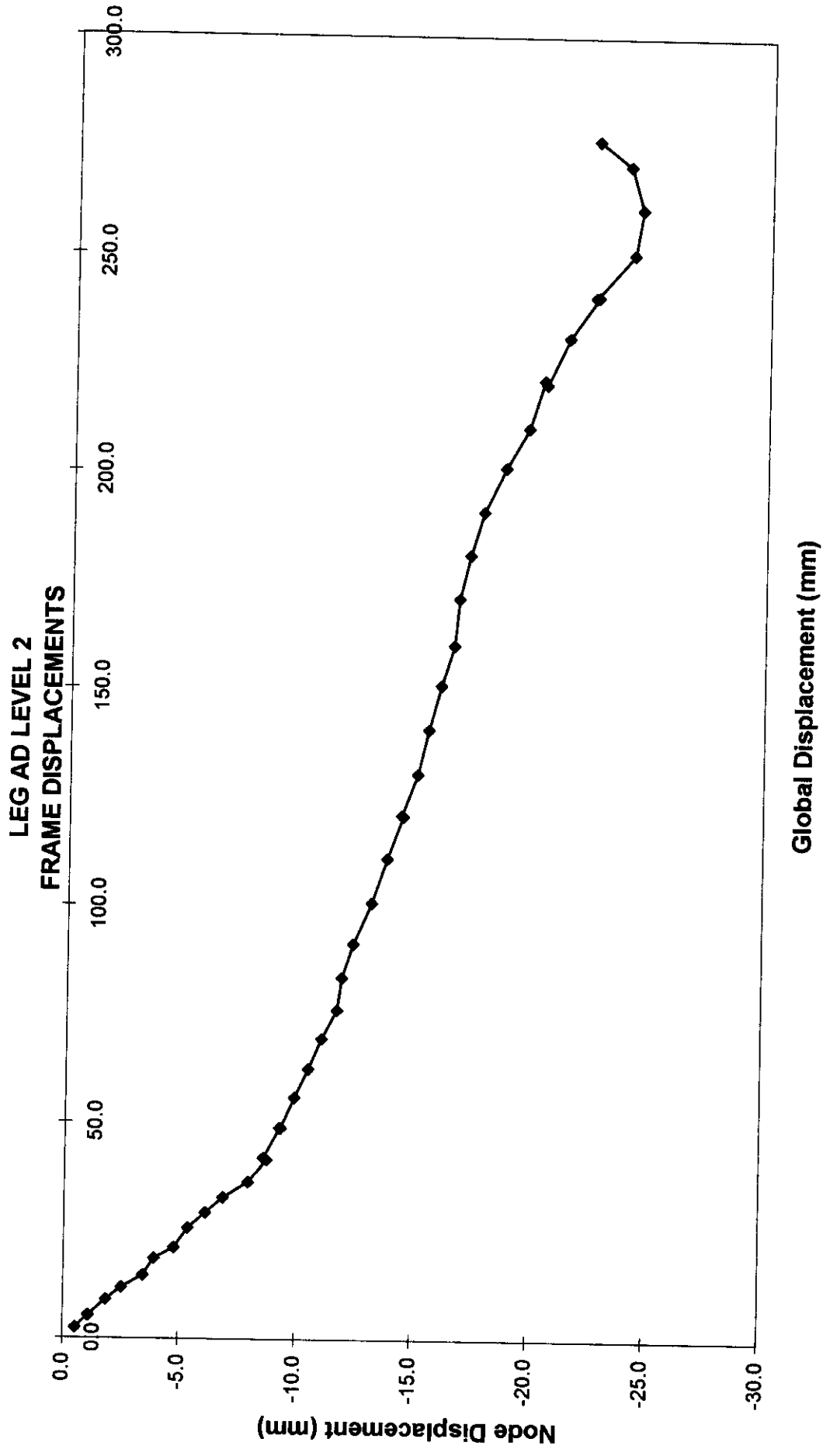
Loadcase 2 - Test

**LEG AC LEVEL 1  
FRAME DISPLACEMENTS**



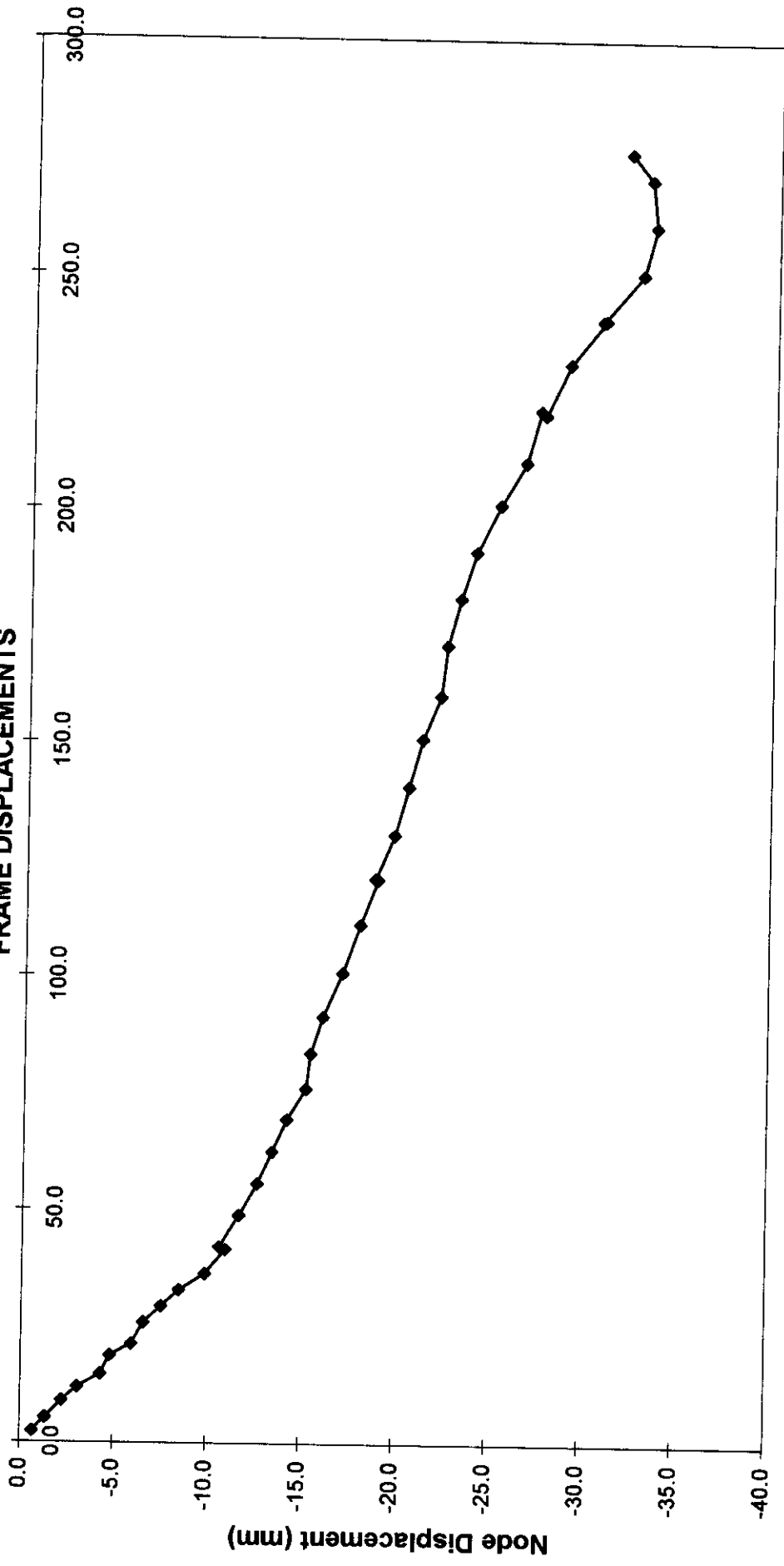
Global Displacement (mm)

Loadcase 2 - Test      ◆ X Measured      ■ Y Measured      ▲ Z Measured



**Loadcase 2 - Test**

**LEG AD LEVEL 1  
FRAME DISPLACEMENTS**

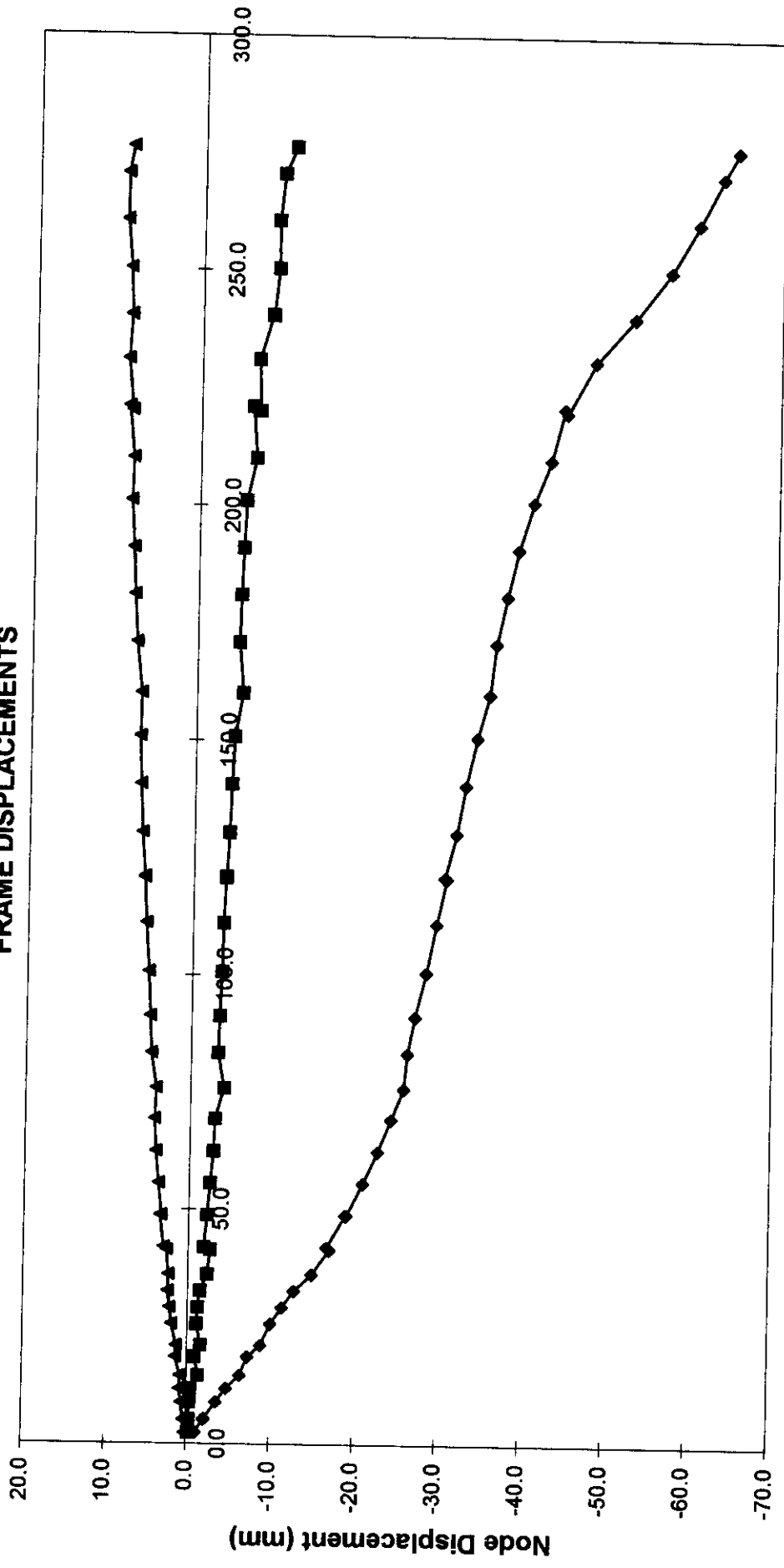


Global Displacement (mm)

◆ X Measured

Loadcase 2 - Test

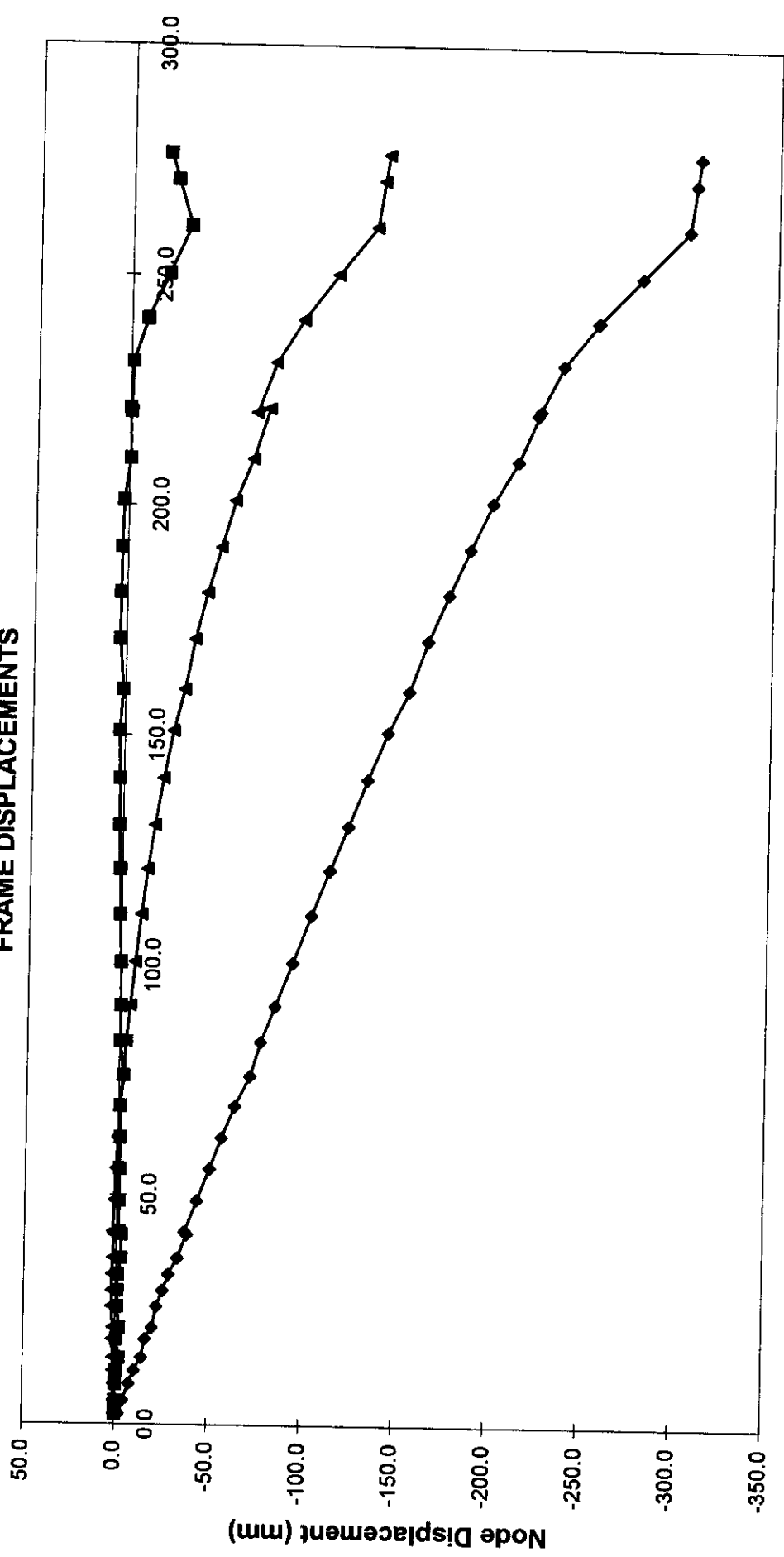
**LEG AE LEVEL 2  
FRAME DISPLACEMENTS**



Global Displacement (mm)

Loadcase 2 - Test      ◆ X Measured      ■ Y Measured      ▲ Z Measured

**LEG AE LEVEL 1  
FRAME DISPLACEMENTS**

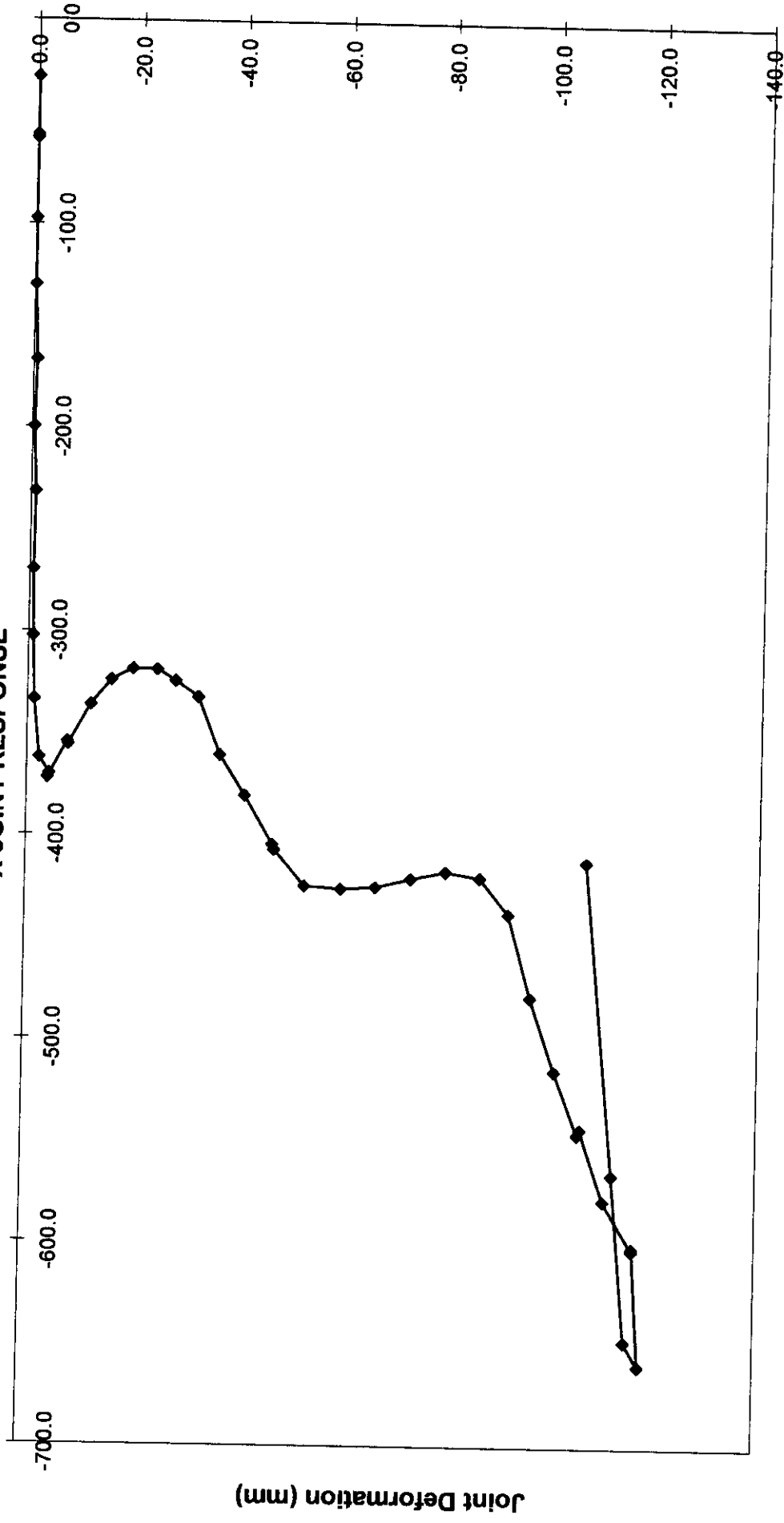


Global Displacement (mm)

Loadcase 2 - Test      —◆— X Measured      —■— Y Measured      —▲— Z Measured



**FRAME E- TOP BAY - COMPRESSION  
X-JOINT RESPONSE**

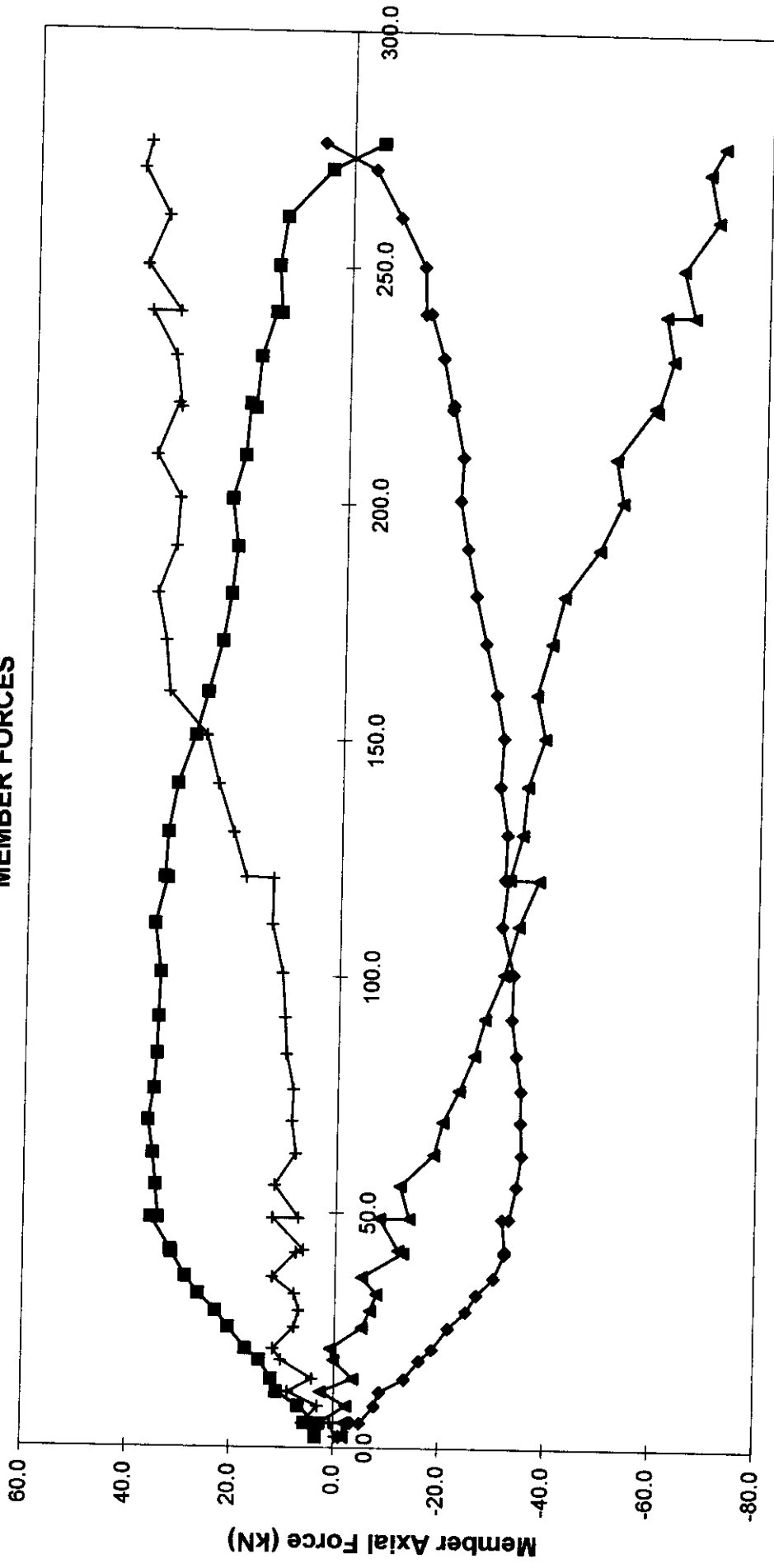


**Axial Force (kN)**

**Loadcase 2 - Test**

◆ N42 Measured

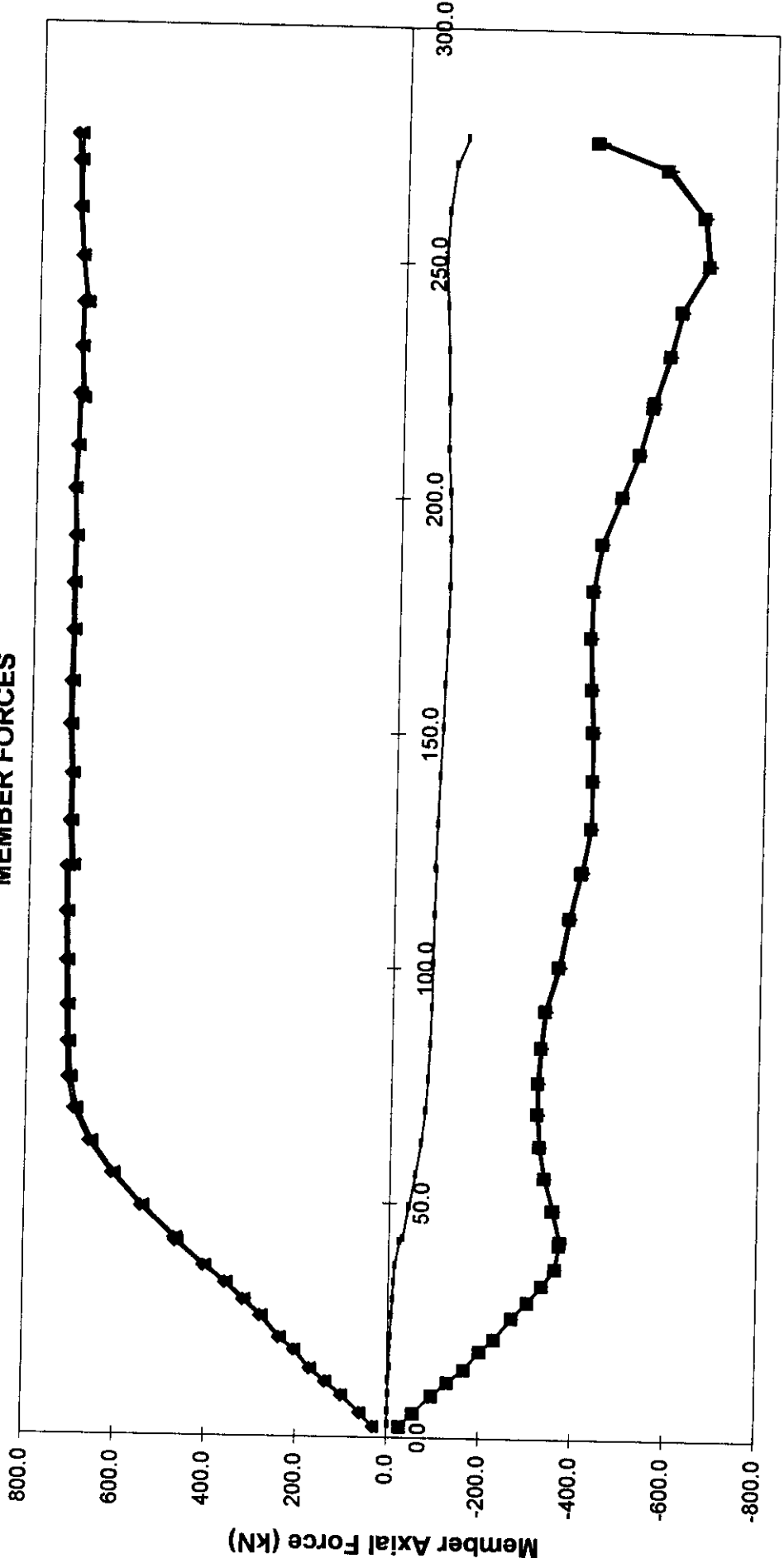
**FRAME D - TOP BAY  
MEMBER FORCES**



**Global Displacement (mm)**

**Loadcase 2 - Test**    ◆—71 Measured    ■—72 Measured    ▲—75 Measured    +—76 Measured

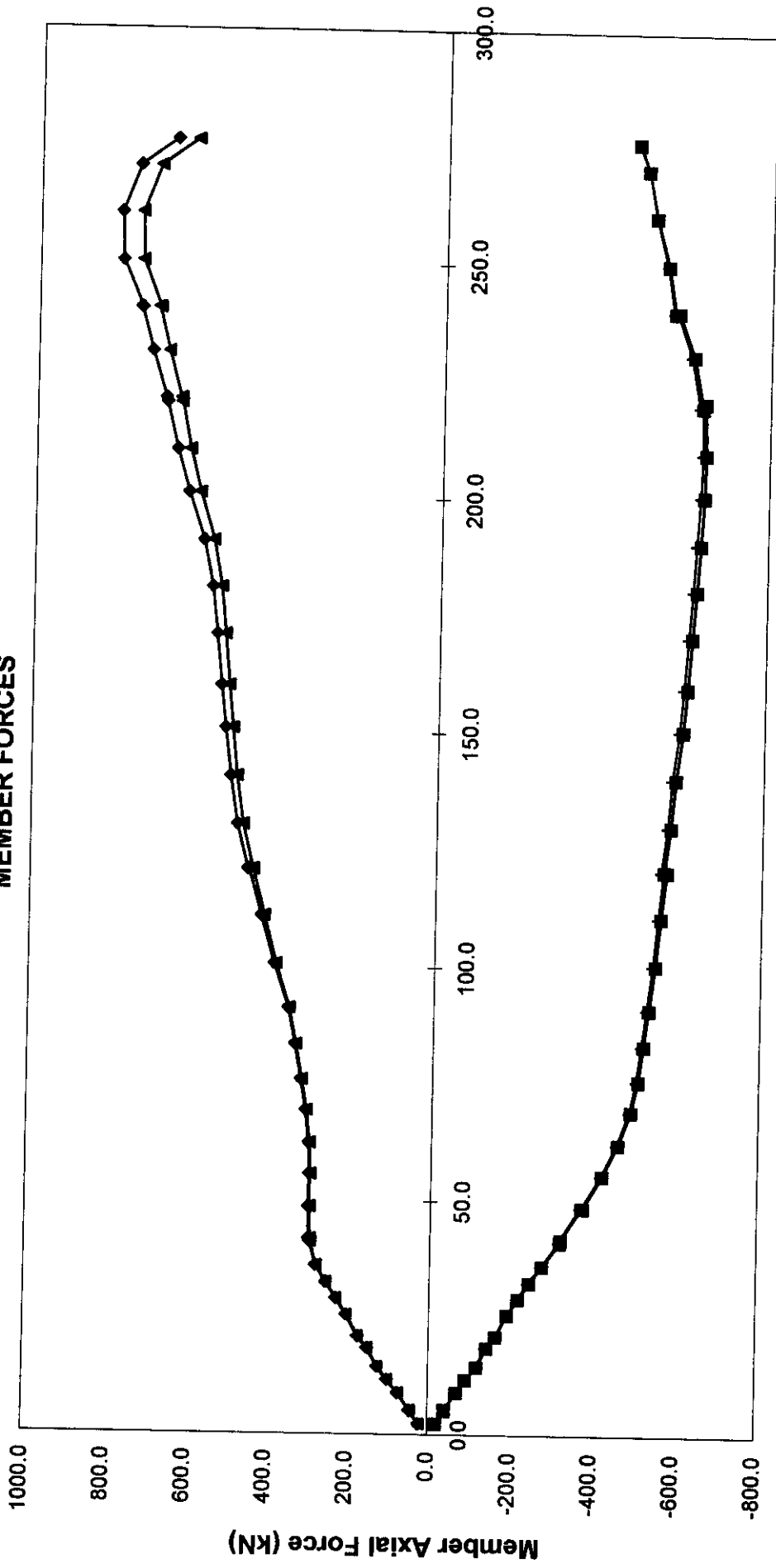
**FRAME E - TOP BAY  
MEMBER FORCES**



Global Displacement (mm)

Loadcase 2 - Test    ◆ 81 Measured    ■ 82 Measured    ▲ 83 Measured    + 84 Measured    — 85 Measured

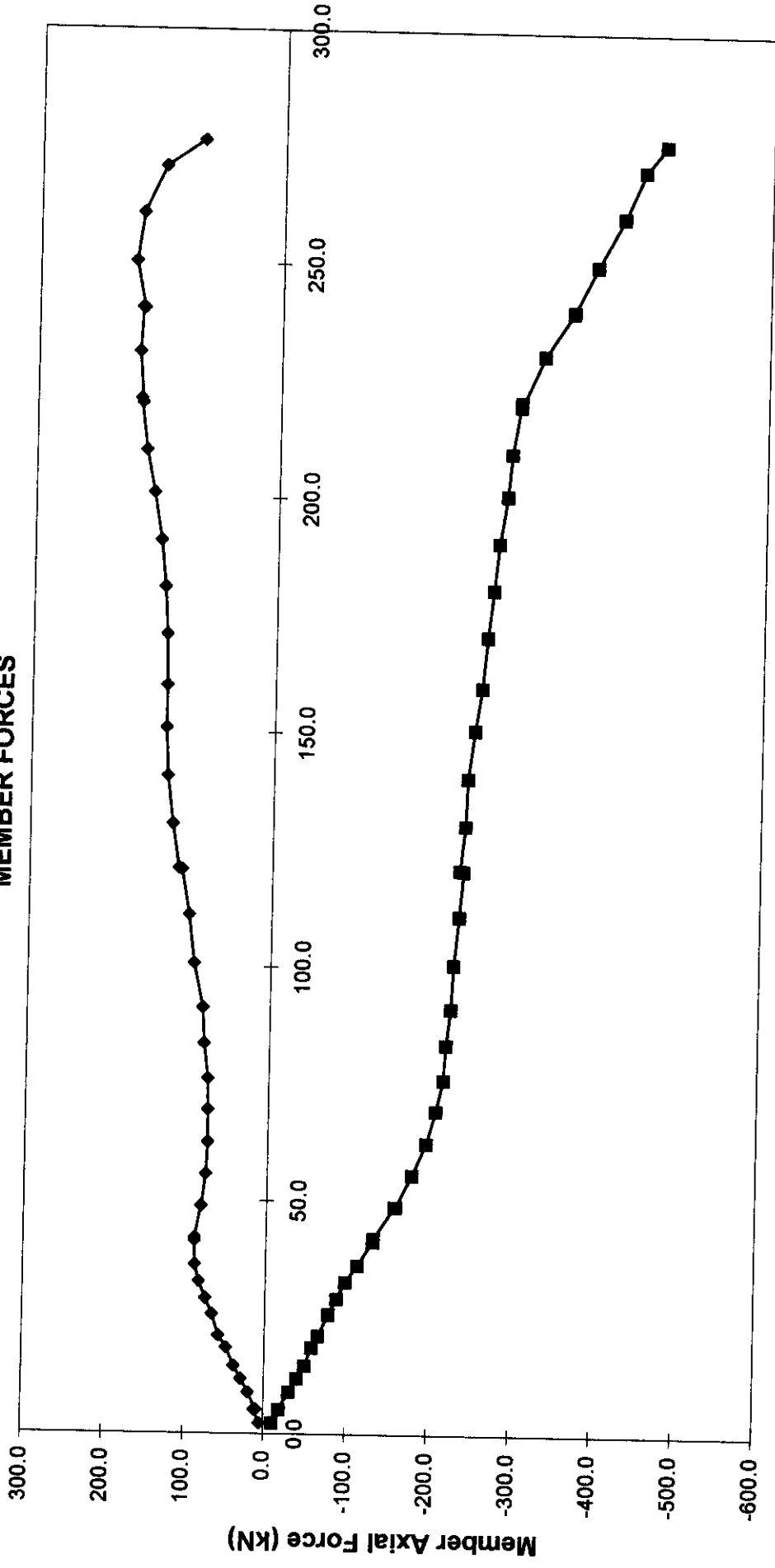
**FRAME E - BOTTOM BAY  
MEMBER FORCES**



Global Displacement (mm)

Loadcase 2 - Test    ◆ 77 Measured    ■ 78 Measured    ▲ 80 Measured    — 80 Measured

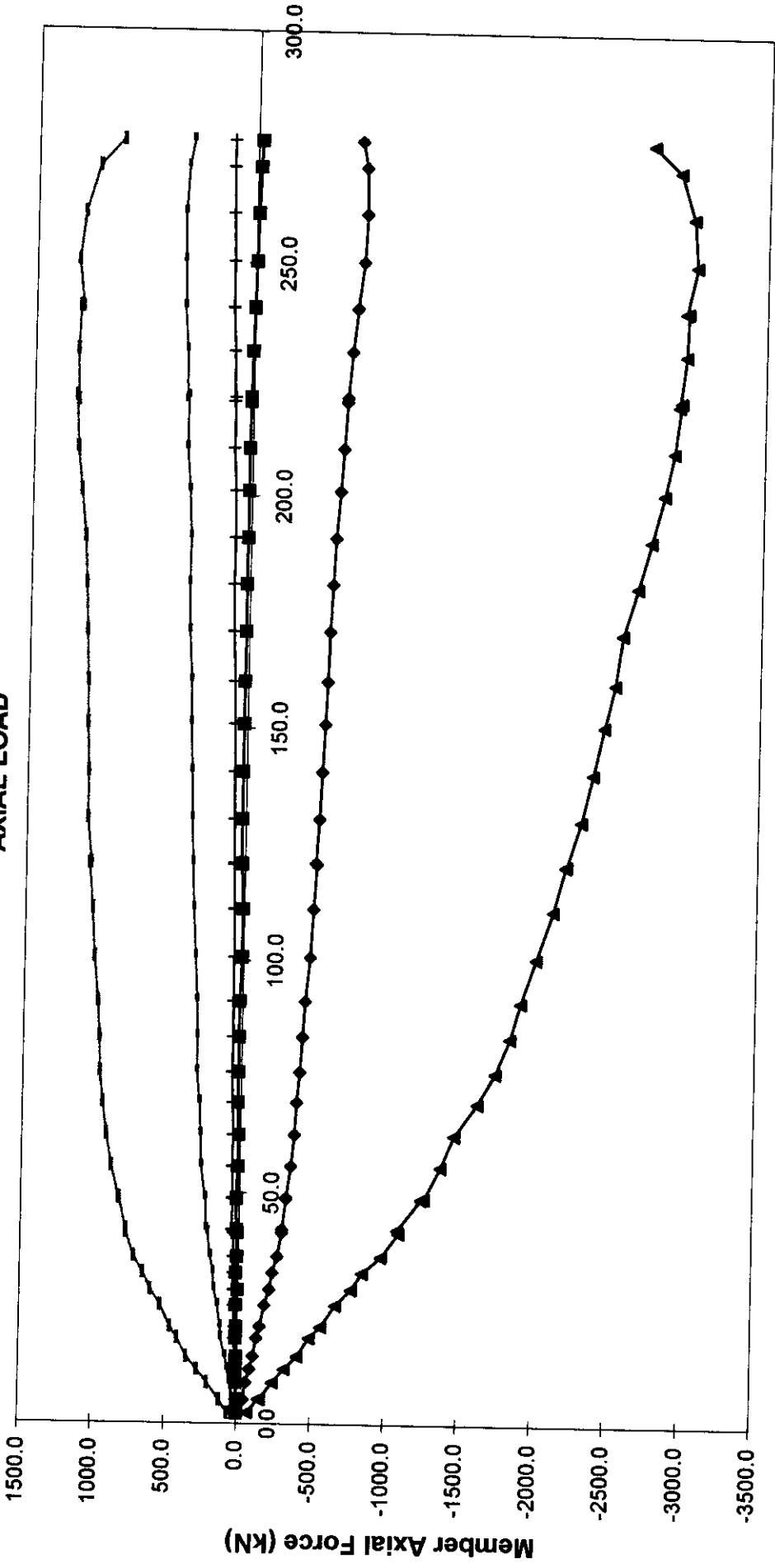
**LEVEL 2 - X  
MEMBER FORCES**



Global Displacement (mm)

Loadcase 2 - Test      —◆— 90 Measured      —■— 93 Measured

**FRAME FEET  
AXIAL LOAD**



**Global Displacement (mm)**

- ◆ 2 Measured
- 5 Measured
- ▲ 8 Measured
- + 32 Measured
- 35 Measured
- 38 Measured

**Loadcase 2 - Test**

## APPENDIX G LOADCASE 3 RESULTS

Plot	Sheet name	Plots / data provided by and supplied to Benchmark Analyst:													
		*	A	B	C	D	E	F	G	H	J	K	L	M	N
<b>Global response</b>															
Pre-test benchmark collation	ALL LC3 Chart (Amm)	X	X	X	X	X	X	X	X	X	X	X	X	X	X
Global response with scan nos	Global Scan Nos	X	X	X	X	X	X	X	X	X	X	X	X	X	X
Global response with failures	Global Annotated	X	X	X	X	X	X	X	X	X	X	X	X	X	X
<b>Displacements</b>															
Rig node uplift c.f.global response	Combined Chart 3	X	X	X	X		X	X		X		X	X	X	
Spatial disp. of 3D frame nodes	**	X		X		X		X	X						
<b>Local joint characteristics:</b>															
Frame A K Node 37 tension	FrC Lev2 Tens														
Frame A K Node 37 compression	FrC Lev2 Comp														
Frame A K Node 38 tension	FrC Lev1 Tens														
Frame A K Node 38 compression	FrC Lev1 Comp														
Frame E X Node 42 compression	FrE TB Comp														
Frame B X Node 16 compression	FrB TB Comp	X			X			X							X
Frame B X Node 18 tension	FrB TB Tens	X			X			X							X
Level 1 X Node 44 tension	Lev1-LC3X Tens	X			X										X
<b>Member Forces</b>															
Frame A X braces L1-L2 FrC-FrD	FrA TDC For	X	X	X	X		X	X	X	X	X		X	X	X
Frame A X braces L1-L2 FrD-FrE	FrA TED For	X	X	X	X		X	X	X	X	X		X	X	X
Frame A X braces L2-L3 FrC-FrD	FrA BDC For	X	X	X	X		X	X	X	X	X		X	X	X
Frame A X braces L2-L3 FrD-FrE	FrA BED For	X	X	X	X		X	X	X	X	X		X	X	X
Frame B X braces L1-L2 FrC-FrD	FrB TDC For	X						X							X
Frame B X braces L1-L2 FrD-FrE	FrB TED For	X						X							X
Frame B X braces L2-L3 FrC-FrD	FrB BDC For														
Frame B X braces L2-L3 FrD-FrE	FrB BED For														
Frame C K braces L1-L2	FrC TB For	X		X						X					X
Frame C K braces L2-L3	FrC BB For	X		X				X	X	X					X
Frame D K braces L1-L2	FrD TB For														
Frame D K braces L2-L3	FrD BB For	X													X
Frame E X braces L1-L2	FrE TB For	X							X					X	X
Frame E X braces L2-L3	FrE BB For														
Level 2 X braces FrD-FrE	Lev 2-X For	X	X												
Level 2 diamond braces FrC-FrD	Lev 2-Dia For	X	X												
Level 1 X braces FrD-FrE	Lev 1-LC3X For	X	X		X			X						X	X
Level 1 diamond braces FrC-FrD	Lev 1-Dia For	X	X												
Frame C legs	Fr C Leg For														
Frame D legs	Fr D Leg For	X												X	
Frame E legs	Fr E Leg For	X												X	
All frame legs at connection to rig	Fr Feet	X						X	X	X					
<b>Bending moments</b>															
Frame A compression braces	FrA... Mom (θ)	X	X												

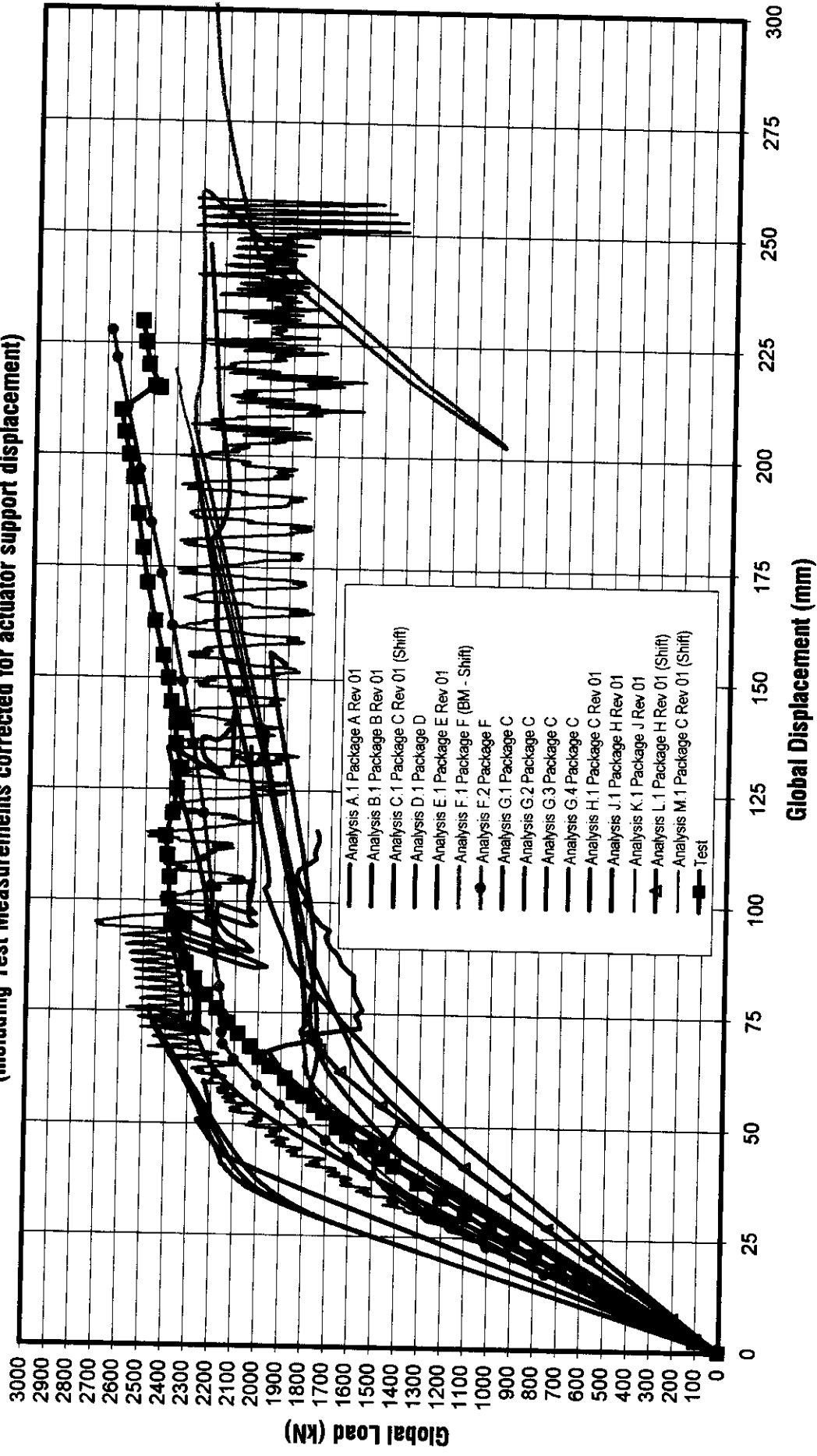
Reference Files:  
 Rig displacements C636\25\063W  
 Loadcase 3 member force plots C636\40\016W  
 Loadcase 3 benchmark comparison C636\32\009W-C

\* Information provided to project sponsors  
 \*\* N21, N22, N25, N26, N29 and N30 Disp

TUBULAR FRAMES PROJECT PHASE III

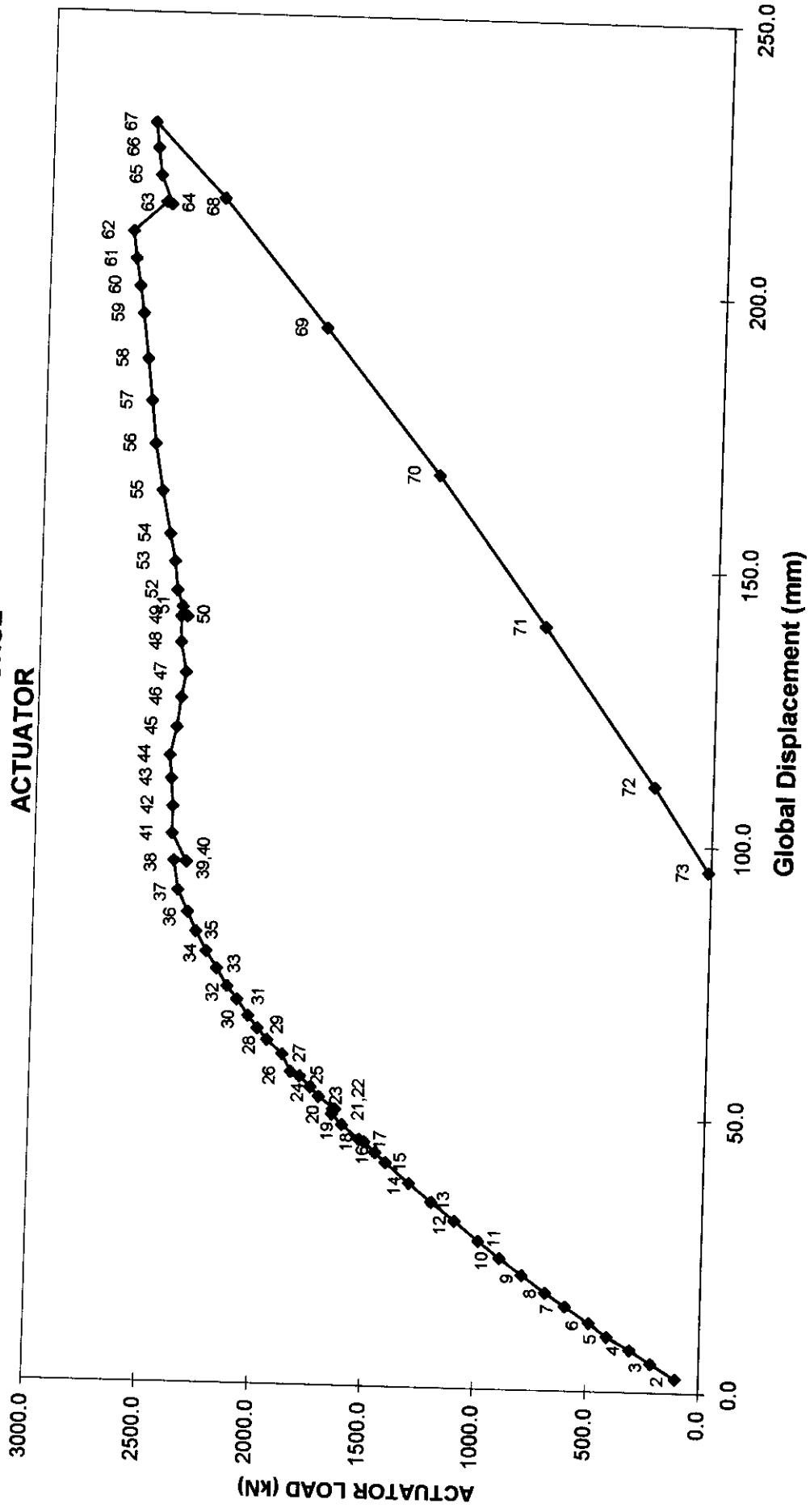
# Global Load vs Global Displacement - Load Case 3 Predictions (Revised)

(including Test Measurements corrected for actuator support displacement)





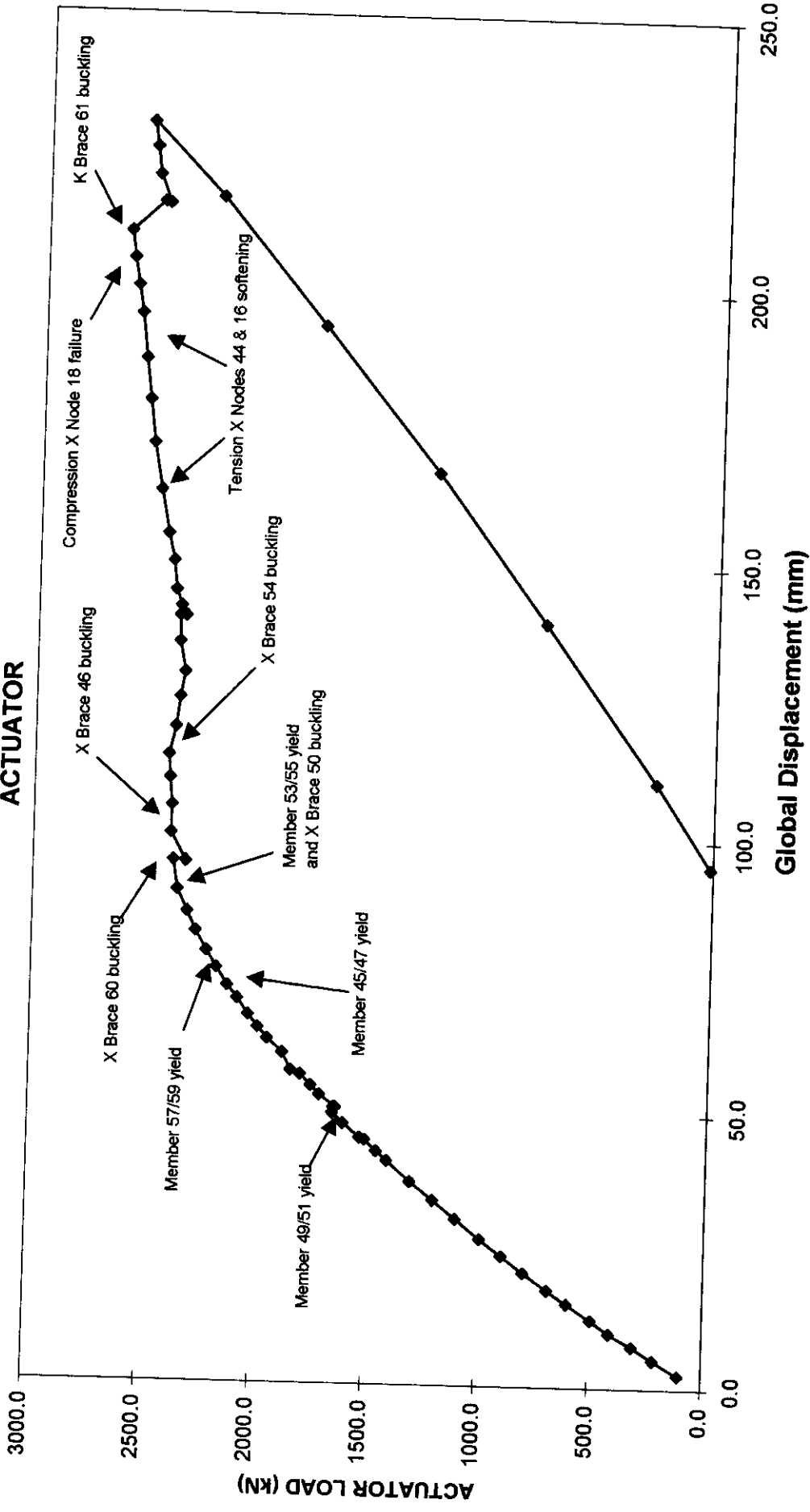
# GLOBAL RESPONSE ACTUATOR



Loadcase 3 - Test

016W.xls GLOBAL Scan Nos 15/08/99

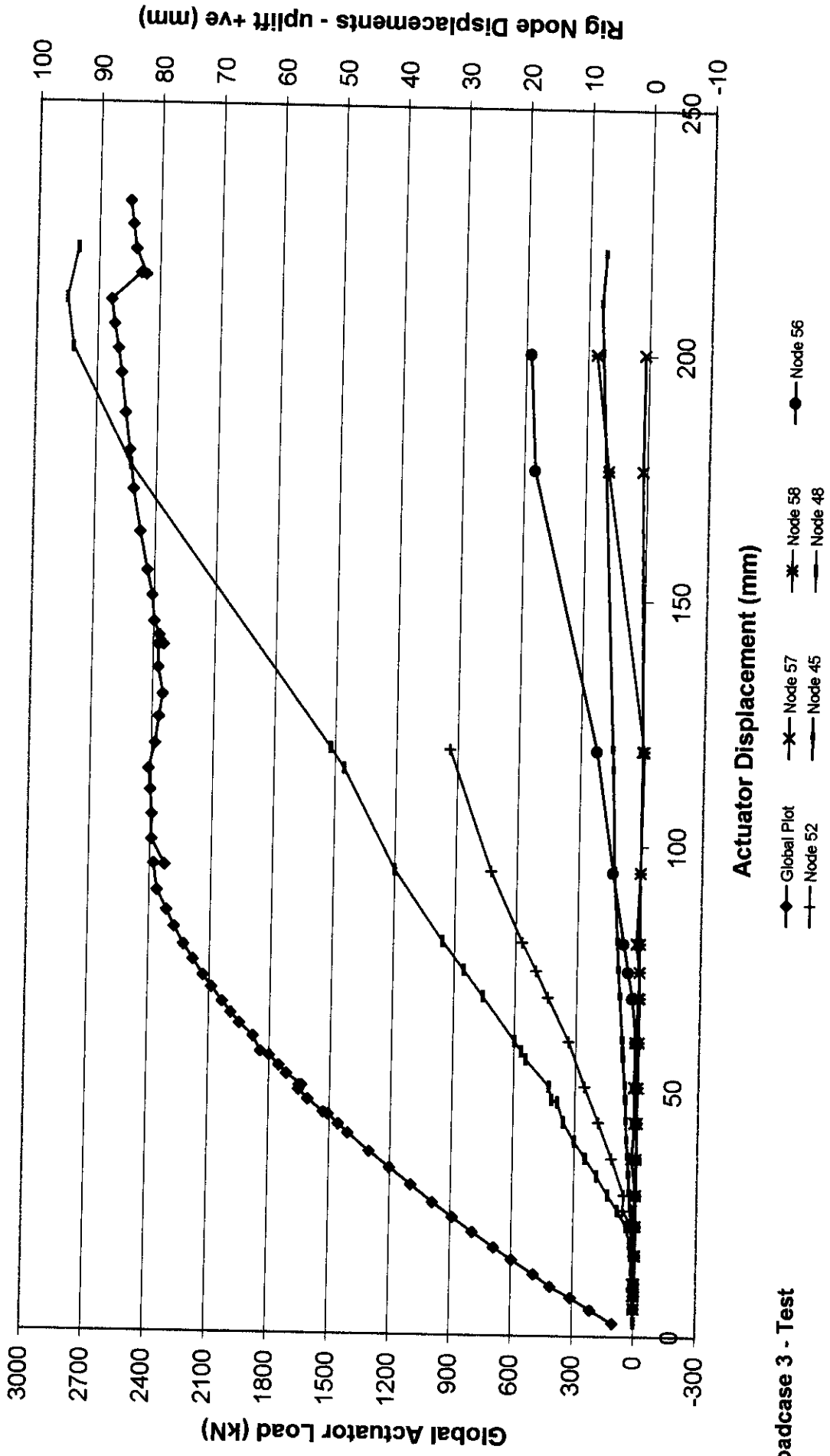
# GLOBAL RESPONSE ACTUATOR



Loadcase 3 - Test

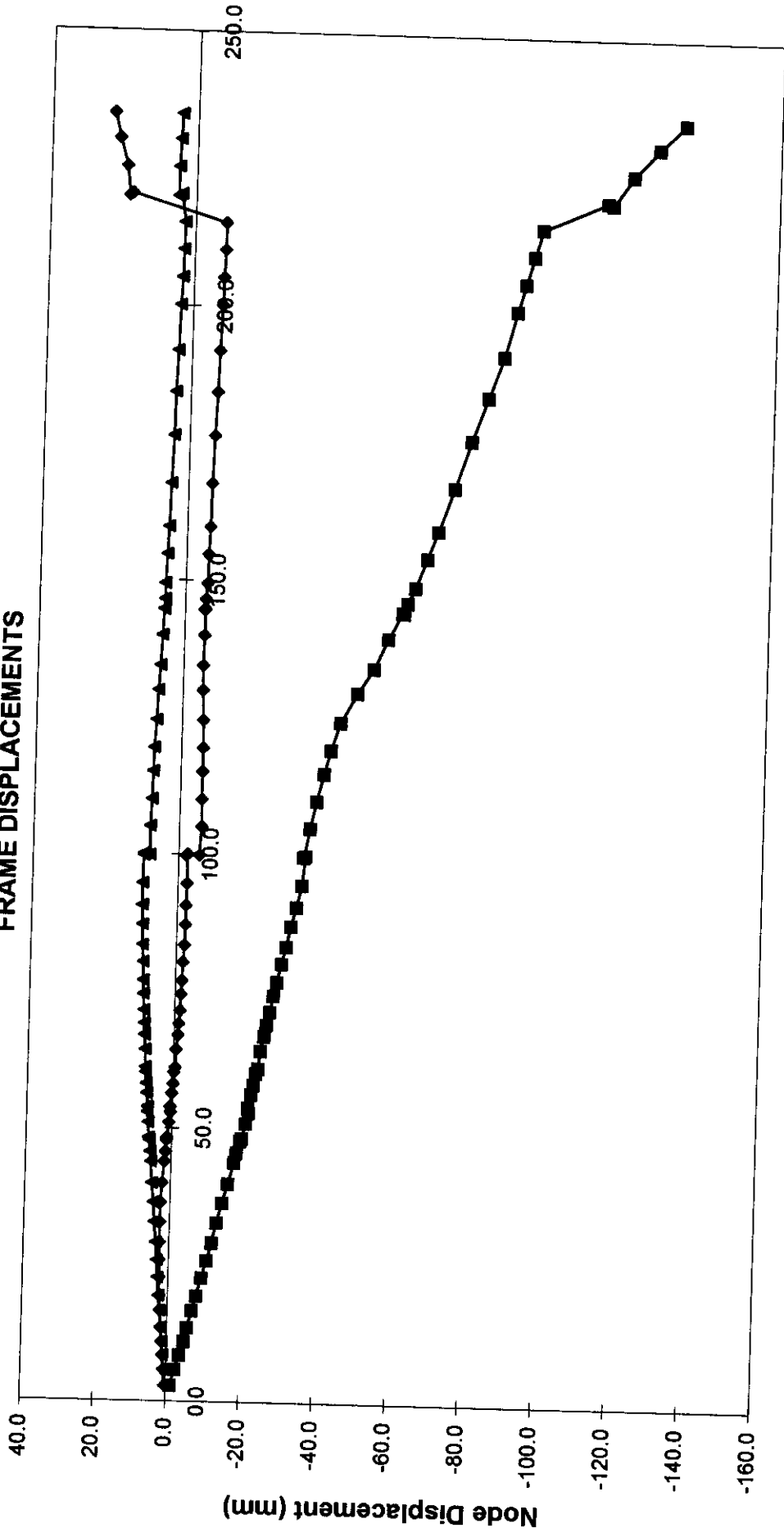
C636\40\016W.xls GLOBAL Annotated 15/08/99

# Nodal Displacements and Global Load versus Global Displacement



Loadcase 3 - Test

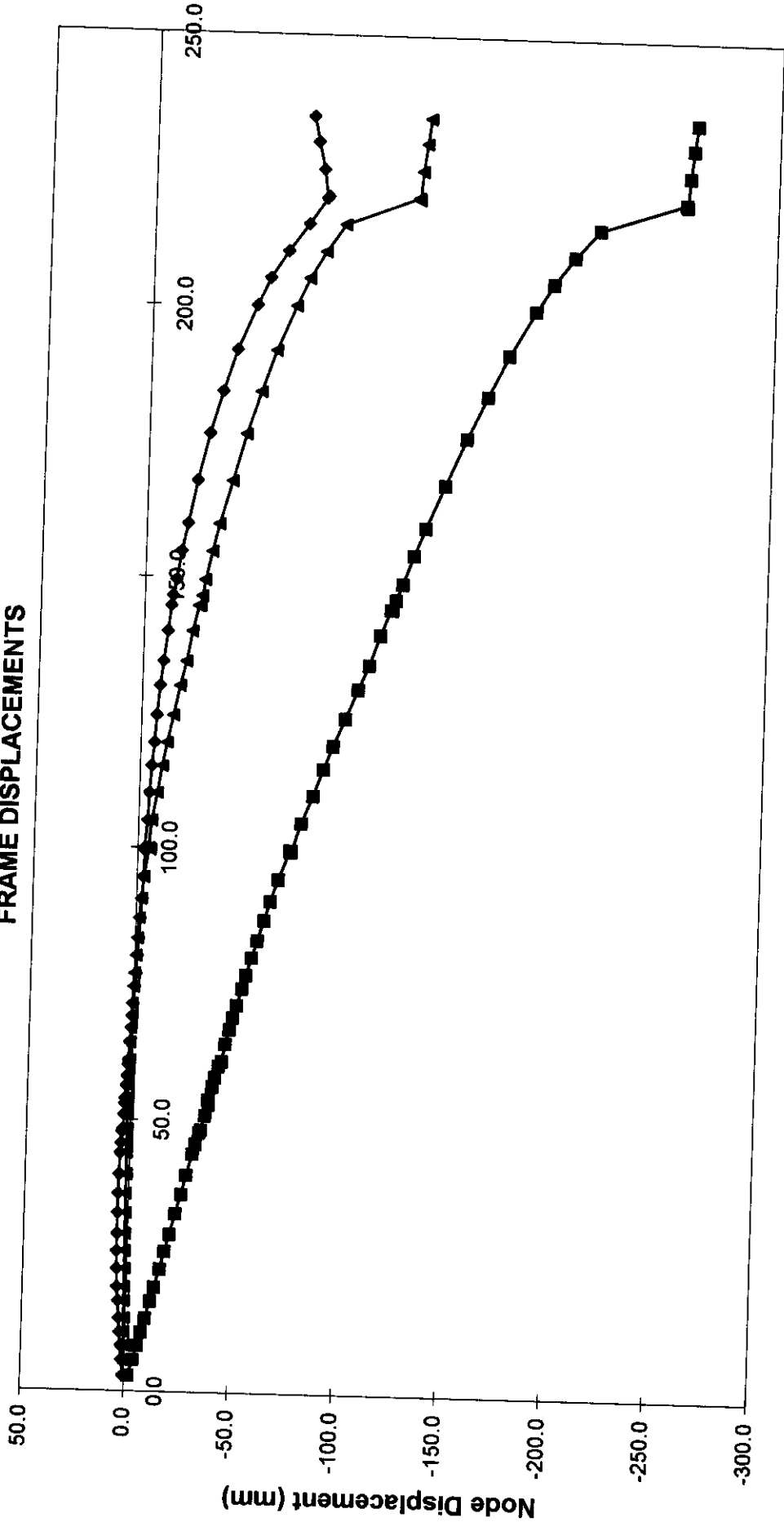
LEG AC LEVEL 2  
FRAME DISPLACEMENTS



Global Displacement (mm)

Loadcase 3 - Test      —◆— X Measured      —■— Y Measured      —▲— Z Measured

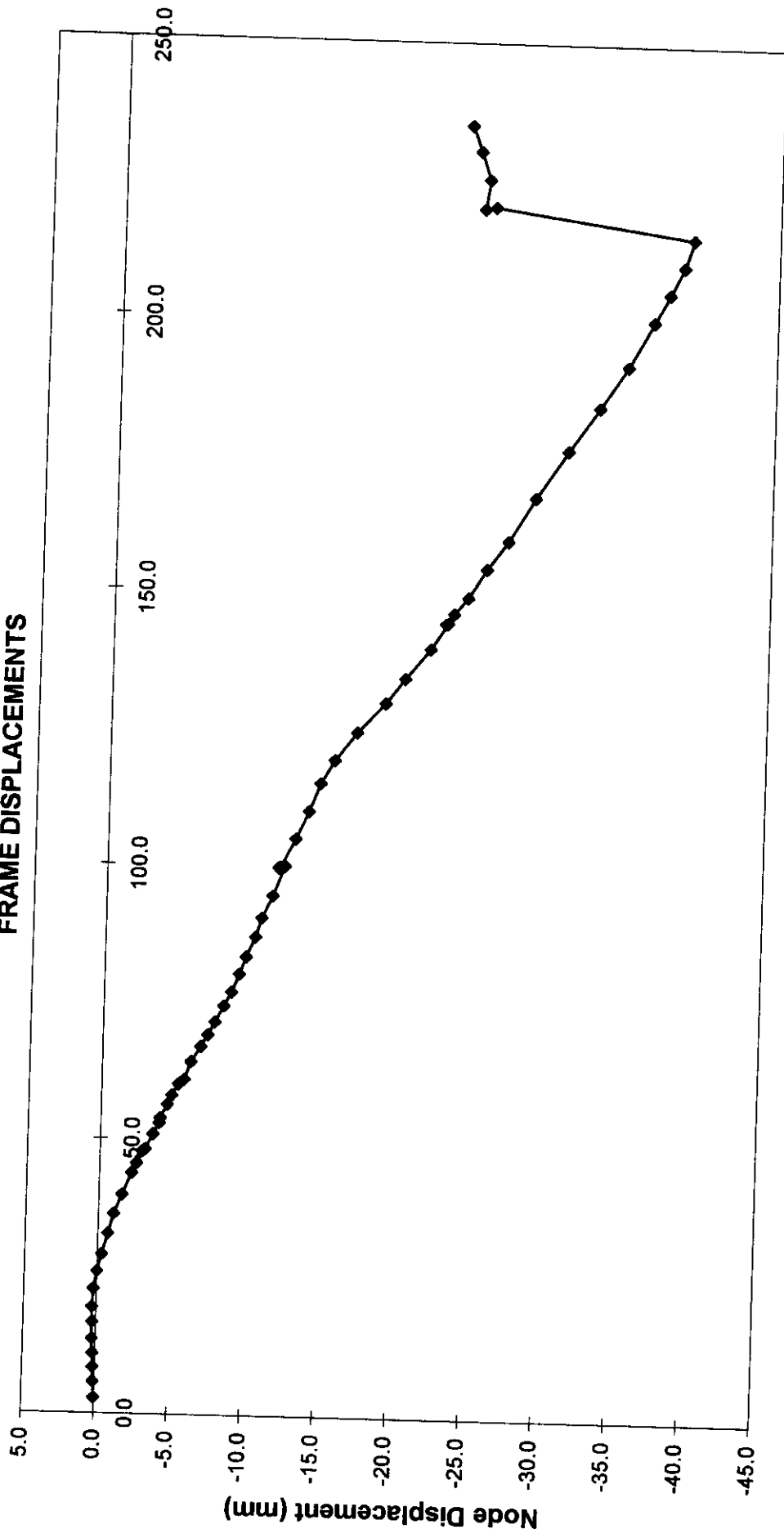
**LEG AC LEVEL 1  
FRAME DISPLACEMENTS**



Global Displacement (mm)

Loadcase 3 - Test      —◆— X Measured      —■— Y Measured      —▲— Z Measured

# LEG AD LEVEL 2 FRAME DISPLACEMENTS

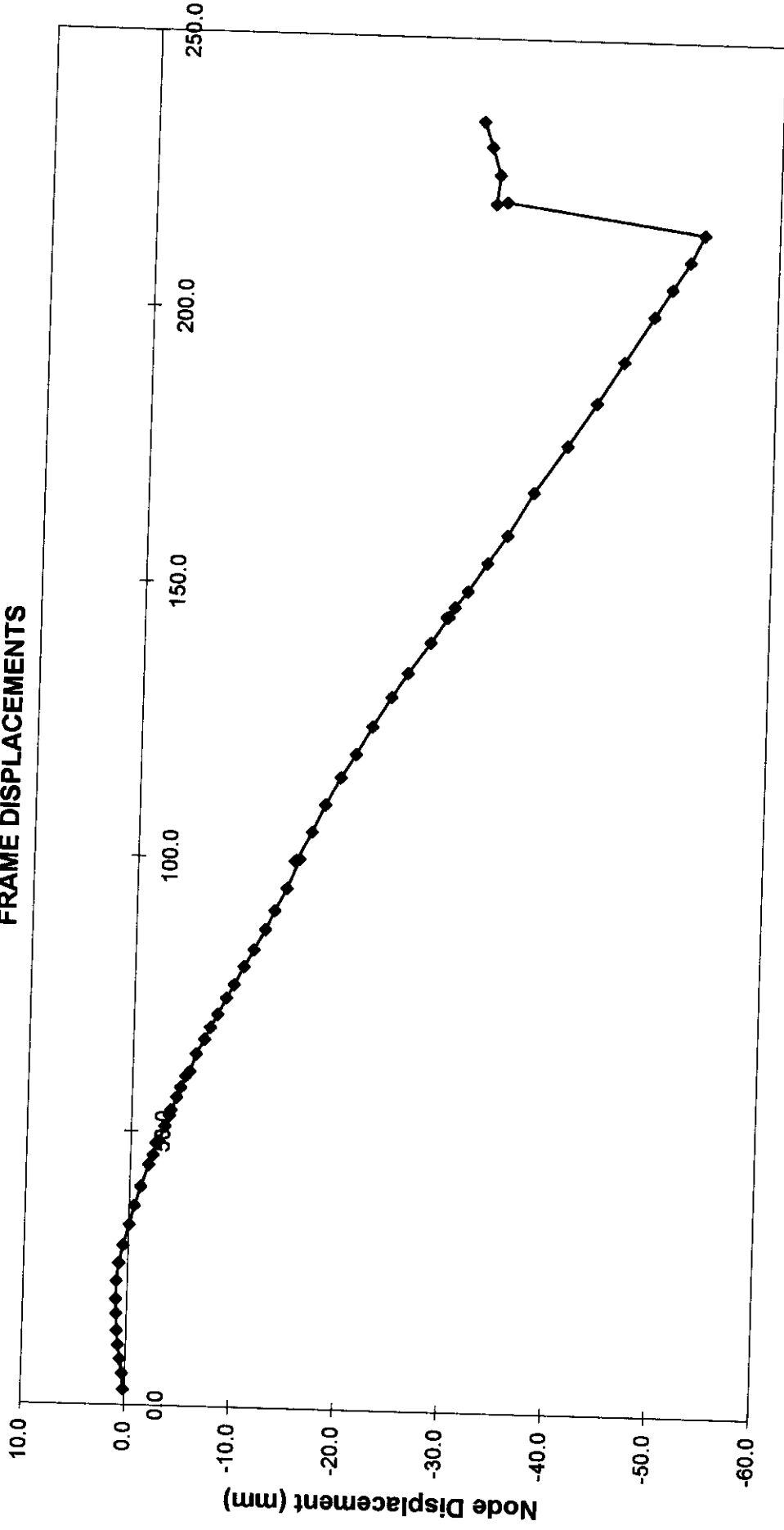


Global Displacement (mm)

Loadcase 3 - Test

—◆— X Measured

# LEG AD LEVEL 1 FRAME DISPLACEMENTS

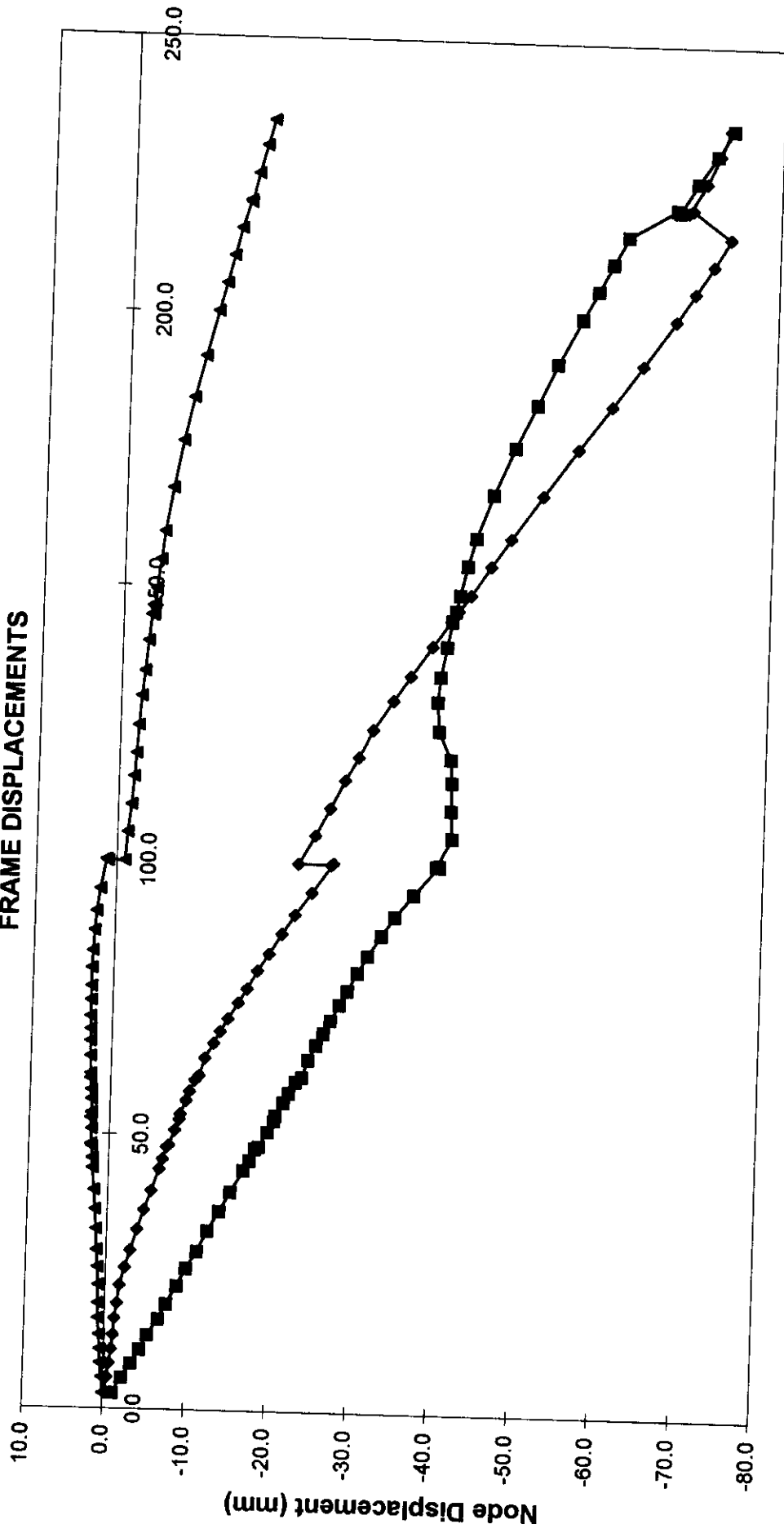


Global Displacement (mm)

Loadcase 3 - Test

◆ X Measured

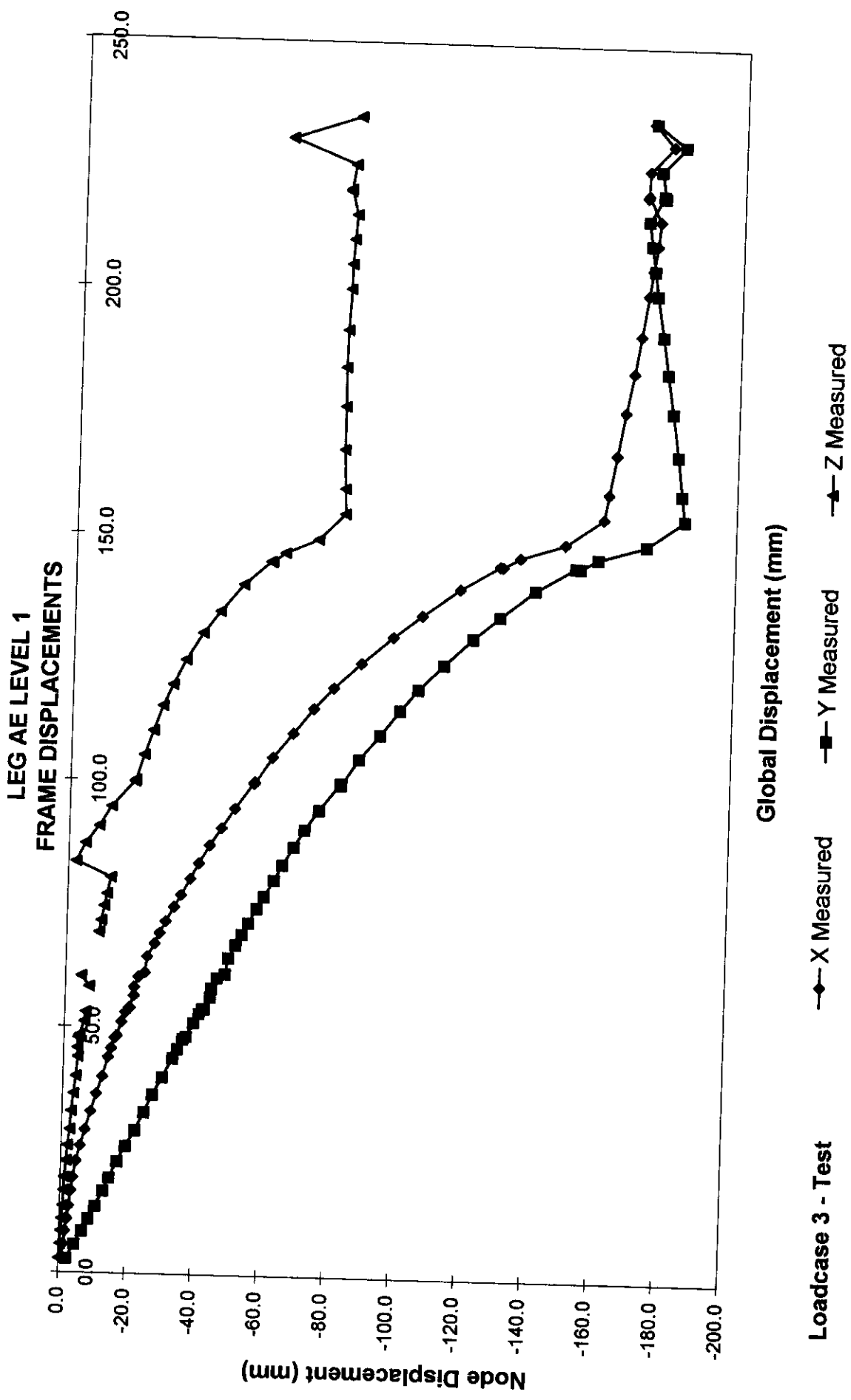
**LEG AE LEVEL 2  
FRAME DISPLACEMENTS**



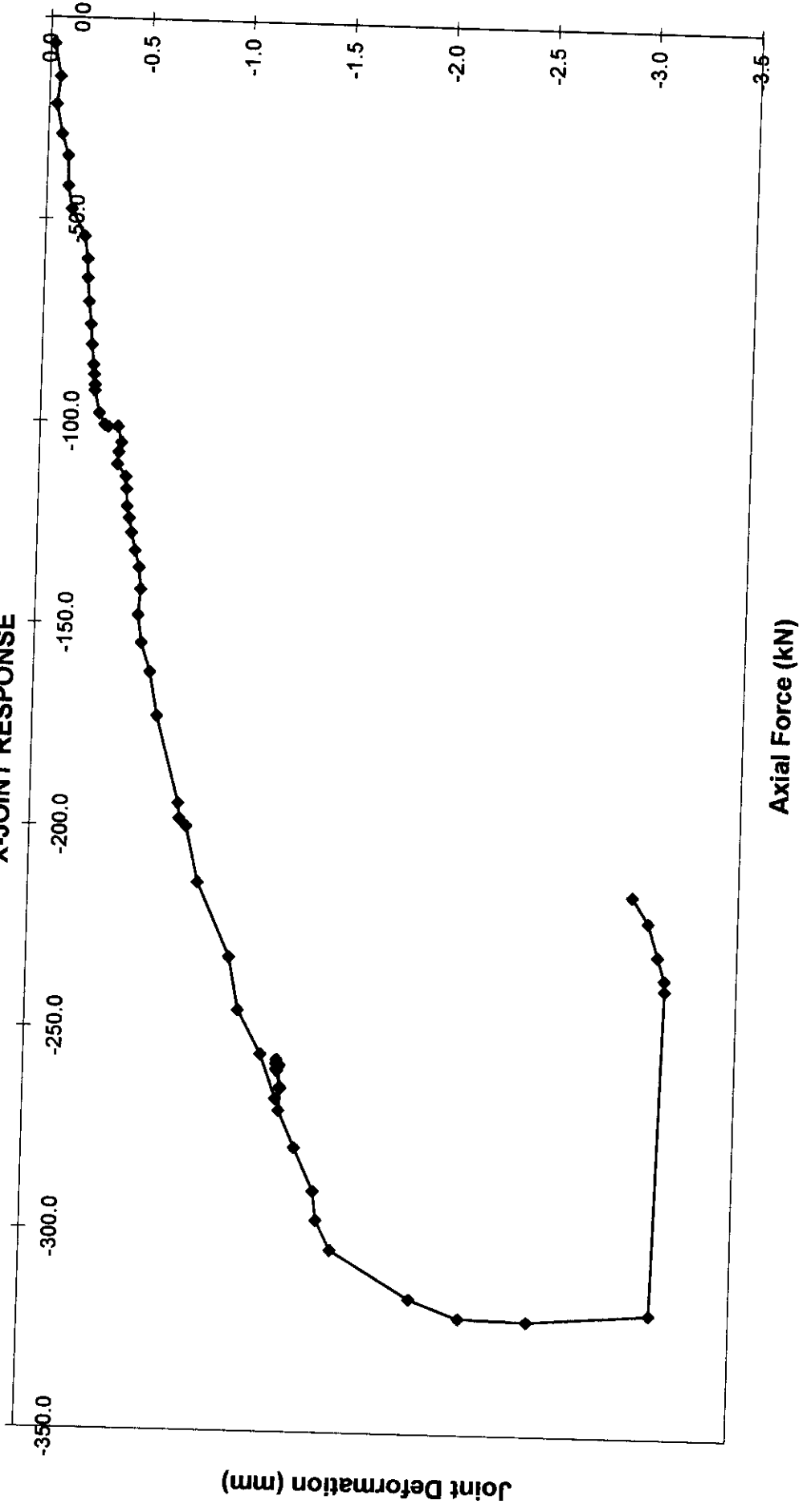
Global Displacement (mm)

Loadcase 3 - Test      —◆— X Measured      —■— Y Measured      —▲— Z Measured



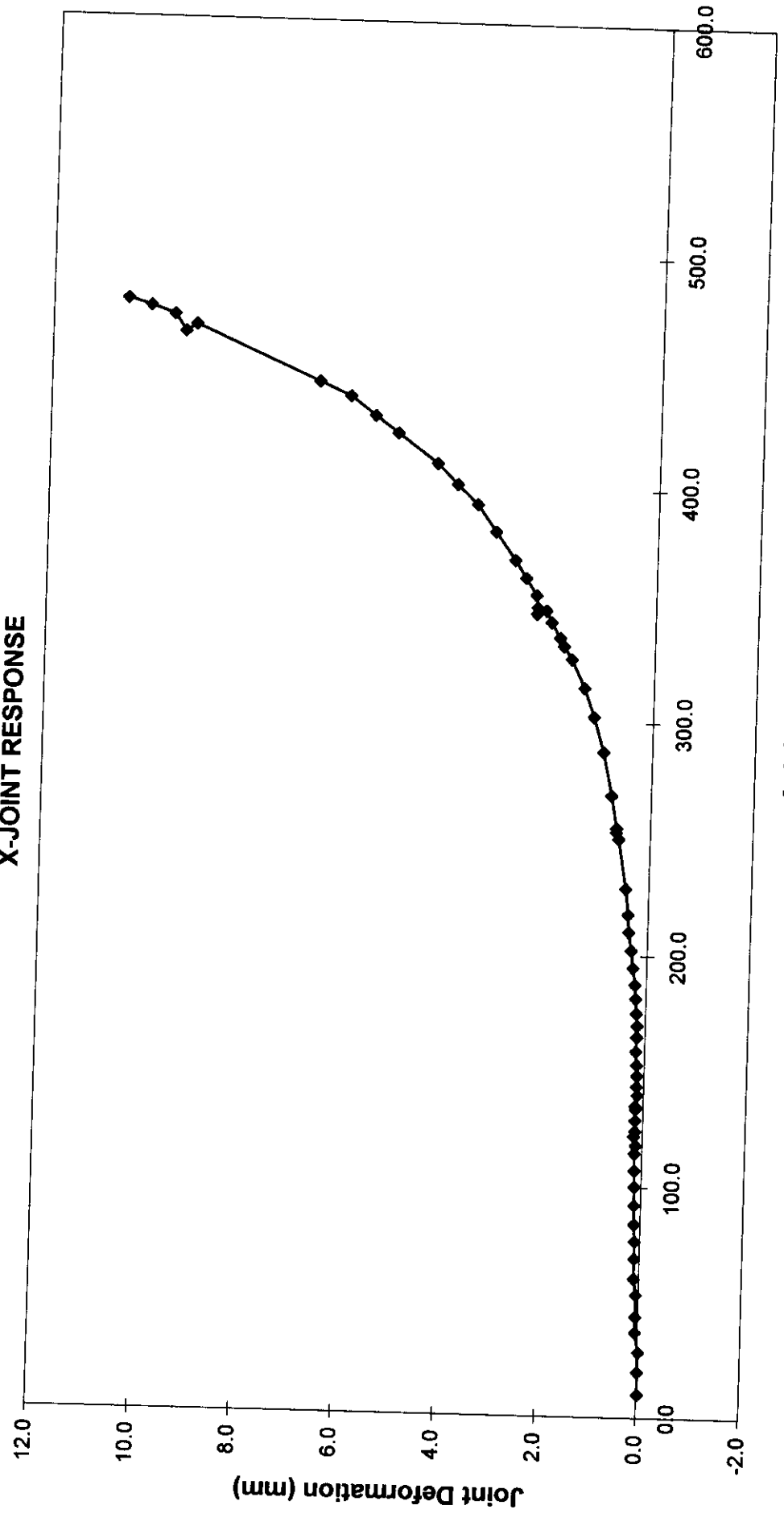


FRAME B- TOP BAY - COMPRESSION  
X-JOINT RESPONSE



Loadcase 3 - Test

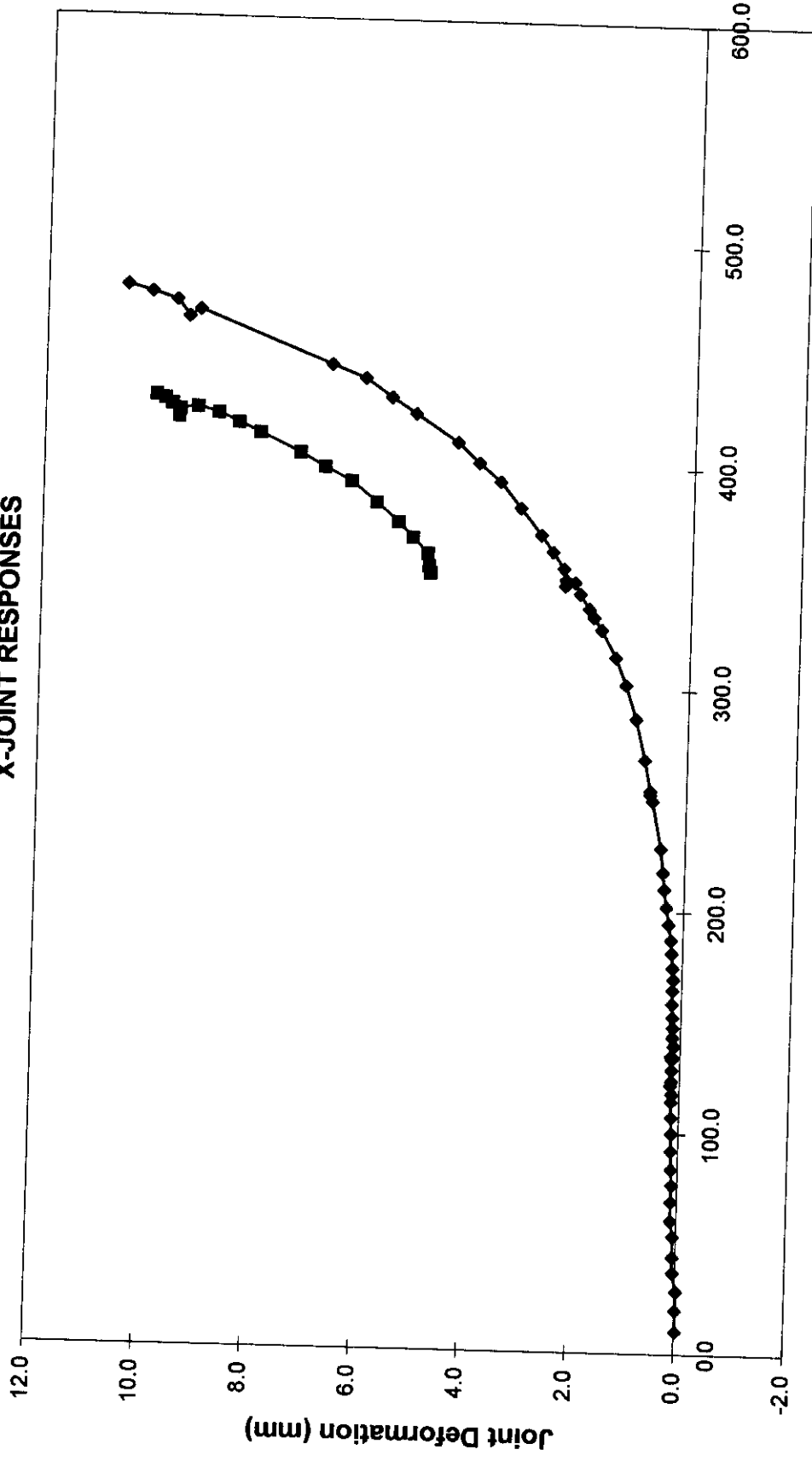
FRAME B- TOP BAY - TENSION  
X-JOINT RESPONSE



Axial Force (kN)

Loadcase 3 - Test

FRAME B - TOP BAY AND LEVEL 1 - TENSION  
X-JOINT RESPONSES

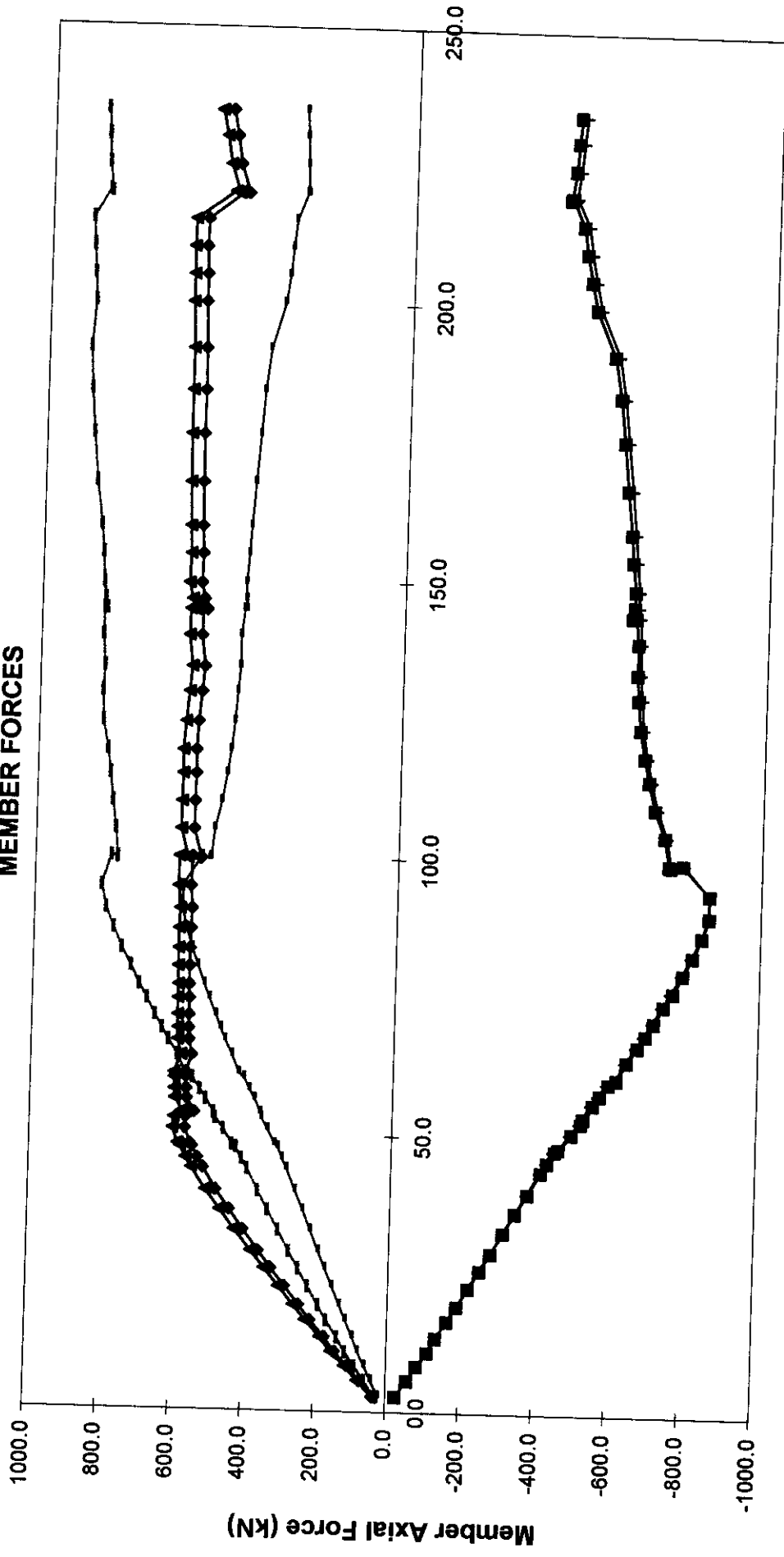


Axial Force (kN)

Loadcase 3 - Test

◆ Node 18    ■ Node 44

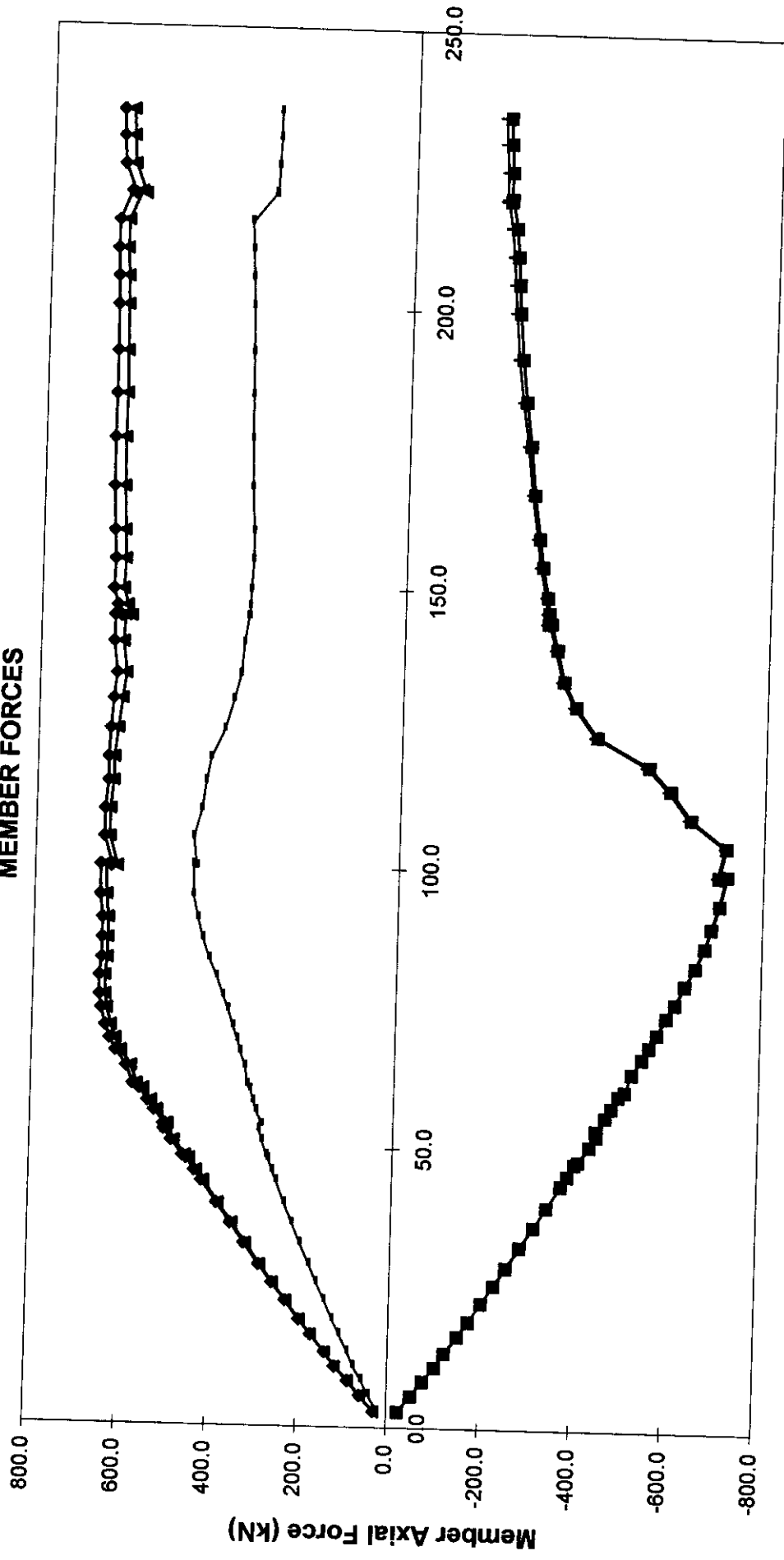
FRAME A - TOP DC  
MEMBER FORCES



Global Displacement (mm)

Loadcase 3 - Test    ◆— 49 Measured    ■— 50 Measured    ▲— 51 Measured    +— 52 Measured    — 43 Measured

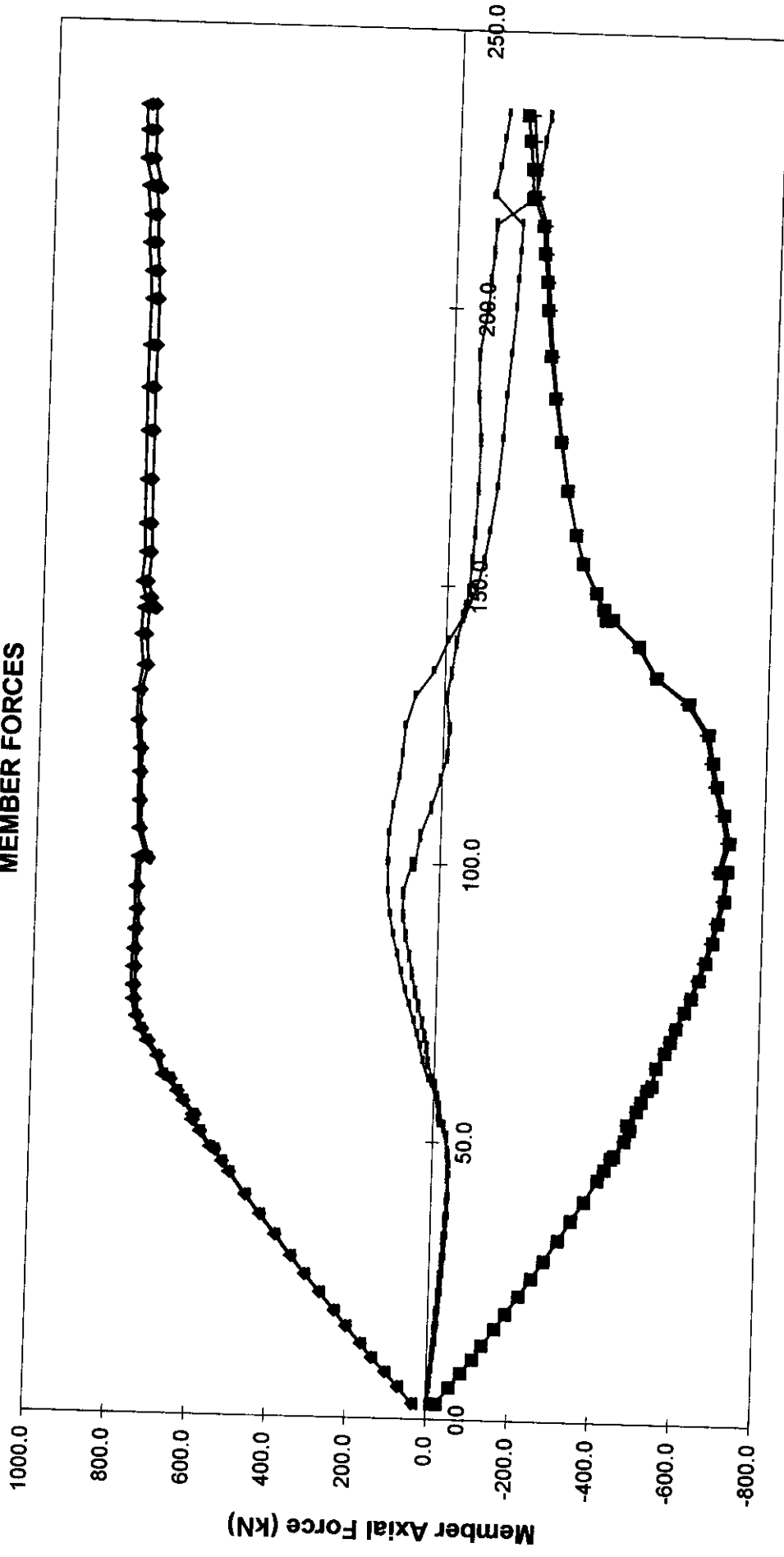
**FRAME A - TOP ED  
MEMBER FORCES**



Global Displacement (mm)

Loadcase 3 - Test    ◆—57 Measured    ■—58 Measured    ▲—59 Measured    ▴—60 Measured    —44 Measured

**FRAME A - BOTTOM DC  
MEMBER FORCES**

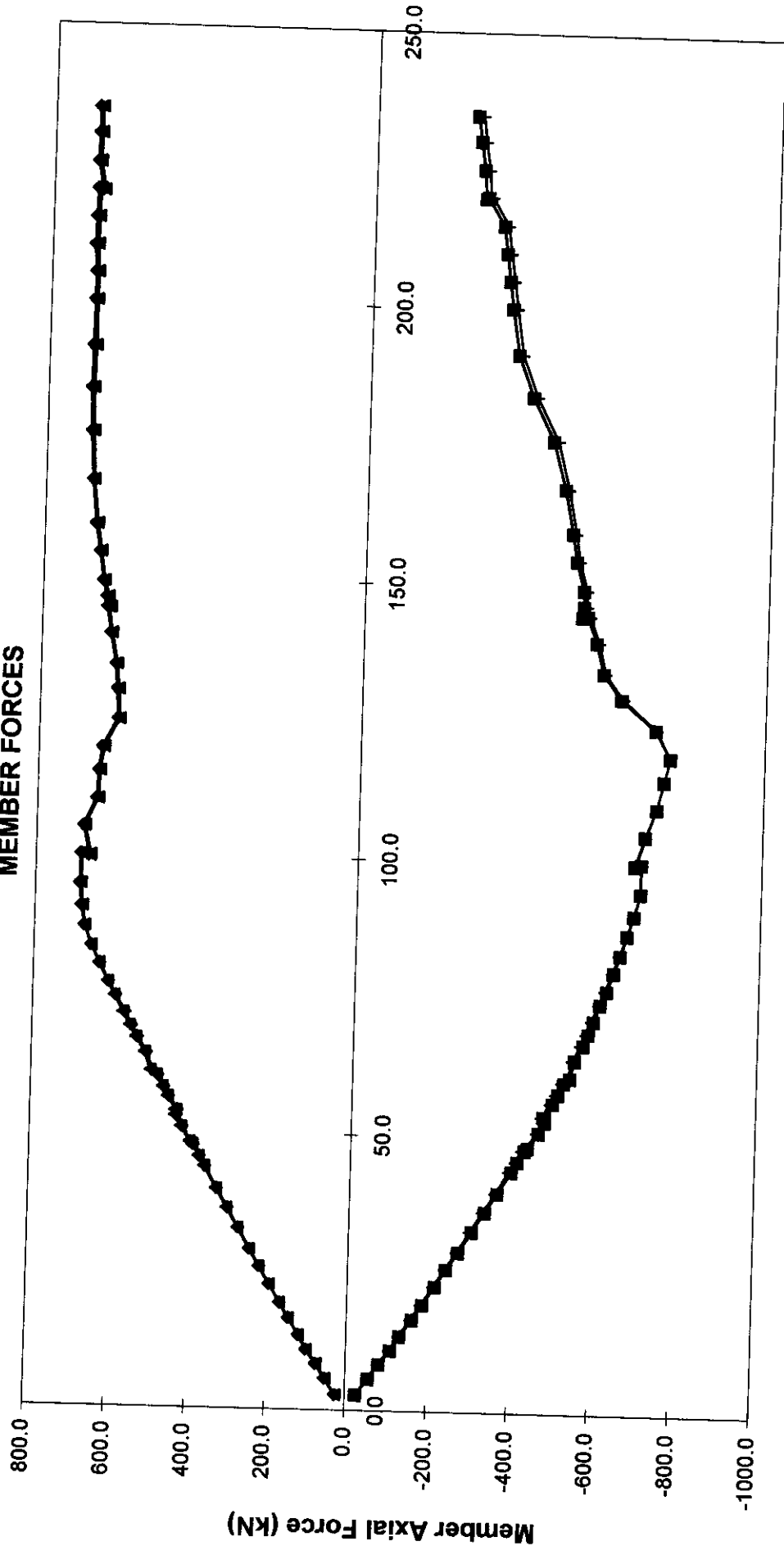


Global Displacement (mm)

Loadcase 3 - Test

—◆— 45 Measured    —■— 46 Measured    —▲— 47 Measured    —+— 48 Measured    —□— 40 Measured    —●— 41 Measured

# FRAME A - BOTTOM ED MEMBER FORCES

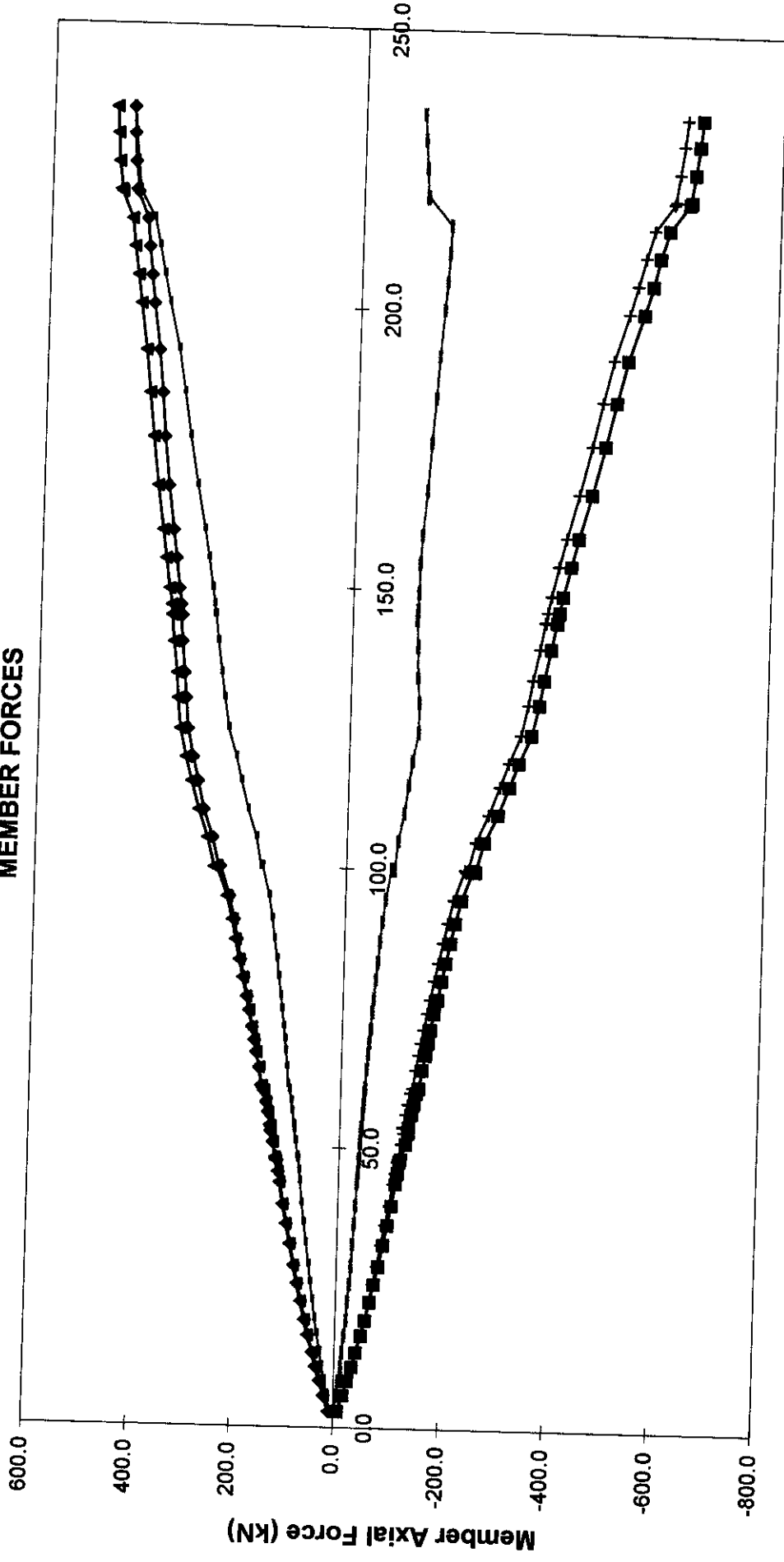


Global Displacement (mm)

Loadcase 3 - Test    ◆ 53 Measured    ■ 54 Measured    ▲ 56 Measured



**FRAME B - TOP DC  
MEMBER FORCES**



Global Displacement (mm)

◆ 19 Measured  
— 12 Measured

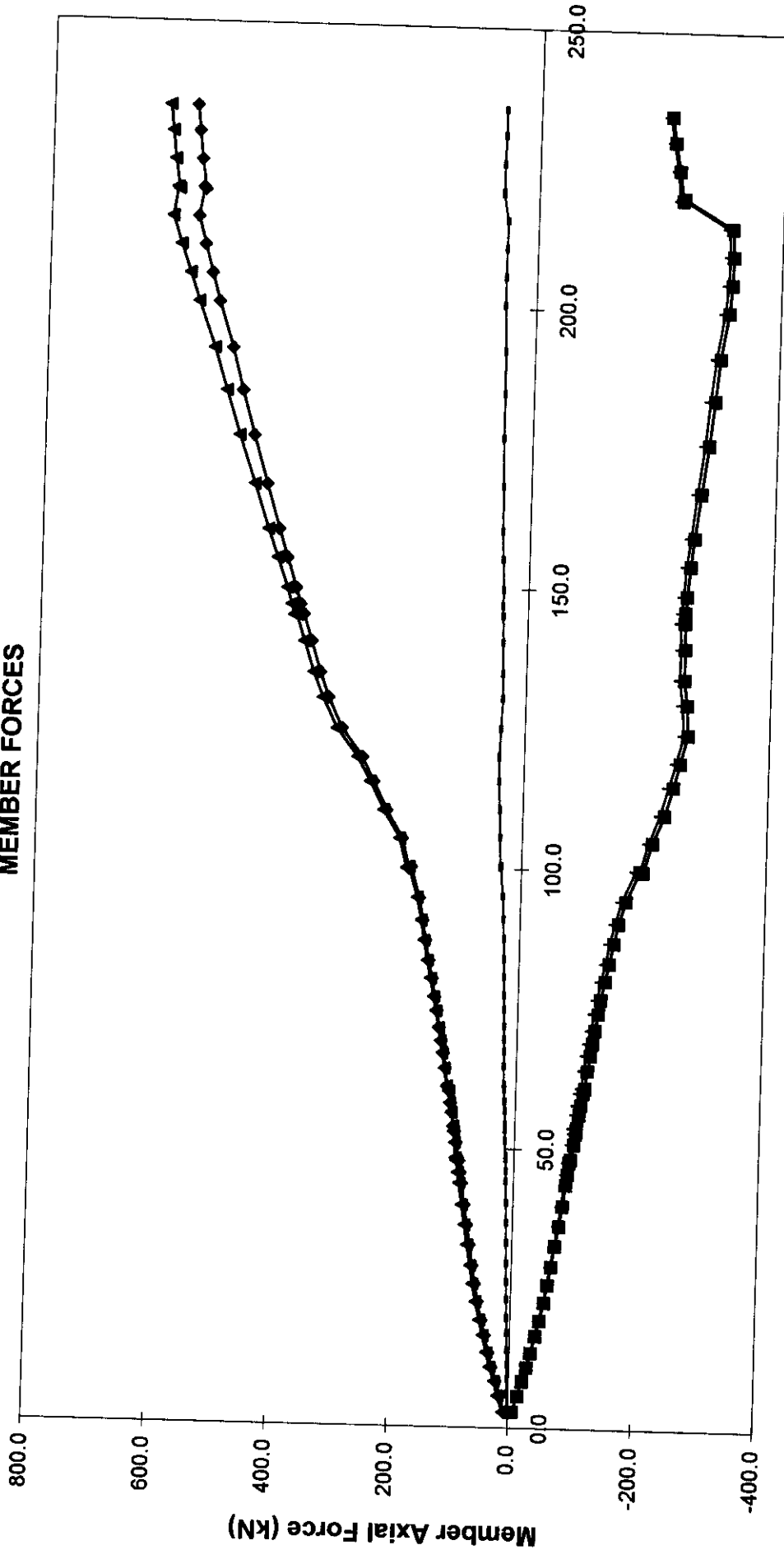
■ 20 Measured  
— 13 Measured

Loadcase 3 - Test

▲ 21 Measured

— 22 Measured

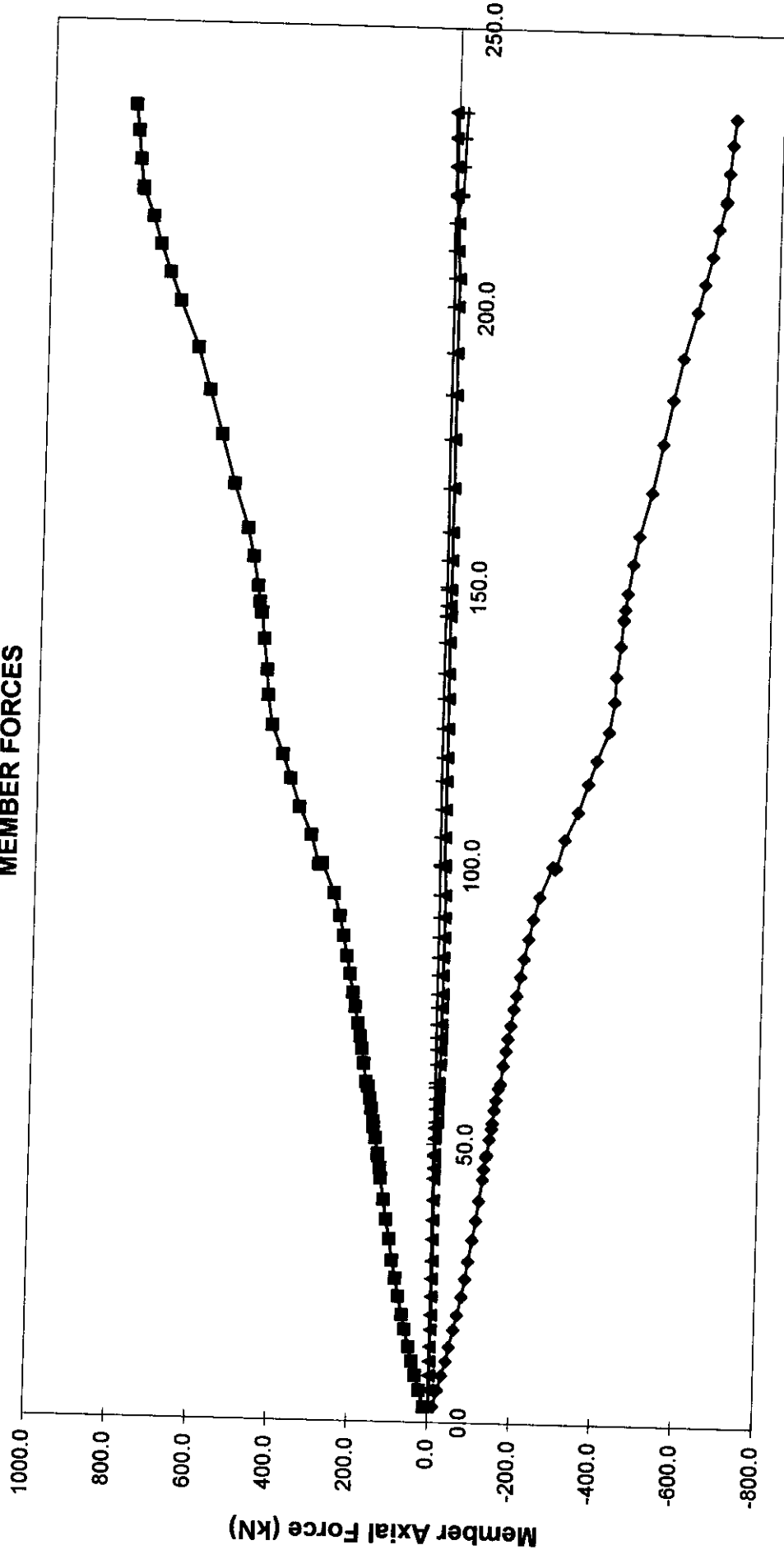
**FRAME B - TOP ED  
MEMBER FORCES**



Global Displacement (mm)

Loadcase 3 - Test    ◆— 27 Measured    ■— 28 Measured    ▲— 29 Measured    — 30 Measured    — 14 Measured

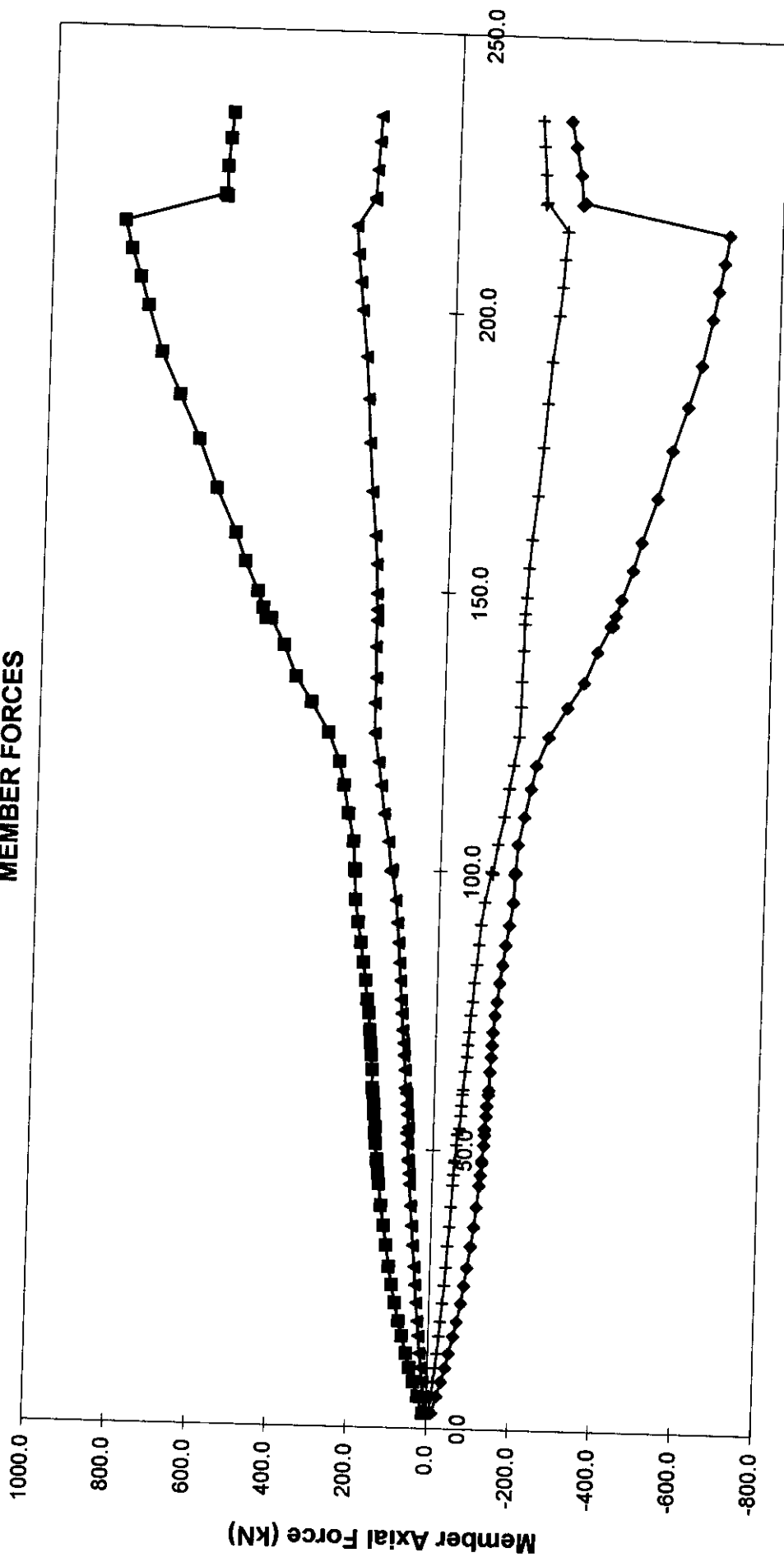
**FRAME C - TOP BAY  
MEMBER FORCES**



Global Displacement (mm)

Loadcase 3 - Test    ◆ 63 Measured    ■ 64 Measured    ▲ 67 Measured    — 68 Measured

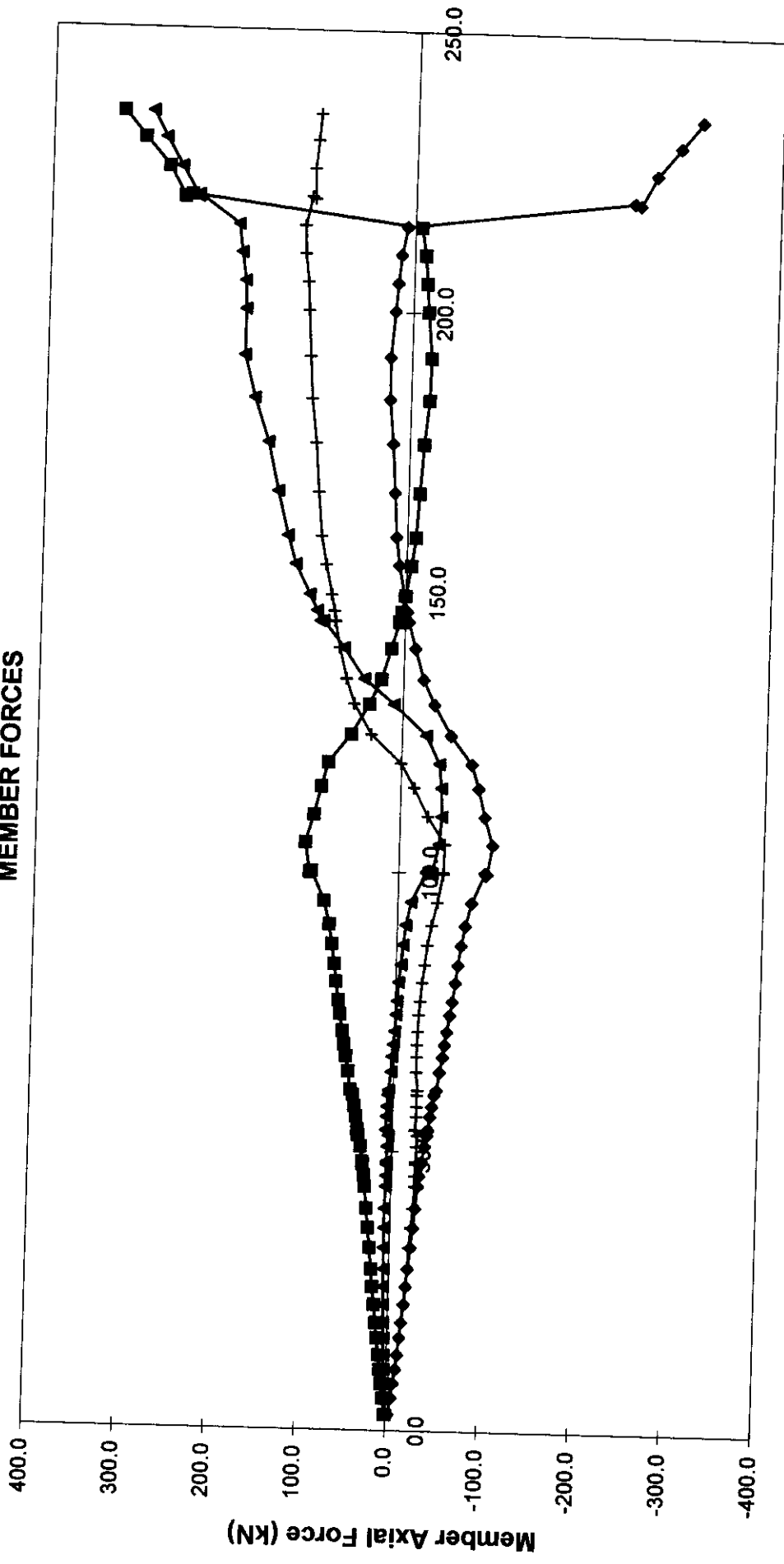
**FRAME C - BOTTOM BAY  
MEMBER FORCES**



Global Displacement (mm)

Loadcase 3 - Test    ◆—61 Measured    ■—62 Measured    ▲—65 Measured    +—66 Measured

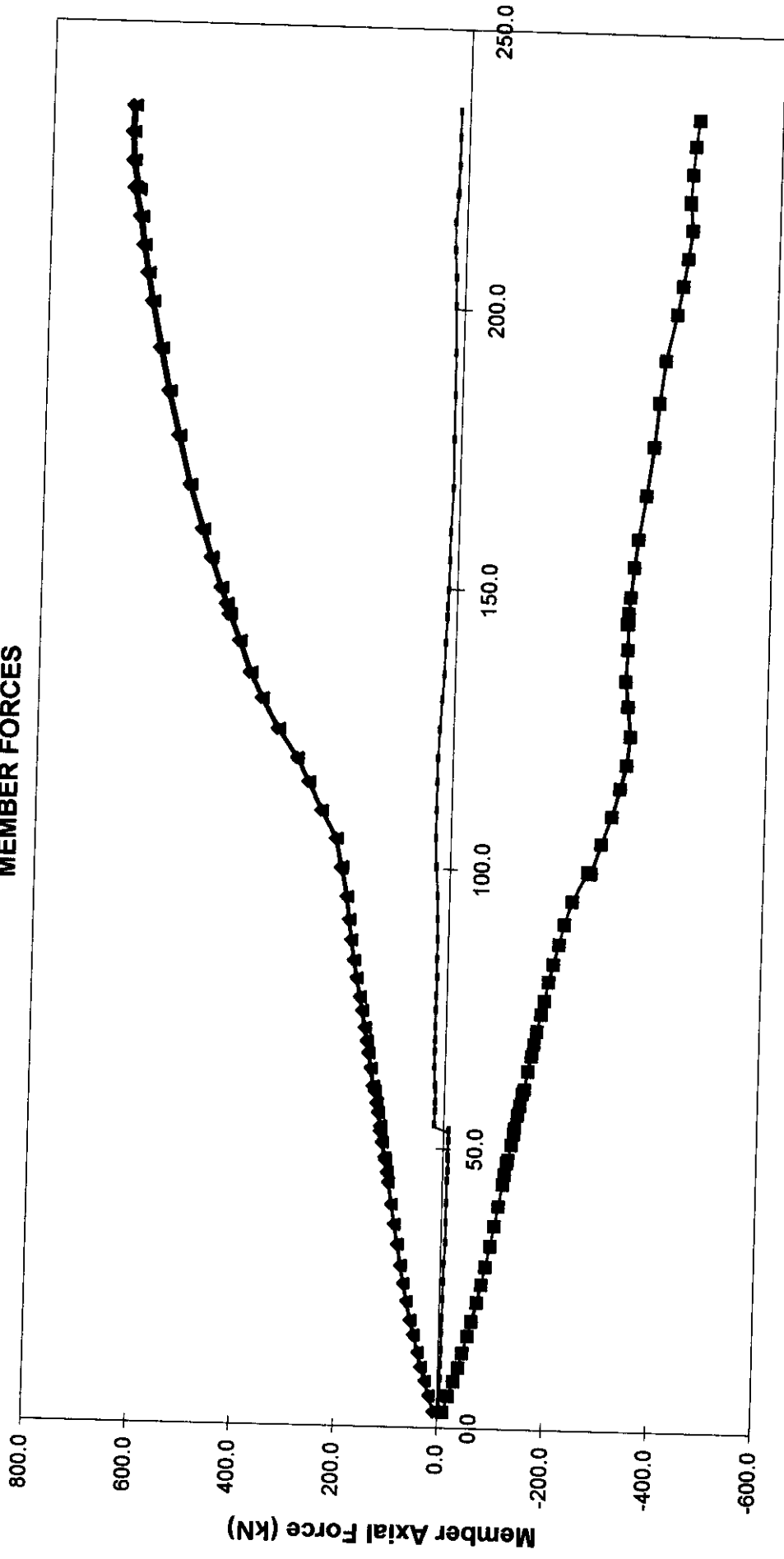
**FRAME D - BOTTOM BAY  
MEMBER FORCES**



**Global Displacement (mm)**

**Loadcase 3 - Test**    ◆ 69 Measured    ■ 70 Measured    ▲ 73 Measured    + 74 Measured

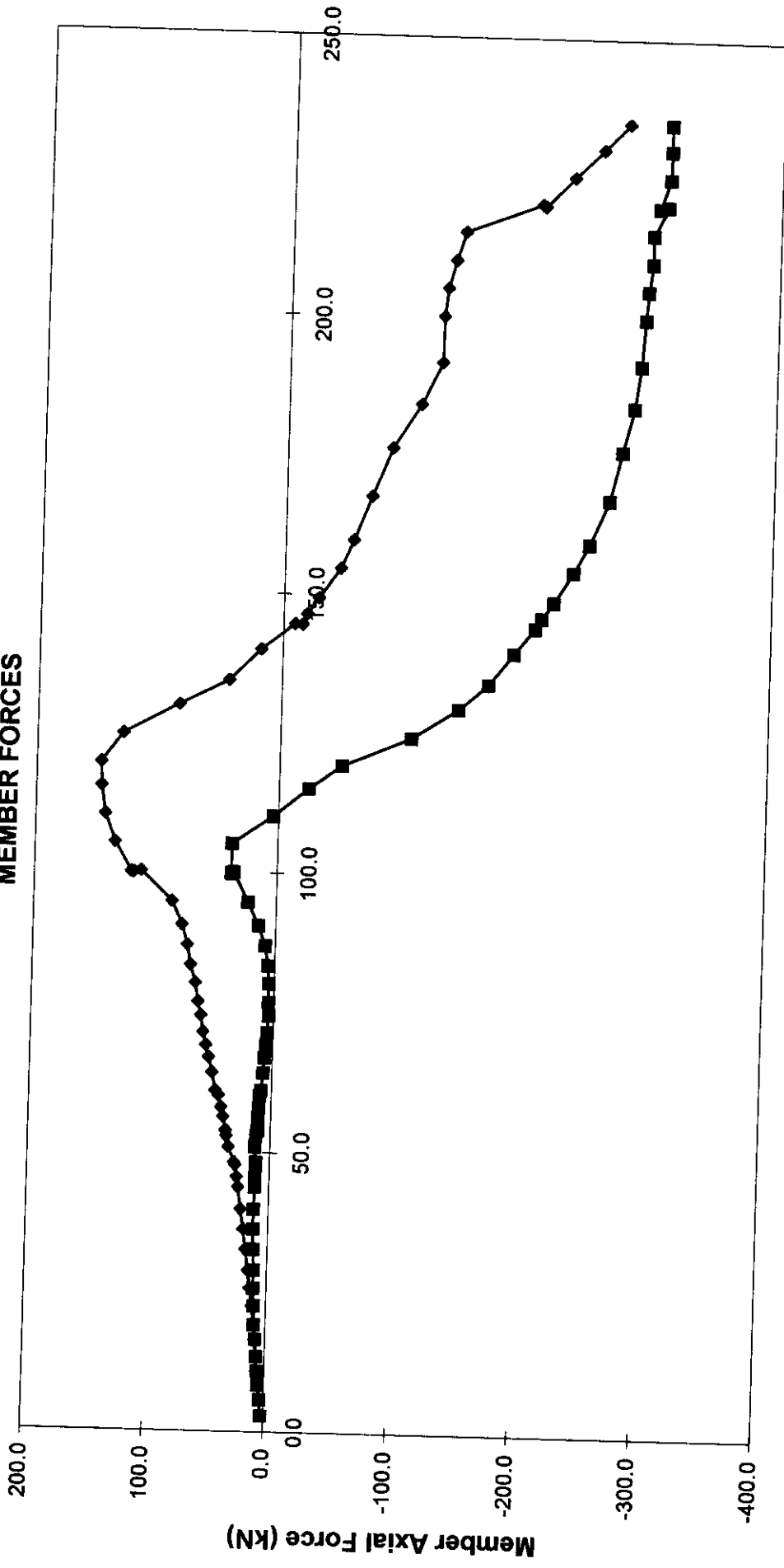
**FRAME E - TOP BAY  
MEMBER FORCES**



Global Displacement (mm)

Loadcase 3 - Test    ◆ 81 Measured    ■ 82 Measured    ▲ 83 Measured    ○ 84 Measured    × 85 Measured

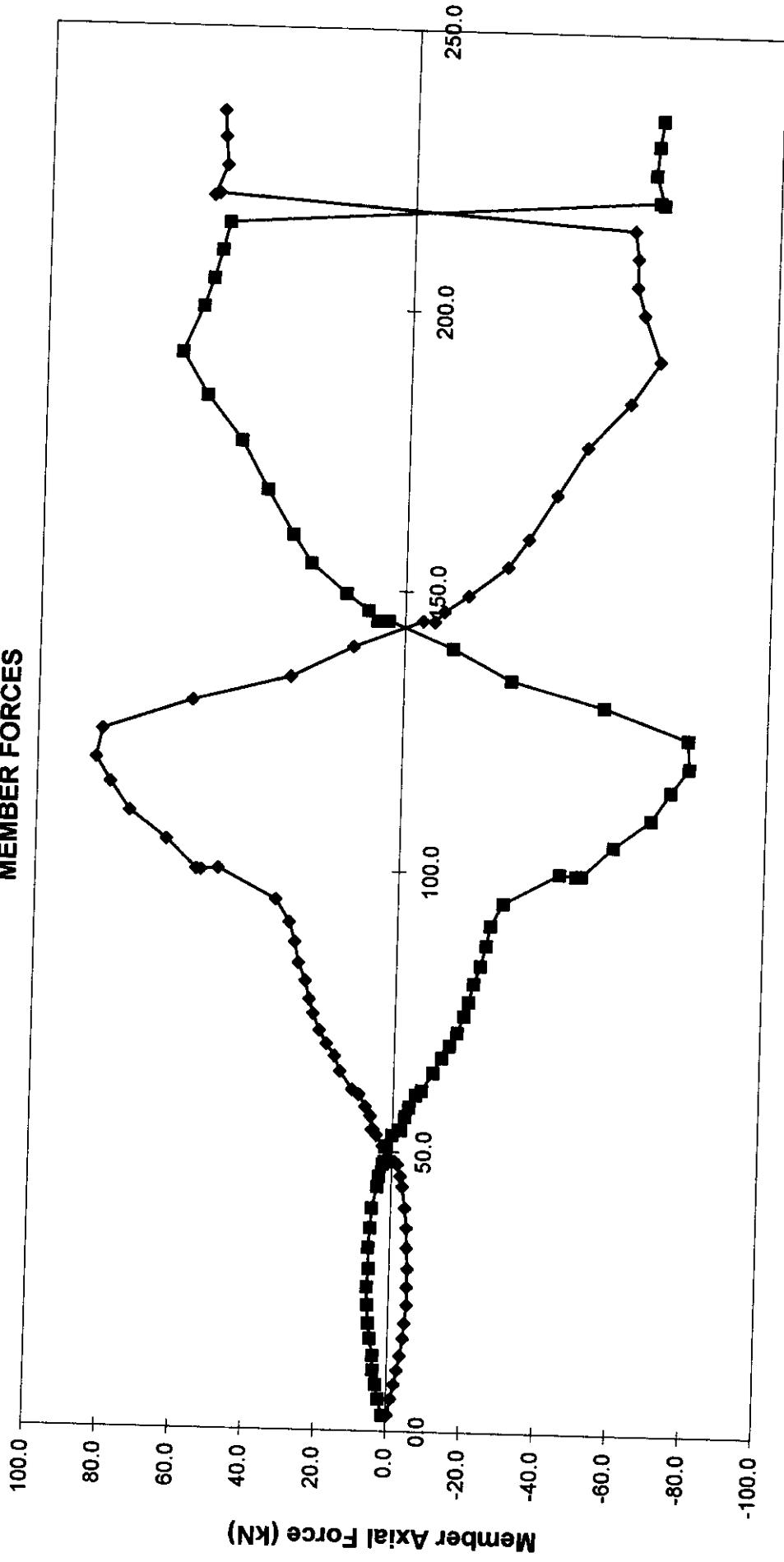
**LEVEL 2 - X  
MEMBER FORCES**



Global Displacement (mm)

Loadcase 3 - Test      —◆— 90 Measured      —■— 93 Measured

**LEVEL 2 - DIAMOND MEMBER FORCES**

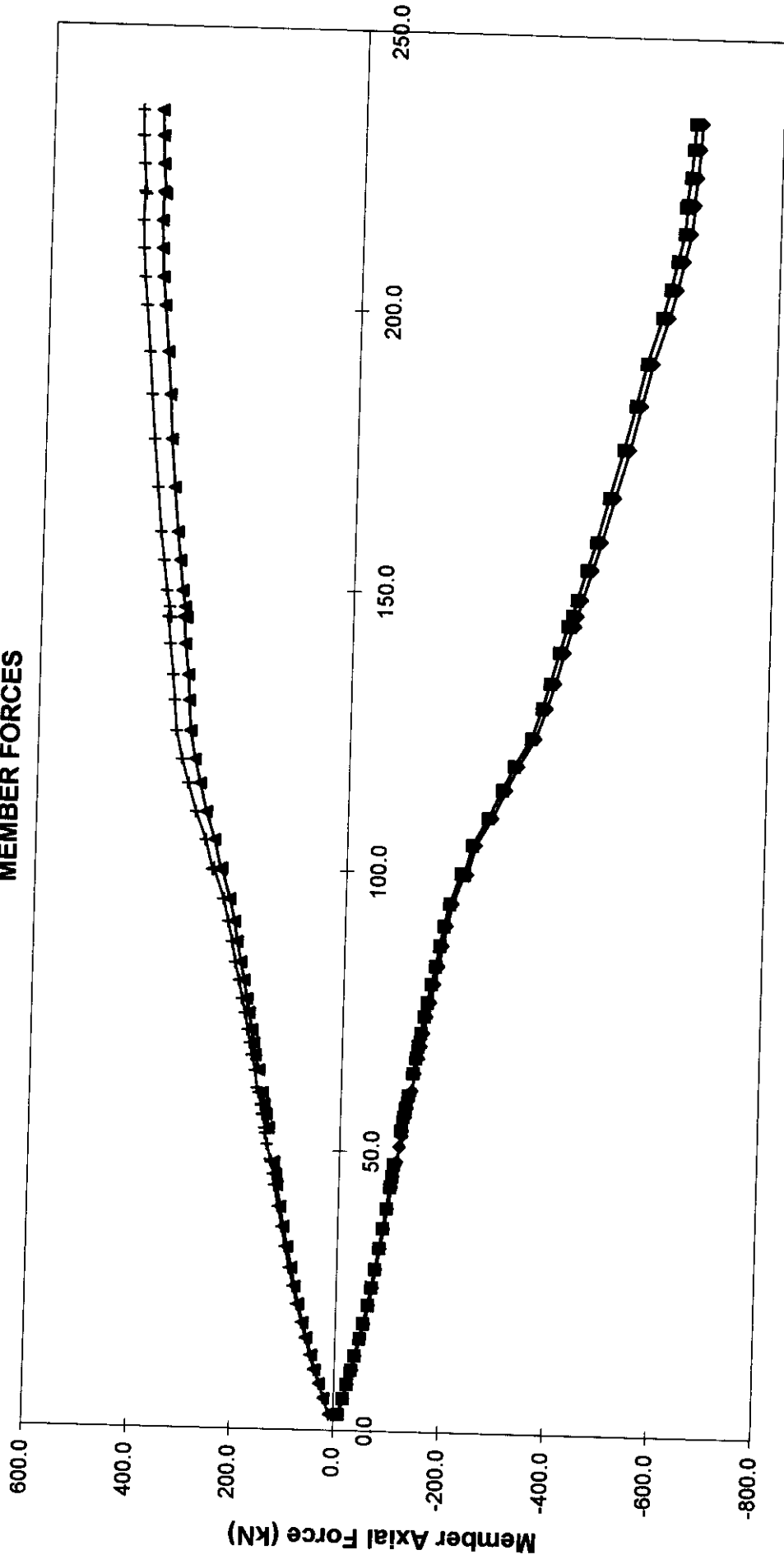


Global Displacement (mm)

Loadcase 3 - Test    ■ 86 Measured    ◆ 87 Measured



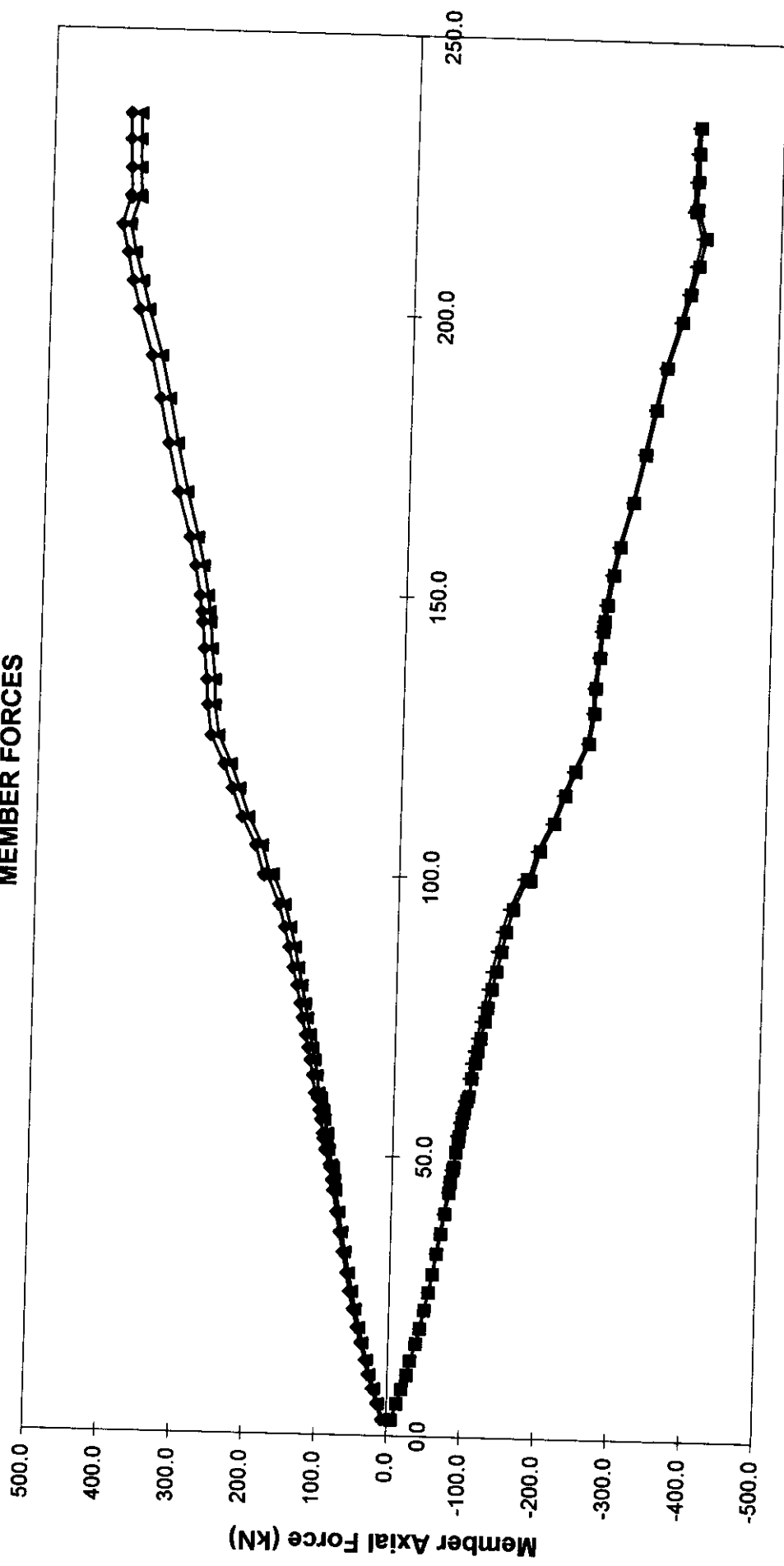
**LEVEL 1 - LC3X  
MEMBER FORCES**



**Global Displacement (mm)**

**Loadcase 3 - Test**    ◆— 98 Measured    ■— 100 Measured    ▲— 99 Measured    +— 101 Measured

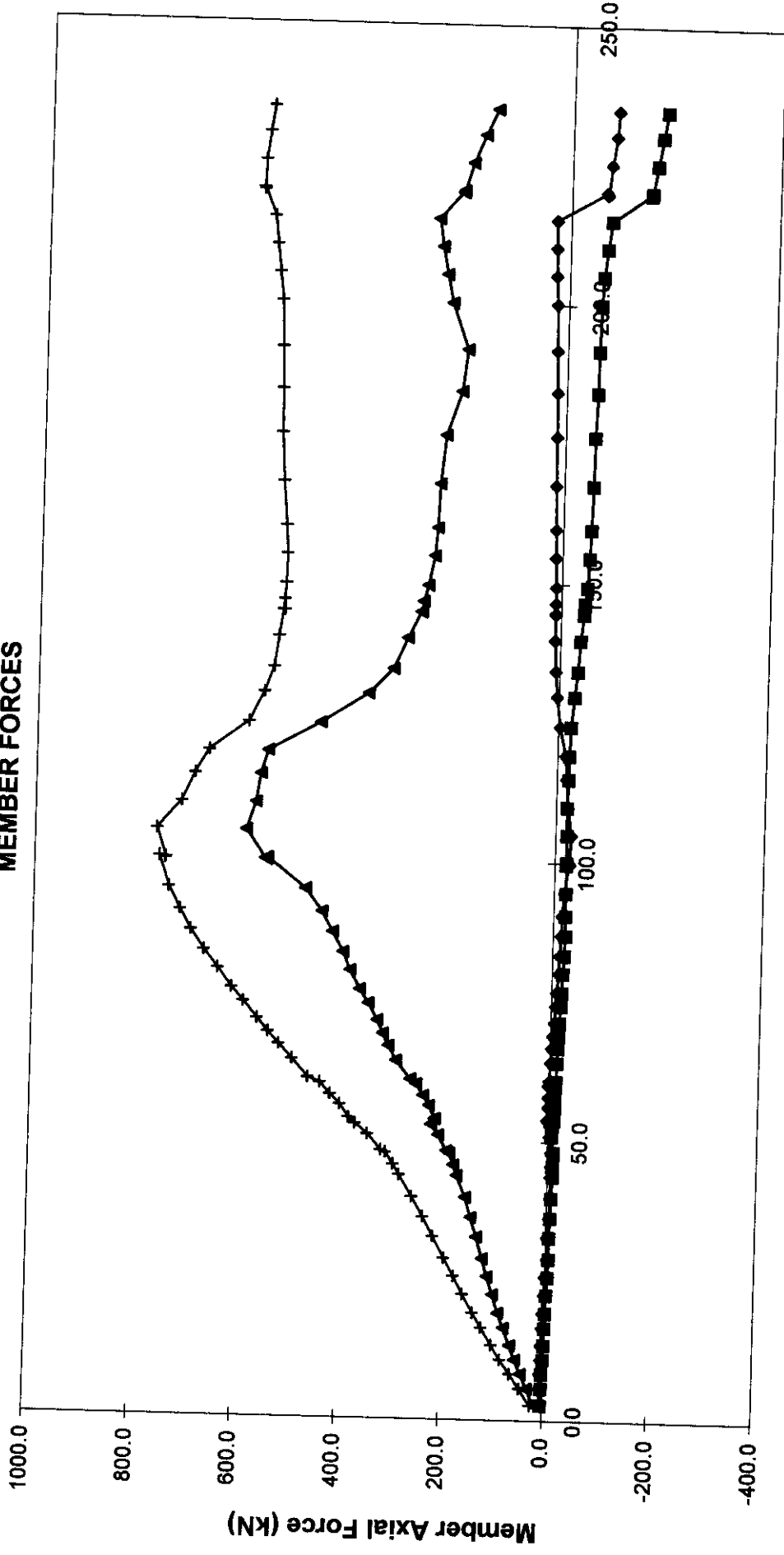
# LEVEL 1 - DIAMOND MEMBER FORCES



Global Displacement (mm)

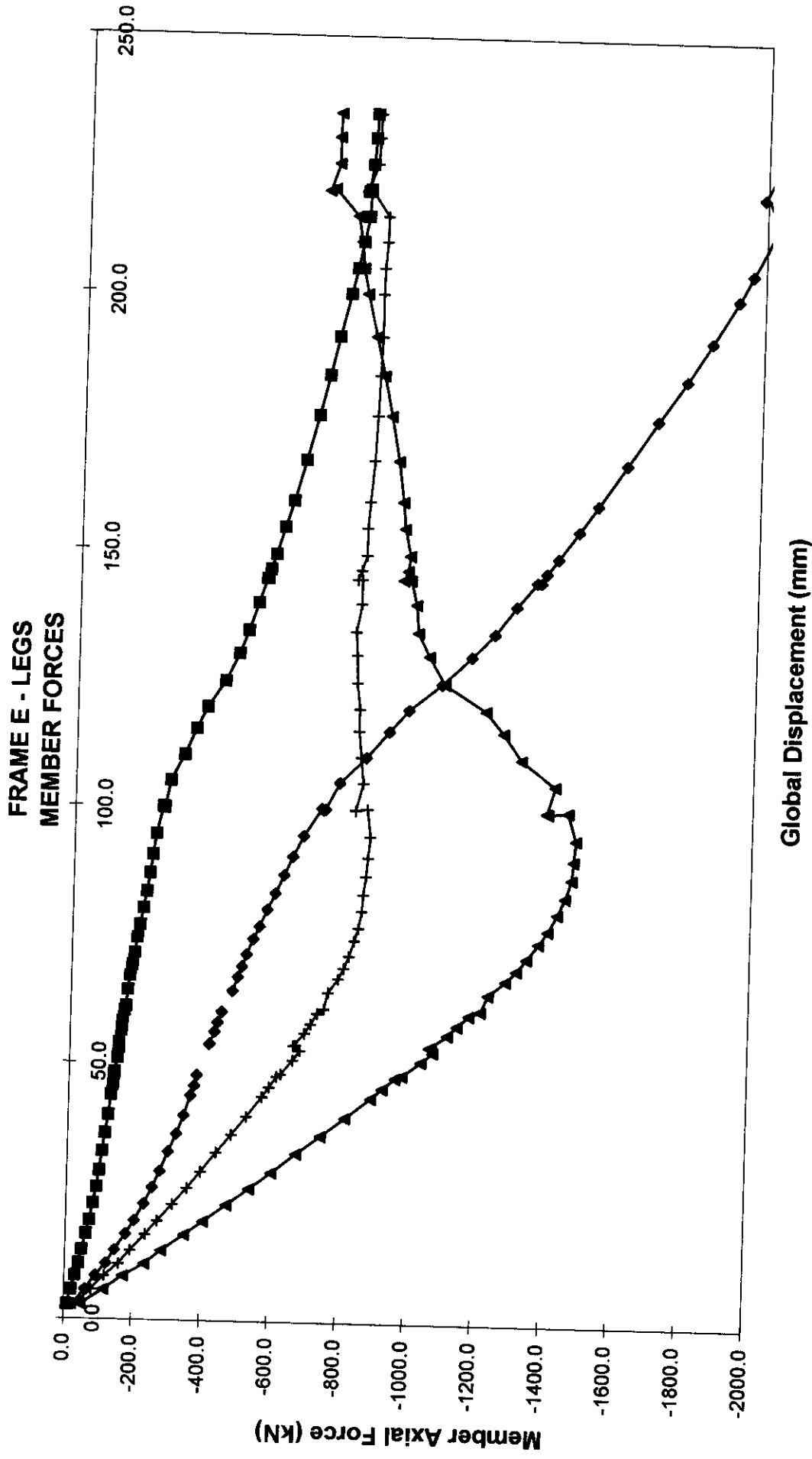
Loadcase 3 - Test    ◆ 94 Measured    ■ 95 Measured    ▲ 96 Measured    × 97 Measured

**FRAME D - LEGS  
MEMBER FORCES**

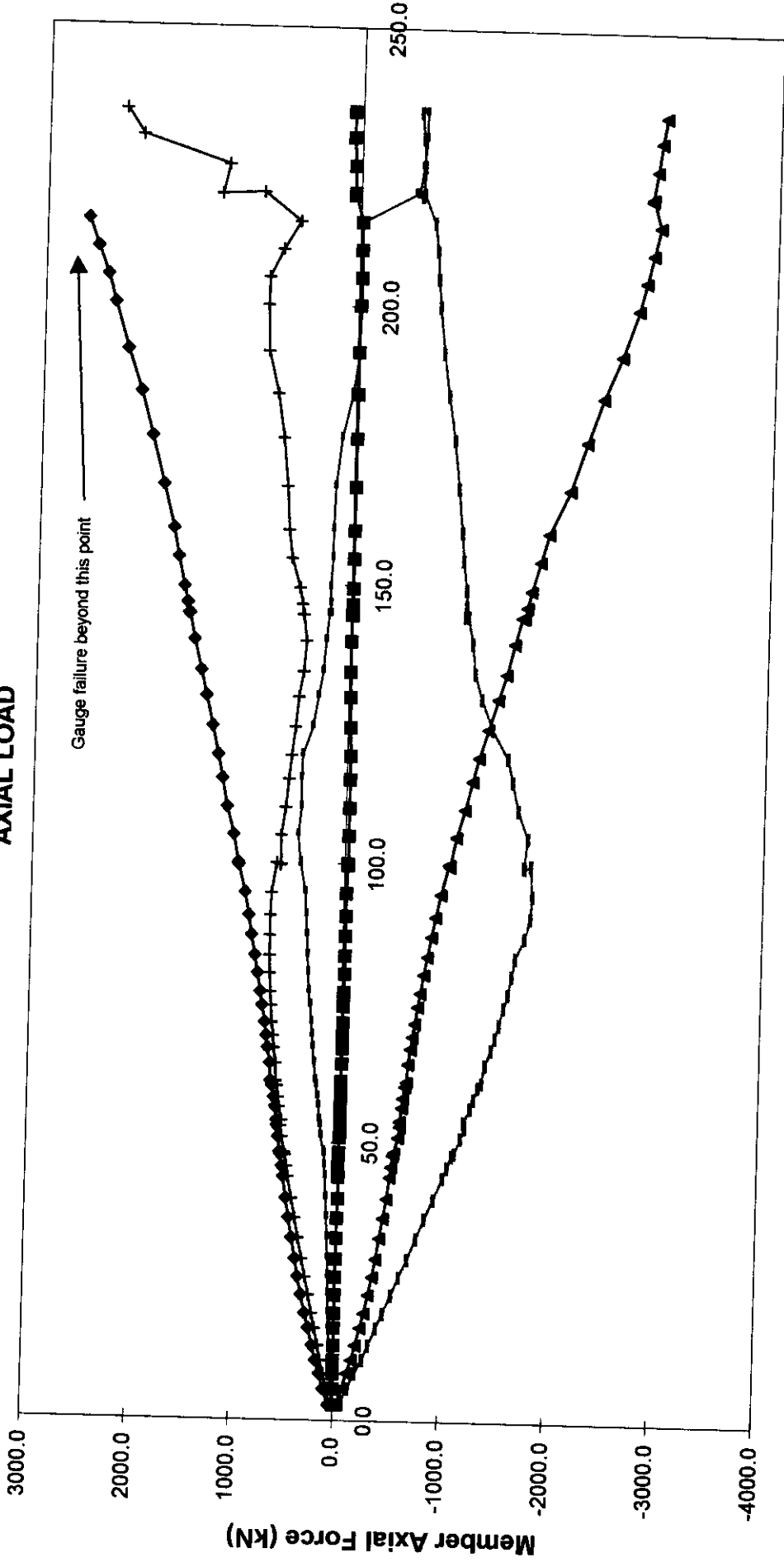


Global Displacement (mm)

Loadcase 3 - Test    ◆—5 Measured    ■—6 Measured    ▲—35 Measured    +—36 Measured



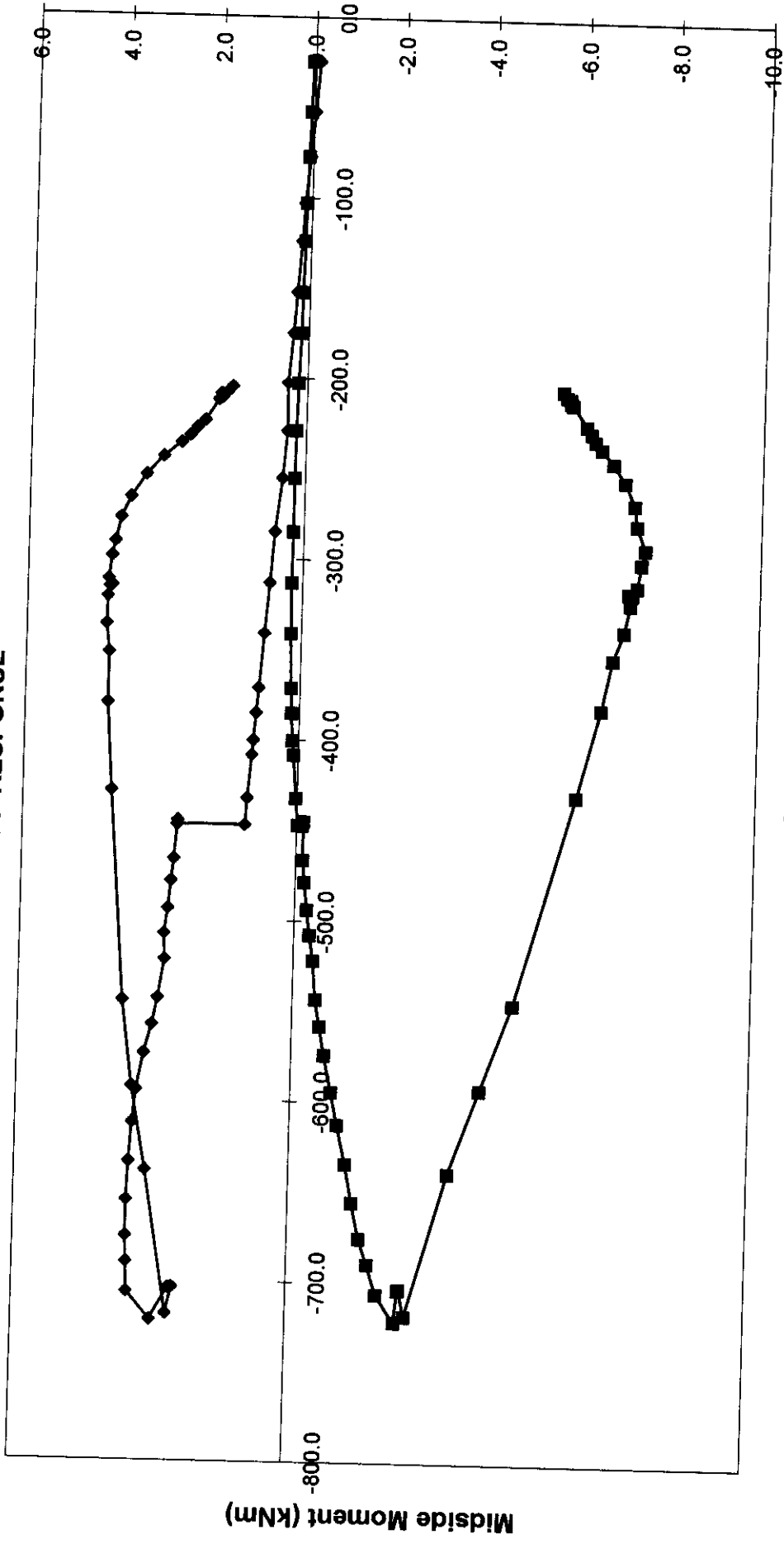
**FRAME FEET  
AXIAL LOAD**



Loadcase 3 - Test

- Global Displacement (mm)
- ◆ 1 Measured
  - 4 Measured
  - ▲ 7 Measured
  - + 31 Measured
  - 34 Measured
  - 37 Measured

FRAME A/ED- TOP BAY - UPPER  
M-P RESPONSE

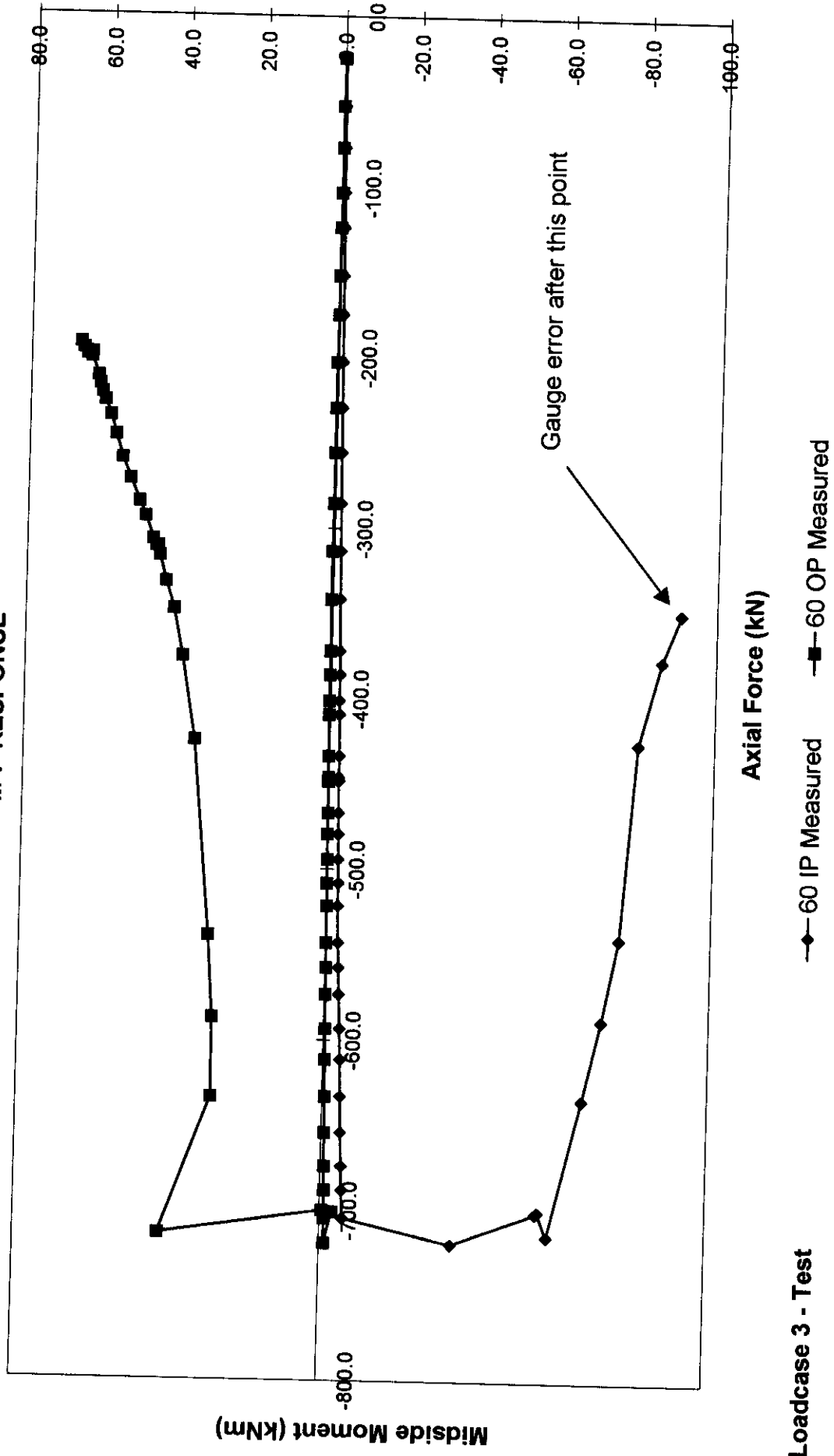


Axial Force (kN)

◆ 58 IP Measured    ■ 58 OP Measured

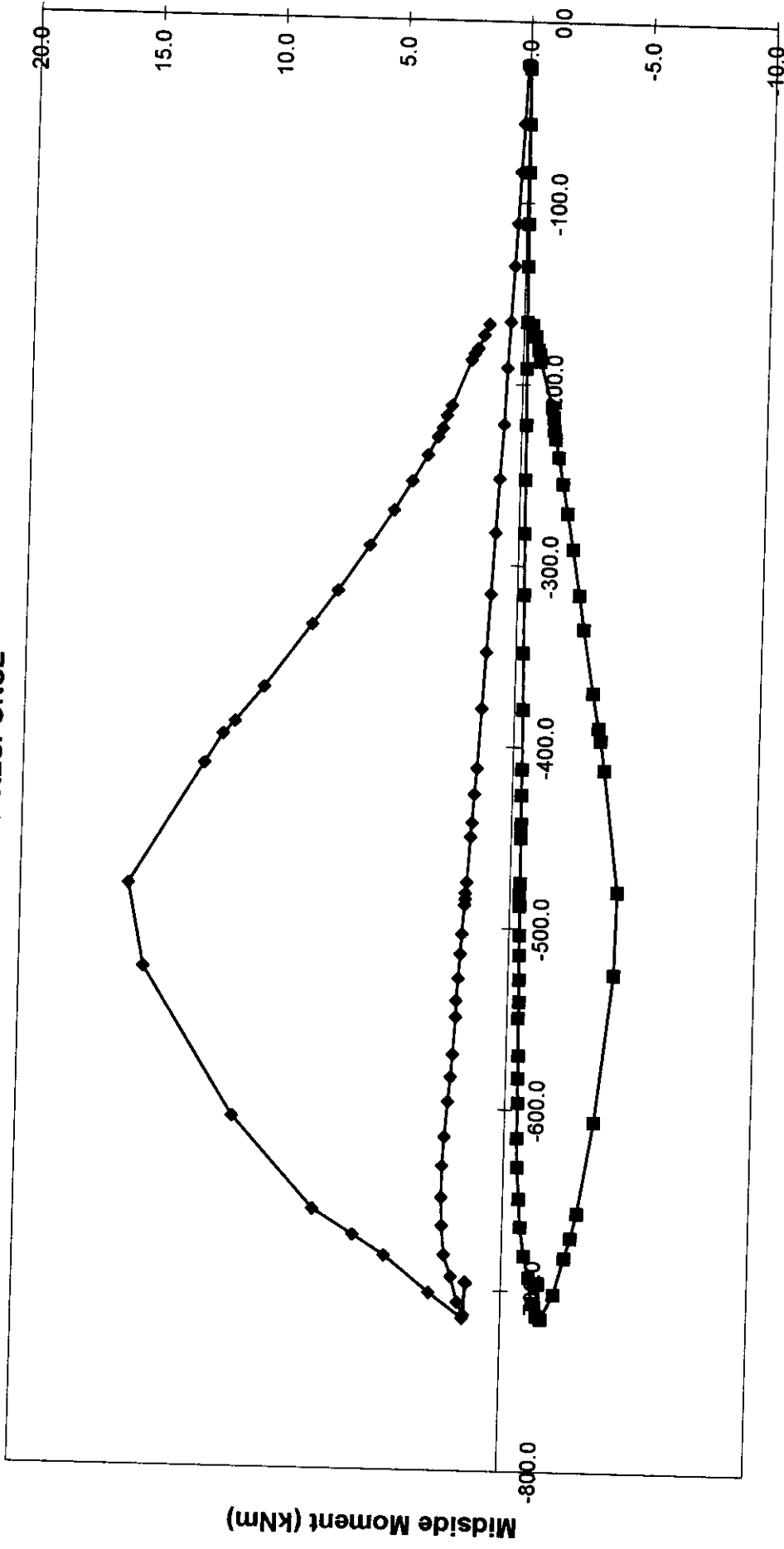
Loadcase 3 - Test

**FRAME A/ED-TOP BAY - LOWER  
M-P RESPONSE**



**Loadcase 3 - Test**

FRAME A/DC- BOTTOM BAY - UPPER  
M-P RESPONSE

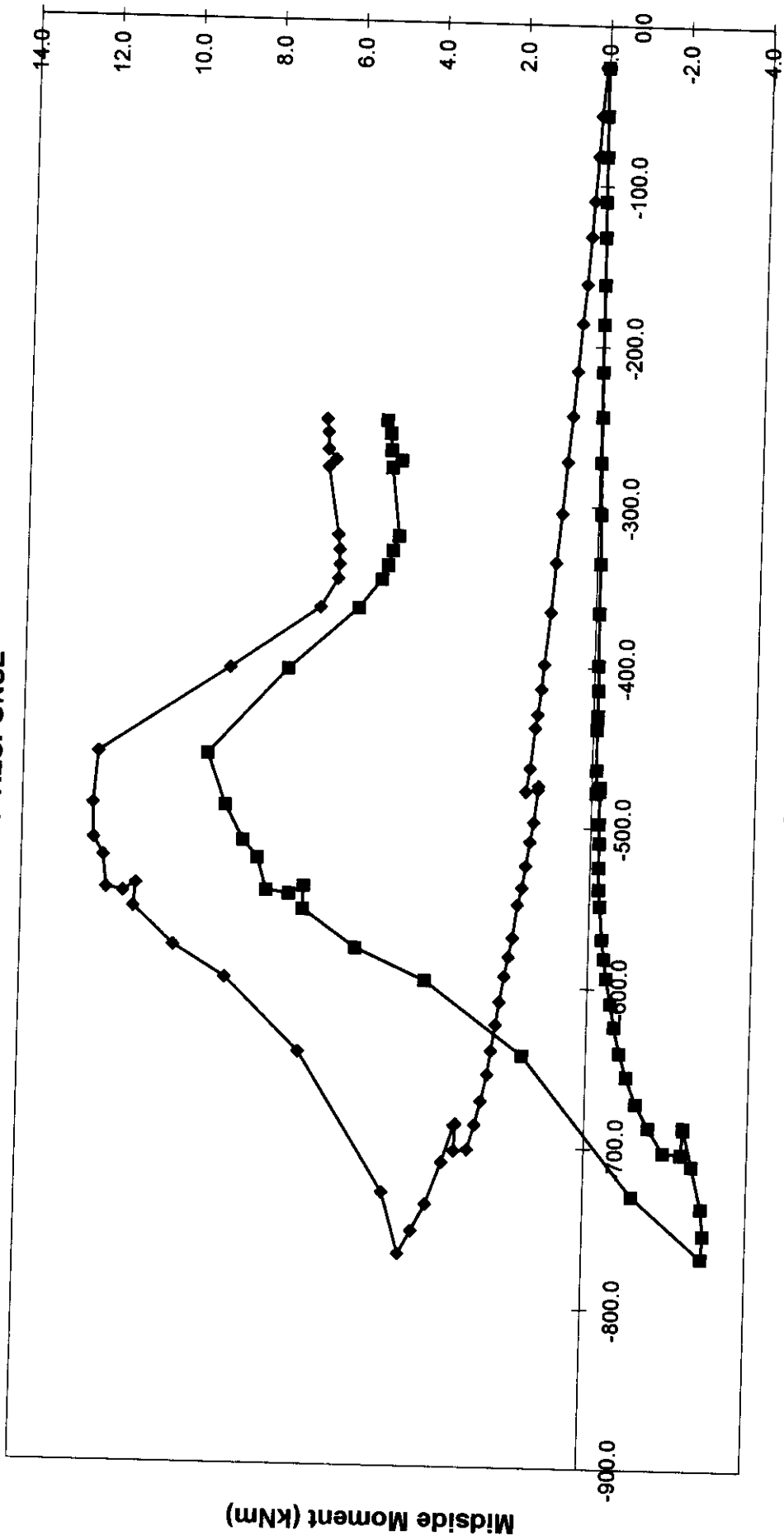


Loadcase 3 - Test      Axial Force (kN)

◆ 46 IP Measured      ■ 46 OP Measured



FRAME A/ED-BOTTOM BAY - UPPER  
M-P RESPONSE

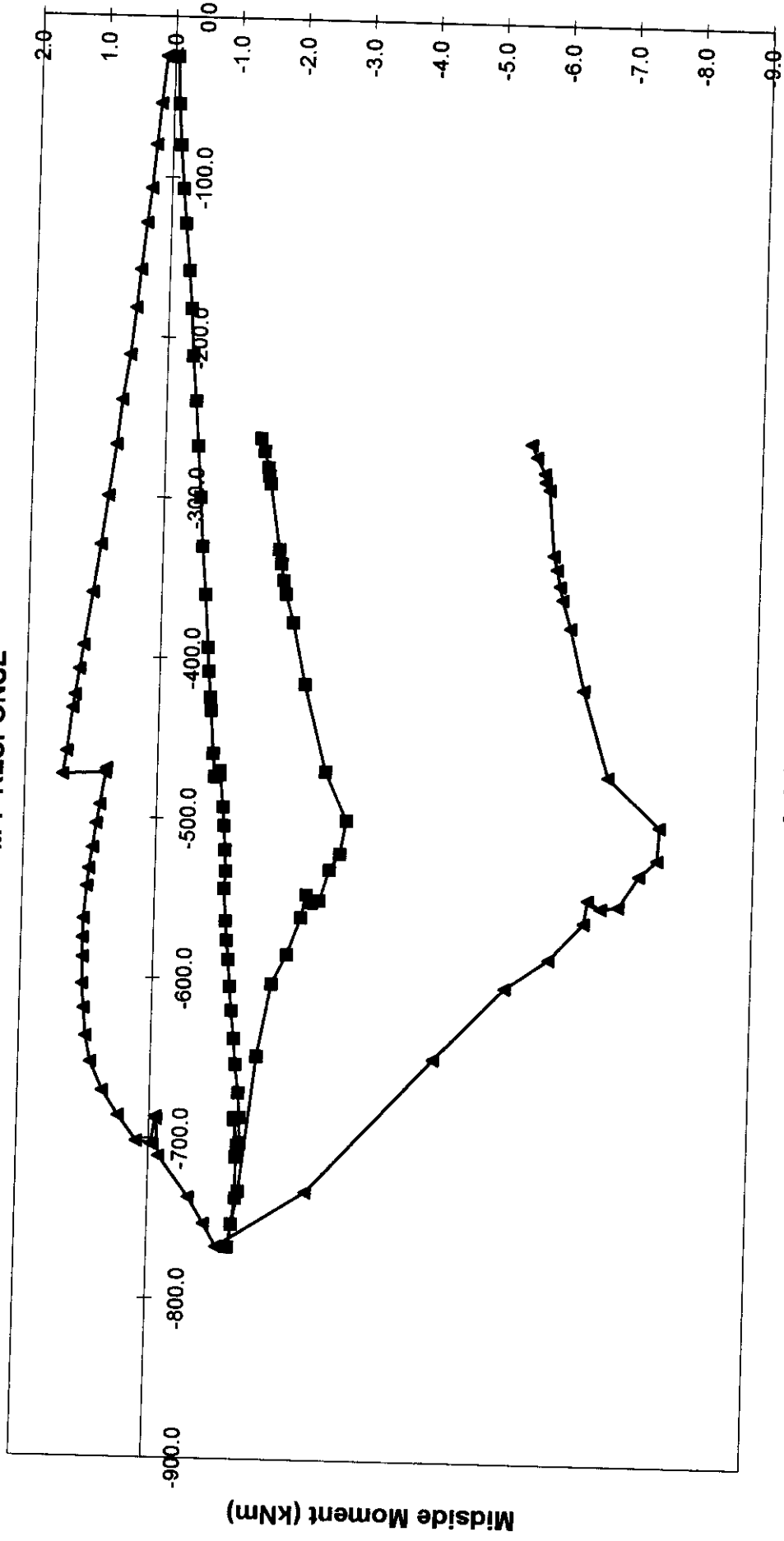


Loadcase 3 - Test

Axial Force (kN)

◆ 54 IP Measured    ■ 54 OP Measured

FRAME A/ED- BOTTOM BAY - LOWER  
M-P RESPONSE

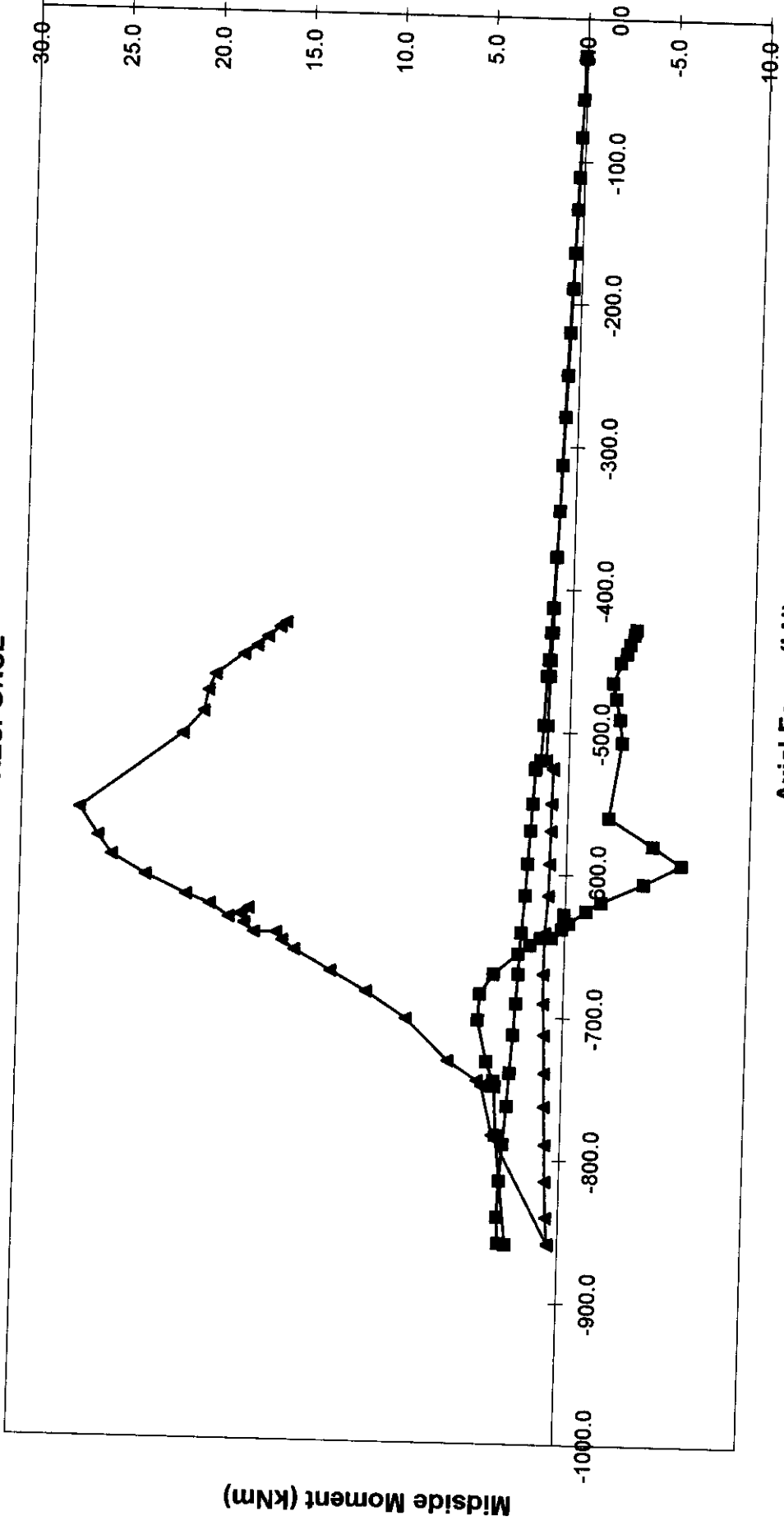


Loadcase 3 - Test

Axial Force (kN)

—■— 56 IP Measured    —▲— 56 OP Measured

**FRAME A/DC- TOP BAY - UPPER  
M-P RESPONSE**

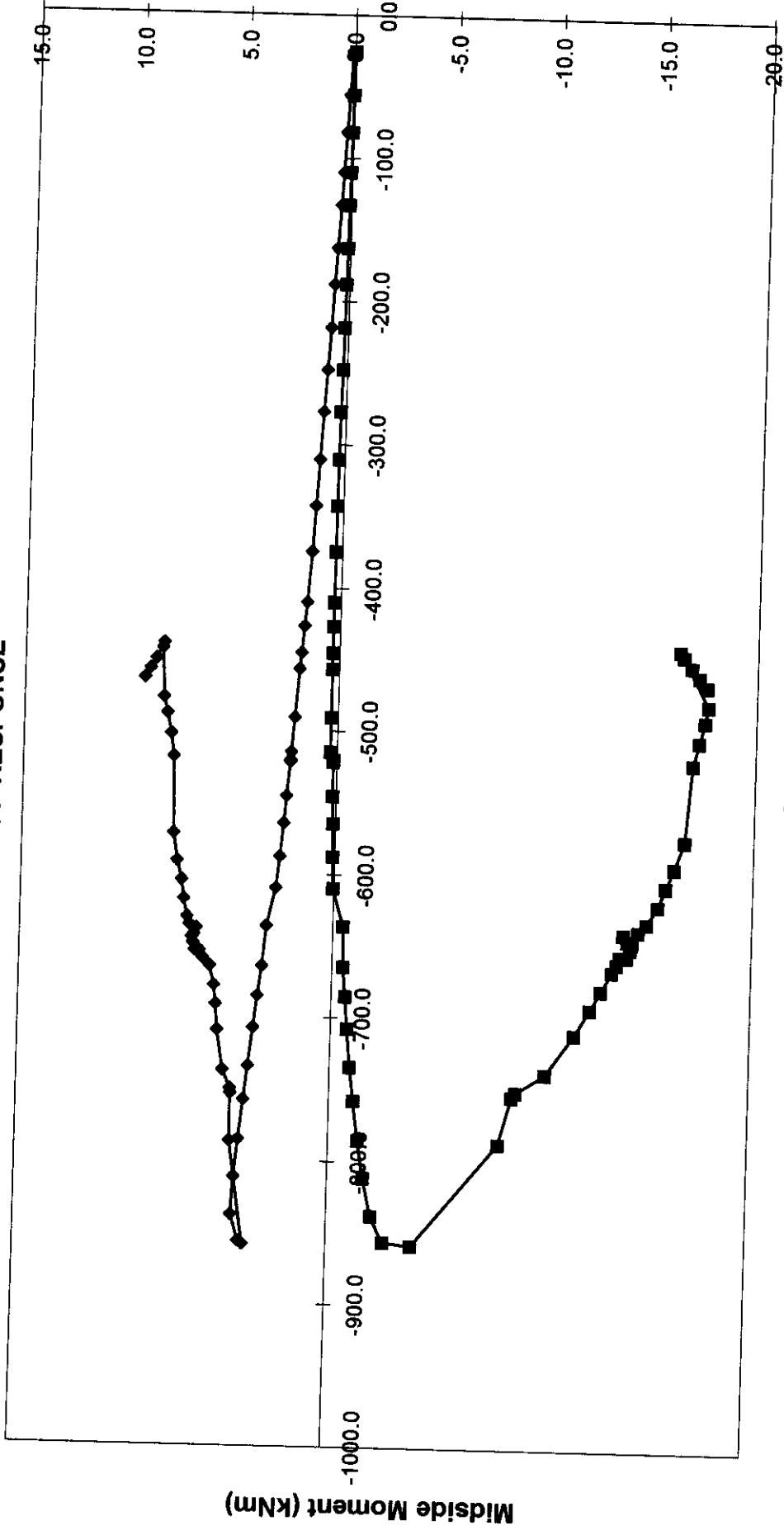


**Loadcase 3 - Test**

**Axial Force (kN)**

—■— 50 IP Measured    —▲— 50 OP Measured

**FRAME A/DC- TOP BAY - LOWER  
M-P RESPONSE**

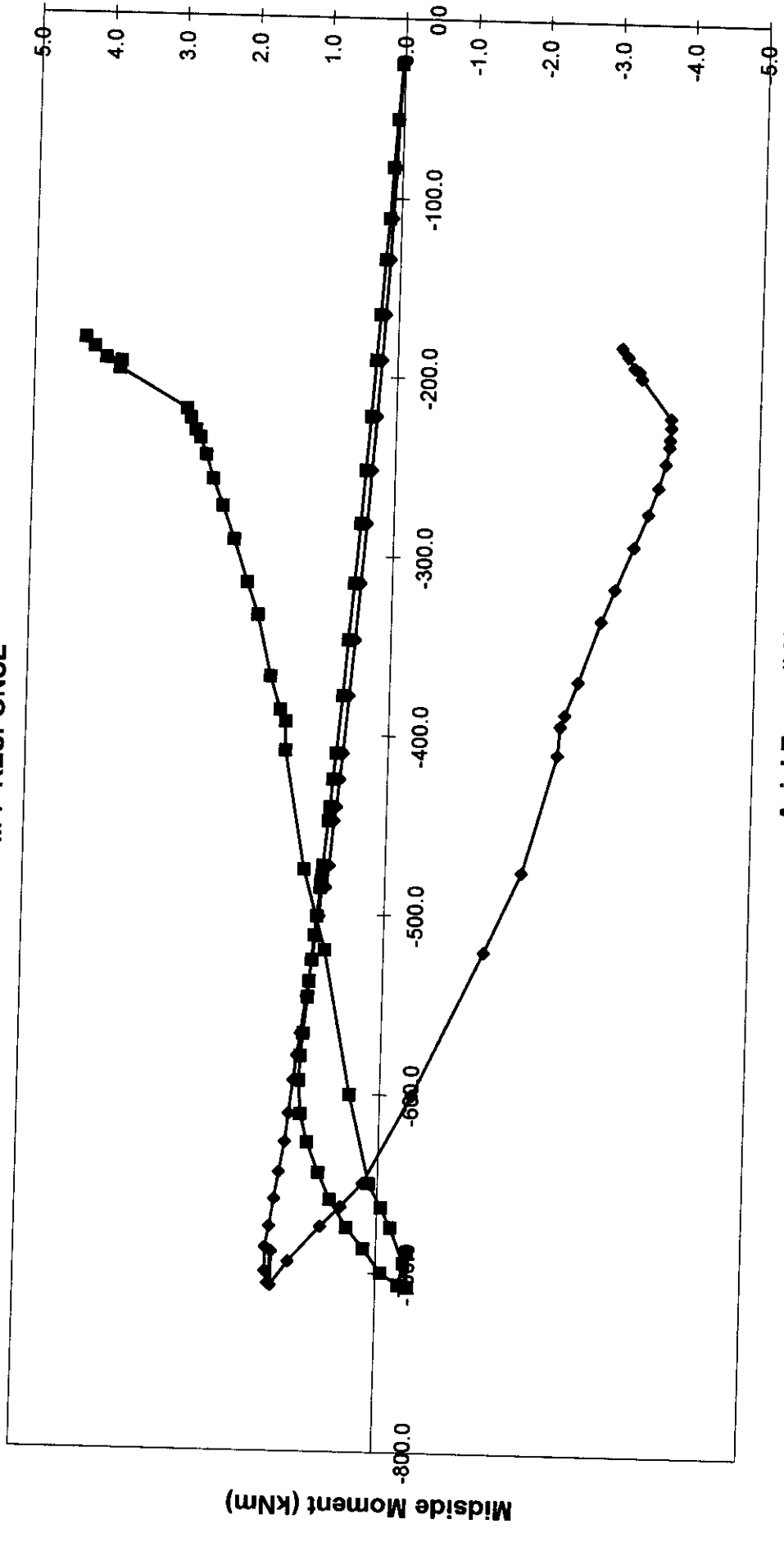


Loadcase 3 - Test

Axial Force (kN)

◆ 52 IP Measured    ■ 52 OP Measured

**FRAME A/DC- BOTTOM BAY - LOWER  
M-P RESPONSE**



**Loadcase 3 - Test**      **Axial Force (kN)**

◆ 48 IP Measured      ■ 48 OP Measured

**APPENDIX H**

**BENCHMARK ANALYSTS' RESPONSE PRO-FORMA**

(C636\32\082U - 2 pages)

# FRAMES PROJECT PHASE III BENCHMARK ANALYSTS FEEDBACK

## Introduction

This proforma is intended to help structure and give complementary feedback from Benchmark Analysts. The intention is to ensure that your own interpretation is properly reflected in the project output. Furthermore, the questions acknowledge the distinction between comparisons with the test and future conduct of offshore jacket analyses.

Please complete Questions 1 to 3 (and 5) and return the form (by email if possible) by 27 August. If you wish, your response to Question 4 may be delayed until 17 September, the date for submission of updated analysis reports.

Please direct your response and any questions to:

Helen Bolt Tel :+44 (0)1628 777707 Email: [bomel@compuserve.com](mailto:bomel@compuserve.com)

## References

1. Benchmark Analysts Blind Predictions – report and analysis
  2. BOMEL Report C636\12\006S Rev B September 1997 'Benchmark Analysis - Project work plan'
  3. BOMEL Report C636\32\002R Rev O February 1998 'Blind predictions of ultimate strength'
  4. BOMEL Report C636\32\066R Rev O July 1999 'Test Report to Benchmark Analysts'
- 

Based on review of Reference 4:

1. How do **you** explain the difference between your blind prediction and the physical response of the frame (components) in each test? (eg: Note difference in the component failure sequence and/or capacities and potential reasons; review global stiffness, etc).

Loadcase 1:

*Enter text here and expand space as appropriate*

Loadcase 2:

.....

Loadcase 3:

.....

2. Based on your response in 1:
- a) are there lessons you will carry forward to future ultimate strength analyses conducted in-house (eg. related to use of the specific software or modelling procedures)?  
.....
  - b) are there lessons which have general applicability and should form part of guidelines for good industry practice?  
.....
3. Based on the initial collation of blind predictions (Reference 3) and subsequent updates (shown in Reference 4)
- a) can you identify pitfalls experienced by others against which good practice guidelines should warn?  
.....
  - b) what advice can you offer client organisations when specifying and/or reviewing ultimate strength analysis?  
.....
4. Based on your best estimate analysis conducted post test, are there remaining discrepancies and to what do you attribute these? (NB these may be due to aspects of the modelling or physical aspects of the test.)  
.....
5. Any other comments.  
.....

---

Form completed by: ..... (name)

For: ..... (company)

Date: .....